Phylogenetic Systematics of the North American Fossil Caninae (Carnivora: Canidae)

Authors: Tedford, Richard H., Wang, Xiaoming, and Taylor, Beryl E.

Source: Bulletin of the American Museum of Natural History, 2009(325) : 1-218

Published By: American Museum of Natural History

URL: https://doi.org/10.1206/574.1

PHYLOGENETIC SYSTEMATICS OF THE NORTH AMERICAN FOSSIL CANINAE (CARNIVORA: CANIDAE)

RICHARD H. TEDFORD

Curator Emeritus, Division of Paleontology
American Museum of Natural History
(tedford@amnh.org)

XIAOMING WANG

Department of Vertebrate Paleontology
Natural History Museum of Los Angeles County, California
(xwang@nhm.org)

BERYL E. TAYLOR

Frick Curator Emeritus
Division of Paleontology
American Museum of Natural History

BULLETIN OF THE AMERICAN MUSEUM OF NATURAL HISTORY
Number 325, 218 pp., 71 figures, 7 tables
Issued September 3, 2009

 ISSN 0003-0090

CONTENTS

ABSTRACT

The canid subfamily Caninae includes all the living canids and their most recent fossil relatives. Their sister taxon is the Borophaginae with which they share an important modification of the lower carnassial, namely the presence of a bicuspid talonid, which gives this tooth an additional function in mastication. Contributing to this function is the enlargement of the posterolingual cingulum of M1 and development of a hypocone. The Caninae diverged from the Borophaginae in the narrowing and elongation of the premolars separated by diastemata and placed in a shallow ramus and narrow muzzle. These latter features allow the Caninae to be recognized in the fossil record as early as the beginning of the Oligocene (34 Ma) and constitute evidence that they represent a monophyletic group.

In striking contrast to the history of the Borophaginae, the Caninae remain confined to a closely similar group of fox-sized species (*Leptocyon* spp.) throughout the Oligocene and showing very limited cladogenesis into the end of the medial Miocene (12 Ma), a span that saw marked adaptive divergence in the Borophaginae and the origin of all its major clades. By 12 Ma (beginning of the Clarendonian Land Mammal age) few fox-sized borophagines remained and most of those held hypocarnivorus adaptations. At that point the Vulpini appear both as mesocarnivores (*Vulpes* spp.) and hypocarnivores (*Metalopex* spp.) reproducing, on a much smaller scale, the range of adaptations shown in the initial radiation of the Borophaginae.

By the end of the Clarendonian (9 Ma) the first members of the tribe Canini appear. Initially this group was represented by the genus *Eucyon*, largely by a single widespread North American species *E. davisi*. Our cladistic analysis predicts that the roots of the South American clade subtribe Cerdocyonina, sister taxon to *E. davisi* and *Canis* species (together, subtribe Canina), must also have been present, but taxa representing this group do not appear in the North America record until the earliest Pliocene (latest Hemphillian, 5 Ma). Species of three genera (*Cerdocyon*, *Chrysocyon*, and possibly *Theriodictis*), now confined to South America, appear in the fossil record of the southern United States and northern Mexico prior to and just after the opening of the Panamanian Isthmus (ca. 3 Ma), indicating that important cladogenesis within the South American clade took place in North America. Species of *Eucyon* make their appearance in the Old World in the late Miocene, and *E. davisi* has a Pliocene record in Asia. Species of this genus undergo a modest adaptive radiation in Eurasia during the Pliocene.

In the late Miocene and early Pliocene two species of *Canis* appear in North America (*C. ferox* and *C. lepophagus*), representing the initial cladogenesis within the genus. These animals are all coyote-sized and represent a broadening of body size range within a mesocarnivorous dental adaptation. Toward the end of the Pliocene and into the Pleistocene in North America a curious and rare group of jackal-like species (*C. thöoides*, *C. feneus*, and *C. cedazoensis*) seem to form an endemic clade arising near *C. lepophagus*. These taxa are dentally similar to jackals, especially *C. aureus*, but share no synapomorphies with them.

The early cladogenesis of *Canis* in the Pliocene of North America produced a somewhat larger form, *C. edwardii*, that appears in the late Blancan at ca. 3 Ma. It also seems to have a sister relationship with *C. lepophagus* and with the coyote *C. latrans*, which appears much later in the record (late Irvingtonian) and quickly becomes distributed across the United States. The golden jackal (*C. aureus*) shares synapomorphies with the coyote and *C. edwardii* but does not appear in the fossil record until the early Pleistocene of North Africa. *Canis edwardii* is extinct by the end of the Irvingtonian.

Large wolflike species of *Canis* seem to be the products of evolution in Eurasia. They appear early in the North American record as immigrants of the crown group of *Canis* that augment the essentially stem group native species of the New World. The first of these is *Canis armbrusteri*, which appears early in the Irvingtonian, initially in the Southwest but later in the eastern United States where it survived into the early Rancholabrean of Florida. This is a large wolf, a sister taxon of *C. lupus*, whose appearance early in the Pleistocene predates the earliest midcontinent occurrence of *C. lupus* by nearly 1 m.y. In the New World *C. armbrusteri* gave rise to the native dire-wolf (*C. dirus*), as evidenced by intergrading morphologies of late Irvingtonian examples that show the transformation to the more hypercarnivorous giant form. The earliest evidence of *C. dirus* is in the midcontinent and it

appears to have displaced *C. armbrusteri* into the eastern part of the continent while it expanded westward and particularly southward into South America during the late Pleistocene. *Canis lupus* itself does not appear in midlatitude North America until the late Rancholabrean (0.1 Ma, last glacial cycle), although it was a resident of Arctic North America since the mid-Pleistocene (ca. 0.8 Ma).

North America has a limited record of canine diversity during the Pleistocene. Most clades of vulpines and canines that reached the Old World during that span underwent significant cladogenesis so that the canid fauna of Eurasia was always more diverse than that of the New World. From time to time waifs from the Old World centers of origin wandered south into midcontinent North America to briefly enrich the fossil record: *Xenocyon* spp. in the late Irvingtonian; *Cuon alpinus* and *Canis lupus* in the late Rancholabrean, along with the living fox species *Vulpes vulpes* (late Rancholabrean) and perhaps the swift-fox earlier in the Pleistocene. The center of evolution of the Caninae thus shifted to Eurasia and to South America when avenues of dispersal to those continents were available at the end of the Cenozoic.

Because of the diversity of Old World forms that became resident in North America, our analysis of the New World fauna has been expanded to include relevant Old World taxa and to present a broader phylogenetic reconstruction than could be offered only on the basis of strictly New World evidence. This expanded view brings in a greater diversity of morphology, which allows us to better separate homoplasy from true homology. We have considered only Old World taxa that are represented by the most complete material so that missing data are kept to a minimum in our analysis. This still affords sufficient taxa so that the major structure of the phylogeny of *Canis* can be discerned.

Our cladistic analysis found two robustly recognized crown clades within *Canis*: the mesocarnivorous *lupus* clade, and the hypercarnivorous *Xenocyon* clade. The first contains the wolf, *C. lupus*, and its sister taxon *C. armbrusteri* + *C. dirus*, with the latter showing some dental features related to hypercarnivory as an autapomorphy. The Chinese late Pliocene wolf *C. chihliensis* appears to be a stem group in the *Lupus* clade and may be closely allied to *C. armbrusteri*. The *Xenocyon* clade is also Eurasian in origin and is marked by character reversals to states primitive within *Canis*. Its earliest record is in the medial Pliocene of eastern Asia (*Xenocyon dubius*), after which it dispersed to western Eurasia in the early Pleistocene (*X. lycaonoides*). In the Pleistocene *Xenocyon* achieved a Holarctic distribution including midlatitide North America (*X. texanus* and *X. lycaonoides*). During this episode of expansion the sister taxa *Cuon* and *Lycaon* arose in Eurasia and Africa, respectively, most likely from isolated *Xenocyon* populations.

In the latest Pleistocene *Cuon alpinus* expanded its range into the middle latitudes of the New World. A number of Pliocene and Pleistocene wolf and coyote-sized Eurasian *Canis* species (*C. arnensis*, *C. etruscus*, *C. palmidens*, *C. mosbachensis*, and *C. variabilis*) were included in our cladistic analysis, but the relationships of those forms were difficult to resolve beyond their paraphyletic relationship to the crown clade.

INTRODUCTION

The long association of man and dog have guaranteed a greater than usual interest in the biology of canids and their phylogenetic relationship among themselves and with other Carnivora. The increasing field and laboratory study of the behavior and molecular systematics of domestic and wild canids have intensified this interest at the present time. It seems especially propitious in light of this interest and the availability of the unprecedented Frick Collection of North American Tertiary canids to review the history of the group based on a critical reevaluation of the evidence from the continent of origin of most living canid clades.

The family Canidae Fischer de Waldheim, 1817, was one of the earliest groups to be recognized by nineteenth century zoologists within the order Carnivora. Although Fischer de Waldheim (1817: 372) proposed this taxon in the form Canini, it is held to be a name at the family rank and hence has priority over Canidae Gray, 1821, following article 36 of the International Code of

Zoological Nomenclature (1985). Various ideas of the relationship of the canids to other carnivoran families (including representatives of other groups now excluded from the order) were based on dentitions, postcranial skeletons, or soft parts and consequently unanimity of classification within the order was lacking. In 1848 H.N. Turner realized that the dentitions and limbs of the Carnivora were intimately linked to specific adaptations and recognized that the structure of the basicranium revealed a suite of characters relatively shielded from feeding and locomotor adaptations. He proposed that the basicranial structures, along with certain features in limbs, teeth, and soft anatomy, could be used to diagnose the families of Carnivora. These observations on living Carnivora were repeated and extended in a more comprehensive manner by W.H. Flower in 1869. These important works laid the fundamental basis for the subdivision of the order Carnivora still in use. Flower recognized, as did Turner, that the terrestrial carnivorans, the fissipeds, could be divided into three groups (called sections by Flower but now regarded as superfamilies). These were based primarily on the presence (Aeluroidea), absence (Arctoidea), or partial development (Cynoidea) of a septum within the hypotympanic cavity of the bulla. In this century the basicranium of the Carnivora has been examined in greater detail by Van Kampen (1905), Van der Klaauw (1931), Segall (1943), Hough (1948), and Hunt (1974), and these studies confirm the empirical grouping of characters in this region into three (or five, Hunt, 1974) morphotypes. In all cases the living Canidae form a uniform group in which the caudal entotympanic makes a substantial contribution to the medial wall of the bulla; the entotympanic-ectotympanic junction is marked by a low septum partially dividing the hypotympanic cavity anteriorly; the bulla has a sutured union with the base of the paroccipital process, with the latter maintaining a free tip; and the internal carotid artery lies in a groove in the median wall of the bulla (see Hunt, 1974, for useful figures illustrating these structures). In a related work (Wang and Tedford, 1994) we have recently reviewed the history of these structures as they pertain to the Canidae. Extensive comparisons made in the literature and in the course of our own research on the Carnivora and with other closely related orders convince us that this suite of basicranial characters, as well as other features of osteology and soft parts, supports the view that the living Canidae represents a monophyletic group. Furthermore, we contend that certain fossil forms, especially those represented by skulls and skeletons, can also be grouped in the Canidae using these same diagnostic criteria.

In this study we regard the Canidae as a monophyletic group based on the criteria mentioned above and explored more fully in our phyletic studies (Wang, 1994; Wang and Tedford, 1994; Wang and Tedford, 1996; Tedford et al., 1995; and Wang et al., 1999). An essential step in our phylogenetic analysis of the Canidae was to discern the larger patterns of relationships within the family. Preliminary analysis of the entire fossil and living canid collection before us indicates that three groups of canids can be recognized whose mutual phyletic relationships are demonstrated by shared-derived cranial and dental characters. Expressed in the form of a cladogram (fig. 1), all living canids belong to a group (subfamily Caninae Fischer de Waldheim, 1817) having a monophyletic relationship with the extinct borophagines (subfamily Borophaginae Simpson, 1945) through possession in both of a clearly bicuspid lower carnassial talonid. The development of a distinct entoconid cusp (conical or crestlike) and consequent broadening of the talonid of m1, the corresponding enlargement of the talon of M1, and reduction of the M1 parastyle distinguish these late Cenozoic canids and constitute the essential diagnoses for the clade that contains them. These subfamilies in turn are linked to a primitive sister taxon, the subfamily Hesperocyoninae Martin, 1989, by the characteristic canid cranial characters. These primitive canids have narrow lower carnassial talonids with a large crestlike and labially situated hypoconid. The talonid is rimmed lingually by a low entoconid crest and the narrow upper molars have prominent parastyles and small, lingually placed hypocones.

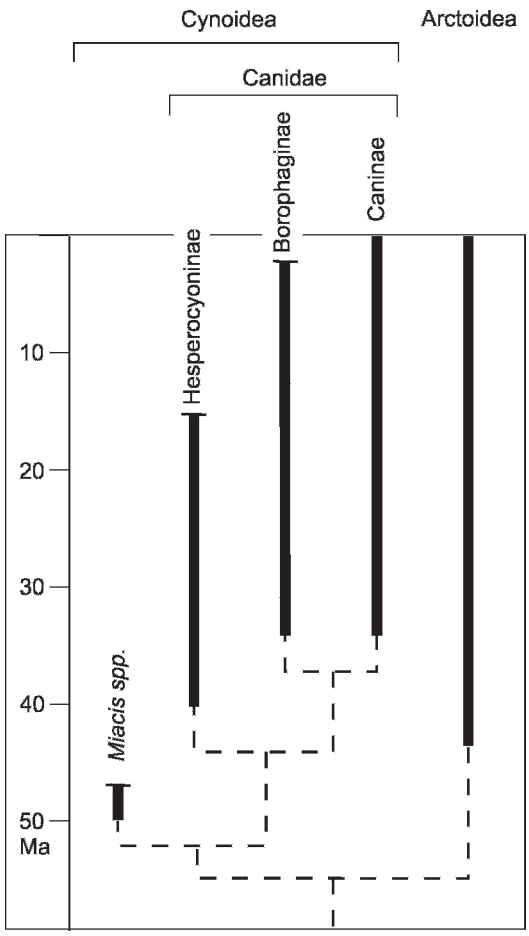

Fig. 1. Cladogram showing the phyletic relationships of the major clades of the Canidae and their temporal ranges. Species of the cynoid *Miacis* are paraphyletic to the Canidae. The Arctoidea (Amphicyonidae, Ursidae, Procyonidae, Mustelidae, and the Phocoidea McKenna and Bell, 1997) serves as the outgroup.

Given these hypotheses of relationships, we recognize that the Canidae first appears in the fossil record in North America in the earliest Chadronian (late Eocene, Wang and Tedford, 1994, 1996), but they do not reach the Old World until late in Miocene time (*Canis cipio* Crusafont, 1950, Turolian, Spain) or in South America until the late Pliocene or early Pleistocene (see Berta and Marshall, 1978, for review and Marshall et al., 1982, for dating). The major part of the recorded history of the Canidae was thus spent within the confines of North and Central America where we infer they experienced three adaptive radiations whose distribution in time was sequential and overlapping (see fig. 2) and whose morphological limits were remarkably repetitive in scope. In the pages that follow we detail the evidence for the systematics and the resulting phyletic reconstruction of the North American Caninae. We comment on the relationship of the North American canines to those of Eurasia and South America because following the Miocene, these continents provided the theaters for much of the evolution that yielded the living canine fauna.

Institutional Abbreviations

ACM	Amherst College Museum (Pratt Museum), Amherst, MA
AMNH	Department of Vertebrate Paleontology, American Museum of Natural History
AMNH(M)	Department of Mammalogy, American Museum of Natural History
ANSP	Academy of Natural Science of Philadelphia, Philadelphia
CMNH	Carnegie Museum of Natural History, Pittsburgh
CWT	Christian Collection, West Texas University, Canyon
DMNH	Denver Museum of Natural History, Denver
F:AM	Frick Collection, Department of Vertebrate Paleontology, American Museum of Natural History
FMNH	Field Museum of Natural History, Chicago
IGM	Museo Instituto de Geologia, Universidad Nacional Autonoma de Mexico, Mexico D.F.
IMNH	Idaho Museum of Natural History, Pocatello
JWT	Johnson Collection, West Texas University, Canyon
LACM	Natural History Museum of Los Angeles County, Los Angeles

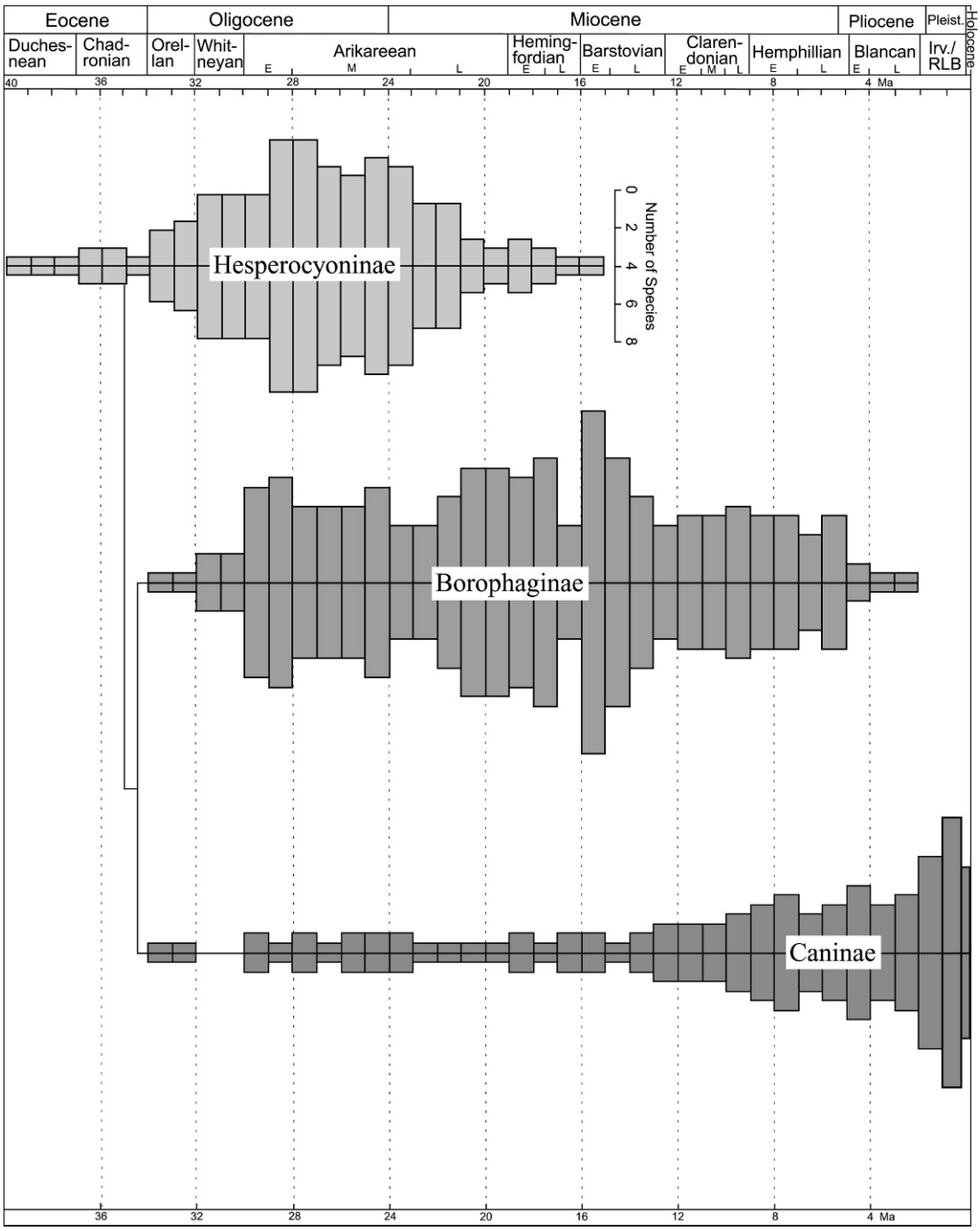

Fig. 2. Diversity at the species level per unit of time (1 Ma) of the three subfamilies of the Canidae. For the subfamily Caninae, only North American taxa are included. For the last 2 Ma interval, the bars are split into an interval of Late Irvingtonian plus Rancholabrean and an interval of Holocene whose diversity is based on living North American canids (see Wang et al., 2004). Diversity data are mostly simplified from our previous compilations (Wang, 1994: fig. 65; Wang et al., 1999: fig. 141) and this study (fig. 66A–B). For long-ranging taxa with gaps in their record, we counted the gaps as presence of the taxa concerned. Note expansion of diversity in succeeding clades near extinction of preceding clades. Time scale shown is that used throughout this study.

LACM(CIT)	Cal Tech Collection, at LACM
MCZ	Museum of Comparative Zoology, Harvard University, Cambridge, MA
MSU	Midwestern State University, Department of Biology, Wichita Falls, TX
NMC,CMN	National Museum of Canada, now Canadian Museum of Nature, Ottawa
NMNH	United States National Museum of Natural History, Smithsonian Institution, Washington, D.C.
OMNH	Oklahoma Museum of Natural History, University of Oklahoma, Norman
SDSM	Museum of Geology, South Dakota School of Mines and Technology, Rapid City
TMM	Texas Memorial Museum, University of Texas, Austin
TRO	Timberlake Research Organization, Lake Wales, FL
UA	University of Arizona, Tucson
UCMP	Museum of Paleontology, University of California at Berkeley
UCR	University of California at Riverside, Department of Geology
UF	University of Florida, Gainesville
UGV	University of Georgia, Department of Geology, Athens
UKMP	University of Kansas, Museum of Natural History, Lawrence
UMMP	University of Michigan, Museum of Paleontology, Ann Arbor
UNSM	Nebraska State Museum, University of Nebraska, Lincoln
UO	University of Oregon, Museum of Natural History, Eugene
USGS	United States Geological Survey, Denver
UW	University of Wyoming, Laramie
UWB	University of Washington, Burke Museum, Seattle
WTUC	West Texas University, Canyon
YPM	Yale Peabody Museum of Natural History, Yale University, New Haven, CT

SCOPE AND METHODS

As in any such study of a group of fossil organisms, determination of the scope of the project is largely dependent on the nature of the database. Remains of carnivorans are rare in any fossil assemblage as a consequence of their position on the trophic pyramid, and it is largely through the intensive fieldwork of the Frick Laboratory, extending over 50 years, that this unprecedented sample has become available. Even so, the collection before us consists mostly of jaw and maxillary fragments, isolated teeth, and postcranial remains, and rarely associated dentitions, skulls, and jaws and very few associated skeletons. The material is not abundant except at a few sites scattered in space and time, so sample sizes are small and those amenable to biometric analysis are frustratingly few.

The systematic section of this work is focused on the delineation and description of specimens of the Caninae that occur in Cenozoic deposits of North America. We have not provided such detailed characterization of Eurasian and South American Caninae beyond the introduction to the morphology of the better known fossil species of *Canis* from Eurasia (see appendix 1). These taxa were selected to give context to the phyletic analysis of their North American contemporaries. Additionally, the scope of our studies was limited to some extent by Nowak's (1979) extensive review of Pleistocene and Recent *Canis* of North America. We have not dealt with Rancholabrean (0.2–0.01 Ma) canids beyond the necessary discussion of taxa whose geologic ranges extend into the Rancholabrean.

In undertaking this study of the fossil representatives of the North American Caninae we found that morphological and biometric comparison of samples of closely related living taxa with their fossil relatives helped us develop morphospecies concepts controlled by a knowledge of the patterns of osteological variation in well-marked living examples. An important initial part of our study involved exploration of the individual and sexual variation in samples of living canids, and this background was called upon repeatedly in making decisions

about the scope of the fossil species proposed herein. Additionally, certain studies of sympatric living canid populations (Wayne et al., 1989; Dayan et al., 1989, 1992) provided information about character displacement (or its lack), especially in lower carnassial size, in species that partition the same environment. These data were used in evaluation of certain large samples (e.g., late Hemphillian of Arizona) of mixed taxa.

The lowest operational taxonomic unit used in this study is the species, which includes a constellation of individuals whose morphology resembles one another more closely than other such groups and whose members show ranges of variation comparable to that demonstrated for living canid species. We have consistently sought morphological rather than mensural bases for definition of our species, but in some cases have had to rely heavily on statistical or proportional differences to avoid forming morphospecies whose range of variation exceeded that known to be typical of living canid populations. In the list of referred specimens we indicate catalog numbers of materials that were not measured with an asterisk (*).

We have made consistent use of the dimensions of the lower first and second molars, as these are the most frequent occurring teeth in our collection. Their lengths have been compared using a modified Dice-Leraas diagram (Simpson et al., 1960: 354) showing the 95% confidence interval, mean, and observed range. The relative size relationships of the m1 and m2 are also depicted on these diagrams, which appear as figures at appropriate places in the text. These data are frequently referred to in our species diagnoses and descriptions to quantify relative size and evaluate the significance of size differences observed among population samples. Important differences in skeletal proportions exist between canid species (e.g., Nowak, 1979, for cranial examples and Hildebrand, 1952, for postcranial examples) and we have found the log-ratio diagram of Simpson (1941) useful to depict proportional relationships among fossil forms complete enough for analysis.

Definitions

We use the conventional terms primitive and derived in descriptions and comparisons of many of the taxa discussed in this work. These terms are used to indicate the phylogenetic relationship between morphological features and taxa in the context of our phylogenetic conclusions. Morphological features of special importance to our phyletic reconstruction are listed and have formal assignment of character-state polarity (see table 1).

The anatomical terminology used in this work derives mostly from the detailed anatomy of the dog of Evans and Christensen (1979). Dental notation follows our previous work (Wang et al., 1999) in which the upper toothrow is indicated in upper and lower row in lower case letters respectively. Frequently used dental morphological terms are indicated in fig. 69. We especially note that in the Caninae and Borophaginae (Wang et al., 1999: 21) the posterolingual cingulum of the M1–M2 may be enlarged and even differentiated as a cusp. In both cases these conditions are referred to as the ''hypocone''.

We employ the terms hyper- and hypocarnivory proposed by Crusafont-Pairo and Truyols-Santana (1956) in a broader sense than the biometric definition of those authors to indicate dental adaptations that emphasize shearing vs grinding. In hypercarnivory the dentition is modified to increase shearing function by elongation of the shearing surfaces of the carnassial teeth accompanied by the reduction or loss of the lower carnassial (m1) metaconid and entoconid and reduction in size of m2–m3 and their lingual cusps. The upper molars show hypocone reduction and differential reduction in size of M2. Hypocarnivory is the antithesis of these trends, especially in that the carnassial blades are shortened and the grinding part of the dentition, the m1 talonid and m2–m3, is enlarged and increases in complexity, and the M1–M2 are enlarged relative to the upper carnassial (P4). A dentition lacking either of these trends is referred to as mesocarnivorous, a condition that usually typifies the primitive condition of the dentition.

Chronological Framework

In this work the calibration of the geologic epoch boundaries follows Berggren et al. (1995, which incorporates the work of Cande and Kent, 1995, cited *in* Wang et al., 1999: 20) in which the Eocene–Oligocene boundary is 33.7 Ma, the Oligocene–Miocene boundary is 23.8 Ma, the Miocene–Pliocene boundary is 5.3 Ma, and the Pliocene–Pleistocene boundary is 1.8 Ma.

The calibration of the boundaries of the North American Land Mammal ages (NALMA) are presently under review, but they do not appear to significantly depart from those accepted by Wang et al. (1999). The Chadronian–Orellan boundary approximates the Eocene–Oligocene boundary at 34 Ma; the Orellan–Whitneyan boundary lies near 32 Ma (rounded from 32.3 Ma, Prothero and Swisher, 1992; Tedford et al., 1996); the Whitneyan–Arikareean boundary lies near 30 Ma (rounded from 30.1 Ma, Tedford et al., 1996); the Arikareean–Hemingfordian boundary is near 19 Ma (rounded from 18.8 Ma, MacFadden and Hunt, 1998); the Hemingfordian–Barstovian boundary is at 16 Ma (rounded from 16.2 Ma, Tedford et al., 2004); the Barstovian–Clarendonian boundary is at 12.5 Ma (Tedford et al., 2004); the Clarendonian–Hemphillian boundary is at 9.0 Ma (Tedford et al., 2004); the Hemphillian–Blancan boundary is at 4.8 Ma (Tedford et al.,2004); the Blancan–Irvingtonian boundary is at 1.8 Ma (rounded from 1.77 Ma, top Olduvai subchron, Matuyama chron, Repenning, 1987; Berggren et al., 1995; and the Irvingtonian–Rancholabrean boundary is at 0.2 Ma (rounded from 0.15 $\pm$ 0.03 Ma estimated by Repenning, 1987: 250–251, for his Rancholabrean I–II boundary; later revised as the ''Irvingtonian III–Rancholabrean'' boundary in a privately circulated addendum of 1988). Subdivisions of the NALMAs proposed in Tedford et al. (1987) have now been revised (Tedford et al., 2004) and are closely similar to those accepted by Wang et al. (1999): the early Arikareean extends from its boundary with the Whitneyan (30 Ma) to a boundary with the medial Arikareean at 28 Ma where faunal turnover results in the extinction of most of the elements of the White River Chronofauna in the Great Plains and the introduction of a number of exotic taxa (allochthones) not closely related to members of the early Arikareean fauna (autochthones). The boundary of the late Arikareean at 23 Ma follows a 3-m.y. gap in the Great Plains biochronologic sequence during which an undocumented span of faunal turnover results in new elements that characterize the late Arikareean. The base of the Hemingfordian, rounded to 19 Ma, witnesses a massive appearance of allochthones and major changes, especially extinctions, that revolutionize the mammal fauna of midlatitude North America. Likewise, the late Hemingfordian beginning at 17.5 Ma continues the appearance of allochthones and is characterized by marked cladogenesis of equine horses initiating the type of assemblages that typify the Miocene Chronofauna of the Great Plains. The beginning of the Barstovian at 16 Ma adds the mammutid Proboscidea to the record and sees further changes in the fauna leading to another pulse of immigration at the beginning of the late Barstovian, 14.8 Ma, in which the major elements of the Miocene Chronofauna are set in place. The Clarendonian is resolved here into an early and late phase. The early phase includes faunas like the Burge of Nebraska (formerly in the Barstovian, Tedford et al., 1987) at 12.5 Ma. The shovel-tusked mastodont *Platybelodon* appears in the record in the late phase beginning at 10 Ma, but the Clarendonian is not a span of vigorous immigration, nor is the beginning of the Hemphillian at 9 Ma, although this is marked by the first appearance of immigrants from South America (sloths). Rising numbers of allochthonous taxa define late Hemphillian at 7.5 Ma, especially larger Carnivora with wide geographic ranges in Eurasia, while the autochthonous ungulate fauna of North America declines. We divide the Blancan into two parts at 3.7 Ma, rounded to 4 Ma, corresponding to Repenning's (1987) Blancan II and III–V marked by the first appearance of muskrats (*Pliopotomys*) in midlatitude North America. The Irvingtonian is likewise divided in two parts at 0.9 Ma, rounded to 1 Ma, corresponding to Repenning's (1987) Irvingtonian I and II–III and the first appearance of the round-tail muskrat (*Neofiber*) and pine vole

TABLE 1
Characters Used in Cladistic Analysis

1) M1 hypocone: (0) small, barely differentiated from lingual cingulum; (1) enlarged, differentiated from lingual cingulum.
2) m1 entoconid: (0) poorly differentiated low crest on lingual border of talonid; (1) discrete conical or crestlike cusp; (2) conical cusp, enlarged, may coalesce with base of hypoconid to block talonid basin; (3) joined to hypoconid by cristids that form a transverse crest; (4) reduced relative to hypoconid, but retains cristid; (5) greatly reduced and lacks cristid.
3) M1 parastyle: (0) large and salient, united with well-developed preparacrista: (1) subdued but remains united with preparacrista; (2) preparacrista directed more anteriorly, lingual to parastyle.
4) Horizontal ramus: (0) deep and thick; (1) shallow and thin.
5) Premolar shape: (0) broad and short; (1) narrow and elongate.
6) p3 posterior cusp: (0) present; (1) weak or absent.
7) Premolar diastemata: (0) closed premolar row; (1) premolars separated by diastemata.
8) P3 posterior cusp: (0) present; (1) very weak or absent.
9) m2 paraconid: (0) present; (1) very weak or absent.
10) m2 talonid length: (0) talonid <90% trigonid; (1) talonid >90% trigonid.
11) P4 shape: (0) broad, protocone large, anterior cingulum strong; (1) slender, protocone small, anterior cingulum weak or absent, particularly across paracone.
12) Paroccipital process: (0) posteriorly directed, free from bulla except at base; (1) ventrally directed, fused with bulla through most of its length.
13) M2 metaconule: (0) present; (1) very weak or absent.
14) p2–p4 anterior cingular cusps: (0) present; (1) very weak to absent; (2) present only on p4.
15) M2 postprotocrista: (0) present; (1) incomplete or absent.
16) m2 anterolabial cingulum: (0) weak; (1) well developed, often reaching labial side of protoconid.
17) Postparietal foramen: (0) present; (1) absent.
18) Cerebellum, dorsal exposure: (0) significant exposure dorsoposteriorly between cerebrum and lambdoidal crest; (1) completely overlapped by cerebrum, not exposed dorsoposteriorly.
19) Nasal length: (0) long, usually extending posteriorly beyond the most posterior position of maxillary-frontal suture; (1) short, not extending beyond maxillary-frontal suture.
20) m1 hypoconulid shelf: (0) absent; (1) present.
21) Metatarsal I: (0) present, with phalanges; (1) reduced to rudiment, lacking phalanges.
22) Humerus, entepicondylar foramen: (0) present; (1) absent.
23) I1–I3 medial cusps: (0) present; (1) absent on I3 only; (2) weak or absent on I1–I2.
24) Paroccipital process: (0) narrow mediolaterally; (1) broad mediolaterally.
25) Zygomatic arch: (0) nearly flat or moderately arched in lateral view; (1) strongly arched dorsoventrally.
26) M1 shape: (0) transversely wide for labial length; (1) narrow for length.
27) m1–m2 protostylid: (0) absent; (1) present.
28) Lower premolars: (0) low-crowned; (1) high-crowned, tips p2–p4 often at same height.
29) Sagittal crest: (0) confined to parietal; (1) extends onto frontal.
30) m2 metaconid: (0) approximately equal in size and height to protoconid; (1) larger and taller than protoconid; (2) reduced in size and height relative to protoconid or absent.
31) Canine shape: (0) long, slender with curved crown; (1) short, robust, crown little curved.
32) Subangular lobe of mandible: (0) absent; (1) present, rounded; (2) present, angular.
33) Paroccipital process: (0) little or no expansion posteriorly; (1) expanded posteriorly, usually with a prominent free tip; (2) large, strong posterolateral expansion.
34) Frontal sinus: (0) absent, presence of depression on dorsal surface of postorbital process; (1) present, may retain depression on dorsal surface of postorbital process; (2) large, penetrates postorbital process and expands posteriorly toward frontoparietal suture; (3) sinus reaches frontoparietal suture.
35) Zygoma: (0) orbital border laterally flared and everted; (1) orbital border not laterally flared or everted.
36) Mastoid process: (0) small, crestlike; (1) large knob or ridgelike.
37) Angular process: (0) attenuated, usually with dorsal hook, fossa for inferior branch of medial pterygoid muscle not expanded; (1) large, usually blunt, without dorsal hook, inferior branch of medial pterygoid muscle expanded often equal to or exceeding fossa for the superior branch.
38) p4 second posterior cusp: (0) absent; (1) present, lies between first posterior cusp and cingulum; (2) undifferentiated from posterior cingulum.
39) Angular process, fossa for superior branch of medial pterygoid muscle: (0) small; (1) large.

TABLE 1
(Continued)

40) Supraoccipital shield: (0) rectangular or fan-shaped in posterior view, inion not overhanging condyles; (1) triangular in shape, inion often pointed and overhangs condyles.
41) Radius/tibia ratio: (0) <80%; (1) 80–90%; (2) >90%.
42) I3: (0) only slightly larger than other incisors, posteromedial cingulum weak or absent; (1) markedly larger than I1–I2, posteromedial cingulum present and enlarged.
43) p3, height principal cusp vs p2, p4: (0) forms ascending series with p2, p4 or is at same height; (1) lies below p2 and p4.
44) P4 protocone: (0) extends anterolingually beyond anterior end of paracone; (1) extends more lingually and not beyond anterior end of paracone.
45) p3, position of crown base vs that of p4: (0) approximately same level as p4 when ramus is viewed laterally; (1) crown base of p3 lies mostly below that of p4.
46) p4, unworn principal cusp: (0) equals or exceeds height of m1 paraconid; (1) lower than m1 paraconid.
47) m1, anterior edge of paraconid: (0) nearly linear and vertical; (1) inclined posteriorly and may be curved.
48) Palate, width at P1: (0) narrow; (1) wide.
49) M1 labial cingulum: (0) well developed and continuous; (1) subdued and often incomplete across paracone.
50) m1 metaconid: (0) not reduced relative to labial cusps; (1) greatly reduced; (2) absent.
51) m3: (0) with two trigonid cusp; (1) with a single, centrally placed trigonid cusp; (2) posterior shelf of trigonid enlarged; (3) m3 absent.
52) Jugal-maxillary suture: (0) obtuse; (1) acute.
53) Anterior palatine foramina length: (0) short, posterior border lies at or anterior to posterior end of canine alveolus; (1) long, posterior border lies posterior to canine alveolus.
54) M1 paracone: (0) not markedly enlarged relative to metacone; (1) paracone markedly enlarged.
55) P4 protocone: (0) little reduced; (1) markedly reduced with small root.
56) M1 lingual cingulum: (0) well developed, extends across protocone; (1) very weak, may be discontinuous across protocone.
57) M1 hypocone: (0) cusp and associated cingulum not reduced; (1) cusp and cingulum markedly reduced; (2) absent.
58) m1 hypoconid: (0) situated laterally on talonid; (1) situated centrally on talonid.
59) M1 metaconule: (0) present; (1) very weak or absent.
60) Frontal, nasal process: (0) long; (1) short.
61) Foramen ovale and alisphenoid canal: (0) separate; (1) in common pit.
62) Optic foramen and anterior lacerate foramen: (0) separate; (1) in common pit.
63) p3, second posterior cusp: (0) absent; (1) present.
64) Stratigraphy: first occurrence of taxa, see text page 167 for temporal subdivisions used in this analysis.

(*Pitymys*). The Rancholabrean is defined classically by the first appearance of *Bison*, which has been difficult to calibrate, but appears in midlatitude North America at ca. 0.2 Ma. The Holocene or Recent is set at 0.01 Ma.

SYSTEMATIC PALEONTOLOGY

Order Carnivora Bowdich, 1821
Suborder Caniformia Kretzoi, 1943
Infraorder Cynoidea Flower, 1869
Superfamily Canidae Fischer de Waldheim, 1817
Family Canidae Fischer de Waldheim, 1817
Subfamily Caninae Fischer de Waldheim, 1817

The diagnostic synapomorphies for the subfamily consist of the following features (branching-point C in Tedford et al., 1995: fig. 2, slightly modified by this study, fig. 1): horizontal rami of the mandible shallow and thin; premolars narrow and elongate; posterior cusplets on p2–p3 weak or absent; P2–P3 and p2–p4 separated by short diastemata; P4 slender, protocone small, anterior cingulum reduced or absent; m1 trigonid elongate (particularly paraconid); paroccipital process directed ventrally and fused with bulla. The species-level cladistic analysis of *Leptocyon* presented herein shows that these features, and several more not included in the previous analysis, are acquired stepwise during the early history of the Caninae, with only the narrow and elongate premolars separated by diastemata marking the initial step separating the canines from borophagines.

The taxa included in this subfamily range from the early Oligocene (Orellan) to the Recent of North America; late Miocene (Turolian) to Recent of Europe; Pliocene to Recent of Asia; Pliocene to Recent of Africa; late Pliocene or early Pleistocene (Uquian) to Recent of South America; and, by human introduction, from 3000 yr BP to present in Australia.

The Caninae, other than *Leptocyon*, were divided by Tedford et al. (1995) into two sister taxa; the tribe Vulpini Hemprich and Ehrenberg, 1832, and the tribe Canini Fischer de Waldheim, 1817. Members of these tribes were united by possession of the following synapomorphies (branching-point D of Tedford et al., 1995: fig. 2): postparietal foramen absent; m1 posterior cingulum often with hypoconulid; m2 anterobuccal cingulum enlarged, metaconid enlarged, may be taller than protoconid; medial cusplet of I3 absent; humerus lacks entepicondylar foramen; and metatarsal I reduced to proximal rudiment. The species-level phylogenetic analysis including fossil taxa reported herein shows that the last three characters listed were acquired during the evolution of species of *Leptocyon*.

Leptocyon Matthew, 1918

Vulpes: Trouessart, 1897: 310 (catalog).
Vulpes: Stirton and McGrew, 1935: 129 (faunal list).
Vulpes: Gregory, 1942: 348.
Vulpes: Macdonald, 1948: 55, fig. 1a–b.
Neocynodesmus Macdonald, 1963: 212.

Type Species: *Leptocyon vafer* (Leidy), 1858.

Included Species: *L. douglassi*, n. sp.; *L. mollis* (Merriam), 1906; *L. delicatus* (Loomis), 1932; *L. vulpinus* (Matthew), 1907; *L. gregorii* (Matthew), 1907; *L. vafer* (Leidy), 1858; *L. leidyi*, n. sp.; *L. tejonensis*, n. sp.; *L. matthewi*, n. sp.; and *Leptocyon* sp. A and B.

Distribution: Orellan to late Clarendonian; Nebraska, Colorado, Montana, South Dakota, Wyoming, Kansas, Nevada, New Mexico, Arizona, California, and Oregon.

Revised Diagnosis: *Leptocyon* differs from *Vulpes* in possession of the following primitive characters: greater postorbital constriction; I1–I3 with medial cusplets; M1 and M2 with stronger parastyle; m1 hypoconulid absent, its entoconid relatively smaller and enlarged only in most derived species; m2 with weaker anterolabial cingulum and metaconid smaller than or equal in size to protoconid in less derived species, postparietal foramen still present in early species; humerus with entepicondylar foramen; ulna and fibula short and more robust with larger distal articular facets for radius and tibia; radius with distal exostosis in early species (Wang and Rothschild, 1992); tibia with longer anteroproximal crest, less anteriorly and distally extended proximolateral and proximomedial articular surfaces for femur; relatively larger entocuneiform and well-developed functional metatarsal I with two phalanges.

Discussion: When Leidy (1858: 21) described *Canis vafer*, he recognized its foxlike features and commented that it did not differ in form from those of the red fox. Trouessart (1897: 310) listed this taxon in his catalog of mammals as *Vulpes vafer*. It was not until 1918 that Matthew delineated the morphological features that separated this species from those of *Canis* and *Vulpes*.

Matthew's (1918: 189) original description of the genus *Leptocyon* was largely based on two lower jaws (AMNH 17201 and 17202; the latter was sent on exchange to the University of Uppsala in 1912) from the early Barstovian Lower Snake Creek Fauna (Olcott Formation, Skinner et al., 1977: 300) in Sioux County, Nebraska. *Leptocyon* species are now recognized in deposits as old as the Orellan (Wang and Tedford, 1996). Several species that are considered to belong to *Leptocyon* (including *L. mollis*, *L. vulpinus*, and *L. gregorii*) were originally described as *Nothocyon*, but its genotypic species is now recognized as an arctoid (Wang and Tedford, 1992). Matthew pointed out the foxlike characters of *Leptocyon* in his diagnosis, including the slenderness of jaw, long premolar region with diastemata between the teeth, premolars with accessory cusps, m1 talonid with low marginal entoconid crest obscurely divided into two cusps, and m2 with vestigial and shelflike paraconid. A combination of several of these features is useful in distinguishing some jaws of *Lepto-*

cyon from *Vulpes*, but of all of the characters cited by Matthew, only the primitively low, conical, and sometimes crestlike entoconid serves to separate most jaws of *Leptocyon* from those of *Vulpes*.

Some later authors (Stirton and McGrew, 1935: 129; Gregory, 1942: 348; and Macdonald 1948: 55) placed *Leptocyon* in *Vulpes*, but Webb (1969: 40) discussed morphological features that can be used to separate *Leptocyon vafer* from *Vulpes* species. Additional evidence permits us to further revise this diagnosis and clearly show how species of the two genera differ. In addition to the low conical or crestlike entoconid on the m1, the talonid in most *Leptocyon* species is U-shaped in transverse section and the hypoconulid is absent, whereas in *Vulpes* the entoconid and hypoconid are larger, coalescing at their bases to modify the talonid basin into a V-shaped transverse section, and the hypoconulid is often present. The m2 of *Leptocyon* differs from that of *Vulpes* in having a weaker anterolabial cingulum.

Neocynodesmus Macdonald (1963) is placed in synonymy with *Leptocyon* because the type of the genus and only known species, *N. delicatus* (Loomis, 1932), shares a number of features with *Leptocyon*. The dental row in the type jaw (ACM 31102) is approximately 40% smaller (appendix 3) than in the next smallest ramus referred to *Leptocyon* and is thus the smallest known canid.

In comparing the upper dentition of *L. vafer* with that of *V. vulpes*, Webb (1969: 40) observed that the protocones on the carnassial and the upper molars are consistently larger and the metaconules weaker than in modern forms. After comparing recent species of *Vulpes* available in the AMNH(M) collection from Europe, Asia, Africa, and North America, we found that the dental features of *Leptocyon*, particularly the earlier species, recall those of *Hesperocyon*. These dental characters are: m1 talonid basin U-shaped in cross-section and hypoconulid absent; m2 with anterolabial cingulum weak to absent, and paraconid present; and M1 and M2 with a relatively strong parastyle and low-crowned paracone and metacone.

Synapomorphous characters that unite *Leptocyon* and *Vulpes* are primarily the foxlike characters initially recognized by Matthew, including the slenderness of the jaw and the long premolar region with diastemata separating the premolars. Of special importance, although misinterpreted by Matthew, are the weak premolar cusplets, which are greatly reduced or absent compared to those in hesperocyonines and borophagines.

As indicated by log-ratio diagram (fig. 3), the skull proportions of *Leptocyon* species show comparable trends. Comparison of Arikareean *L. mollis* and *L. gregorii* with Clarendonian *L. vafer* shows the following differences. In *L. mollis* and *L. gregorii* the braincase is relatively narrower than that of *L. vafer*. The height of the maxilla between the alveolar border and the ventral rim of the orbit and the depth of the jugal are both proportionally less than in *L. vafer*.

The height of the maxilla between the alveolar border and the ventral rim of the orbit and the depth of the jugal are both proportionally less than in *L. vafer*. The larger zygomatic process of the jugal in *L. vafer* is correlated with a deeper and more dorsoventrally expanded depression for the masseter muscle. Furthermore, the skulls of *L. mollis* and *L. gregorii* show more cerebellar exposure on the posterior side of the braincase, and the lip of the external auditory meatus is smaller and projects less laterally than in *L. vafer*. A comparison of the skull of *L. vafer* with that of *V. stenognathus* shows somewhat better agreement than it does with more primitive *Leptocyon*, but *L. vafer* still differs from *Vulpes* in having a relatively deeper jugal and greater height of the maxillary from the toothrow to orbit.

A close resemblance exists between the limbs of *Leptocyon* and *Vulpes*, but the present study shows that the limbs of *Leptocyon* are more primitive, with several features in common with *Hesperocyon* (fig. 9). The entepicondylar foramen is absent in *Vulpes*, but it is well developed on the humerus of *Leptocyon*. Although we lack evidence from associated limbs in most cases, we conclude from the unassociated limbs referred to various *Leptocyon* species that the limb proportions are similar to those of *Vulpes*. The radius appears to be short relative to both the length of the humerus

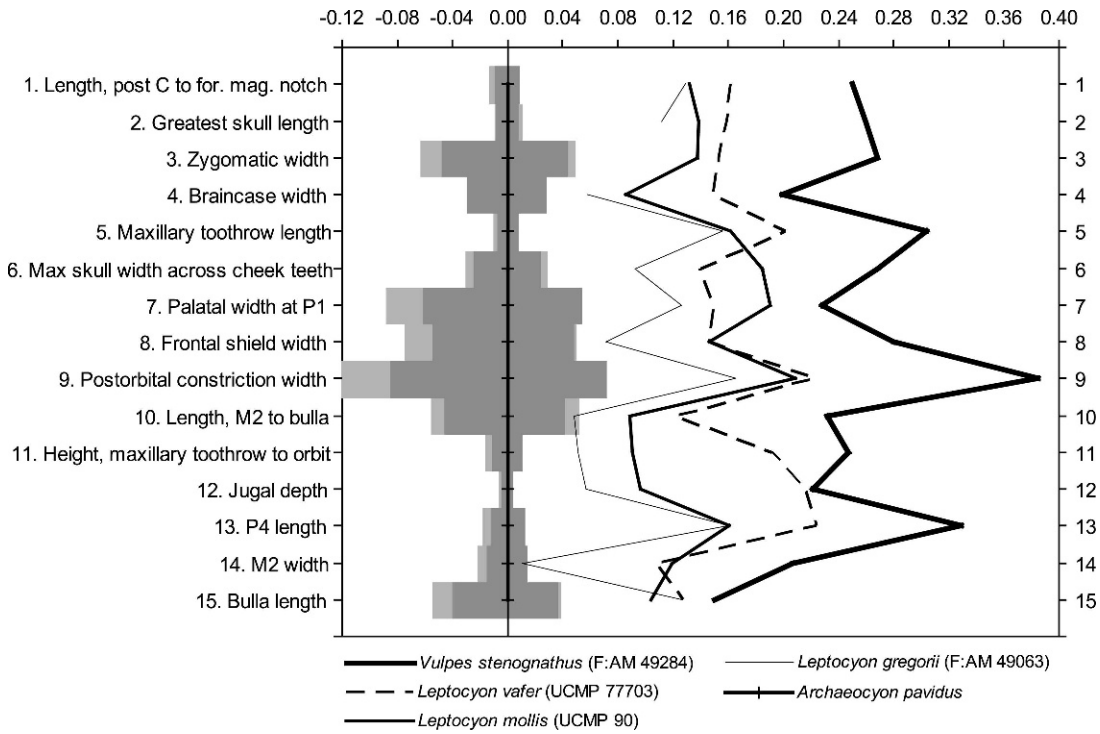

Fig. 3. Log-ratio diagram comparing the proportional relationships of cranial elements (appendix 2) of single individuals of species of *Leptocyon* and *Vulpes* using a primitive borophagine, *Archaeocyon pavidus*, as the standard of comparison. Gray bars extending from the mean are observed ranges (light); the dark bars are $\pm 1\ \sigma$ for the three individuals used to typify the standard (appendix 2).

and the tibia. This is a primitive condition held in common with *Hesperocyon* and all living foxes. The distomedial radial exostosis in *Leptocyon vulpinus* is relatively larger than that of *Vulpes*, but later *Leptocyon* species show smaller exostoses. This osteochondroma is prevalent in *Hesperocyon* and seems to have a hereditary basis (Wang and Rothschild, 1992). Additionally, the ulnae of *Leptocyon* are more robust than those of *Vulpes*. Furthermore, the distal articular facets on both the ulna and radius for their mutual articulation are relatively larger than those of *Vulpes*. The tibia of *Leptocyon vafer* is shorter and the fibula (F:AM 62780) is more robust and less compressed than that of *Vulpes*. Moreover, the tibiae of the *Leptocyon* species differ from those of *Vulpes* in that the anteroproximal crest is relatively longer, and the proximolateral and medial articular condyles for the femur are less anteriorly and distally extended. These features would restrict flexion of the hindlimb as compared to living foxes.

Although our knowledge of the front foot of most *Leptocyon* species is limited to a few unassociated elements, a complete rear foot of *L. vafer* (F:AM 62780) is known from late Barstovian deposits in New Mexico. The tarsals and metatarsals II–V are similar to those of species of *Vulpes* and are well within the range of variation found in recent foxes. It is the first digit of the pes (fig. 9H) that distinguishes *Leptocyon* from *Vulpes* and reveals a surprisingly primitive feature. In *Leptocyon vafer* the entocuneiform is relatively larger than in *Vulpes* species, and metatarsal I is well developed and functional. Metatarsal I is 19.0 mm long and has two small phalanges. The length of metatarsal I is approximately 40% that of metatarsal II. Metatarsal I is unknown in the fossil *V. stenognathus* but in recent foxes it consists of only a short proximal rudiment, although

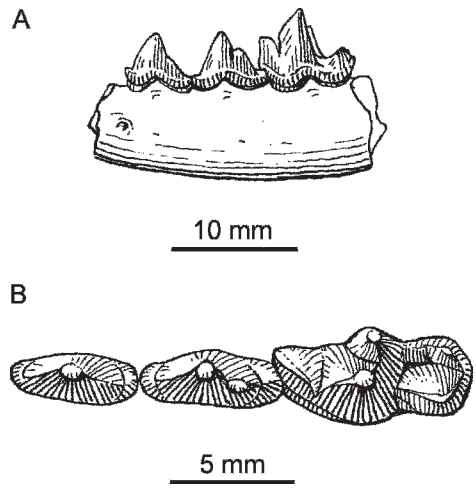

Fig. 4. *Leptocyon* sp. A, UNSM 25354, Orellan, Nebraska. **A**. Lateral view of ramus. **B**. Occlusal view of lower teeth. From Wang and Tedford, 1996: fig. 9.

Lonnberg (1916) reported an individual *V. vulpes* that had both phalanges for this digit. The metatarsal itself had unfortunately been discarded when the animal was skinned.

Primitive limb features of *Leptocyon* held in common with *Hesperocyon* are mainly a proportionally short radius relative to the length of the humerus and tibia, a strong radial exostosis, a robust ulna, a strong fibula, and a functional metatarsal I. Thus, the limbs of *Leptocyon* are less elongate, more robust, and less adapted for running than are those of *Vulpes*.

Leptocyon sp. A
Figure 4

Leptocyon sp., Wang and Tedford, 1996: 447, fig. 9.

Material: UNSM 25354, fragment of left ramus with p3–p4, and m1 from the Orella Member, Brule Formation, White River Group (Orellan), Sioux County, Nebraska.

Description and Comparison: This specimen is the sole evidence for the presence of *Leptocyon* and hence the Caninae at the beginning of the Oligocene. The premolars are the most diagnostic elements in this attribution. The p3 is a thin blade (5.3 mm in length, 2.0 mm in width), and its principal cusp is as tall as that of P4. There are no anterior or posterior cusps, but the anterior cingulum is produced into a cuspule-like structure. The posterior cingulum forms a short shelf but is not produced into a cuspule nor does it join the anterior cingulum along the labial face of the crown. The p3 and p4 touch one another in a slightly imbricate fashion. A prominent posterior cusp is present on p4, set slightly labially from the longitudinal midline of the tooth. Anterior and posterior cingula are present and the labial side of the crown bears a low cingulum. The posterior cingulum extends anteriorly on the lingual side of the tooth to a point opposite the posterior cusp. The crown of p4 is slender (6.0 mm in length, 2.4 mm in width) and is 79% of m1 length, with the principal cusp exceeding the height of the paraconid of m1. The m1 is relatively short (7.6 mm in length, 3.7 mm in trigonid width, 3.4 mm in talonid width) and its talonid is 68% of the trigonid length. The length of the paraconid blade is equal to that of the protoconid; it is deflected inward, forming a closed trigonid. The protoconid is a high cusp made more conspicuous by the shortness of the tooth as a whole. The protoconid is also labially inflated to a greater degree than in other members of the genus. The metaconid is large and its tip lies above that of the paraconid. The talonid is bicuspid, with the entoconid about as high as the hypoconid. Both outline a deep talonid basin partly closed posteriorly by a tiny hypoconulid that arises from the postentocristid. There is a well-developed cingulum that can be traced completely along the labial side of the tooth. The ramal fragment is shallow (about the height of the m1 protoconid), tapering only slightly forward. There is a small posterior mental foramen beneath the short diastema between p2 and p3.

This specimen is slightly smaller than the holotype and referred specimens of *L. douglassi*. It differs from the latter and other species of the genus in the lack of a posterior cusp on p3, the relatively short m1 with a short and inwardly deflected paraconid, a high and labially inflated protoconid, and a conspicuous labial cingulum. Except for the well-developed entoconid, the m1 resembles those of contemporary early Oligocene *Hesperocyon gregarius* rather than later Oligo-

cene *Leptocyon douglassi* with its elongate m1, open trigonid, and subdued labial cingulum.

Discussion: Wang and Tedford (1996) brought this specimen to notice as the earliest defensible member of the Caninae. Its early Oligocene (Orellan) occurrence corroborates the predicted synchronous appearance of members of the sister taxa, the Borophaginae and Caninae. Nevertheless, there are some decidedly primitive features of the m1 that recall *Prohesperocyon wilsoni*, especially the short, closed trigonid and the labial inflation of the high protoconid that together resemble the former taxon more than *Hesperocyon gregarius* and recall the condition of the trigonid in species of *Miacis* (Wang and Tedford, 1994). Despite these primitive features of the trigonid, the broad, strongly bicuspidate talonid and the elongate, slender premolars lacking accessory cusps on p3 and having only a posterior cusp on p4 are characters that ally *Leptocyon* sp. A first with the borophagines and secondly with the canines. This mosaic of features gives some idea of the sequence of character acquisition in an early member of the Caninae as already pointed out by us (Wang et al., 1999).

Leptocyon mollis (Merriam), 1906
Figures 3, 5, 6H–J; appendices 2, 3

Nothocyon geismarianus mollis Merriam, 1906: 13, pl. 2, fig. 1 and pl. 3, fig. 1.

Type: UCMP 90 (AMNH 129683, cast; fig. 6H–J), skull with I3 broken–C, P1 broken, and P2–M2 from the Turtle Cover Member of the John Day Formation, Turtle Cove, John Day River, Grant County, Oregon. This unit spans ca. 29–30 Ma (Fremd et al., 1994), early Arikareean.

Revised Diagnosis: *L. mollis* differs from *L. douglassi* in its larger size and proportionally larger M1 and M2 (fig. 5); from *L. vulpinus* it differs in its smaller and lower crowned premolars; from *L. gregorii* it differs in its wider palate, backward directed, more robust, and salient paroccipital process, in larger and lower crowned P3, in more robust P4 with relatively larger and more anteriorly situated protocone and proportionally larger M1 with more prominent cingulum and slightly stronger parastyle, and in proportionally larger M2 that bears a metaconule.

Description and Comparison: The holotype skull was designated a race of *Nothocyon geismarianus* by Merriam (1906: 13 compared with the referred skull, AMNH 6885, now the holotype of *Cormocyon copei* Wang and Tedford, 1992). He stated: ''Except for the somewhat smaller size, lyrate arrangement of the temporal ridges and somewhat narrower molars, this form is close to *N. geismarianus*'' (Merriam, 1906: 13). For the reasons cited by Merriam, the skull is excluded from *Cormocyon copei*, assigned to the genus *Leptocyon*, and raised to specific rank.

Although the dentition of the type skull is smaller than that of *Leptocyon vulpinus*, the relatively large and broad molars recall those of the latter, rather than the smaller molars of *L. gregorii*. Relatively large molars and a strong M1 parastyle are also characters that distinguish *L. vulpinus* from *L. gregorii*.

Unfortunately, no skull of *L. vulpinus* is known, but *L. mollis* can be compared with the incomplete type skull (AMNH 12872) of *L. gregorii* (see proportional comparison in fig. 3). The type skulls of *L. mollis* and *L. gregorii* are approximately equal in size and proportionally similar except for the broader palate and relatively larger M2 in *L. mollis*. The lyrate temporal ridges of *L. mollis* are more widely separated than in other early species of *Leptocyon* and resemble some examples of *Hesperocyon*. Although more laterally expanded (slightly emphasized by dorsoventral crushing), the cranium of *L. mollis* is elongate as in *L. gregorii*, with the cerebellar exposure similar to that of the latter. Both have tiny postparietal foramina. The morphology of the paroccipital process in this taxon is the most primitive known among the Caninae. Its base is broadly connected to the bulla, but it retains a robust and salient process that is more posteriorly directed than in other species of *Leptocyon*.

When the worn dentition of the type of *L. mollis* is compared with that of *L. gregorii*, the P3 is slightly larger and lower crowned in *L. mollis* and the strong posterior crest has a very weakly differentiated cuspule. More-

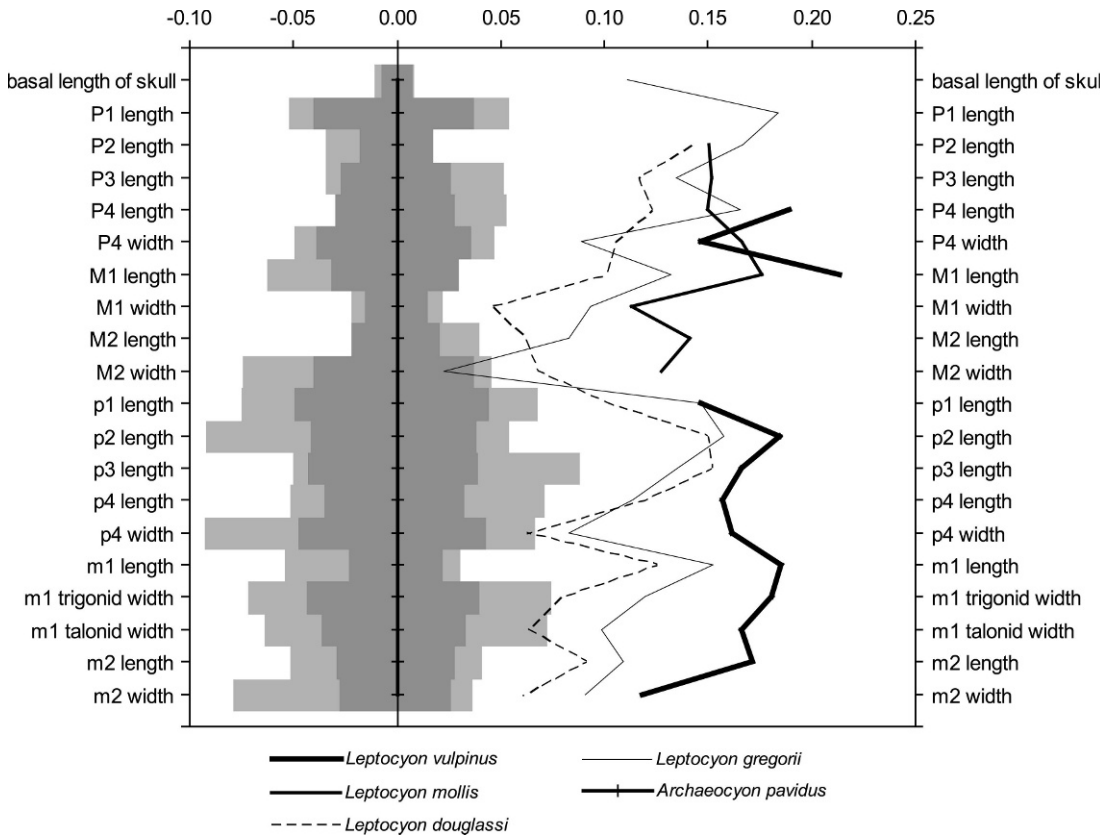

Fig. 5. Log-ratio diagram comparing the means of the cheek tooth dimensions (appendix 3) of four early occurring species of *Leptocyon* against a primitive borophagine, *Archaeocyon pavidus*. Gray bars extending from the means of the standard are observed ranges (light) and $\pm 1\ \sigma$ (dark) of the mean of the sample used.

over, the P4 is more robust in *L. mollis* (fig. 5) with a relatively larger and more anteriorly situated protocone. Allowing for wear, the molars of *L. mollis* are relatively larger. The M1 appears to have almost subequal paracone and metacone with a more prominent buccal cingulum and a stronger parastyle than that of the type of *L. gregorii*. *L. mollis* further differs from the latter in its proportionally smaller and lower crowned premolars.

Leptocyon douglassi, new species
Figures 5, 6A–G, 7; appendix 3

Nothocyon geismarianus: Macdonald, 1970: 55.

Type: NMNH 19931 (fig. 6C–E), cast AMNH 129685, partial palate with P4–M2 and left ramus with c and p2–m2 from the Toston Formation (early Arikareean), 2 2 miles southeast of Canyon Ferry, Lewis and Clark County, Montana.

Etymology: Named for Earl Douglass whose pioneering studies of the fossil mammals of Montana initiated modern knowledge of the Neogene faunas of the northern Rocky Mountains.

Referred Material: From the type area, Toston Formation (early Arikareean), Canyon Ferry, Lewis and Clark County, Montana: NMNH 19106 (cast AMNH 129684), fragments of immature skull and jaw including right partial ramus with p2 unerupted, dp3–dp4 and m2 unerupted, and left detached unworn m1. One mile east of Canyon Ferry: CMNH 1264, right and left mandibular rami with c–m3 (fig. 6A–B); and CMNH 1300, left ramus with i3 root, c–p3 alveoli,

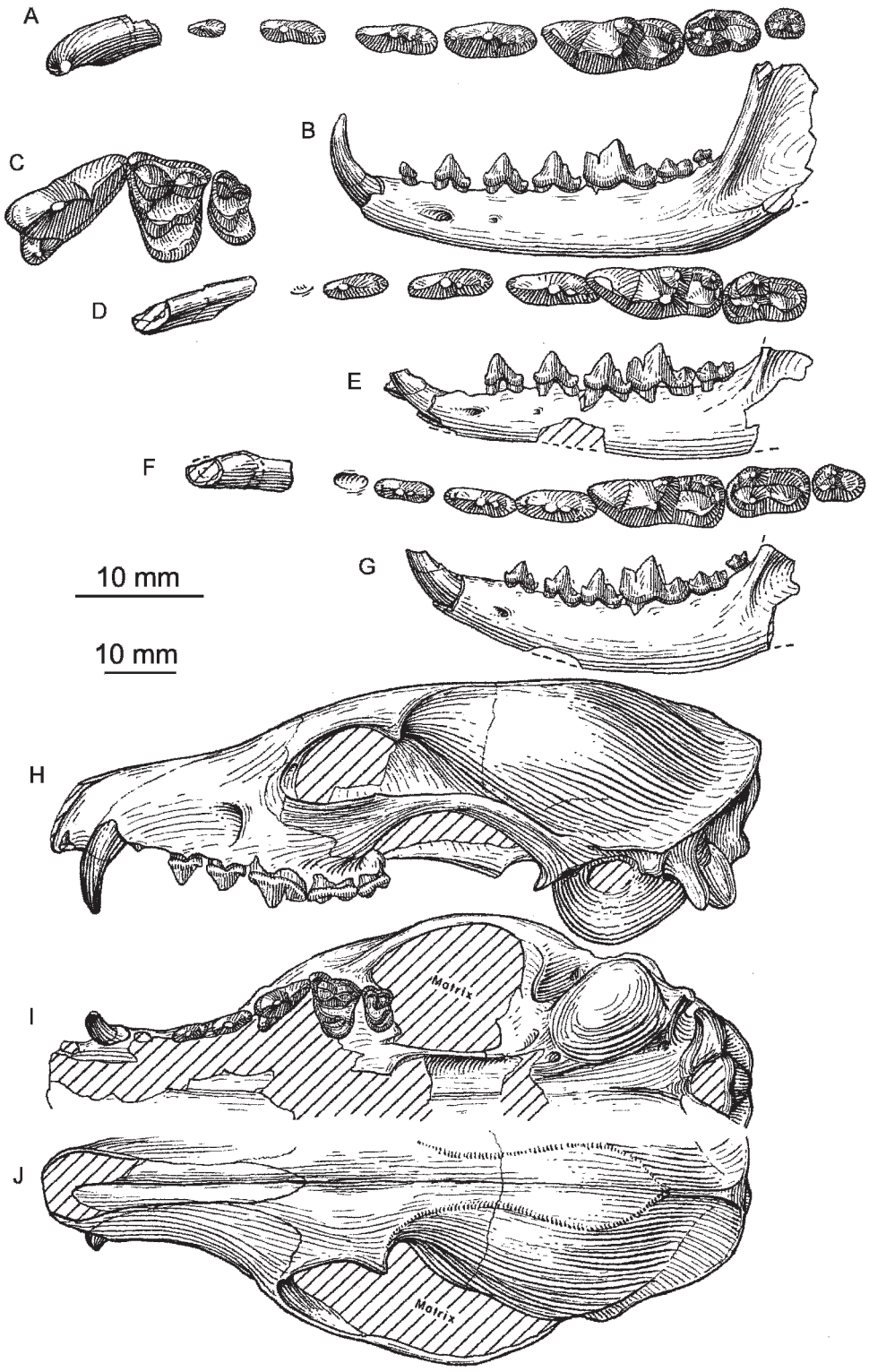

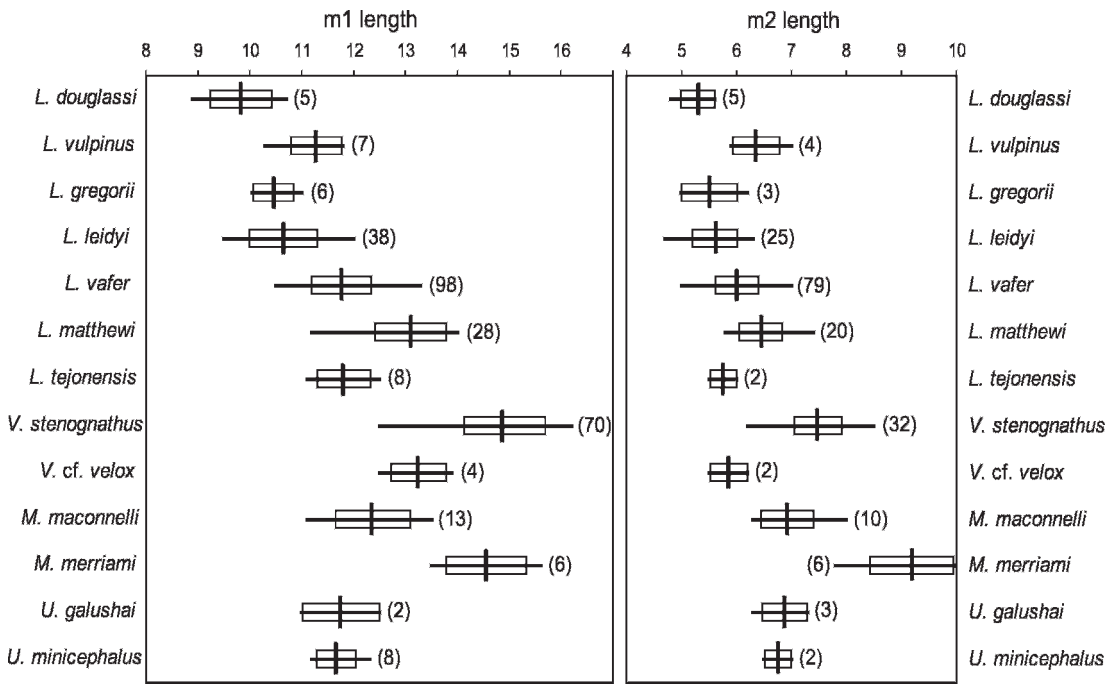

Fig. 7. Graphic comparison of the length of the m1 and m2 of species of *Leptocyon*, *Vulpes*, *Metalopex*, and *Urocyon*. The horizontal bar is the observed range, the small rectangle represents 1 σ from the mean, the vertical line is the mean, and the size of the sample is the number in parentheses.

p4–m2, and m3 alveolus, Earl Douglass Collection, 1902.

White Sulfur Springs (early Arikareean), Meagher County, Montana: F:AM 54196 (fig. 6F–G), left ramus with c broken and p1 alveolus, p2–m3 from deposits considered temporally equivalent to the Gering Formation by Schultz and Falkenbach (1949: 145).

Wounded Knee–Sharps Fauna, Sharps Formation (early Arikareean), South Dakota: LACM 9371, left maxillary fragment with P4–M1 from LACM locality 1955 and referred to *Nothocyon geismarianus* by Macdonald (1970: 55); and LACM 9298, left maxillary fragment with M1 from LACM locality 1980.

UCMP locality V6377, Haystack 8, L-2, Turtle Cove Member, John Day Formation, between the Picture Gorge Ignimbrite and Deep Creek Tuff (29–28 Ma, early Arikareean): UCMP 79365, anterior part of skull lacking canines and incisors, P1 alveolus, P2 roots, left P3, left and right P4, M1–M2.

Distribution: Early Arikareean of Oregon, Montana, and South Dakota.

Diagnosis: *Leptocyon douglassi* differs from all other Arikareean species by its derived p3 lacking posterior cusp, m2 with

←

Fig. 6. A–B. *Leptocyon douglassi*, early Arikareean, Montana. Ramus, CMNH 1264. **A**. Occlusal view. **B**. Lateral view. **C–G**. *Leptocyon douglassi*, early Arikareean, Montana. **C–E**. Type maxillary and associated ramus, NMNH 19931. **C**. Occlusal view, reversed. **D**. Occlusal view. **E**. Lateral view. **F–G**. Ramus, F:AM 54196. **F**. Occlusal view. **G**. Lateral view. **H–J**. *Leptocyon mollis*, Arikareean, Oregon. Type skull, UCMP 90. **H**. Lateral view, reversed (P2 and postorbital process restored from opposite side). **I**. Palatal view, reversed. **J**. Dorsal view, reversed. The longer (upper) scale is for A, C, D, and F, and the shorter (lower) one is for the rest.

long talonid (>90% of trigonid length), and absence of m2 paraconid. Additionally, it differs from *L. vulpinus* in its smaller size and relatively narrower and lower crowned premolars; from *L. gregorii* in averaging smaller in size, M2 having metaconule, and P4 of greater width with stronger protocone; and from *L. mollis* in its smaller size and proportionally smaller M1 and M2.

Description and Comparison: The p2–p4 are widely spaced, elongate, slender, and moderately tall crowned. The lower premolars of the type ramus (NMNH 19931) and those of a referred ramus (F:AM 54196) have stronger anterior cingular cusps than in the type specimens of *L. gregorii* and *L. vulpinus* (compare figs. 6A–E with 11A–E and 8A–C). The anterior cusp is noticeably stronger on p3 and p4, and even the p2 of F:AM 54196 shows a small but distinct anterior cusp. Prominent anterior cingular cusp on the premolars is shared with *Hesperocyon* and members of the Borophaginae. On the other hand, the loss of a posterior cusp on P3 is a derived feature of this early *Leptocyon* species. The P4 of the type (NMNH 19931) is transversely thick with a large protocone and a weak parastylar shelf, similar to that of the type of *L. mollis* and *L. vulpinus* but unlike the slender upper carnassial of *L. gregorii*. The M1 is proportionally smaller than in *L. mollis* (fig. 5) but morphologically similar with an extremely low-crowned paracone and metacone, strong labial cingulum, and a strong parastyle. The M2 is also proportionally smaller than in the type *L. mollis* (fig. 5), but it is morphologically similar with an extremely low-crowned paracone and metacone, strong labial cingulum, and a strong parastyle. The M2 is also proportionally smaller than in the type and has a very low-crowned paracone and metacone, a well-developed protocone, and a strongly recurved talon. The m1 is slender with a strong metaconid and a somewhat more basinlike talonid than in *L. gregorii*. The elongate m2 with a very long talonid contrasts with the shorter talonid length of the m1 in *L. gregorii* and *L. vulpinus*. The m2 has a relatively large subequal protoconid and metaconid but lacks the distinct paraconid present in the type of *L. vulpinus*.

Leptocyon vulpinus (Matthew), 1907
Figures 7, 8A–F, 9A–B; appendices 3, 4

Nothocyon vulpinus Matthew, 1907: 183, fig. 2.
Cynodesmus vulpinus: Macdonald, 1963: 211.

Type: AMNH 12883, left ramus with i1–i2 broken and i3–m2 (fig. 8B–C), right partial ramus, fragmentary premaxilla-maxilla with I1–P1, P3, isolated P4 and M1 broken (fig. 8A), and fore- and hindlimbs including left humerus (fig. 9A), right partial humerus, left radius and ulna (fig. 9B), left partial tibia and distal part of fibula, articulated calcaneum and astragalus, and limb fragments from 4 miles below the post office, Porcupine Creek, referred to Harrison Formation (medial Arikareean) of South Dakota. Matthew (1907: 183) reported the type from the Lower Rosebud beds; Macdonald (1963: 211) listed the type locality as "A.M.N.H. 'Rosebud' 7" and the containing rocks as the "Harrison formation".

Referred Material: Haystack Valley Member (revised, Hunt and Stapleton, 2004), medial Arikareean, John Day Formation, Wheeler County, Oregon. Base of unit, Crazy Woman Knob section, Northwest Museum of Natural History, Portland State University, NM 103/16, fragment of right ramus with m1–m2.

Recorded by the University of Nebraska as from Hemingford Quarry 7B, in the "Upper Marsland Formation" (early Hemingfordian), Box Butte County, Nebraska: UNSM 25416, right ramus with c broken, p2–m3 (p1 missing); UNSM 25611, right ramus with c broken, p2–m3 (p1 missing); UNSM 25453, right ramus with c broken, p3–p4, and m1 (p2 broken, p1, m2, and m3 alveoli). These specimens are from the Runningwater Formation following McKenna (1965: 10) that "the type Runningwater Formation is part of the same unit as that referred to as Upper Marsland by Schultz and others."

Runningwater Formation (early Hemingfordian), Dawes County, Nebraska: F:AM 99352, right isolated M1 from a tributary of Pebble Creek. F:AM 99350, left ramal fragment with m2 and m3 alveoli from Cottonwood Creek Quarry. From Dunlap Camel Quarary, 4.5 miles west of the old town of Dunlap, Dawes County, Nebraska:

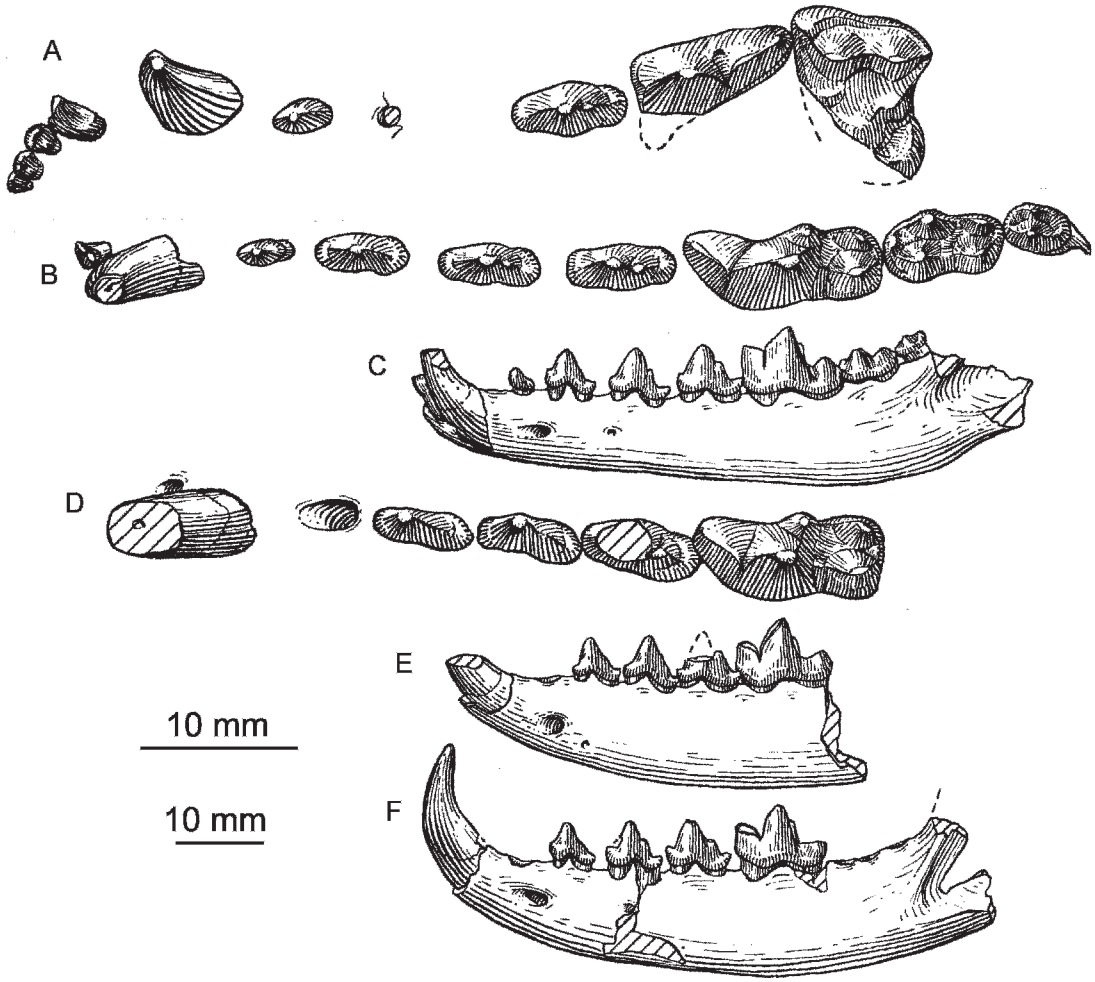

Fig. 8. **A–F**. *Leptocyon vulpinus*. **A–C**. Type skull fragment and ramus, AMNH 12883, late Arikareean, South Dakota. **A–B**. Occlusal views (P3 from opposite side). **C**. Lateral view. **D–F**. Early Hemingfordian, Nebraska. **D–E**. Ramus, UNSM 25611. **D**. Occlusal view, reversed. **E**. Lateral view, reversed. **F**. Ramus, F:AM 49187; lateral view. The longer (upper) scale is for A, B, and D, and the shorter (lower) one is for the rest.

F:AM 49187, right ramus with c–m1, p1, and m2–m3 alveoli (fig. 8F); F:AM 49186, left partial ramus with p4–m3; F:AM 67994, left humerus; F:AM 67994A, left ulna; and F:AM 6799B, right ulna.

Distribution: Medial Arikareean of South Dakota and Oregon, early Hemingfordian of Nebraska.

Revised Diagnosis: *Leptocyon vulpinus* differs from *L. douglassi* and *Leptocyon gregorii* in its larger size, stronger and more distinct parastyle on M1, m1 with trigonid and talonid wider relative to length, and proportionally larger m2 with larger and more distinct paraconid. *L. vulpinus* differs from *L. mollis* in its larger size, as well as larger and taller crowned premolars.

Description and Comparison: Macdonald (1963: 211) placed this species "in *Cynodesmus* because the type does not have lingual cusps on the talonid on m1 between the metaconid and the entoconid, the posterior end of the talonid basin is not closed, and the hypoconid is larger than the entoconid." These characters are also shared with *Leptocyon*, and the type of *L. vulpinus* differs

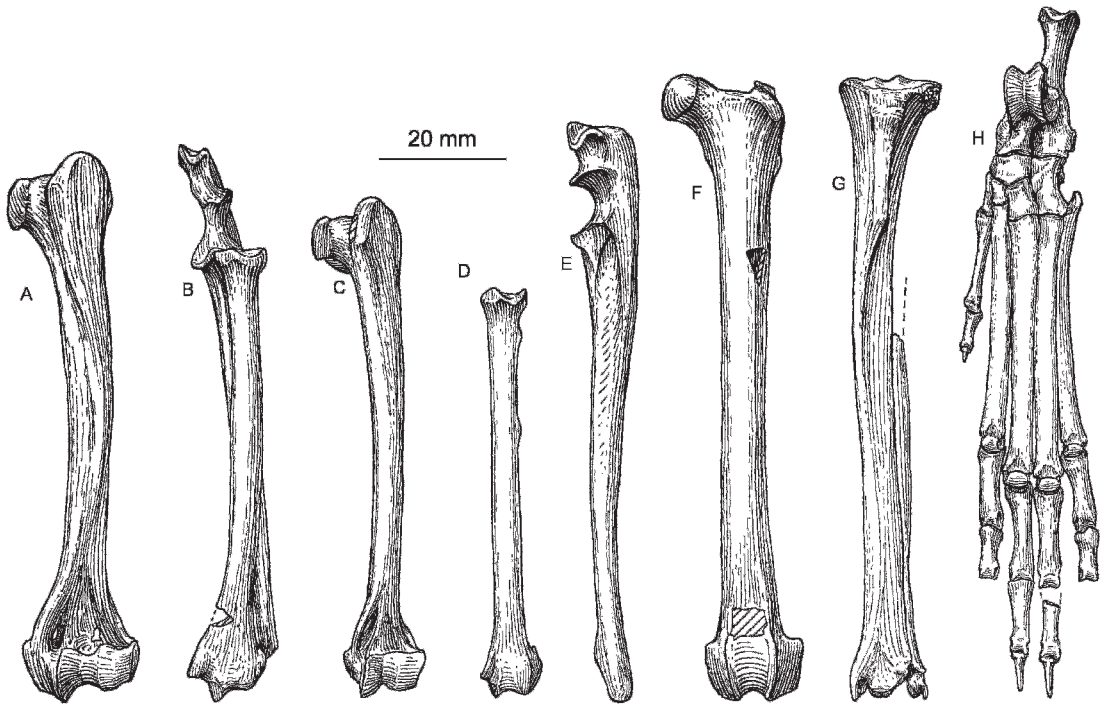

Fig. 9. **A–B**. *Leptocyon vulpinus*, late Arikareean, South Dakota. Type, AMNH 12883 (in part, see dentition fig. 8A–C). **A**. Left humerus, anterior view. **B**. Left radius and ulna, anterior view. **C–E**. *Leptocyon vafer*, late Barstovian, Nebraska. **C**. F:AM 72701, right humerus, anterior view, reversed. **D**. UNSM 51950, right radius, anterior view, reversed. **E**. F:AM 72702, right ulna, anterior view, reversed. **F**. *Leptocyon matthewi*, F:AM 49441, early Clarendonian, South Dakota; left femur, anterior view. **G–H**. *Leptocyon vafer*, F:AM 62780, late Barstovian, New Mexico. **G**. Right tibia, anterior view, reversed, and left partial fibula from opposite side, anterior view. **H**. Articulated right pes, anterior view, reversed.

greatly from the genotypic species of the hesperocyonine *Cynodesmus* (*C. thöoides*, see Wang, 1994). The type of *vulpinus* is assigned to the genus *Leptocyon*, but it differs from all other species of the genus, especially from *L. gregorii* from strata of equivalent age in South Dakota, in its broad P4, larger M1 parastyle, and a proportionally larger m2 with a more distinct paraconid. The M1 parastyle is not only larger, but, unlike that of *L. gregorii*, it appears as a distinct cusp that surmounts the labial cingulum. The lower premolars are large, tall-crowned, and widely spaced. The elongation and height of the premolars approximate those of *L. vafer* but the premolars are more widely spaced in *L. vulpinus*. The lower first molar has a well-developed and somewhat salient metaconid and a large hypoconid that is much larger than the entoconid. The most notable difference between *L. vulpinus* and *L. gregorii* is the large, elongate m2. It is larger relative to m1 than in all other species (fig. 5). Moreover, its paraconid is a well-developed, distinct cusp and not a mere shelf or ridge. For this reason the large subequal protoconid and metaconid are less anteriorly situated than in *L. gregorii*. The Oregon specimen confirms these features of the m1 and m2.

These distinctive morphological characters make it possible to separate *L. vulpinus* from the broadly contemporaneous *L. gregorii* and to extend the temporal range of the species to include specimens from the Runningwater Formation of Nebraska. Four partial rami from the Runningwater Formation are referred to *L. vulpinus*. They show relatively large, elongate, tall-crowned premolars and a robust m1. Unfortunately, only one mandibular ramus (UNSM 25416) possesses the m2. This m2 and an isolated specimen (F:AM 99350) also have a distinct paraconid. Two of

the referred rami have the alveolus for m2, and these again indicate a relatively large tooth approximating the size of that of UNSM 25416.

A combination of primitive and derived characters is seen in the type of *L. vulpinus*. The shape of P4, the well-developed parastyle of M1, and the distinct paraconid on m2 are primitive characters. Postcranial elements of the type (AMNH 12883, fig. 9A–B) also possess numerous plesiomorphic features shared with *Hesperocyon*. The humerus is long relative to the length of the radius, and the entepicondylar foramen is exceptionally large. The distal trochlea is slightly oblique to the shaft, and the lateral articular surface is about twice the width of the medial and the two are separated by a deep groove. Proximally, the greater tuberosity approximates that of the articular surface of the capitulum, and the lesser tuberosity is larger than that of *Vulpes*, with the two being separated by a prominent bicipital groove. An articulated radius and ulna of the type is short and robust and closely resembles that of *Hesperocyon*. Viewed anteriorly, the distal end of the radius is marked by prominent grooves for the extensor tendons. A prominent styloid process extends distally, and a medial radial exostosis is present intermediate in size between that of *Hesperocyon* and *L. vafer*. The distolateral surface bears a large laterally extended articular facet for the ulna. The ulna is robust, with the distal end especially heavy and with a large facet for articulation with the radius.

Incomplete elements of the tibia and fibula are also morphologically similar to those of *Hesperocyon*. The proximolateral condyle of the tibia is transversely broad and widely overlaps the shaft, with a large facet for articulation with the fibula. The distal end of the tibia has a prominent medial malleolus and deep articular grooves for the astragalus that are separated by a strong ridge. The distal end of the fibula articulates weakly with the tibia but possesses a strong articular facet for the astragalus.

Leptocyon delicatus (Loomis), 1932
Figure 12A–B; appendix 3

Pachycynodon delicatus Loomis, 1932: 325, fig. 8.
Neocynodesmus delicatus: Macdonald, 1963: 212.

Type: ACM 31102, left partial ramus with incisor alveoli, c broken, p1 alveolus, and p2–m2 from the "Lower Rosebud beds," Porcupine Creek, South Dakota. Macdonald (1963: 212) concluded that it is impossible to determine if this locality is equivalent to the Monroe Creek or Harrison formations.

Distribution: Known only from the locality of the type, early medial Arikareean of South Dakota.

Revised Diagnosis: Differs from all other species of *Leptocyon* in being approximately 40% smaller; premolar cusplets and cingular cusps generally weaker and especially weaker than those of contemporaneous taxa; m1 metaconid proportionally larger and taller crowned relative to size and height of protoconid; and m2 lacks a paraconid.

Description and Comparison: To our knowledge, the type and only known specimen of *L. delicatus* (Loomis, 1932) is the smallest known canid. Although the canine is broken in the type ramus, its size relative to that of the ramus corresponds to that of *Leptocyon* and the canine is separated from the p1 by a moderately long diastema. The first lower premolar is absent, but the alveolus indicates a small single-rooted tooth that is separated from p2 by a short diastema. The premolars are especially like those of *Leptocyon*: p2–p4 are widely spaced, slender, elongate, and tall-crowned, with the crown height of the p4 exceeding the height of the m1 paraconid. The second premolar lacks an anterior cingular cusp that is present in some species of *Leptocyon*, but it has a minute posterior cingular cusp. Both p3 and p4 have anterior cingular cusps as in contemporary larger species of *Leptocyon*. Additionally, p3 has a minute posterior cusp and p4 a weak posterior cusp. The posterior cusps and cingular cups are relatively weaker than those of other species of *Leptocyon*.

Morphologically, the molars are similar to those of the much larger jaws referred to *L. gregorii* (F:AM 49063) from rocks equated with the Harrison Formation in Wyoming. The m1 is slender with a widely open trigonid and a tall-crowned protoconid as in the latter specimen. The metaconid, however, differs from *L. gregorii* in being proportionally larger and taller crowned relative to the size and height of the protoconid. The features of

the metaconid are plesiomorphous and held in common with *Hesperocyon*. The m1 talonid is narrow and short relative to the length of the trigonid, with a strong hypoconid and a small conate entoconid that are often present in *Leptocyon* and always found in *Vulpes*. The m2 is small relative to the size of the m1 and morphologically resembles that of the above specimen referred to *L. gregorii* (F:AM 49063). An extremely weak anterolabial cingulum is present on m2, as in early occurring species of *Leptocyon*. A distinct paraconid is absent, but a shelf is formed by the joining of weak crests extending anteriorly from the protoconid and metaconid. The protoconid and metaconid are situated anteriorly and subequal in size. A narrow talonid has a well-developed hypoconid and a low crestlike entoconid. X-ray examination of the type shows that the m3 was not present in this individual.

Discussion: Loomis (1932: 325) described *Pachycynodon delicatus* from the Lower Rosebud of South Dakota, and stated, "this tiny lower jaw is almost identical in size with *P. tenius* of the Phosphorites of Quercy, differing only in that the teeth are slightly longer." Macdonald (1963: 212) erected a new genus, *Neocynodesmus*, and designated *P. delicatus* Loomis (1932) its genotypic species. In his study of the Miocene faunas of the Wounded Knee Creek area, South Dakota, Macdonald limited his comparison of the type of *Neocynodesmus delicatus* to that of a new species, *Cynodesmus cooki*, which he described in the same report. Macdonald commented that the "close resemblance of the carnassial to that of *Cynodesmus cooki* suggests that this form may have been derived from that slightly older species." Additional F:AM specimens of "*C.*" *cooki* (now placed in the borophagine genus *Otarocyon* Wang et al., 1999) show that the premolars of *L. delicatus* are more slender with weaker anterior and posterior cingular cusps and less prominent posterior cusp on p3 and p4. Furthermore, the lower carnassial of *L. delicatus* differs markedly from that of "*C.*" *cooki* in the manner typical of the canines in that its m1 is more elongate and slenderer, the trigonid lower, the paraconid less oblique, and the talonid narrower with a much smaller entoconid relative to the size of the hypoconid.

Macdonald failed to compare *L. delicatus* with specimens of *Leptocyon* that also occur in the "Lower Rosebud beds." Except for the lack of an m3, the mandibular and dental features of this tiny ramus are foxlike. Because all canids possess a third lower molar, an X-ray was taken of the type jaw but no unerupted m3 is present. The absence of the m3 prompted a comparison with the mustelids and procyonids. The outstanding general features of the type jaw of *L. delicatus* that separate it from members of those arctoid families are: (1) mandibular ramus shallow, elongate, and tapering anteriorly; (2) premolars elongate, slender, and widely spaced; (3) slender m1 with trigonid tall and open with small, but distinct, entoconid that is generally absent in the mustelids; and (4) m2 large, relative to m1, with strong and subequal metaconid and protoconid, and trigonid about equivalent in length to talonid.

Most of the above features that separate *L. delicatus* from the mustelids and procyonids are shared with *Leptocyon*, including: m1 entoconid distinct; mandibular ramus shallow and thin; premolars narrow and elongate; p4 with weak posterior cusplet; anterior premolars separated by short diastema; m1 without complete labial cingulum; and m2 with weak anterolabial cingulum. The absence of the m3 is considered an anomalous feature in this otherwise canidlike tiny jaw. Although the type is about 40% smaller than the next smallest jaw (CM 1300) referred to *Leptocyon*, it is assigned to this genus because of the listed synapomorphies and the lack of features that would ally it to more derived canine genera.

Leptocyon sp. B

Material: F:AM 97247, right partial ramus with p2–p4 alveoli, and m1 (measurements, table 5) from a roadcut at the half-mile point between Sect. 28 and Sect. 33, T25N, R52W, Box Butte County, Nebraska. The jaw was collected from deposits that were mapped by Cady and Scherer (1946: pl. 1) as the Marsland Formation. Ted Galusha (personal commun., 1975) reported that the

lithology at this site is unlike that of the Marsland Formation, and regional stratigraphic considerations suggest a late Hemingfordian or possibly early Barstovian age for this specimen.

Discussion: The length of the m1 is only 8 mm. It is thus the second smallest known specimen referred to the genus. The m1 is derived with respect to that of *L. delicatus* in that the trigonid is more open and longer relative to the length of the talonid, and the paraconid is less acute. The m1 talonid appears narrow as in *L. delicatus*, but a closer examination shows that postmortem erosion of the lateral surface is partly responsible for this narrowing. The horizontal ramus is slender and extremely shallow, but less elongate than the slightly larger jaw refered to *L. douglassi* (CM 1300) from early Arikareean deposits of Canyon Ferry, Montana. The m1 is slender and morphologically similar to the larger jaws of *L. gregorii* (F:AM 49063) from rocks referred to the Harrison Formation of Wyoming. As in the latter, the trigonid of m1 is long relative in the length of the tooth, the protoconid is tall, the metaconid is moderately developed, and the talonid is relatively short, with the entoconid being markedly smaller than the hypoconid.

Leptocyon gregorii (Matthew), 1907
Figures, 3, 5, 7, 10A–F, 11A–E, 17; appendices 2, 3

Nothocyon gregorii Matthew, 1907: 183, fig. 1.
Hesperocyon gregorii: Macdonald, 1963: 206.
?*Tomarctus* sp. indet.: Macdonald, 1970: 57.

Type: AMNH 12879, posterior two-thirds of a skull with P3–M2, right and left mandibular fragments with p3 and m1–m2 (fig. 11A–E) and limb fragments. Matthew recorded the type from 1 mile east of Porcupine, lower Rosebud beds, South Dakota. Macdonald (1963: 206) listed the type locality as ''A.M.N.H. 'Rosebud' 19'' from rocks thought to be equivalent to the Harrison Formation of Nebraska.

Referred Material: Type area, west of Window Butte, LACM locality 2012, identified as the Harrison Formation (medial Arikareean), South Dakota: LACM 9198, right partial ramus with c, m1 (p1 alveolus and p2–p4 broken), described and measured by Macdonald (1970: 57–58).

Lusk area, rocks referred to the middle Harrison Formation (medial Arikareean), Niobrara County, Wyoming: F:AM 49063, skull with C broken–M2 and left and right mandibular rami with c broken–m3 (fig. 10A–F), north of Keeline, middle brown sand. F:AM 49062, immature right partial ramus with dp3–dp4, m1 unerupted, north of Keeline. North Ridge, along Highway 85, about 10 miles north of Lusk: F:AM 49059, right ramal fragment with m1. North of Jeriah: F:AM 49061, right ramus with c, p1 alveolus, p2–m2.

Distribution: Medial Arikareean of South Dakota and Wyoming.

Revised Diagnosis: *L. gregorii* differs from *L. vulpinus* in smaller size; slender P4, weaker M1 parastyle; smaller premolars; less robust m1 with trigonid and talonid narrower relative to length; and proportionally smaller m2. Differs from *L. leidyi* and *L. vafer* in smaller dentition, retention of m2 paraconid, and proportionally longer and more inflated bullae. *L. gregorii* differs from *L. vafer* in narrower cranium with greater cerebellar exposure, retaining postparietal foramina; weaker m2 anterolabial cingulum; and m2 with subequal protoconid and metaconid.

Description and Comparison: The dentition of *L. gregorii* is significantly smaller than that of *L. vulpinus* (fig. 7) and only slightly smaller than that of *L. leidyi*. *Leptocyon gregorii* retains such primitive features as the paraconid on m2, the postprotocristid (but not metaconule) on M2 and a posterior cusp on p3.

The skull features of *L. gregorii* are provided by the incomplete skull of the type (AMNH 12819, fig. 11A–E) and a referred skull (F:AM 49063, fig. 10A–F). These skulls are compared with the type skull (UNSM 25715, fig. 11F–I) of *L. leidyi* and several heretofore undescribed skulls of *L. vafer*. Crushing and weathering has obscured some of the details of the braincase of the type skull but the description is complemented by the features of the better preserved referred skull. Viewed dorsally, the shape and proportions of the postorbital cranium of *L. gregorii* are similar to those of *Hesperocyon*. As in *Hesperocyon*, the cranium of *L. gregorii*

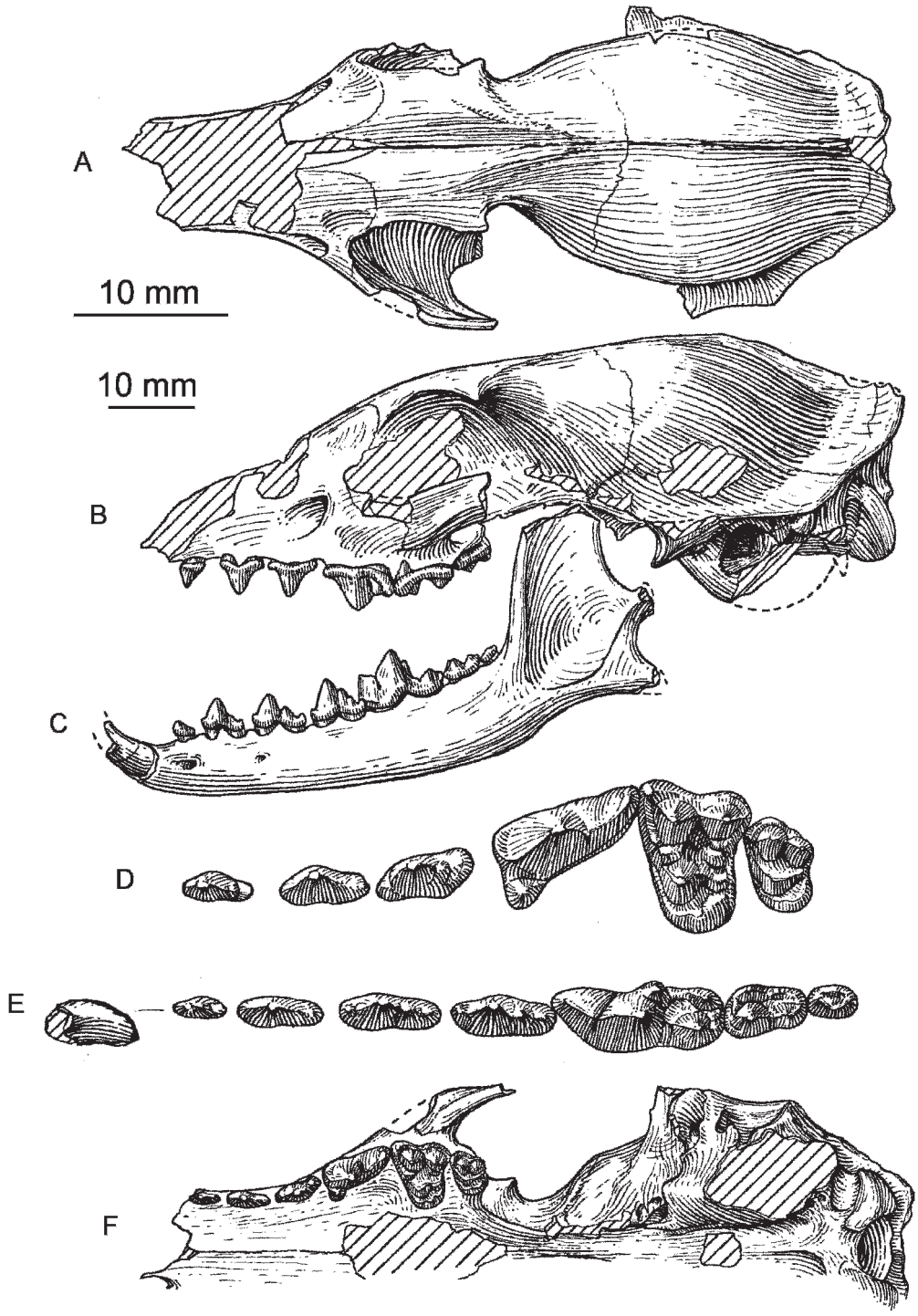

Fig. 10. **A–F**. *Leptocyon gregorii*, Late Arikareean, Wyoming. Skull and associated ramus, F:AM 49063. **A**. Dorsal view. **B–C**. Lateral views. **D–E**. Occlusal views. **F**. Palatal view. The longer (upper) scale is for D and E, and the lower one is for the rest.

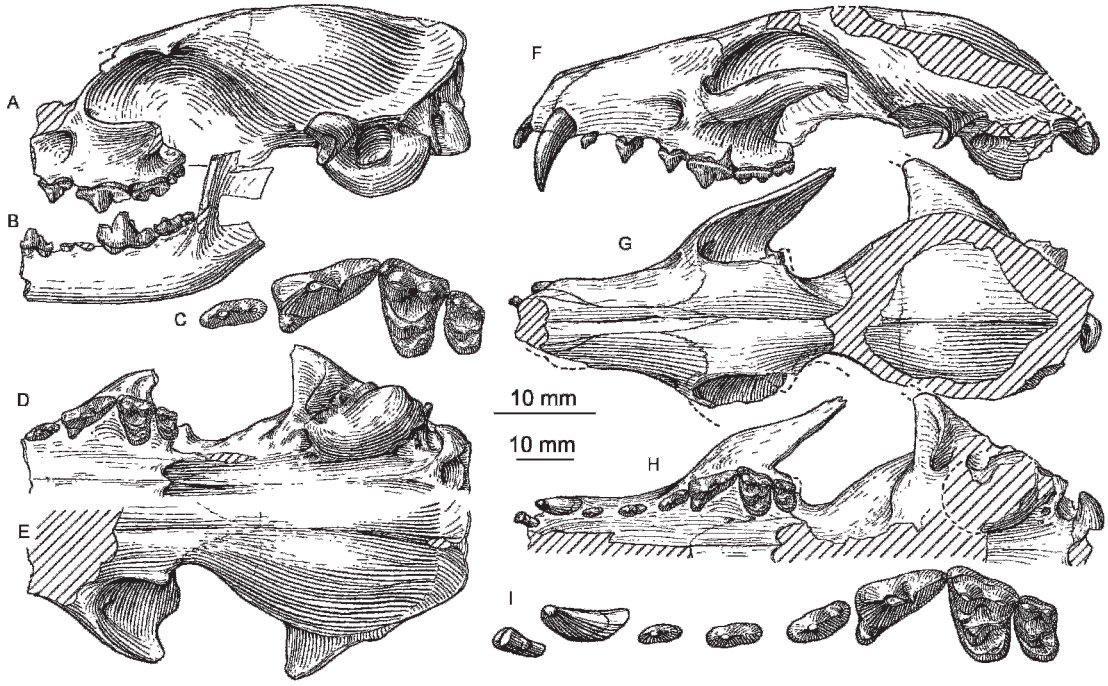

Fig. 11. **A–E**. *Leptocyon gregorii*, late Arikareean, South Dakota. Type skull and associated ramus, AMNH 12879. **A**. Lateral view, reversed. **B**. Lateral view (from both sides). **C**. Occlusal view, reversed. **D**. Palatal view, reversed. **E**. Dorsal view, reversed. **F–I**. *Leptocyon leidyi*, early Hemingfordian, Nebraska. Type skull, UNSM 25715. **F**. Lateral view, reversed. **G**. Dorsal view, reversed. **H**. Palatal view, reversed. **I**. Occlusal view, reversed. The longer (upper) scale is for C and I, and the shorter (lower) scale is for the rest.

is elongate relative to the length of the skull and it retains a small postparietal foramina. Elongation of the cranium approximates that of the type of *L. leidyi*. The nasals converge to a point at the midline well behind (3 mm) the most posterior position of the maxillary-frontal suture in the referred skull. The frontals are narrow and only slightly elevated, and the postorbital processes are weak. Marked postorbital constriction is present in both skulls of *L. gregorii* as in the type of *L. leidyi*. In *L. vafer* the frontals are relatively wider and the postorbital constriction is less. Although the dorsal surface of the braincase is broken in the type of *L. gregorii*, weak lyrate temporal crests can be seen joining behind the frontoparietal suture to form a low sagittal crest. In the referred skull (F:AM 49063) the temporal crests are very weak and best seen where they unite at a point just posterior to the frontoparietal suture. Despite crushing it is evident that the braincase in *L. gregorii* is narrower and the cerebellar exposure is greater than in *L. vafer*. Other measurements of the braincase in the types of *L. gregorii* and *L. leidyi* cannot be made because of crushing.

The auditory bulla in *L. gregorii* is anteroposteriorly longer and relatively larger and more inflated than in either *L. leidyi* or *L. vafer*. Because the bulla is badly broken in the type of *L. leidyi*, little can be determined except for its gross size, which is smaller than that of *L. gregorii*. In the latter, the anterior border of the bulla and the eustachian opening are slightly anterior to the postglenoid process, whereas in *L. leidyi* the broken surface indicates that the entotympanic bone reaches only to the posterior surface of the postglenoid process. Anteriorly, the bulla in *L. gregorii* is marked by a prominent depression at the junction of the ectotympanic and the entotympanic bones. The paroccipital process in *L. gregorii* is nearly vertical,

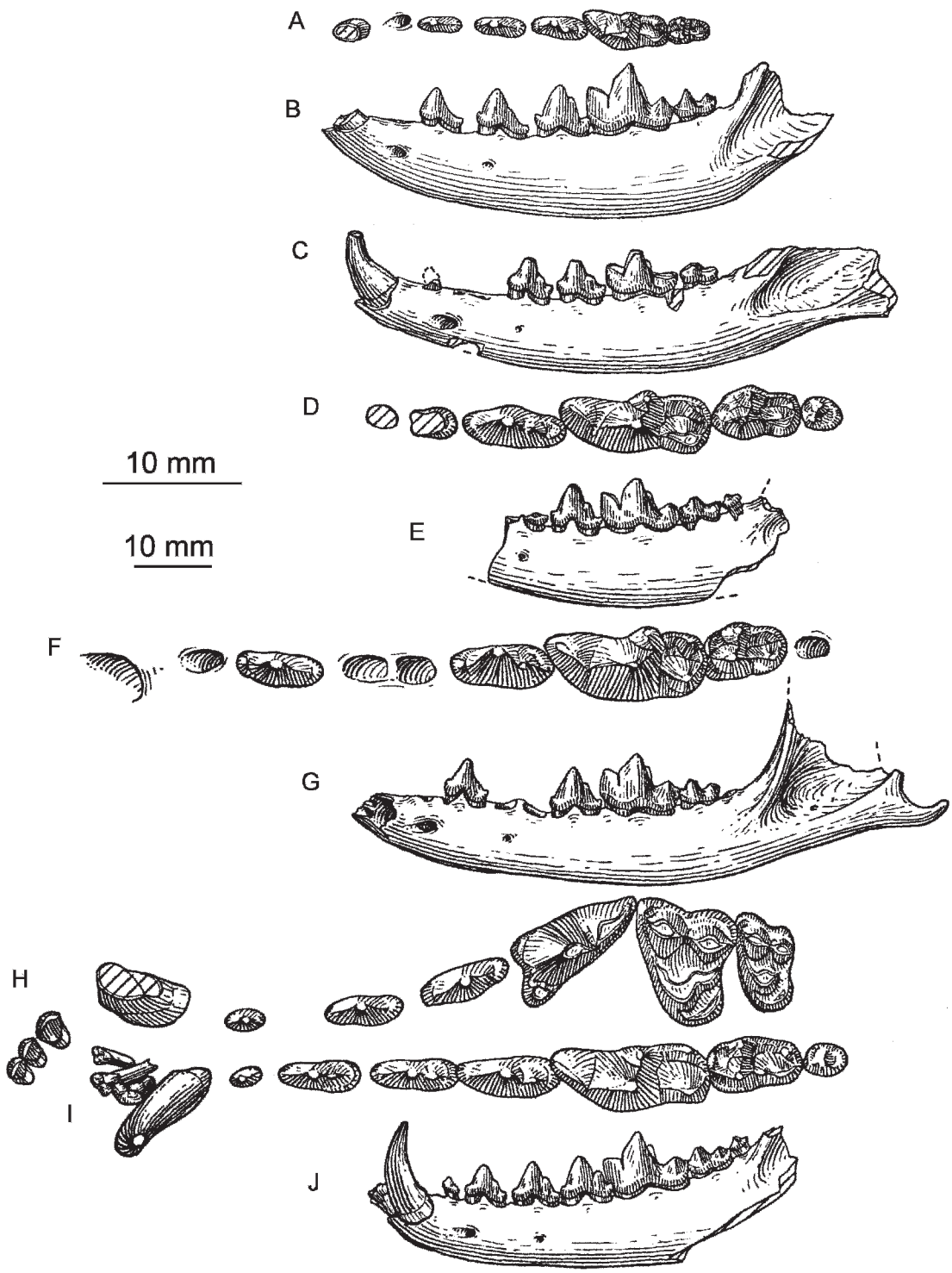

but short and without a free tip. It covers only a small area of the bulla surface. In *L. vafer* this process is also vertical but it is wider and its free tip extends more ventrally; the anterior surface is deeply concave and covers a wider area of the posterior wall of the bulla.

Leptocyon leidyi, new species
Figures 7, 11F–I, 12C–J, 13A–F, 17; appendices 2–4

Leptocyon vafer (Leidy): Matthew, 1918: 190 (in part).
Leptocyon sp.: Galusha, 1975: 56–57.

Type: UNSM 25715, partial skull with I3–M2 (fig. 11F–I), from Hemingford Quarry 12D (early Hemingfordian), Box Butte County, Nebraska. The type was reported by the University of Nebraska State Museum to be from the upper part of the Marsland Formation. We consider these specimens to be from the Runningwater Formation in accordance with McKenna (1965[as in ref]: 10) in that "the type Runningwater Formation is part of the same unit as that referred to as Upper Marsland by Schultz and others."

Etymology: Named in honor of Joseph Leidy, pioneering vertebrate paleontologist, who described the genotypic species of *Leptocyon*.

Referred Material: From the Runningwater Formation (early Hemingfordian) in the general area of the type, Box Butte County, Nebraska: UNSM 25454, right ramus with c, p1–p2 roots, p3–m2, m3 alveolus (fig. 12C–E), Hemingford Quarry 12D; UNSM 25716, left partial ramus with p2–m2 (p3 broken), locality 31, an extension of Hemingford Quarry 12D; UNSM 26146, left isolated M1 and UNSM 26145, left ramal fragment with m1, Hemingford Quarry 7.

Pebble Creek, Runningwater Formation (early Hemingfordian), Dawes County, Nebraska: F:AM 67994C, calcaneum.

From the Runningwater Formation (early Hemingfordian) on the east side of Dry Creek, Box Butte County, Nebraska: F:AM 97245, left partial ramus with p3 alveolus, p4–m1, m2 alveolus.

Middle of the Road Quarry, Red Valley Member, Box Butte Formation (late Hemingfordian), Box Butte County, Nebraska: F:AM 96688, right partial ramus with p4, m1 broken, m2 root (Galusha, 1975: 56).

Sheep Creek Formation (Late Hemingfordian), Sioux County, Nebraska: F:AM 54450, left ramus with p2, p4–m2, and c–p1, p3 and m3 alveoli (fig. 12F–G), Hilltop Quarry. F:AM 54451, right partial ramus with m1–m2, Thistle Quarry. F:AM 54452, right partial ramus with m1. F:AM 67790, right tibia, Greenside Quarry. F:AM 54453, right partial ramus with m1–m2, East Ravine Quarry. F:AM 72671, left femur, Thompson Quarry.

Olcott Formation (early Barstovian), Sioux County, Nebraska: F:AM 54380, palate with I1–M2 (fig. 12H); F:AM 54376, right ramus with p3–m2 (p4–m1 broken), New Surface Quarry. F:AM 54375, mandible with i1–m3 (fig. 12I–J), Echo Quarry. F:AM 54377, right partial ramus with p3–m3; F:AM 72673, right radius, New Surface Quarry. F:AM 72672, right radius; F:AM 72673A, left partial radius; F:AM 72674, right tibia; F:AM 67817, right metatarsal II, Echo Quarry. F:AM 54378, right ramus with c broken–m3, Jenkins Quarry. F:AM 54379, right partial ramus with m1–m2, Humbug Quarry.

←

Fig. 12. **A–B**. *Leptocyon delicatus*, type ramus, AMC 31102, Arikareean, South Dakota. **A**. Occlusal view. **B**. Lateral view. **C–J**. *Leptocyon leidyi*, Early Hemingfordian, Nebraska. **C**. Ramus, UNSM 25454. Lateral view, reversed. **D–E**. Ramus, F:AM 49186. **D**. Occlusal view. **E**. Lateral view. **F–G**. Late Hemingfordian, Nebraska. Ramus, F:AM 54450. **F**. Occlusal view. **G**. Lateral view. **H–J**. Early Barstovian, Nebraska. Upper dentition, F:AM 54380. **H**. Occlusal view, reversed. Ramus, F:AM 54375. **I**. Occlusal view. **J**. Lateral view. The longer (upper) scale is for A, B, D, F, H, and I, and the shorter (lower) one is for the rest.

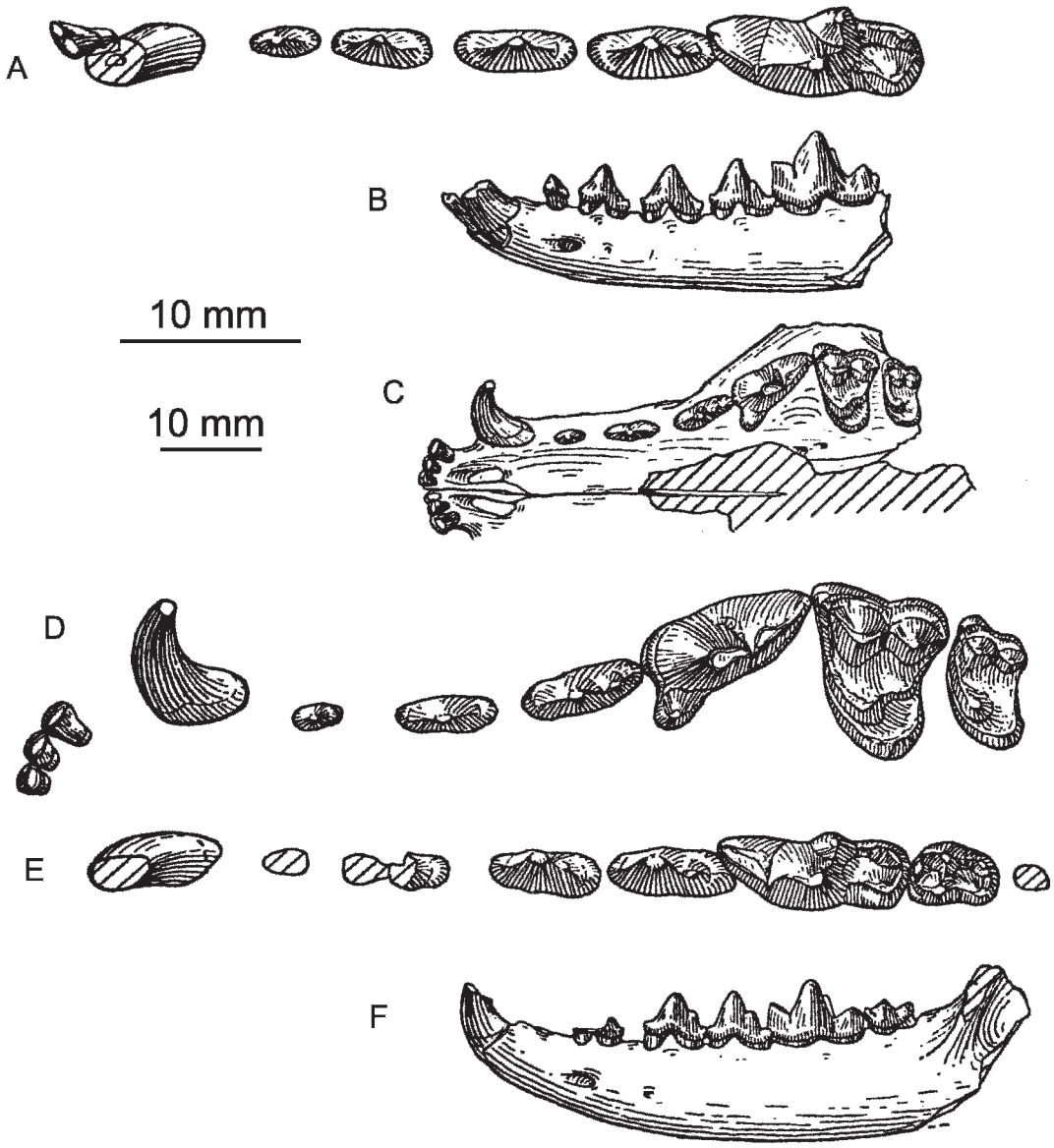

Fig. 13. **A–F**. *Leptocyon leidyi*. **A–B**. Early Barstovian, Colorado. Ramus, F:AM 28345. **A**. Occlusal view (p2 from opposite side). **B**. Lateral view (p2 from opposite side). **C–F**. Late Barstovian, California. Associated upper and lower dentitions, F:AM 27535. **C**. Palatal view. **D**. Occlusal view. **E**. Occlusal view, reversed. **F**. Lateral view, reversed. The longer (upper) scale is for A, D, and E, and the shorter (lower) scale is for B, C, and F.

AMNH 17201, right ramus with p4–m2, Lower Snake Creek beds (referred to *L. vafer* by Matthew, 1918: 190).

Observation Quarry (early Barstovian), ?Sand Canyon Formation, Dawes County, Nebraska: F:AM 25344, left partial ramus with p1–m1.

Lower Madison Valley (early Barstovian), Montana: CMNH 739, right partial ramus with c broken–m1 (p1 alveolus).

Pawnee Creek Formation (early Barstovian), Weld County, Colorado: F:AM 28345, partial mandible with i3, c broken, p1–m1, m2 broken (fig. 13A–B), East Valley No. 1, east side pit.

Skull Ridge Member of the Tesuque Formation (early Barstovian), Santa Fe County, New Mexico: F:AM 27273, right and left partial rami with c broken–m2; F:AM 63134*, right toothless partial ramus, White Operation. F:AM 50177*, left ramal fragment with p4–m2 all broken, White Opertion area. F:AM 50162*, left partial ramus with c–m2 all broken or alveoli, near White Operation. F:AM 63135*, right partial ramus with c–p4 alveoli, m1 broken, m2 alveolus, District No. 1. F:AM 67891, proximal part of radius, and F:AM 67891A, proximal part of ulna, Skull Ridge.

Barstow Formation (early Barstovian), San Bernardino County, California: F:AM 27279, left partial ramus with m1 broken–m2, "Third Division." F:AM 27274, c–m3 (p1 alveolus), no data, preservation suggestive of "Third Division." F:AM 27537A, left partial maxilla with P3 broken–M2; and F:AM 27537, right partial ramus with p4–m3, Green Hills.

Barstow Formation (late Barstovian), San Bernardino County, California: F:AM 50112, left partial maxilla with P4–M2; F:AM 50116, left partial ramus with p4–m3 (m1 broken); F:AM 50110, left partial ramus with p1–m3; F:AM 50111, left ramus with p4–m2, Hidden Hollow Quarry. F:AM 27535, anterior half of skull with I1–M2 and right and left incomplete rami with c–p2 broken, p3–m2, m3 root (fig. 13C–F); F:AM 27536, right and left rami with p2–m3, North End. F:AM 50113, left partial ramus with p4 broken–m2 (m1 broken), Falkenbach horizon, North End. F:AM 50115, partial mandible with broken teeth, below Black Hill Quarry, North End. F:AM 27540, left isolated m1, Skyline Quarry. F:AM 50114, right ramal fragment with m1–m2 both broken, prospect near Chert Ridge. F:AM 27275, partial palate with P2 and P4–M2; F:AM 27276, right and left partial rami with p3 broken–m1; F:AM 27278, left patial ramus with p3 broken–m2, Hemicyon stratum. UCMP 35308, left M2 and right and left ramal fragments with c broken, p1–p2, p4, m1 broken, m2–m3 alveoli, from site 33, UCMP locality V3847. F:AM 27280, right partial ramus with p4 broken–m1, Second Division; and F:AM 27277, left partial ramus with p4–m1, questionably Second Division.

Tributary of Ellison Creek, about 0.75 mile northeast of Willow Grove (late Barstovian), Pine County, Nevada: NMNH 243776, partial palate with P2–P4 all broken and M1–M2.

Distribution: Early to late Hemingfordian of Nebraska, early Barstovian of Nebraska, Colorado, Montana, New Mexico, and California, and late Barstovian of New Mexico, Nevada, and California.

Diagnosis: *L. leidyi* differs from *L. gregorii* in dentition averaging slightly larger (fig. 7), proportionally shorter and less inflated bulla, and tendency to reduce and lose postprotocrista of M2, and loss of paraconid of m2. *L. leidyi* averages smaller than *L. vafer* with 95% confidence interval of m1 length nearly separated (fig. 7); m2 slightly longer relative to length of m1, it lacks enlargement of m2 anterolabial cingulum and short nasals that characterize *L. vafer*, but it shares lack of postprotocrista on M2.

Description and Comparison: The dentition of *L. leidyi* is similar in size to that of *L. gregorii* but smaller than that of *L. vafer* (fig. 7). The morphology of the dentition closely resembles that of *L. gregorii* and only the reduction and loss of the metaconule and postprotocrista on M2 and loss of the paraconid m2 distinguish the two taxa.

The type skull of *L. leidyi* closely resembles that of *L. gregorii* (fig. 11). In both skulls the nasals reach posteriorly beyond the frontal-maxillary suture; the frontals and the postorbital constriction are narrow; and the weak temporal crests unite near the frontoparietal suture to form a low sagittal crest. The basicranial region is shattered and our comparison is thus limited to size. Judging by the distance from the posterior lacerate foramen forward to the eustachian opening, the bulla was anteroposteriorly shorter than that of *L. gregorii*. Moreover, the preserved part of the tympanic bone indicates that it was also less inflated and the occipital bone between the bullae is relatively wider than that of *L. gregorii*. In the type skull of *L. leidyi* the anterior suture for the tympanic

bone is behind the glenoid cavity, whereas in *L. gregorii* it is directly opposite the glenoid cavity. Although the auditory meatus is broken, it appears unlikely that the lip projected laterally to the extent seen in that of *L. vafer*.

In the upper dentition the P1–P3 are anteroposteriorly short, widely spaced, and without posterior cusps. The P4 has a weak parastyle and a well-developed protocone that is situated more anteriorly than that of the type of *L. gregorii*. A moderately strong lingual cingulum extends the full length of the tooth. The morphology of the M1 of *L. leidyi* is similar to that of the type of *L. gregorii*. It is characterized by a low-crowned paracone and metacone, a weak parastyle, and a moderately strong labial cingulum. M1 differs, however, from that of the type of *L. gregorii* in its more quadrate shape and in the reduction of the metaconule. M2 is relatively wider than that of *L. gregorii*, its metaconule is absent in late Hemingfordian examples of *L. leidyi*, and the postprotocrista is lacking as well in Barstovian samples as in *L. vafer*.

The lower dentition and mandible are closest in structure to those of *L. gregorii* where they differ only slightly in size. The mean length of m1 is not significantly different in these taxa (fig. 7). A larger size difference is present between *L. leidyi* and *L. vafer* where the observed ranges of m1 length broadly overlap but the 95% confidence intervals are nearly separated (fig. 7). Additionally, *L. leidyi* has a proportionally longer m2 relative to the length of m1, the premolars are lower crowned, shorter, and have less prominent cusplets, and the m1 talonid is low-crowned. *L. leidyi* shares with *L. vafer* the loss of m2 paraconid but is otherwise plesiomorphic in the lower dentition.

Discussion: The dentition of *L. leidyi* is similar in size to that of *L. gregorii* (fig. 17). The coefficients of variation for some teeth indicated in appendix 3 are high by most standards, probably due to the wide temporal and geographic range of the referred specimens. Examining the statistics, we find the coefficient of variation is high (nearly 10) for the anterior premolars (p1 and p2) and for the length and width of the second upper and lower molars. The sizes of the anterior premolars and the last molars at the ends of the toothrow are generally more variable and the coefficient of variation is often higher than teeth that have anterior and posterior occlusal constraints.

The morphology known for *L. leidyi* appears in most cases to be plesiomorphic with respect to *L. vafer*, and in this respect *L. leidyi* could be considered an approximation of the morphological features of the ancestral stock for later species of *Leptocyon*. It shares the loss of the postprotocrista on M2 with *L. vafer*, a synapomorphy that links those species within *Leptocyon*. *Leptocyon gregorii*, which appears only modestly distinguishable from *L. leidyi* in dental features, is clearly differentiated by its autapomorphy, the markedly inflated bulla.

Leptocyon vafer (Leidy), 1858
Figures 3, 7, 9C–E, G, H, 14G–H, 15A–G, 16A–G, 17, 52, 61A; appendices 2, 4

Canis vafer Leidy, 1858: 21.
Vulpes vafer: Trouessart, 1897: 310 (catalog).
"*Canis*" *vafer:* Matthew, 1909: 115.
Leptocyon vafer: Matthew, 1918: 190.
Canis vafer: Merriam, 1919: 533, figs. 138A, 139B.
Canid indet.: Henshaw, 1939: 17, pl. 2, fig. 2, 2A.
Leptocyon vafer: Henshaw, 1942: 110, pl. 3, fig. 6, 6A.
Vulpes vafer: Macdonald, 1948: 55, fig. 1A–B.
Leptocyon vafer: Webb, 1969: 39, fig. 7.

Type: NMNH 126, right and left rami, c broken, p1–m3 (p3 broken), figured by Leidy (1869: pl. 1, fig. 2, our fig. 14G–H). The type was collected in 1857 by the Warren and Hayden Expedition from the "Loup Fork beds" along the Niobrara River in Nebraska. According to the notes and diaries of Snowden, who accompanied the expedition, Warren and Hayden joined Snowden at the mouth of Bear Creek and continued down the Niobrara River to the vicinity of present day Norden, Nebraska. It is most likely that the type was collected from this section of the Niobrara River. Both the Ash Hollow and the Valentine formations are exposed along this part of the Niobrara River, but the preservation of the type suggests that it is from the Valentine Formation (M.F. Skinner, personal commun., 1972).

Referred Material: Norden Bridge Quarry (Univ. Nebr. locality Bw-106), Cornell Dam Member of the Valentine Formation (early

late Barstovian), Brown County, Nebraska: UNSM 83958*, right ramus with c, p4–m2; NMNH 35296*, right ramus with p1–p3, p4 broken, m1–m2; NMNH 35291*, right ramus with m1–m2 (from Voorhies, 1990: A135).

Crookston Bridge Member of the Valentine Formation (early late Barstovian), Cherry County, Nebraska: UNSM 25717, partial skull with P2–M2; UNSM 25718, partial skull with P2–M2; UNSM 25718, partial skull with I1–M2 (C and P1 alveoli) and right ramus with i3–m3 (p1 alveolus, fig. 14A–D); UNSM 25793, left ramus with c–m2 (p1 and m3 alveoli); UNSM 25719, left ramus with c, m1–m2, and alveoli, Crookston Bridge Quarry. UNSM 32009, right ramus with c, p1–p4 broken alveoli, m1–m2, m3 alveolus, 40 ft above Crookston Bridge Quarry. F:AM 62876, right ramus with p3–m2, Railroad Quarry A. F:AM 25441*, right partial ramus with p4 and m2, Devil's Jump Off Quarry. UCMP 63644, right partial ramus with p4–m1, m2 broken; UCMP 33127, left partial ramus with p1, p2–m1 all broken, and m3 alveolus, listed by Macdonald (1948: 55); UCMP 33126, right partial ramus with p1–m2, m3 alveolus, listed by Macdonald (1948: 55); UCMP 29209, right partial ramus with p3 broken, p4 alveolus–m2, m3 alveolus, listed by Macdonald (1948: 55), and associated left partial ramus with p4, m1 broken, and m3 alveolus; UCMP 29208, isolated teeth including left P4, right M1, left m1, and right m1, Fort Niobrara, UCMP locality V3218. UCMP 32016, isolated right m1, Little Beaver A, UCMP locality V3306. UCMP 29893, isolated right P4, Railway Quarry A, UCMP locality V3307. UCMP 63722, left partial maxilla with M1, boat landing locality. F:AM 62870, left ramus with p2–m2 (fig. 14E–F); F:AM 62871, right partial maxilla with P4–M2; F:AM 62874, left ramus with c broken–m2; F:AM 62888, right partial ramus with m1–m2; F:AM 25440, left partial ramus with m1–m2; F:AM 72706, left metatarsal V, Nenzel Quarry. F:AM 72704, right metatarsal II, F. Schoettger Ranch.

Annies Geese Cross Quarry, Crookston Bridge Member, Valentine Formation (early late Barstovian), Knox County, Nebraska: UGV 68a, right isolated M1; UGV 68b, right isolated P4; UGV 68c, right isolated broken m1; UGV 64, right partial ramus with p2, m1–m2, and alveoli of remaining cheek teeth; UGV 65, right partial ramus with m2, m3 alveolus; UGV 66, right partial maxilla with P4–M1 (both broken); UGV 67, left partial maxilla with M1 broken; UGV 70a, right isolated M1; UGV 70b, left isolated broken M1; UNSM 51951, right partial ramus with c root, p1 alveolus–m1; UNSM 51952, left partial ramus with m2 and alveoli for c–m3; UNSM 51953*, right isolated and broken m1; UNSM 51950, right radius (fig. 9D); and UNSM 51949, left tibia.

Devils Gulch Member of the Valentine Formation (medial late Barstovian), Brown, Cherry, and Keyapaha counties, Nebraska: F:AM 62880A*, left partial ramus with m1 broken–m2; F:AM 72703, left partial tibia, Meisner Slide. F:AM 72701D, left distal part of humerus, near head of Jones Canyon, Dutch Creek. F:AM 62872, left ramus with c–p3 all alveoli, p4–m1 broken–m3, Meisner Slide, ?Burge or Devils Gulch Member. F:AM 62879, left ramus with p3–m2, Fairfield Falls Quarry.

Verdigre Quarry, basal sands Devils Gulch Member of the Valentine Formation (late Barstovian), Knox County, Nebraska: UW 2453, left partial ramus with p1–m2, m3 alveolus; UW 2454, left partial ramus with p4 alveolus and m1–m2, m3 alveolus; UW 2461, right partial ramus with p1–p4 alveoli, m1; UW 2464, left isolated m1; UW 2465, right isolated m1; UW 2466, right isolated m1, UW 2455*, right ramus with p1–p4 alveoli, m1–m2, m3 alveolus; UW 2456, left ramus with c, m2, and all alveoli; UW 2457, left partial ramus with m1 broken–m2 and m3 alveolus; UW 2458, m2 and p2–m1 alveoli; UW 2460, left partial ramus with m2; UW 2459*, left partial edentulous ramus; UW 2467, right isolated P4; and UW 2469, left isolated P4; CMNH 19679, left partial ramus with i1–p3 alveoli, p4–m1, and m2 broken alveolus; CMNH 19675, left detached m1; CMNH 19676, left detached m2; and CMNH 19678, right detached P4.

Valentine Formation (late Barstovian), Fort Niobrara, Cherry County, Nebraska: UNSM 25794, left partial maxilla with P3 alveolus–M2; UNSM 25408, left partial ramus with p1 alveolus–m2 (p2–p4 broken);

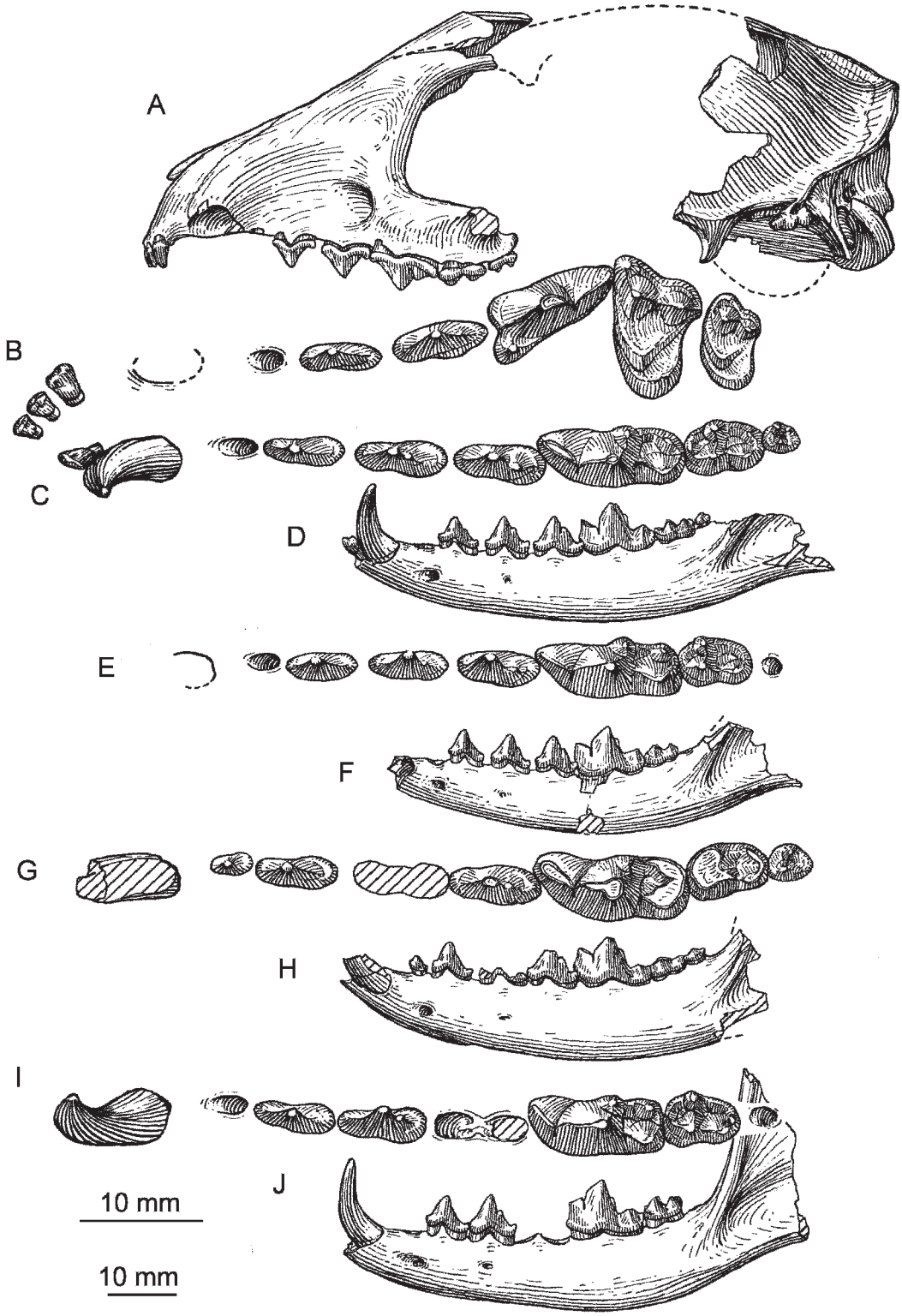

AMNH 8548, right partial ramus with m1, m2 broken, and m3 alveolus; AMNH 8545, left partial ramus with c–p4 alveoli, m1 (broken)–m2, and m3 alveolus; and AMNH 8546, left partial ramus with p1 alveolus, p2, p3 alveolus, p4, and m1 broken.

Rattlesnake Canyon, Valentine Formation (late Barstovian), Brown County, Nebraska: F:AM 25137, right partial ramus with p4–m1.

Driftwood Creek area (late Barstovian), Virgil W. Hay Ranch, 5.5 miles E and 8 miles S of Trenton, Hitchcock County, Nebraska: F:AM 62901, left ramal fragment with m1–m2.

Burge Member of the Valentine Formation (earliest Clarendonian), Cherry, Brown, and Keyapaha counties, Nebraska: F:AM 62886, right partial ramus with p3–m2; F:AM 62887, right partial ramus with m1–m2; F:AM 62885, right partial ramus with p2–m2 (p4 broken); F:AM 62895, left ramus with m3 and all alveoli; F:AM 72702A, left partial ulna, Burge Quarry. F:AM 62884, left partial ramus with m1–m2; F:AM 72701A, left distal part of humerus, Lucht Quarry. F:AM 62889, right ramus with p2–m2 and all alveoli; F:AM 62877, right partial ramus with p4 broken–m1; F:AM 62878, left edentulous ramus, June Quarry. F:AM 62883*, left partial ramus with m2 and c–m1 alveoli, Midway Quarry. F:AM 25444, left ramus with c–m2 (p1, p4, and m3 alveoli, fig. 14I–J), McGuires Canyon. F:AM 62892, right ramal fragment with m2; UCMP 32229, left mandibular fragment with p1–p3 alveoli and p4–m1 (listed and figured by Webb, 1969: 40, fig. 7), Crazy locality. UCMP 64657, right mandibular ramus with c–m2, m3 alveolus (listed by Webb, 1969: 41), Fatigue Quarry. F:AM 72701, right humerus (fig. 9C), south side of Snake Den Canyon, east side of Snake River. F:AM 72702, right ulna (fig. 9E), northeast of falls of Niobrara River, near Cody. F:AM 72705, left metatarsal IV, Mogle Ranch.

Paleo Channel Quarry, temporally equivalent to the Burge Member of the Valentine Formation (earliest Clarendonian), Sheridan County, Nebraska: F:AM 62873, left partial ramus with m1–m2.

Undifferentiated beds (late late Barstovian) of the Ogallala group, Selby Ranch Quarry, 12 miles northeast of Phillipsburg, Phillips County, Kansas: F:AM 49452*, left partial ramus with p4–m1, m2 broken.

Pojoaque Member of the Tesuque Formation (late Barstovian, see Galusha and Blick, 1971: 110; Tedford and Barghoorn, 1993), Santa Fe and Rio Arriba counties, New Mexico: F:AM 62778, partial skull with I1–M1 all broken and partial left ramus with i1–m2 all broken; F:AM 62750, right immature ramal fragment with m1 and associated femur and tibia; F:AM 62756, partial palate with P3–M2; F:AM 62757 and 62757A, left partial maxilla with P4–M2 and left ramus with c broken, p2–p3 both broken, m2; F:AM 62758, right ramus with c broken and p4–m2; F:AM 62764, left partial ramus with m1–m2; F:AM 62763, skull with I1–P1 alveoli, P2–M2, and mandible with c–m3 (fig. 15A–D); F:AM 63136*, right partial ramus with m2 and alveoli, Pojoaque Bluffs. F:AM 62751, left ramus with c–m1 (p1 alveolus and p2–p3 broken); F:AM 62752, mandible with c–m3 all alveoli or broken, Central Pojoaque Bluffs. F:AM 30923*, left broken m1, Jacona Microfauna Quarry, west of Pojoaque Bluffs. F:AM 62754, left toothless maxilla; F:AM 62755*, partial cranium and right and left ramal fragments with m1 broken–m3, west of Pojoaque Bluffs. F:AM 27402C, left partial ramus with p4–m2,

←

Fig. 14. **A–J**. *Leptocyon vafer*, late Barstovian, Nebraska. **A–D**. Associated skull and ramus, UNSM 25718. **A**. Lateral view (combination of both sides and length reconstructed after UNSM 25717). **B–C**. Occlusal views, reversed. **D**. Lateral view, reversed. **E–F**. Ramus, F:AM 62870. **E**. Occlusal view. **F**. Lateral view. **G–H**. Type ramus, NMNH 126. **G**. Occlusal view (restored from both sides). **H**. Lateral view. **I–J**. Ramus, F:AM 25444. **I**. Occlusal view, reversed. **J**. Lateral view, reversed. The longer (upper) scale is for B, C, E, G, and I, and the shorter (lower) one is for the rest.

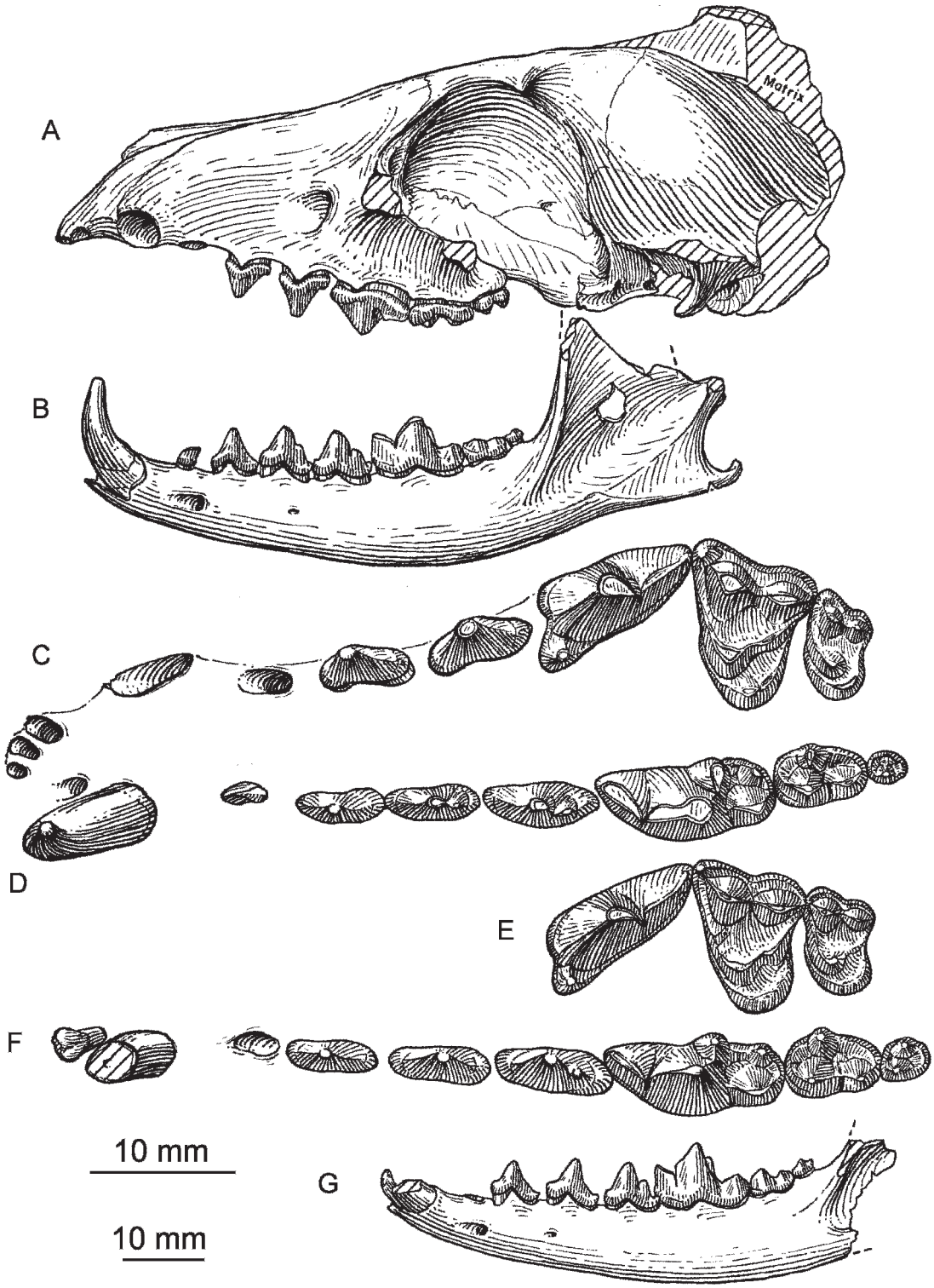

Fig. 15. **A–G**. *Leptocyon vafer*, late Barstovian, New Mexico. **A–D**. Associated skull and ramus, F:AM 62763. **A**. Lateral view, reversed. **B**. Lateral view. **C**. Occlusal view, reversed. **D**. Occlusal view. **E–G**. Associated maxillary and ramus, F:AM 62760. **E–F**. Occlusal views. **G**. Lateral view. The longer (upper) scale is for C–F, and the shorter (lower) scale is for A, B, and G.

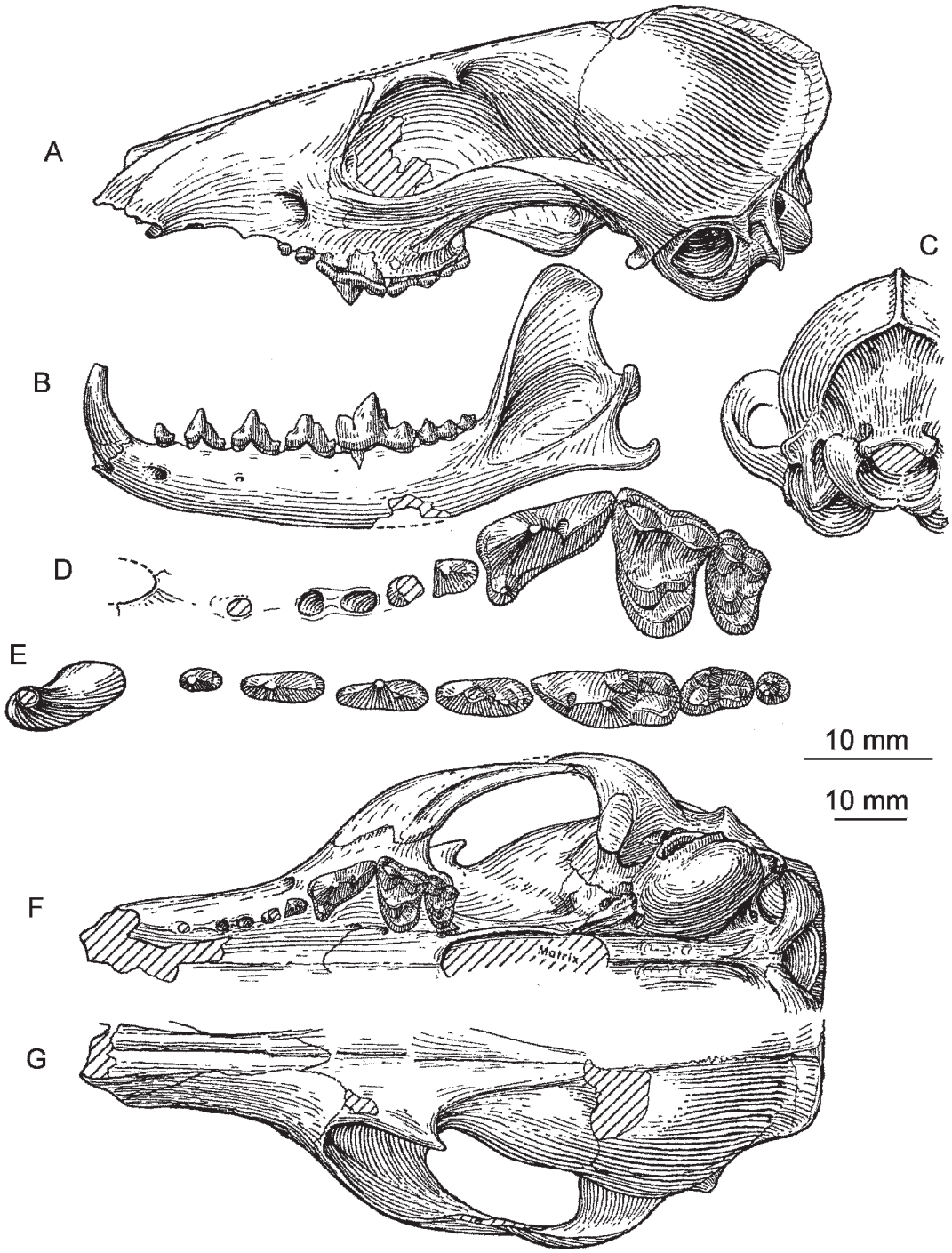

Fig. 16. **A–G**. *Leptocyon vafer*, late Clarendonian, California. Associated skull and ramus, UCMP 77703. **A–B**. Lateral views, reversed. **C**. Occipital view. **D–E**. Occlusal views, reversed. **F**. Palatal view, reversed. **G**. Dorsal view, reversed. The longer (upper) scale is for D and E, and the shorter (lower) one is for the rest.

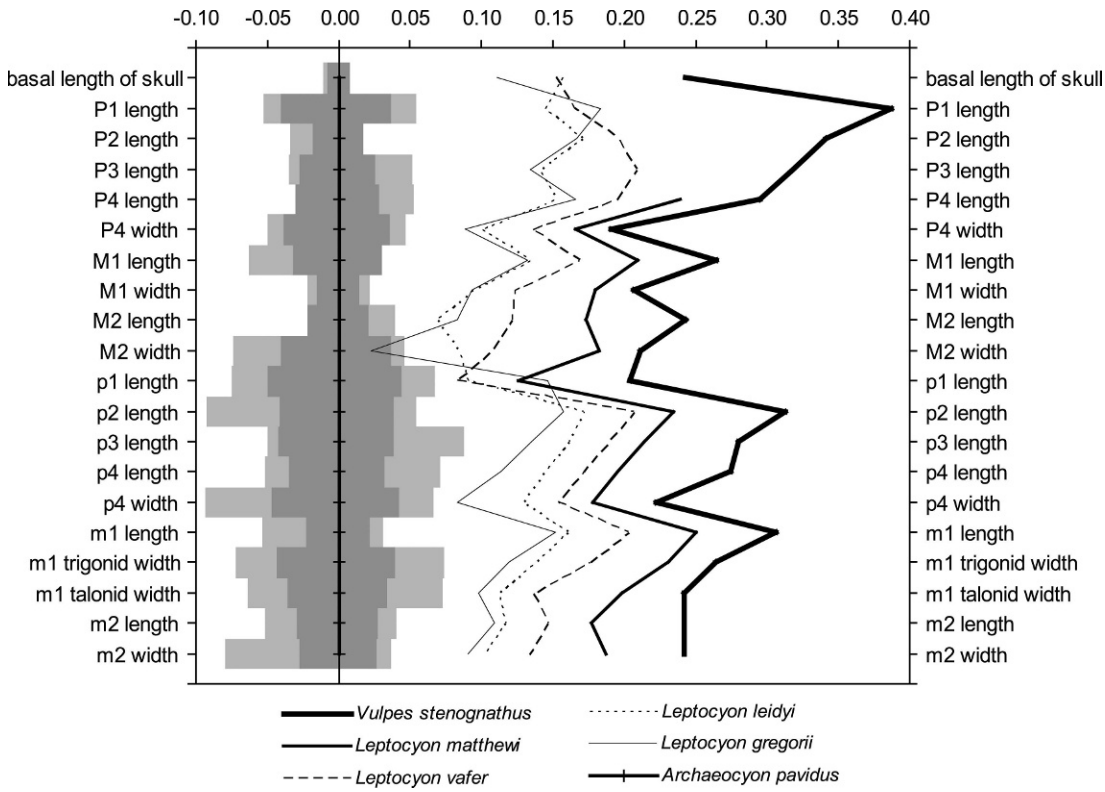

Fig. 17. Log-ratio diagram comparing the means of the cheek tooth dimensions (appendix 3) of four species of *Leptocyon* with *Vulpes stenognathus* using the primitive borophagine *Archaeocyon pavidus* as the standard. Gray bars extending from the mean of the standard are the observed ranges (light) and $\pm 1\ \sigma$ (dark) of the mean of the sample used.

Cuyamunque. F:AM 62761, left ramal fragment with p3 broken–m1, West Cuyamunque. F:AM 27416, skull with P2–M2; F:AM 27402, mandible with i1–m3; F:AM 27402A, right partial ramus with p2 broken–m3 (p3–m1 broken); F:AM 27407, left ramus with c broken–m3 (p1 missing); F:AM 27412, palate with I1–M2 (fig. 61A, incisors) and left partial ramus with p4–m2; F:AM 27401, right partial maxilla with P4 broken–M2; F:AM 27417, right and left partial rami with c–m1; F:AM 27411A, right partial ramus with p3–m2 all broken; F:AM 27412A, left partial ramus with p4–m2; F:AM 27406, right ramus with m1–m2 and all alveoli; F:AM 62774, left partial ramus with p3–p4 (m1 broken); F:AM 27415, right ramus and left partial ramus with c broken–m3 (p4–m1 broken), Santa Cruz. F:AM 62760, left premaxilla and partial maxilla with I2–I3 and P4–M2, left ramus with i3–m3, c broken–p1 alveolus (fig. 15E–G); F:AM 27413, partial skull with P2 broken–M2; F:AM 27411, right ramus with p1–m2 (p2–p3 and m1 broken); F:AM 50201, left partial ramus with p3–m2 (all broken), Santa Cruz, First Wash. F:AM 27421, partial mandible with c root–p3 and p4–m2 (all broken), Santa Cruz, Second Wash. F:AM 50202A* and B*, right and left ramal fragments with p4–m1 (both broken) and m2, Santa Cruz, Third Wash. F:AM 62771, palate with p3–m2, Ojo Caliente. F:AM 62773, right ramus with p1–m2 (p3–p4 broken), middle Ojo Caliente locality. F:AM 62765, left partial ramus with p3–m2 (m1 broken), red layer, Santa Fe. F:AM 27410, left maxillary fragment with P4, Third District. F:AM 27411B, palate with P2–P3 both broken, P4–M2; F:AM 27409, partial palate with P4–M2 and right

partial ramus with m1–m2 and alveoli; F:AM 62848*, left partial maxilla with P4 broken–M1; F:AM 27408, mandible with c–m3 (all broken or alveoli), no data except from Santa Fe area. F:AM 27422, right metatarsal III, Santa Cruz special layer. F:AM 67902, humerus, distal end missing, Santa Cruz red layer. F:AM 67902A, calcaneum; F:AM 27486, right partial humerus, Tesuque Quarry. F:AM 62780, articulated right tibia and left partial tibia and fibula, tarsals, metatarsals, and phalanges (fig. 9G–H), from 60 feet below blue-gray ash, central Pojoaque Bluffs. F:AM 62750, partial humerus, right immature femur and tibia lacking caps, tarsal bone, and fragments, west Pojoaque Bluffs.

Conical Hill Quarry, lower part of the Ojo Caliente Sandstone, Tesuque Formation (late Barstovian), 15 miles northwest of Española, Rio Arriba County, New Mexico: F:AM 62769*, left maxillary fragment with P4–M2; F:AM 62766, partial palate with P2–P3 (both broken), P4–M1 broken; F:AM 62768*, left M2; F:AM 62767, left ramus with c and p2–m2.

Santa Clara and North Santa Clara area, Pojoaque Member of the Tesuque Formation (late Barstovian and possibly Clarendonian), Santa Fe County, New Mexico: F:AM 62790, right and left rami with c (uneruptED)–m3; F:AM 62790A, left edentulous ramus; F:AM 62791, left partial ramus with p4 broken–m2; F:AM 62792*, left immature partial ramus with c broken–dp4, north Santa Clara. F:AM 27414A, right maxilla with P1–M2; F:AM 27414, right partial maxilla with P4–M2; F:AM 27483, right and left partial rami with p4 broken–m3; F:AM 27404, right ramus with c broken–m2 (p2 and p4 broken); F:AM 27405, left partial ramus with m1–m2, Santa Clara. F:AM 62793*, left partial ramus with c–m1 (all broken) and p1 missing, lower beds, Santa Clara locality, northeast of Round Mountain Quarry.

San Ildefonso, upper part of Pojoaque Member of the Tesuque Formation (late Barstovian and possibly Clarendonian), Santa Fe County, New Mexico: F:AM 27420, left ramus with p3–m3; F:AM 27402A, left ramus with c broken–m2 (p2–m1 broken); F:AM 27402B, right and left partial rami with m1 broken–m2; F:AM 27403, left ramus with c broken–m3 (p1 alveolus and m1 broken); F:AM 62826, right and left partial rami, left with c broken, p1, p2–m2 all broken, m3, right partial ramus with c root, p1–p2 alveoli, p3 broken–p4; and F:AM 62824*, right partial ramus with c root, p1–p2 alveoli, p3 root, and p4.

Jemez Creek area, Cerro Conejo Formation (late Barstovian), Sandoval County, New Mexico: F:AM 50189*, left maxillary fragment with P3 and P4 broken M1 and M2 broken, left and right partial rami with c broken–m3 (p2–m2 broken or alveoli) and vertebrae, Canyada de Zia, greenish sand. F:AM 62779*, ramal fragment with p1–p4, and isolated teeth including P4 broken, M1, m1, two canines, and limb fragments including partial radius, partial ulna, right metacarpal IV, both metacarpals V, both calcanea, astragalus, and limb fragments, west tributary of Canyada de Zia, 40 feet above green zone at the top of first set of cliffs. F:AM 50163, right partial ramus, m1 broken–m2, Canyada de Zia, F:AM 50200, right and left partial rami with p3 broken–m3, Rincon Quarry. F:AM 31110, right partial ramus with m1, fourth tributary north of Prospect Fork west side of Canyada de Zia.

North Rio Puerco, Cerro Conejo Formation (Tedford and Barghoorn, 1999, late Barstovian), Sandoval County, New Mexico: F:AM 62845, crushed partial skull with P3–M2; F:AM 62847*, immature right partial ramus with dp3–dp4, F:AM 62846, right partial maxilla with P4–M1, Ceja Prospect, near the head of north fork of Canyada Moquino. F:AM 62849, left ramus with symphysis, i1–p1 all broken, and p2–m2, near the top of red cliffs in Short North Fork of Canyada Moquino.

Siebert Formation (late early Barstovian), San Antonio Mountains, near Tonopah, Nevada: LACM(CIT) 780, right and left rami with c–m2 (p4 broken); LACM(CIT) 2815, partial ramus with p4–m2; additional jaw fragments, broken p4 and milk dentition listed by Henshaw (1942: 110); LACM(CIT) 15978, left partial ramus with m1 broken–m2, m3 alveolus.

Fox Hill, UCMP locality V6021 (early Clarendonian), Cedar Mountain, Mineral

County, Nevada; UCMP 58666, right partial ramus with p4 alveolus–m1, m2 alveolus.

Avawatz Mountains (early Clarendonian), San Bernardino County, California: LACM (CIT) 2308, right partial maxilla with P1–P4, listed by Henshaw (1939: 17, pl. 2, fig. 2, 2a).

UCMP locality 2731, lower part of the Dove Spring Formation (early Clarendonian) Mohave Desert, Kern County, California: UCMP 22319, partial mandible with i1–p2, p3 broken, p4, m1–m2 broken, m3, listed and figured by Merriam (1919: 533, fig. 138a–b). Martha Pocket, UCMP locality V6731, upper part of the Dove Spring Formation (latest Clarendonian), Kern County, California: UCMP 77703, skull with C broken, P1, P2 alveolus, P3 (broken)–M2, and mandible with c–m3 (fig. 16). LACM locality 3580, upper part of the Dove Spring Formation (about 200 m below UCMP 77703, D.P. Whistler, personal commun., 1981; late Clarendonian), Kern County, California: LACM 122324*, fragmentary mandible with m2 and alveoli; LACM 122325*, left ramus p1 alveolus, p1–p2, p3 alveolus, p4–m2; LACM 122326*, left m2.

Distribution: Late Barstovian of Nebraska, Kansas, New Mexico, and Nevada, earliest Clarendonian of Nebraska, early to late Clarendonian of California and Nevada.

Revised Diagnosis: Distinguished from *L. leidyi* by its significantly larger size (95% confidence interval for first lower molars of these taxa nearly separated;fig. 7), m2 shorter relative to m1 (fig. 7) with enlarged anterolabial cingulum and large metaconid, cranium lacks postparietal foramina, shows reduced cerebellar exposure, and nasals do not extend posterior to maxillary-frontal suture. Distinguished from *L. tejonensis* in longer muzzle and more widely spaced and anteroposteriorly longer premolars with stronger accessory cusps. *L. vafer* differs from *L. matthewi* in significantly smaller size, with no overlap of m1 95% confidence intervals (fig. 7) nasals do not extend posterior to maxillary-frontal suture, M2 lacks postprotocrista, m1 lacks hypoconulid shelf, and entoconid not enlarged.

Description and Comparison: The skull of *L. vafer* is based on hitherto undescribed specimens, including two partial skulls, UNSM 25717 and 25718 (fig. 14A–D), from the Valentine Formation in Nebraska, a well-preserved skull and jaws (UCMP 77703, fig. 16) from the upper part of the Dove Spring Formation in California, and two partial skulls (F:AM 62763, fig. 15A–D, and F:AM 62845) from the Pojoaque Member of the Tesuque Formation in New Mexico.

Except for the narrower muzzle, more laterally expanded cranium, and the more robust zygomatic arch, the skull of *L. vafer* for the most part resembles that of *L. mollis* and *L. gregorii* in size and proportions (see fig. 3). The premaxillary and frontal processes are widely separated, and the frontals are unelevated with a slight depression on the dorsal surface of the postorbital process indicating the lack of a frontal sinus as in *Vulpes*. Also like *Vulpes* species, the nasals are short in *L. vafer*, terminating anterior to the frontal-maxillary suture. From the prominent postorbital processes the weak frontal crests extend posteriorly and join near the frontoparietal suture to form a low sagittal crest. Compared to earlier species of *Leptocyon*, the most striking features of the cranium of *L. vafer* are the reduced cerebellar exposure resulting from relative expansion of the neocortex and the consequent loss of the postparietal foramina. The maxillary beneath the orbit and the zygomatic process of the jugal are dorsoventrally deeper in *L. vafer*, and the jugal bears a stronger scar for origin of the masseter muscle than in other species of *Leptocyon* in which this structure is known.

Viewed ventrally, the basioccipital is relatively narrow between the inflated bullae. The medial wall of the bulla slightly underhangs the basicranial bones at the level of the basioccipital-basisphenoid suture. Compared with *L. gregorii*, the bulla is anteroposteriorly shorter, with the lip of the auditory meatus projecting more laterally. The tympanic bulla in *L. vafer* lacks the depression in the ectotympanic anterior to the auditory meatus seen in *L. mollis* and *L. gregorii*. A swelling of the posterolateral border of the entotympanic below the stylomastoid foramen is evident in *L. vafer* (UCMP 77703) and in *L. matthewi* (F:AM 49433). A similar bulge of the entotympanic is more pronounced in *V. stenognathus* (F:AM 75827), which approaches the condition in *V. vulpes*. In *L.*

vafer the paroccipital process is relatively larger than in earlier species of *Leptocyon*. It extends more ventrally with the anterior surface more concave and covering more of the posterior wall of the bulla, foreshadowing the condition in *Vulpes*.

Despite the widespread geographical and temporal range of *L. vafer*, the dentition is remarkably homogeneous in size and morphology. The coefficients of variation (appendix 3) of the total sample range mostly below 7.0 except for the length of P1 and p1. We therefore have assigned these widely separated samples to *L. vafer*.

The limbs of *L. vafer* stand morphologically between those of *L. vulpinus* and those of Hemphillian *Vulpes stenognathus*. Compared to the limbs of *L. vulpinus*, the distal end of the humerus is transversely narrower with a smaller entepicondylar foramen and a smaller entepicondyle (fig. 9). The radius is also less robust with the distal end narrower relative to the shaft and a smaller styloid process (fig. 9). The most striking difference is the smaller distomedial radial exostosis. The hind-limb morphology is known best from an articulated tibia, partial fibula and nearly complete pes (F:AM 62780, fig. 9G–H) from New Mexico. The length of the tibia is shorter than that of *Vulpes* with the length approximating that of the pes. Furthermore, the proximoanterior crest is longer relative to the length of the tibia and the proximal condyles that articulate with the femur are less anteriorly and distally extended. The fibula is less robust than that of *L. vulpinus*, but not as slender and compressed as in *Vulpes*. A functional first digit is present. It bears two phalanges and its length is about 60% of the length of metatarsal II.

Discussion: The genotypic species, *Leptocyon vafer*, was first described by Leidy (1858: 21) as a small species of *Canis* as were most living foxes at that time. Leidy recognized its foxlike features and remarked that they did not differ from those of the red fox. As early as 1897, Trouessart listed this taxon as *Vulpes vafer* in his catalogue of mammals, but Matthew (1909: 115) followed Leidy and listed this species as *Canis vafer* in his faunal lists of the Tertiary Mammalia of the West. Later Matthew (1918: 189) recognized that the morphology of the lower jaw and dentition differed from both *Canis* and *Vulpes*, and he designated *C. vafer* the type species of a new genus, *Leptocyon*. Because of the lack of perception of diagnostic dental features, uncertainty persisted regarding the generic allocation of this species. Merriam (1919: 533) followed Leidy and referred a jaw from the Dove Spring (Ricardo) Formation in California to "*Canis*? *vafer*" and commented that it is "not unlike *Canis*? *vafer* Leidy of the Fort Niobrara Formation." Stirton and McGrew (1935: 129) listed this taxon as *Vulpes vafer* in their list of the Niobrara River Fauna. A fragmentary maxilla from the Avawatz Mountains of California listed as "Canid indet." By Henshaw (1939: 17) was said to possess features that resemble "fairly closely those of *Vulpes vafer* (Leidy)." Three year later, however, Henshaw (1942: 110) recognized Matthew's genus, *Leptocyon*, and referred two jaws from the Tonopah Local Fauna of Nevada to *L. vafer*. Macdonald (1948: 55) reverted to the use of *Vulpes* in referring two partial jaws from the Black Hawk Ranch Local Fauna of California to *Vulpes vafer*.

Thus, *L. vafer* was buffeted among *Canis*, *Vulpes* and *Leptocyon* for over a century. Uncertainty about the generic allocation of this species continued until Webb (1969: 39) effectively diagnosed this taxon and described the dental characters that distinguish *Leptocyon* from *Vulpes*. The additional evidence described herein has enabled us to amplify the description of *L. vafer* and to revise and strengthen the diagnosis for both the genus, *Leptocyon*, and the species, *L. vafer*.

Leptocyon matthewi, new species
Figure 7, 17, 18A–F; appendices 3, 4

Vulpes species: Gregory, 1942: 348.

Type: F:AM 25198, mandible with right and left i1–m3 (fig. 18A–B), from Bear Creek Quarry (late Clarendonian) of Skinner and Johnson (1984), Ash Hollow Formation, strata approximately equivalent to the Merritt Dam Member, Cherry County, Nebraska.

Etymology: Named in honor of W. D. Matthew in recognition of his fundamental work on the Canidae.

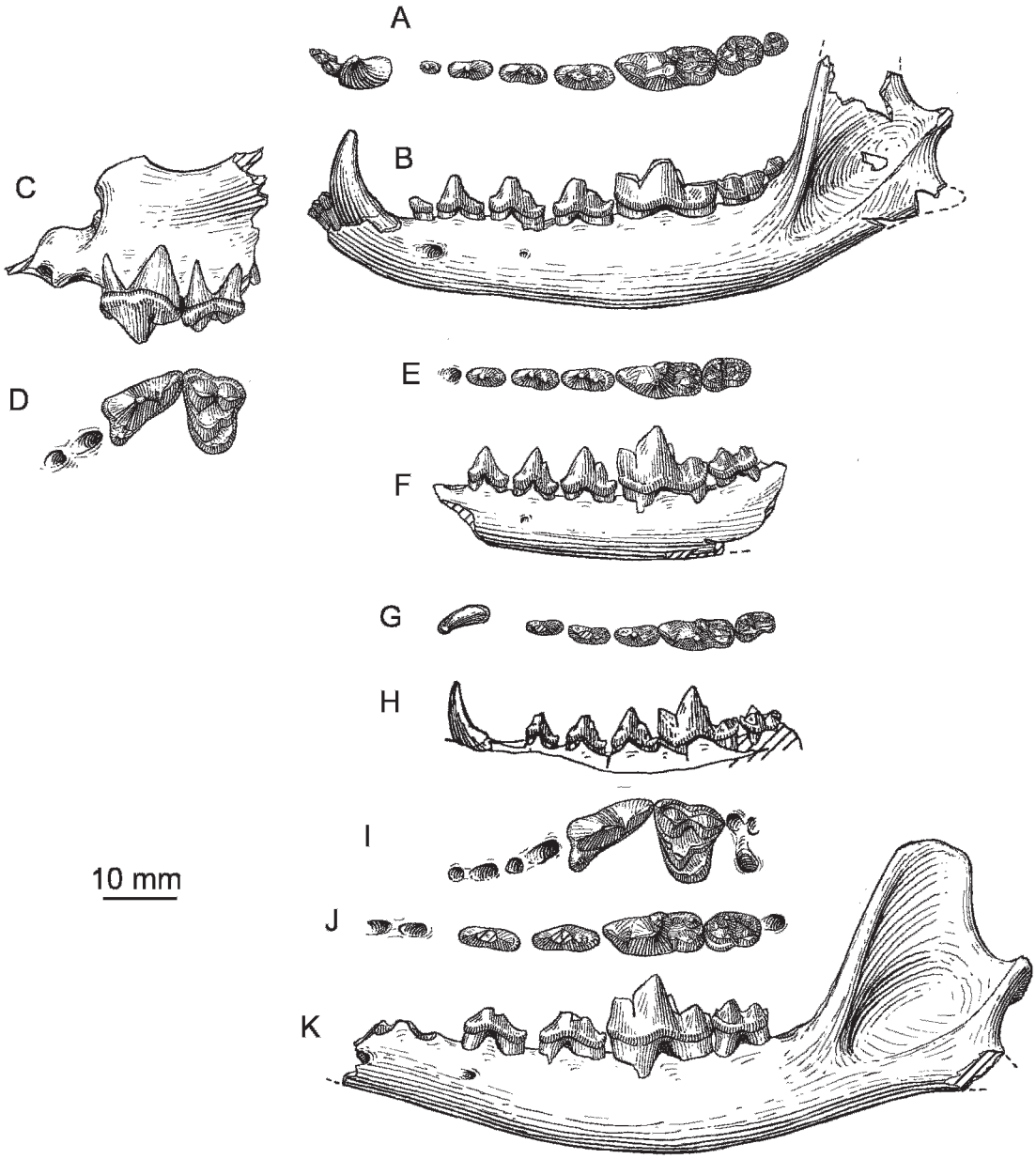

Fig. 18. **A–F**. *Leptocyon matthewi*, Clarendonian, Nebraska. **A–B**. Type ramus, F:AM 25198. **A**. Occlusal view, reversed. **B**. Lateral view, reversed. **C–D**. Maxillary fragment, F:AM 25193. **C**. Lateral view. **D**. Occlusal view. **E–F**. Ramus, F:AM 49165. **E**. Occlusal view, reversed. **F**. Lateral view, reversed. **G–H**. *Leptocyon tejonensis*, early Clarendonian, California. Type ramus, LACM 16719. **G**. Occlusal view, reversed. **H**. Lateral view, reversed. **I–K**. *Vulpes stenognathus*, late Hemphillian, Oklahoma. **I**. Maxillary fragment, F:AM 62938. Occlusal view. **J–K**. Ramus, F:AM 62927. **J**. Occlusal view. **K**. Lateral view.

Referred Material: Big Springs Canyon, undifferentiated beds (early Clarendonian) of the Ogallala Group, temporally younger than the Valentine Formation but earlier than the Ash Hollow Formation of adjacent Nebraska, UCMP locality V3322, site 2, Bennett County, South Dakota: UCMP 33426 and 33427, two partial rami listed by Gregory

(1942: 348) and UCMP 32342, right partial ramus with c broken–p4 (p2–p3 broken).

Undifferentiated beds (early Clarendonian), Ogallala Group, temporally equivalent to the Thin Elk Gravels, Hollow Horn Bear Quarry, Todd County, South Dakota: F:AM 49433, posterior part of skull; F:AM 49426, right isolated P4; F:AM 49434, left partial ramus with p4–Ma; F:AM 49435*, right ramus with m2 and all alveoli; F:AM 49411*, left partial ramus with m2; F:AM 49446*, left partial ramus with p2; F:AM 49440, left radius distal cap missing; F:AM 49441, left femur (fig. 9F); F:AM 494441A, left distal part of tibia; F:AM 49443, right metacarpal III; and F:AM 49443A, left partial metatarsal IV.

Thin Elk or Mission Gravel Pit, Thin Elk Gravels (early Clarendonian), Mellette County, South Dakota: F:AM 72701B, left distal part of humerus.

Clayton and East Clayton Quarry, basal Merritt Dam Member of the Ash Hollow Formation (Medial Clarendonian), Brown County, Nebraska: F:AM 49167, right partial ramus with p3 broken–m2; F:AM 49166, right partial ramus with m1–m2: F:AM 49168, left partial ramus with m1–m2; F:AM 49173, left m1; F:AM 49169, left partial ramus with p2 root–m1 alveolus, m2; F:AM 49171, right partial toothless ramus; F:AM 72707, right partial humerus; and F:AM 72708, right ulna.

Quinn Rhino Quarry 1, Cap Rock Member of Ash Hollow Formation (early Clarendonian), Brown County, Nebraska: F:AM 25130, left partial ramus with p1 alveolus–m2 (p4 and m3 alveoli).

Merritt Dam Member, Ash Hollow Formation (medial and late Clarendonian), Brown and Cherry counties, Nebraska: F:AM 62891, right m1, Gallup Gulch Quarry. F:AM 62881, left partial ramus with p1–p4 roots and M1 broken, Bolling Quarry. F:AM 49175*, right partial ramus with c, p1 alveolus, p2–p3 and p4–m2 alveoli: F:AM 62882*, left partial ramus with c–p1 alveoli, p2, p3–p4 aleoli; UNSM 5025-89, left m1, Pratt Quarry. F:AM 25193, left partial maxilla with P4–M1 (Fig. 18C–D); F:AM 25156, left partial ramus with m1, Xmas Quarry. F:AM 49165, right partial ramus with p2–m2 Leptarctus Quarry (fig. 18E–F). F:AM 25194, left partial ramus with m1–m2 both broken, Kat Quarry. F:AM 25199, left partial ramus with m1–m2, from the talus of high channel with which *Platybelodon barnumbrowni* occurred, west side of Snake River about 1 mile below falls.

Bluejay Quarry (UNSM locality Ap 112). Ash Hollow Formataion (late Clarendonian) in an unnamed post-Cap Rock Member channel, Antelope County, Nebraska. UNSM 47375, left ramus with p1 alveolus, p2, p3 roots, p4–m1.

Laucomer Meber of the Snake Creek Formation (late Clarendonian), Sioux County, Nebraska: AMNH 22039, right ramus with c alveolus–m2 (p1 alveolus and p2–p3 broken), Kilpatrick Pasture Quarry 7. AMNH 20053*, right ramus with c–p4 alveoli, m1 broken, m2, m3 alveolus, Kilpatrick Pasture Quarry b.

Round Mountain Quarry: Chamita Formation (early Clarendonian), Rio Arriba County, New Mexico: F:AM 62811, right ramus with i3–m2 (c broken, p1 alveolus, and m1 broken); F:AM 62806, fragmentary skull with P4–P2; F:AM 62808, left partial maxilla with P4–M1; F:AM 62813, left partial ramus with p3 broken and m1–m2 and associated right (less worn) m1 broken–m2; F:AM 62810*, right M1, broken M2 and metatarsals III, IV and V; F:AM 62812, mandible with c broken–m2 (p1–p4 broken); F:AM 62814, right partial ramus with c–m2 (p3 alveolus and p4 broken); F:AM 62815, left ramus with c broken–m3 (m1 broken); F:AM 62807, right partial maxilla with P3 broken–M2; F:AM 62817, left partial ramus with m1 broken–m3; F:AM 62816, left ramus with i3–p1 alveoli and p2–m2 (all broken); and F:AM 62818, right partial ramus with m1–m2.

Fish Lake Valley (UCR locality RV 7407), Esmeralda Formation (early Clarendonian), Esmeralda County, Nevada: UCR 17005, right and left mandibular rami with i2–m3 (c broken), maxilla fragment with P1, P4 broken, right maxilla fragment with broken M1, left isolated M1, left broken isolated M2, and isolated broken teeth including a canine, premolar and incisors; and UCR 17006, right and left mandibular rami with i1–m2 (i–I2 broken), two isolated incisors, proximal parat of metacarpal II, metacarpal I, scapho-lumar, and a second phalanx.

Distribution: Clarendonian of Nebraska, South Dakota, New Mexico, Arizona and Nevada.

Diagnosis: Differs from *L. vafer* in m1 significantly larger without any overlap of confidence interval (fig. 7); m1 with larger and taller crowned hypoconid, entoconid enlarged, coalescing with base of hypoconid to close talonid basin, hypoconulid shelf present; and m2 smaller relative to length of m1 (fig. 17) with stronger anterolabial cingulum that extends more posteriorly.

Description and Comparison: Not all of the characters listed in the diagnosis can be found in every specimen but a combination of these characters readily distinguishes *L. matthewi* from *L. vafer*. As is characteristic of *Leptocyon*, a strong crest (postprotocrista) unites the M1 protocone and metaconule in *L. matthewi* (F:AM 25193, fig. 18D) and the metaconule is usually smaller than that *Vulpes stenognathus*. Associated remains from Fish Lake Valley (UCR 17005) include an M1 with the parastyle smaller, the buccal cingulum weaker and the paracone noticeably higher crowned than the metacone than seen in either *L. vafer* or *V. stenognathus*. A fragment of the M2, showing most of the talon of UCR 17005 gives the only evidence in this taxon of the nature of the postprotocrista and metaconule of M2. The crista is present, but the conule seems lacking as in *L. vafer*. The m1 is also taller crowned than in *L. vafer* and sometimes (as in UCR 17005) approaches the crown height of this tooth in *V. stenognathus*. Unlike that of *L. vafer*, the m1 entoconid (F:AM 25199 and UCR 17005) is a larger and more distinct cusp resembling that of *Vulpes stenognathus*. The m1 hypoconulid shelf, which is absent in *L. vafer*, is sometimes developed in *L. matthewi*. Although in most specimens it is less developed. The m2 in *L. matthewi* is shorter relative to the length of the m1 than in *L. vafer* (fig. 17), but the most notable difference is the stronger anterolabial cingulum that often extends more posteriorly than in *L. vafer*. The m2 in *L. matthewi*, however, lacks the derived morphology characteristic of *V. stenognathus* and most mesocarnivorous living fox species that includes a stronger anterolabial cingulum and an enlarged metaconid which changes the occlusal outline of this tooth to labially concave and lingually convex.

Compared to *V. stenognathus*, the bulla (F:AM 49433) in *L. matthewi* is larger relative to the size of the cranium, and the lip of the auditory meatus is smaller and projects less laterally. In *L. matthewi* the paroccipital process is transversely narrow, short and its free tip projects posteroventrally in contrast to the broad structure with laterally projecting free tip in *V. stenognathus* and other *Vulpes* species. Furthermore, the limbs referred to *L. matthewi* lack the derived features of *V. stenognathus*. A humerus (F:AM 72707) referred to *L. matthewi* bears an entepicondylar foramen that is lacking in *V. stenognathus*, and a referred ulna (F:AM 72708) is much shorter and more robust than that of the latter.

Although the size of the dentition and the morphology of the first upper and lower molars of *L. matthewi* tend to be somewhat intermediate between those of *Leptocyon* and *Vulpes*, it lacks any derived features of the auditory bullae, paroccipital process, premolars, m2, and limbs that characterize *V. stenognathus* and other foxes.

Leptocyon tejonensis, new species
Figures 7, 18G–H; appendix 3

Type: LACM 16719, right partial ramus with c and p2–m2 from the Bena Gravel (sensu Bartow and McDougall, 1984; Bartow, 1984); formerly referred to the Santa Margarita Formation) early Clarendonian, Comanche Point, South Tejon Hills (CIT locality 303), Kern County, California.

Referred Material: From the type area Bena Gravel, Comache Point, south Tejon Hills (CIT locality 303, except where indicated), Kern County, California: LACM 47670, left partial maxilla with P3–M2; LACM 16721, right partial maxilla with P3 alveolus–M2; LACM 16714, left partial maxilla with P4–M1 both broken; LACM 16730, right partial maxilla with P4 root and M1 broken–M2; LACM 16711, right partial maxilla with M1 broken–M2; LACM 16728, right M1–m2; LACM 16726, right partial ramus with p2–m1; LACM 16718, right m1 broken; LACM 16729, right partial ramus with p4 broken–m1; LACM 16725, left m1; LACM 47669, right partial ramus

with c broken–m1 (p2 broken); LACM 16716, left ramal fragment with m1 broken; and LACM 16715, a lower canine.

Distribution: At present known only from the type locality early Clarendonian of California.

Diagnosis: Derived characters that distinguish *L. tejonensis* from *L. leidyi* and *L. vafer* are shorter muzzle; premolars more closely spaced and anteroposteriorly shorter and taller with less prominent posterior cusp; p4 relatively wide for its length; m2 talonid length greater then 90% of trigonid; and metaconid taller than protoconid than in *L. leidyi* and *L. vafer*.

Description and Comparison: The dentition of *L. tejonensis* is within the size range of *L. vafer* (fig. 7). As indicated by the measurements (appendix 3) it is a homogeneous population sample, and the P4 and all molars are proportionally similar to those of *L. vafer*. The premolars, however, differ noticeably from those of all other species of *Leptocyon* in being more closely spaced, relatively shorter and taller with less prominent accessory cusps. The p4 is noticeably wide for its length (fig. 17). The m2 in the type (LACM 16719, fig. 18G–H), although approximately equal in size to that of *L. vafer*, has a long talonid and its metaconid is larger relative to the size of the protoconid than in other *Leptocyon* species. The metaconid in a second jaw (LACM 16731) is somewhat smaller than that of the type but is still relatively large for *Leptocyon*. Both the short, tall, and simple premolars and the large m2 metaconid are suggestive of the condition in *Metalopex* or *Urocyon*. However, *L. tejonensis* lacks other important derived features that characterize *Metalopex* or *Urocyon*, including the m1 protostylid, strong m2 labial cingulum bearing a protostylid, and the more quadrate upper molars. Because of the absence of the above features, we have allocated this species to *Leptocyon* and view the anteroposteriorly short but tall premolars and enlarged m2 metaconid as having arisen in parallel with *Metalopex* and *Urocyon* species.

Tribe Vulpini Hemprich and Ehrenberg, 1832

The living foxes and fossil taxa attributed to living genera or phyletically related taxa can be grouped as we have indicated on our cladogram (fig. 65). These small canids are distinguished from all other Caninae in possessing a wide paroccipital process that is broadly sutured to the posterior surface of the bulla with a short and laterally turned free tip that barely extends below the body of the process. The presence of a metaconule and postprotocrista on M2 of vulpines represents the culmination of a reversal that began with late *Leptocyon* species to resume the form of the primitive canine M2.

Additional synapomorphies of the Vulpini include enlargment of the m2 metaconid so that it may exceed the protoconid in size, producing a convex lingual outline to the tooth, and further reduction of the parastyle of M1 and loss of its union with the preparacrista. *Metalopex* possesses these critical features and shares with *Vulpes* nasals that end anterior to the maxillary-frontal suture. Additionally, the Vulpini are distinguished from species of *Leptocyon* and united with the Canini (fig. 65) by common possession of three synapomorphies: loss of the medial cusplet on the I3; loss of the entepicondylar foramen on the humerus; and reduction of metatarsal I and loss of its phalanges.

The hypocarnivorous New World *Metalopex* and its living sister taxon *Urocyon* form a clade united by an elongate m2 talonid, high-crowned premolars, a protostylid on m1–m2, more quadrate upper molars, and the peculiar isolation of p2 by longer diastemata than separate other premolars along the very elongate rami of these taxa. These characters also unite these vulpines with the Old World *Protocyon* and *Otocyon* (Tedford et al., 1995).

Vulpes Frisch, 1754

Fennecus Desmarest, 1804.
Megalotis Illiger, 1811.
Vulpis Gray, 1821.
Alopex Kaup, 1829.
Cynalopex H. Smith, 1839.
Leucocyon Gray, 1868.
Mamvulpesus Herrera, 1899.
Xenalopex Kretzoi, 1954.

Type Species: *Canis vulpes* Linnaeus, 1758.

Included North American Species: *V. stenognathus* Savage, 1941; *V. kernensis*, n. sp.; *V. vulpes* (Linnaeus), 1758; *V. lagopus* (Linnaeus), 1758; *V. velox* (Say), 1823; *V. macrotis* Merriam, 1888.

Distribution in North America: Early Hemphillian to Recnt, coterminous United States; Rancholabrean to Recent, Alaska and Canada; late Hemphillian to Recent, Mexico.

Revised Diagnosis: *Vulpes* differs from *Leptocyon* in the following features that constitute synapomorphies with all higher Caninae: medial cusplet on I3 absent; zygoma strongly arched in lateral view; metatarsal I reduced to proximal rudiment; humerus lacks entepicondylar foramen. *Vulpes* shares three synapomorphies with other Vulpini: broad paroccipital process; M1 parastyle very weak and separated from preparacrista; and symplesiomorphic presence of M2 metaconule and associated postprotocrista. Short nasals that rarely extend to level of most posterior position of maxillary-frontal suture is autapomorphic (this feature appears as a homoplasy in a number of *Canis* species).

Discussion: The distinction between *Leptocyon* and *Vulpes*, as indicated above, has long been a problem due to the fact that species of *Vulpes* show many primitive features such as: frontal sinus usually absent, expressed in unelevated frontals with depression creasing dorsal surface of the postorbital process; relatively low-crowned upper molars with subequal paracone and metacone; well-developed labial cingulum on M1 and M2; narrow angular process of the mandible often with hooklike termination; and a relatively short radius relative to tibia length.

Evidence now at hand shows that *Vulpes* can be distinguished from *Leptocyon* on the basis of the derived states of several characters. The above diagnosis indicates important morphological features of *Vulpes* that are derived with respect to *Leptocyon*. The following characters further separate these taxa: relatively larger m1 entoconid; tendency for the m1 entoconid and hypoconid to join at the base or to be linked by a transverse crest; further reduction of parastyle on M1 and M2; more distinct M1 protocone and metaconule; expanded braincase, without cerebellar exposure; and markedly wider postorbital constriction.

Only two species of *Vulpes* are recognized during the late Miocene (Hemphillian). A small species, *V. kernensis*, about the size of *V. velox* (fig. 23A–D), is known only from California. *V. stenognathus* has a widespread geographic distribution that extends from the Pacific Coast across the Great Basin and Great Plains to Florida. Pliocene records of *Vulpes* in North America are surprisingly rare and are restricted to a few specimens described below from the Blancan of the southern Great Plains. Small *Vulpes* specimens that we report from the early Irvingtonian of Nebraska represent the earliest Pleistocene records of the genus. These compare favorably with those of *V. velox*. Such foxes remain the sole representatives of the genus through the early and medial Pleistocene of North America until *Vulpes vulpes* and *V. lagopus* appear in the late Pleistocene.

Vulpes kernensis, new species
Figure 23A–D; appendix 3

Type: LACM 55215, right partial maxillary fragment with P3–M2 (fig. 23A–B) from the Kern River Formation, early Hemphillian, CIT locality 49, southeastern San Joaquin Valley, Kern County, California.

Referred Material: LACM 55216, left partial ramus with p4–m1 (fig. 23C–D) from the type locality.

Distribution: Known only from the early Hemphillian of California.

Diagnosis: Differs from *V. stenognathus* in approximately 20%–25% smaller dentition, P3 and p4 anteroposteriorly shorter, and P4 protocone smaller; differs from *V. macrotis* and *V. velox* in P3 and p4 anteroposteriorly shorter and taller crowned relative to length, p4 weaker posterior cusplet, and M1 paracone taller crowned relative to height of metacone. As in living species, the M1 parastyle is very reduced and the preparacrista is not united with parastyle, and the m1 entoconid has a transverse cristid passing to the base of the hyperconid.

Description and Comparison: The dentition of *V. kernensis* is about 20% smaller than values of *V. stenognathus*. The type maxilla (LACM 55215) is within the size range of *V. velox*. It differs from *V. velox* in

the taller crowned P3 relative to its length, weaker P4 protocone, and relatively taller crowned paracone of M1 relative to the height of the metacone.

The referred jaw (LACM 55216) compares best with that of *V. macrotis*, and the m1 is within the size range of that taxon. Like the P3, the p4 is also anteroposteriorly shorter and taller crowned relative to its length than that of *V. macrotis*. When compared with its length, the height of the m1 crown of *V. kernensis* is taller than that of *V. macrotis*. In these characters, *V. kernensis* closely resembles the Clarendonian *Leptocyon tejonensis*, which is characterized by closely spaced and anteroposteriorly short premolars with weak posterior cusps. Derived characters that distinguish *V. kernensis* from *L. tejonensis* are the taller crowned P3–P4, M1 with smaller parastyle unconnected with the preparacrista and weaker labial cingulum and taller crowned m1 with a more elongate trigonid relative to the length of the talonid, a less oblique paraconid, and an entoconid with a low entoconulid. Additionally, the M2 of *V. kernensis* has both a postprotocrista and metaconule as in most *Vulpes*, rather than the reduced state of these features shown in late *Leptocyon* species. These differences incline us toward the view that *V. kernensis* is a species of *Vulpes* rather than *Leptocyon*. It is coeval with the larger *V. stenognathus* in the early Hemphillian of western North America, but it is not recorded in the late Hemphillian.

Vulpes stenognathus Savage, 1941
Figures 3, 7, 17, 18I–K, 19–22, 27, 52; appendices 2–4

Leptocyon cf. *vafer* (Leidy): Cook and Macdonald, 1962: 562.

Lectotype: OMNH 15167 (formerly OMP 40-4-S24), a right ramus with p2–m3, listed and figured by Savage (1941: fig. 4) as a cotype is here selected as the lectotype. Optima Local Fauna, Ogallala Group (late Hemphillian), near Guymon, Texas County, Oklahoma.

Referred from the Type Locality: Optima Local Fauna, Ogallala Gourp (late Hemphillian), near Guymon, Teas County, Oklahoma: OMNH 15166 (formerly OMP 40-4-S10), right partial ramus with p1–p4, listed as a cotype by Savage (1941: 694); Savage also listed two m1s, four M1s, four M1s, and two M2s as cotypes and figured the following: OMP 40-25-S12, M1 (fig. 2); OMP 40-25-S11, M2 (fig. 3); also figured by Savage, OMP 40-25-S10*, upper canine (fig. 1); F:AM 62942, left P4; F:AM 62940, left partial maxilla with P4–M2; F:AM 62939, right maxilla fragment with P4; F:AM 62938, left partial maxilla with P4–M1 (fig. 18I); F:AM 62956, left p4; F:AM 62950*, associated detached left P4–M2 and right M1–M2; F:AM 62956A, right P4; F:AM 62956B, right P4; F:AM 62944, left maxilla with P2–P4; F:AM 62945, right partial maxilla with P4; F:AM 62941, right partial maxilla with P2–P4; F:AM 62921, right partial ramus with p3–m2; F:AM 62927, left partial ramus with p3–m2 (fig. 18J–K); F:AM 62928, right ramus with p2–m2 (p3 broken); F:AM 62920, right ramus with c (broken)–m2 (broken); F:AM 62926, right ramus with c (broken)–m2; F:AM 62931*, right partial ramus with p2–p4 and m1–m2 (alveoli); F:AM 62957, isolated left m1; F:AM 62961A–F:AM 62961F, seven isolated M1s; F:AM 62961G, H, J–M, six isolated m1s; F:AM 62935, left partial ramus with p4, m2, and alveoli and right partial ramus with p1–m2 (p2–p3 broken); F:AM 30391*, right partial ramus with p1 (p4 and m1 broken); F:AM 30395*, left partial ramus with p3–p4 (p1, p2, and m1 alveoli); F:AM 30396, left ramus, all alveoli; F:AM 30398, right ramus, p2–m3 alveoli.

Thousand Creek Formation (early Hemphillian), Humbolt County, Nevada: LACM 55211, skull fragments and associated dentition including right P4 broken–M1 and M2 broken and right partial ramus with p1 alveolus, p2 broken, p3–m3 alveoli, CIT locality 63; UCMP 84639, left partial maxilla with P1 (alveolus)–P4, UCMP locality V69106; and F:AM 63214, right partial maxilla with P3, P4 broken, M1–M2, north end of Railroad Ridge.

Alturas I, UCMP locality V3594, Alturas Formation (early Hemphillian), Modoc County, California; UCMP 24234, left partial ramus with p3–m1 (p4 and m2 broken).

Burmeister locality, UCMP locality V73061, Rome beds (early Hemphillian), Malheur

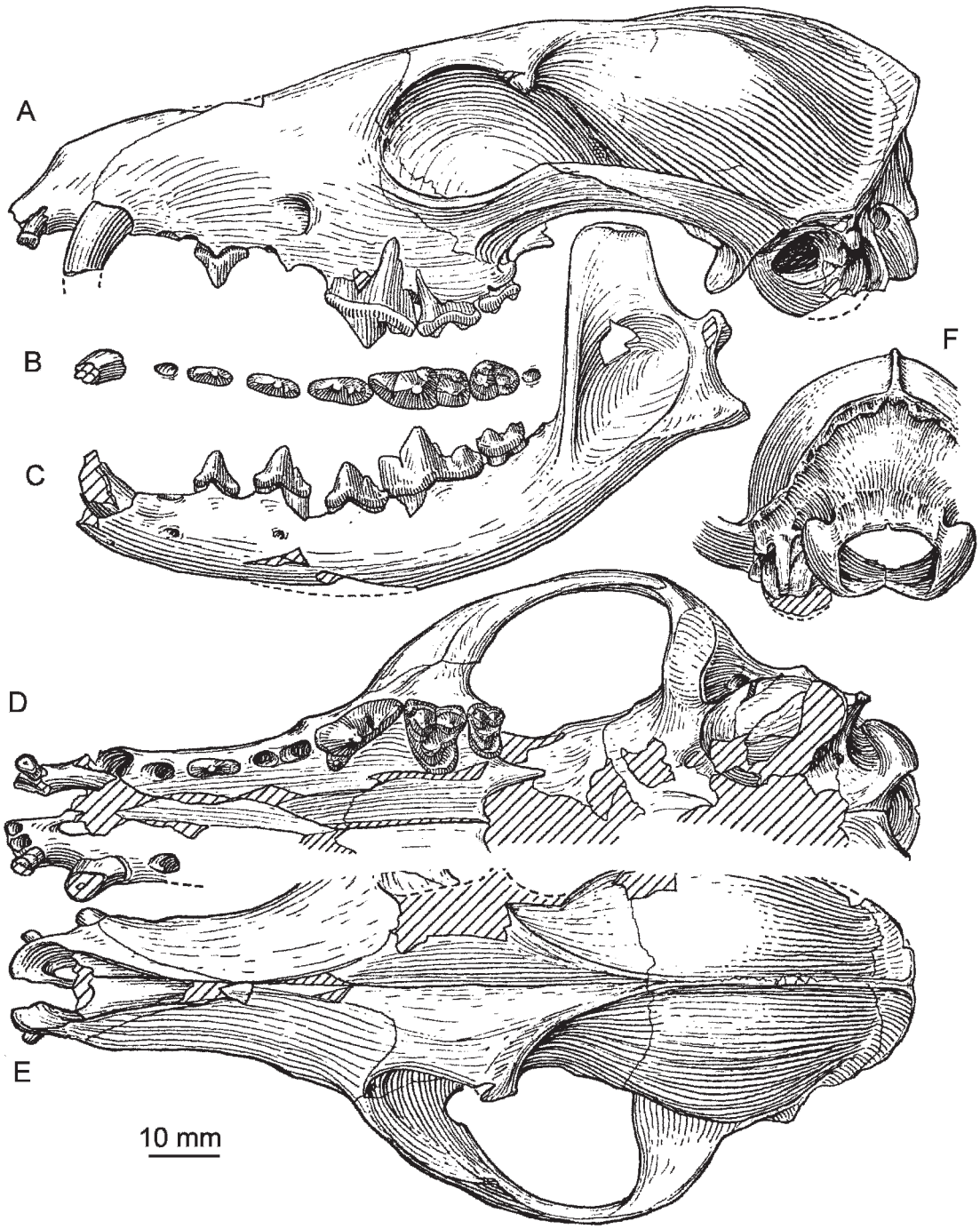

Fig. 19. **A–F**. *Vulpes stenognathus*, late Hemphillian, Nevada. Skull and associated ramus, F:AM 49284. **A**. Lateral view, restored from right side. **B**. Occlusal view. **C**. Lateral view. **D**. Palatal view, restored from right side. **E**. Dorsal view. **F**. Occipital view.

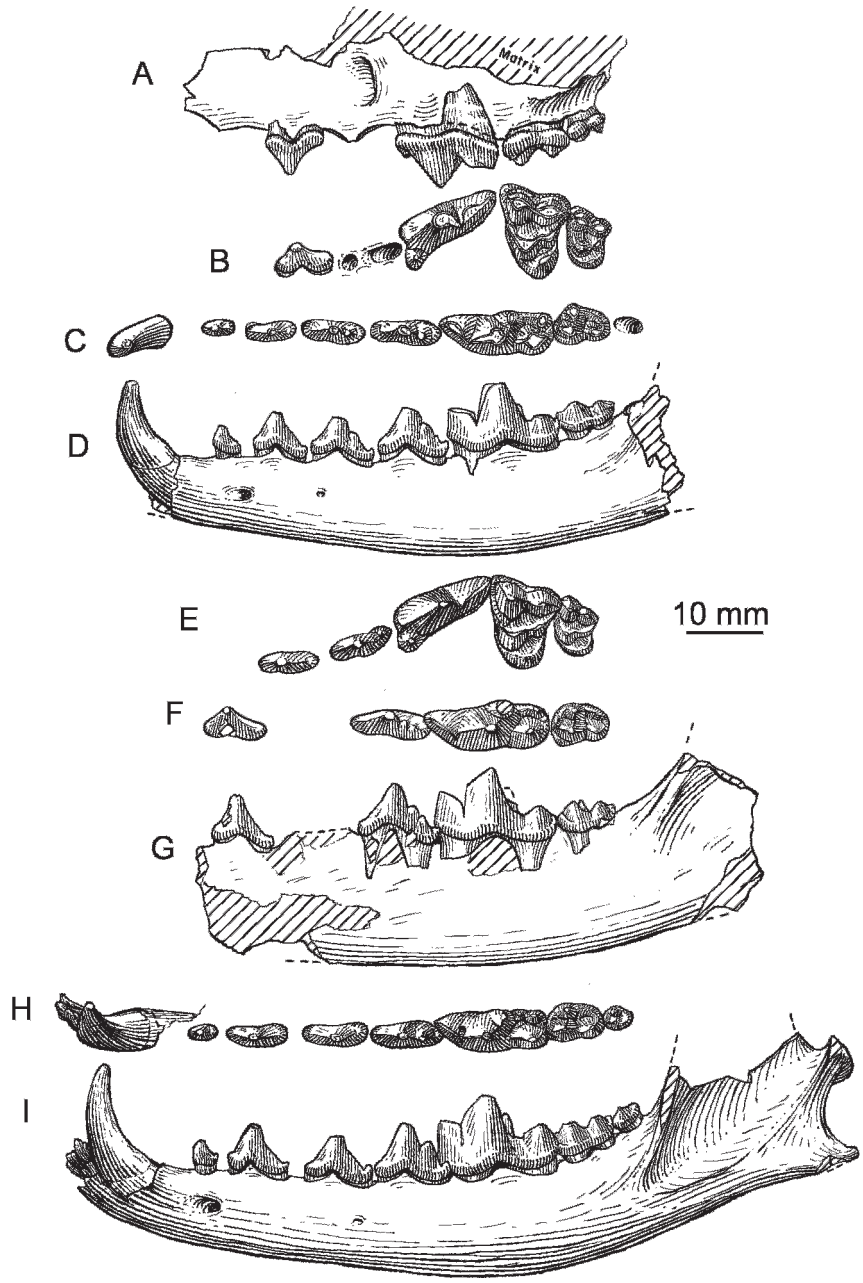

Fig. 20. **A–I**. *Vulpes stenognathus*. **A–G**. Associated maxillary and ramus, F:AM 62990, late Hemphillian, Arizona. **A**. Lateral view, from both sides. **B**. Occlusal view, from both sides. **C**. Occlusal view. **D**. Lateral view. **E**. Maxillary fragment, F:AM 75827. Occlusal view. **F–G**. Ramus, F:AM 75805. **F**. Occlusal view. **G**. Lateral view. **H–I**. Ramus, F:AM 28348, late Hemphillian, Colorado. **H**. Occlusal view, reversed. **I**. Lateral view, reversed.

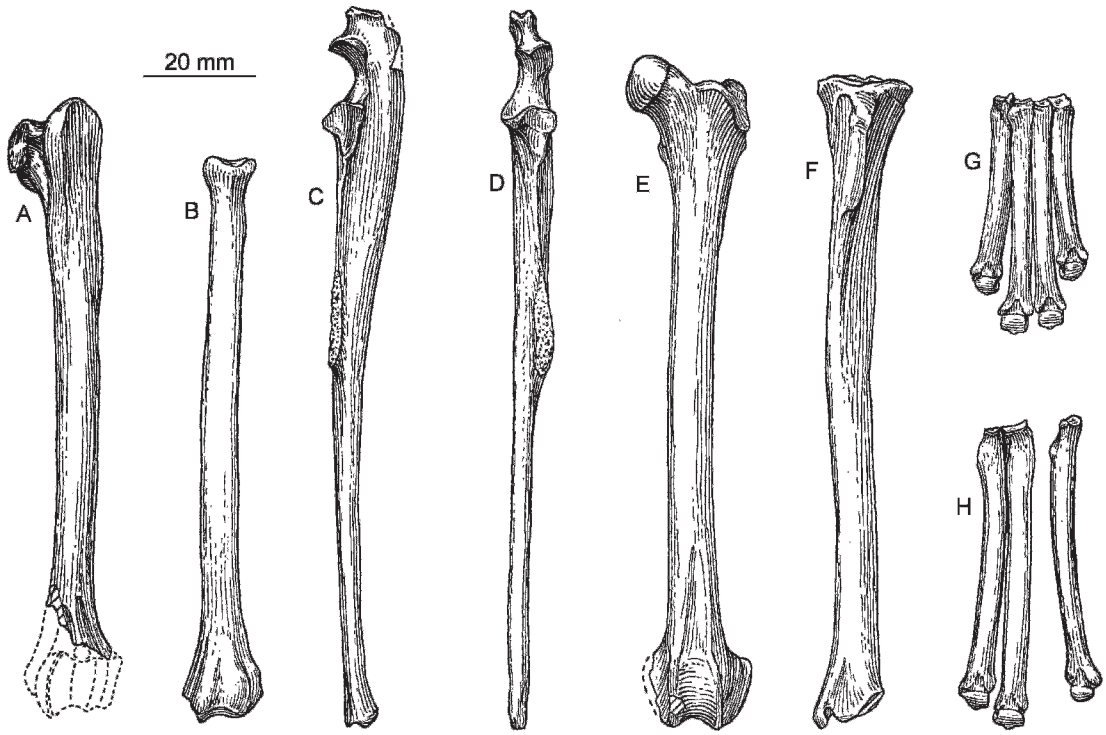

Fig. 21. **A–H**. *Vulpes stenognathus*, late Hemphillian, Arizona. **A**. F:AM 72550; partial left humerus, anterior view. **B**. F:AM 72551; right radius, anterior view, reversed. **C–D**. F:AM 72552; right ulna. **C**. Lateral view, reversed. **D**. Anterior view, reversed. **E**. F:AM 72553, left femur, anterior view. **F**. F:AM 72554, left tibia, anterior view. **G**. F:AM 62990, left metacarpals II, III, IV, and V, anterior view. **H**. F:AM 72580, right metatarsals, II, III, and V, anterior view, reversed.

County, Oregon: UCMP 112195, isolated right P3 and M1.

Rattlesnake 3, UCMP locality 3042, Rattlesnake Formation (early Hemphillian), Grant County, Oregon: UCMP 29969, right m1.

University of Oregon localities 2451 and 2489, Juniper Creek Canyon, Grassy Mountain Formation (early Hemphillian), Malheur County, Oregon: UO 19028, left m1; UO 19029, left P4; and UO 19034, left m2.

Aphelops Draw, Snake Creek Formation (early Hemphillian), Sioux County, Nebraska: AMNH 81021 (HC 519), right m1, described by Cook and Macdonald (1962: 562).

UNSM locality Ft 40, Ash Hollow Formation (early Hemphillian), Frontier County, Nebraska: UNSM 26136, left m1.

Ward's North Valley Pit, Sebits Ranch, Ogallala Group (early Hemphillian), Lipscomb County, Texas: F:AM 101237, immature partial mandible with i3 (unerupted), dc–dp4 and m1–m2 unerupted, and cranial fragments.

From Miami Quarry (= Coffee Ranch of University of California, late Hemphillian), 8 miles east of Miami, Hemphill County, Texas: F:AM 23376D, right isolated P4; F:AM 23376E*, right broken P4; F:AM 23376A*, left broken m1; F:AM 23375, left ramus with p2 (broken)–p4 and alveoli; F:AM 23376, left partial ramus with p2–p3.

From Goodnight area (late Hemphillian), Armstrong County, Texas: F:AM 49323, left m1 and associated calcaneum, Hill Pit 19–20 miles southwest of Claude; F:AM 49321, left broken P4, Hubbard Place Quarry.

From Black Wolf Creek (late Hemphillian), vicinity of Wray, Yuma County, Colorado: F:AM 28348, right and left rami with i1–m3 (fig. 20H–I); F:AM 28349, right

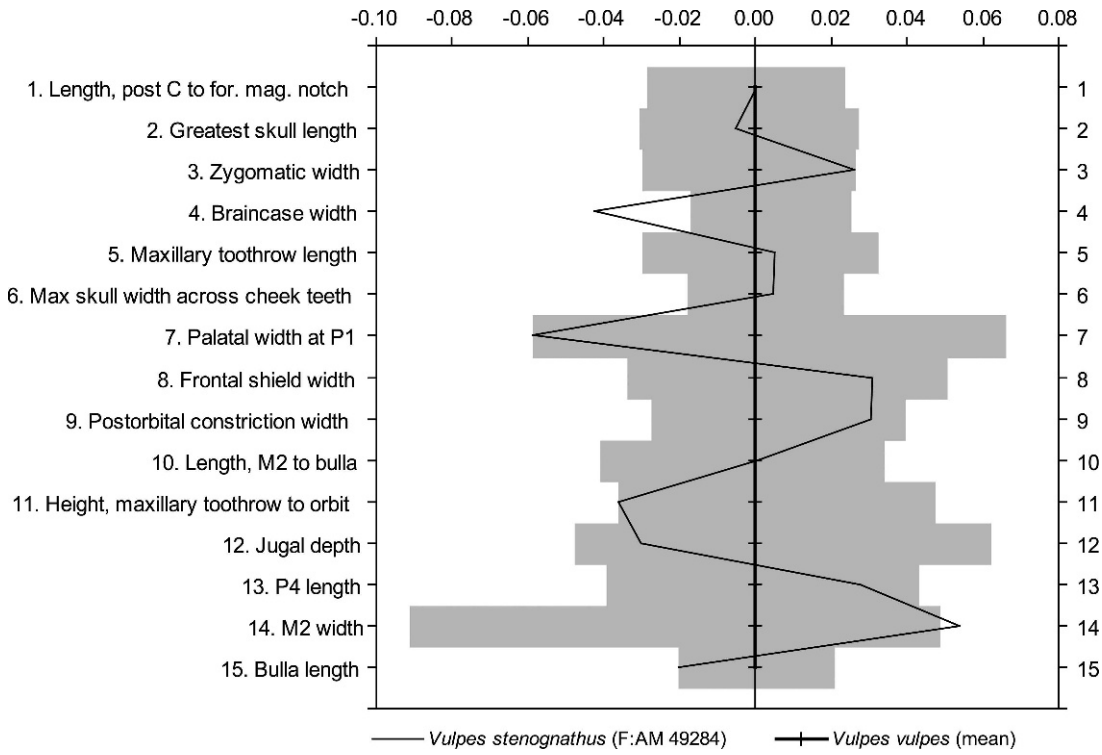

Fig. 22. Log-ratio diagram comparing the proportions of cranial variates (appendix 2) of the late Hemphillian individual of *Vulpes stenognathus* from Nevada (F:AM 49284) with the mean of a sample of 12 individuals (6 adult males and 6 females) of *Vulpes vulpes* from New England. The gray bars extending from the mean are the observed ranges for the indicated variates.

and left partial rami with i1–i3 broken and c–m3 (p1 and p3 alveoli); and F:AM 28349A, left partial maxilla with p4 (broken)–M2 and associated isolated teeth including C, P4, M1 broken, and M2.

Chamita Formation (late Hemphillian), Rio Arriba County, New Mexico: F:AM 27412B, right ramus with c (broken)–m2 (p2, p4, and m1 broken), opposite Alcalde; F:AM 62825, right and left partial rami with c (broken) and p2–m1 (all broken), opposite Lyden; F:AM 62830, right partial ramus with m1–m3 (m3 broken), Lyden; F:AM 62832, right partial ramus with c–p4 (broken or alveoli) and m1, ½ mile North of Lyden Quarry; F:AM 62831, right and left rami with c–p2 broken and p3–m3, ½ mile west of Lyden Quarry; and F:AM 62837, left partial ramus with p2–m2, m3 broken, Alcalde.

Spring Valley near Panaca, Golgotha Water Mill Pothole site (late Hemphillian), Lincoln County, Nebraska: F:AM 49284, partial skull with I1–I2 alveoli, I3–M2 (P1 and P3 alveoli), right and left rami with c–m3, vertebrae, and fragments (fig. 19); F:AM 49285, right and left partial maxillae with P2–M2; F:AM 49283, right ramus with p4–m3, right p4, m1 broken, left p4, m1–m2, isolated incisor, isolated teeth, and ramal fragments; F:AM 49287, right ramus with p4–m2; F:AM 49290, isolated m1 broken, p4, c, i, deciduous premolars; F:AM 49288, left m1; F:AM 62796, partial skull; and F:AM 62797*, right maxilla with M2.

Near Wikieup, Big Sandy Formation (late Hemphillian), Mohave County, Arizona: F:AM 62990, right and left partial maxilla with P2, P4, M1–M2, right and left rami with c, p1–p4, m1–m2, m3 alveoli (fig. 20A–E), both partial humeri, both partial ulnae, partial radius, right and left metacarpals II–V (fig. 21G), two proximal phalanges, astragalus, and miscellaneous fragments; F:AM 72621, left isolated P4; F:AM 62991,

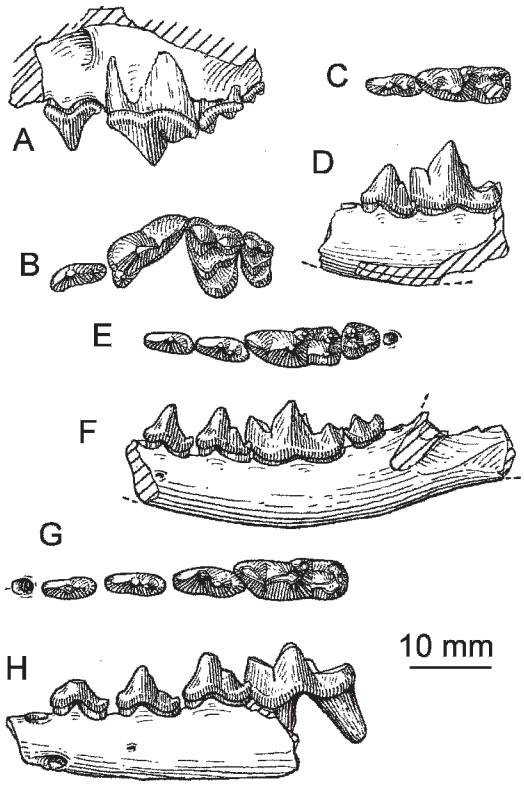

Fig. 23. **A–D**. *Vulpes kernensis*, early Hemphillian, California. **A–B**. Type maxillary fragment, LACM 55215. **A**. Lateral view, reversed. **B**. Occlusal view, reversed. **C–D**. Ramus, LACM 55216. **C**. Occlusal view. **D**. Lateral view. **E–H**. *Vulpes* sp. cf. *V. velox*, Irvingtonian, Nebraska. **E–F**. Ramus, UNSM 26163. **E**. Occlusal view, reversed. **F**. Lateral view, reversed. **G–H**. Ramus, F:AM 25516Z. **G**. Occlusal view. **H**. Lateral view.

left ramus with c (alveolus)–p2 (alveolus), p3–m1 and m2 broken; F:AM 62992, left ramus with c–m2 (p1 alveolus); F:AM 62994, left ramus with p4–m1 and alveoli; F:AM 62995*, left ramus with c, p1–p3 alveoli, p4 (broken)–m2, m3 alveolus; F:AM 62996, right ramus with p3–m2 and alveoli; F:AM 62997, left partial ramus with p4–m1; F:AM 63016D, left partial ramus with m1–m2; F:AM 63050, left m1; F:AM 63036*, right m1; F:AM 72622, left m1; F:AM 72623, left m1; F:AM 72608, left ramus with m2 and alveoli; F:AM 72550, partial left humerus (fig. 21A); F:AM 72651, right radius (fig. 22B); F:AM 72552, right ulna (fig. 21C–D); F:AM 72553, left femur (fig. 21E); F:AM 72578, incomplete metacarpal III; F:AM 72579, metacarpal V; F:AM 72580, associated metacarpals II, III, and V, Bird Bone Quarry (fig. 21H). F:AM 62998, left partial ramus with p1–M1 (p2 alveolus); F:AM 63052, right isolated m1, Clay Bank Quarry. F:AM 62993, right and left partial rami with p4–m2, stratum 3, Gray's Ranch Quarry; and F:AM 72554, left tibia (fig. 21F), Horse Shoe Quarry.

Old Cabin Quarry, Quiburis Formation (late Hemphillian), Pima County, Arizona: F:AM 72655, right ramal fragment with m1 (broken)–m2; F:AM 50691, left ramus with c broken, p1 alveolus–m2 (p2–m1 broken); F:AM 50692, right partial ramus with c–m1, all broken; F:AM 50693, right partial ramus with p3–m2 (all broken); F:AM 50694, right partial ramus with p2–p3 both broken, p4, m1 broken; F:AM 75827, crushed skull with C–M2 (P1 alveolus, fig. 20E); F:AM 63089, skull with P3–M2; F:AM 75823, anterior portion of skull with P2, P4–M2, left ramus with m1–m3, right ramus with p4, m1 broken, right femur, left humerus; F:AM 72828, left and right maxillae with P4–M2; F:AM 50681, left maxilla with P3 (broken)–M2; F:AM 72664, left maxilla with M1–M2; F:AM 72824, left and right maxillae with C–M2; F:AM 75805, left and right rami with p2–m2 (fig. 20F–G); F:AM 75801, left and right partial rami with p2–m3; F:AM 75802, right ramus with p3–m1; F:AM 75803, right ramus with p3–m1; F:AM 50698, right m1; 75826, isolated right M1–M2; F:AM 50687, left P4 (broken)–M2; F:AM 75829, distal end left radius and calcanea; F:AM 75830, 75830a, left femur and two left tibiae; F:AM 75831, left metacarpals II–V, phalanx; F:AM 75832, right metacarpal IV; F:AM 62783, right radius: F:AM 62784, tibia, calcaneum, tarsals; and F:AM 62785, left metacarpal V.

Redington Quarry, Quiburus Formation (late Hemphillian), northwest of Redington, west side of San Pedro River Valley, Pima County, Arizona: F:AM 75800, right ramus with c–m2; F:AM 63099, right ramus with m1.

From the Quiburus Formation (late Hemphillian), Pima County, Arizona: F:AM 63080, right partial ramus with p1–m2 (m1 broken), Leach Dig, ½ mile west of Least

Camel Quarry; and F:AM 72613, right partial ramus with p4–m2 all broken, Rogers Quarry.

Nichol's Mine, upper Bone Valley Formation (late Hemphillian), Polk County, Florida: UF 23994*, right partial ramus with m1–m2.

Lava Mountains Fauna (late Clarendonian or early Hemphillian), Bedrock Springs Formation, San Bernardino County, California, USGS locality LM-16, USGS D669*: right and left rami of mandible with c, p1–4.

Yepomera (late Hemphillian), CIT locality 275, Chihuahua, Mexico: LACM 3534, left partial maxilla with P4 (broken)–M2 alveolus; LACM 30215, M1 broken parastyle.

Distribution: Possibly late Clarendonian of California; Early Hemphillian of Nebraska, Nevada, California, and Oregon; late Hemphillian of Oklahoma, Texas, New Mexico, Colorado, Nevada, Arizona, Florida, and northern Mexico.

Revised Diagnosis: Differs from *V. vulpes* of North America in anteroposteriorly shorter and less robust premolars; p4 often with second posterior cusp; m1 entoconid usually smaller relative to the hypoconid; talonid lacks transverse crest between entoconid and hypoconid, hypoconulid shelf smaller; m2 longer relative to length of m1 with anterolabial cingulum stronger and paraconid shelf larger; muzzle narrower; frontoparietal suture more anterior, with frontal crests joining at suture to form sagittal crest; braincase relatively narrower with frontal region much less expanded; small frontal sinus that penetrates base of postorbital process; and small bulla with less produced lip of auditory meatus.

Description and Comparison: A comparison of *V. stenognathus* with *V. vulpes* shows a few significant morphological differences in the lower dentition as indicated in the diagnosis. The premolars in *V. stenognathus* are anteroposteriorly shorter and less robust. Furthermore, a posterior cusplet is generally present on the p3 of *V. stenognathus* and the p4 often bears a second posterior cusp. In *V. vulpes* the posterior cusp on p3 and the second posterior cusp on p4 are generally absent and, if present, they are comparatively weaker than in *V. stenognathus*. The upper premolars of *V. stenognathus* closely resemble those of *V. vulpes*, including the lack of a posterior cusp on p3. The protocone of P4 tends to be smaller than that of the latter. No consistent morphological features were observed to distinguish the upper molars of *V. stenognathus* from those of the recent species, but on the whole these teeth appear to be larger relative to the size of the skull in *V. stenognathus* (compare P4 length and M2 width vs skull dimensions, fig. 22).

The shallow horizontal ramus is also similar to *Vulpes vulpes*, and the angular process is shallow and attenuated like that seen in living *Vulpes* species. A number of distinguishing features separate the lower molars of *V. stenognathus* from those of *V. vulpes*. Superficially the m1 of *V. stenognathus* resembles that of *V. vulpes*, but the talonid of *V. stenognathus* differs in that the entoconid tends to be smaller relative to the hypoconid and to lack the transverse crest that links it with the hypoconid that is often present in *V. vulpes*. The m1 hypoconulid shelf is also smaller than in *V. vulpes*. The m2 of *V. stenognathus* is larger relative to the length of the m1, with the anterolabial cingulum being stronger and the paraconid shelf larger than in *V. vulpes*.

The skull of *V. stenognathus* (F:AM 49284, fig. 19) is proportionally similar to that of *V. vulpes* except for a narrower (not altogether the result of lateral crushing) and somewhat shorter muzzle (fig. 22). The nasals are short, as in all *Vulpes*, and do not reach the transverse limb of the maxillary-frontal suture. The most distinctive features of the skull separating *V. stenognathus* from North American *V. vulpes* are correlated with the size and expansion of the braincase shown by the red fox (fig. 22). In *V. stenognathus* the width of the frontal shield is similar to that of *V. vulpes*, but the frontoparietal suture is located more anteriorly and thus the frontals are almost 20% shorter along the midline than those of similar-sized skulls of *V. vulpes*. Weak frontal crests join anteriorly near the frontoparietal suture to form a long, low sagittal crest in *V. stenognathus*, whereas in *V. vulpes* the crests join more posteriorly and thus form a shorter sagittal crest. The braincase of *V. stenognathus* is relatively

smaller (see fig. 22) and less laterally expanded than in *V. vulpes*, and the frontal part of the braincase is markedly less expanded. An unexpected result of sectioning the postorbital region of this skull (fig. 57B) was the discovery of a small frontal sinus in the fossil form. Another skull fragment (F:AM 62796), also from Spring Valley, Nevada, shows this sinus as well. The sinus extends laterally into the base of the postorbital process. The nuchal crest is similar to that of *V. vulpes* and the shape of the entire occipital bone closely resembles that of *V. vulpes* except for its lower height relative to its width, which reflects the less expanded braincase of *V. stenognathus*.

Unfortunately the basicranial area of the Nevada skull (F:AM 49284; fig. 19) is badly broken, with the basioccipital missing, and only one broken bulla is present. As nearly as can be determined, the mastoid process, the paroccipital process, and the cranial foramina closely agree with those of *V. vulpes*. The broken bulla, however, has the lip of the external auditory meatus less produced than in *V. vulpes*, and this is confirmed by another crushed skull (F:AM 75827) referred to *V. stenognathus* from Arizona.

Isolated limb elements refered to *V. stenognathus* (fig. 21) also fail to show any morphological features to distinguish them from *Vulpes vulpes*. The proportions of fore- to hindlimb elements (e.g., radius/tibia ratio) are within the range of living foxes. Metatarsal I is unknown in *V. stenognathus*, but its facet indicates that there was as short proximal rudiment that was smaller than the entocuneiform as in later species of *Vulpes*.

Discussion: Savage's (1941) original description of *Vulpes stenognathus* was based on two partial rami and isolated teeth, which he concluded differed from recent *Vulpes* in their larger size, deeper horizontal ramus, and reduced accessory cusps on the premolars. Additional specimens from the type locality, as well as larger samples from other late Hemphillian localities here referred to *V. stenognathus*, do not fully confirm his observations. The measurements and statistics (appendices 2 and 3) for up to 64 dentitions of *V. stenognathus* and 53 specimens of *V. vulpes* from North America with a geographical range from Alaska to Georgia show that the carnassials of the two species are nearly the same size, but the size of the other teeth differ. In *V. stenognathus* the mean values from the premolars and molars (except M1) are mostly smaller for the premolars and larger for the molars than those of *V. vulpes*. This is also indicated for the m1 mean in which *V. stenognathus* has nearly the same length as in *V. vulpes* and the confidence interval for the two taxa overlaps widely, whereas the m2 in *V. stenognathus* is proportionally larger, with the confidence interval only narrowly overlapping that of *V. vulpes*.

The log-ratio diagram (fig. 22) shows that the skull measurements of *V. stenognathus* are, for the most part, within the range of those of the recent sample of *V. vulpes*. As described above, the most distinctive morphological features separating the skulls of *V. stenognathus* and *V. vulpes* are those correlated with the proportions of the muzzle and braincase.

Vulpes sp. cf. *V. velox* (Say), 1823

Figure 7, 23E–H; appendix 3

Vulpes fulvus?: Brown, 1908: 182.
Vulpes, near *V. velox*: Dalquest, 1978: 287.

Material: Beck Ranch Local Fauna, Ogallala Group (early Blancan fide Dalquest, 1978), MSU 9477, right M1; MSU 9473, broken M1; and MSU 8662, M1.

Irvington site 2, UCMP locality V3604, late Irvingtonian, Alameda County, California: UCMP 81733*, fragment of right ramus, c–m1, m2 broken, m3 alveolus; UCMP 81734*, fragment of left ramus m1–m2; UCMP 81735*, talonid left m1; UCMP 81736*, right m1.

Fairmead Landfill site, UCMP locality V93128, late Irvingtonian, Upper Unit C of Turlock Lake Formation, Madera County, California (Dundas et al., 1996): UCMP 170181*, 18 questionably associated teeth, including M1, P4, and other upper premolars and canines*; UCMP 170180*, associated right ramus and right maxillary in matrix block.

Angus Quarry, UNSM locality No-101, late Irvingtonian, unnamed deposits resting on Ogallala Formation, Nuckolls County,

southeastern Nebraska: UNSM 33612, right ramus with c–p1 alveoli, p2, p3 alveolus, p4–m2, m3 alveolus.

Albert Ahrens site, UNDM locality No-104, late Irvingtonian, from pond deposit within Loveland Loess, incised into Lava Creek B Tephra (0.61 Ma), Nuckolls County, southeastern Nebraska: UNSM 2000-91, unworn right m1, unworn left P4, left M1, and right M2 representing different individuals.

"Sheridan beds" (late Irvingtonian), Hay Springs area, Sheridan County, Nebraska: F:AM 25516, right P4; F:AM 25516Z, left partial ramus with c–p1 alveoli, p4–m1 (fig. 23G–H); and UNSM 26163, right partial ramus with p3–m2, m3 alveolus (fig. 23E–F) from Gordon Quarry 1.

Conrad Fissure (late Irvingtonian), Newton County, Arkansas: AMNH 11764, right p4 and left M1 (Brown, 1908: 182).

Distribution: Early Blancan of Texas; late Irvingtonian of California, Nebraska, and Arkansas.

Remarks: The Beck Ranch M1 (MSU 9477) is water-worn, but its major features can be discerned including the larger size of the paracone relative to the metacone, the narrow labial cingulum, and the development of the posterior lingual cingulum, all of which agree with *Vulpes*. The Beck Ranch M1 (anteroposterior diameter, 7.3 mm, transverse diameter, 9.2 mm) is within the range of the *V. velox* sample we have used for comparison (appendix 3).

The two late Irvingtonian rami from Nebraska differ between themselves to a somewhat greater degree than the small sample of *Vulpes velox* used for comparison. UNSM 26163 is a small fox with the length of m1 within the size range of *Vulpes velox*. In both specimens the hypoconid and entoconid are joined by cristids, as in most living foxes. There is an entoconulid between the metaconid and entoconid in both rami. The second lower molar is small relative to the size of m1 and also comparable to that of *Vulpes velox*, but the metaconid is markedly larger than the protoconid, and the talonid is equal to the trigonid in length. The p3 and p4 are smaller and less robust than in the other Hay Springs jaw (F:AM 25516Z) or in *Vulpes velox*. A P4 (F:AM 23516) agrees in both size and weakness of the protocone with *Vulpes velox* and is unlike the larger P4 of *Vulpes vulpes* or *V. lagopus*, which have proportionally larger and more anteriorly situated protocones. In size and morphology F:AM 25516Z and 25516 are very similar to *Vulpes velox*. The Conard Fissure teeth are both appropriate in size and morphology for *V. velox*. Brown (1908: 182) referred to them as "*Vulpes fulvus*?" but noted their smaller size. The measurements show that these teeth are robust but lie, for the most part, within the range of *V. velox*.

The material from the late Irvingtonian of California closely resembles that described from contemporary deposits in Nebraska. Although the southwestern part of North America is inhabited today by the smaller kit fox (*V. macrotis*), the medial Pleistocene remains seem to pertain to a larger animal that in size and morphology agree more completely with the midcontinent swift fox (*V. velox*). By the late Rancholabrean the kit fox was established in the California central valley (Schultz, 1938) and is recorded in the Mohave Desert region to the east (Jefferson, 1991), where it continues to exist. The most useful materials are the jaw fragments from the Irvingtonian site. The teeth are similar to those of *V. velox* and the Hay Springs material figured here in that the m1 talonids have entoconulids that close the talonid basin lingually. The entoconid and hypoconid are united by cristae, leaving a hypoconulid behind the transverse crest. The m2 has a large metaconid that is higher then the protoconid.

Small foxes of this size are known from Pliocene and early Pleistocene strata in Eurasia (Europe: *V. alopecoides* and *V. praeglacialis*, see Bonifay, 1971, and Rabeder, 1976; China: *V. chikushanensis*, see Teilhard de Chardin, 1940; and *V. baihaiensis* Qiu and Tedford, 1990). The early to medial Pleistocene *Vulpes praeglacialis* (Kormos, 1932) resembles the Irvingtonian *Vulpes* sp. cf. *V. velox*, especially in the morphology of the m1 talonid in the presence of cristae connecting the entoconid and hypoconid, presence of an entoconulid, and in the size of the m2 relative to m1 with its well-developed anterolabial cingulum and large metaconid. Kormos (1932), Bonifay (1971),

and Benes (1972) regarded *V. praeglacialis* as the precursor of *V. lagopus* despite the paucity of evidence of specific morphological resemblance. Rabeder (1976), on the other hand, relegated *V. praeglacialis* to a lineage leading from *V. alopecoides* through *V. praeglacialis* to *V. angustidens* Thenius, 1954, to *V. vulpes*, and regarded *V. lagopus* as a morphologically independent lineage phyletically isolated from other foxes. *Vulpes praecorsac* from the medial Pleistocene of eastern Europe further differs in the lower dentition in lacking a transverse crest on m1, showing reduction of the m1–m2 metaconids, and in having larger premolars, features that could ally it with the living red fox as well as the corsac foxes.

These North American specimens are brought together on the basis of size and overall similarity rather than evidence of specific morphological relationships. A considerable gap in age separates the early Blancan Beck Ranch upper molars from the array of materials of late Irvingtonian age. Assiduous searching of available collections on our part has failed to establish a continuity of record for *Vulpes* species between the early Pliocene and medial Pleistocene, just as Kurten and Anderson (1980: 174) had concluded. It thus seems possible that the array of Pleistocene and living *Vulpes* species of North America may all derive from the fox fauna of Eurasia rather than involve forms of proximal New World origin.

Metalopex Tedford and Wang, 2008

Type Species: *Metalopex merriami* Tedford and Wang, 2008.

Included Species: *M. macconnelli*, new species, and *M. bakeri*, new species.

Distribution: Late Clarendonian of Arizona and California, late Clarendonian or early Hemphillian of Oregon and New Mexico, early Hemphillian of Idaho, Nevada, Oregon, and Nebraska, and medial Hemphillian of Texas.

Etymology: Greek: *meta*, near and *alopex*, fox.

Diagnosis: Derived features that distinguish *Metalopex* from *Vulpes* are: mastoid process large; M1 and M2 more quadrate in shape, anteroposteriorly long relative to width; M2 lacks postprotocristid; p2 isolated by longer diastemata; m1 and m2 have protostylids; m2 large relative to m1, more posteriorly extended anterolabial cingulum, and talonid longer relative to trigonid; m3 uniquely elongate, trigonid longer than talonid, that is, relatively large paraconid shelf, protoconid, and metaconid situated more posteriorly.

Primitive characters retained by *Metalopex* include: marked depression on frontals adjacent to postorbital process; basioccipital wide; bulla small; strong medial and lateral cusplets on I2 and medial cusplet on I3; M2 metaconule present despite reduction and loss of connecting postprotocrista; m1 talonid lacks transverse crest between entoconid and hypoconid and also lacks hypoconulid; and m2 with paraconid or strong paracristid.

Discussion: Although the morphological features of *Metalopex* are most typically developed in the type (F:AM 49282) of the genotypic species, *M. merriami*, the smaller species, *M. macconnelli*, which is intermediate in size and cranial proportions (fig. 27) between its contemporary *Leptocyon vafer* and *Vulpes stenognathus*, also clearly exhibits these characters. *Metalopex* differs principally from both *Vulpes* and *Urocyon* in its unique M2, which lacks a postprotocrista but retains the metaconule; in retaining the primitive form of the upper incisors in which I3 still has a medial cusp; in its relatively derived enlargement of the mastoid process (compare posterior views of the crania of *Leptocyon vafer*, fig. 61A, with *Metalopex macconnelli*, fig. 61B); and in the uniquely enlarged m3, which retains the primitive trigonid and talonid.

Metalopex macconnelli, new species
Figures 7, 24A–S, 26A–E, 27, 28, 61B; appendices 2, 3

Type: LACM 55237, crushed skull (fig. 24A–C) with I1–M2 and both ramal fragments including p3–p4 broken, m1 incomplete alveolus, isolated m2 trigonid (fig. 24D), and a broken isolated lower canine from Red Rock Canyon, LACM locality 3552, upper part of the Dove Spring Formation (late Clarendonian), Kern County, California.

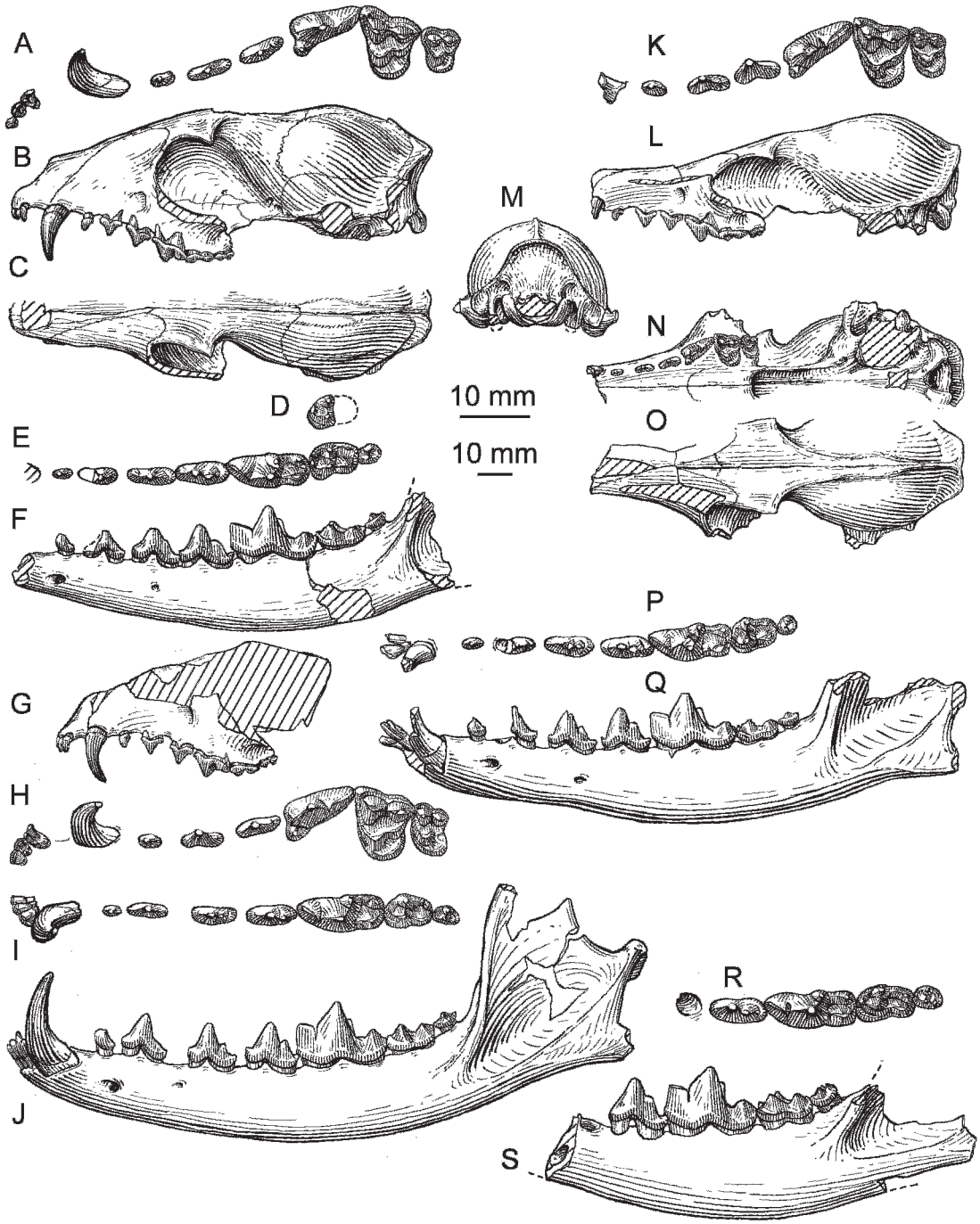

Fig. 24. **A–S**. *Metalopex macconnelli*, late Clarendonian to earliest Hemphillian, California, Arizona, and Oregon. **A–D**. Type skull and trigonid of m2, LACM 55237. **A**. Occlusal view. **B**. Lateral view. **C**. Dorsal view. **D**. Broken m2, occlusal view, reversed. **E–F**. Ramus, LACM 55219. **E**. Occlusal view. **F**. Lateral view. **G–J**. Skull fragment and associated ramus, NMNH 184113. **G**. Lateral view. **H**. Occlusal view. **I**. Occlusal view. **J**. Lateral view. **K–O**. Skull, UA 361-49. **K**. Occlusal view, M2 restored from opposite side. **L**. Lateral view. **M**. Occipital view. **N**. Palatal view. **O**. Dorsal view. **P–Q**. Ramus, UA 359-49. **P**. Occlusal view, canine from opposite side. **Q**. Lateral view. **R–S**. Ramus, NMNH 23883. **R**. Occlusal view, reversed. **S**. Lateral view, reversed. Upper scale pertains to dentitions, lower scale to crania.

Etymology: Named in honor of J. MacConnell, of Diamond Springs, who, with his family, collected the type and generously donated it and many other fine specimens to the Los Angeles County Museum.

Referred Material: LACM 55219, left ramus (fig. 24E–F) with c broken–m3 (p2 broken) from Red Rock Canyon, LACM locality 3552, Kern County, California, upper part of the Dove Springs Formation, 200 m below the occurrence of the type (late Clarendonian). LACM 122323, right and left maxillary fragments, P2–P4, M1–M2, LACM locality 3580, 100 m above the occurrence of the type in rocks of earliest Hemphillian age, Kern County, California. UCMP 33707, left partial ramus with c–m1 alveoli, m2, and m3 alveolus (figured by Macdonald, 1948: fig. 2; fig. 28A–B of this paper).

Walnut Grove Basin, Milk Creek Formation (late Clarendonian), Yavapai County, Arizona: UA 361-49, skull (fig. 24K–M) with C broken–M2; UA 359-49, mandible with i1–i2 both broken, and i3–m3 (c, p2, and p4 all broken, possibly same individual as UA 361-49, fig. 24P–Q); UA 328-49, anterior part of skull with C–M2 and mandible with i1–m2 (p4 and m2 broken); UA 349-49, right and left partial maxillae with P2 alveolus–M2; UA 434-49, left maxilla with C–P3 alveoli and P4–M2 (M1 broken); UA 329-49, right ramal fragment with p4, and m1 broken; UA 408-49, detached canine, p1, p2, p3, and right and left m1s; UA 358-49*, detached p4, fragment of p4, proximal part of radius and ulna, distal fragment of tibia, cuboid, astragulus, and right and left calcanea, Quarry 3. UA 37-49, crushed partial skull with I1–M2, Quarry 1.

From the Milk Creek area, Milk Creek Formation (Clarendonian), Yavapai County, Arizona: F:AM 63065, left partial maxilla with P3 broken–M2 (P4 broken); F:AM 63066, right and left partial rami with p2 root, p3 broken–m3, Manzanita Quarry; F:AM 63067*, right and left partial rami with c broken–p4 (p2, m1, and m2 broken), Cliff Prospect.

Late Clarendonian or early Hemphillian (C.A. Repenning, personal commun.), Malheur County, Oregon: NMNH 23883, right partial ramus (fig. 24R–S) with p4–m3, from Saddle Butte, USGS locality M1099; and NMNH 184113, left anterior fragment of skull with I1–M2 and associated mandible (fig. 24G–J) with i1–m3 from Sand Spring, USGS locality M1419.

Distribution: Late Clarendonian and early Hemphillian of California, late Clarendonian of Arizona, and late Clarendonian or early Hemphillian of Oregon.

Diagnosis: Differs from *M. merriami* in smaller size; lyrate temporal crests that join posterior to frontoparietal suture in short, weak sagittal crest; occiput narrower with lambdoidal crests subdued; bullae larger relative to size of skull; I2 with weaker lateral cusplet and weaker lingual cingulum; dentition lower crowned; M1–M2 less quadrate with stronger labial cingulum on paracone of M1; M2 smaller relative to M1; m1 slenderer with less oblique paraconid, and narrow talonid; and m3 trigonid shorter relative to length of talonid.

Description and Comparison: The morphological features of the type skull (LACM 55237) and referred skull (UA 361-49) of *M. macconnelli*, for the most part, recall those of *Leptocyon*, but the relative enlargement of the mastoid process of the periotic is like that of the genotype, *Metalopex merriami*. The skull characters cited in the diagnosis that distinguish this species from *M. merriami* are in turn similar to those *L. vafer*. Likewise, the mandible is elongate and slender and the angular process (lacking only the tip in the right ramus of NMNH 189113) bears the pterygoid and masseter scars of primitive configuration (Tedford et al., 1995: fig. 5A, "type A" of Gaspard, 1964). The incisors of *M. macconnelli* are simple and possess the basic features of *Leptocyon*. In both taxa, the I2 has a minute medial and lateral accessory cusp on the crown and a faint lingual cingulum. The third upper incisor is about one-third larger than I2 with a more promiment medial accessory cusp and a stronger lingual cingulum. The incisors of the type of *M. merriami* are similar to those of *M. macconnelli*, but the accessory cusps and cingula are stronger in the isolated premaxilla referred to *M. merriami* from Nebraska (UNSM 26115), and the I3 is more compressed.

The premolars in *M. macconnelli* are moderately long but taller crowned relative

to their length than are those of *L. vafer*, but they are shorter crowned than in *M. merriami*. The premolars are slender and widely spaced, with the p2 being the most isolated by diastemata. The P4 is slender, has a well-developed protocone, and is indistinguishable from that of *Leptocyon*.

In *M. macconnelli*, it is principally the molars above and below that differ from *L. vafer* and *Vulpes stenognathus* and possess features in common with *Metalopex merriami*. Compared to a skull of *L. vafer* (UCMP 77703, fig. 16), from about 100 m above the type of *M. macconnelli* in the upper part of the Dove Springs Formation of California, *M. macconnelli* has relatively larger molars with the anteroposterior dimensions of M1 and M2 longer relative to their width. In *M. macconnelli* the lingual cingulum on the M1 and M2 is weaker, especially where it begins at the protocone. The shape of the M1 and M2 is intermediate between that of *L. vafer* and the more quadrate molars of *M. merriami*. The M2 is markedly larger and more quadrate than those of *L. vafer* and *V. stenognathus*, and it retains the metaconule although this cusp is not always linked to the protocone by a postprotocristid.

The m1 of *M. macconnelli* closely resembles that of *L. vafer* (UCMP 77703) from the upper part of the Ricardo Formation of California. Its trigonid is moderately long as in *Leptocyon* and slightly longer with a less oblique paraconid than that of *M. merriami*. It differs mainly from *L. vafer* in its longer talonid that occludes with the more quadrate M1.

The isolated broken anterior half of m2 of the type (LACM 55237) differs from *L. vafer* in that the trigonid is relatively long with a distinct paraconid as in *M. merriami*. A distinct paraconid is present in four of the six m2s listed here, but this is a variable character as shown in two jaws (NMNH 184113 and UA 328-49) in which only a paracristid is present as in *L. vafer*. The above features of the m2 of the type are confirmed by the additional referred mandibular rami. These rami also show the nature of the talonid of m2 which, like that of the genotypic species, show marked elongation, although this is subject to some variation, being especially marked in the Oregon material as further noted below.

The m3 of *M. macconnelli* are markedly larger than those of *L. vafer* and *V. stenognathus*, and it is relatively larger and more elongate than that of *Leptocyon*. A minute paracristid may be present, and the subequal protoconid and metaconid are larger than in *L. vafer*. Moreover, they are situated more posteriorly, making the trigonid longer than the talonid. This unusually large m3 and its long trigonid are characteristic of *Metalopex*.

Macdonald (1948: 56, fig. 2) figured a mandibular fragment from Black Hawk Ranch (UCMP 33707) with only an m2 and alveoli for the other cheek teeth and concluded that it was ''possibly related to *Urocyon*.'' Macdonald listed three additional m2s, which are included in our referred material. He also listed a badly worn upper molar (UCMP 33709) that is not included herein because its extreme wear prevents positive assignment to a taxon. We have recognized additional material from the Black Hawk Ranch Quarry that includes most of the upper and lower molars. These specimens differ from the other materials assigned to this taxon in some ways that deserve additional description and analysis.

The mandibular ramus is no larger than that of *L. vafer*, but the horizontal ramus is deeper below the p1 and comparable to that of other *M. macconnelli*. Judging by the length of the alveoli, the premolars were shorter than most individuals of *M. macconnelli*. A short diastema isolates p2 from p1, and a still longer diastema (4.5 mm) separates p2 from p3.

The m1 in the Black Hawk Ranch sample shows variable development of the protostylid, perhaps more characteristic of *Urocyon* than the much weaker protostylids of the other samples of *M. macconnelli*. The m1 talonid has a distinct entoconulid and the entoconid is smaller and lower crowned than the hypoconid. The m2 is elongate with a relatively long trigonid and a small but distinct paraconid. A well-developed anterolabial cingulum extends posteriorly only to the protoconid where a weak prostylid is present. This is a derived feature that is shared with *Urocyon*. The talonid is elongate

with a well-developed entoconid and hypoconid.

The upper dentition referred to *M. macconnelli* from Black Hawk Ranch includes three P4s, two M1s, and an M2. The P4 (UCMP 112188) is robust with a strong anteriorly directed protocone. The parastyle is not present on the P4 from Black Hawk Ranch, and because of the abrasion of the enamel, it is also uncertain if a labial cingulum was present. The M1 bears a strong lingual cingulum that begins at the base of the paracone and ends posteriorly labial to the metaconule at the base of the metacone. The M1 has a well-developed metaconule connected by the protocrista to the protocone; however, this connection is not present on the M2, where the small metaconule is isolated from the protocone as typical of *Metalopex* rather than *Urocyon*.

Thus, the Black Hawk Ranch sample diverges slightly from others of *M. macconnelli* in the development of the m1–m2 protostylid in a manner foreshadowing the more consistent occurrence of this structure in *Urocyon*. The morphology of one partial ramus (NMNH 23883, fig. 24R–S) also differs from the other jaws of *M. macconnelli* and tends to be intermediate between the latter and the more derived specimens of *M. merriami*.

Although the p4 and m1 of NMNH 23883 compares favorably with the other materials referred to *M. macconnelli*, the last two molars are more like those of *M. merriami*. The m2 (NMNH 23883) is elongate with a distinct paraconid, a labial cingulum that extends to the hypoconid, and it possesses an especially long talonid with a minute entostylid as in *M. merriami*. Its m3 is typically elongate with a long trigonid and a well-developed subequal protoconid and metaconid. We interpret these features as variation within a later occurring population of *M. macconnelli* in view of evidence for considerable variation shown by materials of both species of the genus. As discussed under *M. merriami*, the small samples available for the genus seem to show chronoclinally distributed size and morphological variation that suggest an anagenetic trend that is here somewhat arbitrarily segmented taxonomically.

Metalopex merriami Tedford and Wang, 2008

Figures 7, 25A–I, 28; appendices 2, 3

Vulpes sp.: Becker and McDonald, 1998: 33.
Tephrocyon, near *kelloggi*: Merriam, 1911: 238.

Type: F:AM 49282, partial skull with I3 alveolus–M2, detached premaxillary fragament with I1–I2, and left partial ramus with c alveolus–m3 (p1 alveolus and m1 broken, fig. 25A–D, F–G) from 3 miles north of Line Quarry, just north of the Oregon–Nevada state line, Thousand Creek Formation (early Hemphillian), Harney County, Oregon.

Referred Material: From near the type locality, Line Quarry, Thousand Creek Formation (early Hemphillian), Humboldt County, Nevada: F:AM 61016, left partial ramus with m1 and m2–m3 both broken (fig. 25E). From UCMP locality 1103, Thousand Creek Formation, Humboldt County, Nevada, UCMP 12542, right m2 (Merriam, 1911: fig. 7).

From Mitchell Road, UCMP locality V4825, Rattlesnake Formation (early Hemphillian), Wheeler County, Oregon: UCMP 41084, left isolated M1 and M2.

From Star Valley, IMNH locality 67001, sediments interbedded with Banbury Basalt (early Hemphillian), Owyhee County, Idaho: IMNH 24584, right partial ramus with p4–m2; IMNH 27886*, left partial ramus with c, p1–p4, and m1.

From Kern River, LACM(CIT) locality 49, Kern River Formation (early Hemphillian), Kern County, California: LACM 55217, left partial ramus with c (alveolus)–m2 (p1 alveolus, p2 broken, and p3–p4 alveoli).

From Gabaldon Badlands, 4 miles south of Rio Puerco station (late Clarendonian or early Hemphillian), Valencia County, New Mexico: F:AM 107607*, two fragments of right ramus with c–p2 all alveoli, p3, p4 root, and m1–m2 both broken (Lozinsky and Tedford, 1991: 25, fig. 18D).

UNSM, locality Ft. 48 (early Hemphillian), Ash Hollow Formation, Frontier County, Nebraska: UNSM 521-47*, left partial ramus with c alveolus, p1, p2–p3 both broken, p4 root, and m1–m3 alveoli; UNSM 419-47, right maxillary fragment with M1–M2; UNSM 522-47, left maxillary fragment

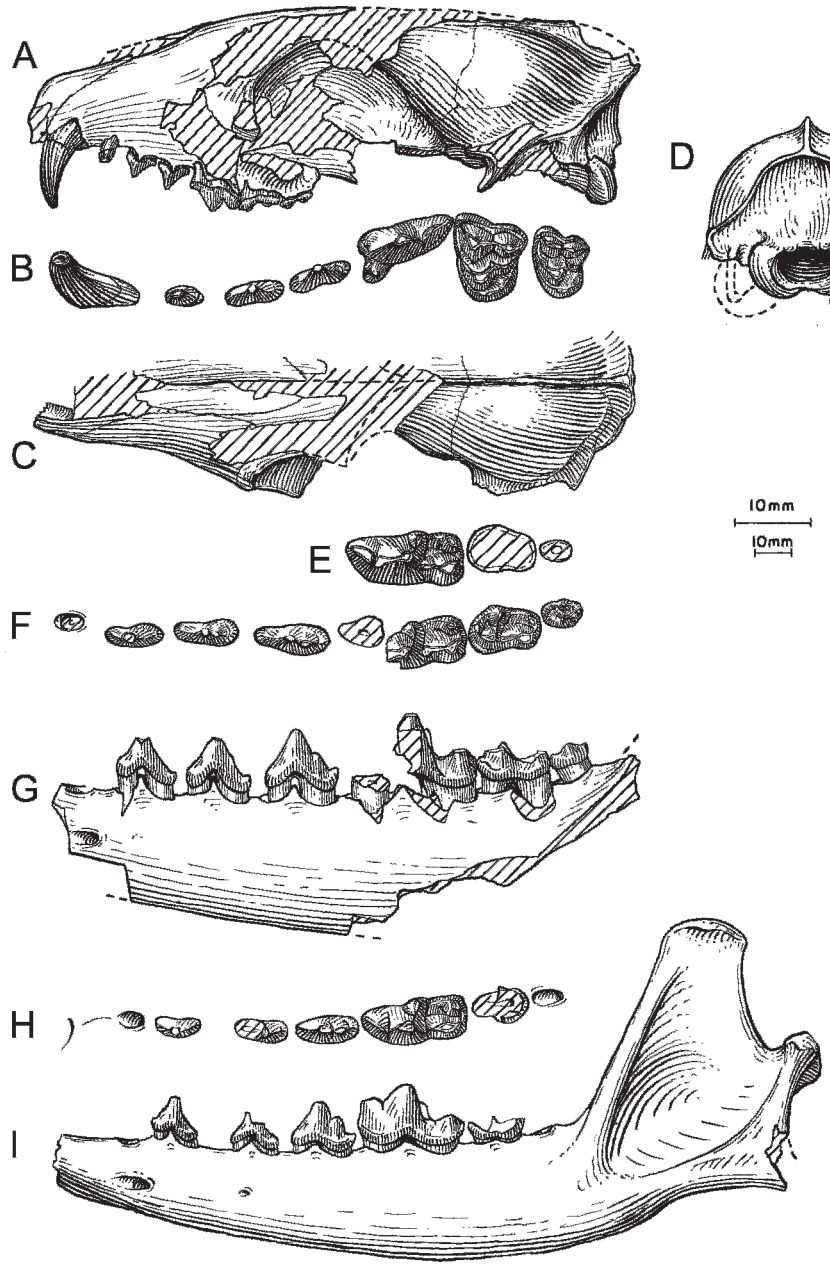

Fig. 25. **A–I**. *Metalopex merriami*, early Hemphillian, Oregon, Nevada, and Nebraska. **A–D**. Type skull, F:AM 49282. **A**. Lateral view, reversed. **B**. Occlusal view, reversed. **C**. Dorsal view, from both sides. **D**. Occipital view, reversed. **E**. Ramal fragment, F:AM 61016. Occlusal view. **F–G**. Ramus, F:AM 49282. **F**. Occlusal view. **G**. Lateral view. **H–I**. Ramus, UNSM 26098. **H**. Occlusal view, reversed. **I**. Lateral view, reversed.

with P2–P3, protocone root of P4, Ft. 48; UNSM 26098, right ramus with c–alveolus, p1–m1 (p2 broken), m2 broken, and m3 alveolus (fig. 25H–I); UNSM 26135, left premaxilla with I1–I3, right and left ramal fragments with c alveolus–p4; UNSM 26136, left m1, Ft. 49. UNSM (unnumbered) right and left rami, right c (alveolus), p1–p3,

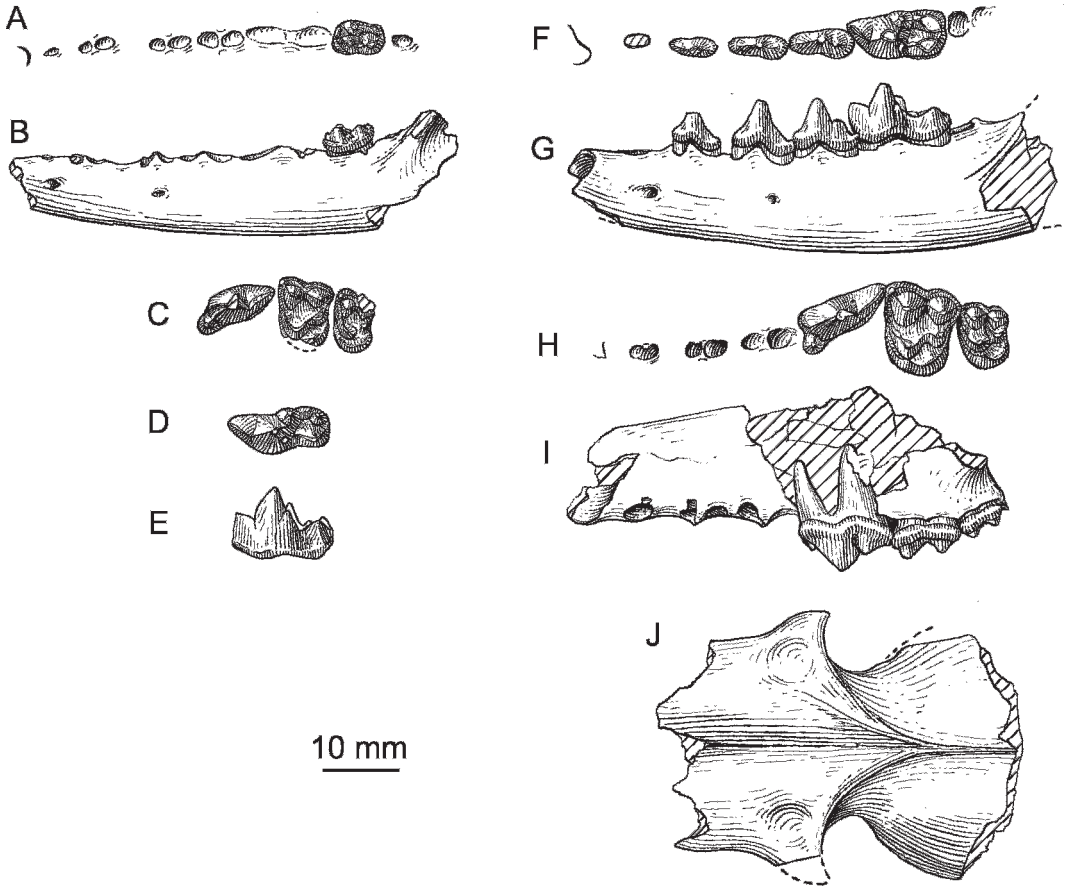

Fig. 26. **A–E**. *Metalopex macconnelli*, late Clarendonian, California. **A–B**. Ramus, UCMP 33707. **A**. Occlusal view. **B**. Lateral view. **C**. Composite view of three isolated teeth: UCMP 112188, p4 occlusal view; UCMP 112191, M1, occlusal view, reversed; UCMP 112194, M2, occlusal view. **D–E**. Lower carnassial, UCMP 112187. **D**. Occlusal view, reversed. **E**. Lateral view, reversed. **F–J**. *Metalopex bakeri*, medial Hemphillian, Texas. **F–G**. Type ramus, F:AM 62970. **F**. Occlusal view. **G**. Lateral view. **H–I**. Maxillary fragment, F:AM 62971. **H**. Occlusal view. **I**. Lateral view. **J**. Skull fragment, F:AM 62970, dorsal view.

anterior half p4, left i1–i3, c, p1 alveolus, p2–p3 broken, Ft. 40.

Distribution: Latest Clarendonian or early Hemphillian of New Mexico, and early Hemphillian of California, Idaho, Nevada, Oregon, and Nebraska.

Diagnosis: Differs from *M. macconnelli* in larger size, wider muzzle, temporal crests joining anterior to frontal parietal suture to form strong sagittal crest; occiput broader with stronger lambdoidal crests; bullae smaller relative to size of skull; I2 with stronger lateral cusplet and stronger lingual cingulum; I3 with stronger medial cusplet, larger lingual shelf, and more laterally compressed; cheek tooth dentition taller crowned; M1 and M2 more quadrate with weaker labial cingulum on paracone of M1; m1 more robust with paraconid more oblique, wider talonid with posterior cingulum extremely weak or absent; m2 larger relative to m1; and m3 trigonid longer relative to length of talonid.

Description and Comparison: In the type skull (F:AM 49282) the premaxilla, maxilla, nasals, and frontals are incomplete and the basicranial area is crushed and broken. The skull is elongate, larger than *V. stenognathus*, and approximates the size of *Eucyon davisi*. Unlike *Vulpes*, the contour of the maxillary surface above P1–P3 is convex as in *E. davisi*.

Furthermore, the skull differs from that of *V. stenognathus* and is similar to *Eucyon davisi* in the wider and more arched palate and the greater dorsoventral height of the maxilla. Unfortunately, the frontals are broken, thus obscuring the maxillary-frontal suture, but the remnants do not contradict an extension of the suture beyond the posterior end of the nasals. A fragment of the frontal with the postorbital process shows the primitive frontal depression adjacent to the process as in *Vulpes*. Moreover, the frontal fragment also reveals that *M. merriami* lacks the frontal sinus seen in *Eucyon*. Enough of the frontals are present to show that the temporal crests join anterior to the parietal suture to form a moderately low sagittal crest similar to that in both *V. stenognathus* and *E. davisi*. In *M. merriami*, the braincase is elongate and expanded. It is markedely wider anterior to the frontoparietal suture than in *V. stenognathus* and *E. davisi*. The supraoccipital shield is broad, with the inion broader than in *V. stenognathus* and similar to that of *E. davisi*. Unlike *Vulpes*, the lambdoidal crests are strong and similar to those of *E. davisi*. The foramen magnum and occipital condyles are larger than in *V. stenognathus* and *Eucyon davisi*, and the mastoid process is knoblike and enlarged as in the Canini. Although the basioccipital area is badly broken, it appears relatively wider than in both *V. stenognathus* and *E. davisi*, and the broken tympanic bullae show that the bullae are small relative to the size of the skull.

A premaxillary fragment (UNSM 26135) has an unworn I2 and I3. The I2 has a well-developed medial and lateral cusplet and the I3 has a well-developed medial cusplet but no lateral cusplet. Both incisors have a lingual cingulum and there is a broad lingual shelf on I3. The complexity of the upper incisors exceeds that of *M. macconnelli*, *E. davisi*, *Leptocyon vafer*, and *V. vulpes*, but the I3 is not enlarged as in the Canini. Compared to both *V. stenognathus* and *E. davisi*, the P1–P3 are smaller relative to the length of the carnassial, more widely spaced, slenderer, and anteroposteriorly shorter and taller crowned. They also lack accessory cusps, but P3 may have a cusp on the posterior cingulum. Morphologically, the P4 closely resembles that of *V. stenognathus* and *E. davisi*, with the anterior border slightly notched due to the projection of the anterobuccal corner and the strong anteriorly directed protocone. The P4, however, is smaller relative to the molars than in both of the above and is more slender than that of *E. davisi*. Unlike *V. stenognathus* and *E. davisi*, the M1 and M2 in *M. merriami* are quadrate in shape, being anteroposteriorly long relative to their width. They are relatively low-crowned, the labial border is strongly indented between the paracone and metacone, there is a prominent labial cingulum, and the small parastyle retains its connection with the preparacrista. The protocone of M1 is relatively large, and a postprotocrista extends to a well-developed metaconule. The hypocone is a long and ridgelike swelling of the posterolingual cingulum, with the cingulum ending posteriorly at or just beyond the metaconule and extending anteriorly to join the anterolingual cingulum across the protocone to the base of the paracone. The M2 of *M. merriami* is even more quadrate than M1 and, like that of *M. macconnelli*, the metaconule is present but there is no postprotocrista connecting it with the protocone. The lingual cingulum extends posteriorly just to the metaconule and anteriorly across the protocone to the paracone.

In *M. merriami* the p2–p4 are slender and tall-crowned for their length, and only p4 consistently possesses a posterior cusp. The p2 is isolated from adjacent premolars by large diastemata as in *M. macconnelli* and species of the *Urocyon* group. The m1 is relatively short and robust with the trigonid shorter relative to the length of the tooth than that of *V. stenognathus* and *E. davisi*. Furthermore, the paraconid is more oblique and the metaconid is stronger and higher relative to the height of the protoconid than in either of these taxa. There is a weak protostylid on m1. The m1 talonid is broad with a relatively low and nearly subequal entoconid and hypoconid. These features of the m1 are accentuated in *M. bakeri*, the youngest member of the *Metalopex* clade. Allowing for wear, the hypoconid is still smaller and lower crowned than that of both *V. stenognathus* and *E. davisi*. A well-developed anterolabial cingulum extends

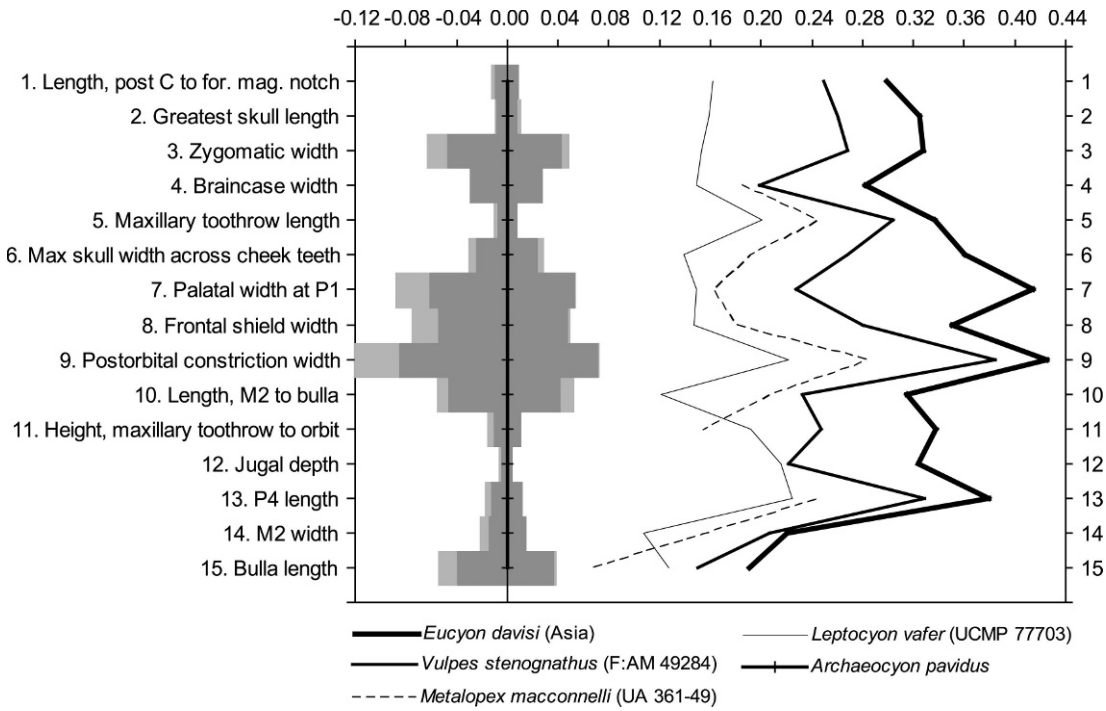

Fig. 27. Log-ratio diagram comparing the proportions of cranial variates (appendix 2) of single skulls of late Miocene Vulpini (*Leptocyon, Metalopex*, and *Vulpes*) and means of near contemporary Canini (*Eucyon*) with the mean of early borophagine *Archaeocyon pavidus* as the standard. Gray bars extending from the mean of the standard are the observed range (light) and $\pm 1\ \sigma$ (dark).

posteriorly across the protoconid and ends on the anterior face of the hypoconid. The m2 trigonid is elongate with a paraconid that is stronger than that of *V. stenognathus*, with the larger metaconid situated slightly posterior to the protoconid. Compared to both *V. stenognathus* and *E. davisi*, the m2 talonid is relatively longer and wider. In *M. merriami* the m3 is also larger and more elongate than that of *V. stenognathus* and *E. davisi*. Moreover, the protoconid and metaconid are distinct subequal cusps that are situated more posteriorly than those of *V. stenognathus* or *E. davisi*, and the trigonid is longer than the talonid.

Discussion: As in the case of *M. macconnelli*, there is considerable variation in size and morphology within and between samples of *M. merriami* from different localities. The fragmentary materials from the Ogallala Group of Frontier County, Nebraska, for example, pertain to four individuals, two of which (UNSM 26098 and 26135) can be usefully measured and are included in appendix 3. The measured specimens are at the extremes of size variation in the dimensions of the lower dentition. The additional materials from the same locality fit in between the measured values, indicating nearly continuous variation. The larger end of the range clearly overlaps the holotype of *M. merriami* (UNSM 521-47 includes alveoli of m1–m3 and these are the size of F:AM 49282). We therefore have referred this material to *M. merriami* despite the near overlap in dimensions of the smallest individuals with *M. macconnelli* and morphological overlap with the more derived *M. macconnelli* specimen (i.e., NMNH 23883).

Except for the Black Hawk Ranch sample of *M. macconnelli*, which foreshadows aspects of the dental morphology of *Urocyon*, the remaining suite of material referred to the two species of *Metalopex* indicates considerable size and morphological intergradation, suggesting anagenetic change from the late

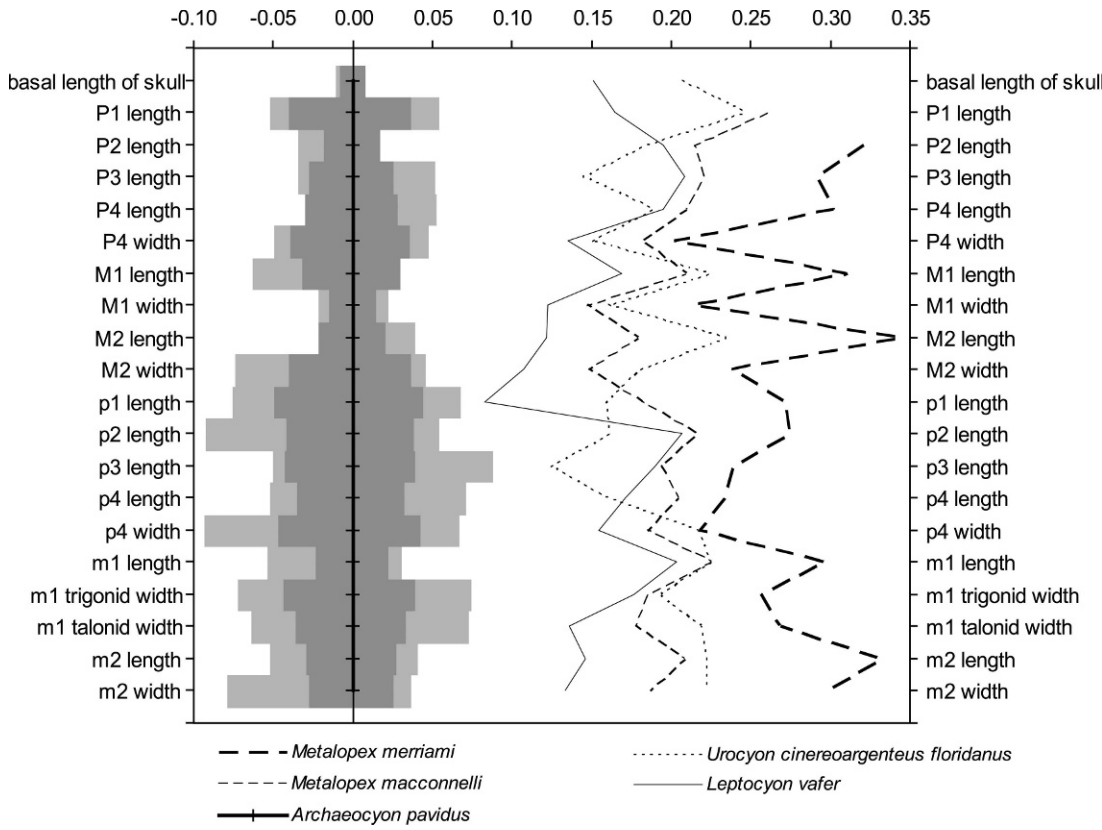

Fig. 28. Log-ratio diagram comparing the means of cheek tooth dimensions (appendix 3) of later vulpines (*Leptocyon*, *Metalopex*, and *Urocyon*) with the mean of the early borophagine *Archaeocyon pavidus* as standard. Gray bars extending from the mean of the standard are the observed ranges (light) and $\pm 1\ \sigma$ (dark).

Clarendonian to the later part of the early Hemphillian (fig. 28). This clade is extended into the medial Hemphillian by *M. bakeri*. What little we know of its morphology seems a clear extension of trends already present in earlier members of the clade.

Metalopex bakeri, new species
Figure 26F–J; appendix 3

Type: F:AM 62970, left partial ramus (fig. 26F–G) with c alveolus, p1 root, p2–p4, mi, m2 alveolus, and associated incomplete frontal (fig. 26J) from the Box T Ranch, Pit 1, Hemphill beds, Ogallala Group (medial Hemphillian), 12 miles northwest of Higgins, Limpscomb County, Texas.

Etymology: Named for C.L. Baker, pioneering geologist of the Cenozoic rocks of the Texas Panhandle early in the 20th Century. His discoveries led to development of the renowned fossil vertebrate faunas of the region.

Referred Materal: F:AM 62971, left maxilla (fig. 26H–I) with C–P3 (alveoli) and P4–M2 from sandy clay, Box T Ranch, West Draw, Hemphill beds, Ogallala Group (medial Hemphillian), 12 miles northwest of Higgins, Limpscomb County, Texas.

Distribution: Only known from the medial Hemphillian of Texas.

Diagnosis: Differs from *M. merriami* in shorter premolars and shorter premolar row without prominent diastemata except those isolating p2; m1 trigonid short, particularly paraconid, talonid markedly wider than trigonid.

Description and Comparison: The dentition of *M. bakeri* is marked by numerous

autapomorphies. The premolars in the type mandibular ramus are markedly shorter and slightly taller crowned than those of *M. merriami*. The p2 is separated from p1 and p3 by short diastemata; the diastemata are shorter than those of *M. merriami*. The m1 is very robust; the width of the talonid is proportionally greater relative to that of the trigonid than in *M. merriami*. This results in a more wedge-shaped carnassial.

The type consists of a mandibular ramus and the dorsal part of the incomplete frontal bone delimited by sutures with adjacent bones anteriorly and posteriorly. These specimens were found associated and are presumed to be one individual. They serve to complement the information on derived *Metalopex* that is missing in *M. merriami*. As in *M. merriami*, the skull is distinguished by the numerous plesiomorphic features. Anterior to the postorbital process the frontals are relatively flat with a prominent depression adjacent to the processes. The depression is small and almost circular in outline, unlike the larger, more elongate frontal depression in most vulpines. Like the latter, the postorbital process is solid, and the frontal sinus is absent. The posterior part of the nasal-frontal suture is shown in this fragment, which indicates that the nasals reached the level of the posteriormost part of the frontal-maxillary suture. The frontals in *M. bakeri* show a marked postorbital constriction, as appears to be the case in *M. merriami*. Like the latter species, the frontal crests join just posterior to the postorbital constriction and well anterior to the frontoparietal suture so that a low sagittal crest is initiated on the frontal bone.

A maxilla (F:AM 62971), referred to *M. bakeri*, shows the alveoli for the canine through P3. Despite the broken condition of the upper canine alveolus, it is evident that the canine was relatively smaller and more compressed than that of *Metalopex merriami*. The alveolus for P1 indicates a relatively robust single root. The alveoli for P2 and P3 are very short anteroposteriorly as in the lower dentition. The P2 alveolus is separated from the alveoli of P1 and P3 by diastemata measuring 3.5 and 2.0 mm, respectively. The spacing of the premolars in the maxilla referred to *M. bakeri* conforms closely to that of the lower premolars in the type. The P4 of *M. bakeri* is elongate and compressed with a rounded anterolabial corner and a weak lingual cingulum. When compared with *M. merriami*, the P4 of *M. bakeri* is similar in form and proportion relative to the molars. Both M1 and M2 are large relative to the carnassial and quadrate in shape as in *M. merriami*. These molars have a low-crowned paracone and metacone and a strong labial cingulum, but the weak parastyle is separated from the preparacrista rather than joined as in *M. merriami*. The M1 has a prominent but low protocone, with the postprotocrista running posteriorly to a well-developed metaconule. The hypocone is anteroposteriorly broad, with the lingual cingulum running laterally to join the labial cingulum at the paracone and ending posteriorly at the metacone. The entire perimeter of the m1 is thus surrounded by a well-developed cingulum. M2 has a large and low protocone and a very small metaconule. As in *M. merriami*, the protocone and metaconule are not connected by the postprotocrista. The hypocone of M2 is also broad anteroposteriorly, and the lingual cingulum extends across the protocone, nearly to the paracone.

Urocyon Baird, 1858

Type Species: *Urocyon cinereoargenteus* (Schreber), 1775.

Included Fossil Species: *U. progressus* Stevens, 1965; *U. minicephalus* Martin, 1974; *U. webbi*, n. sp.; *U. galushai*, n. sp.; and *U. citrinus*, n. sp.

Distribution: Medial Hemphillian to Recent in North America and Recent in Central America and northern South America.

Revised Diagnosis: Differs from other vulpines in the following apomorphies: nasals extend posterior to the frontal-maxillary suture; larger more posterieorly extended depression on dorsal surface of postorbital process accentuated by parasagittal ridges that begin at postorbital processes; frontal crests lyrate, strongly ridged, and joining behind frontoparietal suture; frontal part of braincase more expanded with wider postorbital constriction; medial cusplets on I1–I2 absent; canines with short and little recurved crowns; anterolabial cingulum of P4 often

produced as parastyle; m1 entoconid and hypoconid usually connected by cristids to form transverse crest, hypoconulid relatively large; m2 trigonid shorter with paraconid varying from small (*U. citrinus*) to absent, talonid narrower with hypoconulid varying from distinct cusp to shelf; and in derived species, horizontal ramus with subangular lobe, condyle above alveolar border, and shallow depression ventral to masseteric fossa.

Discussion: *Urocyon* is considered the sister taxon of *Metalopex*. Unlike other vulpines, they have a protostylid on m1 and m2 and a strong labial cingulum on m2 that may be linked with the base of the well-developed protostylid. These synapomorphies are evidence of their phyletic relationship.

As listed in the diagnosis, the morphology of the lower molars of *Urocyon* are more complex, with the consistent presence of the m1 protostylid, the entoconid and hypoconid being generally joined by a transverse crest, and the hypoconulid being larger. The m2 trigonid in *Urocyon* is very short with the paraconid generally absent, although there is a paracristid. In the most derived species of *Urocyon*, there is a shallow depression beneath the masseteric fossa, and a prominent subangular lobe is present, which may be keeled ventrally, strongly angled posteriorly, and spinose.

Urocyon webbi, new species
Figure 29 N–Q; appendix 3

Type: UF 19407, right ramus with c–p1 alveoli and p1–m2 (p3 broken and m3 alveolus, fig. 29N–O) from the Withlacoochee River site 4A (medial Hemphillian), Citrus County, Florida.

Etymology: Named in honor of S. David Webb for his singular contributions to the study of late Neogene mammals of the Americas. We are grateful for his contribution of the type and other important specimens to this study.

Referred Material: From the type locality: UF 19408, right partial maxilla with P3–P4, and M1–M2 alveoli (fig. 29P–Q); UF 20064, left humerus, UF 13859, left radius from the location of the type.

Distribution: Only known from the medial Hemphillian of Florida.

Diagnosis: Differs from species of *Metalopex* in possessing the following apomorphies: P4 with well-developed anterior cingulum and m2 relatively larger with larger paraconid, stronger anterobuccal cingulum and protostylid, and wider talonid with taller crowned entoconid and hypoconid. Great reduction of p2 and associated long diastemata may be autapomorphies for *U. webbi*. *U. webbi* is primitive relative to other species of *Urocyon*, but resembles them in premolar form.

Description and Comparison: The type mandibular ramus of *U. webbi* is larger and more robust than those of other *Urocyon* species and lacks the subangular process so characteristic of them. In *U. webbi* the premolars are anteroposteriorly short, simple, and tall-crowned and remarkably similar to both those of *U. minicephalus* and *U. cineroargenteus floridanus*, with the principal difference being the more robust p4 in *U. c. floridanus*. Comparison of the P4 (UF 19408) of *U. webbi* with that of *U. minicephalus* and *U. c. floridanus* shows that the anterior cingulum is well developed, approaching the condition in *U. c. floridanus*. In *Urocyon minicephalus* there is a distinct parastyle developed from this cingulum.

Like m1, the m2 of *U. webbi* closely resembles that of the type of *U. citrinus*. It is also similar to the m2 of *U. cinereoargenteus scotti*. Primitive features that separate it from *U. citrinus* are a more distinct paraconid and a proportionally smaller metaconid relative to the size of the protoconid. Morphologically, the m2 of *U. webbi* is more like that of *U. c. scotti* than that of *U. minicephalus* and *U. c. floridanus*. It differs from that of *U. c. scotti* in its distinct paraconid, a more anteriorly situated metaconid, and a wider talonid with a well-developed hypoconulid. Compared to the m2 of *U. minicephalus*, that of *U. webbi* is more primitive in being more elongate with the outline of the lingual border less convex. Moreover, the m2 of *U. webbi* also has a distinct paraconid, and the protoconid and metaconid are relatively smaller and situated more posteriorly than in *U. minicephalus*. In *Urocyon webbi*, *U. citrinus*, *U. minicephalus*,

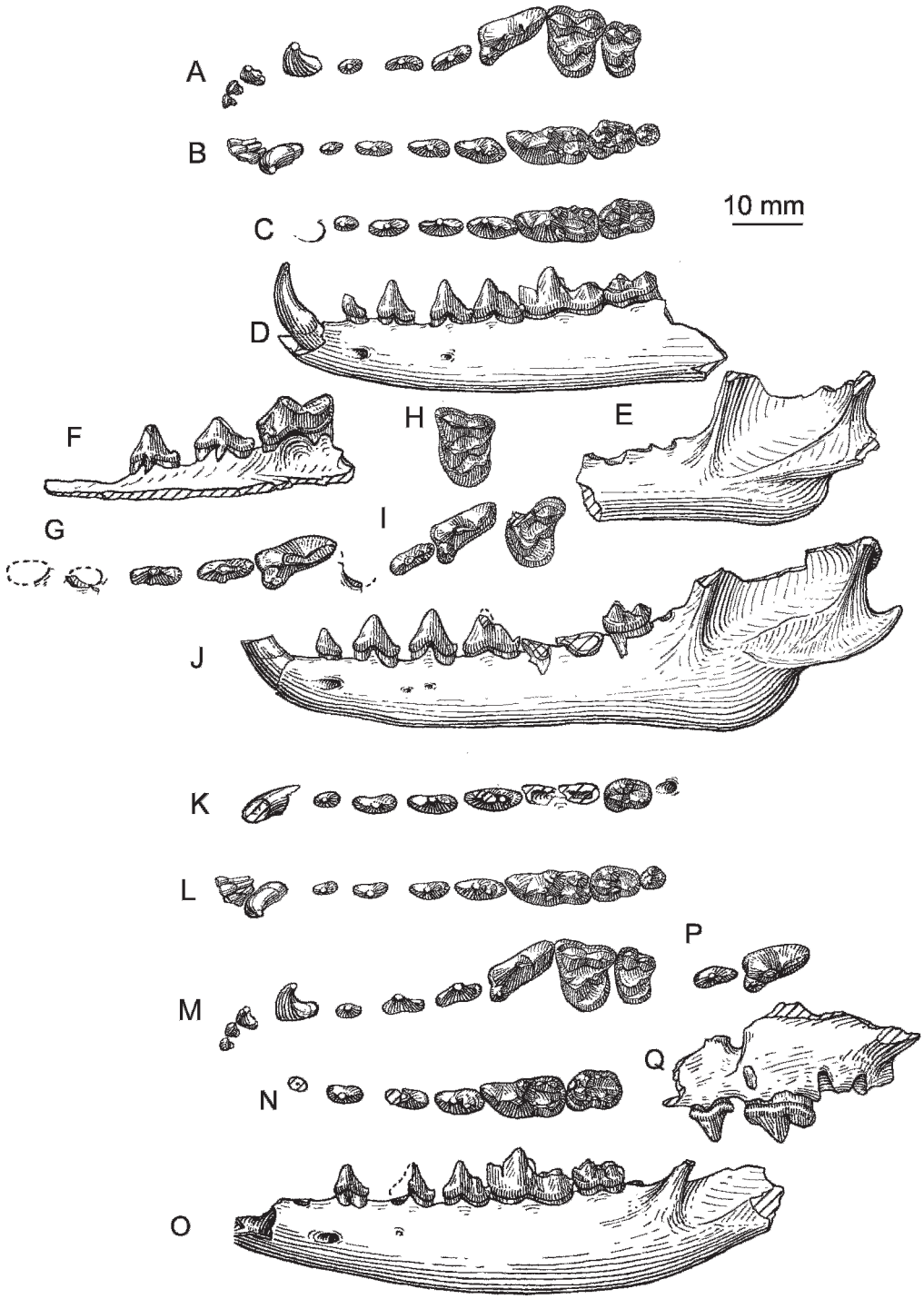

Fig. 29. **A–B**. *Urocyon cinereoargenteus floridanus*, AMNH(M) 183978, Recent, Georgia. **A–B**. Upper and lower dentitions. Occlusal views. **C–E**. *Urocyon citrinus*, early Irvingtonian, Florida. **C–D**. Type ramus, UF 18060. **C**. Occlusal view, reversed. **D**. Lateral view, reversed. **E**. Ramal fragment, UF 18061. Lateral view, reversed. **F–G**. *Urocyon* sp. cf. *U. progressus*, UCMP 112182, early Blancan, Kansas. **F**.

and *U. cinereoargenteus floridanus* the m2 anterobuccal cingulum is well developed and extends posteriorly across the protoconid to terminate near the well-developed protostylid. *Urocyon c. scotti* from the southwestern United States retains some of the primitive features found in *U. webbi*. The protostylid on both m1 and m2 in *U. c. scotti* is relatively weak. Furthermore, the m2 trigonid in *U. c. scotti* is relatively longer with a stronger paraconid crest than in the southeastern taxa of *U. citrinus*, *U. minicephalus*, and *U. c. floridanus*.

The mandibular ramus of *U. webbi* is similar in general shape to that of *Urocyon*, but it lacks the subangular lobe. Compared with other species of *Urocyon*, the horizontal ramus is relatively deeper and markedly deeper beneath p1 and p2. A short diastema isolates p1 from the canine, and a longer diastema isolates the p2. Although the ascending ramus is broken, enough is present to indicate that the masseteric fossa is deep but it lacks the shallow depression ventral to the fossa shown in other *Urocyon* species.

A humerus (UF 20064) is referred to *U. webbi*. It is comparable to that of *U. cinereoargenteus* except for a smaller entepicondyle and a smaller facet on the trochlea for the articular surface for the capitilum of the radius. In keeping with the latter, a referred radius (UF 13859) is longer and decidedly more slender than that of similar-sized individuals of living *Urocyon*.

Urocyon progressus Stevens, 1965
Fig. 29F–G

Urocyon progressus Stevens (in part), 1965: 265, fig. 1A–B.
Urocyon progressus: Bjork, 1974: 25, fig. 2a.

Type: UMMP 37157, left parietal bone, from Rexroad locality 3, Rexroad Formation (early Blancan), Meade County, Kansas. Figured by Stevens, 1965: fig. 1B.

Referred Material: From the type locality: UMMP 37158, incomplete left tibia, figured and nominated paratype by Stevens (1965: fig. 1A), and V56767, edentulous right partial maxilla and jugal, figured by Bjork (1973: fig. 2a). UCMP 112182, right partial maxilla with P1 alveolus and P2–P4 and cranial fragment (fig. 29F–G); and UMMP 37156, left M1, figured and designated a paratype by Stevens (1965: fig. 1C).

Distribution: Only known from the early Blancan of Kansas.

Discussion: The diagnosis given by Stevens (1965: 265) cannot be used to characterize the species, and no additional material has been found that would permit a revision. As discussed by Stevens (1965: 265), the length of the type parietal bone (45.0 mm) is greater than that of the recent *U. cinereoargenteus*. Stevens also stated, ''The maximum distance from the sagittal suture of the fossil parietal to the outer edge of the temporal ridge, at the greatest external curvature, is 12.8 mm.'' This distance is within the range of the living gray fox but greater than that of *U. minicephalus*.

Bjork (1973: 25, fig. 2a) refered a partial maxilla and jugal to *U. progressus*. This specimen was from the type locality and Bjork stated that it may belong to the same individual as the type. The identification of *Urocyon* in the Rexroad Formation is further strengthened by Bjork's observation that the ''maxillojugal suture … is relatively straight as in *Urocyon* which distinguishes it from all other modern genera of canids.''

The right maxillary fragment, UCMP 112182 (fig. 29F–G), also from the type locality, shows the presence of a small midlingual root on both P2 and P3. This variant is occasionally seen in living popula-

←

Lingual view, reversed. **G**. Occlusal view, reversed. **H–K**. *Urocyon galushai*. **H**. JWTU (uncataloged), Cita Canyon beds, late Blancan, Texas. Upper first molar. Occlusal view, reversed. **I–K**. Type, associated maxillary fragment and ramus, F:AM 63104, Irvingtonian, Arizona. **I**. Occlusal view. **J**. Lateral view. **K**. Occlusal view, reversed. **L–M**. *Urocyon cinereoargenteus scotti*, AMNH(M) 136416, Recent, Texas. Occlusal views of upper and lower dentitions. **N–O**. *Urocyon webbi*, medial Hemphillian, Florida. **N–O**. Type ramus, UF 19407. **N**. Occlusal view, reversed. **O**. Lateral view, reversed. **P–Q**. Maxillary fragment, UF 19408. **P**. Occlusal view, reversed. **Q**. Lateral view, reversed.

tions of *Urocyon* (e.g., on left P3 of AMNH(m) 29448). The broken alveolus for P1 indicates a relatively large tooth, and the P1–P2 diastema is also long (5.0 mm). The P4 (length 11.8 mm) is short and broad with a continuous lingual cingulum and anterior cingulum and salient protocone as in *Urocyon*. Although it is larger than most living populations of *Urocyon* and smaller than the range of 53 individuals of *Vulpes* vulpes coming from Alaska to Georgia, it is approached by its near contemporary *U. galushai* from Arizona.

Because of the fragmentary nature and questionable association of the material assigned to this species, it cannot be diagnosed. However, the type parietal bone shows the separated and raised parasagittal crests that are a synapomorphy for *Urocyon* species, and the materials listed here from Rexroad locality 3 form a plausible association that may be confirmed by future discovery.

Urocyon galushai, new species
Figure 7, 29H–K; appendix 3

Urocyon atwaterensis Getz, 1960: 363 (nomen vanium).
Urocyon cf. *progressus* Akersten, 1970: 19.
Urocyon sp.: Dalquest, 1978: 287.

Etymology: Named in honor of the late Ted Galusha, Frick Curator Emeritus, American Museum of Natural History, who collected the holotype and many of the specimens used in this review.

Type: F:AM 63104, right and left partial mandibular rami with c (broken)–m2 (m1 broken and m3 alveolus), maxillary fragment with P3, isolated P4 and M1 (broken), partial scapula, distal end humerus, proximal part of ulna, distal end of tibia, right calcaneum and left partial calcaneum, proximal ends of metatarsals II, IV, and V, and distal end of a metapodial from the 111 Ranch (Dry Mountain) locality (late Blancan latest Gauss Chron and 4 m below correlated Mount Blanco Ash Bed, 2.32 ± 0.15 Ma, Galusha et al., 1984), San Simon Valley, Graham County, Arizona.

Referred Material: Red Light Local Fauna, Love Formation (late Blancan, Akersten, 1970), southeastern Hudspeth County, Texas: TMM 40855-15, partial left ramus with alveoli for p4–m3*.

Beck Ranch Local Fauna, 10 miles east of Snyder (early Blancan fide Dalquest, 1978), Scurry County, Texas: MSU 9475, right P4*; MSU 9476, left P4*; MSU 8569*, left m2*; MSU 9474, left p4*.

Cita Canyon beds (late Blancan), Randall County, Texas: JWTU (uncataloged), M1 (fig. 29H) and broken upper canine.

Vallecito Creek, Upper Diablo-Tapiado Wash, LACM locality 6856, Palm Springs Formation (Blancan), San Diego County, California: LACM 17210, crushed anterior part of skull with I3–P4 represented by alveoli and roots.

LACM locality 1298, Geomys Bed, zone 55.0, Palm Springs Formation (early Irvingtonian), San Diego County, California: LACM 3839, left partial ramus with p1 (root)–m1 all broken, m2 and m3 alveolus. LACM locality 6814, Palm Springs Formation (early Irvingtonian), San Diego County, California: LACM 53678, left partial ramus with m1 (broken), m2, and m3 (alveolus).

Distribution: Early to late Blancan of Texas, late Blancan of Arizona and California, and early Irvingtonian of California.

Diagnosis: Autapomorphies that distinguish *U. galushai* are: elongate and deep horizontal ramus, p1–p2 large relative to other teeth, and ascending ramus with wide separation of condyloid crest and masseteric line.

Differs from *Urocyon citrinus* in derived features: large premolars; smaller m2 with shorter trigonid, shorter paracristid, and shorter talonid lacking both entoconulid and distinct hypoconulid. Differs from *U. minicephalus* and *U. cineroargenteus* in larger, taller crowned premolars; m2 more elongate, narrower, longer trigonid, better developed paracristid, weaker anterobuccal cingulum, weaker protostylid; elongate horizontal ramus; ascending ramus with greater separation between condyloid crest and masseteric line; and more rounded subangular lobe.

Description and Comparison: The type mandibular ramus of *U. galushai* is elongate with a comparatively deep horizontal ramus. It is larger than that of *U. minicephalus* and is also larger than the average for *U. cinereoargenteus*. The ascending ramus is broken

and missing above the level of the coronoid process, but enough is present to show that the lateral surface is marked by a greater separation of the condyloid crest and masseteric line. The angular process is also large in these specimens, but the process is attenuate and hooked distally (fig. 29J) and the insertions of the pterygoid musculature have the primitive form seen in other vulpines. Both the type of *U. galushai* from Arizona and the similar-sized referred mandible from the Blancan of Texas have a rounded subangular lobe with a rugose medial surface rather than the abruptly projecting subangular process characteristic of later *Urocyon*.

The lower premolars are relatively larger, more elongate, and taller crowned than in *U. minicephalus* and *U. cinereoargenteus*. The m2 in *U. galushai*, as in *U. citrinus*, is primitive and similar to that of *U. cinereoargenteus scotti* and unlike that of *U. c. floridanus* and *U. minicephalus*. Compared to the two latter taxa, the m2 of *U. galushai* and *U. c. scotti* is more elongate and less complex. The protoconid and metaconid are relatively smaller and situated more posteriorly with the paraconid either a small cusp or a distinct cristid. Moreover, the m2 is less robust, has a narrower talonid, and the anterolabial cingulum and protostylid are both weaker than in *U. c. floridanus* and *U. minicephalus*.

In addition to the Blancan mandibular fragment described by Akersten (1970: 19), an isolated M1 and broken canine from the Cita Canyon beds in the Panhandle-Plains Historical Museum collection are also referred to *U. galushai*. The M1 (JWTU uncataloged, fig. 29H) differs from that of the type of *U. galushai* in its weaker labial cingulum at the base of the metacone and its relatively larger hypocone. The hypocone is anteroposteriorly longer and higher crowned, differing from the M1 referred to *U. progressus* in the same way. Although the lingual cingulum narrows at the anterior base of the protocone, it is much stronger than that of the type M1 of *U. galushai* or *U. progressus*, and the cingulum is continuous across the labial surface of the protocone. Despite the above differences, the Blancan M1 from Texas is referred to *U. galushai* because an examination of a recent population of *U. c. floridanus* from Thomas County, Georgia, showed that the M1 is variable in these same feataures. Unfortunately, no comparison can be made with any corresponding elements of *U. citrinus*. Hence, the most diagnostic of the Blancan specimens from Texas is the mandibular fragment with rounded subangular lobe that is similar to that of *U. galushai* and unlike the sharply angled subangular lobe of living *Urocyon*.

Of the four isolated teeth from the Beck Ranch, the m2 is the most diagnostic. It is smaller than that of the type of *U. galushai* and morphologically like that of *U. c. scotti*. The m2 is elongate and slender and less robust and less complex than that of *U. c. floridanus*. Compared to the latter, the protoconid and metaconid are smaller and situated less anteriorly with a well-developed paracristid. The anterolabial cingulum is small and the protostylid weak as in *U. galushai* and similar to that in *U. c. scotti*.

Discussion: Getz (1960: 363) based *U. atwaterensis* on a M2 from the Borchers Local Fauna (late Blancan), Meade County, Kansas, and stated, "The M2 has a well developed cingulum and is wider than Recent forms. A small cusp is present between the protocone and metacone." It can be demonstrated with a series of recent specimens of *U. cinereoargenteus* that the strength of the cingulum on M2 is somewhat variable, as in the development of the metaconule ("the small cusp between the protocone and metacone"). *U. atwaterensis* is therefore considered a nomen vanum.

U. galushai appears more derived than the later occurring *U. citrinus* athough they share a rounded subangular lobe. When compared with *U. minicephalus* and *U. cinereoargenteus floridanus*, it is primitive in most characters that can be observed. On the other hand, *U. galushai* is unique in its elongate horizontal ramus with large anterior premolars and the presence of a widely separated condyloid crest and masseteric line. These characters serve to isolate it from other species of *Urocyon*.

Urocyon citrinus, new species
Figure 29C–E; appendix 3

Type: UF 18060, right (fig. 29C–D) and left partial rami with parts of i1–i3 alveoli

and c–m2 from Inglis site 1A (early Irvingtonian), Citris County, Florida.

Referred Material: From the type locality: UF 18061, right mandibular fragment with m1 broken alveolus, m2 and m3 alveoli, and angle of mandible with subangular lobe (fig. 29E); UF 18062, right calcaneum; UF 18063, proximal end left tibia; and UF 18064, right metatarsal IV from the type locality.

Distribution: Only known from the type locality, early Irvingtonian of Florida.

Diagnosis: A synapomorphy that *U. citrinus* shares with *U. galushai* is rounded subangular lobe on the mandibular ramus. Pleistocene and Recent species of *Urocyon* have a distinctly angular subangular process. We have been unable to recognize any autapomorphies for this taxon, although it clearly belongs to the genus as discussed below.

Differs from *U. galushai* in the following plesiomorphies: smaller premolars, and larger m2 with longer trigonid, stronger paracristid and small paraconid, longer bicuspid talonid with entoconulid, and distinct hypoconulid. Differs from *U. minicephalus* in the following plesiomorphies: less robust p4; m1 more elongate; and m2 relatively larger, trigonid longer, paraconid small, and talonid longer with distinct entoconulid. Differs from *U. c. floridanus* in the following plesiomorphies; slenderer p4; m1 narrower, metaconid relatively smaller, protostylid weaker, entoconulid stronger; and m2 lingual border less convex and buccal border less concave, trigonid longer, paracristid stronger, metaconid and protoconid smaller with protoconid situated more posteriorly and nearly opposite metaconid; and talonid relatively wider. Differs from *U. c. scotti* in the following plesiomorphies: larger m2 with longer trigonid, stronger paracristid, and small paraconid, and wider talonid.

Description and Comparison: The dentition of the type mandibular ramus of *U. citrinus* has characters in common with both *Urocyon webbi* and *U. minicephalus*. The lower premolars of *U. citrinus* are anteroposteriorly short and tall-crowned and resemble those of both *U. webbi* and *U. minicephalus*. The p4 of *U. citrinus* is less robust than that of the latter. The premolars, however, are more evenly and closely spaced. In both *M. macconnelli* and *U. webbi* the p2 is separated from p1 and p3 by an unusually long diastema (see fig. 29N).

Although the m1 of *U. citrinus* is less robust than that of *U. webbi*, it is similar in length and unlike the shorter proportioned m1 of *U. minicephalus*. Moreover, the m1 protostylid in *U. citrinus* is stronger and comparable to that of *U. minicephalus*. As in *U. webbi*, the m1 talonid in *U. citrinus* is elongate but the entoconid and hypoconid are transversely connected, a derived feature that is shared with *U. minicephalus* and recent taxa. A hypoconulid or hypoconulid shelf is present as in both *U. webbi* and *U. minicephalus*.

The elongate m2 of the type of *U. citrinus* is primitive and closely resembles that of *U. webbi*. As in the latter, the m2 protoconid and metaconid are situated posteriorly and the trigonid is long. A tiny paraconid lies at the end of the paracristid in a more labial position than in *U. webbi*. Furthermore, in both *U. webbi* and *U. citrinus* the m2 talonid is long with a small entoconulid, a distinct entoconid and hypoconid, and a small hypoconulid. From the above description it is evident that the m2 of *U. citrinus* has numerous morphological features in common with *U. webbi*, all of which are primitive. A strong anterobuccal cingulum on the m2 of *U. citrinus* extends posteriorly to a well-developed protostylid, a derived feature present in some individuals of *Metalopex macconnelli* as well as *Urocyon* species.

Interestingly, most of the above primitive features of the m2 of *U. citrinus* are shared to some degree with the living western gray fox, *U. cinereoargenteus scotti* (fig. 29L). The m2 of *U. c. scotti* is also rather elongate and less complex than that of *U. c. floridanus* (fig. 29B). The m2 protoconid and metaconid tend to be smaller and situated more posteriorly, somewhat similar to that of *U. citrinus*, with either a small paraconid or a strong paracristid running forward from the protoconid. In general, the m2 in *U. c. scotti* is less robust, with both the anterolabial cingulum and the protostylid weaker than in *U. minicephalus* and *U. c. floridanus* and more like that of *U. citrinus*.

The mandibular ramus of *U. citrinus* is similar to that of *U. minicephalus*. A frag-

mentary mandibular ramus (UF 18061, fig. 29E) from the type locality has a rounded subangular lobe that is an inwardly turned sharp ridge ventrally as in species of *Urocyon* except *U. galushai*.

Discussion: The type of *U. citrinus* resembles the type of *Urocyon webbi*, but this is due, for the most part, to retention of primitive features of the *Urocyon* group. Emphasis is placed on the derived morphological features that *U. citrinus* shares with other species of *Urocyon*, such as: the presence of a transverse crest joining the m1 entoconid and hypoconid, the presence of an m1 hypoconulid, and the well-developed mandibular subangular lobe. Interestingly, the dentition of *U. citrinus* most closely resembles that of *U. c. scotti* among living gray fox populations, a fact that suggests that this western race retains primitive dental features that were lost or modified in the evolution of the eastern race since the early Pleistocene.

Urocyon minicephalus Martin, 1974
Figure 7, 30; appendices 2, 3

Type: UF 13146 (fig. 30A, D–E), nearly complete skull except for premaxillaries, broken nasals and zygomae, with P1–M2 from Coleman IIA Loal Fauna (late Irvingtonian), Sumter County, Florida.

Referred from the Type Locality: UF 67849 and 67852, two left maxilla with P4–M1; UF 67851, left premaxilla and partial maxilla with I1–I3 alveoli, C–P2; UF 67850, left partial maxilla with P4–M2; UF 13148, left partial premaxilla and maxilla and right partial maxilla with P3–P4 and detached teeth of two or more individuals including two right upper P4s; UF 13143* and 67848*, two postorbital crania; UF 67855*, right edentulous ramus; UF 67863*, left posterior part of ramus; UF 67856, left partial ramus with p1 alveolus–m2; UF 67854, right ramus with C, P1–P2 alveoli, P3–M2, m3 alveolus; UF 13140 (Fig. 30B–C), right partial ramus with c, p1–p2 alveoli, p3–p4, m1–m2, and m3 alveolus; UF 67858, left partial ramus with p2–m1; UF 67857, left partial ramus with p2–m1; UF 67857, left partial ramus with p3 (broken)–m2; UF 67861*, left partial ramus with i1–i3 alveoli, c–p1, and p2–p3 alveoli; UF 67862*, left partial ramus with p2 and c–p1, and p3–m2 alveoli; UF 67859, left partial ramus with m1 and m2–m3 alveoli; UF 67860, left partial ramus with p2–p4 and c–p1, p3, and m1 all alveoli; UD 67853, right ramus with c–p1 alveoli, p2–m1, and m2–m3 alveoli.

McLeod Lime Rock Mine, Smith Pit, pocket "A" (late Irvingtonian), Levy County, Florida: F:AM 67296, left partial maxilla with P4; F:AM 67297, right ramus with c–m1 and m2–m3 alveoli; F:AM 95190, partial scapula; F:AM 68024, left humerus; F:AM 68024A, left humerus; F:AM 68024B, left partial humerus; F:AM 68024C, right radius; F:AM 68024D, left partial radius; F:AM 68024E, right distal part of tibia: F:AM 68024G, right calcaneum.

Distribution: Only known from the late Irvingtonian of Florida.

Revised Diagnosis: Derived relative to *U. progressus* in shorter parietals. Differs from *U. citrinus* in possessing the following apomorphies: m1 less elongate, and m2 relatively smaller with shorter trigonid, paraconid absent, and shorter and angled subangular lobe. Differs from *U. galushai* in the following apomorphies: smaller, lower crowned premolars; m2 trigonid shorter, smaller paraconid shelf, stronger anterolabial cingulum, stronger protostylid; and mandibular ramus less elongate with less expanded masseteric fossa and angled subangular lobe. Differs from *U. cinereoargenteus floridanus* in the following plesiomorphies: smaller skull, narrower frontals, greater postorbital constriction, narrower braincase, less widely separated frontoparietal crests, narrower occiput; M1 with lower crowned paracone and metacone, weaker labial cingulum, smaller paraconule; smaller metaconule; m1 protostylid weaker; and m2 metaconid less posterior and almost directly opposite protoconid, protostylid weaker. Differs from *U. c. scotti* in the following plesiomorphies: smaller skull with relatively wider muzzle, narrower frontals, greater postorbital constriction, narrower braincase, less lyrate parasagittal crests, narrower occiput. Apomorphies that distinguish *U. minicephalus* from *U. c. scotti* are: P4 stronger protocone, stronger anterolabial cingulum; M2 metaconule greatly reduced or absent; and m2 less elongate,

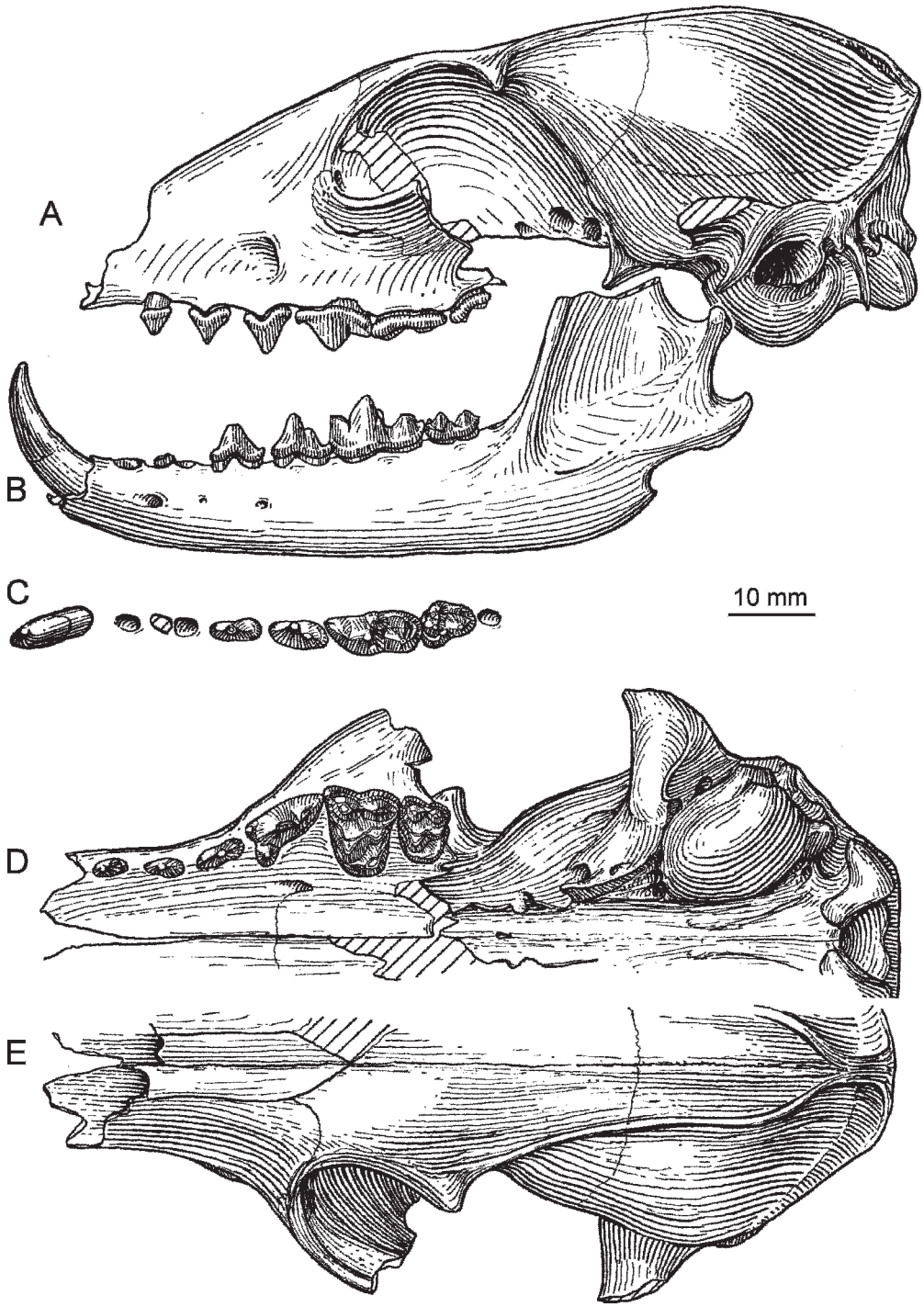

Fig. 30. **A–E**. *Urocyon minicephalus*, late Irvingtonian, Florida. **A**. Type skull, UF 13146, lateral view. **B–C**. Ramus, UF 13140. **B**. Lateral view, reversed. **C**. Occlusal view, reversed. **D–E**. Type skull, UF 13146. **D**. Palatal view. **E**. Dorsal view.

relatively wider, shorter trigonid, stronger anterolabial cingulum, stronger protostylid.

Description and Comparison: Martin (1974: 70) described the skull of *U. minicephalus* as differing from the living gray fox "in the relatively closely allied sagittal crests and narrower occiput." Additional primitive characters that distinguish the skulls of *U. minicephalus* from those of *U. c. floridanus* are wider muzzle, narrower frontals, and a less expanded braincase. The upper dentition of *U. minicephalus* is very similar to that of *U. c. floridanus* except the P4 in which the protocone is larger than the average Florida gray fox and the anterolabial cingulum is stronger. In the P4 of the type of *U. minicephalus* this cingulum is produced into a small, but distinct, parastyle that is present in some of the living gray foxes examined. The M1 and M2 of *U. minicephalus* are more primitive in being more complex than those of *U. c. floridanus* with a smaller paraconule of both upper molars, and the M2 bears a small metaconule.

The lower dentition of *U. minicephalus* averages smaller than that of *U. c. floridanus*, and the m1 is primitive in being less robust with a weaker protostylid. Two jaws (UF 67855, 67856) of *U. minicephalus* with unworn m2s have an extremely short trigonid with the metaconid directly opposite the protoconid. In contrast, the more apomorphic m2 in *U. c. floridanus* has a larger metaconid that is situated slightly posterior to the protoconid, making the trigonid longer and the lingual border of m2 more convex.

The morphology of the lower dentition of *U. minicephalus* is more like that of *U. c. floridanus* than that of *U. c. scotti* or even *U. citrinus* from the early Irvingtonian of Florida. The premolars, especially p4, of *U. minicephalus* are more robust, and the p2–p3 diastema is shorter than in the type jaw of *U. citrinus*. Except for a slightly stronger protostylid, the m1 is very similar to that of *U. citrinus*. Derived features separating *U. minicephalus* from *U. citrinus* are seen in the m2, which in *U. minicephalus* is less elongate with the trigonid shorter and the paraconid absent. Furthermore, the talonid in *U. minicephalus* is also shorter and lacks the distinct entoconulid.

No morphological features were observed to distinguish the limbs of *U. minicephalus* from the McLeod Lime Rock Mine from those of *U. cinereoargenteus*.

Discussion: Although the morphology of the skull of *U. minicephalus* is primitive and differs markedly from that of *U. c. floridanus*, the dentition is derived and very similar to that of the latter. The dentition of the late Irvingtonian *U. minicephalus* is more like that of the recent eastern race of the gray fox than that of the more primitive *U. citrinus* from the early Irvingtonian of Florida or the living western race, *U. c. scotti*.

Tribe Canini Fischer de Waldheim, 1817

The living dogs, wolves, coyotes, jackals, and so-called foxes or zorros of South America were morphologically characterized as the sister group of the Vulpini at branching-point H in figure 2 of Tedford et al. (1995). The critical features that mark the Canini as a monophyletic group include the consistent enlargement of the frontal sinus, often accompanied by the correlated loss of the depression in the dorsal surface of the postorbital process; the posterior expansion of the paroccipital process; the enlargement of the mastoid process; and the lack of lateral flare of the orbital border of the zygoma.

In this work we assume the monophyly of the South American Canini based on our previous investigation (Tedford et al., 1995) while acknowledging the contradictions posed by biomolecular systematic work (Wayne et al., 1997) regarding the polyphyly of some taxa. The core taxa within the "South American foxes" of Wayne et al. (1997) remain phyletically associated in combined analysis of morphologic and molecular evidence (Wayne et al., 1997: fig. 7). The most parsimonious combined evidence tree is reasonably robust in bootstrap analysis, and its form contains groups of sister taxa common to both approaches.

Beyond the early appearance of a clade of large hypercarnivores (*Protocyon* and *Theriodictis*; Berta, 1988) related to the recently extinct Falkland Island fox (*Dusicyon australis*), the South American fossil record adds little information on phylogeny other than

that contributed by the living taxa. The span of this record approximates the latest Pliocene and Pleistocene (Tonni et al., 1992, 1999) and is largely restricted to Andean and southern South America (Berta, 1987). Amazonian records are limited to the latest Pleistocene.

We have, however, been able to recognize fossil species in North America that can be placed in or close to living species of *Cerdocyon* and *Chrysocyon*, and possibly the extinct *Theriodictis*, that indicate these South American forms had representatives in the Northern Hemisphere in the earliest Pliocene and early Pleistocene, respectively. This evidence implies that clades within the South American Canini were forming in northern latitudes well before 3 Ma when the opportunity to move south across the Panamanian Isthmus first arose (Keigwin, 1978). Taxa identified as *Canis* sp. and *Pseudalopex* sp. appear first in Argentina (Tonni et al., 1992), and by the earliest Pleistocene most of the South American clades are in place. Sequence divergence data for the South American canids (Wayne et al., 1997) leads to similar conclusions regarding the appearance of this fauna. Similarly, *Nyctereutes* appears in eastern Asia at the beginning of the Pliocene (Tedford and Qiu, 1991), indicating westward expansion of this putative South American clade into the Old World before the opportunity to invade South America arose. Because of strong evidence from morphology and history we have formalized the ''South American canids'' as a new subtribe, Cerdocyonina, to emphasize its probable monophyly.

The phylogenetic analysis presented herein shows that species of the extinct genus *Eucyon* Tedford and Qiu (1996) have a sister relationship to all other species of *Canis* rather than lying at the base of the Canini. This clade (subtribe Canina, new rank) was restricted to North America for most of the late Miocene, but in the latest Miocene *Eucyon* appeared in Europe (*E. monticinensis* Rook, 1992) and by the early Pliocene achieved a Holarctic-wide distribution with local centers of evolution yielding endemic Old World species (e.g., *E. zhoui* Tedford and Qiu, 1996) and taxa of higher rank (e.g., *Nurocyon* Sotnikova, 2006).

The Canina also contains species of *Canis*, *Cuon*, *Lycaon*, and *Xenocyon*. *Canis* expanded its range to Eurasia early in the Pliocene and by the Pleistocene was present in Africa as well. Its species arose in many quarters of the Old World, with those present in arctic Beringia eventually extending their ranges southward during the Pleistocene into mid-latitude North America to augment the autochthonous canid fauna. *Cuon* and *Xenocyon* were rare visitors to North America during the Pleistocene, and the presence of species of these Old World genera has been mentioned by Repenning (1967) and Youngman (1993).

Subtribe Cerdocyonina, new subtribe

The recognition of the monophyly of the South American canids (except *Urocyon* and *Canis*) and the inclusion with them of the Eurasia *Nyctereutes*, the ''raccoon-dog'' has made the erection of the Cerdocyonina a plausible taxonomic statement (Tedford et al., 1995). These taxa, representing diverse adaptations, can be diagnosed by the following synapomorphies: angular process of the mandible wide, may lack hooklike termination, expansion accommodates widened insertions for pterygoid muscle segments, especially that for the medial branch of the internal pterygoid; posterior cusp of p3 weak or absent; and m1 hypoconid and entoconid, joined by cristids.

The Cerdocyonina lacks the strongly arched zygoma and often the second posterior cusp on p4 between the cingulum and the large first cusp, which marks them as primitive relative to *Eucyon* and its sister taxon the subtribe Canina, which shares these synapomorphies.

Cerdocyon Smith, 1839

Carcinocyon J. A. Allen, 1905.

Type Species: *Cerdocyon thous* (Linnaeus), 1766.

Included Species: *C. texanus*, new species, and *Cerdocyon*? *avius* Torres and Ferrusquía, 1981.

Distribution: Tropical South America (see Langguth, 1969: fig. 1 for map) for *C. thous* and closely allied late Pleistocene forms,

earliest Pliocene of New Mexico and Texas for *C. texanus*, and early Pliocene of Baja California Sur for *C.*? *avius*.

Revised Diagnosis: As indicated by Tedford et al. (1995), the synapomorphy that unites *Cerdocyon* with *Atelocynus* and *Speothos* and distinguishes it from more plesiomorphic South American Canini (*Dusicyon*, *Pseudalopex*, and *Lycalopex*) is the further expansion of the angular process of the mandible and enlargement of the fossa for the inferior ramus of the median pterygoid muscle. Additionally, other synapomorphies specifically unite *Cerdocyon* and its sister taxon *Nyctereutes* such as presence of a subangular lobe of the mandible and short and recurved canines of small diameter. *Cerdocyon* differs from most cerdocyonines in that its palate does not extend behind the toothrow. The same is true for fossil species of *Nyctereutes*, but in the living *N. procyonoides* the palate is long.

Discussion: *Cerdocyon texanus*, and to a lesser extent *C.*? *avius* (Torres and Ferrusquía, 1981), possesses derived dental and mandibular features that are unlike any other members of the North American Canina but are shared with *Cerdocyon* and, in some instances, other South American canids and Eurasian *Nyctereutes*. The North American fossil taxa referred to *Cerdocyon* are morphologically similar to *C. thous* in that they share the following derived characters: canines short and strongly curved backward; m1 and m2 with mesoconid on crista obliqua (in *C. texanus*); upper first molar broad and large relative to the size of the upper carnassial with strongly developed conules; rounded subangular region and deep angular process. All of these characters are shared with *Nyctereutes*, except that the subangular lobe is more similar to certain Eurasian early Pliocene species attributed to *Nyctereutes* (*N. donnezani* and *N. tingi*). Later species of *Nyctereutes* have a more highly developed subangular lobe.

Cerdocyon texanus, new species
Figure 31A–D; appendix 3

Cerdocyon, n. sp. B, Torres and Ferrusquía, 1981: 711.

Cerdocyon channingensis Torres and Ferrusquía, 1981: table 1, nomen nudum.

Vulpes stenognathus: Morgan et al., 1997: 102.

Type: F:AM 62985, right partial ramus with c (alveolus)–m3 (p1 broken) from Rentfro pit 1, Ogallala Group (latest Hemphillian), 6.4 km southwest of Channing, Hartley County, Texas. The type and referred maxilla, F:AM 62984, may be one individual.

Referred Material: F:AM 62984, partial premaxilla and right maxilla with left I1–I3, and right I1–M1 (broken) from the type locality.

North Fork of Walnut Canyon, Grant County, New Mexico, Walnut Canyon Local Fauna (latest Hemphillian), Formation B (of Morgan et al., 1997), Gila Group, NMNH P26861, right ramus, c root, p1–p4 alveoli, m1 lacking part of paraconid and protoconid, and associated left ramal fragment with alveoli of p3–m1 (described as *Vulpes stenognathus* by Morgan et al., 1997: 102, fig. 5a–b).

Distribution: Known only from the latest Hemphillian (earliest Pliocene) of Texas and New Mexico.

Diagnosis: Autapomorphies that distinguish *Cerdocyon texanus* from *C. thous* are: I3 more compressed with stronger lingual cingulum; P1–P3 more elongate and taller crowned; P4 more elongate and slender with stronger and more anterolingually directed protocone; p1 large, may be double-rooted; p4 with well-developed second posterior cusp; m1 trigonid longer relative to length of carnassial, entoconulid larger; m2 anterolabial cingulum stronger and posteriorly extended behind hypoconid, metaconid nearly opposite protoconid, with both cusps subequal in size, talonid wider and longer relative to length of trigonid.

Description and Comparison: Unlike *Vulpes* and *Canis*, but as in *Cerdocyon* and *Nyctereutes*, the lower canine crown in *C. texanus* is short and strongly curved posteriorly. The lower premolars are anteroposteriorly shorter relative to their crown height than those of *Vulpes* and *Canis*, and except for their slightly taller crowns, they resemble those of *Cerdocyon thous* and the living species of *Nyctereutes*. The p1 in *C. texanus* is double-rooted in the type. An occasional jaw of *Cerdocyon thous* and *Lycalopex vetulus* has a p1 with longitudinally grooved roots that suggest fusion of an originally two-

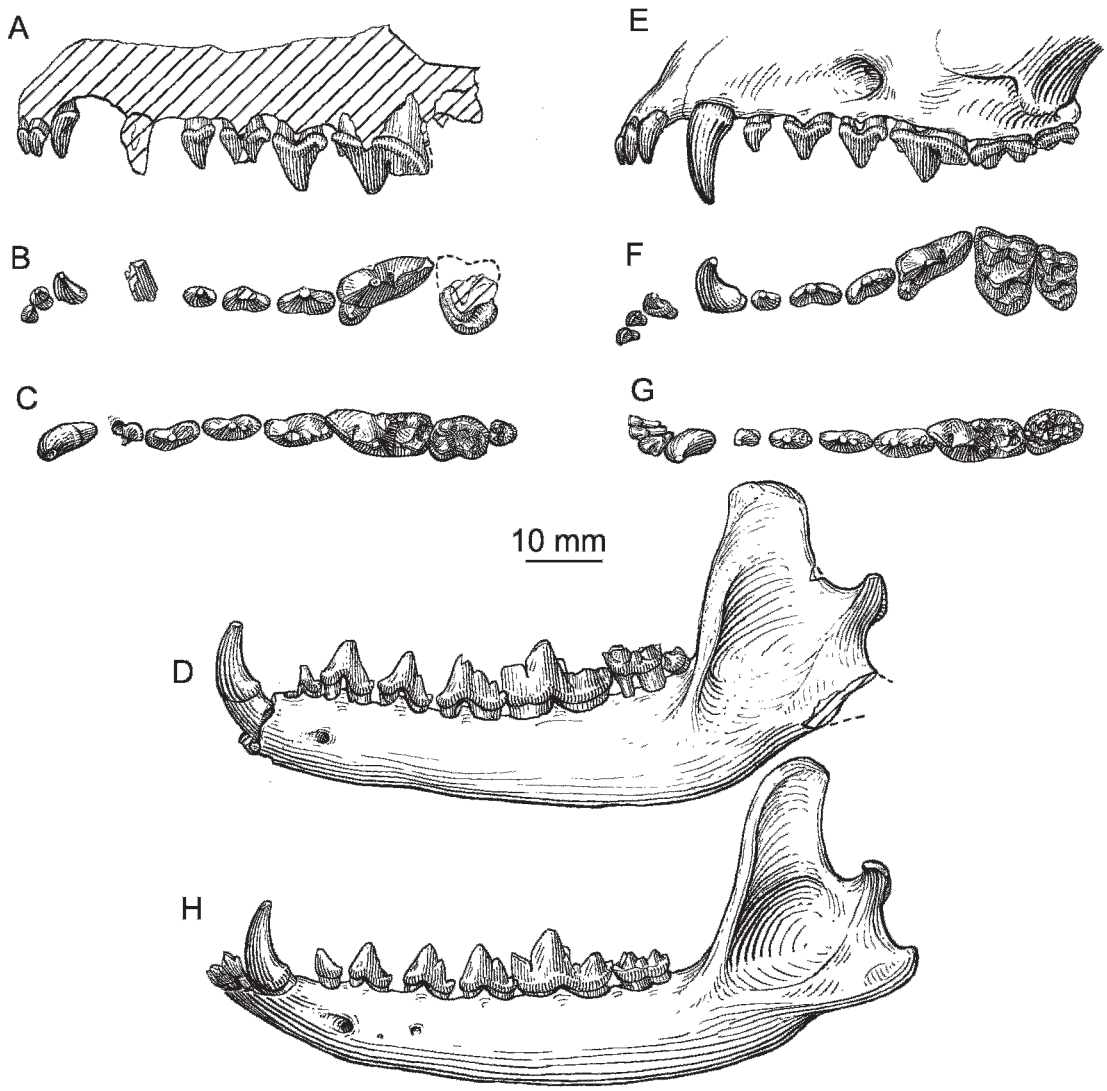

Fig. 31. **A–D**. *Cerdocyon texanus*, late Hemphillian, Hartley County, Texas. **A–B**. Maxillary fragment, F:AM 62984. **A**. Lateral view, reversed. **B**. Occlusal view, reversed. **C–D**. Type ramus, F:AM 62985. **C**. Occlusal view, reversed. **D**. Lateral view, reversed. **E–H**. *Cerdocyon thous*, AMNH(M) 14636, Recent, Colombia, South America. Skull and associated ramus. **E**. Lateral view. **F**. Occlusal view. **G**. Ococlusal view, reversed. **H**. Lateral view, reversed.

rooted tooth. The p2 consists of a tall central cusp and lacks a posterior cusp as in *C. thous*. The p3 of *C. texanus* has a small posterior cusplet. This cusp is highly variable in *C. thous* and ranges from absent (AMNH(M) 36503) to strong (AMNH(M) 14663, fig. 31H). The p4 is larger than that of *C. thous* and has two well-developed posterior cusps between the principal cusp and the cingulum. The second posterior cusp is larger than that occasionally found in *C. thous*. This cusp is also sometimes found in *Lycalopex*, and it may be present on the very differently proportioned p4 of *Vulpes stenognathus*. It is consistently present in *Eucyon davisi* and species of *Canis*.

The m1 of *C. texanus* is more elongate than that of *C. thous*, and the talonid is especially longer relative to the length of the carnassial. The m1 protoconid is tall and seems to lack a protostylid. In *C. thous* the protostylid is frequently seen in unworn lower carnassials. Both *C. texanus* and *C. thous* have a mesoconid on the crista obliqua of m1, a derived feature shared with the smaller species of *Pseudalopex*, *Lycalopex*, and *Nyctereutes*. The m1 metaconid is strong in both *C. texanus* and *C. thous*, and an entoconulid is present in both taxa but is largest in *C. texanus*. The m1 talonid in *C. texanus* is elongate and shares derived features of the Canini including the joining of the well-developed entoconid and hypoconid by cristids to form a transverse crest and a strong hypoconulid shelf. In *C. thous* the transverse crest between the entoconid and hypoconid is weaker than in *C. texanus*, but a distinct hypoconulid is sometimes present on the m1. The morphology of the m1 talonid is very similar to that in *Nyctereutes*, although the development of the transverse crest is variable in species of *Nyctereutes*.

The m2 of *C. texanus* is a distinctive molar with a combination of primitive and derived characters that is unlike any other member of the Canini. The trigonid in *C. texanus* is elongate with a distinct paraconid. These primitive features are also present in *C. thous* and *Nyctereutes*. The metaconid in *C. texanus* lies opposite the protoconid, and the cusps are subequal in size. A more derived condition is seen in the m2 of *Nyctereutes* and *C. thous* in which the metaconid is relatively larger and slightly posterior to the protoconid. The m2 of *C. texanus* has the strong labial cingulum that ends behind the hypoconid. A strong cingulum is also present on the m2 of *Nyctereutes* and *C. thous*, but it extends only to the posterior part of the protoconid. The m2 of *C. texanus* has a well-developed entoconulid, which is unique among known North American Canina. This derived feature, however, is shared with living species of *Cerdocyon*, *Pseudalopex*, *Lycalopex*, and *Nyctereutes*. In *C. texanus* the m2 is elongate, wide, and larger relative to m1 than in *C. thous* and *Nyctereutes*. It has a weak entoconid that contrasts with the strong hypoconid, and the hypoconulid is absent. In *C. thous* the m2 talonid is narrower and the entoconid ranges in size from weak (AMNH(M) 14663, fig. 31G) to absent (AMNH(M) 36503). The protoconid and metaconid are joined by a cristid on the m3 of *C. texanus*, *C. thous*, and *Nyctereutes*.

The referred maxilla (F:AM 62984) likely represents the same individual as the type ramus. It lacks most of the bone surrounding the toothrow, but a fragment of the jugal shows that the ventral border of the zygoma is rather concave, and a prominent scar for the masseter muscle is present as in *C. thous*. A part of the palatine is also preserved behind the M2 roots and this indicates, as in *C. thous* and fossil *Nyctereutes* spp., that the palate did not extend beyond the toothrow. The incisors are present and the I3 in *C. texanus* is more compressed and has a stronger lingual cingulum than in *C. thous*. The first and second incisors, although in early wear in F:AM 62984, have the medial and lateral cuspules seen in *Cerdocyon*. *Nyctereutes* also retains these cuspules as do other Canini. Although fractured, it is still evident that the upper canine is short and proportionally similar to that of *C. thous*. P1–P3 are anteroposteriorly short, slender, and tall-crowned. They are less elongate than those of *Vulpes* and *Canis*, but longer and taller crowned than those of *C. thous* or species of *Nyctereutes*. Both P2 and P3 have minute styles on the posterior cingula. Posterior cingular styles are also found on the P2 and P3 of *C. thous*, but the style on P2 is smaller. Compared to *C. thous* and *Nyctereutes*, the P4 of *C. texanus* is longer and more slender, has a stronger and more anterolingually directed protocone, and has an anterolabial shelf with a low cingulum. In *C. texanus* the P4 lingual cingulum is broken away along the paracone but it is well developed along the metacone and approximates that of *C. thous* or *Nyctereutes*. Although broken, enough is present of the M1 to show that it is a relatively large molar with a large protocone and a strong postprotocrista that reaches a well-developed metaconule as in *C. thous*. Judging by the broken surface, it seems that a paraconule was also present as in *C. thous*. Enough remains of the M1 hypocone to show that it

was large and connected to a strong labial cingulum that extends anterolaterally around the base of the protocone and possibly to the paracone as in *C. thous* and *Nyctereutes*. The hypocone is anteroposteriorly long with some indication that it is divided to form a distinct hypoconal cusp as in *C. thous*. The general shape of the M1 and the strong protocone and metaconule are also similar to the M1 of *Atelocynus*.

The mandibular ramus of *C. texanus* is relatively deep and robust as in some of the larger and older male individuals of *C. thous*. As in the latter, the horizontal ramus narrows very little anteriorly and is relatively deep beneath p2. The ascending ramus in both taxa is very erect and both have a deep masseteric fossa and a prominent masseteric crest. The subangular region of the ramus in *C. texanus* is rounded with a strong medial digastric scar. The subangular notch in *C. texanus* is most similar to that of *C. thous*. These are derived features that are shared with *Cerdocyon thous*, *Speothos*, *Nyctereutes donnezani*, and *N. tingi*. Although the angular process is broken in *C. texanus*, it does not appear to be as deep as in *Nyctereutes* but may be similar to more primitive South American canids grouped as "*Pseudalopex*" in the phyletic analysis of Tedford et al. (1995). On the medial side of the angular process part of the fossa for the superior ramus of the median pterygoid muscle is present. All indications are that the superior fossa is similar in size to the rugose area that serves as the insertion for the inferior ramus of the median pterygoid muscle in the Cerdocyonina at the morphological level shown by species of "*Pseudalopex*" (particularly "*P.*" *griseus*) and, apparently, *Nyctereutes donnezani* and *N. tingi*. The mandibular condyle is situated well above the level of the toothrow as in *C. thous*, *Nyctereutes*, and *Speothos*. The coronoid process is dorsoventrally shorter but anteroposteriorly about as long as in *C. thous*.

The jaw fragments from southwestern New Mexico, originally described as *Vulpes stenognathus*, occur in deposits with a closely similar fauna as the type locality of *C. texanus* in the Texas Panhandle (Morgan et al., 1997). This specimen differs from *V. stenognathus* (as does the type) in its deeper ramus with little forward taper, strong symphyseal union, and shallow flexure of the inferior border behind the symphysis. The m1 is wide for its length, showing a prominent entoconid and entoconulid and a strong union of the talonid cusps. The specimen differs from the type of *C. texanus* in having a single-rooted p1, but the alveolus is elongate as in *C. thous*, implying a stout root, or coalesced roots, similar to the type in size.

Discussion: It is clear from the above comparisons that as far as the dentition and mandible are concerned, *C. texanus* resembles *Cerdocyon thous* and species of *Nyctereutes*, especially the early Pliocene Eurasian taxa *N. donnezani* and *N. tingi* (Tedford and Qiu, 1991). There is much about the dentition that is collectively unique to *C. texanus* as listed in the diagnosis, but the sum total of features lies with *Cerdocyon*. We have referred this taxon to *Cerdocyon*, but it may represent a member of the stem group in the cladogenesis of *Cerdocyon* and its sister taxon *Nyctereutes*.

Cerdocyon? *avius* Torres and Ferrusquía, 1981

Cerdocyon, n. sp. A, Torres and Ferrusquía, 1981: 710.

Type: IGM 2903, a right ramus lacking the ascending portion, with c broken, p1 alveolus, p2 broken, p3–p4 alveoli, m1 trigonid broken, m2 alveolus, m3, and isolated left p2, and left M1, with associated partial skeleton including the atlas, 5th cervical, thoracic vertebrae 5–11 and 13, lumbar 4, caudals 8–11, a fragment of a scapula, right and left humeri, proximal end of right ulna, distal end of right and left radii, carpals and metacarpals, pelvis, right femur lacking distal epiphysis, right and left astragali, right calcaneum, and left cuboid, navicular and phalanges.

Collected from IGM locality BCS-46 on Rancho Algodones, 20 km north–northeast of San Jose de Cabo, Baja California Sur (Torres, 1980), from rocks formerly assigned to the "Salada Formation" and now regarded as the Refugio Formation. These nearshore marine deposits contain a shark and molluscan fauna associated with the de-

scribed canid, *Notolagus* sp., and an indeterminate myomorph rodent, the mammals are grouped as the Algodones Local Fauna (Torres, 1980). These marine deposits lie about 12 km southwest of the continental deposits containing the early Blancan Las Tunas Local Fauna described by Miller (1980). The two sites probably occur in nearly coeval facies of the Pliocene deposits filling the fault-bounded trough between the Sierra de la Trinidad on the east and the Sierra de la Victoria on the west. An early Blancan age is suggested for the Algodones Local Fauna.

Revised Diagnosis: *Cerdocyon*? *avius* is distinguished from *C. texanus* by its single-rooted p1; smaller dentition set in longer and deeper horizontal ramus; slightly better defined subangular lobe; m1 with more reduced metaconid, lack of crest connecting talonid cusps; and absence of an entoconulid.

Etymology: *Avius*, Latin, meaning out of the way, alluding to the remote location of a member of a South American canine genus.

Discussion: Although the detailed description and comparisons of this taxon are contained in the thesis of Torres (1980), a summary was published by Torres and Ferrusquía (198l), sufficient to establish the name *C. avius* introduced in table 1 of their paper. They point out that the mandible bears a subangular lobe, an expanded median pterygoid fossa of the angular process, a single-rooted p1, a small and short-crowned lower canine, and a skeleton that is 10% larger than living examples of *Cerdocyon thous*, with the proportions of the appendicular elements similar to and as robust as the latter, with the details of the morphology and proportions of the calcaneum similar to *Cerdocyon* and *Pseudalopex* species. These comparisons suggest membership in the Cerdocyonina along with *Cerdocyon texanus*.

However there are no morphological features of the material referred to *C.*? *avius* that clearly indicate its reference to *Cerdocyon* rather than *Nyctereutes*, nor do the tooth indices used by Torres and Ferrusquía (1981) provide a point of differentiation from species of *Nyctereutes* (using data on *N. donnezani* from Soria and Aguirre, 1976) or other canids, such as *Urocyon*, in which the molars are relatively large compared with the carnassials. Furthermore, photographs of the holotype (courtesy of F. Prevosti, La Plata, Argentina) show the medial view of the ramus and the angular process, which is slender with an upwardly directed, hooklike termination. The fossa for the superior branch of the median pterygoid is large, and that for the inferior branch is smaller. These proportions are primitive for Canini, such as those shown by the primitive South American canines and *Nyctereutes tingi*.

Chrysocyon Smith, 1839

Type Species: *Canis brachyurus* Illiger, 1815.

Included Species: *Chrysocyon brachyurus* and *C. nearcticus*, new species.

Distribution: For *C. brachyurus*, Ensenadan (medial Pleistocene) to Recent, South America (Berta, 1987, 1987). For *C. nearcticus*, n. sp. early or medial Blancan (early Pliocene) of southern California, Arizona, and Chihuahua.

Revised Diagnosis: *Chrysocyon* shares a number of synapomorphies (Tedford et al., 1995) with all other Cerdocyonina, including zygomatic arch with wide masseter muscle scar and corresponding enlarged insertion for medial masseter ventral to masseteric fossa of ascending ramus, and coronoid process with long base relative to height. It shares with more derived members of South American clade blunt angular process, fossa for inferior ramus of median pterygoid expanded, and M1–M2 more quadrate in occlusal outline so they appear transversely narrow for their length. A number of autapomorphies distinguish *Chrysocyon* from other South American canines: it primitively retains palate shorter than toothrow; like *Canis*, its forelimb is long relative to hindlimb (the radius/tibia ratio is greater than 90%), although it shows great limb elongation (humerus + radius more than 50% of head-body length).

Discussion: Berta (1981, and more explicitly in 1988) proposed that *Chrysocyon* was a member of the clade containing *Canis*, a sister group to the other South American canines, mainly on the basis of its elongate forelegs, which have *Canis*-like proportions, and on the interpretation of the size of the frontal sinus and muscle scars on the angular

process of the mandible. We have reevaluated these characters based on collections in the Department of Mammalogy of the American Museum of Natural History and find that the latter two features have the characters found in the South American clade (Tedford et al., 1995). There is a frontal sinus, but it does not extend beyond the postorbital constriction nor does it markedly inflate the postorbital processes or penetrate the tips of those processes. The angular process is deep and short and shows a large area for insertion of the inferior ramus of the median pterygoid muscle as is typical of most Cerdocyonina. For these reasons we (Tedford et al., 1995) have returned the maned wolf to relationship with the South American taxa as Langguth (1969) and Clutton-Brock et al. (1976) had previously concluded.

A recent study of the mitochondrial DNA (Wayne et al., 1997) of a fairly comprehensive suite of living canids has explicitly linked the maned wolf and the South American bush dog (*Speothos*) as a sister taxon of either the Canina or the Canina plus the Cerdocyonina. A combined analysis of our morphological data (Tedford et al., 1995) and the 2001 base pairs of the canid mtDNA (Wayne et al., 1997: fig. 7) placed the maned wolf and bush dog as sister taxa, but relegated them to a position basal to the Cerdocyonina, the whole of which is a sister taxon of the Canina.

More recently Bininda-Emonds et al. (1999) presented a ''supertree'' comparing biomolecular and morphologic data by parsimony analysis to produce a composite tree of all living canid species. The resulting tree (their fig. 9) shows *Chrysocyon*, *Atelocynus*, *Speothos*, and *Cerdocyon* in a multichotomy with the dhole and hunting dog plus *Canis* species and the remaining South American taxa (*Dusicyon* and *Pseudalopex*). This result is not substantially different from that of Wayne et al. (1997), but it reduces the resolution of relationships of nearly half the total South American taxa to uncertainty at the tribal level.

In 2004 Zrzavý and Řičánková considered morphologic and molecular datasets to assess their relative reliability and utility in phylogenetic interpretations of living canids. They utilized 65% of the osteological characters used by Tedford et al. (1995), combining them with some features discovered by Clutton-Brock et al. (1976) and Berta (1987). Additionally, they combined the former with developmental, behavioral, and cytogenetic characters, all 188 of which were labeled ''morphological characters.'' The molecular data were based on three mitochondrial genes: cytochrome b and cytochrome c oxidase subunits I and II.

In their analysis of this dataset, the crown clade was labeled ''DC'' (dog clade) and included species of *Canis* and the ''South American DC'', but with the sister taxa *Chrysocyon* and *Speothos* as an outgroup to these. The *Vulpes* clade is also paraphyletic. *Fennicus* and *Allopex* are monophyletic and immersed within the *Vulpes* species clade. *Otocyon* and *Nyctereutes* are outgroups to all of the above, and the *Urocyon* species constitute a stem group of the living Canidae.

The fossil record, as interpreted here, shows that the problematic foxes at the base of the cladogram in combined analyses are all of early appearance, mostly late Miocene or early Pliocene. Their relationship to living Canina is distant in space (North America, Eurasia, Africa) as well. Their behavior in phyletic analysis may be the result of this history in contrast to the crown group whose history begins in the late Pliocene at the earliest and on continents already under the influence of Quaternary climates.

Chrysocyon nearcticus, new species
Figure 32A–D; appendix 3

Canis edwardii: Nowak, 1979: 84.

Type: UA 12610, left partial ramus with i1, c (roots), p1–p2, p3 (roots), p4–m2, m3 (alveolus) lacking the posterior part of the coronoid process and the tip of angular process (fig. 32C–D) from UA locality Sand Wash 1, Gila Group (early or medial Blancan), 8 km north of Duncan, Greenlee County, Arizona.

Etymology: For its occurrence in the Nearctic zoogeographic province (Sclater, 1859).

Referred Material: LACM(CIT) 1680, anterior part of left ramus with parts of c, p1–p2, and associated incisors, and LACM

(CIT) 149, fragment of left horizontal ramus with p3–m3 (fig. 32A–B). These fragments seem to be parts of a single ramus as established by contacts of the lateral wall of the ramus and are treated as such in the following description: CIT locality 105, unnamed deposits (early Blancan), about 4.7 km north of Minaca, valley of the Rio Papagochic, 250 km west–northwest of Chihuahua City, Chihuahua, Mexico. These remains were referred to *Canis edwardii* by Nowak (1979: 84).

Aguanga Fauna, Temecula Arkose (early or medial Blancan), 26 km east of Temecula, Riverside County, California: F:AM 31854, left ramal fragment with p3.

Distribution: Early or medial Blancan (early Pliocene), southeastern Arizona and southern California; early Blancan, western Chihuahua, Mexico.

Diagnosis: Synapomorphies that unite *C. brachyurus* and *C. nearcticus* are: lower premolars large relative to size of lower carnassial with significant diastemata separating p2 from adjacent premolars; ramus relatively slender and elongate in premolar region and base of coronoid process long (distance from m3 to condyle) relative to height; lower carnassial with small metaconid and talonid with weak transverse crest; m2 with weak anterobuccal cingulum, crown large relative to m1 with metaconid subequal in size to protoconid. *C. nearcticus* is distinguished from *C. brachyurus* in that premolars have more primitively elongate form, not short and high-crowned as in *C. brachyurus*; metaconid of m2 not disproportionally enlarged; and talonid wider relative to trigonid.

Description and Comparison: The rami referred to *Chrysocyon nearcticus* are very similar in size to those of *Canis edwardii*. Comparison of these taxa reveals the major points of difference as follows. First, the rami of *Chrysocyon* are relatively elongate and slender. These proportional relationships are most marked in the length and depth of the ramus below the canine and anterior part of the premolar row and in the great length of the ascending ramus (expressed as distance from the posterior wall of the m3 alveolus to the end of the condyle: 54.0 mm, UA 12610). The premolars are separated by diastemata and more slender, elongate, and higher crowned than in *C. edwardii*, yet large relative to the size of the molars. The p3 from Aguanga, California, is grouped here because of its slender but high-crowned form, and enough of the ramus remains to show the diastemata separating it from adjacent teeth. It shows a weakly differentiated cusp situated high on the rear of the principal cusp. The p4 has a strong posterior cusp and a second cusp is present in the holotype of *C. nearcticus*, but not the referred specimen. The anterior premolars seem to lack posterior cusps. These teeth resemble those of *Canis* and *Eucyon*, especially in having a second cusp on p4, and they contrast with the short, broad, and high-crowned premolars with low posterior cusp on p3–p4 found in *Chrysocyon brachyurus*. The p4 is higher than the paraconid of m1, unlike in *C. edwardii* and other large *Canis* species.

Chrysocyon species have relatively lower crowned carnassials than in *Canis*, with the paraconid in particular having a nearly vertical anterior border and being low relative to the protoconid. The metaconid is reduced and the talonid has a weak transverse crest between the hypoconid and entoconid. The m2 is large relative to the m1 in the *Chrysocyon* species, and the anterolabial cingulum is weak when compared with *Canis*. *Chrysocyon nearcticus* has a relatively small metaconid on m2, only equal to the height of the protoconid. In *C. brachyurus* the m2 has a larger metaconid, equal in size to the protoconid. Its base markedly inflates the lingual border of the tooth. This may be an autapomorphy for the living maned wolf correlated with the development of relatively large molars. An early stage in this transformation is seen in *C. nearcticus* in which the m2 is large relative to the m1. Correspondingly, the m3 in *C. nearcticus* is a relatively large oval tooth with subequal protoconid and metaconid and well-developed labial cingulum (LACM(CIT) 149: length $\times$ width, 6.5 $\times$ 5.5 mm).

Discussion: The discovery of fossil species closely resembling species of the living South American canids *Cerdocyon* and *Chrysocyon* in early Pliocene rocks of southern North America indicates the extent of the phyletic differentiation of the Canini at that

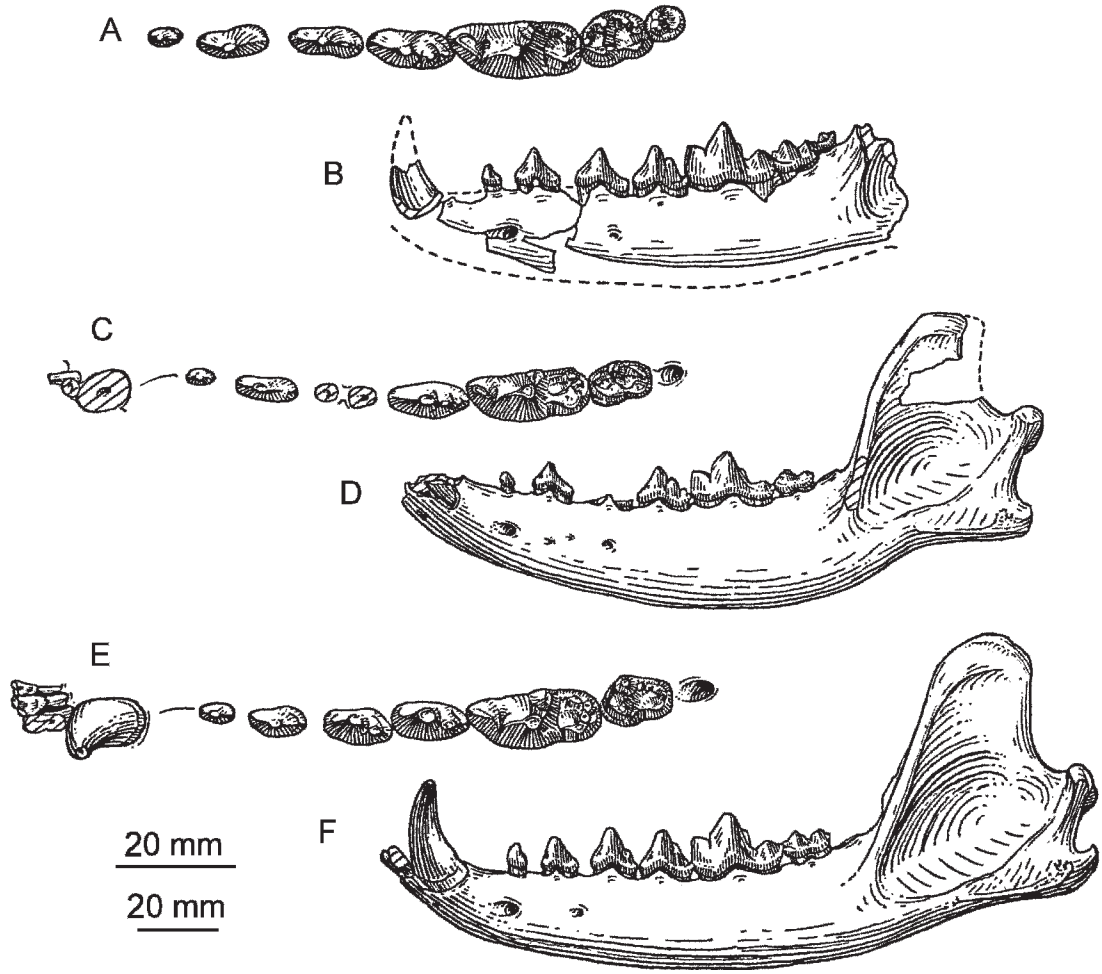

Fig. 32. **A–D**. (above) *Chrysocyon nearcticus*. **A–B**. LACM(CIT) 1680 (rostral part of ramus with c, p1–p2) and LACM(CIT) 149 (fragment of horizontal ramus with p3–m3) combined as one individual, Blancan, Chihuahua, Mexico. **A**. Occlusal view. **B**. Lateral view. **C–D**. Type ramus, UA 12610, Blancan, Greenlee County, Arizona. **C**. Occlusal view. **D**. Lateral view. **E–F**. (above) *Chrysocyon brachyurus*, Recent, Brazil, AMNH(M) 36962. Ramus. **E**. Occlusal view. **F**. Lateral view. **G–L**. (right) *Theriodictis* ?*floridanus*. **G–I**. Type, right ramal fragment, UF 19324, early Irvingtonian, Citrus County, Florida. **G**. Occlusal view. **H**. Lateral view. **I**. Internal view. **J–L**. Right ml, UF 133922, Late Blancan, Sarasota County, Florida. **J**. Occlusal view (stereopair). **K**. Lateral view. **L**. Internal view. The longer (upper) scale is for A, C, and E, and the shorter (lower) scale is for B, D, and F.

time. The record of *Chrysocyon* described above rests only on the morphology of the lower jaws and lower dentition and hence not on the many cranial and postcranial autapomorphies recognized for the genus. To a certain extent the distinctive jaw and lower dental features represent a series of correlated characters common to dolichocephalic canids (e.g., *Canis simensis* or *Vulpes ferrilata*) and as such could represent parallel development of features in a taxon only distantly related to *Chrysocyon*. However, the correspondence in details of morphology are striking and the exceptions that distinguish *C. nearcticus* are features that are primitive for the Canini.

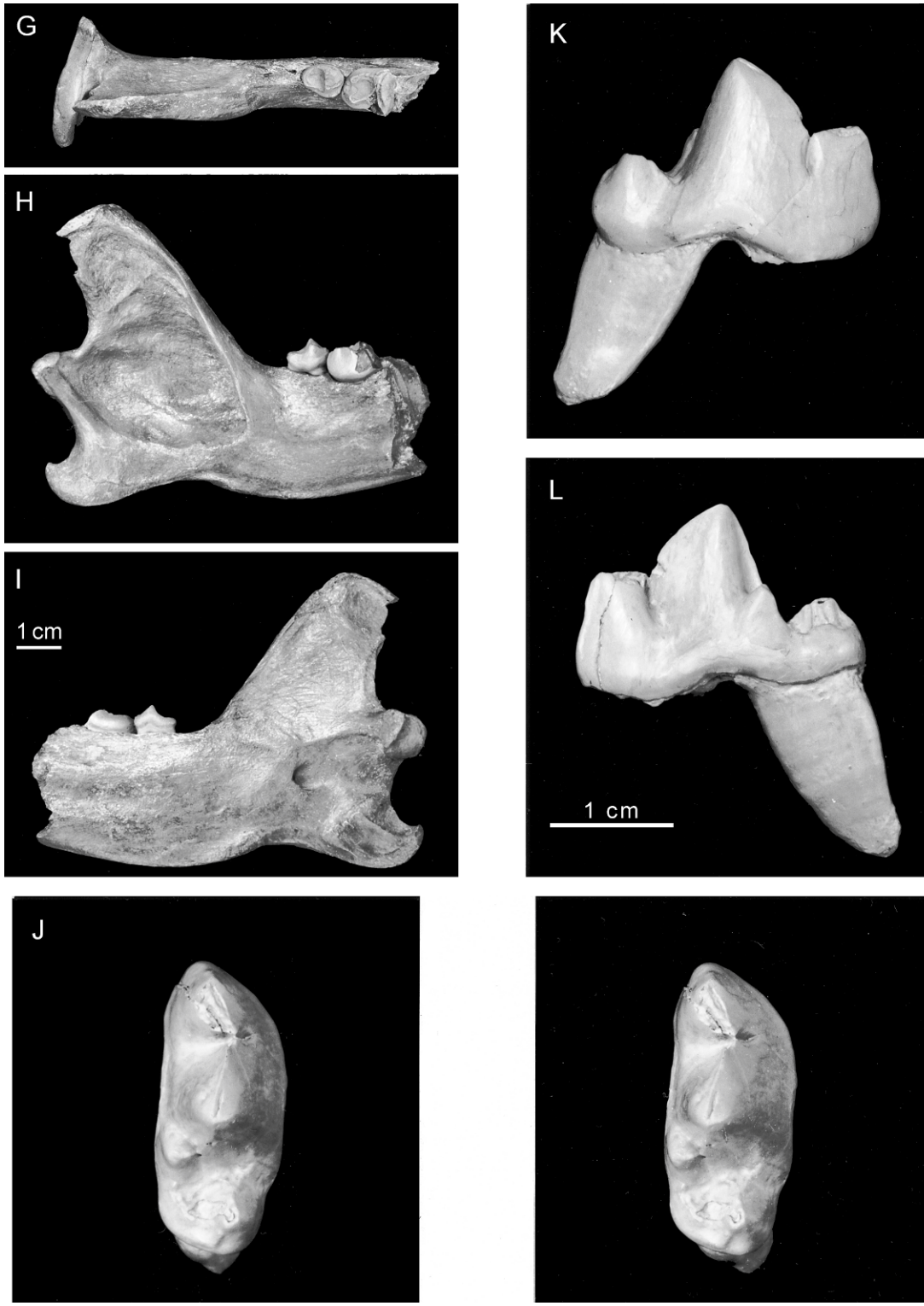

Fig. 32. *Continued.*

Theriodictis Mercerat, 1891
Figure 32G–L; appendix 3

Dinocynops F. Ameghino, 1898.
Pleurocyon Mercerat, 1917.
Canis (*Theriodictis*) L. Kraglievich, 1928.

Type Species: *Theriodictis platensis* Mercerat, 1891.

Included Species: *T. tarijensis* (Ameghino), 1902, and *T.*? *floridanus*, n. sp.

Distribution: For *T. platensis*, Argentina, Ensenadan and Lujanian (medial to late Pleistocene); for *T. tarijensis*, Bolivia, late Ensenadan and/or early Lujanian; for *Theriodictis* sp. (formerly *Amphicyon argentinus* F. Ameghino, 1904), Argentina, possibly Montehermosan (Pliocene), but more likely Ensenadan (medial Pleistocene) fide Berta (1988: 76); and for *T.*? *floridanus*, southeastern United States, late Blancan and early Irvingtonian.

Revised Diagnosis (Berta, 1988: 64): Frontal sinus penetrates postorbital process and extends to frontoparietal suture; deep zygoma with wide masseteric scar; palatines extend posteriorly beyond toothrow; M1–M2 hypocones reduced; M2 small relative to M1 with reduced metacone; coronoid process anteroposteriorly long, dorsoventrally low; angular process expanded dorsoventrally; large fossa for inferior branch of medial pterygoid; m1 lacks metaconid but retains small entoconid; m2 small relative to m1, lacking anterolabial cingulum, strong paracristid and relatively unreduced metaconid.

Discussion: Recognition of the presence of this genus or a closely related taxon is based on two specimens, both elements of the lower jaw, from late Pliocene and medial Pleistocene deposits in Florida. Fortunately these specimens contain some of the more diagnostic features of the Cerdocyonina, particularly the hypercarnivorous adaptations within the clade that also contains the extinct *Protocyon* and the recently extirpated Falkland Island fox (*Dusicyon*).

Theriodictis*? *floridanus, new species
Figure 32G–L; appendix 3

Type: UF 19324, fragment of right ramus with talonid of m1, m2 and partially bone-filled alveolus of m3, complete ascending ramus. Inglis 1A Local Fauna, Citrus County, Florida, early Irvingtonian.

Referred Specimen: UF 133922, right m1, Macasphalt Shell Pit, 8 km east of Sarasota, west side of I-75, Sarasota County, Florida, late Blancan.

Distribution in North America: Late Blancan to early Irvingtonian of Florida.

Diagnosis: Only posterior ramus and parts of m1–m3 known. Synapomorphies grouping *T.*? *floridanus* with other *Theriodictis* spp. are m1 with tiny entoconid, talonid narrow, hypoconid labial (not central), connected to entoconid by transverse cristid; m2 short relative to m1, especially in length of talonid, protoconid and metaconid subequal, paracristid diagonal, paraconid lacking, anterolabial cingulum extends to posterolabial side of protoconid; talonid narrow, and no talonid cusps; m3 apparently single-rooted, but lost in life, alveolus nearly filled with cancellous bone; angular process large, especially fossa, for insertion of inferior ramus of median pterygoid.

Description and Comparison: These specimens could be regarded as variants of the more fully tribosphenic lower molars of *Canis* if it were not for their peculiar morphology and the form of the ascending ramus, which lie cladisticaly within the Cerdocyonina. Reference to *Theriodictis* is based on the few characters that can be compared between the Florida specimens and the more complete dentitions known of the Pleistocene Bolivian and Argentinian species. That this comparison is necessarily incomplete is denoted by the question mark placed after the genus name. *Therodictis*? *floridanus* is close to the size of *T. platensis* and *T. tarijensis*.

Important diagnostic features of the ascending ramus of *T.*? *floridanus* include the depth of the ramus beneath the junction of m1 and m2 (28.0 mm), followed by a strong digastric process at the ventral margin of the ramus. The angular process is deep (25.0 mm) and blunt, with a small hooklike process at the dorsal end. The internal side shows well-defined fossae for the superior and inferior branches of the median pterygoid muscle, in which the inferior fossa is larger than the superior fossa in the characteristic cerdocyonine manner. There is a

strong rugosity for the medial as well. Externally, the masseteric fossa is strongly impressed into the coronoid process, and the masseteric crest below is rimmed ventrally by a well-formed masseteric fossa. The coronoid process is long (45.0 mm) and low (31.0 mm).

The morphology of the m1 is similar to *Theriodictis* spp. in reduction of the entoconid and formation of a cristid connecting the hypoconid with it (a synapomorphy with the Canina). The metaconid, although small, is still present in *T.*? *floridanus*, corresponding to its primitive nature; otherwise, the dentition has mostly achieved the hypercarnivorus features of later *Theriodictis*.

If we have correctly interpreted this taxon, it agrees with other evidence from southern North America showing the extent of the radiation of the Cerdocyonina into clades that represent nearly the range of adaptations of the group.

Subtribe Canina Fischer de Waldheim, 1817, new rank

Our analysis of the crown group of the Canini resulted in the separation of the South American clade as the Cerdocyonina, new subtribe, a monophyletic group whose phylogeny was explored by Berta (1988) and Tedford et al. (1995). The remaining taxa in the crown group include the species of *Canis* and its sister taxon *Eucyon*. These form the terminal clade of the Canidae, the subtribe Canina, new rank. This subtribe is defined by two synapomorphies: a zygoma that is strongly arched dorsoventrally, and the usual presence of a second posterior cusp on p4 lying between the first posterior cusp and the cingulum.

Eucyon Tedford and Qiu, 1996

Type Species: *Canis davisi* Merriam, 1911.

Included North American Species: *Eucyon davisi* (Merriam), 1911, and *E.*? *skinneri*, new species.

Distribution in North America: Late Clarendonian of Nebraska and Hemphillian of Kansas, New Mexico, Oklahoma, Texas, Arizona, Nevada, Oregon, California, and northern Mexico.

Revised Diagnosis: *Eucyon* has no autapomorphies but is distinguished from the fossil and living Vulpini and the Cerdocyonina by possession of synapomorphies also present in all other members of the Canina: frontal sinus invading base of postorbital process removing ''vulpine-crease'' or depression from dorsal surface of process; paroccipital process expanded posteriorly usually with salient tip; mastoid process enlarged as knob or ridgelike prominence; loss of foxlike lateral flare and eversion of dorsal border of orbital part of zygoma.

Primitive characters retained by *Eucyon* relative to those of most species of *Canis* are: frontal sinus less posteriorly extended, ends anterior to frontoparietal suture and does not completely invade postorbital process; supraoccipital shield fan-shaped, inion broad and not strongly overhanging condyles; I3 less enlarged relative to I2 with weaker posteromedial cingulum; M1 paracone and metacone subequal in size; M2 metaconule weak or absent, postprotocrista present; m1 entoconid and hypoconid usually not joined by transverse crest; angular process of mandibular ramus less expanded with smaller fossa for inferior pterygoid muscle; forelimb short relative to hindlimb, radius/tibia ratio less than 80%; and humerus often with entepicondylar foramen.

Derived features linking *Eucyon* with *Canis* include: zygomatic arch strongly arched rather than gently curved, and p4 with second posterior cusp.

Discussion: In general, the morphology of *Eucyon* is similar to that of *Vulpes*, as they share numerous primitive features. However, *Eucyon*, like the South American cerdocyonines, possesses a small frontal sinus that does not fully penetrate the postorbital process, and it does not extend as far posteriorly as in most species of *Canis*. *Eucyon* does share with *Canis* species two synapomorphies lacking in the cerdocyonines, namely, the presence of a second posterior cusp on p4, and the strongly arched zygoma.

In North America, *Canis* is not known until the late Hemphillian. *Canis ferox* Miller and Carranza-Castañeda (1998) tends to be morphologically intermediate between *Eucyon davisi* and *Canis lepophagus*. The former shows the derived enlargement of the frontal sinus that distinguishes it from *E. davisi* and supports its relationship to *Canis*.

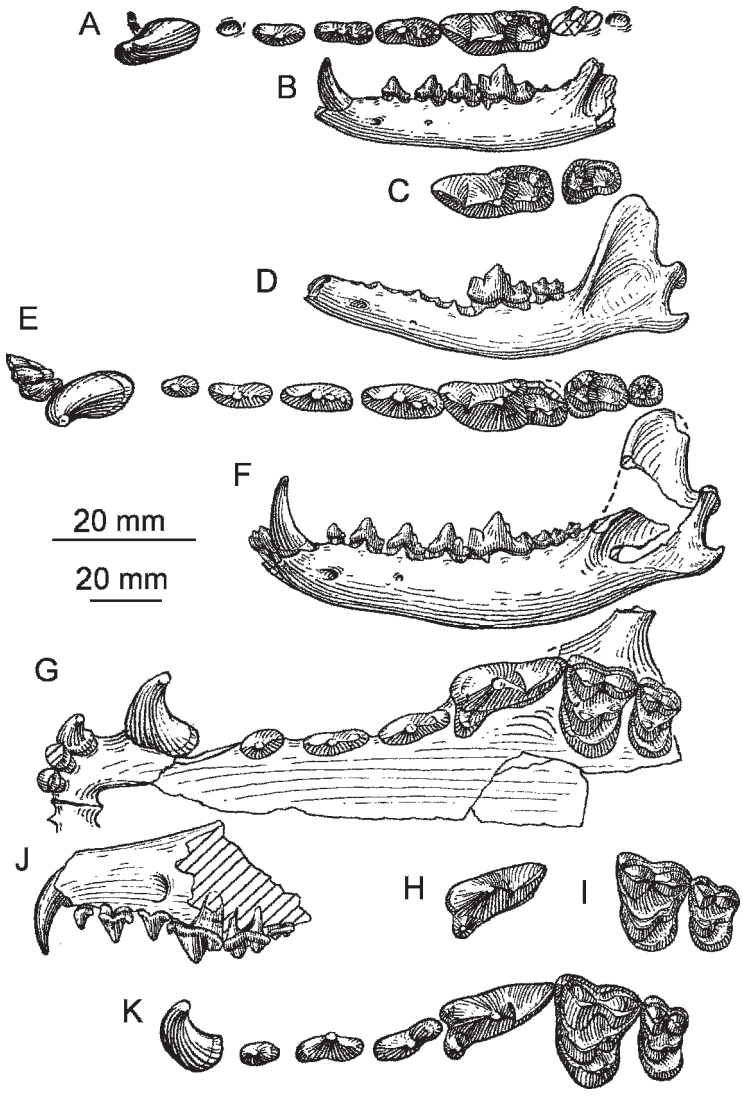

Fig. 33. **A–B**. *Eucyon skinneri*. Type mandible, F:AM 25143, late Clarendonian, Nebraska. **A**. Occlusal view. **B**. Lateral view. **C–T**. *Eucyon davisi*. **C–D**. Late Hemphillian, Oregon. Ramus UOF 3241 (type of *Canis condoni*), and m1, UOF 2353. **C**. Occusal view. **D**. Lateral view of UOF 3241 with UOF 2353 inserted into m1 alveolus. **E–G**. Early Hemphillian, Oregon, palate and associated ramus UOF 26742. **E**. Occlusal view. **F**. Lateral view. **G**. Occlusal view. **H**. Late Hemphillian, Oregon, UOF 2727. Upper carnassial. Occlusal view. **I**. Early Hemphillian, Oregon, UCMP 545 (type of *Canis davisi*). First and second upper molars. Occlusal view. **J–O**. Late Hemphillian, Sherman County, Kansas. **J–K**. Maxillary fragment, F:AM 49464. **J**. Lateral view. **K**. Occlusal view.

Eucyon*? *skinneri, new species
Figure 33A–B; appendix 3

Type: F:AM 25143, partial mandible with i1–i3 alveoli and c–m2 (p1 and m3 alveoli and m2 broken) from the Hans Johnson Quarry, Merrit Dam Member, Ash Hollow Formation (late Clarendonian), Cherry County, Nebraska.

Etymology: Named in honor of the late Morris F. Skinner, Frick Curator Emeritus, American Museum of Natural History, who

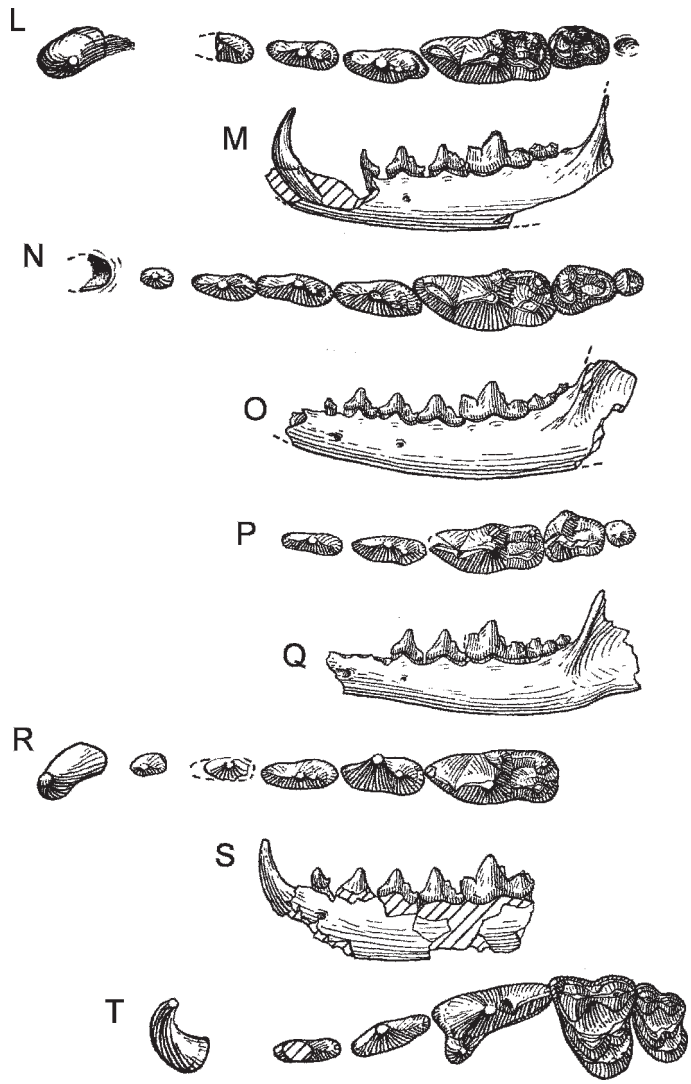

Fig. 33. *Continued.* **L–M**. Ramus, F:AM 49462. **L**. Occlusal view. **M**. Lateral view. **N–O**. Ramus, F:AM 49466. **N**. Occlusal view. **O**. Lateral view. **P–T**. Late Hemphillian, Texas County, Oklahoma. **P–Q**. Ramus, F:AM 62932. **P**. Occlusal view. **Q**. Lateral view. **R–S**. Ramus, F:AM 62951. **R**. Occlusal view. **S**. Lateral view. **T**. Maxillary fragment, F:AM 62954, occlusal view. The longer (upper) scale is for A, C, E–I, K, L, N, P, R, and T, and the shorter (lower) scale is for the rest.

discovered the type and many of the other specimens used in this review.

Distribution: Late Clarendonian of Nebraska.

Diagnosis: Synapomorphies that unite *Eucyon*? *skinneri* with *E. davisi* and other Canina are: m1 with well-developed entoconid and small hypoconulid. Primitive characters retained by *E.*? *skinneri* and differentiating it from *E. davisi* are: smaller size; shorter jaw; less elongate, lower crowned, and more robust premolars; p4 with small second posterior cusp; m1 trigonid proportionally shorter, protoconid lower crowned, hypoconid and entoconid lower crowned.

Description: The horizontal ramus retains a *Leptocyon*-like slenderness (depth beneath m1–m2 junction: 15.2 mm; beneath p1–p2: 10.5 mm) with the largest mental foramen beneath the short diastema separating p1

from p2, and a second foramen occurs beneath p3. The symphyseal union extends back to the posterior root of p2 where there is a slight inflection of the ventral side of the ramus. The canine is robust as in *E. davisi* and larger than that of the contemporaneous *Leptocyon matthewi*. The p1 alveolus shows that it was a robust, single-rooted tooth about the size of that of the smaller jaws referred to *E. davisi*. A very short diastema (2.6 mm) separates the canine and p1 alveolus; the length of this diastema is less than that of *E. davisi*. The p2 and p4 are more closely spaced; their transverse diameters are greater relative to their lengths than in *E. davisi*. The p2 consists primarily of a central cusp without a distinct posterior cusp. The p3 is intermediate in size to p2 and p4, and it has a weak anterior cusp, but a well-developed posterior cusp and a small cusp on the posterior cingulum. The p4 is similar to p3, but more robust, with a relatively stronger posterior cusp. It has a small second cusp on the posterior side of the first posterior cusp as seen in some *E. davisi* and in species of *Canis*.

The first lower molar is short and robust with the length less than that of *E. davisi*. The length of the trigonid is shorter relative to the length of the talonid than in the latter. The tooth is low-crowned with the heights of the protoconid and the hypoconid markedly lower than in *E. davisi*. The metaconid is strong and the talonid is wide and basinlike with a low hypoconid and entoconid. The height of the latter two cusps is less than in *E. davisi*. The metaconid is strong and the talonid is wide and basinlike with a low hypoconid and entoconid. The height of the latter two cusps is less than in *E. davisi*. The size of the hypoconid is proportionally smaller relative to that of the entoconid. As in *E. davisi*, the hypoconid and entoconid lack the transverse crest between them. There is an entoconulid differentiated from the postmetacristid as also seen in some individuals of *E. davisi*. Another character of note is the presence of an enlargement of the cingulum at the posterior base of the m1 hypoconid. This enlargement of the cingulum, or hypoconulid shelf, is not present in *Leptocyon matthewi* and is less developed than in *E. davisi*.

Discussion: The taxa to which *E.*? *skinneri* bears a close morphological resemblance are *Leptocyon matthewi* and *Eucyon davisi*. A comparison of the type of *E.*? *skinneri* with jaws of *L. matthewi* shows that its mandible and dentition are larger and more robust. It is, however, the morphological features of the m1 that really distinguish the type of *E.*? *skinneri* from *Leptocyon* and show its affinity with *Eucyon*. Compared to *L. matthewi*, the talonid of the m1 of *E.*? *skinneri* is proportionally wider with a better developed entoconid and an enlargement of the posterior cingulum. In *Leptocyon*, the m1 talonid is narrower and the entoconid is usually not as well developed as in the type of *E.*? *skinneri*. Like *Leptocyon* and *Eucyon davisi*, the type of *E.*? *skinneri* lacks a transverse crest between the entoconid and hypoconid of m1. The presence of a well-developed entoconid and a small hypoconulid or hypoconulid shelf are both derived characters that are shared with *E. davisi*. However, the p4 of the type has a distinct, but tiny, second posterior cusp characteristic of *E. davisi*. Lack of fuller knowledge of *E.*? *skinneri* causes us to question its assigment to the genus *Eucyon*.

Eucyon davisi (Merriam), 1911
Figures 27, 33C–T, 34A–Q, 35A–S, 36A–B, 39, 40, 43–44, 50–52, 60C, 61C; appendices 2–4

Canis(?) sp.: Merriam, 1906: 5, fig. 1.
Canis(?) *davisi* Merriam, 1911: 242.
Leptocyon shermanensis Hibbard, 1937: 460.
Canis condoni Shotwell, 1956: 733.
Eucyon davisi: Tedford and Qiu, 1996: 36.

Type: UCMP 545, M1–M2 in a fragment of a right maxilla (fig. 33I) that Merriam designated the type of *C.*(?) *davisi* in 1911: 6 "was obtained between Cottonwood Creek and Birch Creek in the southeast corner of Wheeler County, Oregon (Locality No. 887, Univ. Calif. Coll. Vert. Paleo.). At this locality the Mascall Formation is capped by the Rattlesnake beds. This specimen was obtained on an exposure of Mascall beds immediately below a Rattlesnake outcrop. It was not in the matrix, and we cannot be absolutely certain that it had not originally come from the Rattlesnake beds above."

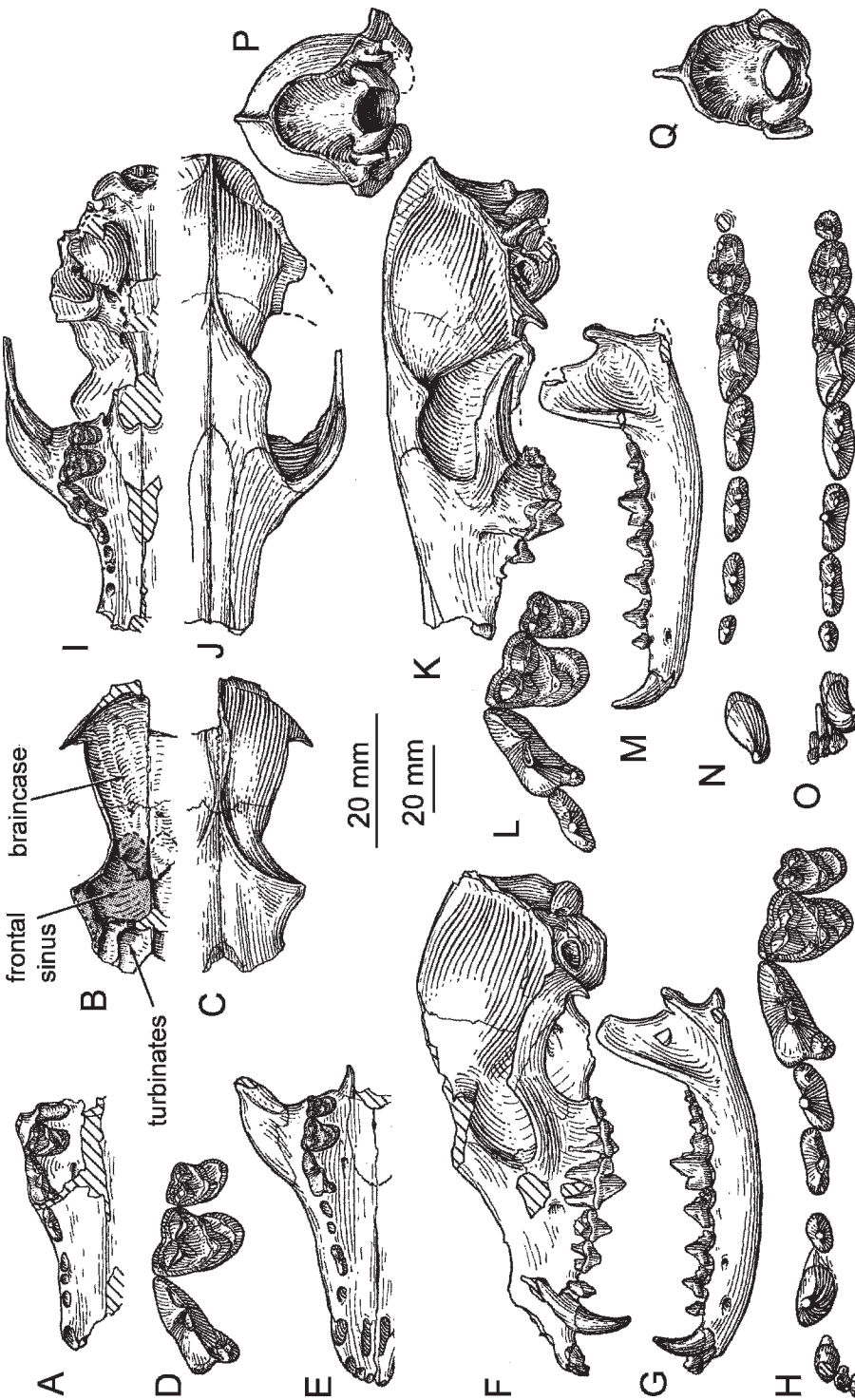

Fig. 34. **A–Q**. *Eucyon davisi*, late Hemphillian, Arizona. **A–C**. Cranial fragments, F:AM 63005. **A**. Palatal view. **B**. Internal view of cranium frontal sinus shaded. **C**. Dorsal view of cranium. **D–E**. Palate, F:AM 63004. **D**. Occlusal view. **E**. Palatal view. **F–H** and **O**. F:AM 63010. **F–G**. Skull and mandible, lateral views, reversed. **H**. Occlusal view, reversed. **I–L**. F:AM 63009, reconstructed skull. **I**. Palatal view. **J**. Dorsal view. **K**. Lateral view. **L**. Occlusal view, reversed. **M–N**. F:AM 63009B, ramus associated with F:AM 63009. **M**. Lateral view. **N**. Occlusal view. **O**. F:AM 63009, occipital view. **P**. F:AM 63183, late Hemphillian, Kansas, occipital view of skull fragment. **Q**. F:AM 63183, Late Hemphillian, Kansas, occipital view of skull fragment. The longer (upper) scale is for D, H, L, N, and O, and the shorter (lower) one is for the rest.

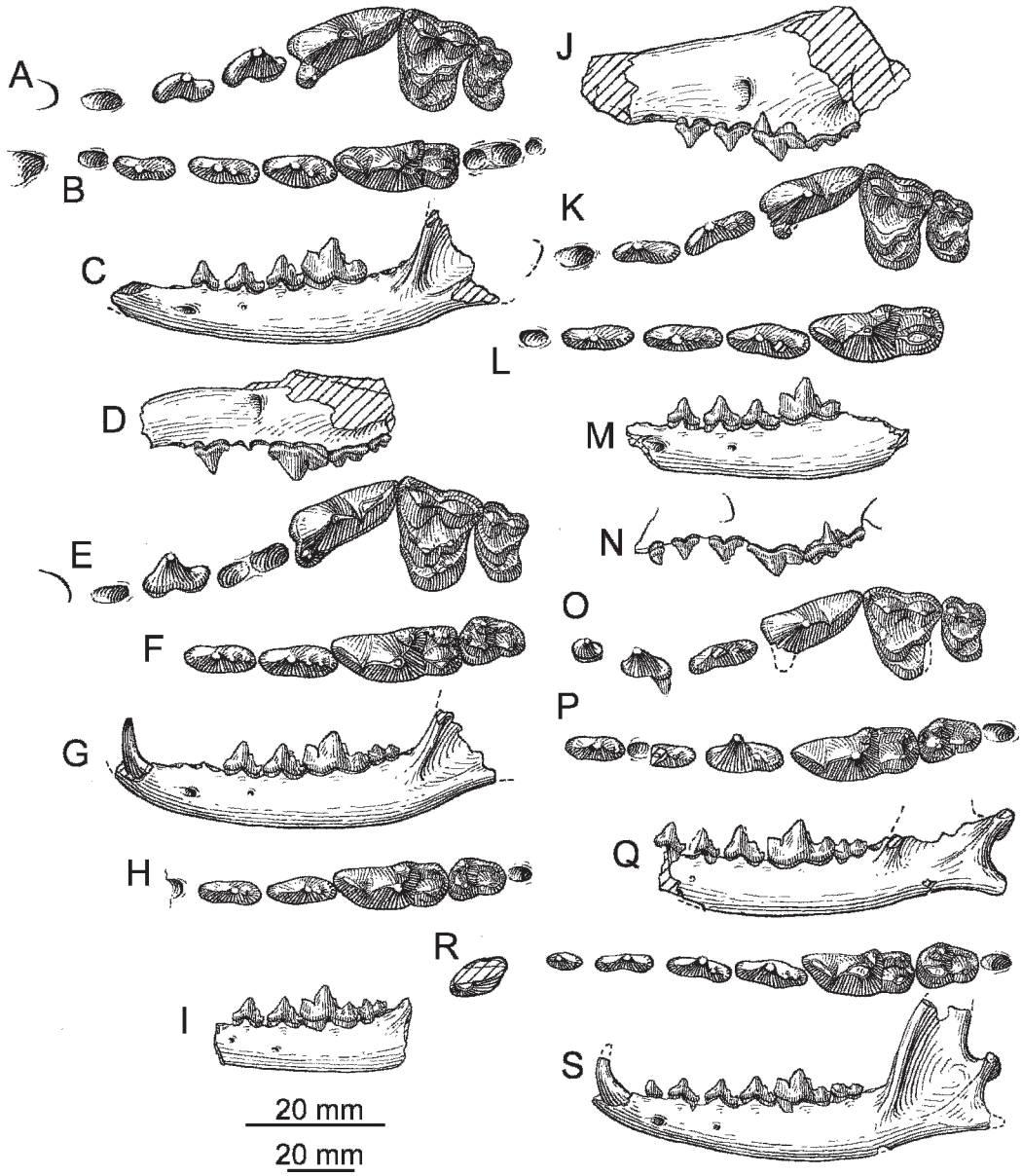

Fig. 35. **A–S**. *Eucyon davisi*. **A–G**. Late Hemphillian, Arizona. **A–C**. Associated upper and lower dentitions, F:AM 63058. **A**. Occlusal view. **B**. Occlusal view, reversed. **C**. Lateral view, reversed. **D–G**. Associated upper and lower dentitions, F:AM 63056. **D**. Lateral view, reversed. **E**. Occlusal view, reversed. **F–G**. Left ramus (p3 and p4 drawn from opposite side). **F**. Occlusal view. **G**. Lateral view. **H–M**. Miami Quarry, Texas. **H–I**. Ramus, F:AM 23353. **H**. Occlusal view. **I**. Lateral view. **J–M**. Associated upper and lower dentition, F:AM 23373. **J**. Lateral view, reversed. **K–L**. Occlusal views, reversed. **M**. Lateral view, reversed. **N–Q**. Associated upper and lower dentitions, F:AM 62981, Channing, Texas. **N**. Lateral view. **O**. Occlusal view. **P**. Occlusal view, reversed. **Q**. Lateral view, reversed. **R–S**. Ramus, F:AM 49294, Nevada. **R**. Occlusal view. **S**. Lateral view. **Q**. F:AM 63183, late Hemphillian, Kansas, occipital view of skull fragment. The longer (left) scale is for A, B, E, F, H, K, L, O, P, and R, and the shorter (right) one is for the rest.

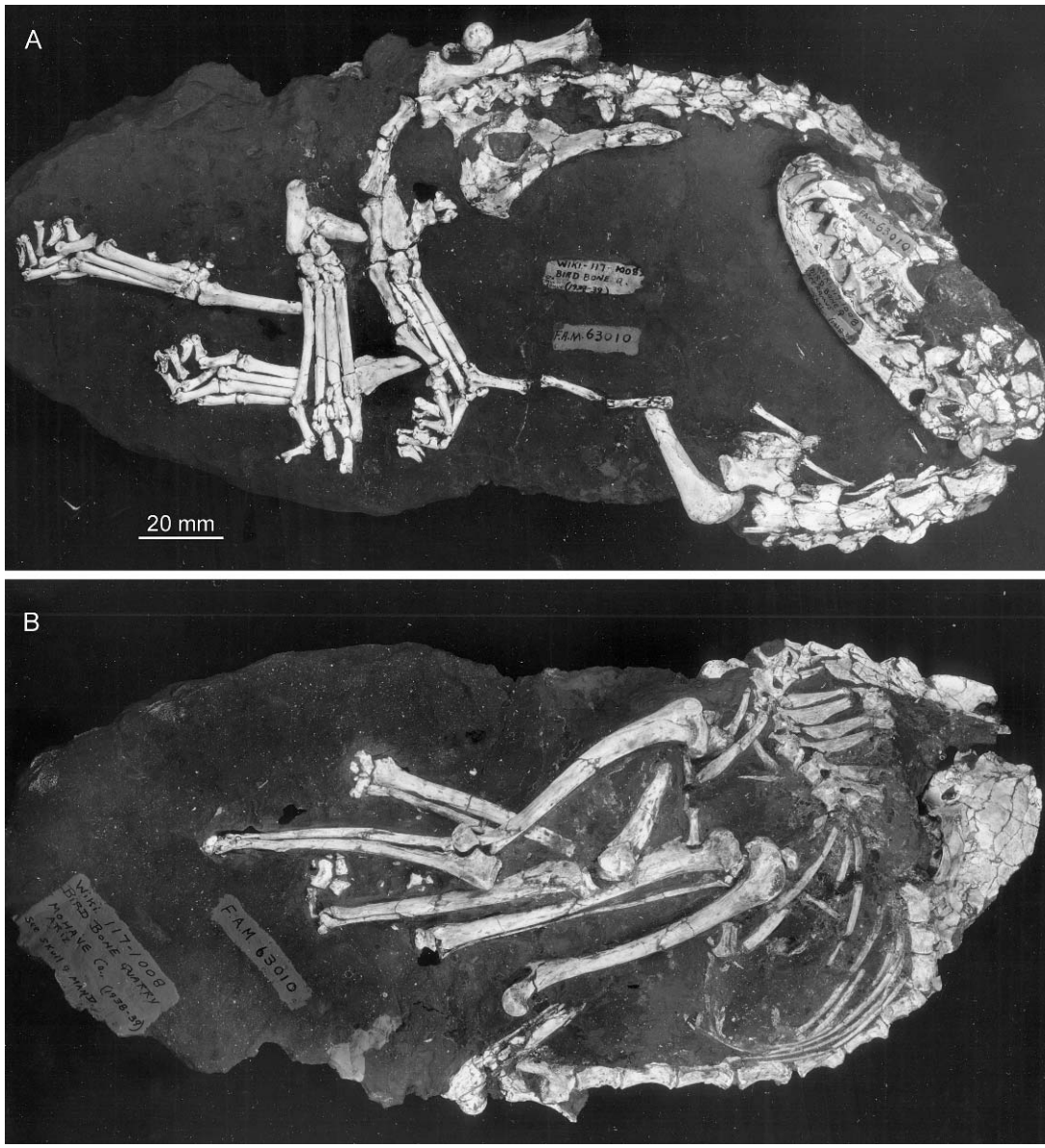

Fig. 36. *Eucyon davisi* skeleton in situ, F:AM 63010, Bird Bone Quarry, Big Sandy Formation (late Hemphillian), near Wickieup, Mohave County, Arizona. **A**. Right side (left side of skull and mandible) of nearly complete skeleton. **B**. Left side. Skeleton photographed in ultraviolet light to fluoresce the bones against matrix (illustration by C. Tarka). Both views to same scale.

Referred North American Material: Thousand Creek Formation (early Hemphillian), CIT locality 63, Humboldt County, Nevada: LACM 55210, left ramal fragment with p4; LACM 55209, right ramal fragment with m2; LACM 55208, left ramal fragment with p2 root–p4; LACM 55207, right ramal fragment with c–p1 alveoli, p2–p3 broken, and p4; and LACM 55206, left maxillary fragment with P2–P3 alveoli, P4, M1–M2, right maxillary fragment with M1 broken–M2. Line Quarry, Humboldt County, Nevada: F:AM 49286*, left maxillary fragment with P2 alveolus, P3 and P4 broken. LACM locality 1221, Hum-

boldt County, Nevada: LACM 103220, left ramus with c–p3 alveoli, p4–m1, m2 alveolus. Thousand Creek, Humboldt County, Nevada UCMP locality V69113, UCMP 112197, right ramus with c alveolus, p1–p2 (broken), p3 (alveolus)–p4, m1; and UCMP locality V78064, UCMP 121862, left M1.

Juniper Creek Canyon, Grassy Mountain Formation (early Hemphillian), Malheur County, Oregon: UO 19027, right isolated M1; UO 26743, right partial ramus with p1–m2, UO locality 2451; and UO 19950, left partial maxilla with M1–M2, UO locality 2469.

Little Valley, Grassy Mountain Formation (early Hemphillian), Malheur County, Oregon: UO 26742, fragments of skull including partial premaxilla with I1–I3, right and left partial maxillae with P1–M2 (fig. 33G), right (fig. 33E–F) and left rami with i1–m3, detached teeth including two canines, much of the atlas and axis vertebrae, scapula, humerus fragment, distal ends of radius and ulna, scapholunar, magnum, four metacarpals, and phalanges, UO locality 2381.

Hoffman Blowout, Shutler Formation (Late Hemphillian), 6 miles southwest of Boardman, Morrow County, Oregon: LACM 55212, right isolated m1.

McKay Reservoir, UO locality 2222 (late Hemphillian), Malheur County, Oregon: UO F3241, left ramus with c–m1 alveoli, m2, m3 alveolus (type of *Canis condoni* Shotwell, figured by Shotwell, 1956: fig. 6K, this paper fig. 33C–D, with UO F2353, m1, inserted into alveolus); UO F2353, isolated m1 (figured by Shotwell, 1956: fig. 6L, this paper fig. 33C, inserted into UO F3241); UO F2727, right isolated P4 (fig. 33H); UO F2107, left isolated P4; UO F3672, right isolated P4; UO F3254, left isolated m2; UO F3264, isolated lower incisor; UO F3672, right isolated P4, UO F3254, left isolated m2; UO F3264, isolated lower incisor; UO F2458, isolated p2; UO F3266*, isolated p2; UO F3262, broken canine; and UO F3253, isolated unerupted C. SDSM locality V802: SDSM 13127*, left ramus with alveoli of c–p4, m3, and crowns of m1–m2; and SDSM 57973*, left maxillary fragment with alveolus of P3, crowns of P4 and M1–M2.

Optima Local Fauna, Ogallala Group (late Hemphillian), near Cuymon, Texas County, Oklahoma: F:AM 62961-I, -N, -O, three isolated m1; F:AM 30397*, left ramus with p3–m2 alveoli; F:AM 30427*, right ramus with p1, p2–p4 alveoli, left ramus with p3–p4, m1 (alveolus); F:AM 30393*, right ramus with m2 broken; F:AM 30394*, partial left ramus with broken c–p4; F:AM 62929, left ramus with p2–m1; F:AM 62922*, right ramus with c, p2–m2; F:AM 62936, left ramus with p2–m1; F:AM 62937, left ramus with c, p1 alveolus, p2–p3, p4 alveolus, and m1; F:AM 72802, left femur, left tibia, tarsal bones, metatarsals II–V, phalanges; F:AM 72803, right radius; F:AM 72803A, right radius; F:AM 72804, left metacarpal II; F:AM 72804A, right metacarpal V; F:AM 72805, right metatarsal III; F:AM 62932, right ramus with p3–m3 (fig. 33P–Q); F:AM 62930, left ramus with p2–p3, m1; F:AM 62934, left and right rami with p3, m1–m2; F:AM 62950, right ramus with p3 broken–m1; F:AM 62951, right ramus with c–m1 (fig. 33R–S); F:AM 62952, partial left maxilla with p2–p3, p4 (broken), m1; F:AM 62958–62958C, isolated p4s; F:AM 62954, left maxilla with C–M2 (fig. 33T); F:AM 62960, isolated M1; F:AM 62953, left maxilla with P4, M1–M2 broken; and F:AM 62933 fragments of right and left rami, c, p2–p4, m1–m2.

Chamita Formation (late Hemphillian), Rio Arriba County, New Mexico: F:AM 27485, left ramus and right ramal fragment with c–m3 (p1 alveolus and m2 broken), 5 miles north of San Juan; F:AM 62836, right and left partial maxillae with P3 and M1–M2, right ramus with i1–m1, m2 broken, and calcaneum, 5 miles north of San Juan; F:AM 62835, left maxillary fragment with M1–M2, San Juan locality, upper tuffaceous zone; F:AM 27375, mandibular fragment and symphysis with i1–p3 broken and p4, Battleship Mountain.

Edson Quarry, Ogallala Group (late Hemphillian), Marshall Ranch, Sherman County, Kansas: KUMP 3608, right partial ramus with incisor alveoli, c–p4, and m1 broken (type of *Leptocyon shermanensis* Hibbard, figured by Hibbard, 1937: fig. 1); F:AM 49464, palate with C–M2 (fig. 33J–K); F:AM 49458, left maxilla with P3–P4; F:AM 49462,

left ramus with c, p2 broken–m2 (fig. 33L–M possibly part of the holotype mandible of *L. shermanensis*); F:AM 49463, right ramus with p3, m1–m2; F:AM 49466, left (fig. 33N–O) and right rami with p1–m3; F:AM 49461, right ramus with dp2–dp4, m1–m2 erupting, calcanea, scapula fragment, right metatarsals III–V, left metatarsals II–IV, phalanges; F:AM 49465, left and right rami with c–m2; F:AM 63183, partial occiput (fig. 34Q); F:AM 63184, isolated canine; F:AM 49456, isolated incisors, canines, M1–M2, left and right rami, p1–m2, isolated teeth, left tibia, left limb, calcaneum, astragalus, left metatarsals II–V, tarsals, proximal and distal phalanages, right femur, right tibia, right fibula, calcaneum, astragalus, right metatarsals II–V, phalanges, vertebrae; F:AM 49457, right ramus with m1–m2 both broken; F:AM 49470, palate with C–P4, deciduous teeth, vertebrae; F:AM 49469*, right ramus of old individual with p2 broken–m3, m2 broken; F:AM 72828A, left tibia; F:AM 72832, calcaneum; F:AM 72832A, astragalus; F:AM 63177, calcaneum; F:AM 63188, distal end radius; F:AM 63177, left metatarsal IV; F:AM 72830, right metatarsal IV; F:AM 63186, right metatarsal V; F:AM 63187, right metatarsal II; F:AM 63185, left metacarpal II; F:AM 72826, left radius, right metacarpals II–V, distal end of ulna, phalanges, and sesamoid; F:AM 63177B, distal phalanx; F:AM 63190, medial phalanx; F:AM 63176, proximal, medial, and distal phalanges; F:AM 63181, distal phalanx; F:AM 72829, left metacarpal V; F:AM 63179, distal phalanx; F:AM 72831, right metatarsal V; and F:AM 63189, right metatarsal IV. F:AM 63178, left upper canine, 2 miles south of Main quarry, Marshall Ranch (Rhino Hill Quarry).

Goodnight beds, Ogallala Group (late Hemphillian), Goodnight area, Armstrong County, Texas: F:AM 49319, left partial ramus with p2 alveolus, p3–p4, and m1 alveolus, Hill Quarry, 20 miles southwest of Claude; F:AM 49322, right maxilla with M1–M2, McGehee Place Quarry; and F:AM 49320, right isolated P4 and left isolated M1, Christian Pit 2.

Miami Quarry (= Coffee Ranch Quarry), Ogallala Group (late Hemphillian), 8 miles east of Miami, Hemphill County, Texas: F:AM 23373, right maxilla with C–P1 alveoli and P2–M2 (fig. 35J–M) and right partial ramus with p1 alveolus–m1; F:AM 23353, left partial ramus with p3–m2, m3 alveolus (fig. 35H–I); F:AM 23374, left partial maxilla with P1–P4 alveoli and M1–M2; F:AM 23373A, left isolated P4; F:AM 23376F, right isolated M1; F:AM 23374B*, m1 broken; F:AM 23376B*, m1 broken; and F:AM 23376C, right m2.

Axtel locality, UCMP locality V5319, Ogallala Group (latest Hemphillian), Rendall County, Texas: UCMP 112196, right isolated M1.

Rentfro Pit, Ogallala Group (Latest Hemphillian), 4 miles southwest of Channing, Hartley County, Texas: F:AM 62981, crushed skull with P1–M2 (fig. 35N–O), right partial ramus with p2–m2 (p3 broken), m3 alveolus (fig. 35P–Q), and atlas: and F:AM 62980, left partial ramus with m1 broken–m3.

Gravel pit on the Virgil Clark place (latest Hemphillian), 2.5 miles southeast of Higgins, Texas, in Ellis County, Oklahoma: F:AM 22296, right ramal fragment with p4–m1 alveoli and m2.

Bird Bone Quarry, Big Sandy Formation (late Hemphillian), near Wikieup, Mohave County, Arizona: F:AM 63007, partial skull with P3–M2; F:AM 63004, anterior portion of skull with P2, P4–M2 (fig. 34D–E), and isolated teeth; F:AM 63039, anterior portion of skull with P2–M2; F:AM 63019, partial skull with P1–M2, left and right rami with p3–m3; F:AM 63038, palate with P2–M2, left and right rami with p2–m2, isolated c; F:AM 63033, left and right maxillae with P4–M2; F:AM 63034, left and right maxillae with P1–M2 (P3 alveolus) and left ramus with p2–p3; F:AM 63020, left and right maxillae with C, P4–M2, left and right rami with m1, vertebrae; F:AM 63012, right maxilla with P2 and P4; F:AM 63021, right maxilla with C, P4–M2; F:AM 63013, left and right maxillary fragments of old individual with P2–P4 and M1–M2; F:AM 62999, left ramus with p4 broken–m2; F:AM 63000, right ramus with m1–m2; F:AM 63001, left ramus with c–m2; F:AM 63002, left ramus with p3 broken–m2, m1 (broken); F:AM 63015, left and right rami with p1–m1; F:AM 63016B, right ramus with p3–m2; F:AM 63016C, left ramal

fragment with m1; F:AM 63016D*, right ramus with p1–p2; F:AM 63022, left ramus with m1; F:AM 63023, right partial ramus with p4–m2; F:AM 63025, left ramus with p2–m1; F:AM 63026, left ramus with p2–m2; F:AM 63027, right ramus with p2, p4–m1 (all broken), and m2; F:AM 63028C, left partial ramus with p4–m1 broken, m2; F:AM 63041, left ramus with p2–m2; F:AM 63042, right ramus with p1–m3; F:AM 63051*, left and right rami with m1; F:AM 63056, left and right (fig. 35D–E) maxillae with P2, P4–M2, and left (fig. 35F–G) and right rami with c, p3–m2, isolated teeth; F:AM 63057, right maxilla with P4–M2, left and right rami with m1; F:AM 63063, right maxilla with P4–M2; F:AM 63046, left and right rami with p3 broken–m2; F:AM 72593*, left ramus with p3–p4 (all broken), m2, and all alveoli; F:AM 72594*, left ramus, all alveoli; F:AM 72595*, right ramus with m2; F:AM 72605, right ramus with p1–p4; F:AM 72609*, right ramus with p3; F:AM 63010, crushed skull (fig. 34F, H) and mandible (fig. 34G, O) with complete dentition and articulated skeleton (fig. 36A–B); F:AM 63058, left and right (fig. 35A) maxillae and premaxilla with I3 broken, P2–M2, left and right (fig. 35B–C) rami with p2–m1, isolated canine, and right m2; F:AM 63005, anterior portion of skull with P3–M1 (fig. 34A) and cranial fragment (fig. 34P); F:AM 63191, left maxilla with M1, left and right partial rami with all alveoli, distal femur cap, distal end of tibia, metatarsals II, IV–V, metapodial fragments, proximal and distal phalanges, two isolated p4, isolated m1 broken, vertebrae, cuneiform, cranial and maxillary fragments; F:AM 63192*, left partial ramus with p4–m3 alveoli, radius, caudal vertebrae; F:AM 63196, calcaneum; F:AM 63198, metatarsal II; F:AM 63199*, isolated left m1; F:AM 63203*, isolated right p2 and premolar fragments; F:AM 63200*, right p4, metacarpals III (left and right), V, and II (left and right partial), distal end of tibia, proximal ends of left and right radius, proximal end of ulna, proximal and medial phalanges, vertebrae, limb and dentary fragments; F:AM 63201, astragalus and cuboid; F:AM 63202, astragalus; F:AM 63206, left calcaneum and astragalus, left metatarsals II–IV, one proximal, two medial, and two distal phalanges, right metatarsals II–III, V (broken), two proximal, two medial, two distal phalanges, carpals, distal end left and right tibiae, partial pelvis, caudal vertebrae; F:AM 72555, right humerus; F:AM 72558, right humerus; F:AM 72559, right humerus; F:AM 72561, right radius; F:AM 72562, left radius; F:AM 72563, left radius; F:AM 72564, left radius; F:AM 72567, right ulna; F:AM 72568, right ulna; F:AM 72570, left femur; F:AM 72572, right tibia; F:AM 63019A, right humerus, proximal end left humerus, left femur, distal head right femur, right tibia (three pieces), left tibia, left and right calcanea, right astragalus, distal ends of three metapodials, three phalanges, scapula and pelvic fragments, vertebrae; F:AM 72583, left metacarpal IV; F:AM 72583A, left metacarpal IV; F:AM 72584, right metacarpal V; F:AM 72584A, left metacarpal V; F:AM 72585, left metatarsal II; F:AM 72585A, right metatarsal II; F:AM 72586, left metatarsal III; F:AM 72587, left metatarsal III, F:AM 72586A, left metatarsal V; F:AM 72587A, right metatarsal II; F:AM 72587B, left metatarsal III; F:AM 72588, right metatarsal IV; F:AM 72589, right metatarsal IV; F:AM 72589C, left metatarsal IV, right metatarsal V; F:AM 72590, left metatarsal V; F:AM 72590A, left metatarsal V; F:AM 72590B, left metatarsal V; F:AM 72573, left metatarsals II–V; F:AM 72575, left metatarsals II–V, two phalanges; and F:AM 63207, calcaneum and astragalus.

Clay Bank Quarry, Big Sandy Formation (late Hemphillian), near Wikieup, Mohave County, Arizona: F:AM 63031, crushed partial skull with C–M2, left and right rami with p2–m2; F:AM 63008, partial skull with P4 broken–M2, right ramus with p3 broken–m2, distal and left humerus, proximal end right femur, calcaneum, phalanges; F:AM 63008X, right ramus with p2 broken, p4 broken, m1, right ramus with p3–m2 (p4 broken), left maxillary fragment with P4–M1 broken; F:AM 63008Y, anterior portion of skull with P2, P4–M2; F:AM 63006, right maxilla with P4, M2, cranial fragments; F:AM 63011, left maxilla with P2, P4–M2; F:AM 63009, skull with P3–M2 (fig. 34P), two astragali, phalanges, and caudal vertebrae; F:AM 63009A*, right ramus with p4 broken–m2; F:AM 63009C*, right ramus with p2 broken, m1 broken; F:AM 63003,

left and right rami with p1–m3; F:AM 63009B, left ramus with c–m2 (fig. 34M–N); F:AM 63014, left ramus with p2–m1; F:AM 63016A, right ramus with p3 broken–m2; F:AM 63018, left ramus with p2–m3 (p3 broken); F:AM 63024, right ramus with p3–p4 both broken, m1–m2, and m3 broken; F:AM 63028, isolated m1; F:AM 63028A, left ramus with p1–m2; F:AM 63028B, left ramus with p2–m1; F:AM 63028D, right isolated m1; F:AM 63028E, left ramus with m1–m2; F:AM 63028M right ramus with p2–p3, p4 alveolus, m1–m2, m3 alveoli; F:AM 63028G, left ramus with p4–m1; F:AM 63028H, right m1; F:AM 63028I, right ramus with m1–m2; F:AM 63028J, right ramus with p3 broken–m1 and m2 broken; F:AM 63028K*, right ramus with p3 broken, m1; F:AM 63030, anterior portion of skull and ramus with C–M3, limb fragments; F:AM 63029, left ramus with p3–m2; F:AM 63032, right ramus with m1–m2; F:AM 63036*, right isolated m1; F:AM 72604, left ramus with c–m2; F:AM 72592, left ramus with p2–m2; F:AM 72596, right ramus with p1–m2; F:AM 72601, left ramus with p4 broken, m1–m2; F:AM 72591, right ramus with c, p2–m2; F:AM 72597, left ramus with p2 broken–m1 (p3 broken); F:AM 72602, left ramus with p3–m1; F:AM 63047, right ramus with p4–m2; F:AM 63049, left ramus with m1–m2; F:AM 63044, right ramus with p1–p2, p4–m2 all broken; F:AM 63045, right ramus with c, p1 alveolus, p2–p4, m1, m2 broken; F:AM 63043, right ramus with p1–m2; F:AM 63017, left m1; F:AM 63017A, left ramus with p2–m1; F:AM 63197, metatarsal IV, phalanges; F:AM 72557, distal end right humerus; F:AM 72560, right radius; F:AM, left radius; F:AM 72570A, right femur; F:AM 72571, left tibia; F:AM 63208, left ulna; F:AM 63009D, left humerus; F:AM 63009E, right humerus; F:AM 63009F, right ulna; F:AM 63009G, distal end left radius, proximal end right radius, and partial proximal end left ulna; F:AM 63009H–L, right femur; F:AM 63009M, left femur; F:AM 63009N, left tibia; F:AM 63009O, right tibia; F:AM 63009P, left tibia; F:AM 63009Q–R, right tibii; F:AM 63009S, calcaneum, astragalus, right metatarsals II, III, V, phalanges, scapula and pelvic fragments, vertebrae; F:AM 63017B, left and right humeri; F:AM 63017C, proximal end right radius, distal end left radius; F:AM 63017D, left and right ulnae; F:AM 63017E, proximal end right femur; F:AM 63017F, proximal end left and right tibiae; F:AM 63017G, right tibia; F:AM 63017H, calcaneum, astragalus, isolated teeth, metapodials, scapula fragments, vertebrae; and F:AM 63208, left ulna.

Grey's Ranch Quarry, Big Sandy Formation (late Hemphillian), Mohave County, Arizona: F:AM 63040, right ramus with c–p4, m1 broken; F:AM 63040A, right partial maxilla with M1–M2 (associated with F:AM 63040 and possibly one individual); F:AM 63048, left ramus with p3–m3; F:AM 72603, right maxilla with C broken, P2 broken, right ramus with p4–m2 (m1 broken); F:AM 63204, astragalus; F:AM 63204A, astragalus; F:AM 63204B, calcaneum; F:AM 63205, astragalus; F:AM 63205A, astragalus; F:AM 63205B, calcaneum; F:AM 63193, calcaneum; F:AM 63194, calcaneum; and F:AM 63195, distal end of tibia.

Old Cabin Quarry, Quiburus Formation (late Hemphillian), near Redington, Pima County, Arizona: F:AM 72661, crushed skull with C–M2, left ramus with p2 and p4–m3 all broken, right humerus, astragalus; F:AM 72662, crushed partial skull with right C–P1 (broken), P2–M2, and left I2–P2, P3–P4 broken; F:AM 72663, left maxilla with P4–M2; F:AM 50685, right maxilla with P2–P4; F:AM 50686, left maxilla with P2–M2; F:AM 50688, right M1–M2; F:AM 75825*, crushed palate with C, P2–M2; F:AM 75836, crushed skull with P4 broken, left and right rami with c–m1, m2 broken, left and right humeri, metatarsals, astragalus and phalanx, scapula; F:AM 75796, skull with P4–M2; F:AM 75841, crushed skull with C–M2; F:AM 75838, skull with P2–M2; F:AM 75797, crushed skull with C, P2–M2; F:AM 75837, palate with P1–M2, right ramus with p2–p4 and m1–m2 both broken; F:AM 75843, palate with P3–M2; F:AM 75844, left maxilla with P3–M2; F:AM 75846, right maxilla with P4–M2; F:AM 75810, left and right rami with c–m3; F:AM 75811, left and right rami with c–m2; F:AM 75818, left ramus with p3–m3; F:AM 75845, right maxilla with P3–M2, left and right rami with p1–m3; F:AM 75799, left ramus with c–m2; F:AM 75806, left ramus with p4 broken–m3;

F:AM 75807, right ramus with p1–m1; F:AM 75809*, c broken, p4–m2 all broken; F:AM 75812, left and right rami with m1–m2; F:AM 75813*, left ramus with p4 broken–m3; F:AM 75815, right ramus with p3–m3, left ramus with m1 broken–m2; F:AM 75816, left and right rami with p2 broken, p4 broken–m1; F:AM 75817, right m1; F:AM 72656 and 72656A, right and left rami with i3–m2 and m3 alveoli; F:AM 72657, left isolated m1; F:AM 50696, left isolated m1; F:AM 50697, right isolated m1; F:AM 72659, right isolated m1; F:AM 50695, right isolated m1; F:AM 72658, left ramal fragment with p4–m1; F:AM 75798, right partial ramus with c–m2; F:AM 50689*, left partial ramus with p1 alveolus p2–p3, p4 alveolus, m1–m2; F:AM 99373, partial skeleton including scapula, two humeri, two radii, one partial ulna exposed, metacarpals II–III, metatarsals II–V, two incomplete and broken metapodials, and articulate vertebrae; F:AM 73833B, right humerus; F:AM 75833C, left humerus; F:AM 75833D, right humerus, F:AM 75852, distal end right humerus, left tibia, astragalus, left metatarsals II–V; F:AM 75853, right tibia; F:AM 75834, left tibia, right radius, left ulna; F:AM 75849, articulated right metacarpals II–V; F:AM 75850, right metacarpals II–III; F:AM 75854, articulated metatarsals III–V; F:AM 75833, left humerus; F:AM 75833A, right humerus and fragments of radius and femur; F:AM 75833E, left humerus; F:AM 63209, right humerus.

Redington Quarry, Quiburus Formation (late Hemphillian), northwest of Redington, San Pedro River Valley, Pima County, Arizona: F:AM 63094, crushed skull with P2, P4–M2; F:AM 75840, fragmentary skull and rami, limbs, F:AM 75808*, crushed partial skull with broken teeth; F:AM 75804*, left ramus with c–p1, p4–m2, upper dentition with P2–P4 all broken and M1; F:AM 75835, crushed maxillae with C–P4 all broken, M1–M2, and partial ramus with i1–m2 all broken; F:AM 75839*, right maxilla with I1–M2; F:AM 63096, right partial maxilla with I1–M2; F:AM 75814*, left and right rami with c–m2; F:AM 63087, left ramus with p1–p2, m1; F:AM 63097*, right ramus with p2–p4 and m1 broken; F:AM 63086, isolated right M1, right ramus with m1; F:AM 63088, isolated right m1; F:AM 63088A*, right ramus with p2–p4; F:AM 63093*, right M1, left m2; F:AM 63095, right ramus with p4–m2; F:AM 62786*, right ramus with p2 broken–p4, m1 broken; F:AM 62789*, left ramus with p4; and F:AM 75851; left femur, left tibia, and calcaneum; and F:AM 108427, right humerus.

San Pedro Valley, Quiburus Formation (late Hemphillian), 13 miles south of Mammoth, San Pedro Valley, Pima County, Arizona: F:AM 63081, left partial maxilla with P3–M2, Hilltop Dig; F:AM 63084, left partial ramus with c–p1 and p3–m2 all broken, Least Camel Quarry, Camel Canyon; F:AM 63085*, left partial ramus with c–m1 all broken, Least Camel Quarry, Camel Canyon; F:AM 63090, right partial ramus with c–p4, m1 broken, Camel Canyon; and F:AM 63083*, right ramal fragment with p4 root–m1 broken.

Bidahochi Formation (late Hemphillian), Keams Canyon, Navajo County, Arizona: F:AM 23392, right partial ramus with m1 and m2–m3 alveoli.

Golgotha Water Mill Pothole locality (late Hemphillian), Spring Valley near Panaca, Lincoln County, Nevada: F:AM 49294, left (fig. 35R–S) and right rami with c–m2; F:AM 49291A, left ramus with m2; F:AM 49291A*, juvenile right ramus, deciduous premolars; F:AM 49293*, right ramus with all alveoli; F:AM 49296, right maxilla with P4, left ramus with p2–m2; F:AM 49297, right ramus with p3–m1; F:AM 62794, proximal end right ulna; F:AM 62794A, right metacarpal V; F:AM 62794B, left metacarpal III; F:AM 62794C, right metacarpal V; F:AM 62794D, left metacarpal IV; F:AM 62794E, right metacarpal IV; F:AM 62794F, calcaneum; F:AM 62794G, distal end of ulna; F:AM 62794H, phalanges; F:AM 62795, right isolated m1; F:AM 62795A, left isolated m1; F:AM 62795B*, right isolated p4; F:AM 62795C, isolated C; and F:AM 62795D, left isolated i3.

Turlock locality 4, UCMP locality V5837, Mehrten Formation (late Hemphillian), Stanislaus County, California: UCMP 52423, partial palate with P2–M2.

Pinole site 2, UCMP locality V3425, Pinole Formation (late Hemphillian), Alameda

County, California: UCMP 62408, left partial ramus with p4 alveolus, m1–m2, m3 alveolus; UCMP 60667, left partial ramus with m1; UCMP 64836, left partial ramus with p2 broken, p3 alveolus–m2, m3 alveolus; and UCMP 58333, right ramus with c broken–p1 alveolus and p2–m2, m3 alveolus.

Fort Green Mine (Agrico), Polk County, Florida, Bone Valley Formation (late Hemphillian): UF 45884*, fragment of right ramus, m1–m2, m3 alveolus.

Yepomera (latest Hemphillian), Chihuahua, Mexico: LACM 30206*, isolated right broken M1, CIT locality 276; and LACM 30216*, right premaxilla and partial maxilla with I1–C alveoli, P1–P2, and P3 anterior root, CIT locality 287.

Distribution in North America: Early Hemphillian of Oregon and Nevada; late Hemphillian of Kansas, New Mexico, Oklahoma, Texas, Arizona, Nevada, Oregon, California, Florida, and northern Mexico.

Revised Diagnosis: *Eucyon davisi* differs from *E.*? *skinneri* in its larger size; longer jaw; more elongate, taller crowned premolars; p4 with second posterior cusp; m1 trigonid relatively longer, protoconid taller crowned, entoconid and hypoconid taller crowned, and larger hypoconulid shelf.

Eucyon davisi differs from *Canis ferox* and *C. lepophagus* in its smaller size and less robust skull and jaws; frontal sinus ends well before frontoparietal suture; jugal shallower relative to length of skull; width of skull across cheek teeth greater relative to length of skull; sagittal crest weaker; inion wider (never narrows to a point); premolars less robust; p4 anterolabial border generally less rounded; M1 paracone and metacone lower crowned and nearly subequal in size with stronger labial cingulum and stronger parastyle; m1 talonid without transverse crest between entoconid and hypoconid and hypoconulid shelf relatively smaller; angular process of mandible less expanded with smaller fossae for pterygoid muscle; and radius/tibia ratio less than 80%.

Description and Comparison: Numerous dentitions are referred to *E. davisi*, but a good skull representing the North American populations is still unknown. A brief description of the skull is herein based principally on three crushed skulls (F:AM 63010, 63007, and 63009, one of which (F:AM 63009) we have reconstructed (fig. 34I–K, P)) and a partial palate with an associated cranial fragment (F:AM 63005, fig. 34A–C) from the late Hemphillian Big Sandy Formation near Wikieup, Arizona. Chinese specimens of the species (Xiagou, Nihe subbasin, Gaozhuang Formation, early Pliocene, Yushe, Shanxi Province, Tedford and Qiu, 1996) are used to augment the comparisons where the North American evidence is inadequate.

The skull of *E. davisi* is intermediate in size to that of *Vulpes vulpes* and *Canis latrans*. Compared to *C. lepophagus*, the zygomae in *E. davisi* flare more laterally with a more marked eversion of the dorsal border. The frontals in *E. davisi* are narrower and less elevated, and the sinuses are less elongate and less posteriorly extended than in *C. lepophagus*. In the Chinese material (F:AM 97056), there is a dorsal inflation of the sinus behind the postorbital processes. Uninflated temporal crests join at or just anterior to the frontoparietal suture to form a low sagittal crest. The sagittal crest is weaker and the supraoccipital shield is narrower and more rounded and extends less posteriorly than in *C. lepophagus*. The basioccipital in *E. davisi* is narrow between the bullae, and the condyles are small. Compared to the size of the skull, the bullae average relatively and actually longer than those of *C. lepophagus* and the lip of the auditory meatus is smaller and less laterally extended. The upper incisors of *E. davisi* are simple, with only minute medial accessory cusps on I1 and I2, and a faint lingual cingulum is present on I1 and I2. The I3 is only slightly larger than I2 and lacks a medial accessory cusp, but it has a stronger lingual cingulum. The incisors are similar to those of *Vulpes* and relatively smaller than those of *Canis*. Although the premolars show considerable variation, they can be characterized as elongate, slender, and less robust than those of *C. lepophagus*. P3 is generally without a posterior cusp, but a minute cusp may occasionally be present. The morphology of the P4 varies in the Wickieup sample from the slender carnassial with a strong anterolingually directed protocone, a sharp anterolabial border and a deeply notched anterior border (F:AM 63058, fig. 35A) to a

robust carnassial with a smaller and less anteriorly situated protocone, and a more rounded anterolabial border (F:AM 63056, fig. 35E). The former variant is predominant in the available *E. davisi* samples and these features are plesiomorphous. The latter variant is the dominant form of the P4 in the *C. lepophagus* populations known to us. Both M1 and M2 in *E. davisi* have a low-crowned, nearly subequal paracone and metacone and a strong labial cingulum. M1 also has a prominent parastyle, a weak paraconule, and a strong protocone with a postprotocrista that joins the metaconule. A weak but distinct cingulum extends lingually from the base of the paracone across the base of the protocone and becomes continuous with the hypocone, ending at the metaconule. In most specimens the M1 is transversely narrow relative to its length as in the type of *E. davisi*. The M2 has a well-developed protocone and a greatly reduced metaconule, which may be limited to a low swelling at posterior extension of the postprotocrista. In some specimens the metaconule is absent as well as the postprotocrista. A distinct lingual cingulum extends from the paracone to the metaconule. Compared to *C. lepophagus*, the paracone and metacone are lower crowned and nearly subequal in size.

The horizontal ramus is shallower and less robust than that of *C. lepophagus*. Two mental foramina are present; the anterior foramen is below the p1 or below the diastema between p1 and p2. The smaller posterior foramen is below p3 with its position varying between the roots of this premolar. The deep masseteric fossa has a well-outlined anterior margin and most of the ventral margin is marked by a distinct masseteric crest. The angular process of the mandible is less expanded, and the fossa for the inferior pterygoid muscle is smaller than in *Canis*.

In *E. davisi* i1 is a simple peglike tooth. The i2 is slightly larger and has a small lateral accessory cusp. The i3 is still larger with a prominent lateral accessory cusp as in *Vulpes* and unlike the more robust incisors with stronger accessory cusps seen in *Canis*. The lower premolars are elongate and generally slender with the crown height varying from moderate to tall. A small posterior cusp is sometimes present on p2 (e.g., F:AM 63010, fig. 34G, O). The p3 posterior cusp varies from absent (e.g., F:AM 62932, fig. 33P–Q) to strong in F:AM 63010 (fig. 34G, O) and F:AM 63056 (fig. 35F–G) within a single population. Additionally, the p4 has a second posterior cusp in front of the cingulum. The tip of the major cusp of p4 lies at or above the paraconid of m1. The m1 trigonid in *E. davisi* varies from moderately short with a somewhat oblique paraconid (F:AM 23373, fig. 35H) to elongate with a less oblique shear (F:AM 63041). The protoconid is tall and a close examination will occasionally reveal a faint protostylid ridge. The hypoconid is larger than the entoconid and the two cusps are very rarely joined by a weak transverse crest (F:AM 63010, fig. 34O). On the first lower molar, the hypoconid and entoconid vary from being closely proximate at their bases (F:AM 63056, fig. 35F) to widely separated cusps (F:AM 23353, fig. 35H). The position of the entoconid is usually slightly posterior to that of the hypoconid, and a small entoconulid is sometimes present. Considerable variation is seen in the development of the hypoconulid. A small hypoconulid shelf is usually present (F:AM 63010, fig. 34O), but this varies to near absence (F:AM 63056, fig. 35F). In *C. ferox* the talonid is about as in *E. davisi*, but in *C. lepophagus* the m1 hypoconid and entoconid are usually joined by a transverse crest, and the hypoconulid shelf tends to be larger and a cusp is occasionally present.

The m2 in *E. davisi* is usually larger, relative to the size of the m1, than that of *C. lepophagus*. A distinct paraconid is not present, but a strong crest (paracristid) extends anteriorly from the protoconid to the anterior cingulum. The well-developed anterolabial cingulum ends at the base of the protoconid. The metaconid is slightly smaller than the protoconid, with its position slightly posterior to the protoconid. The talonid is marked by a well-developed hypoconid, a small entoconid, and sometimes a small entoconulid. The m3 is a small tooth with an oval occlusal outline. It consists of two small cusps, the protoconid and metaconid. The protoconid is the larger and is situated slightly anterior to the metaconid. A weak

crest runs anteriorly from the protoconid to the anterior border of the m3.

Based on the measurements of an articulated skeleton of *E. davisi* (F:AM 63010, fig. 36A–B and appendix 4) the length of the limb bones can be compared to those of *Leptocyon*, *Vulpes*, and *Canis* (fig. 52 and appendix 4). The relative proportions of the limb bones closely follow those of *Leptocyon vafer* (fig. 52). The presence of an occasional entepicondylar foramen of the humerus of *Eucyon* is a primitive feature relative to *Canis*. In *Eucyon* this foramen is usually absent, but when present, it is small relative to the size of the humerus with an extremely weak bridge enclosing the foramen. Unlike the limbs of Recent *Canis* species, the radius of *E. davisi* is short relative to the length of the humerus and tibia. The radius/tibia ratio of the articulated skeleton (F:AM 63010) is 78.7%, within the upper part of the range of such values for living *Vulpes* species. Additional primitive skeletal features of *E. davisi*, comparable to those of *Vulpes*, but unlike *Canis*, are a more robust ulna, a more erect olecranon process with a less concave anterior border, and a stronger posterior tuberosity (fig. 39C). Furthermore, the fibula of *E. davisi* also tends to be relatively stronger than that of its contemporary *V. stenognathus*. The tibia/femur ratio (F:AM 63010: 101.6%) in *E. davisi* approximates that in living species of *Canis* and is less than that in *Vulpes*. Metatarsal I in *E. davisi* is reduced to a short proximal rudiment, as in both recent *Vulpes* and *Canis*. Unfortunately, a comparison is impossible between the metatarsal I of *E. davisi* and *V. stenognathus* because it is unknown in the latter. However, an examination of the metatarsal II of *V. stenognathus* (F:AM 72580) shows that the articular facet for metatarsal I is relatively larger, and especially anteroposteriorly longer, than that of *E. davisi* and *V. vulpes*. This indicates that the proximal end of the metatarsal I of *V. stenognathus* was larger than that of *E. davisi*. Thus, the metatarsal I of *V. stenognathus* may have been intermediate in size between the functional digit I of *Leptocyon* and a proximal rudiment in *V. vulpes*. Such evidence also suggests that the metatarsal I of *E. davisi* may have been more reduced than that of its contemporary, *V. stenognathus*.

Discussion: Merriam (1906: 5) tentatively referred to the genus *Canis* a partial maxilla (UCMP 545, fig. 33I) with M1–M2 apparently from the early Hemphillian Rattlesnake Formation of eastern Oregon. In 1911, he selected this maxilla as the type of *C. davisi* and referred additional teeth to that taxon from the early Hemphillian Thousand Creek Formation in northwestern Nevada. Merriam compared the type of *C. davisi* with the living coyotes of eastern Oregon and reported that the upper molars were a little smaller but the M2 was relatively larger and its metacone was about equal in size to the paracone. He described the M1 of *C. davisi* as having a laterally compressed and sharp paracone and metacone, with the protocone joining the incipient paraconule and metaconule to form a V-shaped ridge. We have found that these molars are also lower crowned, have stronger parastyles, and stronger labial cingula than the coyotes. These characters, and those noted by Merriam, serve to distinguish the upper molars of *Eucyon davisi* from those of *Canis*.

The type of *Leptocyon shermanensis* Hibbard, 1937, is from the late Hemphillian, Edson Quarry, Kansas. According to Hibbard (1937), the length of the m1 in the type is 17.3 mm and it lies within the size range of seven Edson specimens in our collection in which the m1 ranges from 17.0 to 18.0 mm in length. This sample differs markedly from both *Leptocyon* and *Vulpes* in its larger size, deeper horizontal ramus, especially beneath the p1, and more robust premolars. Moreover, the posterior cusps on p3 and p4 are stronger than in *Vulpes*. Regarding the broken m1 in the type, Hibbard stated that the entoconid is weakly developed and there is no indication of a hypoconulid. We also note the lack of a transverse crest connecting the hypoconid and entoconid in Hibbard's type. In the F:AM Edson sample the m1 entoconid varies from moderate to strong, and a weak transverse crest and a weak hypoconulid shelf are sometimes present. A partial palate (F:AM 49464, fig. 33J–K) in our topotypic sample is larger but morphologically similar to the type of *E. davisi*. The paracone and metacone are low-crowned, and the parastyle and labial cingulum are strong as in the type of *E. davisi*. A well-

developed protocone in both M1 and M2 joins a strong metaconule in M1 and a greatly reduced metaconule in M2. Another specimen (F:AM 49456) having M2 lacks both the metaconule and postprotocrista. The morphology of the Edson sample is very similar to other late Hemphillian specimens herein referred to *E. davisi*.

Shotwell (1956: 733) described *Canis condoni* from the late Hemphillian McKay Reservoir Local Fauna in Northeastern Oregon and the type is a lower jaw with m2 (UO F3241). His description of this taxon was also based on an isolated m1 fitting almost perfectly into the alveolus on the type jaw (fig. 33C–D). According to Shotwell's diagnosis, the type m2 is transitional between that of *Tomarctus* and *Canis* in the presence of a small paraconid that is separated from the protoconid "by a minute valley." We question the presence of a distinct paraconid and prefer to consider it the paracristid extending anteriorly from the protoconid. Hence, the morphology of the m2 is not really transitional but within the limits of variation in samples of *E. davisi* and species of *Canis*. The weak transverse crest between the entoconid and hypoconid and the small hypoconulid in the referred m1 are also characteristic of other samples of *E. davisi* and hence we refer *C. condoni* to that species.

Canis Linnaeus, 1758

Thos Oken, 1816.
Vulpicanis de Blainville, 1837.
Lyciscus Smith, 1839.
Sacalius Smith, 1839.
Oxygous Hodgson, 1841.
Lupulus Gervais, 1855, not de Blainville, 1843, a nomen nudum.
Simenia Gray, 1868.
Dieba Gray, 1869.
Macrocyon Ameghino, 1881.
Luppullella Hilzheimer, 1906.
Schaeffia Hilzheimer, 1906.
Alopedon Hilzheimer, 1906.
Stereocuon Mercerat, 1917.
Aenocyon Merriam, 1918.
Megacyon von Koenigswald, 1940.
Oreocyon Krumbiegel, 1949, not *Oreocyon* Marsh, 1872, a creodont.
Dasycyon Krumbiegel, 1953, replacement for *Oreocyon* Krumbiegel, 1949.

Type Species: *Canis familiaris* Linnaeus, 1758.

Included North American Species: *Canis lupus* Linnaeus, 1758; *C. latrans* Say, 1823; *C. dirus* Leidy, 1858; *C. armbrusteri* Gidley, 1913; *C. lepophagus* Johnston, 1938; *C. edwardii* Gazin, 1942; *C. cedazoensis* Mooser and Dalquest, 1975; *C. ferox* Miller and Carranza-Castañeda, 1998; *C. thöoides*, new species and *C. feneus*, new species.

Distribution in North America: Late Hemphillian to Recent (late Miocene to Recent).

Revised Diagnosis: Synapomorphies that unite species of *Canis* with those of *Cuon*, *Lycaon*, and *Xenocyon* and serve to distinguish them from all other members of the Canina are: frontal sinus large, penetrates postorbital process and extends posteriorly to frontoparietal suture; supraoccipital shield triangular in shape, inion usually pointed and overhanging condyles; I3 crown and cingulum enlarged; superior fossa of angular process for median pterygoid expanded; p4 with second posterior cusp; m1 entoconid united with hypoconid by cristids; and forelimb long relative to hindlimb.

Canis is primitive relative to *Cuon*, *Lycaon*, and *Xenocyon* in its relatively larger canines and lack of such dental adaptations for hypercarnivory as m1–m2 metaconid and entoconid small or absent; M1–M2 hypocone small; M1–M2 lingual cingulum weak; M2 and m2 small, may be single-rooted; m3 small or absent; and wide palate.

Discussion: The oldest remains from North America that can definitely be attributed to the genus *Canis* are those described below from the late Hemphillian of western North America. Previously referred to *Canis* in the Late Miocene of western Europe was the holotype maxillary fragment and a subsequently referred lower carnassial (Pons-Moya and Crusafont, 1978) of *Canis cipio* Crusafont, 1950, from late Turolian deposits of the Teruel Basin of Spain. The fragmentary nature of these remains limits observation of most of the derived features of *Canis* or the *Canis* group, and, accordingly, the generic allocation of *C. cipio* has been recently questioned (Rook, 1992), and we provide a further analysis in the conclusions of this work.

Canis ferox Miller and Carranza-Castañeda, 1998
Figures 37A–G, 38A–Q, 40, 43, 44, 52; appendices 2–4

Canis lepophagus: Bjork, 1970: 13.
Canis davisi: Gustafson, 1978: 36.
Canis lepophagus (in part): Nowak, 1979: 71.
Canis ferox Miller and Carranza-Castañeda, 1998: 549.

Type: IGM 1130, nearly complete skull, highly fragmented, but little distorted, with badly eroded left and right P3–M2, associated, left ramus better preserved, with c alveolus, p1 broken, p2 alveolus, p3, p4 broken, m1–m2, m3 alveolus, atlas fragment, partial 3rd cervical, three fragmented thoracic vertebrae, left scapula, nearly complete left and right humeri, fragmented of right ulna, right metacarpals IV and V, nearly complete left femur, patella, nearly complete right tibia, left calcaneum, cuboid, navicular and cuneiform, left and right proximal ends of 2nd metatarsals, two proximal, two medial, and five distal phalanges. Figured by Miller and Carranza-Castañeda (1998: figs. 4, 5). From the Rancho San Martin locality (GTO-42), 2 km northeast of the village of Rancho Viejo and 12 km north of the city of San Miguel Allende, Guanajuato, Mexico, in the lower part of the Rancho Viejo beds (late Hemphillian).

Paratype: F:AM 49298, skull with right I1–I3, C–P1 alveoli, P3–M2 and left I1–P1 alveoli, P2–M2; isolated left I3 and P1; right and left mandibular rami, with i3–m3, axis and 3rd cervical, one thoracic and two caudal vertebrae, and fragment of pelvis from the Golgotha Water Mill Pothole site (late Hemphillian), from unnamed deposits in Spring Valley, near Panaca, Lincoln County, Nevada,

Referred Material: Optima Local Fauna (late Hemphillian), near Guymon, Texas County, Oklahoma: F:AM 62955, left isolated P4; and F:AM 30468, left isolated M1.

Leyden loality, Chamita Formation (late Hemphillian), Rio Arriba County, New Mexico: F:AM 27388, left partial ramus with p3–p4 alveoli and m1–m2.

Bird Bone Quarry, Big Sandy Formation (late Hemphillian), near Wikieup, Mohave County, Arizona: F:AM 63032, palate with incisor alveoli, left canine and P1 alveoli, right P2–P3 broken, left P2–M1, right P4, M1 broken, M2 (fig. 38A); F:AM 63035, right and left (fig. 38C) rami with right teeth broken, left c–m2; F:AM 73606, left partial ramus with c broken, p1 alveolus, p2–p4, m1 broken; F:AM 72556, left humerus; F:AM 72566, left radius; F:AM 72569A, left ulna; F:AM 72581, left metacarpal II; F:AM 72577, metacarpals II, III, and incomplete metacarpal IV; F:AM 72572A, left tibia; F:AM 72572C, left tibia; F:AM 72572B, left tibia; F:AM 72610, left metatarsal II; F:AM 72585B, left metacarpal II; F:AM 72611, left metatarsal II; F:AM 72587D, left metatarsal II; F:AM 72589B, left metatarsal IV; and F:AM 72589A, right metatarsal IV.

Clay Bank Quarry, Big Sandy Formation (late Hemphillian), near Wikieup, Mohave County, Arizona: F:AM 63060, right partial ramus with c–m2; 61612*, left partial ramus, with p4–m1 broken, m2, and m3 alveolus.

Gray's Ranch Quarry stratum 3, Big Sandy Formation (late Hemphillian), near Wikieup, Mohave County, Arizona: F:AM 63059, left partial ramus with p1 alveolus, p2, p3 alveolus p4–m1, m2 alveolus; F:AM 63061, right and left rami with right p3–p4, m1–m3 alveoli, left m1–m2, m3 alveolus (fig. 38B); and F:AM 72572A, left tibia.

Redington Quarry, Quiburus Formation (late Hemphillian), northwest of Redington on the west side of the San Pedro River Valley, Pima County, Arizona: F:AM 75848, crushed skull with I3 (alveolus)–M2 and right ramus with c–M2 (broken) (p1 alveolus–p2 broken); F:AM 75821, left ramus with c (broken)–m3 (P1 alveolus and m1 broken), probably same individual as F:AM 75848; F:AM 75822, right partial ramus with m1–m2.

Old Cabin Quarry, Quiburus Formation (late Hemphillian), near Redington, Pima County, Arizona: F:AM 75847, crushed left and right maxillae with I3–M2 (P2–P3 broken); and F:AM 75819, left and right partial rami with c (broken)–m3 (p1–p2 and p4 broken) and right maxillary fragment with M1 (broken)–M2.

Yepomera, CIT locality 275 (latest Hemphillian), Chihuahua, Mexico: LACM 30205, left m1.

Devils Nest Airstrip, UNSM locality Kx-113, Ogallala Group (late Hemphillian),

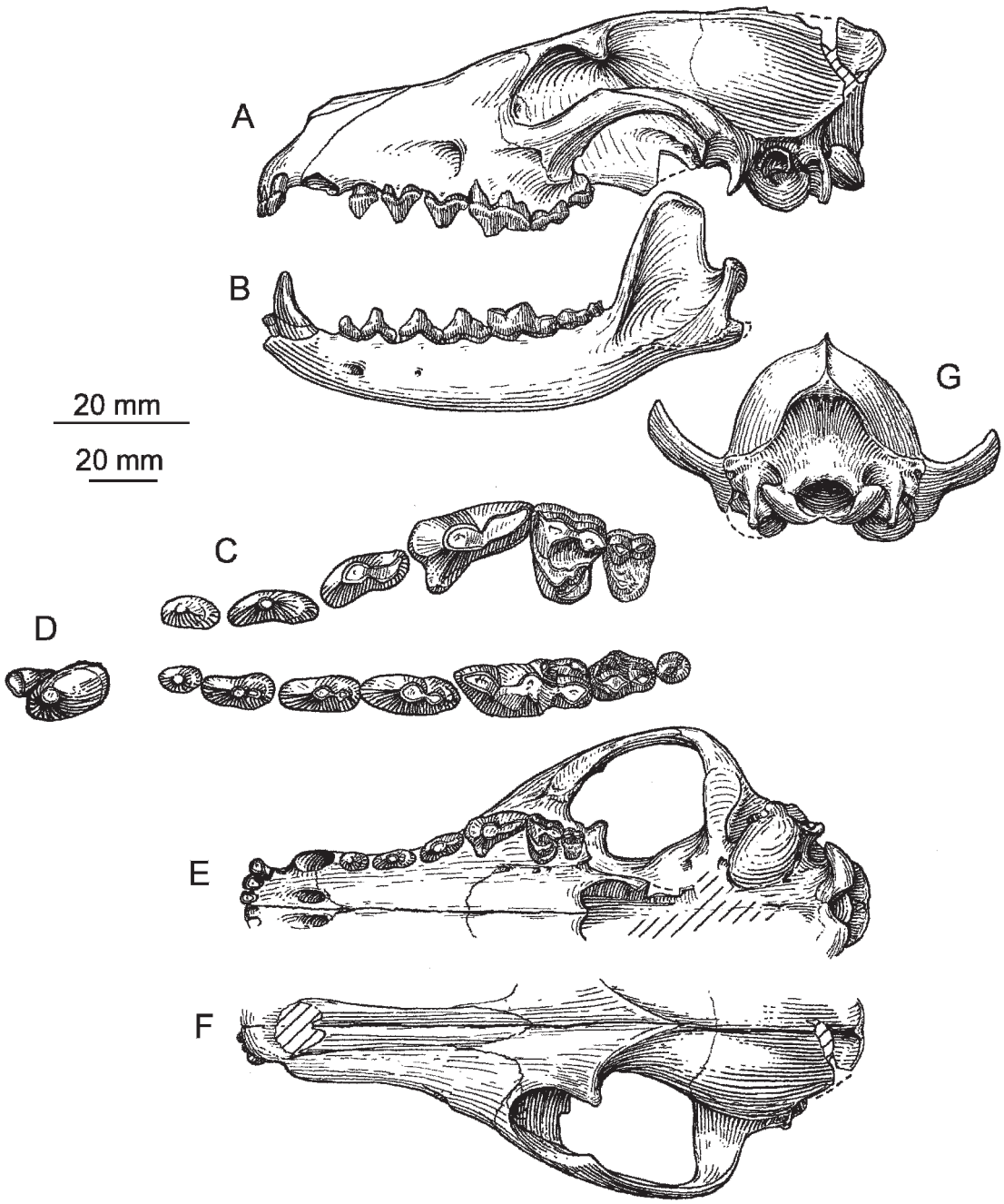

Fig. 37. **A–G**. *Canis ferox*. Paratype skull and ramus, F:AM 49298, late Hemphillian, Nevada. **A–B**. Lateral views. **C–D**. Occlusal views. **E**. Palatal view. **F**. Dorsal view. **G**. Occipital view. The longer (upper) scale is for C–D, and the shorter (lower) scale is for the rest.

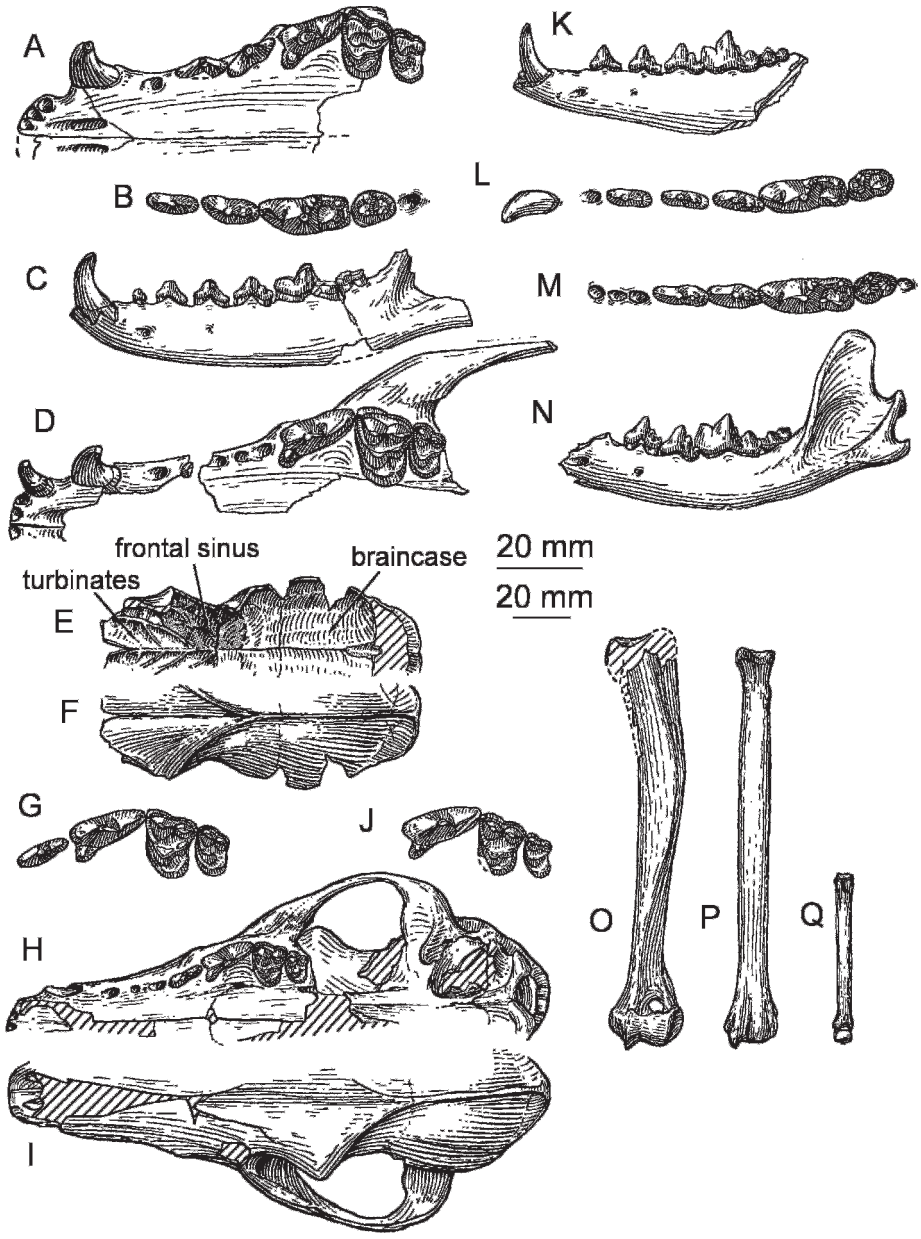

Fig. 38. **A–Q**. *Canis ferox*. **A–C**. Late Hemphillian, Arizona. **A**. Palate, F:AM 63062, occlusal view. **B**. Ramus, F:AM 63061, occlusal view (restored from both sides). **C**. Ramus, F:AM 63035, lateral view. **D–F**. UNSM 1022-73, late Hemphillian, Nebraska. **D**. Palatal view, reversed. **E**. Internal view of dorsal side of cranium (restored from both sides). **F**. Dorsal view of cranium (restored from both sides). **G–I**. Skull, UNSM 26107, Blancan, Nebraska. **G**. Occlusal view. **H**. Palatal view. **I**. Dorsal view. **J**. Maxillary, UMMP V52280, Blancan, Idaho, occlusal view. **K–L**. Ramus, UMMP V53910, Blancan, Idaho. **K**. Lateral view. **L**. Occlusal view. **M–Q**. Ramus and associated limb bones, UNSM 4261, Blancan, Nebraska. **M**. Occlusal view. **N**. Lateral view. **O**. Humerus, anterior view (reversed). **P**. Radius, anterior view (reversed). **Q**. Metacarpal III, anterior view (reversed). The longer (upper) scale is for A, B, D, G, J, L, and M, and the shorter (lower) scale is for the rest.

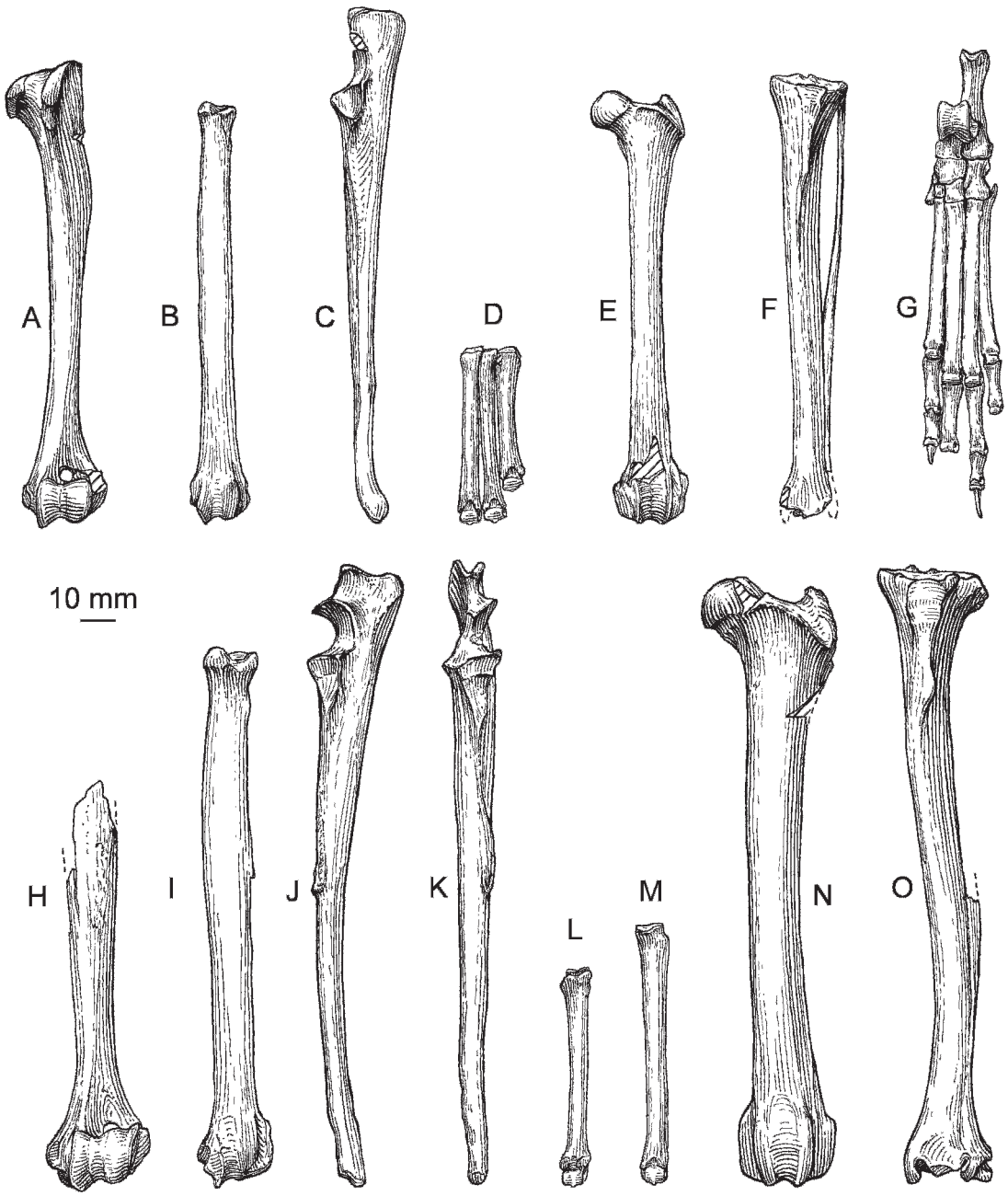

Fig. 39. **A–G**. *Eucyon davisi*. **A–D**. Late Hemphillian, Arizona. **A**. F:AM 63019A, humerus, anterior view, reversed. **B**. F:AM 72564, radius, anterior view. **C**. F:AM 72564, ulna, medial view. **D**. F:AM 72576, metacarpals III, IV, and V, anterior view, reversed. **E–G**. F:AM 72802, late Hemphillian, Oklahoma. **E**. Femur, anterior view. **F**. Tibia and fibula, anterior view. **G**. Pes, anterior view. **H–O**. *Canis edwardii*, F:AM 63100, associated limb bones (see skull and jaws, fig. 48), Irvingtonian, Arizona. **H**. Humerus, distal end, anterior view, reversed. **I**. Radius, anterior view, reversed. **J**. Ulna, lateral view, reversed. **K**. Ulna, anterior view, reversed. **L**. Metacarpal III, anterior view, reversed. **M**. Metatarsal III, anterior view. **N**. Femur, anterior view, reversed. **O**. Tibia, anterior view.

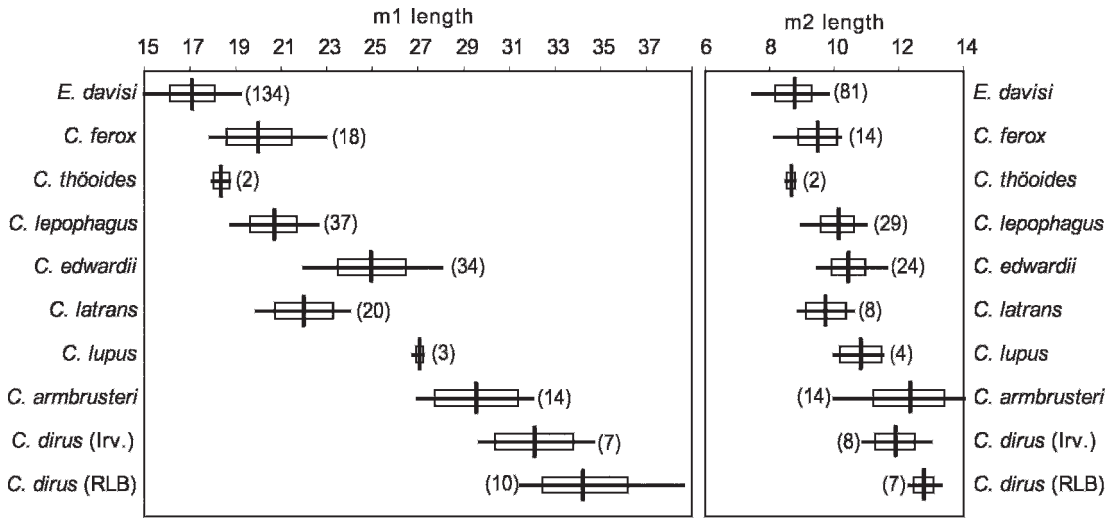

Fig. 40. Graphic comparison of the length of m1 and m2 of species of *Eucyon* and *Canis*. The horizontal bar is the observed range, the small rectangle represents $\pm 1\ \sigma$, the vertical line is the mean, and the size of the sample is the number in parentheses.

Knox County, Nebraska: UNSM 1022-73, paratial skull including most of the frontal, parietal, and interparietal region (fig. 38E–F), broken basioccipital region, incomplete premaxilla and maxillary fragment with I1–I2 alveoli, and I3–C, and right and left partial maxillae with P3 (broken), P4 (alveolus), and P4–M2 (fig. 38D).

Rexroad Local Fauna, locality 3, Rexroad Formation (early Blancan), Rexroad Ranch, Meade County, Kansas: UMMP 37132, P4, M1 broken, and p3. This was referred to *C. lepophagus* by Nowak (1979: 72).

Bender Local Fauna, above massive caliche in the Rexroad Formation and below the Angel member of the Ballard Formation, Rexroad Formation (early Blancan), Bender Ranch, Meade County, Kansas: UMMP V60942, right and left partial rami with p2, m1 (broken)–m2 (all other teeth represented by alveoli or roots), and associated isolated teeth including two canines, premolars, m1, and tooth fragments.

Hagerman Fauna, Glenns Ferry Formation (medial Blancan), Twin Falls County, Idaho: UMMP V452222, left partial ramus with c (alveolus)–p4 (p1 alveolus), USGS Cenozoic locality 19213 (DWT 427); UMMP V53910, right and left rami with incisors alveoli–m2 (p1 alveolus), UMMP locality UM-Ida 70-65 (fig. 38K–L, figured by Bjork, 1970: fig. 8c); UMMP V54995, right partial maxilla with P4, UMMP locality UM-Ida 19-65; UMMP V56282, right ramal fragment with m1 (broken) m2–3 (alveoli), UMMP locality UM-Ida 80-65; UMMP V56401, left partial maxilla with P4–M2, UMMP locality UM-Ida 11-67 (figured by Bjork, 1970: fig. 8b); and UMMP V52280, left partial maxilla with P4–M2 (fig. 38J), USGS Cenozoic locality 20765. These specimens had been referred to *C. lepophagus* by Bjork (1970) and Nowak (1979: 70–71).

White Bluffs Fauna (early Blancan), 35–45 ft above White Bluffs Tuff, Ringold Formation, Franklin County, Washington: UWB 28747*, lower canine fragment; UWB 402289*, lower canine fragment; UWB 40393*, m1; UWB 35114*, P4; UWB 40288*, P4; UWB 40393*, m1, UWB 40393*, m1; UWB 41969*, m1; UWB 33061*, p4 (referred to "*Canis*" *davisi* by Gustafson, 1978: measurements table 12). Rankin Canyon, LACM locality 4574, Franklin County, Washington: LACM 143527*, right ramus with p1–p2 alveoli, p4–m1; Ringold Formation, LACM locality 588D: LACM 143528*, left ramus with m1 and partial alveolus of m2; LACM 143529*, left m1.

Lisco Member of the Broadwater Formation (medial Blancan), Garden County, Nebraska: UNSM 26107, partial skull (fig. 38G–I) with I1–P3 (alveoli) and P4–M2, locality Gd-13, Lisco Quarry 4; UNSM 26114, right and left partial rami with c (broken)–m3 (alveolus), p1 and p3 (alveoli), Gd-12, Lisco locality C, Quarry 1; UNSM 4258, right and left partial rami with p2–m2, Gd-14, Lisco locality C, Quarry 2; UNSM 4261, right ramus with p2 (alveolus)–m2 (m3 alveolus) (fig. 38M–N), partial scapula, humerus (fig. 380), partial ulna, radius (fig. 38P), incomplete metacarpal II, one complete (fig. 38Q) and one partial metacarpal III, incomplete metacarpal IV, metacarpal V, partial pelvis, partial femur, partial tibia, calcaneum, astragalus, metatarsal IV, phalanges, vertebrae, and fragments, Gd-14, Lisco locality C, Quarry 2; UNSM 88522*, right ramus with i3, c, p1 (alveolus), p2–p3, m1–m2, and possibly associated anterior part of skull with complete, but largely disarticulated, dentition, Gd-14, Lisco Quarry 2; and UNSM 88528*, palate with right and left P4, M1, M2 and associated left ramus with p1–p3, p4 (root), m1 (broken), m2–m3, Gd-14, Lisco Quarry 1. Nowak (1979: 72) referred UNSM 26107 and 26114 to *C. lepophagus*.

Distribution: Late Hemphillian of Mexico, New Mexico, Arizona, Nevada, Oklahoma, and Nebraska, early Blancan of Washington, early to medial Blancan of Kansas, and medial Blancan of Idaho and Nebraska.

Revised Diagnosis: The expanded frontal sinus, enlargement of the angular process for insertion of the superior ramus of median pterygoid, triangular shape of supraoccipital shield, and union of the parasagittal crests anterior to the frontoparietal suture differentiates *C. ferox* from *Eucyon* sp.; other features such as the size of skull and skeleton stand intermediate between *E. davisi* and *C. lepophagus*.

Discussion: Miller and Carranza-Castañeda (1998) proposed *C. ferox* for an associated skull, ramus, and partial skeleton from the late Hemphillian of central Mexico following comparison with the *E. davisi* sample at the American Museum of Natural History and the type and topotypic sample of *C. lepophagus* in the Panhandle Plains Museum, Canyon, Texas. They thought that *C. ferox* was closer to *C. lepophagus*, differing primarily in smaller size and in proportional relationships of the skull, dentition, and some elements of the skeleton. We agree with this conclusion and add a number of other samples from the Great Plains, Washington, and Idaho that similarly show such intermediate features.

Because of the lack of uncrushed skulls of North American *E. davisi*, it is difficult to compare the skull features with those of the type and paratype of *C. ferox*. However, the skulls referred to *E. davisi* from the Chinese Pliocene (Tedford and Qiu, 1996) are used to provide supplementary data. It is evident that the two skulls (F:AM 49298 and 75848) of *C. ferox* are larger and more massive with a wider muzzle than those of *E. davisi*. The width of the braincase and especially that of the postorbital constriction of *C. ferox* are markedly narrower relative to the length of the skull (fig. 43). The frontal sinus cavity is narrow but extends to the end of the long narrow postorbital constriction. A septum partially separates the frontal sinus of the postorbital process from the main body of the frontal sinus. In *C. ferox*, the sagittal crest is stronger, its parasagittal components unite well before the frontoparietal suture, and the supraoccipital is triangular in outline, narrower, and projects more posteriorly than in *E. davisi*. A palate and partial cranium of *C. ferox* of late Hemphillian age from Nebraska (UNSM 1022-73, fig. 38D–F) can be compared with that of *E. davisi* (F:AM 63005, fig. 34A–C) from the late Hemphillian deposits near Wikieup, Arizona. The frontal sinuses are similar in size, as they are also to an early Blancan skull (UNSM 26107, fig. 38I) from the Lisco Member of the Broadwater Formation in Nebraska. In both of these specimens the inion is fan-shaped as in *E. davisi*, but in the type of *C. ferox* the inion is more triangular and may have overhung the condyles as in some individuals of *C. lepophagus*.

Among the canid dentitions of late Hemphillian age from Wikieup, Arizona, there is a group that is significantly larger than those referred to *E. davisi* (fig. 40). Judging by the size of the canine teeth, both sexes are

included in the sample and thus the larger size of these specimens as a whole is not attributable to sexual dimorphism. Although many of the lower carnassials from Arizona are worn, the talonids, as in most *E. davisi*, lack the transverse crest between the entoconid and hypoconid, and there is only a low hypoconulid shelf. This primitive condition is also occasionally present in specimens of *C. lepophagus* of Blancan age. Otherwise, the specimens are morphologically intermediate between those of *E. davisi* and *C. lepophagus*. Furthermore, the premolars are extremely elongate and vary from slender (F:AM 63060) to robust (F:AM 63035, fig. 38C). The premolars are more elongate and generally more robust than those of contemporary specimens of *E. davisi*, but again within the size range of those of *C. lepophagus*. The mandibular ramus is also more robust, and the horizontal ramus is deeper than in *E. davisi*. The angular process of the mandible is similar to that of *E. davisi* and less robust than that of *C. lepophagus* with a smaller fossa for the inferior ramus of the median pterygoid muscle.

Dentitions of *C. ferox* from the Lisco Member (medial Blancan) of the Broadwater Formation at the Lisco Quarries in Garden County, Nebraska, are, on average, smaller and less robust than those of *C. lepophagus* from the referred Lisco Member of the Broadwater Formation farther west in Morrill County, Nebraska. In both size and morphology the dentition from the Lisco Quarries closely resembles those described by Bjork (1970: 13) from the Hagerman Fauna (medial Blancan) and attributed by him to *Canis lepophagus*. Some of the better specimens of these Hagerman *C. ferox* are included in the hypodigm here, and according to Bjork, the total sample consists of a group of 19 individuals with a stratigraphic range of 320 feet in the Glenns Ferry Formation. That portion of the Glenns Ferry section lies in the later part of the Gilbert Chron (4.2–3.6 Ma) of the geomagnetic polarity time scale (Neville et al., 1979, recalibrated by Cande and Kent, 1995). Because of the favorable comparison of the Hagerman Fauna canids with those from the Lisco Member from Garden County, the latter are tentatively considered as members of a medial Blancan fauna. Voorhies and Corner (1986: 75) also concluded that the fauna of the Lisco Quarries was significantly older than the fauna of the Broadwater Quarries and of "early Blancan" age following comparison of *Megatylopus*(?) *cochrani* with similar forms from Washington (Ringold Formation) and Kansas (Rexroad Formation). They also report the presence of *Pliopotamys minor* in the Lisco Quarries, an immigrant arvicoline rodent typical of Blancan III faunal unit of Repenning (1987) that includes the Hagerman and younger Ringold (Taunton) faunas also paleomagnetically correlated with the later part of the Gilbert Chron.

The minimum size and the mean value of the m1 and m2 of *C. ferox* from the Rexroad Formation, the Glenns Ferry Formation, and the Lisco Quarries of the Broadwater Formation in Garden County are smaller than those of the larger topotypic population of *C. lepophagus* from Cita Canyon (late Blancan) of Texas (fig. 40). The 95% confidence interval for the length of the m1 and m2 partially overlaps the lower end of the interval of the Cita Canyon population. In contrast, the *C. lepophagus* samples from the Broadwater Quarries in Morrill County, Nebraska, are similar in size (appendix 3) and morphology of the skull and dentition to the topotypic sample of *C. lepophagus* from the late Blancan of Cita Canyon.

Further inspection of the dentitions from the Hagerman Fauna and the Lisco Quarries of Garden County indicates that not only are they smaller than that of *C. lepophagus* from Cita Canyon, but in some ways the morphology recalls that of the dentition of *E. davisi*. Specimens from both the Hagerman Fauna and the Lisco Quarries in Garden County have slender premolars similar to those of *E. davisi*. The P4 has the protocone anterolingually directed, and the anterolabial shoulder projects more anteriorly and is less rounded than is generally found in *C. lepophagus* from Cita Canyon. The foregoing features result in the anterior border of the P4 being deeply notched. In some specimens (UMMP V56401 and V52280, fig. 38J), the M1 is anteroposteriorly long relative to its transverse diameter as in *E. davisi*, a condition occasionally seen in

C. lepophagus from Cita Canyon (WTC 530 and 560J). Furthermore, the M1 paracone and metacone are relatively low-crowned with a strong labial cingulum and a small parastyle. The hypocone is strong and continuous, with the lingual cingulum joining the labial cingulum at the base of the paracone. The lower carnassial is intermediate in size and morphology between *E. davisi* and *C. lepophagus*, with the entoconid and hypoconid either separate or weakly joined by a transverse crest. A distinct hypoconulid is absent although a small hypoconulid shelf may be present.

Limbs referred here to *C. ferox* are longer (appendix 4) and more robust than those of *E. davisi* (compare fig. 38O–Q with fig. 39A–B, D), and for the most part are within the size range of those of *C. lepophagus* from Cita Canyon (fig. 52). The unassociated limbs imply that the relative proportion of elements (fig. 52) are closely similar to those of *C. lepophagus* and differ from *C. edwardii* and *C. latrans*.

Thus, this heterogeneous late Hemphillian to medial Blancan sample, which is morphologically intermediate between the Hemphillian *E. davisi* and late Blancan *C. lepophagus*, is predominantly characterized by plesiomorphic characters. The dentition is larger but morphologically similar to that of *E. davisi* and compares favorably with only a few of the Blancan dentitions from Cita Canyon of *C. lepophagus*. The expanded frontal sinus, enlarged angular process, triangular supraoccipital shield, and sagittal crest originating on the frontals are characters shared with *C. lepophagus* and features that distinguish *C. ferox* from *E. davisi*.

Canis lepophagus Johnston, 1938
Figures 40, 41A–G, 42A–J, 43, 44, 52; appendices 2–4

Canis lepophagus Johnston, 1938: 383–390, pls. 1–3.
Canis latrans lepophagus: Giles, 1960: 369.

Type: WTUC 881, skull with I1–M2 (fig. 41A–C) from North Cita Canyon (type locality of the Cita Canyon beds), stratum no. 2, Ogallala Group (late Blancan), Randall County, Texas.

Referred Material from Type Locality: WTUC 722, skull with I1–P4 (alveoli or broken), M1–M2, and ramus with c–m2 (il–i3 and m3 alveoli or broken); WTUC 760, skull with I1 (broken)–M2 (fig. 41D–F); WTUC 2523, skull with P1–M2, C alveolus broken and provisionally associated left ramus: WTUC 2527, pl (alveolus healed), p2 broken, and p3–m3; WTUC 558, mandible with incisor alveoli, c–pl broken, p2–m3; WTUC 558a, right ramus with c–pl (alveolus), p2 (broken)–m3 (alveolus); WTUC 558b, left ramus with i1–i3 (alveoli), c (broken), pl (alveolus healed), p2–p4 (alveoli), and m1 (broken)–m3 (alveolus); WTUC 558c, left ramus with pl (alveolus healed), p2, p3 (alveolus), p4–m2 (broken), and m3 (alveolus); WTUC 558d, i1 (alveolus)–c alveolus, p2–m2; WTUC 560i, right maxilla with P4–M2 (alveolus); WTUC 560j, right maxilla with P3 (alveolus)–M2; WTUC 560k, left m1; WTUC 5601, right ramus with p4 alveolus, m1 and m2 alveolus; WTUC 530, left maxilla with M1–M2; WTUC 1038, left maxilla with M1–M2; WTUC 2495, left isolated p4; WTUC 1027a, right and left rami with i2 (broken)–m3 (alveolus); WTUC 1027b, left ramus with i1–i2 (alveoli) and i3–m3 (m1 broken); WTUC 1027c, right ramus with i1–i3 (alveoli) and c–ml (broken); WTUC 2287, right and left rami with c–m2; WTUC 2423, right ramus with p4–m2 and m3 alveolus; WTUC 2494, right ramus with p4 (broken)–m1 (broken) and m2–m3 (alveolus); WTUC 2631, left ramus with p4 (broken)–m2; WTUC 2717, right ramus with c–m3 (alveolus); WTUC 1027d, right ramus with i1–c (alveoli) and p1–m3 (fig. 42B–C); WTUC 559, left ramus with i1 (broken)–m3 and c broken; WTUC 559a, right ramus with i1–i3 (alveoli) and c (broken)–m3 (alveolus) (fig. 42A); WTUC 560, right and left rami with c–m1 and m2–m3 (alveoli) (fig. 42D–E); WTUC 560a, right ramus with i2–i3 (alveoli), c broken, p1–p2, p3 root, p4–m1 (broken), m2 (alveolus), and m3 (broken); WTUC 560b, right ramus with p3–m3 (alveolus); WTUC 560c, right ramus with il–i3 (alveoli), c–p3 (broken), and p4–m1 (broken); WTUC 560d, right ramus with p3 (broken and alveolus), p4 (alveolus), m1–m2, and m3 alveolus; WTUC 560e, left ramus with p4 (alveolus) and m2; WTUC 560f, left ramus with p1 (broken) and m3 (alveolus); WTUC 560g, right and left rami with i1–i3 (alveoli), c

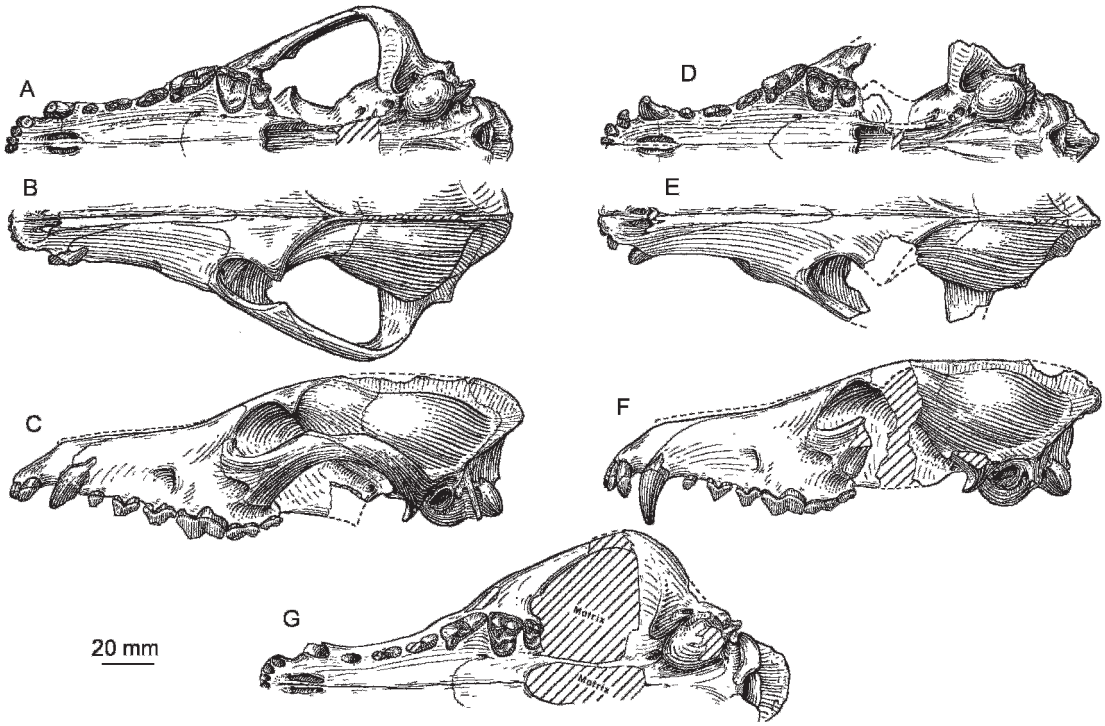

Fig. 41. **A–F**. *Canis lepophagus*, crania, late Blancan. **A–F**. Cita Canyon, Randall County, Texas. **A–C**. Type, WTUC 881. **A**. Palatal view, reversed. **B**. Dorsal view, reversed. **C**. Lateral view, reversed. **D–F**. WTUC 760. **D**. Palatal view, reversed. **E**. Dorsal view, reversed. **F**. Lateral view, reversed, bulla restored from left side. **G**. *Canis lepophagus*, cranium, early Blancan, F:AM 49295, Lincoln County, Nevada, palatal view.

(broken), p2 (broken), p3–m1, and m2–m3 (alveoli); WTUC 560 h, left ramus with c (broken), p2, m2, and alveoli; WTUC 1531, right isolated M1; WTUC 560m, right ramus with m2–m3 (alveolus); WTUC 560n, right ramus with m1 (broken)–m2; WTUC 560o, right isolated m2; WTUC 560p, right isolated m2; WTUC 2532, left ramus with m1–m2; WTUC 2532a, right ramus with p3 (alveolus broken)–m1 (alveolus) and m2; WTUC 2530, left isolated m1; JWT 1062m, radius; CWT 2446, radius and ulna; CWT 2574, radius; ulna; CWT 2573, femur; CWT 2525, partial humerus; JWT 1908, partial humerus; JWT 573, tibia; CWT 2526, tibia; JWT 614, metacarpal II; no number, metacarpal III; CWT 2411, metacarpal II; JWT 565, metacarpal IV; JWT 565, metacarpal IV; JWT 614, metacarpal IV; JWT 565, metacarpal V; CWT 2446, metacarpal V; CWT 2430, metatarsal II; CWT 2572, metatarsal II; CWT 2442, metatarsal III; CWT 2572, metatarsal III; JWT 565, metatarsal IV; JWT 565, metatarsal V; CWT 2442, metatarsal V; CWT 2572, metatarsal V; and JWT 614, metatarsal V.

Rita Blanca beds, between 11 and 13 km southeast of Channing (late Blancan), Oldham County, Texas: F:AM 62986, left isolated P4; F:AM 99374, metatarsal V, from Bevins Pit 1; F:AM 62987*, right and left partial rami with c, p2, and alveoli, from Proctor Pit B.

Red Light Local Fauna (late Blancan), Love Formation, Hudspeth County, Texas: TMM 40664-3*, right ramus, c, p1–p4 alveoli; TMM 40664-9*, left ramus, p1 roots; TMM 40664-11, part of right radius and right metacarpal II.

Camp Rice Formation (late Blancan or early Irvingtonian), Mesilla Basin, south of Las Cruces, Doña Ana County, New Mex-

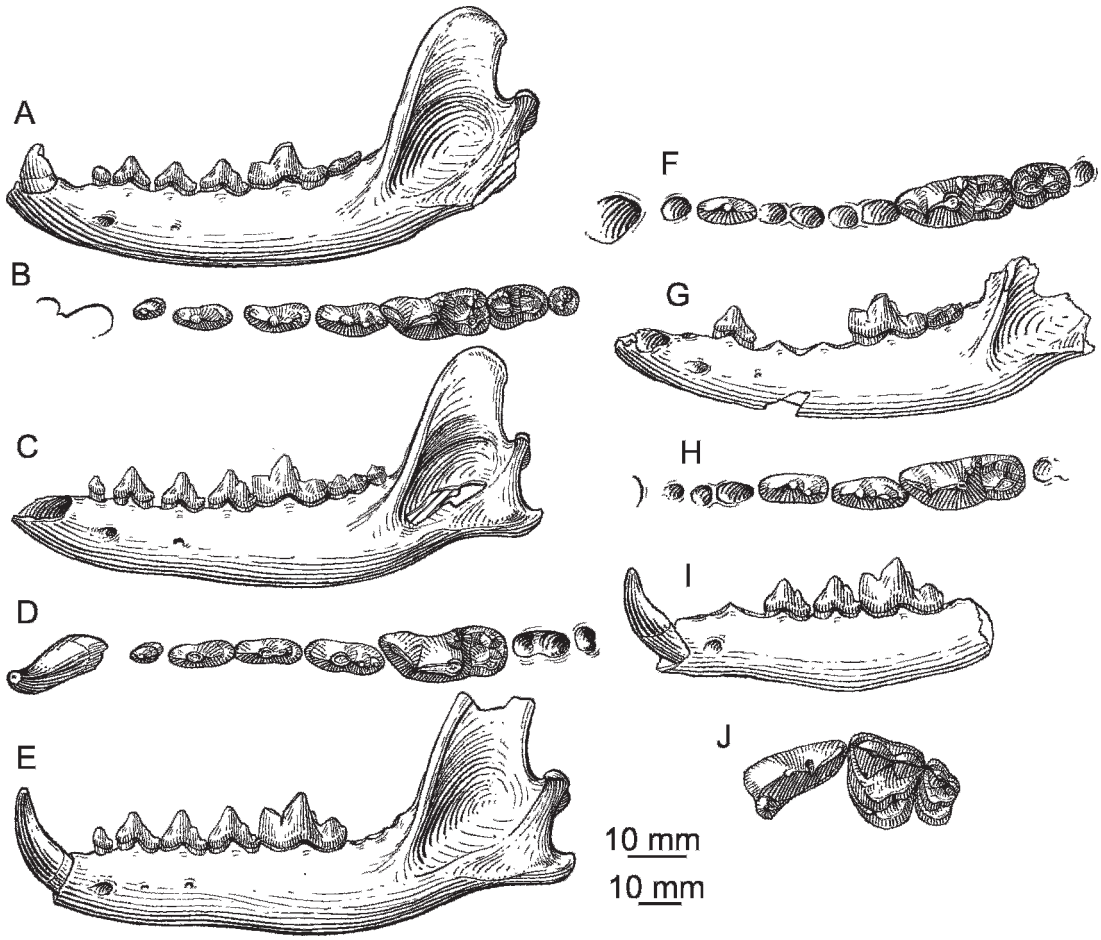

Fig. 42. **A–J**. *Canis lepophagus*, late Blancan. **A–E**. Rami, Cita Canyon, Randall County, Texas. **A**. WTUC 559a, lateral view, reversed. **B–C**. WTUC 1027d. **B**. Occlusal view, reversed. **C**. Lateral view, reversed. **D–E**. WTUC 560. **D**. Occlusal view. **E**. Lateral view, restored from opposite side. **F–J**. Broadwater, Morrill County, Nebraska. **F–G**. Ramus, UNSM 26116. **F**. Occlusal view. **G**. Lateral view. **H–I**. Ramus, UNSM 4260. **H**. Occlusal view, reversed. **I**. Lateral view, reversed. **J**. Maxillary teeth, UNSM 26113, occlusal view. The longer (upper) scale is for B, D, F, H, and J, and the shorter (lower) one is for the rest.

ico: F:AM 22251*, right partial ramus with p1 alveolus, p2, p3–p4 both broken, well-worn m1–m2, and m3 root.

Sand Draw Fauna, east of Jackrabbit Hill, Keim Formation (medial Blancan), Brown County, Nebraska: UMMP V57321, fragments of skull, right premaxilla, and maxilla with I1–M1 (broken) (I2 and P1 alveoli and I3, P2–P3 broken), right and left rami with c–m3, p1 alveolus (figured by Skinner and Hibbard, 1972: fig. 48).

Lisco Member, Broadwater Formation (late Blancan), locality Mo-5, Morrill County, Nebraska: UNSM 26112, crushed skull with I1–I3 (alveoli), c (broken), P1–P2 (alveoli), and P3 (broken)–M2; UNSM 26111, crushed skull with I1–IC (alveoli) and P1–M2; UNSM 26113, left partial maxilla with P4–M2 (fig. 42J); UNSM 26116, left ramus with i3, c–p1 alveoli, p2, p3–p4 alveoli, m1–m2, m3 alveolus (fig. 42F–G); and UNSM 4260, right partial ramus with c–p2 (alveoli) and p3–m2 alveolus (fig. 42H–I).

Big Spring Local Fauna (late Blancan), Long Pine Formation, UNSM locality Ap

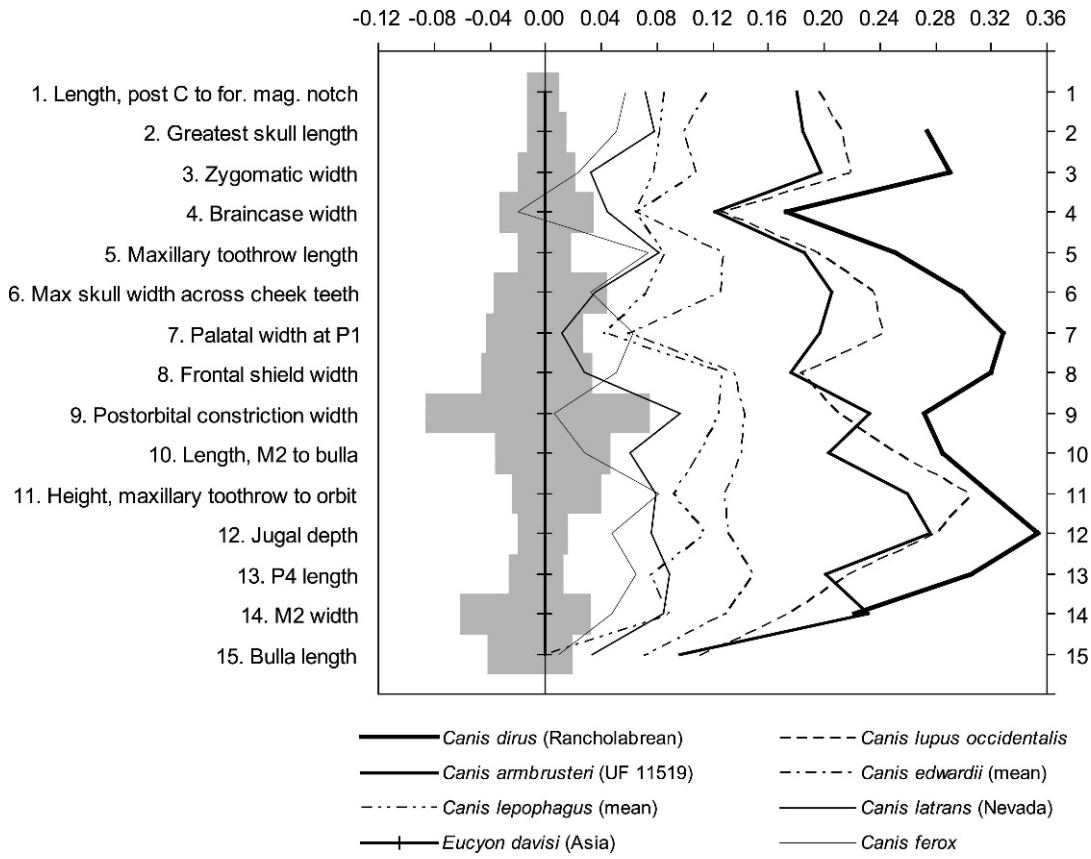

Fig. 43. Log-ratio diagram comparing the proportions of cranial variates (appendix 2) of the skulls of various species of *Canis* with the mean of *Eucyon davisi* from a single locality near Xiakou, Yushe Basin, Shanxi, China, as the standard of reference. Gray bars extending from the mean of the standard are the observed range. Data from table 3: *Canis dirus*; the Rancholabrean sample cited by Nowak (1979); *Canis lupus occidentalis*, mean of 9 individuals from northern Canada; *Canis armbrusteri*, a single individual (UF 11519); *Canis edwardii*, mean of 5 individuals; *C. lepophagus*, mean of 7 individuals; *C. latrans*, mean of a sample of 12 individuals from Nevada; and *C. ferox*, the paratype, F:AM 49298.

103, Antelope County, Nebraska: UNSM 46893, right ramus with p4, m1–m2, m3 alveolus; and UNSM 52306*, fragment of left ramus with p1 (root), p2–p3 (root).

Meade County State Park, Deer Park Local Fauna, Missler Member, Ballard Formation (late Blancan), Meade County, Kansas: UMMP V31945*, two right and one left isolated, broken M1s. Other specimens from the same locality in the KU collections referred by Nowak (1979: 71–72).

Tehama Formation (late Blancan), Beck Ranch site 1, UCMP V3022, Tehama County, California: UCMP 29828, m1 (attributed to *Canis* sp. by VanderHoof, 1933).

Double Butte, 6.25 m below the Double Butte Quarry, Panaca Formation (early Blancan), Lincoln County, Nevada: F:AM 49295, crushed skull with I1–IC alveoli, P1–P3 broken and P4–M2 (fig. 41G), and limb fragments.

Glenns Ferry Formation (late Blancan): LACM 1246, left partial ramus with p2 (alveolus)–m2, CIT locality 118, Grandview Fauna, 21 km northwest of Grandview, Owyhee County, Idaho. LACM 1343, left partial ramus with c and p1 (alveolus)–m3 alveolus (p2 and m2 alveoli) from CIT locality 122, Flatiron Butte Local Fauna, Barker Ranch, south side of Snake River,

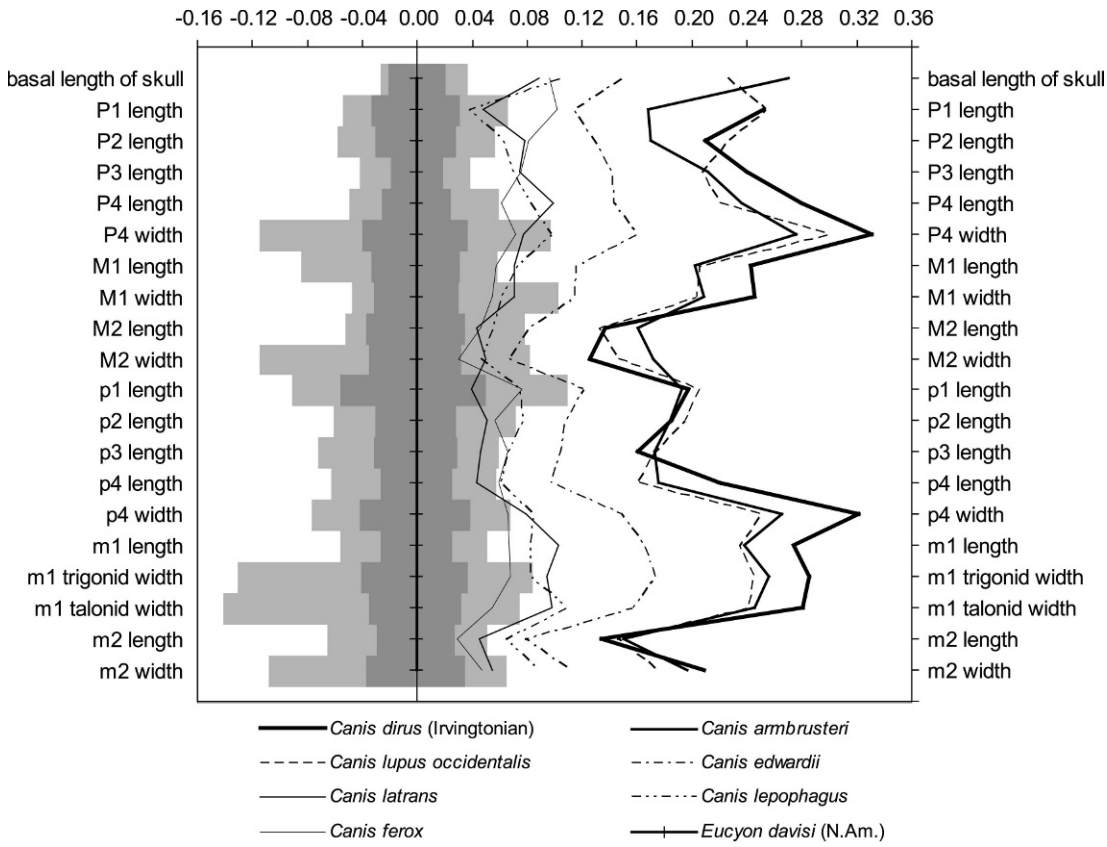

Fig. 44. Log-ratio diagram comparing the cheek tooth dimensions (appendix 3) of species of *Canis* against the mean of the North American sample of *Eucyon davisi*. Gray bars extending from the mean of the standard are the observed ranges and the dark bars show the standard deviation ($\pm$ 1σ). Data from table 4: *Canis dirus*, Irvingtonian sample of 8 individuals; *C. armbrusteri*, sample of 15 individuals of Irvingtonian age; *C. lupus occidentalis*, 10 individuals from northern Canada; *C. edwardii*, mean of 34 individuals, including the type; *C. latrans*, mean of 38 individuals from Nevada; *C. lepophagus*, mean of 37 individuals, including the type; and *C. ferox*, mean of 18 individuals, including the type and paratype.

6 km east of Bruneau-Mountain Home Bridge, Owyhee County, Idaho.

Santa Fe River, site 1A (late Blancan), Columbia and Gilchrist counties, Florida: UF 10424, right ramus, I1–I3, c, p1, alveoli, p2–p4, m1–m3; UF 10423, left ramus, p4–m1; UF 10837, left ramus, c–p2 alveoli, p3, p4–m1 alveoli; UF 10833*, edentulous right ramal fragment c–p4 alveoli; UF 10836*, edentulous right ramal fragment with c–m1 alveoli (Kurtén, 1974: 6, table 4).

Saint David Quarry, Saint David Formation (late Blancan), 4 km east of Saint David, Cochise County, Arizona: F:AM 63091, crushed partial skull with P4–M1 and all alveoli; F:AM 72612, left M1, Benson area, Saint David Formation (late Blancan), Cochise County, Arizona.

Tusker Fauna, 111 Ranch at Dry Mountain locality (late Blancan) near Safford, Graham County, Arizona: F:AM 63102*, skull fragments including partial premaxilla* and maxilla with C–P3 alveoli and broken, and calcaneum; F:AM 63103*, left partial ramus with p3 (broken)–m1 (broken).

El Golfo de Santa Clara, northwestern Sonora, Mexico (Blancan): IGM 13103* (Yuma), partial right ramus with p3–p4 (broken), m1–m2, m3 alveolus.

Distribution: Early Blancan of southern Nevada; medial Blancan of Nebraska; late Blancan of Texas, Kansas, Nebraska, California, New Mexico, Arizona, Idaho, Florida, and northwestern Mexico.

Revised Diagnosis: Derived characters that distinguish *C. lepophagus* from *E. davisi* are larger size and more robust skull and jaws; frontal sinus extends more posteriorly; sagittal crest stronger with contribution from frontal; inion narrower and sometimes pointed; m1 talonid with entoconid and hypoconid usually linked by transverse crest; hypoconulid shelf relatively larger but with distinct cusp rarely present; angular process of mandible more robust; and longer forelimb relative to hindlimb (radius/tibia ratio >80% but <90%).

Canis lepophagus shares the above derived features with *C. ferox*, but it differs in more consistent m1 hypoconid-entoconid union through cristids, and reduction of M1 parastyle.

C. lepophagus differs from many larger species of *Canis* in its primitively small size; small I3 relative to I1–I2; P4 protocone more anteriorly directed; p4 lacks a posterolingual shelf and is higher than paraconid of m1; m3 retains two trigonid cusps; less inflated frontal sinus; relatively wider frontal shield; and relatively wider braincase.

Primitive characters that distinguish *C. lepophagus* from *C. latrans* are: greater postorbital constriction; zygomatic process dorsoventrally deeper with broad scar for masseter muscle; smaller bulla with less laterally extended tubular auditory meatus; P4 protocone situated more anteriorly; m1 less elongate with trigonid shorter relative to length of talonid and weaker hypoconulid; m2 larger relative to m1, metaconid lower crowned, and anterolabial cingulum stronger; less elongate limbs especially forelimb, with radius/tibia ratio exceeding 80% but less than that of *C. latrans*, where ratio usually exceeds 90%.

Description and Comparison: Among the topotypic Cita Canyon collection of *Canis lepophagus* are two female and two male skulls. The type WTUC 881 (fig. 41A–C) and WTUC 760 (fig. 41D–F) are females by virtue of their small canines, the slenderness and elongation of their skulls, narrow muzzles, less expanded frontal shield, and weaker sagittal crests. Males are represented by the skulls of WTUC 722 and WTUC 2523 and a maxillary fragment, WTUC 558d, in which the diameter of the canine is 9.4 mm. The males seem to have proportionally larger bullae; particularly noticeable is the posterior expansion of the bullae. The lambdoidal crests are more laterally extended in the males, and in both sexes the inion extends posteriorly well beyond the condyles. In WTUC 760, a female skull (fig. 41D–F), the inion is unusually narrow and pointed, suggesting that the range in variation is comparable to that of other species of *Canis*. Temporal crests join anterior to the frontoparietal suture to form a strong continuous sagittal crest. The form of the zygoma conforms to the pattern seen in *Canis* and differs strongly from that of *E. davisi* in lacking the primitive flaring and eversion of the orbital part of the arch. The masseteric scar on the zygoma is strongly developed in both sexes, often terminating ventrally in a crest or knoblike process.

The premolars are large in this species and show considerable variation, with the males having the larger and more robust teeth. The P3 lacks a posterior cusp in most individuals although it may at times be present, as in the holotype, WTUC 881 (fig. 41C). Measurements reveal considerable variation in the P4 dimensions, and here again the males seem to have slightly larger and more robust teeth. In all cases the P4 narrows posteriorly so that the transverse diameter across the paracone is greater than across the metacone. The P4 protocone is anterolingually directed and usually forms the most anterior part of the tooth. The M1 has a well-developed continuous labial cingulum that is sometimes produced into a low parastyle. The paracone is larger and taller than the metacone, but the difference in size is not as extreme as in most species of *Canis*. A distinguishable paraconule and a strong metaconule are present. Considerable variation in the proportion of the length to width of the upper M1 seems to result, in part, from the variable development of the hypocone and the cingulum. In individuals where the M1 cingulum can be observed (WTUC 1531, 1038, 530, 56011-J) the lingual cingulum is continuous from the hypocone across the face of the protocone to

the paracone, where it joins the labial cingulum. In most individuals the M1 appears transversely wide relatively to its length; however, in a few individuals (WTUC 530 and 560J) the M1 is markedly narrower, approaching the condition commonly observed in *E. davisi*. Compared with the size of M1, the M2 seems relatively large with a comparatively strong labial cingulum that is particularly well developed around the paracone. The paracone is slightly larger and taller than the metacone, and the conules are weakly developed. The hypocone is strong and continuous with the anterior cingulum, which extends across the face of the protocone, and may reach the anterolabial cingulum.

The horizontal ramus is relatively deep for its size and somewhat more robust, particularly anteriorly, in the males. Two mental foramina are present, with the anterior foramen the larger and lying consistently beneath the diastema between p1 and p2. The posterior mental foramen is small and its position varies between the anterior and posterior roots of p3. The masseteric fossa is deep with a well-marked anterior and ventral margin. The coronoid process tapers only slightly dorsally, and a posterior hook is frequently present. A strong angular process is conspicuously marked by muscular insertions, especially for the enlarged superior branch of the median pterygoid muscle. The process still terminates in a prominent dorsal hook. The form of the angular process closely resembles that of other species of *Canis* and contrasts markedly with the slender, foxlike process of *E. davisi*.

The lower premolars are relatively large, with the largest in the males. They vary from elongate and low-crowned (WTUC 559a, fig. 42A) to higher crowned (WTUC 560, fig. 42D–E). Individuals with the highest crowned premolars also have the most prominent posterior cusps on p3 and p4. None shows posterior cusps on p2. The p4 may show a small second posterior cusp lying immediately anterior to the cingulum in both the high- and low-crowned individuals (JWT 559A, WTUC 560, JWT 1027d, and JWT 558). The tip of the unworn crown of p4 consistently lies at or above the paraconid of m1 regardless of relative crown height. For the most part the tips of the premolars form a rising gradient front to back, with their crown bases lying at approximately the same level.

The lower carnassials have a wide talonid but show some variation in the obliqueness of the paraconid shear. The angle of the paraconid varies from that typical of the other Pleistocene and Recent canids to a more oblique shear present in WTUC 560 (fig. 42E). The anterior face of the paraconid is nearly vertical. A weak protostylid ridge is developed in at least one individual (WTUC 560d) and a weak anterolabial cingulum is sometimes developed. The hypoconid is larger than the entoconid and they are usually joined by a low transverse crest separating the talonid into anterior and posterior basins. A hypoconulid was seen in only one specimen (JWT 5601) but a hypoconulid shelf is usually present. The entoconid is situated slightly posterior to the hypoconid, and a small entoconulid may be present.

The m2 is widest anteriorly, with the talonid narrowing posteriorly. An anterolabial cingulum usually occurs but is not strongly developed. A paracristid is ordinarily present and may be produced into a cuspule forming the anterior part of the m2. This cuspule is removed shortly after wear begins. The protoconid and metaconid are subequal in height, with the metaconid slightly posterior to the protoconid. The hypoconid is present but a distinct entoconid is lacking, and the posterior and lingual part of the talonid is marked by a crest bearing low cuspules. The m3 is oval in shape with a distinct metaconid and protoconid, sometimes connected by a cristid, lying just posterior to the center of the tooth.

Discussion: In his description of *Canis lepophagus*, Johnston (1938: 385) observed that this taxon is slenderer in the general proportions of the skull and skeleton than in living *C. latrans*. He also noted that the sagittal and lambdoidal crests of *C. lepophagus* are stronger, and the braincase is not expanded. Giles (1960: 377) made a multivariate analysis of six mandibular rami of *C. lepophagus* from Cita Canyon. From this study he concluded that *C. lepophagus* "seems to rate only subspecific distinction within *C. latrans*." Nowak (1979: 69) observed that the skulls of *C. lepophagus*

averaged smaller than *C. latrans*, but overlapping occurred in most measured dimensions. Nowak also noted that the braincase was smaller and less inflated dorsoposteriorly, and he regarded this form as a species separate from *C. latrans*.

We have compared the measurements of four skulls of *C. lepophagus* from Cita Canyon with 12 skulls (6 male and 6 female) of *C. latrans* from Nevada in a log-ratio diagram (fig. 43). Based on this small sample, the only skull dimension of *C. lepophagus* that diverges sharply from those of *C. latrans* is the width of the frontal shield. It is relatively wider in *C. lepophagus* as noted by Nowak (1979). We also agree with Nowak that the braincase is narrower anteriorly.

Although *C. lepophagus* retains a number of primitive features in common with *Eucyon davisi*, it is an advanced canid and shares a number of derived features with larger species of *Canis*: posterior expansion of the frontal sinus; supraoccipital narrowed dorsally, sometimes reduced to a point at the inion; m1 talonid with transverse crest usually present between entoconid and hypoconid; angular process of the mandibular ramus robust and hooklike with a large scar for the superior ramus of the median pterygoid muscle; and the forelimbs assigned to *C. lepophagus* suggest that they were moderately elongate relative to hindlimbs with the radius/tibia ratio greater than 80%, but shorter than in some other species of *Canis*, in which the radius/tibia ratio may exceed 90% (e.g., *C. lupus* and *C. latrans*). However, *C. lepophagus* lacks several synapomorphies that *C. latrans* shares with *C. lupus* and is thus considerably removed from the close relationship implied by previous authors. Its lack of autapomorphies, however, suggests a stem (or ''ancestral'') position relative to the radiation of *Canis* crown group species.

Canis thöoides, new species
Figure 40, 45A–C, 52; appendices 3, 4

Type: F:AM 63101, right (fig. 45B–C) and left rami with c–m3, maxillary fragments and isolated teeth including right (fig. 45A) and left C–M2 (P1 broken), partial scapula, right humerus and left partial humerus, left radius and articulated incomplete ulna, right incomplete radius and ulna, left articulated metacarpals I–V and most phalanges, both incomplete tibiae, partial fibula, calcaneum, astragalus, and articulated metatarsals II–V with most phalanges. Flat Tire Fauna, Dry Mountain locality (late Blancan), 32 km southeast of Safford on the east side of the San Simon Valley, Graham County, Arizona.

Etymology: Greek: *thos*, jackal; *oides*, similar in form.

Referred Material: Saint David locality, Saint David Formation (late Blancan), San Pedro Valley, east of Saint David, Cochise County, Arizona: F:AM 63092, right partial ramus with p3–m2.

Distribution: Known only from the late Blancan of Arizona.

Diagnosis: *Canis thöoides* differs from *C. lepophagus* and resembles more derived species of *Canis* in its wide premolars, especially p4 with its posterolingual cingular shelf; like *C. aureus*, it differs from *C. ferox* in possessing primitive states of derived features of that and other crown group species. The P4 protocone extends anterior to the paracone; I3 not markedly enlarged, with weak median cingulum; p4 principal cusp exceeds m1 paraconid in height; m1 anterior face of paraconid vertical or nearly so; m3 bicuspid. The isolation of all premolars by diastemata seems an autapomorphy in *C. thöoides*.

Description and Comparison: In the course of this work we found three canid taxa of late Blancan to early Rancholabrean age that appear to be morphologically similar to the Asian golden jackal, *Canis aureus*. Two of these taxa are known from the remains of single individuals, but the third, and oldest, *C. thöoides*, although known from only two individuals, is better represented dentally and skeletally.

As indicated in the diagnosis, the dentition of *C. thöoides* (fig. 45A–C) differs little in size or morphology from *C. aureus*, particularly with regard to Asian populations. The only consistent differences are: in *C. thöoides* P2–P3 and p2–p4 are wider and higher crowned than in *C. aureus*. In comparison with their length, the premolars of *C. thöoides* are separated by prominent diastemata, with p2 often isolated by longer diastemata; also, the protocone of P4 lies anterior to anterior face of paracone. These are mostly primitive

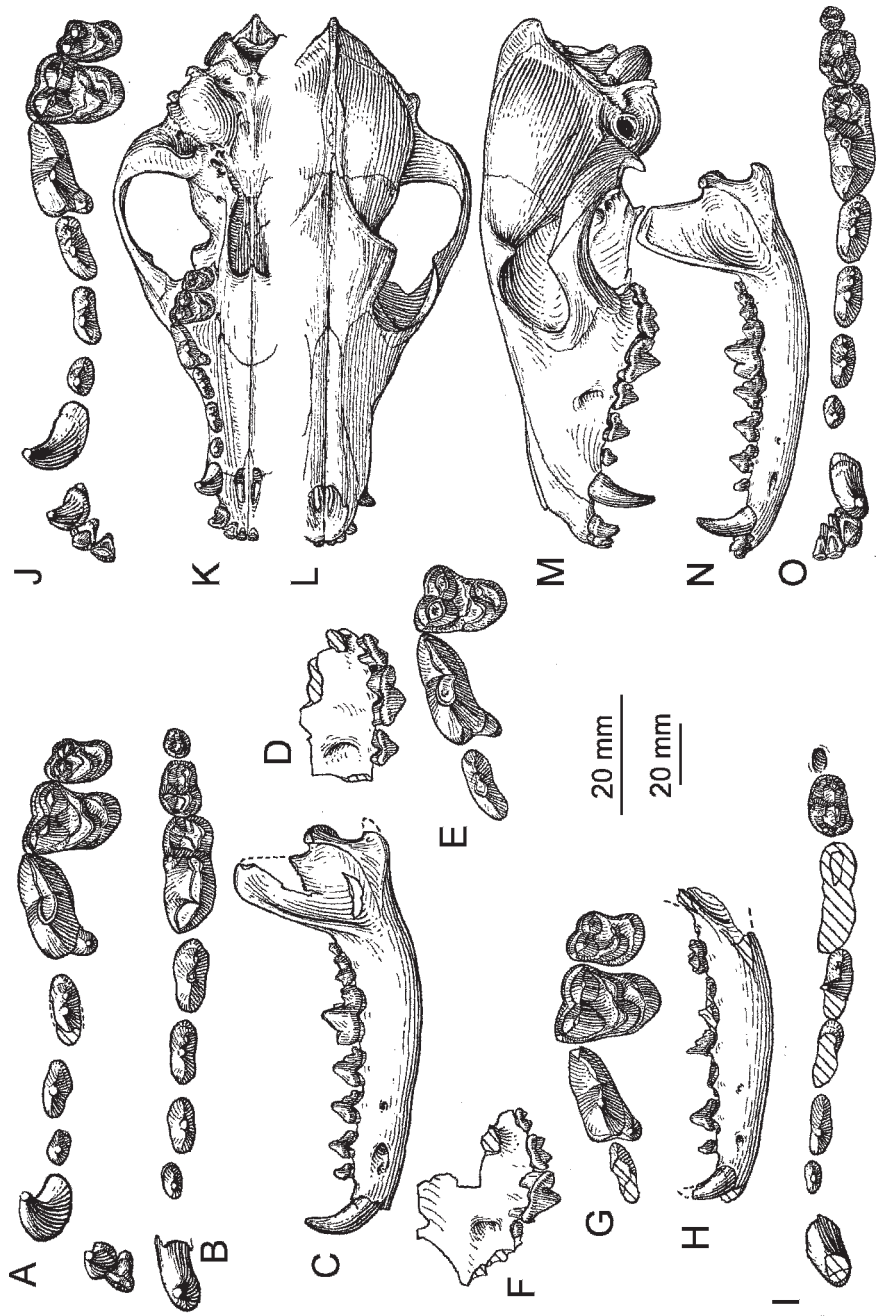

Fig. 45. **A–C**. *Canis thöoides*, Irvingtonian. **A–C**. Type, ramus and maxillary, F:AM 63101, late Blancan, Graham County, Arizona. **A**. Maxillary, occlusal view. **B**. Ramus, occlusal view, reversed. **C**. Ramus, lateral view, reversed. **D–E**. *Canis cedazoensis*. Type, maxillary, TMM 41536-41, Rancholabrean, Aguascalientes, Mexico. **D**. Lateral view, reversed. **E**. Occlusal view, reversed. **F–I**. *Canis feneus*, type, maxillary and ramus, F:AM 25515, late Irvingtonian, Sheridan County, Nebraska. **F**. Maxillary, lateral view. **G**. Maxillary, occlusal view. **H**. Ramus, lateral view (combination of both sides). **I**. Ramus, occlusal view. **J–O**. *Canis aureus aureus*, skull and mandible, AMNH(M) 81041, Recent, Abyssinia. **J**. Occlusal view. **K**. Palatal view. **L**. Dorsal view. **M**. Lateral view. **N**. Ramus, lateral view. **O**. Ramus, occlusal view. The longer (upper) scale is for A, B, E, G, I, J, and O, and the shorter (lower) one is for the rest.

characters. Even the isolation of the premolars by longer diastemata is present in *C. latrans* and in individuals of *E. davisi* in which it is related to a longer muzzle as in *C. thöoides*. Ontogenetically older individuals of *C. aureus* also occasionally show this feature.

The P4 of *C. thöoides* is stout (width across the paracone is approximated by that across the metacone) and the relatively small protocone lies anteriorly. The cingulum is confined to the labial and lingual bases of the metacone. A paraconule is not differentiated in the M1 as it is in *C. aureus*, nor is the lingual cingulum continuous across the protocone as in individuals of *C. aureus*. Likewise, in *C. aureus* the paracone is noticeably larger than the metacone of M1 but not as markedly so as in the coyotes and wolves. The labial cingulum is continuous across the face of the tooth as in *C. aureus*, and the parastyle is no larger in *C. thöoides* than in the golden jackal. The M2 is similar to that in *C. aureus* in size and shape relative to M1. There is a broad labial cingular shelf in both taxa. As in *C. aureus*, the postprotocrista does not quite reach the posterior border of the tooth where a slight swelling represents the metaconule.

The p3–p4 have posterior cusps, and the p4 of F:AM 63092 shows a tiny second posterior cusplet lacking on the type, but present in *C. aureus*. There is a marked widening of the p4 posteriorly due to the development of a posterolingual cingular shelf. The m1 is robust, with its talonid as wide or wider than the trigonid. Cristids from the hypoconid and entoconid join these cusps although they are weakly expressed in F:AM 63092. The entoconid lies slightly behind the hypoconid and there is a hypoconulid shelf developed posterior to the transverse cristids. The anterolabial cingulum on m2 is well developed and passes posteriorly across the labial face of the protoconid in F:AM 63092, but not in the type. The cingulum is confined to the anterolabial face of the protoconid of m2 in *C. aureus*. A small paraconid is present in F:AM 63092, but it seems lacking in the type. Similar variation is present in *C. aureus*. The length of the talonid is less than 90% that of the trigonid, and the hypoconid, but not an entoconid, is differentiated from the ridge surrounding the talonid basin. The m3 is oval to nearly circular in occlusal outline and bears two trigonid cusps set opposite or slightly oblique to one another as in *C. aureus*.

The partial skeleton of the holotype gives information on the forelimb elements of *C. thöoides* in comparison with *C. aureus*. The proportions of the radius to humerus show that *C. thöoides* has a markedly shorter radius relative to the length of the humerus than in *C. aureus* or *C. latrans*, whereas the length of radius to metacarpal III is comparable in all these taxa. The length of the radius with respect to the tibia (88%) lies within the values for the golden jackal (87%–93%) and just below that for coyotes (89%–92%), implying a derived long distal forelimb in *C. thöoides* yet not reaching modern levels in its relationship with the proximal forelimb (fig. 52). This is a primitive feature only exceeded by the longer forelimbs of coyotes and wolves.

Discussion: It is interesting to see a jackal-like form as a product of the Blancan radiation of *Canis* species in North America. This clade appears to continue into the early and medial Pleistocene with the poorly known *C. feneus* and *C. cedazoensis*. Although jackals are today confined to southern Eurasia and Africa, they are rare in the fossil record (Turner, 1990). The recent announcement of the discovery in Morocco (Geraads, 1997) of a taxon of late Pliocene age (2.5 Ma) thought to be close to *C. aureus* seems on the other hand to be a primitive form closer in size and morphology to *Eucyon davisi* previously recorded in deposits of similar age in China (Tedford and Qiu, 1996) and more recently in Macedonia (Koufos, 1997). The reference of fragmentary jackal material from the early Pleistocene site at l'Ain Boucherit, Morocco, to *C. aureus* (as *C. anthus primaevus*) by Arambourg (1979) may be the oldest African record of this taxon. Jackals are apparently unrecognized in the Pliocene or early–medial Pleistocene of Eurasia.

Canis feneus, new species
Figure 45F–I; appendix 3

Type: F:AM 25515, both partial maxillae with P3 (broken)–M3 (fig. 45F–G) and parts of both mandibular rami with c, p1–p2, p3–p4, and m1 alveoli, right m2, and m3 alveolus

(fig. 45H–I). "Sheridan beds" (late Irvingtonian), Hay Springs area, Sheridan County, Nebraska.

Etymology: Latin: *fenem*, hay, with reference to the type locality.

Referred Material: From the type locality: F:AM 95313, right femur missing its proximal end is tentatively referred.

Distribution: Known only from the late Irvingtonian of western Nebraska.

Diagnosis: Differs from *C. thöoides* and *C. aureus* in the following features: upper and lower premolars very slender for their length; P4 small relative to M1, slenderer especially across the metacone; M1 with weak parastyle and preparacrista; ramus slender, but deep; p4 with well-defined second posterior cusp; m2 has strong paraconid, labial cingulum surrounds protoconid and ends at hypoconid.

Description and Comparison: In addition to the features noted in the diagnosis, the maxillary fragment, which seems little distorted, rises nearly vertically above P4; the external margin of the slitlike infraorbital foramen slants anteriorly, and the anterior root of the zygoma lies opposite the junction of M1–M2 as in *C. aureus*. The posterior end of the palate lies at the level of the midline of M2 as in *C. aureus*.

The P3 has most of the crown broken away, but there is no cingular cuspule or evidence of the posterior cusp present in *C. aureus*. In addition to the relatively small size and slender form of the P4, the protocone is also small with a conical tip. Breakage across the anterior end of this tooth does not hide the angled anterolabial border or the fact that the protocone just protruded beyond the anterior border of the paracone as in *C. thöoides* but unlike in *C. aureus*.

The paracone of M1 is noticeably taller and larger than the metacone, and both are somewhat laterally compressed cones. There is a weak parastyle and corresponding preparacrista, but these are not as well developed as in *Eucyon davisi*. The hypocone is large and connected by the lingual cingulum with the metaconule. Anteriorly, the lingual cingulum is well defined across the protocone where it joins the preprotocrista at the base of the paracone. The paracone and metacone of M2 are low and of nearly equal size, surrounded labially by a shelflike cingulum without stylar cusps. A strong lingual cingulum and hypoconal shelf are prominent and, although the protocone retains a postprotocrista, the metaconule is absent. All of these features are also those of *C. thöoides* and *C. aureus*.

The horizontal ramus is deep for a small animal with such slender teeth. The premolars are not strongly graded in length backward as they are in *C. aureus*, but more as in *C. thöoides*, and the p2 is set off with slightly longer diastema as in *C. thöoides* and older individuals of *C. aureus*. A strong anterior mental foramen occurs beneath p1 and smaller foramen beneath the anterior root of p3. Only the m2 remains of the molar row and it is distinguished by retention of a paraconid and the posteriorly extended labial cingulum as indicated in the diagnosis. The metaconid was similar in size and only slightly taller than the protoconid, and there is a well-defined hypoconid and a beaded crest on the lingual part of the talonid without a clearly defined entoconid.

Discussion: *Canis feneus* is nearly a contemporary of *C. cedazoensis* yet it shows morphological traits that represent a more mesocarnivorous, or perhaps even hypocarnivorous, adaptation. If these animals, known only from the fragmentary remains of single individuals, are correctly diagnosed, their presence suggests that a previously unrevealed diversity of jackal-like canids occupied North America in the early and medial Pleistocene.

Canis cedazoensis Mooser and Dalquest, 1975

Figure 45D–E; appendix 3

Canis cedazoensis Mooser and Dalquest, 1975: 787, fig. 2.
Canis cedazoensis: Nowak, 1979: 68.

Type: TMM 41536-41 (originally O. Mooser collection FC 634, AMNH cast 105201), right partial maxilla with P3–M1 and M2 alveolus (fig. 45D–E) form strata referred to the Tacubaya Formation in Arroyo Cedazo (early Rancholabrean), 3 km southeast of Aquascalientes, State of Aquascalientes, Mexico.

Distribution: Only known from the Rancholabrean of Mexico. Attributed to the

Sangamon interglacial (stage 5 as determined by ^{18}O) by Pinsof (1996).

Revised Diagnosis: *Canis cedazoensis* differs from *C. aureus* and *C. thöoides* in M1 anteroposteriorly shorter relative to length of P4 with reduced hypocone and labial cingula; M2 alveoli indicate smaller size tooth relative to M1.

Description and Comparison: Mooser and Dalquest (1975: 787, fig. 2) reported that this taxon is intermediate in size to the coyote and fox, and that it may have filled the niche occupied in the Old World by the jackals. They compared the type maxilla with nearly 100 Recent coyote skulls from Texas and found that some of the coyotes had the upper carnassial as short, but never as narrow, and "no coyote had the M1 as small as that of *C. cedazoensis*." Nowak (1979: 68) followed Mooser and Dalquest in allocating this species to *Canis*, but because the type was fragmentary and worn, he did not evaluate the taxon.

No comparisons were previously made with the living jackals, but we have found that *C. cedazoensis* is close in size and aspects of morphology to *C. aureus*, although differing from it in significant ways. Like *C. aureus*, the P3 has a weak posterior cusp. The P4 is proportionally similar and has a relatively larger protocone that, as in *C. aureus*, barely protrudes beyond the anterior end of the tooth. The greatest difference lies in the relative size and form of M1 and M2 (as inferred from its alveoli). The M1 is small relative to P4 taking into account wear and missing enamel on the labial and lingual sides of the tooth. Nevertheless, the labial cingulum is not as well defined as in *C. aureus*, nor is there an anterior cingulum lingually. The hypocone and associated cingulum are reduced and confined posterior to the protocone. Although there is considerable wear on the principal cusps, the paracone is clearly larger than the metacone as in *C. aureus*. The alveoli for the paracone and metacone of M2 lie in a line nearly transverse to the sagittal plane, indicating that the M2, like the M1, was transversely wide for its length, and likely had a much reduced metacone and hypocone. The interdental facet for M2 on M1 is mostly lingual to the M1 metastyle, also suggesting a small tooth situated more lingually than in *C. aureus*.

The morphology of *C. cedazoensis* suggests a jackal-like canid with dental tendencies toward more hypercarnivorous adaptations than seen in any jackal or in the two other North American jackal-like species (*C. thöoides* and *C. feneus*) that have been recognized in the course of these studies.

Canis edwardii Gazin, 1942
Figures 39H–O, 40, 43, 44, 46A–H, 47A–F, 48A–F, 50–52; appendices 2–4

Canis edwardii Gazin, 1942: 499, fig. 41.
Canis cf. C. *lupus*: Hibbard and Dalquest, 1966: 20.
Canis priscolatrans Cope (in part): Kurtén, 1974: 7, 11.
Canis edwardii: Nowak, 1979: 82.

Type: NMNH 12862, partial skull with I1–M2 (fig. 46E–F) and incomplete rami with i1–m2 (fig. 46G–H) from about 3.2 km northeast of Curtis Ranch homestead, Saint David Formation (earliest Irvingtonian), San Pedro Valley, Cochise County, Arizona.

Referred Material: Curtis Flats, Saint David Formation (earliest Irvingtonian), Cochise County, Arizona: F:AM 67301, right partial ramus with m1 (broken)–m2; F:AM 103409, left ramal fragment with p3–p4 (both broken); NMNH 12864, right partial maxilla with P3–M2 from 4.8 km northeast of Curtis Ranch; AMNH 21806*, left ramus with c–m3 alveoli; and AMNH 23393*, badly broken left ramus with c–m1.

Tusker fauna, 111 Ranch at Dry Mountain locality (late Blancan), near Safford, Graham County, Arizona: F:AM 63100, skull with I1–M2 (I2 alveolus) (fig. 48A–C), right partial ramus with c (root broken)–m3 (alveolus) (fig. 48D–F), and associated skeletal elements, including right partial humerus (fig. 39H), both radii (fig. 39I) and ulnae (fig. 39J–K), metacarpals II–V (metacarpal III, fig. 39L), right femur (fig. 39N), both tibae (fig. 39O), metatarsals III–V (metatarsal III, fig. 39M), calcaneum, phalanges, and vertebrae.

Whitlock Mountains (UA locality 9806), south of Dry Mountain (late Blancan), near Safford, Graham County, Arizona: UA

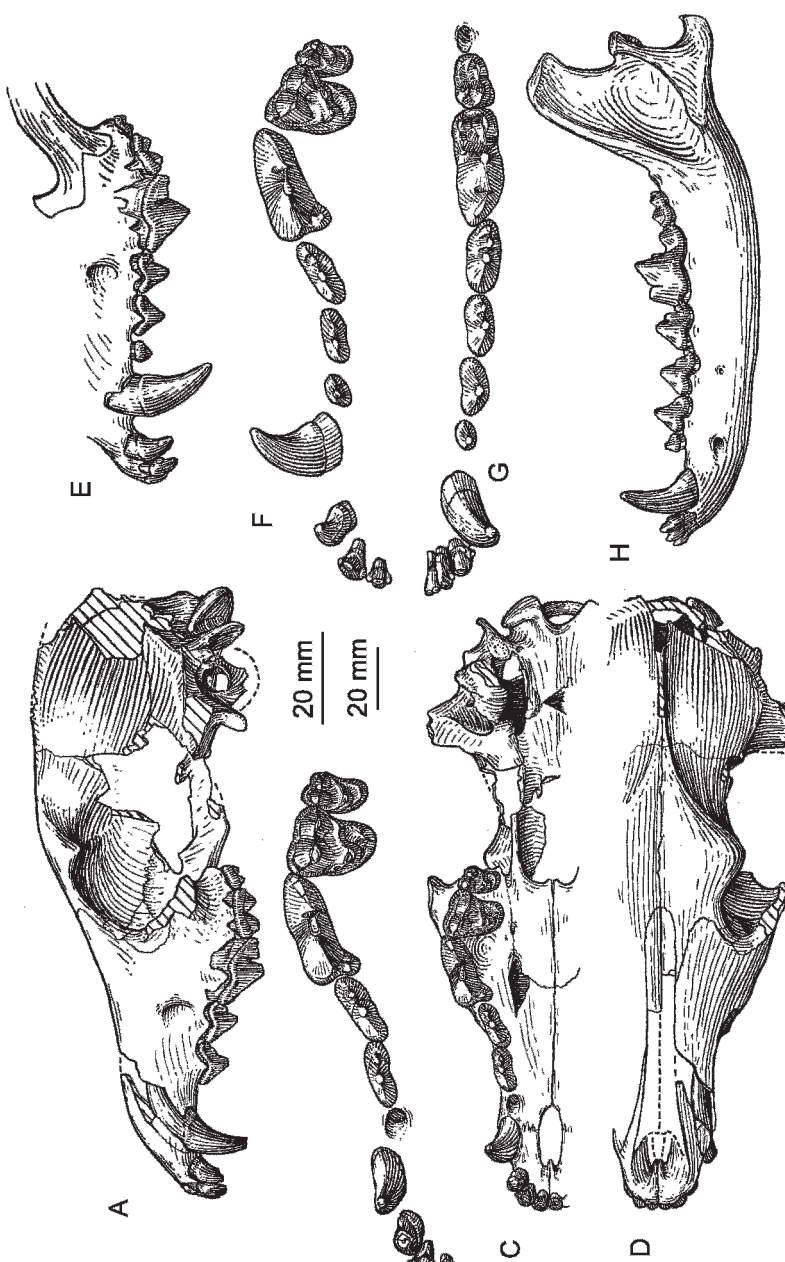

Fig. 46. **A–H**. *Canis edwardii*. **A–D**. Skull, NMNH 23898, Irvingtonian, southeastern Oregon. **A**. Lateral view. **B**. Occlusal view. **C**. Palatal view. **D**. Dorsal view. **E–H**. Palate and ramus, type, NMNH 12862, Irvingtonian, San Pedro Valley, Arizona. **E**. Lateral view. **F**. Occlusal view. **G**. Occlusal view, reversed. **H**. Lateral view, reversed. The longer (upper) scale is for B, F, and G, and the shorter (lower) one is for the rest.

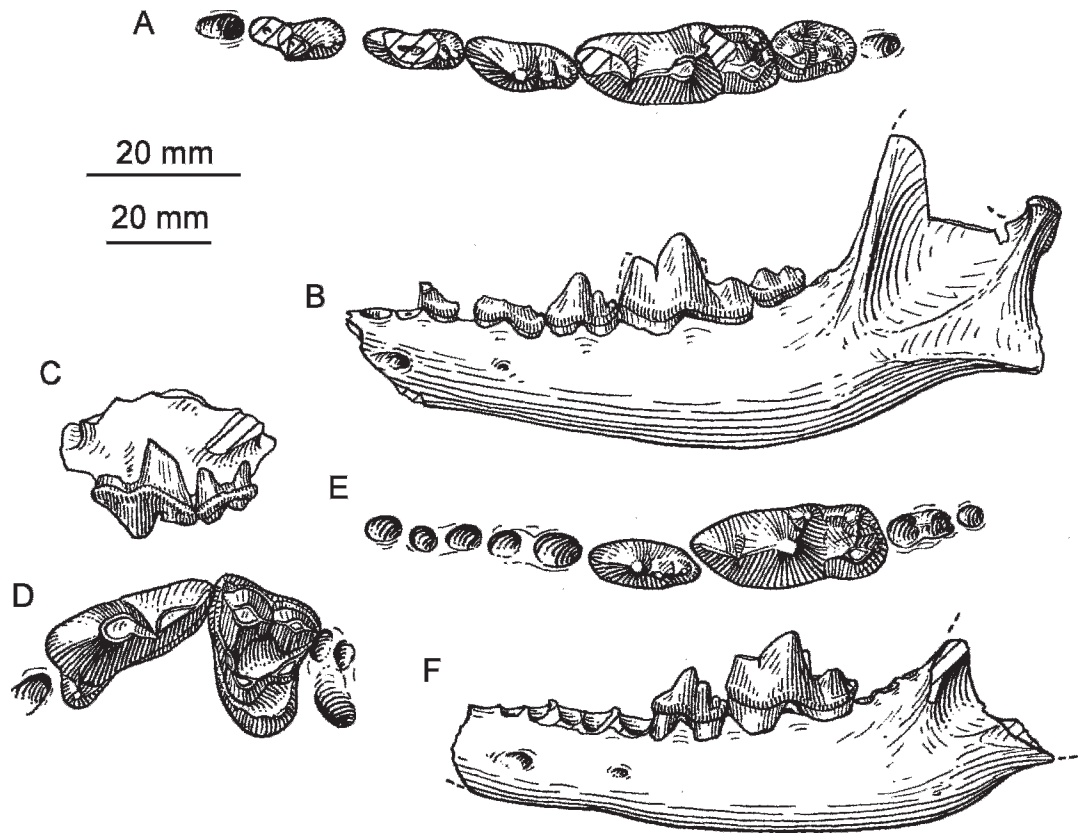

Fig. 47. **A–F**. *Canis edwardii*. **A–B**. Ramus, NMNH 10210B, Irvingtonian, Coconino County, Arizona. **A**. Occlusal view. **B**. Lateral view. **C–F**. Maxillary and ramus, Irvingtonian, Citrus County, Florida. Maxillary, UF 18046. **C**. Lateral view, reversed. **D**. Occlusal view, reversed. **E–F**. Ramus, UF 19323. **E**. Occlusal view, reversed. **F**. Lateral view, reversed. The longer (upper) scale is for A, D, and E, and the shorter (lower) scale is for the rest.

23402, crushed skull (restored) and mandible showing most dentition except I1–I2, M2, i1–i3, c, m2, associated partial cervical vertebrae 3–7, fragment of left scapula, clavicle, first rib, and proximal part of right ulna.

Stagomastodon locality, Saint David Formation (latest Blancan), Curtis Ranch, Cochise County, Arizona: UA 1632, left ramal fragment with p2–p3, m1, and p4 (broken); and UA 3231, left ramal fragment with m1, m2 broken, and m3.

Cita Canyon beds (late Blancan), Randall County, Texas: WTUC 1936, fragment of right frontal, isolated right C, and right and left partial maxillae with P4–M2; CWT 2574, radius; CWT 2526, tibia; and CWT 2572, metatarsal III.

Sand Draw Quarry, Keim Formation (medial Blancan), north of Ainsworth, Brown County, Nebraska: F:AM 95189*, right fragmentary maxilla with P3.

Big Spring Local Fauna, Long Pine Formation (late Blancan), UNSM locality Ap 103, Antelope County, Nebraska: UNSM 2136-78, isolated left M1.

Haile 12B (late Blancan fide Hulbert and Morgan, 1993: table 8.1), Alachua County, Florida: UF 11516, partial skull consisting of right maxillary, jugal, anterior part of squamosal with glenoid fossa and anterior part of ectotympanic, frontal shield, anterior part of parietal including sagittal crest to interparietal, P4, M1–M2. This specimen was attributed to *C. rufus* by Nowak (1979: 88), who did not list the specimen number

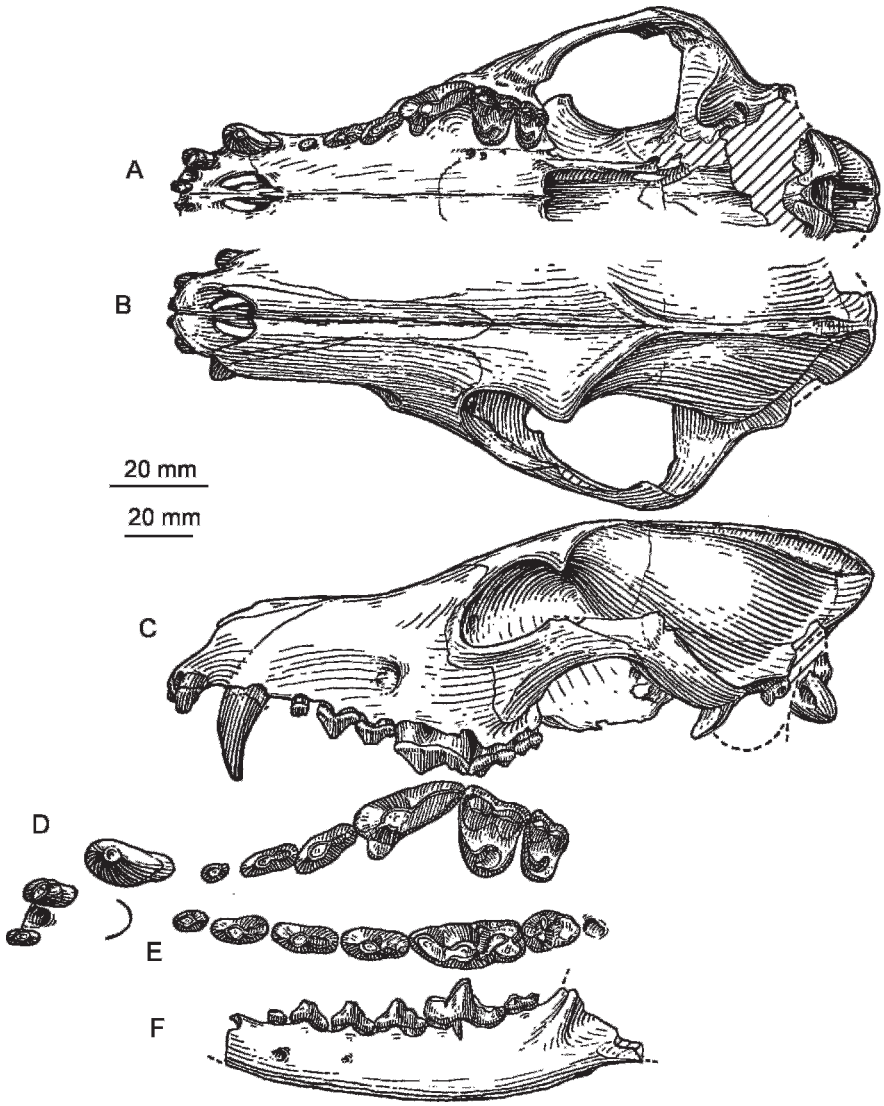

Fig. 48. **A–F**. *Canis edwardii*. Skull and mandible, F:AM 63100, Irvingtonian, Graham County, Arizona. **A**. Palatal view, reversed. **B**. Dorsal view. **C**. Lateral view. **F**. Occlusal view, reversed. **F**. Lateral view, reversed. The longer (upper) scale is for D and E, and the shorter (lower) one is for the rest.

and who incorrectly listed the site as Haile 7A and the age as Rancholabrean. It subsequently was attributed to *C. edwardii* (his *C. priscolatrans*) by Nowak (2002: 107), who then correctly listed the site as Haile 12B and the age as late Blancan, but who incorrectly listed the site (Nowak, 2002: 127) as Haile 12A.

Reigle Gravel Pit, west of Plainview, north of Highway 20, Antelope County, Nebraska: UNSM locality Ap-133, unnamed early Irvingtonian gravel deposits of glacial origin overlying the Blancan Long Pine Formation: UNSM 2555-90, associated left lower teeth, p3–p4, m1 found together in situ.

Waneta site, near McCook, Chase County, Nebraska, UNSM locality Ch-102, late early Irvingtonian crystalline gravels incised into the Ogallala Group that appear to be continuous with similar beds along the

Republican River, including the site near Orleans in Harlan County, Nebraska, type area of the Sappa Ash (equivalent to Mesa Falls Ash of Yellowstone, 1.2 Ma): UNSM 48590, right ramus with c–p4 alveoli, m1–m2, m3 alveolus including ascending ramus.

Williams site, Hitchcock County, Nebraska, UNSM locality Hk-113, stratigraphy and late early Irvingtonian age as for UNSM localities Ch-102 and Rw-105: UNSM 3011-97, labial half of crown of right m1.

McCook Clam site, Red Willow County, Nebraska, UNSM locality Rw-105, stratigraphy and late Irvingtonian age as for UNSM localities Ch-102 and Uk-113: UNSM 88523, left ramus with partial alveolus for p3, p4 alveolus, m1 broken, m2, m3 alveolus; UNSM 88524, left maxillary fragment with P3–P4, M1–M2; and UNSM unnumbered, right m2.

Mike Jones site, UNSM locality Fn-104, Republican River near Cambridge, Furnace County, Nebraska, late early Irvingtonian gravels incised into the Ogallala Group: UNSM 88527, right ramus, p1 root, p2–p3, p4 broken, m1–m2; UNSM 5357-92, m2.

Anita Fauna (early Irvingtonian), fissure fill in Kaibab Limestone, Coconino County, Arizona: NMNH 10210B, left ramus with p1 alveolus, p2–p3 broken, p4–m1–m2, m3 alveolus (fig. 47A–B); NMNH 10210C*, left ramus with p4.

Vallecito Creek Fauna, Palm Springs Formation (early Irvingtonian), San Diego County, California: LACM 20591, isolated C, anterior part of the left P4 broken and right P4 (possibly two individuals); LACM 20591, isolated C, anterior part of left P4 broken and right P4 (possibly two individuals); LACM 6250, right and left maxillae with P3 (broken)–M2 and right and left rami with i1–p4 broken and alveoli of m1–m3; LACM 8235, right and left partial rami with c broken–p1, p1–m1 broken, and m2; LACM 6236, left partial ramus with p3–m2 broken; LACM 6770, right maxilla fragment with M1 broken–M2; LACM 3258, right and left partial rami with c broken, p1–p4 alveoli, p4–m1 broken, and m2 alveolus; and LACM 3805, metatarsals II, III, and IV.

Seventeen Palms (Irvingtonian), Palm Springs Formation, Imperial County, California: F:AM 31853, left partial maxilla with P4–M1.

Mecca Hills (Irvingtonian), Palm Springs Formation, Coachella Valley, Riverside County, California: LACM 1148, left partial maxilla with P3 (broken)–M2 (badly worn).

El Casco Local Fauna (early Irvingtonian, 1.3–1.4 Ma; Albright, 1999), Riverside County, California: F:AM 17863, right partial ramus with c (alveolus)–m1 (broken) (p1 and p4 roots); F:AM 17864, right partial ramus with m1 (broken)–m2 root; F:AM 17865, left partial ramus with c (broken)–p1–p3 broken, p4–m1.

USGS locality M1367, Bruneau Formation (late Irvingtonian), Owyhee County, Idaho: NMNH 184126, left partial ramus with p4 broken and m1–m3.

Rome, USGS locality M1080 (Irvingtonian), Malheur County, southeast Oregon: NMNH 23898, skull with I1–M2 (P1 missing) (fig. 46A–D).

Gilliland Local Fauna (earliest Irvingtonian), lower part of the Seymour Formation, 11 km west of Vera, Knox County, Texas: UMMP 46483*, articulated partial maxillae and premaxillae with I1–P2 (P3 broken) and both partial rami with i1–p4; and UMMP 46460, cranial fragment including the left interparietal, parietal and both temporal bones and incomplete glenoid area, broken bulla, and base of paroccipital process; MSU 8676*, right edentulous partial ramus with alveoli for c–m4; and UMMP 46479*, left upper canine.

Arkalon Gravel Pit (late Irvingtonian), Crooked Creek Formation, just above Lava Creek B (Perlette Type O) tephra (0.61 Ma), 2.4 km east of Arkalon Station of the Rock Island Railroad, Seward County, Kansas: UMMP V29068, associated limbs of a single individual, radius, femur, tibia, calcaneum, metatarsals III and V (Hibbard, 1953).

Inglis site 1A (earliest Irvingtonian, sensu Morgan and Hulbert, 1995), Citrus County, Florida: UF 19323, right partial ramus with p4–m1 and alveoli for p1–p3, m2–m3 (fig. 47E–F); UF 19324, right partial ramus with m1 (talonid)–m2; UF 19404, left isolated m1; UF 18050, left p3; UF 18049, right P4; UF 18046, right partial maxilla with P4–M1, M2 (alveolus) (fig. 47C–D); UF 67846*, left partial maxilla with M1; UF 19405, left

M1; UF 19406, left M1; UF 18051*, left premaxilla with I1–I2 alveoli and I3; UF 18052*, right lower canine; UF 18047, right partial maxilla with M2; UF 18048, left M2 and a right M2 germ (two individuals); UF 18054, atlas; UF 18056, left radius; UF 67845A, right radius (smaller individual); UF 22566, left proximal part radius; UF 22567, right distal end of radius; UF 67843, left partial ulna; UF 18055A, left partial ulna; UF 67844B, right partial ulna; UF 22568, left partial ulna; UF 22569, left partial ulna; UF 18057, left metacarpal III; UF 22570, left metacarpal IV; UF 18057A, left metacarpal IV; UF 45457, left metatarsal V; UF 45458, left metatarsal V; UF 45459, left metatarsal V; UF 22571, distal end left tibia; UF 22572, distal end left of tibia; UF 22573–22576, four astragali; UF 18059, left calcaneum; UF 22577, right metatarsal III; UF 22578, left metatarsal IV; UF 45457, left metatarsal V; UF 45458, left metatarsal V; and UF 45459, left metatarsal V. Most of the dental remains listed above were attributed to *C. rufus* by Nowak (1979: 88), and later to *C. edwardii* by Nowak (his *C. priscolatrans*, 2002: 127–128).

Rigby Shell Pit (late early Irvingtonian), Bermont Formation, Sarasota County, Florida: UF 40090, right maxillary fragment with P4 and well-worn M1–M2; UF 40091, fragment of right ramus with p1 root, p2, p3 root, p4 broken, m1–m3 alveoli.

Wolf Hill locality, Bone Valley (late Irvingtonian), Polk County, Florida: TRO 1441, skull fragments and detached teeth with I1–M1 and M2 (broken).

Leisey Shell Pits, Hillsborough County (early Irvingtonian), Florida: UF 81665, maxillary fragment with P4, M1–M2 (figured by Berta, 1995: fig. 1C); UF 81666, right maxillary fragment with M1–M2; UF 81664, right maxillary fragment with P3; UF 81663, left maxillary fragment with P1–P2; UF 124531, right maxillary fragment with M1; UF 63667, left ramus with c alveolus, p1, p2 broken, p3–p4, m1; UF 64399, left ramus with m1, m2–m3 alveoli; UF 81670, right ramus with p3–p4, m1; UF 84752, right m1, UF 87285, right m1; UF 81689, right m2; UF 87297; left m2; UF 81672, left m1; UF 81662, left P4; UF 81668, right P4; UF 81669, right M1; UF 81657, right M1; UF 81657, right M1; UF 81661*, metastyle of left P4; UF 81658, right p4; and UF 81659, right P4 (the last four specimens listed as *C. armbrusteri* by Berta, 1995: 465); and postcranial elements listed by Berta (1995: 466).

Haile 21A (Newberry Quarry), Alachua County (late early Irvingtonian sensu Morgan and Hulbert, 1995), Florida: UF 62563 (cast), left ramus with p3–p4, m1–m2, m3 alveolus; UF 62564 (cast), left ramus with p1–p4 alveoli, m1–m2, m3 alveolus; UF 62562 (cast), right ramus with i1–i3, c, p1 alveoli, p2–p4, m1–m2, m3 alveolus; UF 62568, right ramus with m1 talonid, m2; UF 63175, left ramus with p1–p4, m1–m2; UF 63174, edentulous partial right ramus, alveoli for i1–i3, c, p1–p4; UF 124539, left p4; UF 63527, fragment of right ramus, p4 roots, m1 broken, m2 alveolus; UF 63311, right p4; UF 62567, right m1; UF 62561 (cast), fragment of right premaxillary, maxillary with I1 root, I2 alveolus, I3, C, P1 and associated left maxillary with C, P1–P2 alveoli, P3–P4, M1–M2; UF 124537, left P4; UF 63159, left radius; UF 62588, left humerus lacking distal end; UF 63162, left metacarpal II; UF 63309, left metacarpal V; UF 62585, associated left metatarsals II–IV; UF 62584, right metatarsal IV; UF 63526, left metatarsal II; UF 63098, left tibia; and UF 63100 left femur.

Crystal River Power Plant, UF locality Citrus 8 (late early Irvingtonian sensu Morgan and Hulbert, 1995), Citrus County, Florida: UF 17074, right maxillary fragment with P3 alveolus, P4, M1, M2 alveolus. Attributed to *C. rufus* by Nowak (1979: 88) and to *C. edwardii* (his *C. priscolatrans*) by Nowak (2002: 128).

El Golfo de Santa Clara, northwestern Sonora, Mexico (late Blancan): IGM 10163* (HJG 793), right maxillary fragment with P4, M1–M2, and associated left maxillary fragment with P4; IGM 10047* (HJG 777), edentulous left ramal fragment with c, p1–p4, and anterior part of m1 alveoli.

Distribution: Medial Blancan of Nebraska; late Blancan of northern Mexico, Arizona, Texas, Nebraska, and Florida; and early to late Irvingtonian of Texas, Kansas, Nebraska, Oregon, Idaho, Arizona, California, and Florida.

Revised Diagnosis: *Canis edwardii* is distinguished from *C. ferox* by a suite of

synapomorphies the former shares with *C. latrans* and the wolves: tip of p3 principal cusp lies below those of adjacent premolars and its cingulum lies entirely below that of p4; principal cusp of p4 lies below paraconid of m1, anterior face of m1 slants posteriorly; paracone of M1 is larger than metacone; maxillary-jugal suture is acute; m3 is single-cusped; and incisive foramen may extend posterior to canine alveolus.

Canis edwardii is larger than *C. latrans* and differs in skull and some tooth proportions as well as lacking two synapomorphies that group *C. latrans* with the wolves: elongation of distal part of forelimb (radius/tibia ratio <90%), and sagittal crest extends onto frontal bone.

Description and Comparison: Among the diverse materials listed above that we ascribe to *C. edwardii*, there are five useful skulls: two of which are from late Blancan deposits of southeastern Arizona, the type from slightly younger rocks (earliest Irvingtonian) not far away in southern Arizona, a fourth from late Blancan deposits of Florida, and the fifth from Irvingtonian deposits in southeastern Oregon. In cranial proportions these specimens show considerable diversity, but that is to be expected from their temporal (about 2 m.y.) and geographic range, as well as from sexual and ontogenetic variation (although all are adults). Compared to *C. latrans*, these animals are larger in all dimensions and the proportional relationships of the cranial elements are similar (fig. 43). We found no systematic changes in these proportions within the time range covered by the five skulls.

Based on all the referred specimens, *C. edwardii* is characterized morphologically as follows: the incisive foramen is long and extends posterior to the canine alveolus; the infraorbital foramen is slitlike and opens above the posterior root of P3; the jugal-maxillary suture is acute; the nasals extend behind the most posterior extent of the maxillary-frontal suture; the frontal sinus is expanded with modest inflation of the postorbital processes and associated parasagittal crests, extending nearly to the frontoparietal suture; the parasagittal crests join to form a low sagittal crest at the frontoparietal suture; posteriorly, the sagittal crest gains in height onto the interparietal; the broad shield formed by the nuchal crests is a dorsally truncated triangle when viewed from the rear; the mastoid shelf and process are not strongly developed; the paroccipital processes are vertically directed and have short free-tips, the processes are transversely narrow and cover only a small part of the posterior surface of the bulla; the bullae are moderately inflated and may just extend anterior to the postglenoid process; the basioccipital is narrow and parallel-sided; the palate extends to just posterior to or opposite the M2; the largest posterior palatal foramen lies on the maxillary-palatine suture opposite the paracone of P4 or farther behind at the posterior end of that tooth.

The upper incisors are large, I1–I2 have lateral and medial cusps, and I3 is markedly larger and has no subsidiary cusps, only a well-developed median cingulum. The upper premolars are large, elongate, low-crowned, and closely spaced, and the only diastemata of any length separates P1 from C and P2. The P3 frequently has a small posterior cusp, but the Rome specimen (NMNH 23898) shows a P2 with a tiny posterior cusp as well. The P4 is slender, with its protocone prominent and anterolingually directed, but it does not extend beyond the anterior border of the tooth. The M1 has a paracone that is larger than the metacone but not markedly enlarged, the protocone is situated opposite the paracone, the protoconule is barely differentiated, and the metaconule a little more so, but not prominent, so that the postprotocrista is only slightly enlarged at its position. There is a strong hypocone situated posterolingually connected to the lingual cingulum, which passes across the protocone to the parastyle. Posteriorly, the lingual cingulum ends at the position of the metaconule. A strong labial cingulum is present, terminating anteriorly in a low parastyle to which the preparacrista is attached. The M2 has the paracone larger than the metacone, as well as a shelflike labial cingulum. A postprotocrista passes to the posterior border, but the metaconule is very small or lacking. The lingual cingulum and hypocone form an internal shelf. The shape of this tooth is usually oval but may be markedly attenuated

lingually by posterolingual expansion of the hypocone (e.g., NMNH 23898, fig. 46B).

The holotype is the only specimen that shows the lower incisors, all of which have lateral cusps; the canine is large and recurved. The lower premolars are large, elongate, and low-crowned, as are their upper counterparts. They are uncrowded and p2 may be separated by diastemata. There is no inflection of the premolar row as present in the wolves. The p2 lacks a posterior cusp, but p3–p4 have such cusps, although other examples show that they may be absent on p3. The tip of the principal cusp of p3 lies below p2 and p4; its posterior cingulum lies below the base of the crown of p4. The p4 consistently has a tiny second posterior cusp just anterior to the posterior cingulum. The tip of the principal cusp of the p4 lies below the tip of the paraconid of m1. The anterior face of the m1 paraconid slants or curves backward and the trigonid is relatively open. The talonid is close to the same width as the trigonid; its hypoconid is prominent, laterally situated; the entoconid, markedly smaller, lies somewhat posterior to the hypoconid and is connected to it by a low cristid. The talonid may be open lingually between the entoconid and metaconid or the gap closed by a low entoconulid. A low cingulum is often found on the labial side of the talonid. A talonid shelf is consistently present, and a hypoconulid may be present behind the hypoconid. The m2 is relatively large with an anterolabial cingulum and a metaconid that is smaller than the protoconid and slightly posteriorly placed relative to the protoconid. The protoconid has a paracristid that extends to the anterior cingulum, although there is no paraconid. The talonid may be wide with a prominent hypoconid and lingual crest studded with small cuspules but no differentiated entoconid, or it may be attenuated posteriorly and consist only of a hypoconid. The m3 is preserved in only a few specimens. It is a single-cusped tooth with a lingual crest passing from this cusp to the lingual border, but no metaconid is differentiated along this crest.

The horizontal ramus is relatively shallow, but it does not markedly decrease in depth anteriorly. The largest mental foramen lies beneath p1 or between p1 and p2; a smaller foramen lies between the roots of p3. There is a shallow inflection of the lower border of the ramus behind the symphysis. The masseteric fossa is deep, especially anteroventrally and against the anterior rim, and a masseteric line is developed. The coronoid process is shorter than high, corresponding to the short temporal fossa of the skull. As in other species of *Canis*, the medial side of the angular process shows a large fossa for the superior ramus of the median pterygoid muscle and below it a smaller roughened area for the inferior ramus. The process is markedly attenuated posteriorly and ends in an upturned hook.

We have unassociated limbs referred to *C. edwardii* from four sites: Cita Canyon, Texas, and Leisey Shell Pit, Haile 21A, and Inglis 1A in Florida. Two important associated skeletons are from the late Blancan of Arizona (F:AM 63100, fig. 39H–O) and the late Irvingtonian Arkalon site in southwestern Kansas (UMMP V 29068, fig. 52). They represent the extremes in size and sample nearly the limits of the geological range of this species. The Kansas specimen was discussed by Kurtén (1974), and although unaccompanied by cranial or dental remains, seems properly referred to *C. edwardii* on the basis of similarity of its elements to those from other sites where dentitions are available. As Kurtén (1974) has pointed out, the Arkalon skeleton of *C. edwardii* (*C. priscolatrans* in his taxonomy) is a robust form as befits its overall size, and the allometry follows the pattern of *C. lepophagus*, as exemplified by the relationship of the proximal width of the radius to its total length (Kurtén, 1974: fig. 6). The mutual proportions of the forelimb elements (radius and metacarpal III) show that the forelimb of the Arkalon individual of *C. edwardii* was elongated as in the living coyotes. The radius lies below the range of *C. latrans* relative to the tibia (radius/tibia ratio $<90\%$). In particular, the smaller Arizona specimen (F:AM 63100) shows a significantly lower radius/tibia ratio (85%). Both specimens, however, differ little from the hindlimb proportions of *C. latrans*. The larger radius in the Arkalon individual hints at changes in limb proportions within *C. edwardii* during its long geological range.

Discussion: Cope (1899: 227–228) described *Canis priscolatrans* from three "superior molars of a single individual" (all ANSP 57), a right M1 and M2 in early wear, and a right P4 (not a "pm1" as he designated it) also in early wear. These were obtained from the Port Kennedy "bone deposit" in upper Merion Township, Montgomery County, Pennsylvania, and are of late Irvingtonian age.

The cotypes of *Canis priscolatrans* have dimensions falling inside those of *C. edwardii*, and the "conules in the M1 are not distinct" as noted by Cope (1899: 227), a feature that is alluded to in his diagnosis (Cope, 1899: 228), both of which agree with the condition in *C. edwardii*. However, we set aside this possible synonymy on the basis of the very incomplete knowledge of the taxon *C. priscolatrans* afforded by the cotypes in comparison to the type of *C. edwardii* and hold the former as a nomen dubium.

Canis latrans Say, 1823
Figures 40, 43, 44, 49A–H, 50–52;
appendices 2–4

Canis cf. *priscolatrans* Cope (in part): Gidley and Gazin, 1938: 23.
Canis irvingtonensis Savage, 1951: 231, figs. 8a–b, 9a–b, 10.
Canis priscolatrans Cope (in part): Kurtén, 1974: 6, 11.

Referred Pre-Rancholabrean Material: UCMP locality V3604, Irvington site 2 (Irvingtonian, late Matuyama Chron, older than 0.73 Ma), Bell Sand and Gravel Co. Quarry, 1.3 km southwest of Irvington, Alameda County, California: UCMP 38805, right partial ramus with p1 (alveolus) p2–m2, m3 alveolus (type of *C. irvingtonensis*); UCMP 38748, left ramus with i1–p1 alveoli and p2–p3 (alveolus); UCMP 38804, left radius (paratype of *C. irvingtonensis*); UCMP 81737*, part of left M1; UCMP 56090, cranium lacking inion, condyles, bullae, and tips of postorbital processes.

Fairmead Landfill, UCMP site V93128, Turlock Lake Formation (late Irvingtonian, Dundas et al., 1996), Madera County, California: UCMP 140413, left maxillary fragment with M1–M2, and posterior part of frontal bone.

"Sheridan beds" (late Irvingtonian), Rushville and Gordon area, Sheridan County, Nebraska: From UNSM locality Sh-3, Rushville Quarry 1: UNSM 2913, right partial ramus with p1–p4 alveoli and m1–m2 (broken); from UNSM locality Sh-5, Gordon Quarry 1, Pit 3: UNSM 21435, right ramal fragment with i3–m1; from UNSM locality Sh-5: UNSM 21437, left partial ramus with i1–p1 alveoli, p2–p3 and p4 (alveolus)–m1 (broken); from UNSM locality Sh-4, Quarry 4B: UNSM 451-76, fragment of left ramus with p1 alveolus, p2 roots, p3–p4; from UNSM locality Sh-4, Quarry 4B: UNSM 452-76, right m1; from UNSM locality Sh-3: UNSM 6.3.8.33 NP, left m1; from UNSM locality Sh-5: UNSM 21434, left maxillary fragment P3 alveolus, P4; from UNSM locality Sh-5: UNSM 15250-38, left P4; from locality Sh-4, Quarry 4B: UNSM unnumbered, left M1.

Rock County Gravel Pit (Irvingtonian), Rock County, Nebraska: F:AM 87248, left ramal fragment with p4 (alveolus)–m1 (broken).

Mullen Pt 1 (late Irvingtonian, see Martin, 1972, for discussion of the faunal composition and age of the Mullen sites), UNSM locality Cr-10, Cherry County, Nebraska: UNSM 26115, right ramus with c–m2 and m3 alveolus (fig. 49C–D).

Conard Fissure (late Irvingtonian), 24 km south of Harrison, Newton County, Arkansas: AMNH 12394, a left unerupted m1.

Rock Creek, Tule Formation (late Irvingtonian), 14.5 km southwest of Silverton, Briscoe County, Texas: JWT 2303, right partial maxilla with M1 (paracone broken away)–M2; F:AM 95314, left humerus; F:AM 95315, right metatarsal IV; and YPM 10080, right M1.

Slaton Quarry Local Fauna (late Irvingtonian, 0.5–0.6 Ma, Dalquest and Schultz, 1992), west side of Yellowhouse Canyon, 7.6 km northeast of Slaton, Lubbock County, Texas: MSU 6522, maxillary fragment with posterior half P3, P4–M1; MSU 5043, right ramal fragment with canine alveolus, p2–p3.

Cumberland Cave (late Irvingtonian), 6.5 km northwest of Cumberland, Allegany County, Maryland: NMNH 7660, partial skull (fig. 49A) with I1–M2 represented by alveoli, roots, or broken teeth; NMNH 494384, right ramus, c–p2 alveoli, p3–p4,

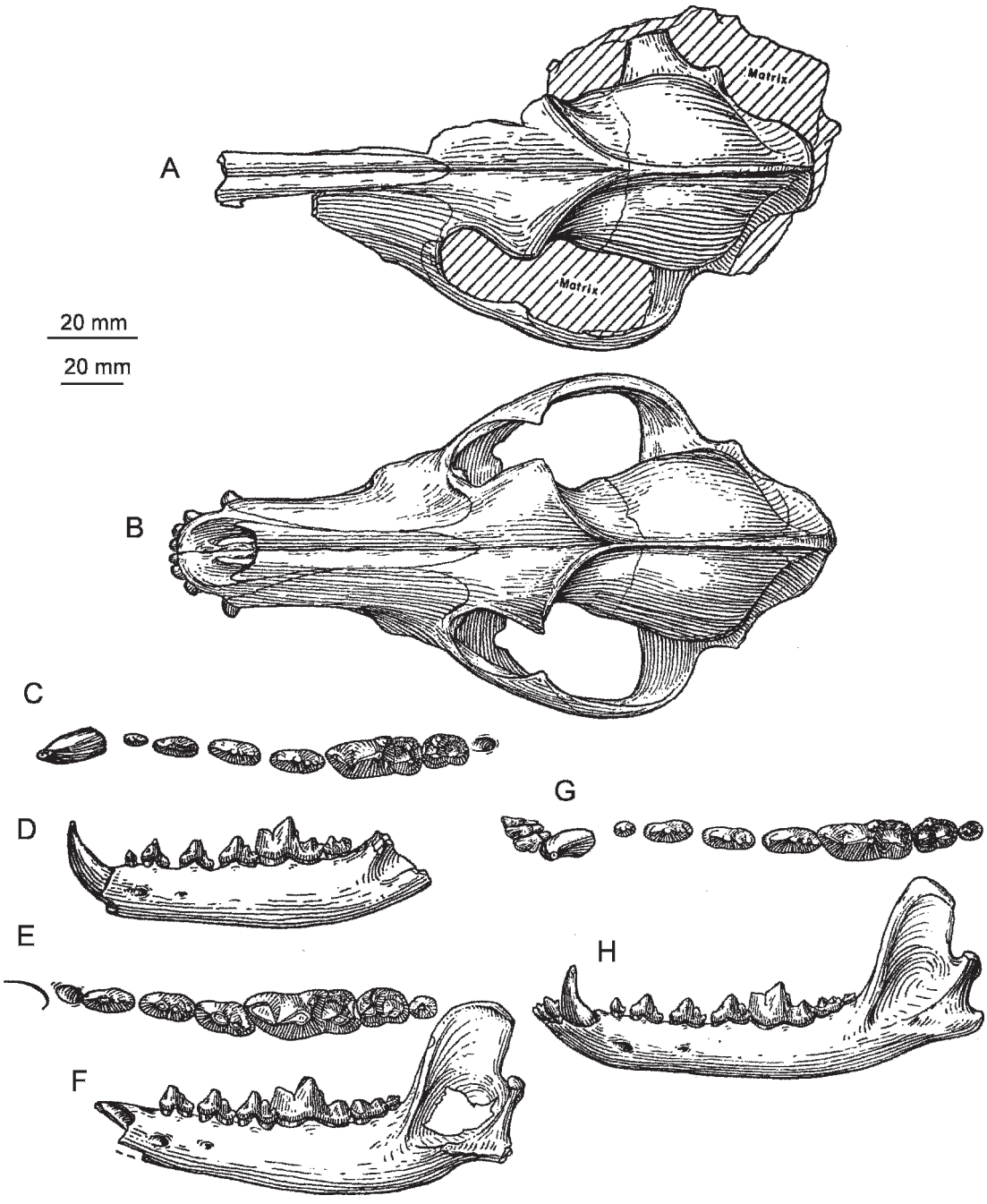

Fig. 49. **A**. *Canis latrans*, skull, NMNH 7660, early Irvingtonian, Maryland, dorsal view. **B**. *Canis latrans*, AMNH(M) 149560, Recent, Nebraska, dorsal view. **C–D**. *Canis* cf. *C. latrans*, ramus, UNSM 26115, Irvingtonian, Nebraska. **C**. Occlusal view, reversed. **D**. Lateral view, reversed. **E–F**. Ramus, F:AM 25514M, Irvingtonian, Nebraska. **G–H**. *Canis latrans*, ramus, AMNH(M) 148273, Recent, Nebraska. **G**. Occlusal view. **H**. Lateral view. The longer (upper) scale is for C, E, and G, and the shorter (lower) scale is for the rest.

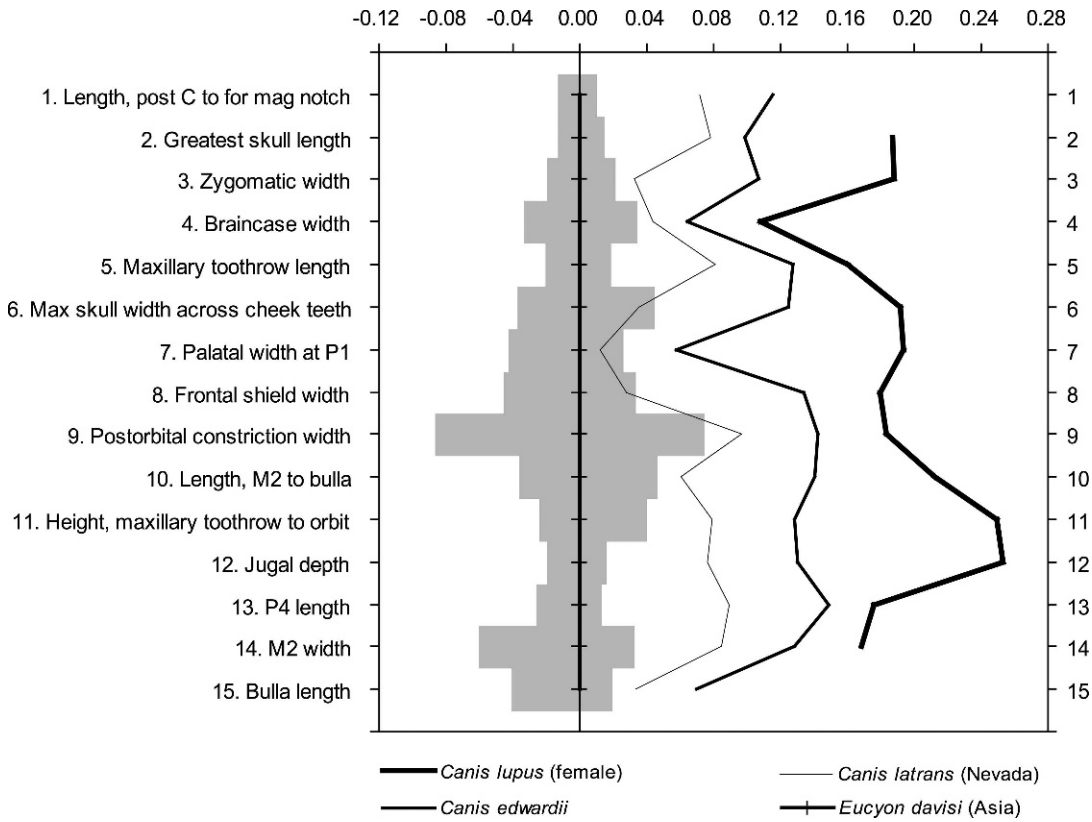

Fig. 50. Log-ratio diagram comparing the proportions of the means of cranial variates (appendix 2) of the skulls of various species of *Canis* with a sample of *Eucyon davisi* (n = 7) from a single locality near Xiakou, Yushe County, Shanxi, China, as the standard of reference. Means of *Canis lupus* (northern and western sample of females, n = 146, Nowak, 1979: appendix B), *C. edwardii* (n = 5), and *C. latrans* (n = 12) shown. Gray bars extending from the mean of the standard are the observed ranges.

m1–m2, m3 alveolus; NMNH 494385, right M1.

Hamilton Cave (late Irvingtonian, 0.74–0.85 Ma), Pendleton County, West Virginia: NMNH 336123, left M1 (between Cheeta Room and Smilodon 2 site); NMNH 494386, left metacarpal III; NMNH 494387, right astragalus; NMNH 494388, left m1 (near Smilodon site); NMNH 494389, right m1 (Smilodon 2 site); NMNH 494390, right m1 (Smilodon 2 site). Porcupine Cave (late Irvingtonian, 0.35–0.48 Ma), Park County, Colorado: Anderson (1996) listed material that resided in the CM, DMNH, and UCMP collections at that time. We examined CM 49121, fragment of left maxillary and M1 broken and M2 from the Badger Room. Recently obtained material in the DMNH collection (a skull, 30676) from the Badger Room confirms the identification of *C. latrans* there (Bever, 2005).

Distribution: Late Irvingtonian of California, Colorado, Nebraska, Arkansas, Texas, West Virginia, and Maryland. Rancholabrean to present of North and Central American (see Nowak, 1979).

Discussion: Nowak (1979: 73–82) gave a much more comprehensive survey of the later Pleistocene coyotes than we attempt here. Our purpose in further describing and figuring some of the specimens listed above is to compare the earliest records of *C. latrans*-like forms with their contemporaries and immediate antecedents. We do not deal with the much larger Rancholabrean and Holocene records reviewed by Nowak (1979). All of our referred specimens fall within the size range of living *C. latrans*. They are

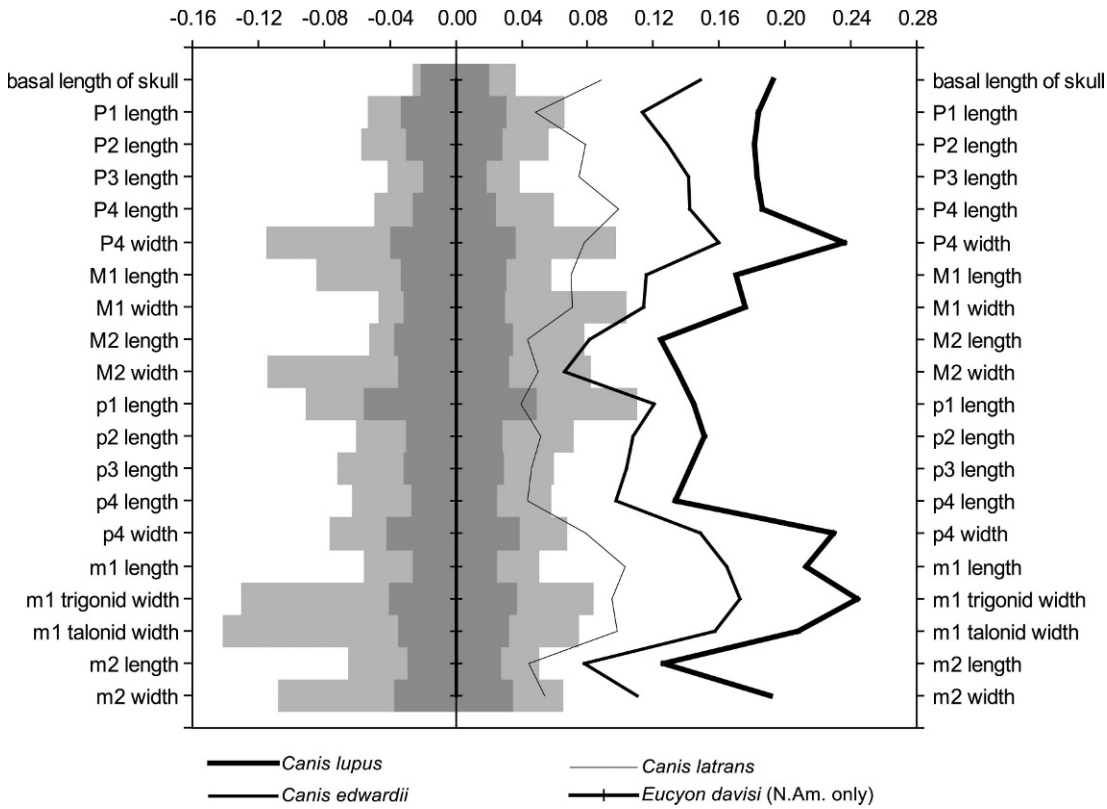

Fig. 51. Log-ratio diagram comparing the means of cheek tooth dimensions (appendix 3) of species of *Canis* against the North American sample of *E. davisi* (see appendix 3) as the reference. *Canis lupus*, western Canada, mean of 10 individuals, *C. edwardii* (n = 34), and *C. latrans* (n = 38) are shown. Gray bars extending from the mean of the standard are the observed ranges (light) and $\pm 1\ \sigma$ (dark).

smaller than the isolated teeth (ANSP 57) selected and figured by Cope (1899: fig. 3, 3d, and 3e) as the cotypes of *C. priscolatrans*.

Savage (1951: 231) based *C. irvingtonensis* on a mandible with a deep horizontal ramus and closely spaced, broad, and massive premolars. A radius was also chosen as a paratype, and from this evidence Savage "visualized that this shorter-jawed, shorter-limbed, stockier animal from Irvington [was] a coyote with habitus tending to be somewhat different from known coyotes." Nowak (1979: 73), however, found that the tooth and mandibular measurements of the type fell within the range of variation of late Pleistocene and Recent specimens of *C. latrans*, and concluded that it warranted no more than subspecific distinction. The radius, however, appears proximally wide for its length, unlike living coyotes (Kurtén, 1974: fig. 6).

A coyotelike skull (NMNH 7660, fig. 49A) from the late Irvingtonian deposits of Cumberland Cave in Maryland, referred to *C. priscolatrans* by Gidley and Gazin (1938: 23) and *C. latrans* by Nowak (1979: 80), has a smaller dentition, as judged by the roots, than either *C. priscolatrans* or *C. edwardii*. Gidley and Gazin pointed out that this skull is close in size to that of *C. latrans* but slightly more robust, particularly in the frontal region. The nasals are short, as in most *C. latrans*, not reaching beyond the maxillary-frontal suture. The zygomatic arch is very robust and measures 15.5 mm at the shallowest point anterior to the postorbital process. A broad scar for the masseter muscle is present, and the jugal-maxillary suture forms an acute angle at the base of the arch. The height of the maxilla between the toothrow and the orbit is 29.3 mm. The frontal

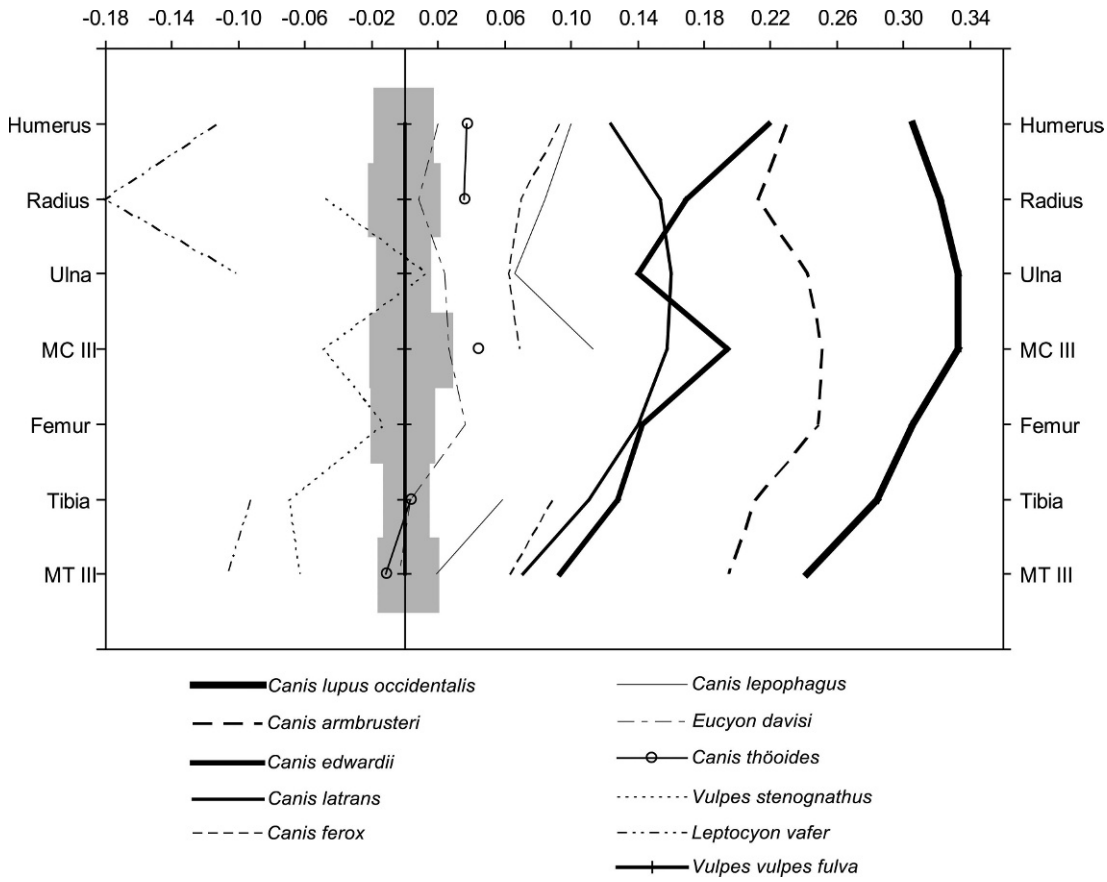

Fig. 52. Log-ratio diagram comparing the mean lengths of limb bones of canines relative to an eastern North American sample of *Vulpes vulpes fulva* (n = 5, gray bars give observed range) as the standard. Most fossil taxa represented by single individuals except *Canis armbrusteri*, where the Cumberland Cave sample consists of a maximum of 22 individuals. *Canis lupus occidentalis* from Alberta, n = 5; *C. latrans* from western United States, n = 6; see appendix 4.

shield is about 50.4 mm wide and moderately inflated. Especially noticeable is the expanded braincase (59.7 mm wide at the parietosquamosal suture) that is markedly wide anterior to the frontoparietal suture as in coyotes. At the point of the greatest postorbital constriction the skull measures 38.7 mm. The short frontal crests join at the frontoparietal suture to form a strong sagittal crest rather than in front of this suture as in most *C. latrans*. The supraoccipital shield is broad and the inion is less narrowed than in *C. latrans*. Some of the above features of the Cumberland Cave skull that differ from *C. latrans*, including the strong sagittal crest and the broad supraoccipital shield, are primitive characters. Otherwise, the Cumberland Cave individual, although estimated to be a young adult by Nowak (1979: 80), has a large skull with an expanded braincase that closely resembles that of *C. latrans*.

Recently obtained material from Cumberland Cave, Maryland, includes a ramus with p3–p4, m1–m2 (NMNH 494384), and an isolated M1 (NMNH 494385) whose dimensions clearly fall into the range of *C. latrans*. The p3 is low with a posterior cusp. The p4 has a second posterior cusp independent of the posterior cingulum. The first posterior cusp lies in line with the principal cusp and the second cusp, rather than labially as in

many *C. latrans*. The m1 entoconid is situated at the posterolingual corner of the talonid, oblique to the hypoconid. These cusps are united by cristids. The talonid basin is closed lingually by the entoconulid crest. The m2 has a well-developed anterolabial cingulum that passes posteriorly across the protocone on to the talonid. The metaconid of m2 is only slightly oblique to the protoconid and smaller than the latter. Depth of the ramus below m1–m2 is 20.0 mm. The isolated M1 is about the right size for the skull (NMNH 7660). Morphologically it closely resembles that of *C. latrans*, including the anteriorly directed preparacrista that lies medial to the parastyle.

Somewhat older (early late Irvingtonian) materials from Hamilton Cave, West Virginia, include four m1s more robust than that in the ramus just described from Cumberland Cave and rather like the type of *C. irvingtonensis* and the sample from late Irvingtonian "Sheridan beds" exposed along the Niobrara River in Sheridan County, northwest Nebraska. These lower carnassials have talonid basins that open lingually in front of the entoconid.

A maxilla fragment (JWT 2303), humerus, and metatarsal IV are listed here as *C. latrans* from the later Irvingtonian part of the Tule Formation at Rock Creek, Texas. The length and width of the broken M1 are estimated to be 11.0 and 13.5 mm, respectively; the M2 measures 6.0 and 9.3 mm. These measurements are slightly smaller than those of an M1 (YP 10080) from Rock Creek, which was figured as *Canis ?priscolatrans* by Troxell (1915: fig. 19). Troxell recorded the length and greatest transverse diameter of this M1 as 12.0 and 17.0 mm, respectively. Judging from Troxell's figure, the greatest transverse diameter was probably taken obliquely from the paracone to the hypocone. The paracone in JWT 2303 is broken, but the transverse diameter would still be less than that of the M1 figured by Troxell. However, the measurements of the teeth and the limbs from Rock Creek, Texas, are within the range of those of *C. latrans* and smaller than those of the other two larger taxa ("*C. dirus*" and "*C.*" *texanus*) that Troxell recognized at this locality.

The referred material includes a late Irvingtonian ramus (UNSM 26115, fig. 49C–D) from near Mullen, Nebraska, which was referred by Kurtén (1974: 7) to *C. priscolatrans*. Kurtén also referred the types of both *C. irvingtonensis* and *C. edwardii* to *C. priscolatrans*. These types are both larger and the premolars are more closely spaced and more robust than those in the Mullen jaw. The Mullen ramus shows a few derived characters typical of coyotes: premolars separated by diastemata; p2 isolated by longer diastemata than other lower premolars; p4 crown lies below level of tip of m1 paraconid; anterior face of m1 paraconid slants backward; m1 hypoconid and entoconid connected by cristids; and m2 metaconid not significantly enlarged over the size of the protoconid. The lengths of the m1 and m2 (20.1 and 8.9 mm, respectively) of the Mullen jaw are similar to the Cumberland Cave specimen and within the lower part of the range of *C. latrans*. Additional measurements of the lower molars of Irvingtonian coyotes include an unerupted m1 (AMNH 12394, length, 20.02 mm; trigonid width, 7.2 mm; talonid width, 6.7 mm) from Conard Fissure, Arkansas, that indicates a small form, but within the range of samples of living coyote populations (Nowak, 1979: appendix C).

Discussion: Although the evidence is fragmentary, there are convincing indications of the presence of a taxon lying within the morphological and metrical limits of living *C. latrans* as early as late Matuyama time (Irvington, California; Porcupine Cave, Colorado; Cumberland Cave, Pennsylvania; and Hamilton Cave, West Virginia). These early examples include robust individuals at the upper limits of the living coyote populations. Together they possess a number of cranial features typical of coyotes: the incisive foramina do not reach beyond the canine alveoli; the short nasals reach only to the most posterior limit of the frontal-maxillary suture; the short palate reaches only the m2 and does not extend posterior to it; the postorbital processes are not markedly inflated; the parasagittal crests are little inflated and join close to the frontoparietal suture; the cranium is inflated anteriorly (enlargement of the prorean gyrus of the neocortex), forming a prominent "shoulder" to the anterior part

of the braincase in dorsal view, and consequently the postorbital constriction is short and broad; the frontal sinus does not reach the frontoparietal suture; the paroccipital process is nearly vertical, not markedly extended posteriorly, and has a short and laterally directed free-tip.

Canis armbrusteri Gidley, 1913
Figures 40, 43, 44, 52, 53A–D, 54A–F, 55A–D; appendices 2–4

Canis priscolatrans (in part): Cope, 1899: 227, fig. 3a, 3b, 3f.
Canis occidentalis?: Brown, 1908: 182.
Canis armbrusteri: Patterson, 1932: 334.
Canis priscolatrans (in part): Kurtén, 1974: 7.
Canis lupus: Martin, 1974: 71–77, figs. 3.11, 3.12.
Canis armbrusteri: Nowak, 1979: 90.

Type: NMNH 7662, left partial ramus with p4–m2, figured by Gidley, 1913: fig. 2, 2a (our fig. 53C–D) from Cumberland Cave (late Irvingtonian), Allegany County, Maryland.

Referred Material: From the type locality, Cumberland Cave (late Irvingtonian), Allegany County, Maryland: NMNH 11886, skull with P3–M2 (fig. 53A–B); NMNH 12888, crushed skull with P2–M2 broken; NMNH 7994, posterior part of skull with P4–M2; NMNH 11887, posterior part of skull with P3 (broken)–M2 and partial ramus with p1 (broken)–m2 (p3 and m1 broken); NMNH 11881, anterior part of skull with C (alveolus)–M2 and left partial ramus with c (broken)–m2 (p2 alveolus). Gidley and Gazin (1938: 16–17) listed and measured: NMNH 11883, partial skull with C–M2 (P2 alveolus); NMNH 11885, partial skull with P1 and P4–M2; NMNH 8168, ramus with c–m2; NMNH 8169, ramus with p3–m3; NMNH 8172, ramus with c–m2 (p1 missing); NMNH 10210A*, left partial ramus with c, p2, p4, m2–m3 (both broken), and alveoli; NMNH 10210C*, left partial ramus with c–m1 (all broken or represented by alveoli); NMNH 4889, left ulna; NMNH 7995, associated right humerus, radius, ulna, and metacarpal III; NMNH 8167, associated right tibia, left and right metatarsal III; and unnumbered four humeri, an ulna, a radius, four metacarpal IIIs, three femora, and a tibia are present in the NMNH collection from Cumberland Cave in 2002 (F. Grady, personal commun., NMNH). FMNH 14790*, right M1–M2 (figured and described by Patterson, 1932).

Leisey Shell Pit 1A, upper part of Bermont Formation (late early Irvingtonian sensu Morgan and Hulbert, 1995), Hillsborough County, Florida: UF 81654, left maxillary fragment with P3 alveolus, P4–M1, M2 alveolus (figured by Berta, 1995: fig. 1A); UF 81655, right maxillary fragment with M1–M2; UF 81656, right P4; UF 67091, right C; UF 87283, left ramal fragment with p3 alveolus, p4; UF 95647, right ramal fragment with p1–p3 alveoli, p4, m1 broken, m2; and UF 81660, left m1 broken.

Haile 21A, Newberry Quarry (late early Irvingtonian), Alachua County, Florida: UF 63623, left M1.

McLeod Lime Rock Mine, Smith Pit, pocket "A" (medial Irvingtonian sensu Morgan and Hulbert, 1995), Levy County, Florida: F:AM 67286, restored partial skull with C–P1 alveoli, P2–M2, and M3 alveolus (fig. 54A–B) and associated mandible with right c–p1 (alveoli), p2–m1, m2–m3 alveoli, left c alveolus, p1–p3 roots, p4, m1 broken, m2, m3 alveolus, both coronoid processes broken away (fig. 54C–D); F:AM 68017, left distal half of humerus; F:AM 68017D, right ulna; F:AM 68017E, proximal half of right ulna; F:AM 68017A, left radius; F:AM 68107B, proximal and distal ends of right radius; F:AM 68108B, left partial femur; F:AM 68108A, right femur; F:AM 68108C, proximal part of right tibia; F:AM 68108D, proximal and distal ends of left tibiae; F:AM 68020Q, right astragalus; F:AM 68020N, left calcaneum; F:AM 68020O, right calcaneum; F:AM 68020C, right metacarpal V; F:AM 68020D, metacarpal V: F:AM 68020, left metacarpal IV; F:AM 68020B, right proximal part of metacarpal IV; F:AM 68020F, right metatarsal II; F:AM 68020I, left metatarsal IV; F:AM 68020K, right partial metatarsal IV; F:AM 68020L, left metatarsal IV; F:AM 68020R–S, two first phalanges (most of the foregoing limbs may represent the same individual as the skull and mandible); F:AM 67291, right ramus with c alveolus, p1, and p2 alveolus–m3 (fig. 54E–F); F:AM 68018, right femur; and F:AM 68020P, right calcaneum.

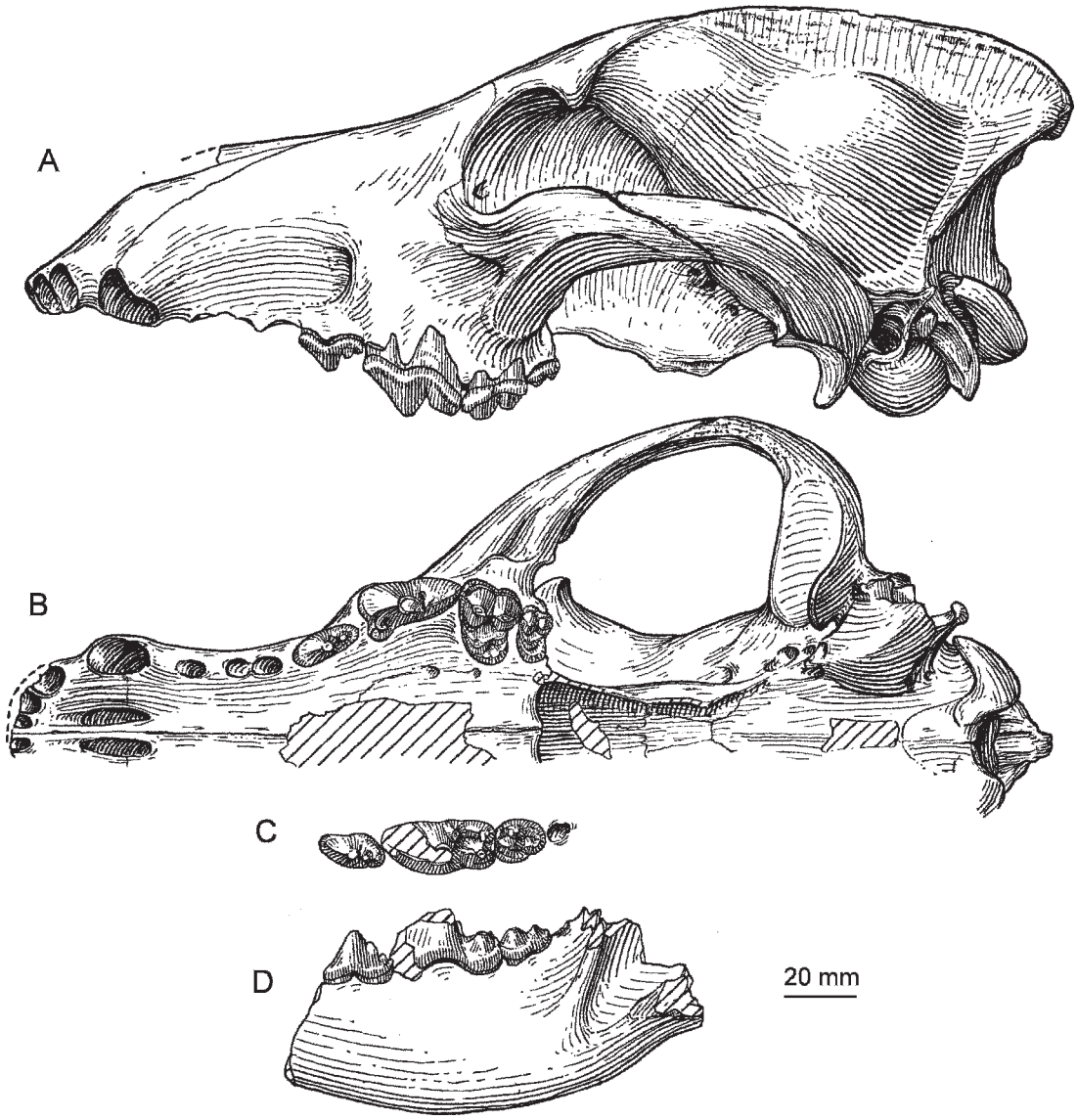

Fig. 53. **A–D**. *Canis armbrusteri*, late Irvingtonian, Maryland. **A–B**. Skull, NMNH 11886. **A**. Lateral view. **B**. Palatal view. **C–D**. Ramus, type, NMNH 7662. **C**. Occlusal view. **D**. Lateral view.

Coleman site 2A (latest Irvingtonian sensu Morgan and Hulbert, 1995), Sumter County, Florida: UF 11519, partial skull with C alveolus–M2 (P1 alveolus), left premaxilla–partial maxilla with I1 broken alveolus–C broken alveolus and two detached upper canines (fig. 55A–B); UF 12120, fragment of right ramus, p2–p4 alveoli, m1, m2 alveolus; UF 11518, fragment of right ramus, m1–m2, m3 alveolus; UF 12114, two right p4; UF 12121, two right m1, right m2; UF 11520, right and left partial rami with c–p2 and p4–m3 (fig. 55C–D); UF 12125, right humerus; UF 12122, right tibia; and UF 12120, right metacarpals IV–V, left metatarsal IV. Described by Martin (1974) as *Canis lupus*.

Anita Fauna (early Irvingtonian), fissure fill in Kaibab Limestone, Coconino County, Arizona: NMNH 10201A*, left partial ramus

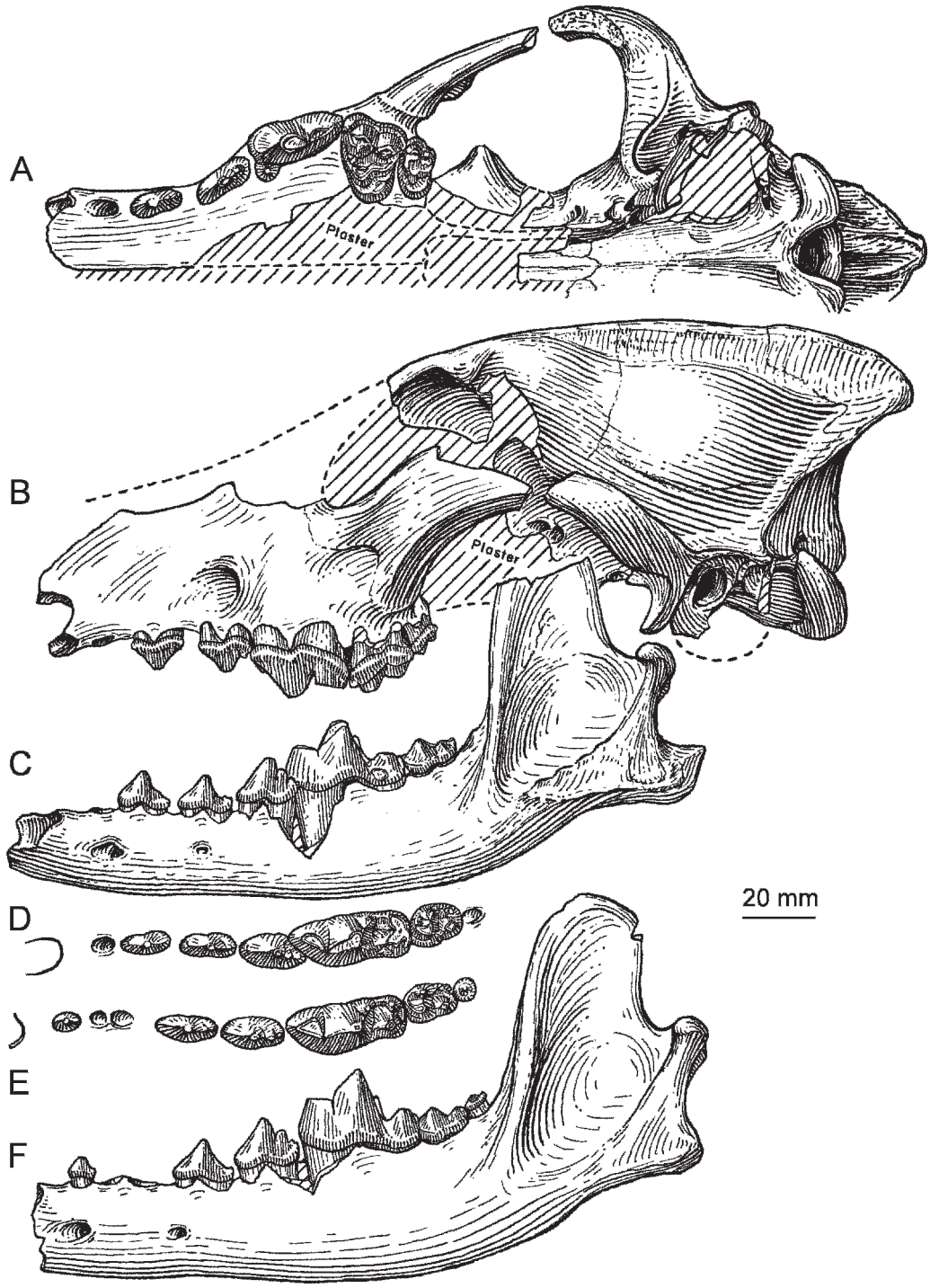

Fig. 54. **A–F**. *Canis armbrusteri*, Irvingtonian, Florida. **A–D**. Skull and ramus, F:AM 67286. **A**. Palatal view, reversed. **B**. Lateral view, reversed. **C–D**. Ramus. **C**. Lateral view. **D**. Occlusal view. **E–F**. F:AM 67291. **E**. Occlusal view, reversed. **F**. Lateral view, reversed.

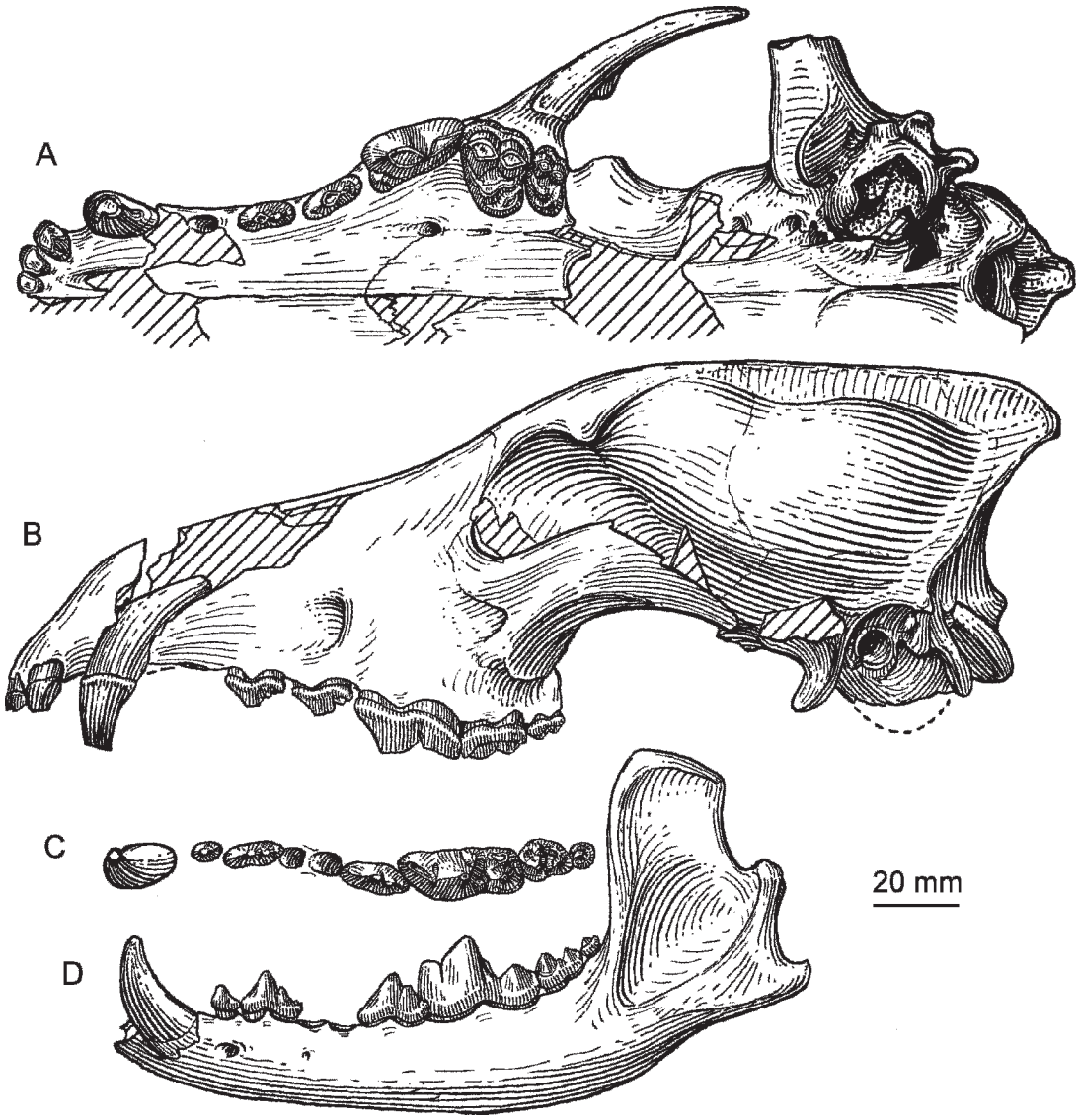

Fig. 55. **A–D**. *Canis armbrusteri*, Irvingtonian, Florida. **A–B**. Skull, UF 11519. **A**. Palatal view. **B**. Lateral view. **C–D**. Ramus, UF 11520 (drawing combines both sides of mandible). **C**. Occlusal view. **D**. Lateral view.

with p4, m1 lost in life; AMNH 14360, left partial ramus with partial alveolus of m1 and m2–m3.

W.C. Stouts Ranch, Crooked Creek Formation (late Irvingtonian), 2 km southeast of Arkalon station on the Rock Island Railroad, Seward County, Kansas: F:AM 95181, crushed partial skull with M1–M2, and associated partial skeleton including both humeri, partial radius, both partial ulnae, partial femur, both partial tibiae, one with incomplete fibula, astragalus, calcaneum, incomplete metatarsals II–IV, phalanges, and vertebrae.

Rock Creek, Tule Formation (late Irvingtonian), 14.5 km southwest of Silverton, Briscoe County, Texas: YPM 10079*, tibia, phalanx, rib, and P3 (Troxell, 1915: 626–

634); TMM fragment of right premaxillary, right upper canine and associated right P3, P4 broken, and M1* described by Cope (1895: 453–454) from the W.F. Cummins collection (now in the Texas Memorial Museum) from the ''Equus horizon of the Tule Canyon on the Staked Plains of Texas,'' and presumably from the Tule Formation at the above locality. JWT 678, right partial ramus with p1–p2, p3 broken–p4 alveolus, m1, and m2–m3 alveoli; and JWT 688, right partial maxilla with P4 root, M1 broken, and M2 partial alveolus.

Conard Fissure (late Irvingtonian), Newton County, Arkansas: AMNH 11761, fragment of left ramus, alveoli for p3–m3; AMNH 11762, fragments of left and right astragali and right m2; AMNH 11762a, fragment of right P4 lacking protocone and anterior border; AMNH 90981, posterior cranial fragment, gnawed by rodents; AMNH 96633, distal end right humerus. Identified as *Canis occidentalis*? by Brown (1908: 182).

Port Kennedy Cave (late Irvingtonian), Montgomery County, Pennsylvania: The following isolated teeth (ANSP) including a broken right P4, a canine, and phalanx were a part of the syntypic series of *Canis priscolatrans* figured by Cope (1899: pl. 1B, fig. 3a, 3b, and 3g, respectively). In the course of his description of *C. priscolatrans*, Cope also mentioned unnumbered limb bone fragments ''very large, exceeding those of the largest wolf known to me.''

Haile 7A (early Rancholabrean sensu Morgan and Hulbert, 1995: table 2), Alachua County, Florida: UF 11845, associated right and left rami with p1–m2, left maxillary fragment with P2–M1, fragments of the cranium and left ascending ramus. Identified as *C. rufus* by Nowak (1979: 88).

Distribution: Early Irvingtonian of Arizona; late early to late Irvingtonian and early Rancholabrean of Florida; late Irvingtonian of Kansas, Texas, Arkansas, Maryland, and Pennsylvania.

Revised Diagnosis: *Canis armbrusteri* shares with *C. lupus* and *C. dirus* the following synapomorphies: incisive foramina extend posterior to limit of canine alveoli, strong posterior expansion of paroccipital process, posterior expansion of frontal sinus to frontoparietal suture, and very reduced M1 parastyle lacking union with preparacrista. It differs from *C. lupus* in that it retains premolars in which P3 and p2–p3 usually have posterior cusps, and the second posterior cusp of p4 is separate from the posterior cingulum. Like *C. dirus*, it also differs from *C. lupus* in having short-crowned and relatively straight canines, the metaconid of m1–m2 reduced, and a reduced P4 protocone. Although a sister taxon to *C. dirus*, *C. armbrusteri* lacks the other hypercarnivorous dental features characteristic of *C. dirus* including a primitively retained labial cingulum on M1.

Description and Comparison: *C. armbrusteri* was originally described by Gidley (1913: 98) based on three incomplete jaws from Cumberland Cave, which he thought differed from those of *C. lupus* in the greater depth of the jaw, a smaller canine, simpler p2 and p3 usually without posterior cusps, the presence of an additional posterior cusp on p4, and a relatively larger m1 talonid. Gidley also wrote that, compared to *C. lupus*, the m1 paraconid is less expanded at the base, and the metaconid is larger and situated higher on the protoconid and is narrower. Additional material obtained later shows that some of the characters listed in Gidley's original diagnosis of *C. armbrusteri* are variable within the Cumberland Cave population of that species. The depth of the horizontal ramus is no greater in some *C. armbrusteri* (F:AM 67286) than in *C. lupus*. Based on all of the specimens that we have examined, the p4 of *C. armbrusteri* always has an additional posterior cusplet on the cingular shelf anterior to the dorsally produced posterior cingulum. In mature individuals diastemata are present between the anterior premolars of *C. armbrusteri*, especially between p2 and p3.

Patterson (1932) described two upper molars from Cumberland Cave and pointed out the relative large size of M2 and the variability in the size of the M1 hypocone. He wrote that the reduction in the size of the M1 hypocone does not reach the stage common to *C. dirus* from Rancho La Brea.

Gidley and Gazin (1938: 15) referred additional materials, including skulls, to *C.*

armbrusteri from the type locality. They figured four skulls (NMNH 7994, 11886, 11883, and 11885) and discussed additional morphological features that strengthened the diagnosis of *C. armbrusteri*. Compared to similar-sized skulls of *C. lupus occidentalis*, Gidley and Gazin found that the skull of *C. armbrusteri* has a slender muzzle, broad heavy frontals, a prominent sagittal crest, and the inion in the largest skull (NMNH 11886) "projects backward to a marked degree, but not nearly so much as in the Rancho La Brea wolves" (i.e., *C. dirus*). Our comparison of the proportional relationships of 14 cranial measurements taken on the Cumberland Cave samples of *C. armbrusteri* by Nowak (1979: appendix B) with the mean values for *C. lupus occidentalis* from Alberta and Northwest Territory of Canada and Alaska in the Department of Mammalogy collection (AMNH) shows (fig. 43) rather close proportional resemblance between these taxa except for the narrow muzzle (width of palate at P1) and palate, short temporal opening (length M2 to bulla), shallow maxillary below the orbit, and wider M2 in *C. armbrusteri*. Although *C. dirus* has a relatively reduced M2 and greater width across the frontals and muzzle, its relatively shallow maxillary and short temporal fossa resemble *C. armbrusteri* rather than *C. lupus*.

Comparison of proportions of the dentition of *C. armbrusteri* and *C. dirus* and the living populations of *C. lupus occidentalis* referred to above (fig. 44) reveals that, except for the small P1–P2, the dentition agrees in proportional relationships with *C. l. occidentalis* and lacks the degree of hypertrophy of P4 and p4 shown in *C. dirus* compared to other teeth.

Cope (1895) described a fragmentary upper dentition from the Tule Formation of Rock Creek, Texas, under the name *C. indianensis* Leidy, 1869 (a synonym of *C. dirus*), and later Merriam (1912) compared this material favorably with *C. dirus* from Rancho La Brea except for the alveolar evidence of a large protocone root on P4. Additional materials of later Irvingtonian age at Rock Creek have been described by Troxell (1915), including a P3 and limbs that he also referred to *C. dirus*. The collections of the Panhandle Plains Museum from Rock Creek include fragments of a maxillary and ramus that corroborates the occurrence in the Tule Formation of a large canid whose morphology and dental dimensions fall within those for *C. armbrusteri* and below the range reported for *C. dirus* by Merriam (1912). Morphologically the M1 of JWT 688 (length × width, approximately 16.5 × 20.5 mm) resembles Cope's specimen in having a small hypocone and very reduced anterolingual cingulum that is discontinuous across the protocone. In these ways it resembles *C. dirus*, as discussed below. The M2, judging from its alveoli, is relatively large however. Likewise, the lower carnassial of JWT 678 (length, 31.5 mm; width trigonid, 12.0 mm; width talonid, 11.0 mm) lies below the range of *C. dirus*, but is similar in size to those of late Irvingtonian *C. dirus* from Nebraska. The premolars (length and width p2, 13.7, 5.5 mm; p3, 14.7, 5.8 mm) are shorter and narrower than in *C. dirus*, and they lack posterior cusplets and are not separated by diastemata. They lie within the range of *C. armbrusteri*. Thus, this material, although approaching *C. dirus* in aspects of the morphology of M1, retains more primitive proportions and morphology in the rest of the available dentition. It is possible that this material samples an early population of *C. dirus* like that more clearly seen in the Nebraskan late Irvingtonian. Better preserved specimens are needed from Rock Creek, and so we follow the conservative course of referring this material to *C. armbrusteri*.

Based on his study of the material from the late Irvingtonian Coleman 2A site in Florida, Martin (1974: 77) concluded that *C. armbrusteri* is synonymous with *C. lupus*, and thus *C. dirus* and *C. lupus* were the only wolves in the middle and late Pleistocene deposits of North America. However, the morphology of this sample agrees better with *C. armbrusteri*, as Nowak (1979: 92) concluded. The Coleman 2A sample is chronologically not far removed from the Cumberland Cave type series. It serves to reinforce certain morphological features characteristic of late examples of this species. In the skull (fig. 55A–B) the muzzle is narrow, the postorbital processes are moderately inflated but with a nearly flat frontal shield, the

nasals reach just beyond the posterior limit of the maxillary-frontal suture, the inflated parasagittal crests join at or just ahead of the frontoparietal suture, and the inion overhangs the condyles but does not achieve the hooklike form seen in *C. dirus*. The paroccipital process is slender, posteriorly expanded but not strongly produced ventrally; the jugal-maxillary suture at the anterior base of the zygoma is acute; the bullae are moderately inflated and reach forward just to the postglenoid processes; and the palate ends just behind M2. The rami are notably slender anteriorly, even in older adults (UF 11520 young adult, fig. 55C–D, depth at p1/2 of 19.6 mm, depth at m1/2 of 25.5 mm; UF 11518 old adult, depth at m1/2 of 28.0 mm). The premolar row is nearly straight and the premolars show little imbrication. In UF 11520 the P2 and p2 possess posterior cusps, a rare variant in *C. armbrusteri*. The lower dentition shows little evidence of hypercarnivory beyond the small size of m1–m2 metaconids and entoconids, and the m3 is unicuspid but retains a large lingual cingular shelf. The P4 is wider, the M1 labial cingulum less prominent, and the lingual cingulum across the M1 protocone is absent in comparison with the early Irvingtonian Leisey Shell Pit sample, which otherwise resembles the Coleman 2A individuals in size.

The Haile 7A skull and jaw fragments (UF 11845) of early Rancholabrean age are the latest well-preserved material of *C. armbrusteri* available from North America. The young adult skull fragments show the parasagittal crests meet at the frontoparietal suture so that there is no frontal contribution at this stage in ontogeny. The mastoid process is tiny, smaller than in the Coleman 2A sample. The upper dentition shows modifications transitional to *C. dirus* in M1: loss of anterolingual cingulum and much of the labial cingulum, tiny parastyle, but the hypocone is still large and essentially continuous with the posterior cingulum. The upper premolars are small and separated by diastemata; the P2–P3 have posterior cusps. The mandible is shallow anteriorly as in other *C. armbrusteri* (depth at p1/2 of 23.6 mm, depth at m1/2 of 33.8 mm). Lower premolars 2–3 are low-crowned and lack posterior cusps as in the McLeod sample, and p4 has a second posterior cusp anterior to the cingulum. The metaconid is reduced on m1–m2, but the m1 talonid is bicuspid. This individual is clearly an example of *C. armbrusteri*.

The best sample of limb bones of *C. armbrusteri* was obtained from Cumberland Cave, the type locality. Measurements of the lengths of these elements were kindly forwarded by Fred Grady of NMNH in 2002. None of these was described by Gidley and Gazin (1938) beyond the remark that the limb bones "are equally as long but slenderer than corresponding elements of various individuals of the Brea wolf in the National Museum collections."

Discussion: Nowak (1979: 90) concluded that *C. armbrusteri* was distinct from *C. lupus*. He thought that *C. armbrusteri* evolved from the basal stock of primitive wolves represented by *C. edwardii* and that the presence of these large wolves in Irvingtonian sites suggested that divergence of *C. armbrusteri* occurred early in the Pleistocene. *Canis edwardii* does show a number of synapomorphies with the larger wolves and coyote, including reduction of the m2 metaconid; p3 principal cusp positioned lower than those of adjacent premolars, crown base of p3 lies below p4; p3 with posterior cusp (reversal); and paracone of M1–M2 markedly enlarged over metacone. However, the skull proportions of *C. edwardii*, as shown on the log-ratio diagram (fig. 43), diverge widely from those of *C. armbrusteri*, which, in turn, closely parallel those of *C. dirus* and *C. lupus*. Only the proportionally narrower muzzle and simple P2–P3 and p2–p3 of *C. armbrusteri* deviate from both *C. dirus* and *C. lupus* and agree with *C. edwardii*. Additionally, the skull of *C. armbrusteri* is narrower across the frontals and the cheek teeth than seen in *C. dirus*. In general, however, the measurements of *C. armbrusteri*, *C. dirus*, and *C. lupus* form a general grouping on the log-ratio diagrams (figs. 43 and 44) and diverge from those of *C. edwardii*, *C. latrans*, and *C. lepophagus*.

Canis armbrusteri represents the first lineage of wolf-sized Canina to appear in the North American record, with its earliest occurrence near the beginning of the Pleistocene (earliest Irvingtonian, Anita fissure fills, Arizona, correlated tentatively with the Old-

uvai Subchron, Lundelius et al., 1987). This slightly predates the first occurrence of large wolves in Europe, that is, *C. falconeri* Forsythe-Major, 1877 (Tasso Fauna of Italy, Azzaroli et al., 1988; Masini and Torre, 1989; see appendix 1), in just post-Olduvai, early Pleistocene (late Villafranchian) time. However, in eastern Asia, large *Canis* is known from the later Pliocene in China (*C. chihliensis*, appendix 1). The latter taxon appears to represent a sister lineage to the Holarctic and North American forms represented by *Canis lupus*, *C. armbrusteri*, and its derivative *C. dirus* (fig. 65). The abrupt appearance in the early Pleistocene of North America of large *C. armbrusteri* suggests that this is an immigrant taxon from an Asian source, much as *C. lupus* was later in the Pleistocene.

Canis dirus Leidy, 1858
Figures 40, 43, 44, 56A–F; appendices 2, 3

Canis primaevus Leidy, 1854: 200 (preoccupied by *C. primaevus*, Hodgson, 1833).
Canis dirus Leidy, 1858: 21.
Canis indianensis Leidy, 1869: 368.
Canis mississippiensis Allen, 1876: 49.
Canis ayers Sellards, 1916: 152.
Aenocyon dirus Merriam, 1918: 533.
Aenocyon dirus nebrascensis Frick, 1930: 7 (nomen nudum).
Canis armbrusteri Nowak, 1979: 93 (in part).

Late Irvingtonian Material: Hay Springs Area, ''Sheridan beds'' (late Irvingtonian), Sheridan County, Nebraska: F:AM 25511, anterior part of skull with I1–I3 alveoli and C–M2 (P1 alveolus) (fig. 56B, E); F:AM 25511M, right isolated P4 (fig. 56A); F:AM 25511L, left isolated and broken M1; F:AM 25509, right partial ramus with p3–m2 (m2 broken) (fig. 56F); F:AM 25510, left partial ramus with m1 (broken)–m3 (alveolus); F:AM 95306 and 95308, two metacarpals II; F:AM 95309, partial metacarpal II; F:AM 95310, astragalus; F:AM 95311, calcaneum; and F:AM 95312, first phalanx. Hay Springs Quarry 2, UNSM locality Sh-2, UNSM 2912, right ramus with partial c alveolus, p1–p4, m1–m2, m3 alveolus; Rushville Quarry 3, UNSM locality Sh-3, UNSM 15486-38, left M1; Rushville Quarry 4, UNSM locality Sh-4, unnumbered right M1; UNSM 4026-71, right and left M1; UNSM 4062-71*, left p3; Gordon Quarry 5, UNSM locality Sh-5, UNSM 25691, left maxillary fragment with P4 and M1 (identified as ''*C. armbrusteri*'' by Nowak, 1979: 93); UNSM 21431, right ramus with c, p1–p2 alveoli, p3–p4, m1 alveolus; UNSM 21432, right p4; UNSM 8137-41*, unerupted left p4; UNSM 21436*, premaxillary fragment with I2–I3; UNSM 21439*, right p4; and UNSM 10337-39, right femur.

Albert Ahrens site, UNSM locality No-104, site in ponded sediments between two bodies of red (''Loveland'') loess incised into Lava Creek B tephra (0.61 Ma), late Irvingtonian, Nickolls County, Nebraska: UNSM 3269-94, left maxillary fragment with P4, M1–M2, and base of zygoma; UNSM 2223-90, talonid of right m1; and UNSM 2233-90, little worn left m2.

Mullen, Pit 1, UNSM locality Cr-10, middle Loup River, latest Irvingtonian, Cherry County, Nebraska: UNSM 26117, left ramus with p2–p4, m1–m2, m3 alveolus, and ascending ramus; UNSM locality Cr-10, Pit 3, UNSM 39337, right maxillary fragment with well-worn M1–M2 (''*C. dirus*'' in Martin, 1972: 174; ''*C. lupus*'' in Nowak, 1979: 101); UNSM 6.31.8.31 NP, left femur.

Irvington site 2, UCMP locality V3604 (late Irvingtonian), 1.3 km southeast of Irvington, Alameda County, California: UCMP 38749, left ramal fragment with m1 broken–m3 alveolus; UCMP 41779*, trigonid of right m1; UCMP 58032*, a mandible in a concretion, right and left m2–m3, roots of other cheek teeth; UCMP 38784, anterior part of a skeleton lacking skull and mandible, but with fragments of most limbs and some vertebrae; UCMP 38806, distal end of right humerus; UCMP 67930, proximal end of baculum; and UCMP 58033, inion of skull.

Fairmead Landfill locality, UCMP locality V93128, upper part of Turlock Lake Formation (late Irvingtonian), Madera County, California: UCMP 140265, partial right ramus of mid-aged adult (probable female) with p1–m2 (Dundas et al., 1996: pl. 1, fig. A); UCMP 156047, mandible of old adult (probable male) lacking right i1, left i1–2, left and right m3, and left ascending ramus with m1–m2; UCMP 156048, fragments of a skull including right maxillary with C alveolus, p1–p4, paracone of M1, left maxillary with M1

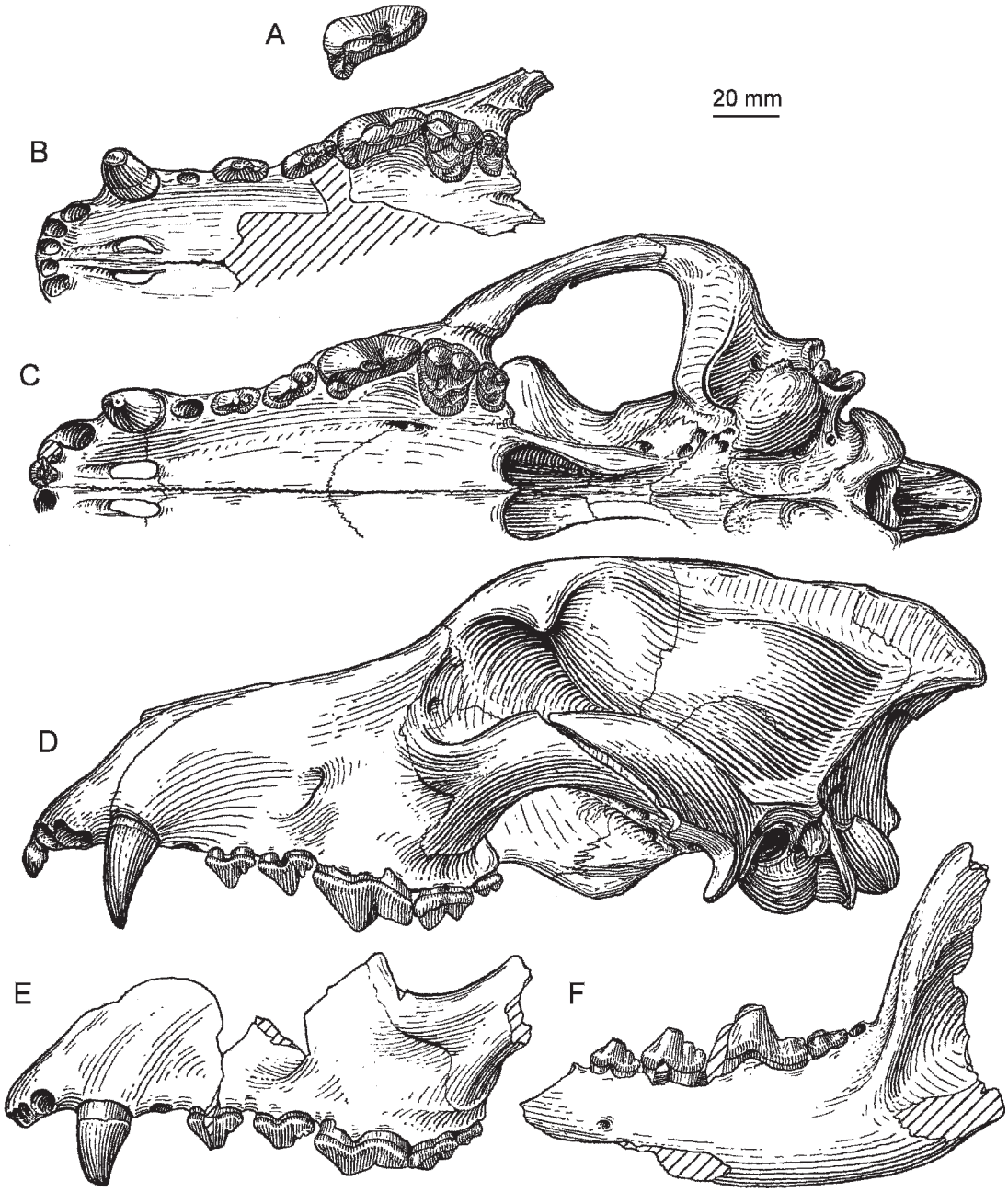

Fig. 56. **A–B**. *Canis dirus*, Irvingtonian, Sheridan County, Nebraska. **A**. Upper carnasial, F:AM 25511M, occlusal view, reversed. **B**. Skull, F:AM 25511, palatal view. **C–D**. *Canis dirus*, skull, AMNH 15867, Rancho La Brea, Rancholabrean, California. **C**. Palatal view. **D**. Lateral view. **E–F**. *Canis dirus*, Irvingtonian, Sheridan County, Nebraska. **E**. Skull, F:AM 25511, lateral view. **F**. Ramus, F:AM 25509 (restored from F:AM 25510) lateral view, reversed.

paracone broken, complete M2, and fragment of P4 and part of right ear region.

Distribution: Late Irvingtonian of California and Nebraska; Rancholabrean of Canada, United States, Mexico, Venezuela, Ecuador, Bolivia, and Peru.

Revised Diagnosis: *Canis dirus* is distinguished by a number of autapomorphies related to hypercarnivory: loss of m2 anterolabial cingulum; wide palate; greatly reduced m1–m2 metaconids and entoconids; greatly reduced M1–M2 hypocones; very weak or discontinuous anterolingual cingulum across M1 protocone. It shares with *C. armbrusteri* two synapomorphies: short and little recurved canine, and a reduced P4 protocone. With *C. lupus* it shares four additional synapomorphies: paroccipital process strongly expanded posteriorly; frontal sinus reaching the frontoparietal suture; long incisive foramina that extend to or behind canine alveoli; M1 parastyle very weak, preparacrista directed anteriorly, not to parastyle.

Description and Comparison: We agree with Frick (1930) that the late Irvingtonian wolf from the Hay Springs area in Sheridan County, Nebraska, may represent the earliest record of the largely Rancholabrean *C. dirus*. Unfortunately, the cranial evidence is limited to the preorbital part of a skull (F:AM 25511, fig. 56B, E) with a toothrow length falling within that of *C. armbrusteri*. However, two of the skull measurements (the palatal width at P1 of 41.5 mm, and the height of the maxillary between the M1 alveolar border and the ventral border of the orbit of 42.3 mm) are larger than in *C. armbrusteri* and equivalent in size to those of *C. dirus* (see appendix 2).

The dentition of the Hay Springs individual is smaller than that of *C. dirus* and within the size range of *C. armbrusteri* (fig. 40), but it shares a number of derived characters with *C. dirus*. In F:AM 25511, the incisors are missing and the canine is robust and short-crowned. The first upper premolar is missing. The second (length × width, 14.8 × 6.9 mm) and third (length × width, 17.2 × 7.5 mm) upper premolars both have posterior cusps as in *C. dirus* and are likewise more robust than in *C. armbrusteri*. The P4 (F:AM 25511M, length × width, 30.5 × 12.5; F:AM 25511, 27.5 × 11.4 mm) is slightly smaller than Rancholabrean *C. dirus* but within the size range of *C. armbrusteri*. Unlike the latter, the anterolabial surface of the paracone is more rounded and the protocone is reduced as in *C. dirus* and *C. lupus*. Like P4, the morphological features of M1 are also very similar to those of *C. dirus*. The M1 (length × width, 17.8 × 20.2 mm) is small relative to the size of the P4, more as in *C. dirus* than in *C. armbrusteri*. The labial cingulum is also much weaker than in *C. armbrusteri* and, like *C. dirus*, it is nearly absent across the paracone. After an allowance is made for wear, the heights of the paracone and metacone seem to be about as in *C. armbrusteri*, and the paracone is not quite as enlarged as in *C. dirus*. As in *C. dirus*, the hypocone is smaller, the conules poorly developed, and the anterolingual cingulum is weaker and not continuous with the hypocone across the protocone. Additional examples of some of these teeth in the UNSM collection from Hay Springs agree in the stated features. Some variability in these characters is expected, but Martin (1974: 72) stated that "in *C. dirus* the anterolingual cingulum [of M1] does not reach the hypocone, but ends at the protocone. In samples of living wolves that approximate the average size of *C. dirus* (*C. lupus pambasileus* and *C. lupus occidentalis*), the cingulum fails to reach the hypocone on only 4 out of 75 individuals." Gidley and Gazin (1938: 17) also observed some variability in the size of the M1 hypocone in *C. armbrusteri* and stated, "this character is variable and in some dentitions where the heel of M1 is narrower the hypocone is not so prominent. However, the reduction of the hypocone in these cases does not reach the stage common in *C. dirus* of Rancho La Brea." The M2 is significantly more reduced relative to M1 than in *C. armbrusteri* (fig. 44) and in accord with the degree of reduction seen in Rancholabrean *C. dirus*. Reduction of the labial cingulum and hypocone account for most of the change in proportions of this tooth. The metaconule seems to be lacking but not the postprotocrista.

Characters of the lower dentition are seen in two incomplete and probably associated rami (F:AM 25509 and 25510), with p3–m2 represented, and in other material from the

Hay Springs area in the UNSM collection, and they show that the lower teeth lie within lower range of values given for *C. dirus* by Kurtén (1984). The p3 and p4 (F:AM 25509: length p3, about 15.0 mm; p4 length × width, 19.0 × 10.0 mm) are no longer than in *C. armbrusteri* but tend to be wider in relationship to their length. The p3, however, has a posterior cusp, which is characteristic of *C. dirus* and not usually present in *C. armbrusteri*, although Gidley and Gazin (1938: fig. 20) figured a ramus of *C. armbrusteri* from the type locality with a well-developed posterior cusp on p3. The p4 of F:AM 25509 has a second posterior cusp that lies on the cingulum as described for some individuals of *C. dirus* by Merriam (1912: 230). It also has a wide posterolingual shelf as in *C. dirus*. The M1 (F:AM 25509; length, about 32.0 mm; width trigonid, 12.1 mm; width talonid, 12.9 mm) has the paraconid broken away, the metaconid is very small, the entoconid is barely differentiated from the posterolingual ridge of the talonid, and the hypoconid, although the dominant talonid cusp, is still laterally located with a short hypoconulid shelf lying medial to it. The worn m2 (F:AM 25509, length × width, 12.0 × 9.3 mm; F:AM 25510, 12.0 × 9.8 mm) tends to be smaller relative to M1 than that of *C. armbrusteri*, but larger than in *C. dirus*. The anterolabial cingulum is lacking, the metaconid is greatly reduced, and the talonid narrows posteriorly, implying the loss of the entoconid although the tooth is too worn for confirmation.

University of Nebraska State Museum 2912 is the smallest individual in the Hay Springs sample. It has a shallow ramus (depth beneath m1–m2, 29.5 mm; compared to F:AM 25510, 36.4 mm) and uncrowded premolars. The p1–p3 lack posterior cusps, as in *C. armbrusteri*. The second posterior cusp of p4 is not clearly differentiated from the cingulum, and it has a posterolingual shelf. However, the m1 shows typical *C. dirus*-like morphology in which the metaconid and entoconid are reduced, the hypoconid is connected to the entoconid by a cristid, and a hypoconulid shelf occurs behind the transverse cristid. The m2 likewise has the metaconid reduced relative to the protoconid, but a small entoconid remains on the narrow talonid; there is a well-formed anterolabial cingulum. The premolars and m1 of this specimen lie just outside the range for length of the samples of *C. dirus* measured by Kurtén (1984: table 4) and Nowak (1979: appendix C) but inside for the width. The m2 dimensions are within the lower range for *C. dirus*, and although the depth of the ramus falls within the range of *C. lupus*, the teeth are absolutely larger. This specimen forms a morphological link between *C. armbrusteri* (premolar morphology) and *C. dirus* (dental proportions and molar morphology).

The Hay Springs material was the basis for Frick's undescribed taxon *Aenocyon dirus nebrascensis*, a name that appeared in a faunal list of extinct forms from Nebraska. Nowak (1979: 93) referred the same material to *C. armbrusteri*, but we find that it has more characters in common with *C. dirus* and differs from *C. lupus* in its wider muzzle, greater distance between the M1 alveolar border and the ventral border of the orbit, smaller P4 protocone, reduced M1 hypocone and lingual cingulum, weaker M1 labial cingulum, and great reduction of metaconid of m1–m2. Because of these derived characters shared with *C. dirus*, and the general agreement in dental size, we refer these specimens to that taxon.

In her review of the large Quaternary canids of South America, Berta (1988) redescribed *Canis gezi* L. Kraglievich, 1928, from Argentine deposits of Ensenadan age (early to medial Pleistocene, correlated with the Matuyama and early Brunhes chrons, Tonni et al., 1992, 1999) that correspond with the late Blancan and Irvingtonian of North America. Berta (1988: 55) compared *C. gezi* with late Irvingtonian *C. dirus* (referred to as "*C.* cf. *dirus*") and found these taxa "most similar" among North American large canids. In a cladogram, Berta (1988: fig. 28) placed *C. gezi* and the Irvingtonian *C. dirus* as sister taxa, but relegated Rancholabrean *C. dirus* to a closer relationship with *C. nehringi* F. Ameghino, 1902, from deposits of Lujanian age (late Pleistocene, Brunhes Chron, Tonni et al., 1992, 1999).

The reevaluation of the late Irvingtonian material in this work provides a link between *C. armbrusteri* and Rancholabrean *C. dirus*, suggesting that the South American forms

may form a collateral lineage with *C. dirus* during the medial and late Pleistocene. However, the Argentine and North American lineages are united by many dental similarities related to developing hypercarnivory as well as cranial similarities (some related to size increase) including such peculiarities as the union of the optic and anterior lacerate foramina in a common pit. This latter feature is apparently also shared with *C. armbrusteri*, further suggesting a common source for the two clades.

Despite suggestions of the "origin" of *C. dirus* in South America (Kurtén and Anderson, 1980; Dundas, 1999), a case can be made for a collateral South American lineage (*C. gezi* and *C. nehringi*) that would be united by such synapomorphies as elongate jaws and exceptionally small, low-crowned, and simple premolars with prominent premolar diastemata. As in *C. armbrusteri*, p2 and p3 are nearly the same length (in *C. gezi* the p4 is only a little longer) with the p3 strongly set below p2 and p4 and its posterior cingulum completely below the base of the crown of p4. The m2 primitively retains an anterolabial cingulum in both species. This lineage does not show a striking increase in size with time, but it does acquire somewhat more complex premolars, and the cranium of *C. nehringi* shows a more *C. dirus*-like conformation (both holotypes appear to be male individuals based on relative canine dimensions). This lineage was the only large *Canis* in South America until the appearance of *C. dirus* in the later Pleistocene. The dire wolf seems to have been restricted to the north and west coasts of South America. Its remains have not been found in the very fossiliferous Pampean Pleistocene deposits of Argentina that produced *C. gezi* and *C. nehringi*, nor have remains of these species been found elsewhere in South America.

Canis lupus Linnaeus, 1758
Appendix 3

Canis lupus Linnaeus, 1758.
Canis lupus lunellensis Bonifay, 1971.

Medial Pleistocene North American Material: From Cripple Creek Sump (Olyorian, late Irvingtonian), near Fairbanks, Alaska: F:AM 67186, left ramus with i1–i3 alveoli, i2 root, c–m2, and m3 alveolus; F:AM 67183, right ramus with i1–p3 alveoli and p4 broken, m1–m2, and m3 alveolus; F:AM 67181, left ramus with i1–i3 alveoli, c, p1 alveolus, p2–m2, m3 alveolus; F:AM 67173, left maxillary fragment with part C alveolus, p1–p3 alveoli, P4–M2; F:AM 97107, fragment of right ramus with i1–i3, c, p1–p3 alveoli, p4, m1 alveolus; F:AM 97109, left ramus with i1–i3, c, p1–p4, m1 alveolus; F:AM 97091 and 97091A, two left partial humeri; F:AM 97093, 97093A, and 97093B, left proximal and two distal ends of right radii; F:AM 97095, 97092, 97092A, and 97092B, three right partial ulnae; F:AM 68008C, right partial ulna; F:AM 97095 and 97095A, left partial ulna and partial femur; F:AM 90974A and 90974B, right partial femur, right and left partial tibiae; F:AM 68010A, right incomplete tibia; F:AM 68010D, right tibia; F:AM 68012O, right metacarpal V; F:AM 68012J, left metacarpal V; and F:AM 68013F, left calcaneum.

From Old Crow River, northern Yukon, northwestern Canada, CRH locality 47, unit 2, beneath Surprise Creek Tephra in rocks of normal polarity attributed to the Jaramillo Subchron, Matuyama Chron, medial Pleistocene (1.11 Ma, see Repenning, 1992, for discussion): CMN 39490, right M1.

Distribution: Earliest North American record is medial Pleistocene (Olyorian, equivalent in part to late Irvingtonian) in the Arctic at Old Crow locality CRH 47 in Yukon, Canada. More material is available in slightly younger beds at the Cripple Creek Sump locality near Fairbanks, Alaska. Midcontinent records begin in the late Rancholabrean.

Description and Comparison: The unworn right M1 from the Yukon (CMN 39490) is the oldest (Jaramillo) material attributed to *C. lupus* from North America. This early *C. lupus* is presently represented only by a single upper cheek tooth (M1, length, 17.4 mm, width, 20.2 mm). The available specimen shows a number of dental features that are synapomorphic with *C. lupus*. Notable among these are the hypertrophy of the paracone with respect to the metacone [table 1, character 54(1)], enlargement of hypocone [1(1)], preparacrista di-

rected anteriorly, lingual to the parastyle [3(2)], and reduction of the metaconule [59(1)].

The gold-bearing alluvial deposits of the region west of Fairbanks, Alaska, have produced large quantities of Quaternary mammalian fossils. The largest samples reside in the Frick Collection at AMNH and at the University of Alaska. The exigencies of collection of this material during hydraulic mining of the deposits provided few opportunities for stratigraphic allocation of the remains. Moreover, most of this work was carried out in the 1930s and early 1940s before a consistent stratigraphy had been developed for the Quaternary deposits. Troy Péwé's monumental studies (1975a, 1975b, 1989) were the first synthesis of the stratigraphy of the Quaternary deposits in the Fairbanks area. This was later refined with the application of tephrochronology and magnetostratigraphy (Westgate et al., 1990) so that it is now possible to see that the gold-bearing deposits extend, with hiatuses, from the medial Pliocene through the Pleistocene.

Unfortunately, very few of the large collections of mammals can be clearly related to this stratigraphic scheme and their ages are consequently uncertain. However, there is one locality, on Cripple Creek, at the dredging site call the Sump, that yielded a suite of mammalian remains from a more circumscribed lower part of the local column. At the Cripple Creek Sump, faulting has preserved a section of the Fox Gravels and the lower part of the overlying Gold Hill Formation. Closely associated occurrences of the Ester Ash Bed in the lower Gold Hill Formation yielded an isothermal plateau fission track age of 0.81 ± 0.07 Ma (Westgate et al., 1990). At nearby Gold Hill this part of the sequence lies in a reversed magnetozone correlated with the latest phase of the Matuyama Chron.

This chronology corresponds with the late Irvingtonian of mid-latitude North America, although the Alaskan fauna of this time contains many taxa that do not appear south of the continental glacial barrier until the Rancholabrean (e.g., *Bison*, *Ovibos*, *Ovis*, and *Panthera leo*). The fauna at the Cripple Creek Sump (verified with F:AM records and examination of specimens) includes: *Lepus* sp., *Ochotona* sp., *Castor* sp., *Xenocyon lycaonoides*, *Canis* cf. *lupus*, *Panthera leo*, *Ursus arctos*, *Taxidea taxus*, *Mammut* sp., *Mammuthus* sp., *Cervus* cf. *elaphus*, *Rangifer* sp., *Alces* cf. *latifrons*, *Bison* cf. *priscus*, *Bootherium bombifrons* (McDonald and Ray, 1989), *Praeovibos recticornis* and *P. priscus* (McDonald et al., 1991), *Ovibos* sp., *Ovis* sp., *Saiga tartarica* (Harington, 1981), *Camelops* sp., and *Equus* sp. In its composition it more closely corresponds with the Olyor faunas of adjacent northeastern Siberia (Sher, 1986), especially in the co-occurrence of *Xenocyon*, *Canis* cf. *lupus*, lion, *Saiga*, *Bison*, *Praeovibos*, and *Alces* cf. *latrifrons*. North American elements in this New World Olyorian fauna include the badger *Taxidea*, the lamine camel *Camelops*, and the endemic ovibovine *Bootherium*.

As far as dental measurements are concerned, the Cripple Creek Sump wolves are clearly nested within a suite (n = 12) of *C. lupus lycaon* from Minnesota in the AMNH(M) collection. They lie below most values of *C. l. occidentalis* (n = 11) from Alberta and Montana, but fall close to the two females of *C. lupus* from northeastern Siberia in the AMNH(M) collection. The Sump specimens have dentitions that lie above the range of samples of the medial Pleistocene wolf *C. mosbachensis* from Europe (see appendix 1): length of m1: Untermassfeld, Germany (n = 16, 23.3–25.8 mm; Sotnikova, 2001); Stránska Skála, Czechoslovakia (n = 18, 20.5–24.1 mm, Musil, 1972); Mosbach, Germany (n = 5, 22.4–24.7 mm, Adam, 1959: table 4); Hundesheim, Austria (n = 3, 23.9–24.0 mm, Thenius, 1954: table 4); Heppenloch, Germany (n = 2, 24.0–26.0 mm, Adam, 1959: table 4), and Westbury-sub-Mendip, England (n = 7, 21.5–25.7 mm, Bishop, 1982: table 28).

Only a few ramal fragments and a single maxillary are known from the Cripple Creek Sump. The rami provide most of the characters: none of the incisors are known and the canines are so worn that they provide no basis for description. The lower premolar row curves medially as is typical of *C. lupus*. The premolars are separated by diastemata and are closely similar in individual length, forming a series that increases posteriorly at

about 1 mm per tooth. The p2 may have a posterior cusp, and the p3 consistently does so. The p4 has a tiny second posterior cusp lying in front of, or discernible from, the posterior cingulum in three of the four rami in which it can be observed. This is a primitive feature in *Canis* sp., more consistently present in *C. mosbachensis* than in *C. lupus*, where this cusp cannot be differentiated from the posterior cingulum. The tip of p4 lies below the paraconid of m1; p3 lies below p4 and p2; and the p4 lacks a strong posterolingual shelf as in *C. mosbachensis*. The m1 and m2 show no peculiarities except for the better developed anterolabial cingulum on m2 of the Sump fossils. The largest and most anterior mental foramen lies below the anterior root of p2, with the smaller one below p3. The horizontal ramus gently tapers forward, and there is a shallow inflection in the ventral border behind the symphysis. The masseteric fossa is deep, especially anteriorly, and extends beneath m3; ventrally it is marked by a strong masseteric crest. The angular process is typical of *Canis*.

The left maxillary fragment, F:AM 67173, bears P4, M1–M2, and parts of the palate and alveoli for P1–P3. From this specimen the following cranial measurements, in millimeters, can be approximated following the craniometry adopted herein: LPM 79.0, MW about 76, PW P1 about 30, P4L 23.2, WM2 11.5. These dimensions fall within the Minnesota sample of *C. lupus* used for this work. As in *C. lupus*, the infraorbital foramen lies above the posterior root of P3 and the largest posterior palatine foramen lies on the maxillary-palatine suture opposite the paracone of P4; a smaller second foramen lies within the edge of the palatine opposite M1. The most anterior position of the palatine notch lies opposite the rear of M2. The P4 has a stout protocone that extends slightly anterolingually but does not extend beyond the anterior margin of the tooth. The M1 has a conspicuously enlarged paracone and a low parastyle connected to the paracone by the preparacrista; the labial cingulum is subdued but largely present. The talon is narrow, but it includes a differentiated weak metaconule, a trace of the paraconule, and a low protocone. The hypocone is also subdued, and the lingual cingulum joins the metaconule and extends around the protocone to the parastyle. The M2 is relatively large compared with M1, and the paracone is considerably larger than the metacone. No conules are developed from the protocristae. The lingual and labial cingula nearly completely encircle the tooth except across the metacone. The hypocone is not a differentiated cusp.

Wolves close in size and morphology to the *Canis* sample from the Cripple Creek Sump appear in Europe near the close of the medial Pleistocene (''Mindel-Riss'' interglacial, sensu Bonifay, 1971, ca. 0.4 Ma), where a sample from the Lunel-Viel Cave of southern France (Herault) was designated *Canis lupus lunellensis* by Bonifay (1971). This taxon was differentiated from living wolves solely on its smaller size. The length of m1 of 10 individuals ranged from 23.8 to 27.4 mm, the m2 (n = 9) from 9.6 to 10.8 mm. The m1 and m2 fall mostly below the range of Cripple Creek Sump. However, the single upper dentition from the Sump lies within the range of the dental measurements of *C. l. lunellensis* (taking into account differences in the measurement of width due to choices of reference points). Morphologically the Sump wolves closely resemble living North American wolves of comparable size as well as *C. l. lunellensis*.

Thus, the Alaskan material of medial Pleistocene age indicates the presence of a population that clearly belongs to *Canis lupus*. If the geological attribution of this material is correct, and its age is ca. 1.0 Ma, wolves similar to the living species were part of a high-latitude Arctic fauna (Olyorian) that existed contemporaneously with other species of *Canis* in the Irvingtonian of the middle latitudes of North America.

Xenocyon Kretzoi, 1938

Sinicuon Kretzoi, 1941: 118.
Canis (*Xenocyon*) Rook, 1994: 71.

Type Species: *X. lycaonoides* Kretzoi, 1938.

North American Species: *X. texanus* (Troxell), 1915, and material referred here to *X. lycaonoides* Kretzoi, 1938.

Distribution of North American Species: Late Irvingtonian of Texas; Olyorian (medial Pleistocene) of Alaska and Yukon.

Diagnosis (follows Schütt, 1974, and Sotnikova, 2001): Canids of large size, comparable to *C. lupus*; horizontal ramus deep and robust; coronoid process low relative to length; cheek toothrow straight, lacking inward inflection at premolar-molar junction seen in *C. lupus*; canines with short crowns; M1 with weakly developed labial and lingual cinguli, hypocone small, conules weakly developed; M2 not markedly reduced relative to M1, metaconule absent, postprotocrista present; lower premolar row lacks diastemata; p2 and p3 without posterior cusp; p4 with posterior cusp; posterior cingulum of p3 lies below base of crown of p4; p4 with second posterior cusp anterior to cingulum; tip of p4 lies at or above tip of m1 paraconid; m1 metaconid greatly reduced, entoconid represented by a low crest or absent, yet hypoconid often retains trace of connecting cristid, hypoconid nearly centrally positioned on talonid; m2 not markedly reduced relative to m1, metaconid greatly reduced but present, hypoconid present and labially placed on talonid, entoconid not differentiated from lingual talonid crest; anterolabial cingulum weak or absent; m3 present and bicuspid.

Discussion: In describing the fauna of the medial Pleistocene fissure fills at Gombaszög (Gombasek), Hungary, Kretzoi (1938: 132) designated the right M1 of a large canid the holotype of *Xenocyon lycaonoides*, n. gen., n. sp., and, in the same work, but on page 128, he designated a left ramal fragment with a p4 and trigonid of m1 "*Canis*" *gigas*, n. sp. In a review of the fauna based on later collections, Kretzoi (1941: 112) recognized that these fragments belong to a single taxon and took the name with page precedence, making "*C.*" *gigas* the genotypic species. He pointed out the dental similarities to *Cuon* and *Lycaon* (the most striking are related to hypercarnivory), but noted that *Xenocyon gigas* was significantly larger and retained m3. The latter feature was indicated by a right ramal fragment with the m3 alveolus (Kretzoi, 1941: pl. V, fig.1). A year later, Kretzoi (1942) realized that *Canus gigas* was a preoccupied name and renamed the genotypic species *C. spelaeoides*. When Musil (1972) described the *Xenocyon* sample from Stránska Skála he used the name *X. spelaeoides* Kretzoi, 1942, as the material was clearly referable to that Gombaszög species. Furthermore, as the genus *Xenocyon* was based on *X. lycaonoides* Kretzoi, 1938, recognition that *C. gigas*, described in the same paper, was the same taxon is no grounds for submersion of *lycaonoides* and thus the homonomy of *C. gigas* is not relevant. For this reason we follow later workers (beginning with Schütt, 1973) in using *Xenocyon lycaonoides* as the name for the genotypic species.

In a revision of the Lycaoninae (Gray), 1868 (included in Caninae by McKenna and Bell, 1997), Kretzoi (1941) erected *Sinucuon* for *S. peii*, n. sp. based on "*Cuon*, sp. nov." of Pei (1939) from Choukoutien locality 18. He was apparently unaware that this taxon had already been described from locality 18 as *Cuon dubius* by Teilhard de Chardin in 1940. Later, Schütt (1974) referred *C. dubius* to *Xenocyon*, thus extending the geological and geographic range of the genus into the late Pliocene of China. Thenius (1954: fig. 33b) proposed *Cuon dubius stehlini* based on isolated teeth from Rosiéres (Cher), France, in which the presence or absence of m3 could not be seen. Schütt (1973) held this taxon as a synonym of *X. lycaonoides*. To further confound the confusion between *Xenocyon* and *Cuon*, there is a large true *Cuon*, *C. alpinus priscus* Thenius, 1954, that occurs with *X. lycaonoides* at Mosbach II (Weisbaden), Germany (Schütt, 1973).

In 1994 Rook, following a suggestion of Torre (1967), reduced *Xenocyon* to a subgenus of *Canis* and relegated the large early Pleistocene taxa as *C. falconeri* Forsyth-Major (1877) from the Upper Valdarno deposits in Tuscany, Italy; *C. antonii Zdansky*, 1924, from Honan, China; and *C. africanus* Pohle, 1928, from Olduvai Gorge, Bed II, Tanzania, to a supraspecific group (i.e., a clade) termed *Canis* (*Xenocyon*) ex gr. *falconeri*, whose constituent taxa were "semispecies … representing the extremes of the geographic range of the taxon" (Rook, 1994: 72). The diagnosis of this group differed from that of *Xenocyon* sensu stricto by the primitive states of most of the dental features

detailed above, although the metaconids of m1 and m2 were said to be relatively reduced, the upper molars had a marked tendency toward brachyodonty, and the neural cranium was relatively short. Based on the evidence presented, a good case can be made for the phyletic union of the named taxa, but our phyletic results show a more divergent relationship (see below and fig. 65).

Present evidence indicates that *Xenocyon* is represented in the late Pliocene only by *X. dubius*, a taxon so far unrecognized beyond its type site near Beijing. *Xenocyon lycaonoides*, the genotypic species, has a wide geographic range from Europe across Asia into northern North America in the medial Pleistocene. An endemic form, *X. texanus* (Troxell), 1915, occurred at the same time in the New World middle latitudes.

Xenocyon texanus (Troxell), 1915
Fig. 57A–C; appendix 3

Canis texanus Troxell, 1915: 627.
Protocyon texanus: J.L. Kraglievich, 1952: 62.
Protocyon texanus: Kurtén and Anderson, 1980: 172.

Type: YPM 10058, fragment of a left ramus with canine, p1–p4, m1–m3 (Troxell, 1915: fig. 18); paratypes: YPM 10058, right M1 lacking most of the paracone and metacone (Troxell, 1915: fig. 20); left humerus (Troxell, 1915: fig. 23); anterior scapular fragment; left metatarsal IV; right cuneiform; right pisiform. YPM Mylodon-Camel Quarry, head of Rock Creek, Tule Formation (late Irvingtonian), Briscoe County, Texas.

Distribution: Know only from the type locality.

Revised Diagnosis: Distinguished from *Xenocyon lycaonoides*, the only other species of the genus to occur in North America, by slightly larger size, m1 talonid wider relative to trigonid; hypoconid more marginal on the talonid; and M1 metaconule more salient than in most *X. lycaonoides*.

Description and Comparison: Except for the relatively minor differences signaled in the diagnosis, the morphology of the holotype clearly allies this taxon with *X. lycaonoides*. The crown of the canine is broken, but enough remains to show that it was short and only gently recurved. The premolars are uncrowded, and the p2 is isolated by diastemata. The premolar crowns are short and broad across their posterior roots and, although p3 may have had a minute posterior cusp, at the present state of wear only p4 does so and it has a tiny second cusp that surmounts the cingulum. The tip of p3 lies just below p2 and its posterior cingulum lies below that of p4. The tip of p4 may not have reached the height of the paraconid of m1 in the unworn state. The anterior face of the m1 curves backward, and wear has opened a broad carnassial notch. The trigonid of m1 is only slightly wider than the talonid, the metaconid is small, and the hypoconid, clearly the largest talonid cusp, is not as centrally placed on the crown as in *X. lycaonoides* or the smaller, early Pleistocene *X. dubius* of China. Much of the enamel is broken away on the lingual surface of the talonid, and that has carried away any remnant of the entoconid. The m2 has likewise been damaged lingually, but that does not obscure the small size of the metaconid relative to the protoconid and the lack of a distinct entoconid. There is no anterolabial cingulum. The m3 has a central cusp (protoconid), a ridge leading lingually from it and a tiny cusp (metaconid) at its lingual side.

The horizontal ramus is deep as in *X. lycaonoides*, and the premolar row is not deflected medially relative to the molars as in *C. lupus*. A large mental foramen lies beneath p1–p2, with a smaller one beneath the anterior root of p3. The masseteric fossa is deep anteriorly and ends just behind m3.

Discussion: Berta (1988: 98) questioned Kraglievich (1952) and Kurtén and Anderson's (1980) assignment of *Canis texanus* to *Protocyon* Giebel, 1855, citing the retention of the metaconid on m2, despite its loss on m1, as characteristic of species of the latter genus. She instead assigned this taxon to *Cuon*, further supporting the differences between the latter and *Protocyon* on cranial and mandibular grounds. However, she failed to note that *C. texanus* retains the m3, a feature lacking in all species of *Cuon*. The only large hypercarnivorous canine genus with the constellation of features described above is *Xenocyon*. Moreover, *X.*

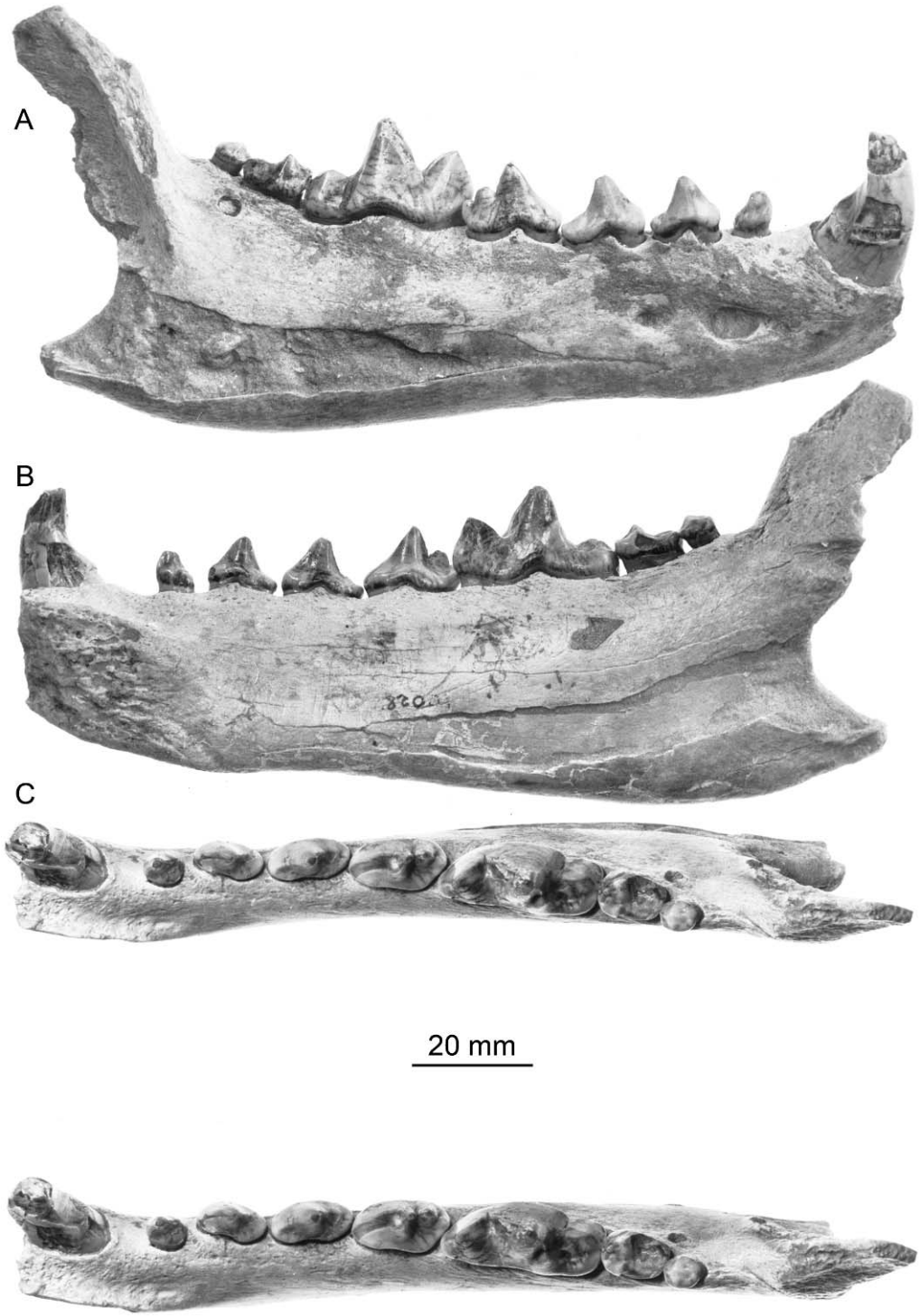

Fig. 57. **A–C**. *Xenocyon texanus*, late Irvingtonian, Briscoe County, Texas. **A**. Left ramus, holotype, YPM 10028, lateral view, reversed. **B**. Lingual view, reversed. **C**. Occlusal view, stereo pair.

texanus lies morphologically close to *X. lycaonoides* of Arctic North America and possibly represents an extralimital variant of the widespread *X. lycaonoides*.

Xenocyon lycaonoides Kretzoi, 1938
Figure 58A–C; appendix 3

"*Canis*" *gigas* Kretzoi, 1938: 128.
Xenocyon lycaonoides Kretzoi, 1938: 132.
Xenocyon gigas: Kretzoi, 1941: 112.
Xenocyon spelaeoides Kretzoi, 1942: 345, to replace *C. gigas*, preoccupied.
Cuon dubius stehlini Thenius, 1954: 18.
Xenocyon spelaeoides: Musil, 1972: 85.
Xenocyon lycaonoides: Schütt, 1973: 63.
Cuon rosi Pons-Moya and Moya-Sola, 1978: 55.
Cuon sp., Harington, 1978: 61.
Cuon sp., Youngman, 1993: 141.
Canis (*Xenocyon*) *lycaonoides*: Sotnikova, 2001: 622.

Type: MNM FA 20 (PV4), unworn right M1, from site 3a, a terra rossa–filled fissure in the limestone quarried at Gombaszög, Hungary (Kretzoi, 1938: pl. III, fig. 4).

Referred from Type Locality: MNM FA 19, fragment of a left ramus with broken p4 and trigonid of m1 (holotype of "*Canis*" *gigas* Kretzoi, 1938: 128, pl. II, fig. 10); MNM PV 5, fragment of a right ramus, lacking ascending part, with incisor, canine and p1–p4 alveoli, m1 talonid, m2, and alveolus of m3 (Kretzoi, 1941: pl. V, fig. 1).

Referred from North America: Cripple Creek Sump, Fox Gravels or lower Gold Hill Formation (Olyorian, approximately equivalent to late Irvingtonian, medial Pleistocene), near Fairbanks, Alaska: F:AM 67180, fragment of a right ramus with i1–i3, c, p1–p3 alveoli, p4 broken, m1 paraconid broken, m2, m3 alveolus (fig. 58A–B); and F:AM 97110, fragment of left ramus with alveolus of talonid of m1, m2, m3 alveolus, and ascending ramus.

NMC 14353, a fragment of a right ramus with posterior part of p1 alveolus, alveoli of p2–p3, crown of p4, and anterior part of m1 alveolus. This specimen was obtained from the Old Crow River site 14N, Yukon Territory, Canada (67°51′N, 139°46′W). Five C14 dates on mammal bone from this site range from 22 to36 Ka (Harington, 1978), but the presence of the giant pika (*Ochotona* cf. *whartoni*) and Olyor horse (*Equus* cf. *verae*) and *Xenocyon lycaonoides* indicates the presence of an older fauna of medial Pleistocene age.

Quaternary nonglacial deposits, Wellsch Valley, New Mountain site (late Irvingtonian) about 10 km northwest of the town of Stewart Valley, Saskatchewan, Canada: NMC 17824*, left maxillary fragment with part of posterior alveolus of P4, M1 with labial and posterior borders broken away, M2 lost in life, alveolus filled with cancellous bone; NMN 17825*, fragment of right premaxillary, alveoli for I1–I2, I3 well worn, broken anteriorly, anterior part of canine alveolus present. Reported as "*Borophagus diversidens*" by C.S. Churcher in Barendregt et al. (1991) and in previous contributions on the Wellsch Valley Fauna cited in that work.

North American Distribution: Medial Pleistocene (Olyorian) of Alaska and Yukon; late Irvingtonian of south-central Canada.

Revised Diagnosis: Rami distinguished from those of *X. dubius* Teilhard de Chardin, 1940, by larger average size; premolars not as elongate, wider, and higher crowned; p2 lacks posterior cusp; second posterior cusp on p4 smaller, often closely appressed to cingulum; m2 with metaconid smaller relative to protoconid and narrower talonid.

Description and Comparison of North American Material: The Alaskan ramal fragments compare favorably with the array of *L. lycaonoides* material discussed in the literature cited above. Right ramus, F:AM 67180, was mentioned by Repenning (1967: 307, footnote 6 to table 8) as "*Xenocyon gigas*" following McKenna's identification of it with *Xenocyon* (cited by Péwé and Hopkins, 1967: 269, footnote d to table). It was briefly described and figured by Youngman (1993). This specimen falls in the lower size range of *X. lycaonoides*, but agrees in all available characters. As in that taxon, there is often a short diastema between p2 and p3, and the anterior root of p2 lies slightly labial to the p1 in a weakly imbricated fashion. Otherwise there is no break in the linear form of the dental row. The horizontal ramus is deep anteriorly, here being only a gentle taper forward. The subangular or digastric insertion of the ventral surface of the ramus just behind the toothrow is developed as in other

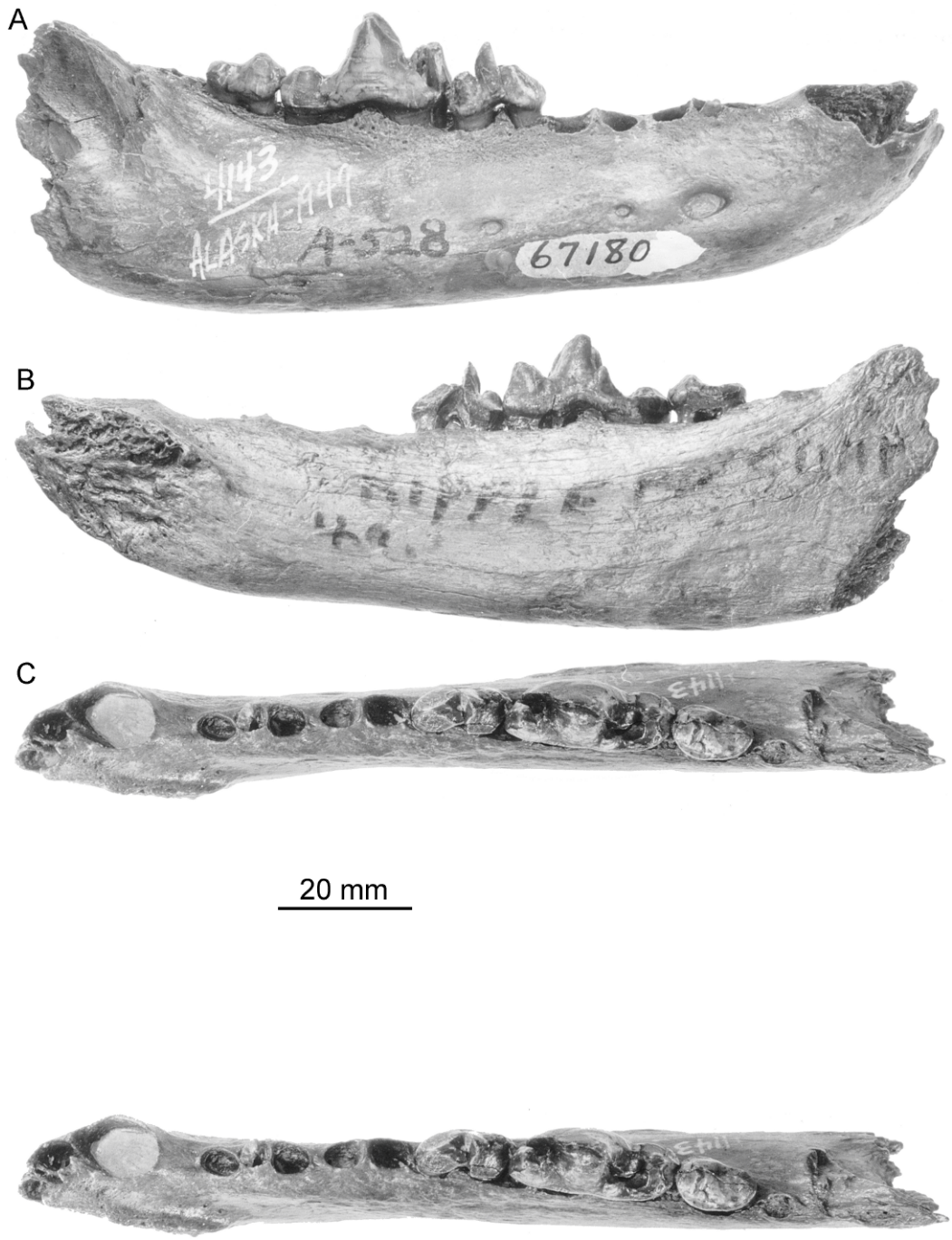

Fig. 58. **A–C**. *Xenocyon lycaonoides*, Olyorian (medial Pleistocene), Cripple Creek Sump, Alaska, F:AM 67180. **A**. Right ramus, lateral view. **B**. Lingual view. **C**. Occlusal view, stereo pair.

X. lycaonoides specimens, and the anterior end of the masseteric fossa lies relatively high at the base of the ascending ramus. This fossa ends anteriorly, just behind the m3 alveolus. This region of the ramus is more completely preserved in F:AM 97110, but in a young adult jaw that has not yet reached adult proportions. The posterior part of the anterior alveolus and all of the posterior alveolus of m1 are preserved and show that the crown of this tooth was large, although probably not exceeding 32 mm in length judging from the length of the posterior root (16 mm). The coronoid process is short and high, the angular process has much growing cancellous bone, as does the tip of the coronoid, and the condyle is small. Clearly this region was actively growing since acquisition of the permanent dentition. This specimen is identified as *X. lycaonoides* chiefly on the morphology of m2, which has a very reduced metaconid and short and narrow talonid.

The individual represented from Old Crow River is also a very young adult; the jaw evidently has not reached adult size as the teeth are closely spaced, p2 is imbricated, and the ramus is shallow. A large mental foramen lies beneath the anterior root of p2, and there are two additional foramina approximately at mid-level on the ramus: one beneath the anterior root of p3, the other beneath the posterior root of the same tooth. Other *X. lycaonoides* individuals also show these foramina, although the most posterior may be below p4 (as in F:AM 67180). There is a shallow inflection in the ventral border of the ramus just behind the symphysis. The morphology of the p4 provides the most definite identification of either *Xenocyon* or *Cuon* rather than *Canis lupus* in the presence of a discrete second posterior cusp filling the space between the first posterior cusp and cingulum, and in the presence of an anterior cingulum with a low cusp. The proportions of the p4 (length, 14.8 mm, width, 6.7 mm from a cast) and large size of the anterior premolars implied by their roots (p2 about 11.0 mm, p3 12.7 mm) exceed those of the larger forms of *Cuon alpinus* (*C. a. priscus* and *C. a. fossilis*) or *C. javanicus antiquus*. Except for the shallower jaw, the specimen agrees best with *X. lycaonoides*, based on the morphology of the p4, the size and relationships of the p1–p3, and the distribution of the mental foramina.

The Saskatchewan specimens consist of two fragments from an old individual, one that lost M2 in life. The premaxillary (NMC 17825) and maxillary (NMC 17824) could represent a single individual as far as preservation and wear on the teeth are concerned. The premaxillary contains I3, which, although badly worn, still shows a clear remnant of the medial cingulum. The M1 is badly broken, but the large paracone and metacone can be seen. The protocone is relatively small and lacks a conule on the preprotocrista. The hypocone is very small, placed on the lingual cingulum posterior to the protocone; the cingulum connects with the postprotocrista at the site of the metaconule; and a very subdued lingual cingulum extends anteriorly across the protocone to the anterior border opposite the site of the paraconule. The maxilla extends backward, forming a shelf where the M2 would lodge. It terminates in cancellous bone.

Discussion: The right ramus (F:AM 67180) allowed the first identification of the presence of *Xenocyon* in the New World (Repenning, 1967; Péwé and Hopkins, 1967) and supported the presence of substantially older Pleistocene deposits in the Fairbanks area of Alaska. This specimen was figured and described by Youngman (1993), who thought that it should be referred to *Cuon* despite the retention of m3 and less modified molars. Likewise, the Canadian M1 agrees best with *Xenocyon lycaonoides* in size and in the presence of a hypocone and lingual cingulum.

We have discussed the age of the Cripple Creek Sump site in our description of the *Canis lupus* from that locality, but the age of the Wellsch Valley site needs further comment. The identification of the large canid as *Xenocyon*, rather than *Borophagus*, removes the necessity, on this basis, for an age older than the Pliocene–Pleistocene boundary. The known range of large *Xenocyon lycaonoides* seems limited to the medial Pleistocene in the Old World. The younger age also removes the necessity of having the Wellsch Valley occurrence of *Microtis paroperarius* represent the oldest in North America (Repenning, 1987). The fission-track and paleomagnetic

dating of the Wellsch Valley sequence is also resolved in favor of the fission-track date of 0.69 ± 0.11 Ma for the ash that lies at a reversed to normal magnetic polarity boundary. Barendregt et al. (1991) favored the latter as the Matuyama–Brunhes reversal. The electron spin resonance (ESR) dates on elephant enamel from below the ash of 274 ± 35 Ka (Zymela et al., 1988) are too young, as suspected, but not as markedly discordant as they would have been if this section sampled the Matuyama Chron in the vicinity of the Olduvai Subchron as suggested by the previous identification of the canid.

Cuon Hodgson, 1837

Chrysaeus Smith, 1839: 167.
Primoevus Hodgson, 1842: 39.
Primaevus Gray, 1843.
Cuon Agassiz, 1846: 113.
Cynotherium Studiati, 1857: 657.
Anurocyon Heude, 1888: 102.
Crassicuon Kretzoi, 1941: 118.
Semicuon Kretzoi, 1941: 119.

Type Species: *Cuon primaevus* Hodgson, 1837.

Distribution in North America: *Cuon alpinus* Rancholabrean (latest Pleistocene), northeastern Mexico.

Diagnosis: The osteological differentiation of species of *Cuon* from those of *Xenocyon*, and the morphologically related *Lycaon pictus*, lies principally in the extreme hypercarnivory of *Cuon* spp.: loss of m3; reduction of m2 to single or poorly differentiated double-rooted condition with further simplification of crown involving great reduction and loss of metaconid so that it resembles m3 of other canines; loss of m1 entoconid and any remnant of the cristid connecting it with hypoconid, and further reduction of metaconid to very small size and loss (usually as individual variation in *Cuon* populations); anterior premolars also with prominent, high-crowned principal cusps, p2 and p3 usually with posterior cusp; large p4 whose principal cusp is as high or higher than m1 paraconid, and presence of shelflike anterior cingulum that may be produced into anterior cusp; M1 lacking hypocone, although there may be remnant of posterolingual cingulum; M2 very reduced, but retaining tribosphenic form.

Discussion: The living kinds of *Cuon* are variously interpreted as races or full specific taxa: *C. primaevus* (Hodgson, 1837), from the Himalayas and Tibetan Plateau; *C. alpinus* (Pallas, 1811), from northern Asia (Urals to Altai); *C. dukunensis* (Sykes, 1831), the dhole of peninsular India and the Deccan Plateau; and *C. javanicus* (Desmarest, 1820), from southeastern Asia and the larger islands of Indonesia west of Wallace's Line. Pocock (1936) advocated union under *C. javanicus*, but most authorities now use the specific name *C. alpinus* for all living *Cuon*. In the fossil record *Cuon* appears in the medial Pleistocene of Europe as *C. alpinus priscus* (Thenius), 1954, and in southeastern Asia as *C. javanicus antiquus* (Matthew and Granger, 1923). Late Pleistocene northern Eurasian forms are usually placed in *C. alpinus fossilis* (Nehring, 1890) or, in the latest Pleistocene, *C. alpinus europaeus* (Bourguignat, 1868). In the course of describing the material of *Cuon alpinus fossilis* from late Pleistocene deposits at Heppenloch, Germany, Adam (1959) viewed the record of *C. alpinus* in Europe as a clade (Formenkreis) beginning with *C. a. priscus*, passing through *C. a. fossilis* to *C. a. europacus*, with progressive modifications of the molar dentition, especially m2 to a unirooted condition and loss of metaconid; the p4 increases in crown height and prominence of the anterior cusp. The North American examples described below belong to the terminal part of this clade.

Cuon alpinus Pallas, 1811
Figure 59A–C; appendix 3

Cuon alpinus: Kurtén and Anderson, 1980: 172.
Cuon sp.: Youngman, 1993: 141.

Material: From San Josecito Cave, Nuevo Leon, northeastern Mexico; LACM(CIT) locality 192, carbon 14 dating (Arroyo-Cabrales et al., 1995) indicates that the cave fill excavated by CIT ranges from 27 to 11 Ka: LACM 110984, left M1; LACM 28081, fragment of a right ramus with c–p4 alveoli, m1, m2 alveolus; LACM 28082 (site L13) fragment of a right ramus, c root, p2–p3, p4 root; LACM 28083, fragment of a right ramus, p1 root, p2 tip broken, p3–p4, m1, anterior part m2 alveolus; LACM 28084, fragment of right ramus, p1–p2

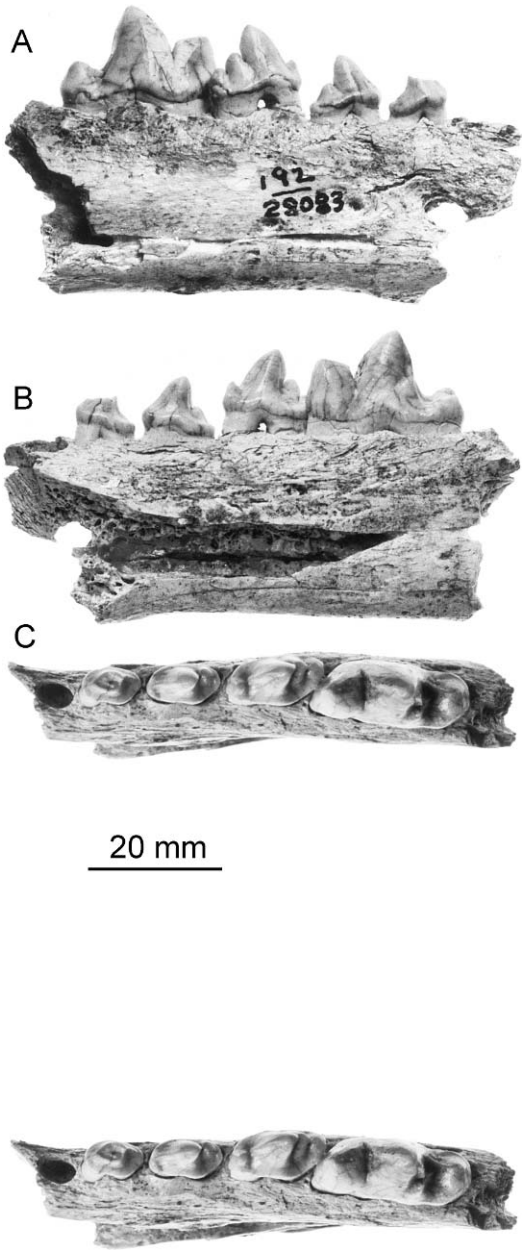

Fig. 59. **A–C**. *Cuon alpinus*, Rancholabrean, San Josecito Cave, Nuevo Leon, Mexico, LACM (CIT) 28083. **A**. Right ramus, lateral view. **B**. Lingual view. **C**. Occlusal view, stereo pair.

partial alveoli, p3–p4, m1–m2 partial alveoli; LACM 28085, fragment of left ramus, m1, and alveolus of m2; and LACM 28086 (site B2.60), fragment of left ramus, c–p1 alveoli, p2–p3 roots, p4 alveolus, m1, m2 alveolus.

Description and Comparison: The upper dentition is represented only by a M1; it has the typically short talon of the genus. The tooth lacks conules, the hypocone is very reduced, and a lingual cingulum is absent on the protocone. The labial cingulum is present and complete and there is a low parastyle connected to the paracone by the preparacrista.

The horizontal rami are robust, deep, especially anteriorly. A shallow medioventral extension of the symphysis is present, and the ventral border has an inflection behind the symphysis. The largest mental foramen lies below the anterior root of p2, and there is a smaller foramen beneath p3 and sometimes also a small foramen below p4 as occasionally seen in other species of *Cuon*. The anterior part of the masseteric fossa is deeply indented so that the anterior rim overhangs the fossa. The premolars lack diastemata and p1–p2 and p2–p3 may be imbricated. All premolars have anterior cinguli, but only that on p4 is produced into a prominent anterior cusp that is canted medially in the manner of a carnassial paraconid. Premolars 3 and 4 have posterior cusps and p4 has a second cusp lying just in front of the posterior cingulum. The crown of p4 tips backward and its principal cusp is taller than the m1 paraconid. This tilt results in the base of the crown of p4 lying well above the base of p3, but the p3 principal cusp does not lie below that of p2. The anterior face of the m1 paraconid slants backward, and the metaconid is low and very reduced and is only slightly higher than the hypoconid. The talonid is unicuspid but the hypoconid lies a little labial to the midline. It is compressed laterally into a crest that reaches forward to the base of the protoconid. The crista obliqua is very low and is directed to the base of the metaconid. There is only a low crest lingually, which rises to a union with the tip of the hypoconid. No specimen shows the m2, but the alveoli have an interradicular crest that indicates the presence of a weakly two-rooted tooth. There is no m3.

This sample compares most favorably with *C. alpinus europaeus* from the latest Pleistocene of Europe. It agrees closely in size with

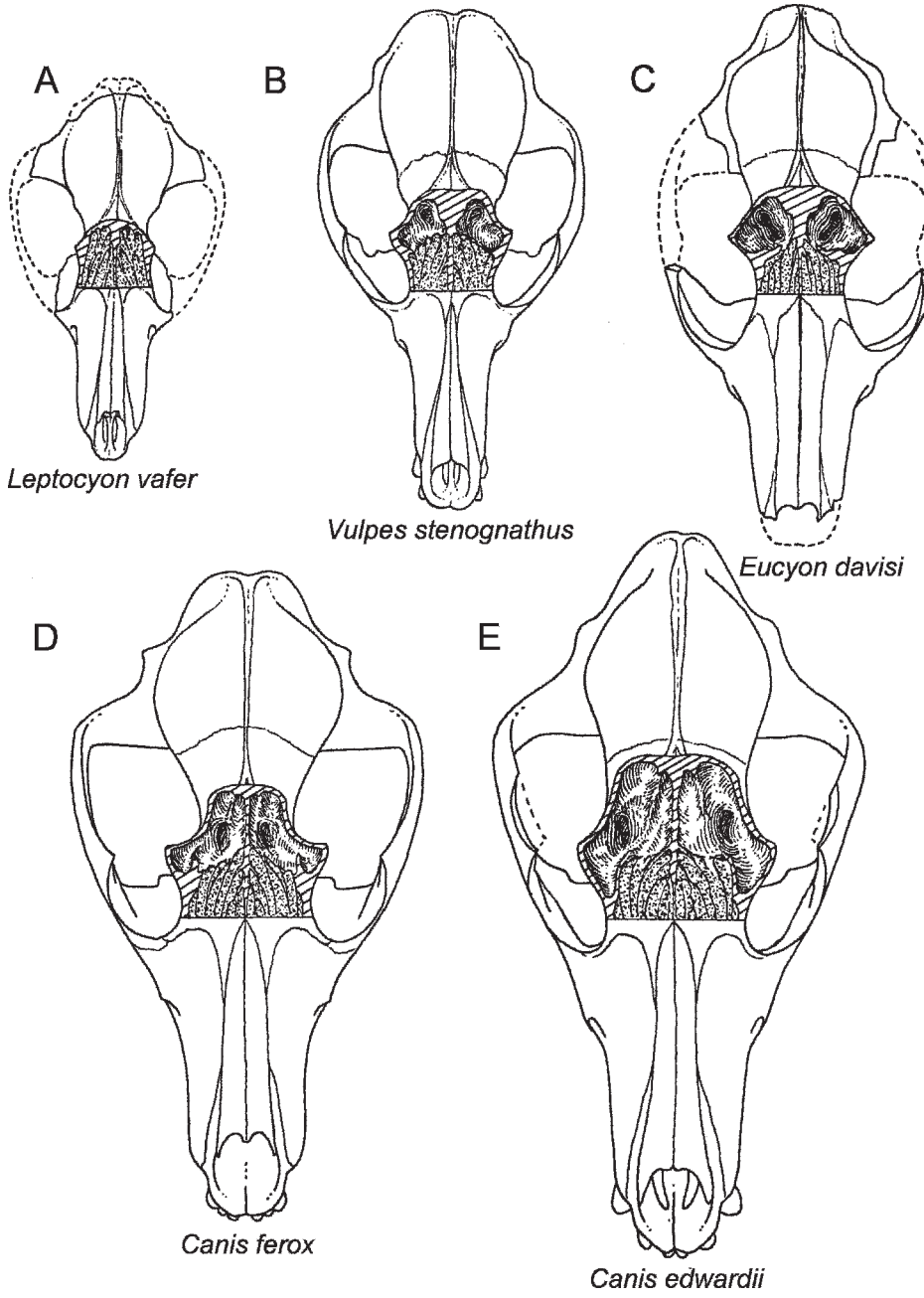

Fig. 60. Comparative dorsal views of the skulls of fossil canine species sectioned to show the extent and form of the frontal sinus (character 34, table 1), frontal turbinates stippled, frontal sinus shaded. **A**. *Leptocyon vafer*, F:AM 62763, lacking a frontal sinus. **B**. *Vulpes stenognathus*, F:AM 49284, showing the small frontal sinus unique to this taxon. **C**. *Eucyon davisi*, F:AM 63009, with frontal sinus that penetrates the postorbital processes [character state 34(1), table 1]. **D**. *Canis ferox*, F:AM 49298, paratype. **E**. *Canis edwardii*, F:AM 63100, showing the expanding sinus typical of primitive members of the genus *Canis* [character state 34(2), table 1]. Drawn to common scale.

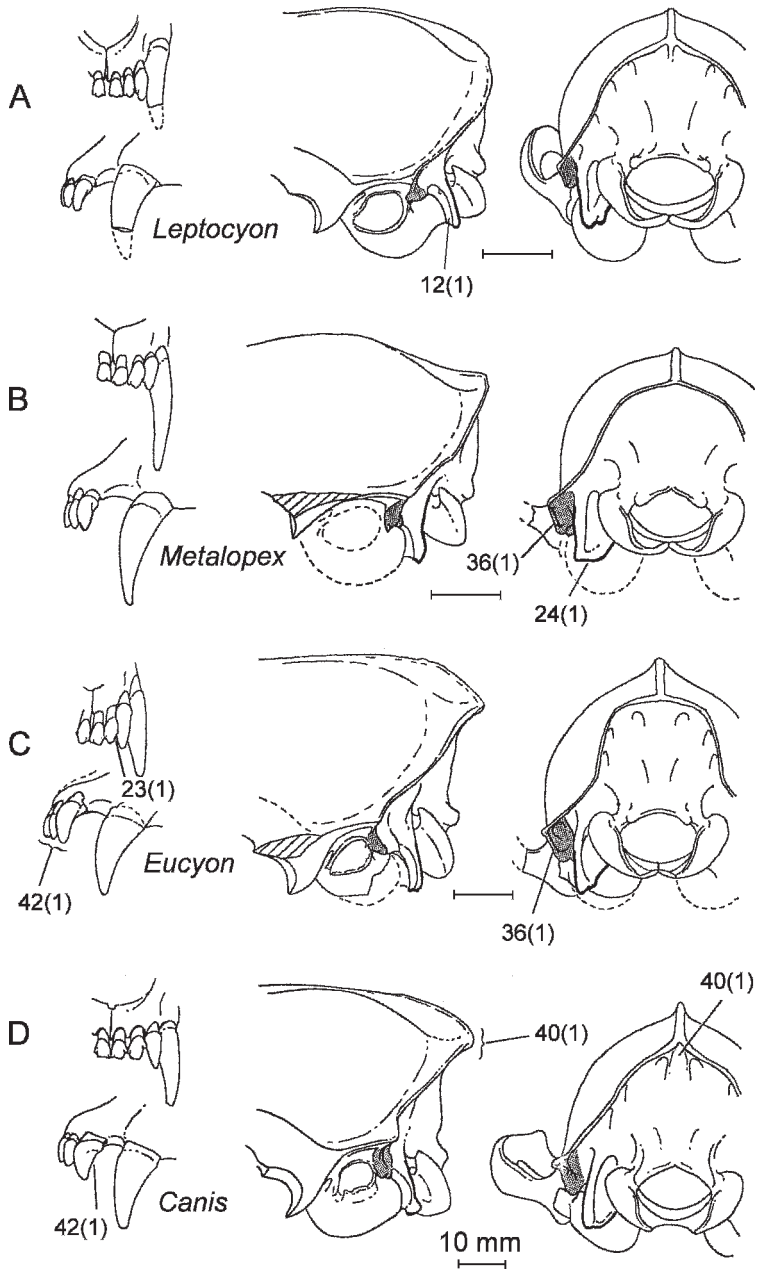

Fig. 61. Comparative views of the left upper incisors and canine (anterior view above lateral view) and the left side of the braincase (lateral view to the left of posterior view), mastoid process stippled, paroccipital process accentuated to show several features used in phyletic analysis (characters states numbered to correspond to table 1). **A**. *Leptocyon vafer*, incisors, F:AM 27412, cranium, UCMP 77703, showing the primitive condition in incisor and canine form and the relative size of the supraoccipital, mastoid, and paroccipital. **B**. *Metalopex macconnelli*, LACM 55237, holotype, cranium, UA361-49, incisors; cranium retains primitive upper incisors, broad paroccipital process of the vulpines [character 24(1)] but shows large mastoid process [character 36(1)] typical of the canines. **C**. *Eucyon davisi*, F:AM 63010, incisors; cranium composite of F:AM 63009 and 63183, showing enlarged I3 relative to I1–I2 [character state 42(1)], medial cuspule I3 lacking [character state 23(1)], large mastoid process [character

samples allocated to that taxon (Adam, 1959: table 2) and particularly in the morphology of the p4 with its large anterior cusp. Nevertheless, there are some peculiarities of the m1 talonid that would need closer comparison than can be undertaken, and so the San Josecito specimen is referred simply to *Cuon alpinus* without subspecific designation.

Discussion: It is a zoogeographic surprise to see a single record of *Cuon* in North America at a mid-latitude late Rancholabrean site. The presence of several individuals is in accord with the pack-hunting behavior of the living dholes, but with hundreds of known sites of this age scattered across the United States and Mexico, the occurrence of this taxon in only a single place is a sobering reminder of the paucity of our real knowledge of the fossil record of even the youngest sites. Today *Cuon* ranges into northeastern Asia and is thus poised to traverse Beringia during favorable low sea-level episodes. So far only *Xenocyon* has been recorded in Alaska and northern Canada. Perhaps competitive exclusion forced *Cuon* into southern North America to avoid wolves and *Xenocyon* at higher latitudes.

PHYLETIC ANALYSIS

Introduction

In our previous analysis of the genera of living canids (Tedford et al., 1995) we used 57 characters to demonstrate the phylogenetic relationships of 16 genera among themselves and to the two extinct canid clades, the Hesperocyoninae and Borophaginae. The present species-level analysis used 48 (84%) of these morphological characters plus an additional 15 features. Inclusion of the fossil record necessitates strong reliance on dental features (59% of total), as these structures are often the only elements available for comparative work. In using dental structures as a basis for phyletic analysis, it must be kept in mind that the close relationship between morphology and function may lead to the independent development of similar structures. This is especially so in the Canidae where the modification of the primitive canid carnassials is limited to just a few pathways of adaptation with hypo-and hypercarnivory at the extremes. Such covariances present a constellation of characters that, as homoplasies, are strongly orienting in cladistic analysis. This is particularly problematic within the *Canis* clade, where the variation within populations can include significant numbers of hypercarnivorous individuals in demes basically mesocarnivorous. In these cases analysis must look beyond these adaptations to other features not so homoplastically labile. In other cases, careful analysis will reveal that the acquisition of hypercarnivory does not involve the same structures in identical ways so that the individual pathways toward that adaptation can be distinguished. The confusion between *Protocyon* of South America and *Cuon* and *Xenocyon* of Holarctica is a case in point (see discussion of *X. texanus*, above).

As in our previous reviews, character polarity is established via outgroup comparison. As outgroups we used *Prohesperocyon* and *Hesperocyon gregarius* as basal cynoids and hesperocyonines, respectively, and the species of *Archaeocyon* as basal borophagines. Character state coding followed the convention in which "0" is the primitive state; "1", "2", and so forth are derived states. These features were unordered in the parsimony analysis and thus independent of their implication as an evolutionary progression. In the following description of the characters used in the analysis we organize

←

36(1)] and primitive narrow, salient paroccipital process, and fan-shaped supraoccipital shield. **D**. *Canis aureus*, AMNH(M) 88712, I3 enlarged with posterior cingulum [character state 42(1)]; supraoccipital shield triangular in shape and inion overhangs condyles [character 40(1)]. All drawings to a common size for ease of comparison; specimens selected to conform to a median size to minimize allometric relationships imposed by individuals of markedly different relative size. Ten millimeter scale for each taxon shown.

TABLE 2
Matrix Detailing the Distribution of Character States vs Taxa
See text.

	1	2	3	4	5	6
	12345678901234567890123456789012345678901234567890123456789012345678901234					
Hesperocyoninae	000000000000000000000000000000000000000000000000000000000000000000000000					
Borophaginae	111000000000000000000000000000000000000000000000000000000000000000000001					
Leptocyon mollis	1?1?1??1??000?0?000????000?00?0?0000???0?0?0???00??0?00000000?2					
Leptocyon douglassi	111110111102000??00?????000?000?00??0????000000000?0000000??02					
Leptocyon vulpinus	110110100002?000???0?00??000?000?????0???00?000?000?0000000???03					
Leptocyon gregorii	111110100011100000002??000000000000000002?000000000000000000003					
Leptocyon leidyi	111110111012111002?00?00??000?000?00?000?000000000000000000??04					
Leptocyon vafer	111110111011111111100000000000000000000000000000000000000100005					
Leptocyon matthewi	1211101?1011110111?1?0?0?000000000000000?2?000000000?000000???06					
Vulpes stenognathus	121110111011010111111111000000000100000000000000000000000000?08					
Metalopex macconnelli	12111011010101111110??01?1100000000010000?000000002000000??07					
Metalopex merriami	121111110101011111?0??0??111100002?1?0?0??000000002?00000000??08					
Urocyon webbi	12?1111?010??1?1???0?????211?110?????0????00000??0?0??0??0????09					
Urocyon galushai	1?111111110??1?1?????1???111?111?????0????000???00???000000???0A					
Urocyon citrinus	?3?1111111???1?1???1?????211?111?????0????0?000??00??00000????0C					
Urocyon minicephalus	131111111101012?11101?1?1011101120000000??000000000000000?000D					
Urocyon cinereoargenteus	1311111111011101110111121011101120000000000000000000000000000000E					
Cerdocyonina	131111111011110111011111000000000111110000000000000000000000000009					
Eucyon davisi	121110111011110111011110100000001111010000000000000000000000000008					
Canis ferox	12111011101111011101?1101000100012110111100000000000000000000?009					
Canis thöoides	131110101012?1101???1111??000?000????0111100000?000??000000???0B					
Canis lepophagus	13111010101111011101?1101000100012110111100000000000000000000000A					
Canis aureus	131110101011110111111111010001000121101111111111100001000000000D					
Canis arnensis	13111010101111011111??1010001000?3110111?10100000000000000???0C					
Canis etruscus	13111010101111011101??10100012001311011111111000002?01000000100C					
Canis falconeri	131110101011110112?1????000?210????011??111101111?0??000001???0C					
Canis antonii	13111010101111011111??10100002101311?111?111101111000000010000B					
Canis edwardii	13111010101111011101?1101000020012110111111111100001010000002?00B					
Canis mosbachensis	131110101011110111011112?0001200?2??011111111110000101000000??0D					
Canis palmidens	131110101011110111111110?0000200131101117?111111001?010000000000B					
Canis variabilis	13111010101111011111?1101000020012110111111111100001010000000000D					
Canis chihliensis	14111010101111011101??10100010001310011?111101111100110000000000B					
Canis latrans	131110101011110111111111010001200121101112111111000010100000000D					
Canis armbrusteri	132111101011110111012?1?0100012102311011121111110011111100001111C					
Canis dirus	132110101011110111011110100012102311011121111111111111111011111D					
Canis lupus	132110101011110111011110100012002311021121111111101111000000000D					
Xenocyon lycaonoides	14111010101111011100??10?000121023110110?101101111000101111000C					
Cuon javanicus	151100001011121111001110010102101211011121011001123011012110000C					
Lycaon pictus	151100101011121111001110010102101211011121011001122111011110000D					

the features by morphological region but indicate by their character number the approximate position of their first occurrence on the cladogram. Reference to these characters in the character list (table 1) and matrix (table 2) is in boldface type. These are followed by their equivalent (if any) (in lightface type) corresponding to the analysis of the Canidae by Tedford et al. (1995). Most of the following characters have been discussed in connection with our generic phylogeny, but they are repeated here for completeness. The wider comparisons made for this work resulted in some omission of characters and revision of the derived states in others.

Character Analysis

Skull: Compared with other Carnivora, the form of the canid skull is stereotypical and primitive, with the antorbital portion of the skull making up about 40% of the total length. Shortening of the antorbital part of the skull is part of a functional complex, including widening of the anterior palate (**48**; 41). Changes in the anterior palate of interest phylogenetically are the lengthening of the anterior palatine foramina beyond the canine alveolus [**53(1)**] as seen among the more derived species of *Canis*. Shortening of the nasal bones [**19(1)**; 19(1)] is seen in vulpines and some canines where the nasals end anterior to the most posterior position of the maxillary-frontal suture. Since this occurs in taxa with skulls of primitive form, it is not correlated with shortening of the antorbital portion of the skull. In canids the nasal process of the frontal wedges in between the nasals and maxillaries, and may eventually contact the premaxillary in borophagines. Within the crown group, a single clade (*C. dirus* and *C. armbrusteri*) is typified by having a very short frontal nasal process [**60(1)**], the antithesis of the primitive condition in the Canidae.

The phylogenetically important aspects of the form of the frontal sinus (**34**; 32) are fully discussed and illustrated in Tedford et al. (1995: 3–5, fig. 3), and we have found these features equally useful in treating the fossil record where skulls are available (fig. 60A–E). *Leptocyon* species clearly lack a frontal sinus, and they are foxlike in having this primitive condition [**34(0)**; 32(0)] manifested by a shallow depression or groove creasing the dorsal surface of the postorbital process. Although *Vulpes stenognathus* has a small frontal sinus as an autapomorphy, the condition becomes generally present only in members of the Canini. The South American Canini (Cerdocyonina) and *Eucyon* have a small sinus largely limited to the midline so that the dorsal surface of the postorbital process often retains the vulpinelike depression [**34(1)**; modified from 32(1)]. Members of the genus *Canis* show enlargement of the frontal sinus with lateral invasion of the postorbital process (removing the vulpine crease) and posterior expansion into the postorbital constriction, inflating this region of the cranium [**34(2)**; 32(2)]. Further expansion posteriorly inflates the postorbital constriction dorsally and ultimately reaches the frontoparietal suture [**34(3)**].

Canids primitively have a moderately arched or nearly flat zygoma when viewed laterally [**25(0)**; 4(0)], and the orbital portions of the zygomae are laterally flared and their jugal surfaces are everted to form a shelflike structure [**35(0)**; 35(0)]. These primitive conditions remain in *Leptocyon* and the Vulpini, but with the basal Canini, the South American taxa (Cerdocyonina), the zygomae lack the lateral flare and eversion [**35(1)**; 35(1)], and with *Eucyon* and *Canis* the zygomae become markedly arched in lateral view [**25(1)**; 4(1), mistakenly coded in table 2 of Tedford et al., 1995; recoding this feature has no effect on the form of their cladogram]. In the *Canis* crown group the union of the maxillary and jugal forms an acute angle [**52(1)**], whereas in other Canidae (including the outgroups) the angle between the orbital and masseteric wings of the jugal is obtuse [**52(0)**].

The postparietal foramen [**17(0)**; 11(0)] is primitively present in the Canidae, but in the Caninae this structure disappears [**17(1)**; 11(1)] in the more derived *Leptocyon* species and their descendants. This seems correlated with an increase in the posterodorsal exposure of the cerebellum, as the latter overlaps the cerebrum [**18(1)**] at the same node in the cladogram (fig. 65).

Primitively the sagittal crest in canids is confined to the parietal bone [**29(0)**], but in

derived members of all subfamilies the parasagittal crests emanating from the postorbital processes unite in front of the frontoparietal suture to extend the sagittal crest onto the frontal bone [**29(1)**]. In the Vulpini the derived state appears as an autapomorphy in *Metalopex merriami*, otherwise this condition typifies most species of *Canis*, although it is reversed in some species in the crown group.

In the Canidae the supraoccipital bones (fig. 61) primitively form a rectangular or fan-shaped shieldlike structure when viewed from the rear [**40(0)**; 55(0)]. In these cases the inion fails to overhang the condyles when the skull is viewed laterally. The derived condition in which the inion is produced posteriorly beyond the condyles and the supraoccipital shield is triangular in form is a useful synapomorphy [**40(1)**; 55(1)] for most species of *Canis*. These features are not consistently correlated with ontogeny and size since even small species of *Canis*, such as the golden jackal (*C. aureus*), possess the derived state.

The paroccipital process (fig. 61) is primitively associated with only the posterodorsal surface of the large bulla of the Canidae. The process is directed posteriorly and, consequently, it has a considerable portion of its length free of the bulla in primitive hesperocyonines and borophagines (our outgroups), as well as in the most primitive canines in which the structure is known (*Leptocyon mollis*). In *Leptocyon gregorii* and younger members of *Leptocyon* the paroccipital process has turned ventrally [**12(1)**; 10(1)], increasing the union between the process and the bulla with the base of the process being hollowed out for reception of the bulla. In the vulpines the paroccipital process widens laterally, embracing a larger part of the posterior bulla wall [**24(1)**; 18(1)], with its free-tip being very short and laterally turned. In the Canini the process is vertically directed and its body appressed to the bulla but the process is expanded posteriorly and has a prominent free-tip [**33(1)**; 31(1)]. In some members of the crown group of *Canis* the paroccipital process is larger and shows a strong posterolateral expansion [**33(2)**; 31(2)].

The Canini has the mastoid process (fig. 61) enlarged into a knob- or ridgelike structure [**36(1)**; 33(1)]. This is not simply correlated with size since small canines, similar in size to the larger vulpines, have large processes. The exceptions to this trend are species of the vulpine hypocarnivore *Metalopex*, which share this feature as a generic synapomorphy. In this case there is presumably a parallel development of muscles involved in lateral movements of the head.

Within the *Canis* clade the foramen ovale and posterior opening of the alisphenoid canal may be closely associated and lie in a common pit [**61(1)**] in some taxa. A similar proximity of the optic and anterior lacerate foramen [**62(1)**] causes them to arise from a common opening in the orbital fissure. These features characterize the *Canis armbrusteri–C. dirus* clade.

MANDIBLE: Most hesperocyonine and borophagine canids have primitive deep and thick horizontal rami [**4(0)**; 4(0)], even in some of the smaller taxa. Canines, on the other hand, show shallow and thin jaws [**4(1)**; 4(1)] that support the extended and relatively delicate premolar series. This latter condition [**7(1)**; 7(1)] is emphasized by the consistent separation of the premolars by diastemata, a derived feature in the Canidae, and a synapomorphy grouping all members of the Caninae.

In species of the more hypocarnivorous clades (species within *Urocyon* and *Otocyon* among the vulpines, and *Cerdocyon* and *Nyctereutes* among the Cerdocyonina) the digastric insertion on the ramus is enlarged to form a distinct process called the ''subangular lobe'' by Huxley (1880: 251). Within the *Urocyon* clade, the process is initially rounded in outline [**32(1)**; 24(1)], but in the most derived species it is angular in outline [**32(2)**] and sometimes bears a spine.

Primitively (in *Leptocyon* and all vulpines) the angular process of the mandible is slender, attenuated, and often terminates in a dorsal hook [**37(0)**; 38(0)]. Uniquely in the Cerdocyonina, the process is large, usually blunt, and lacks the dorsal hook, and the fossa for the inferior branch of the medial pterygoid muscle is large, often equal to or exceeding the size of the fossa for the superior branch [**37(1)**; 38(1)]. In members of the genus *Canis* the large angular process

shows a differential enlargement of the insertions of the medial pterygoid in which the fossa for the superior branch is enlarged and consistently exceeds the size of the fossa of the inferior branch [**39(1)**; 54(1)]. The morphology of the medial side of the canine angular process differs from the hesperocyonines (Wang, 1994: fig. 61) and especially most borophagines (Wang et al., 1999: 316) in which the ridge separating the fossae for the inferior and superior branches of the medial pterygoid is pocketed on its dorsal surface extending the superior insertion medially.

UPPER TEETH: Primitively the upper incisors of canids gradually increase in size from I1 to I3. In the Caninae their crowns are flattened cones bearing medial and lateral cusplets but lacking posterior cingula, and the I3 is a high cone with a medial cusplet (fig. 61). Members of the Vulpini and Canini are united by the lack of the medial cusplet on I3 [**23(1)**; 17(1)]. In the more derived *Urocyon* species the medial cusplets on I1–I2 are also weak or absent [**23(2)**; 17(2)]. The I3 is markedly larger than I1–I2 in the more derived members of *Canis*, and its posteromedial cingulum is present and often enlarged [**42(1)**; 53(1)].

Among the Caninae there are clades characterized by relatively small and more gently curved canine teeth [**31(1)**; 27(1)] in both sexes. This condition is present in hypocarnivores like the vulpines *Urocyon* and *Otocyon*, and the Cerdocyonina *Cerdocyon* and *Nyctereutes*, as well as in hypercarnivores like *Cuon*, *Lycaon*, and *Xenocyon* as well as the large *Canis* clade containing *C. armbrusteri* and its sister taxon *C. dirus*.

Primitive Caninae have upper and lower premolars that are narrow and elongated [**5(1)**; 6(1)] rather than relatively short as in hesperocyonines and borophagines. These teeth are set in slender, shallow jaws and are usually separated by diastemata in the character complex that typifies the Caninae as a whole. The Caninae shows loss of the posterior cusps of the premolars from the front to the back of the jaw. Primitively the P2 lacks this cusp and with further reduction within *Leptocyon* this cusp is lacking or very weak on P3 as well [**8(1)**]. This condition characterizes the Vulpini, but the primitive, well-developed cusp on P3 returns early in the *Canis* clade [coded as reversal, **8(0)**].

The upper carnassial, or P4, of canines retains the form common to most Caniformia. It is more elongate and narrower across the paracone, its anterior cingulum is weaker, and its protocone is smaller than in the Borophaginae [**11(1)**; 9(1)]. In the hypocarnivorous *Urocyon-Metalopex* clade the carnassial is slightly molarized, returning to an approximation of its primitive shape [thus coded as a reversal, **11(0)**]. Modification of the P4 protocone occurs within *Canis*, in which the primitive canid protocone that extends anterolingually beyond the anterior end of the paracone is shortened so that it is more lingual in position and does not extend beyond the paracone [**44(1)**; 39(1)]. A further modification of the P4 seen in *Canis armbrusteri* and *C. dirus* is the marked reduction in size of the protocone and its root [**55(1)**]. This reduction is seen in some other hypercarnivorous Carnivora, but curiously not in the canines *Xenocyon*, *Cuon*, or *Lycaon*, which otherwise are well-adapted hypercarnivores.

The primitive canid M1 is transversely elongate (i.e., transversely wide for its anteroposterior length), but in both hypo- and hypercarnivorous canines the transverse width is shortened so that it becomes narrow with regard to the length [**26(1)**; 30(1)]. Primitively the M1 has a well-developed labial cingulum bearing a prominent parastyle connected directly to the paracone by the preparacrista; the paracone and metacone are subequal in size; the lingual cingulum is complete across the protocone and often bears a small hypocone (or enlargement of the lingual cingulum) posterolingual to the protocone; and subequal para- and metaconules are differentiated from the pre- and postprotocristae. The Caninae shows changes in this form, including: enlargement of the size and differentiation of the M1 hypocone from the lingual cingulum [**1(1)**; 1(1)]; reduction of the parastyle while remaining connected to the paracone through the preparacrista [**3(1)**; 3(1)], or the preparacrista may shift anteriorly, losing its connection with the parastyle to reach a more lingual connection with the anterior cingulum [**3(2)**]; the labial cingulum becomes subdued and often incom-

plete across the paracone [**49(1)**; 46(1)]; the paracone is markedly enlarged relative to the metacone [**54(1)**; 45(1)]; the lingual cingulum becomes subdued and may be discontinuous across the protocone [**56(1)**]; the hypocone cusp and its containing cingulum become markedly reduced [**57(1)**; 44(1)] or absent [**57(2)**; included in 44(1)]; and the metaconule may be very weak or absent [**59(1)**]. Many of these features are paralleled by those of the M2, but its modification begins earlier in canine phylogeny; the M2 metaconule may be very weak or absent [**13(1)**] and the connecting postprotocrista may also be incomplete or absent [**15(1)**] as a correlated transformation.

LOWER TEETH: As in the examples discussed above, the primitive canine horizontal ramus is shallow and thin [**4(1)**; 5(1)]; the premolars, usually separated by diastemata [**7(1)**; 8(1)], are narrow and elongate [**5(1)**; 6(1)] and usually low-crowned, although in some clades (the hypocarnivorous *Urocyon* species and hypercarnivorous *Cuon* and *Lycaon* clade) these teeth are higher crowned, with their tips often lying at the same height [**28(1)**; 20(1)]. The lower canine may depart from its primitive laniary form and become shorter crowned and only gently curved [**31(1)**; 27(1)] in both hypo- and hypercarnivores. The lower premolars show reduction of subsidiary cusps in the Caninae, with the anterior cingular cusps being very weak to absent on p2–p4 [**14(1)**; 22(1)]. Only p4 consistently has a posterior cusp; that on p3 is usually absent [**6(1)**; 7(1)] except in the *Urocyon* species and in some species of *Canis*. Variably there is a second posterior cusp on p3 just anterior to the posterior cingulum [**63(1)**] in the sister taxa *Canis armbrusteri–C. dirus*.

Within *Canis* the crown base of p3 lies entirely below the base of the p4 crown [**45(1)**] and consequently the height of its principal cusp lies markedly below that of p2 and p4 [**43(1)**]. All Caninae above the South American Cerdocyonina have a p4 with a small second posterior cusp lying between the first posterior cusp and the cingulum [**38(1)**; 34(1)], and in the wolves (*C. lupus*) this cusp cannot be differentiated from the cingulum [**38(2)**], serving as an autapomorphy for that taxon. Additionally, the height of the principal cusp of p4 lies beneath that of the m1 paraconid [**46(1)**]. This feature characterizes the crown group of *Canis*.

The lower carnassial, or m1, like the occluding upper carnassial, provides many useful characters to cladistic analysis. The biomechanical interactions of this pair of teeth constrain the possible extent of morphological innovation in the Caninae, giving rise to considerable homoplasy that may confound use of these features in analysis. The principal divergence in form from the primitively open trigonid and bicuspid talonid [coded as m1 entoconid discrete, conical, or crestlike, **2(1)**; 2(1)] shared by borophagines and canines leads on the one hand toward hypocarnivory, with enlargement and elaboration of cusps of the talonid, and on the other toward hypercarnivory, with the narrowing of the talonid and reduction and loss of lingual cusps of the trigonid and talonid.

Initially, the lingual cusp of the talonid, the entoconid, is enlarged until its base coalesces with that of the hypoconid to block the talonid basin [**2(2)**; 2(2)]. The enlarged entoconid may be joined to the hypoconid by cristids from both cusps forming a transverse crest subdividing the talonid basin [**2(3)**; 2(3)]. We see state 3 in the derived *Urocyon* species and as a feature appearing early in the differentiation of *Canis* species. In hypercarnivores the entoconid is reduced relative to the hypoconid but retains the connecting cristid [**2(4)**] as in *Xenocyon*. Finally, in *Cuon* and *Lycaon* the entoconid is further reduced, often to a crest, lacks the cristid [**2(5)**], and essentially returns to the morphology of hesperocyonines. Conversely, the hypocarnivorous vulpines *Metalopex* and *Urocyon* add a protostylid to the trigonids of both m1 and m2 [**27(1)**; 28(1)], a feature also seen in *Nyctereutes*. A further elaboration of the talonid is the development of a hypoconulid shelf [**20(1)**; 13(1)], a posterior extension of the talonid in the region of the hypoconulid at the rear of m1 that may or may not include a discrete cuspid. This occurs just before the separation of the Vulpini and Canini. Later it is subject to some homoplasy involving reversal in both clades. It may be eliminated altogether as the talonid becomes functionally unicuspid in the most hypercarnivorous canines.

Associated with the reduction in the height of the principal cusp of p4, relative to that of the m1 paraconid, is the marked tendency for the anterior edge of the paraconid to be inclined posteriorly either in a linear or curved manner [**47(1)**]. These features appear to be correlated with the lingual shift in the orientation of the upper carnassial protocone [**44(1)**], which appears just in advance of these changes in the lower dentition and at the base of the clade containing the larger species of *Canis*. Hypercarnivorous large canines such as *Protocyon*, *Speothos*, *Canis dirus*, and *Xenocyon*, *Cuon*, and *Lycaon* species have greatly reduced or lost m1 and m2 lingual cusps in developing a nearly linear array of cusps anteroposteriorly along the molar row. We code this only as a great reduction of the m1 metaconid [**50(1)**; 42(1) in part] and its eventual loss [**50(2)**]. Associated with the latter features is the shift of the m1 hypoconid to a central or near central position on the talonid [**58(1)**] seen in the most hypercarnivorous taxa in the *Canis* crown group.

The m2 has some features of its own that are not correlated with the morphological changes of m1. These include the reduction of the paraconid, which becomes very weak or absent [**9(1)**] early in canine history; the size relationships of the protoconid and metaconid, including a metaconid taller than the protoconid [**30(1)**; 14(1)] or reduced relative to the protoconid [**30(2)**; 14(2)]; the relative proportions of the talonid vs trigonid, with the talonid being less than 90% of the length of the trigonid in primitive canines (most *Leptocyon* species) and more than 90% of the length of the talonid [**10(1)**] in the hypocarnivorous vulpines; and the degree of development of the anterolabial cingulum, which is weakly expressed primitively in the canines but becomes well developed, reaching the labial side of the protoconid [**16(1)**; 12(1)] in most canines above the basal species of *Leptocyon*.

The m3, primitively a single-rooted tooth, bears two trigonid cusps, usually identified as the protoconid and metaconid, connected by a transverse cristid. In the more derived species of *Canis* the metaconid is absent and the tooth becomes unicuspid with a protoconid centrally placed and often surrounded by a cingulum [**52(1)**]. In the hypocarnivorous *Metalopex* species the m3 is uniquely enlarged posteriorly by a shelflike cingulum [**51(2)**]. This tooth is lost altogether [**51(3)**; 51(1)] in the hypercarnivores *Speothos*, *Cuon*, and *Lycaon*.

POSTCRANIAL: A few postcranial elements were found to be useful in cladistic analysis and to be represented in more than 25% of the taxa coded. Above *Leptocyon*, the canines tend to lose the entepicondylar foramen of the humerus [**22(1)**; 16(1)] and to reduce the metatarsal I to a rudiment lacking phalanges [**21(1)**; 15(1)]. Cursorial canines increase the length of the radius relative to the tibia above the value of 80% that characterizes *Leptocyon* and the vulpines as well as most South American Canini (except, of course, *Chrysocyon*) and the stem canine *Eucyon*. A radius at least 80%–90% of the length of the tibia [**41(1)**] characterizes *Canis* species, with values greater than 90% [**41(2)**; 47(1)] found in the *Canis* crown group. The loss of the metacarpal I is found only in *Lycaon pictus* among living Caninae, although Rook (1994: 76) has claimed circumstantial evidence that the first metacarpal was ''vestigial if not absent'' in material referred to *Canis falconeri* from Italy. Details of the morphology of the front foot were not so widely observable among fossil taxa and hence this character was not utilized in the analysis.

CHRONOLOGY: In order to use chronological first occurrence to test the relative morphological order to taxa resulting from cladistic analysis, we added such data (character **64)** to the matrix. This was accomplished by transporting the MacClade program (versions of Maddison and Maddison, 1992) and manually searching the composite morphological and temporal data matrix for the shortest tree. The temporal units are defined in the ''Scope and Methods'' section of this work. The subdivisions used in table 2 are as follows: 1, Orellan; 2, early Arikareean; 3, medial Arikareean; 4, early Hemingfordian; 5, late Barstovian; 6, early Clarendonian; 7, late Clarendonian; 8, early Hemphillian; 9, late Hemphillian; A, early Blancan; B, late Blancan and late Pliocene; C, early Irvingtonian and early Pleistocene; D, late Irvingtonian and medial Pleistocene.

Phylogeny

In this study of the Canidae, we employ parsimony analysis of our morphological data as a starting point, not because we think that nature is inherently parsimonious, but because it provides the simplest explanation of the data with the minimum number of untested hypotheses. It is also well to remember that the cladistic analysis fundamentally depicts character resemblances in a hierarchy of acquisition of derived features. This hypothesis of polarity gives the cladogram an ascending trajectory and establishes a rationale for the hypothesis that the special morphological relationships among the taxa in question approximate an evolutionary pathway.

In addition to two canid outgroups (Hesperocyoninae and Borophaginae) represented by a composite of characters common to their stem taxa, we examine the relationships of 37 taxa, one of which is a monophyletic clade (''South American canids'', Tedford et al., 1995; subtribe Cerdocyonina, new taxon, this paper). Taxa subjected to analysis included those described in the systematic section of this report, for which at least 50% of the characters used in this analysis could be observed. Additionally, several Eurasian species of the *Canis* group were added to the matrix where they are represented by usefully complete material. Most of these species have been described and illustrated in the literature and many have been examined by us (sources of information on these taxa are brought together in appendix 1). The rationale for adding these forms lies in the recognition that the Pliocene–Pleistocene record of *Canis* is more completely represented in the much larger and more ecologically diverse Eurasian continent. Placing the North American history without this essential context would ignore the significance of Eurasia in the evolution of *Canis*.

Sixty-three morphological characters representing 143 character states were used in this analysis (table 1). The PAUP program (version 3.1.1 of Swofford, 1993) was used to search for the shortest trees, and the character support for each node was mapped using ClaDos (version 1.2 of Kevin C. Nixon). Analysis was initiated by heuristic search of the entire matrix (excluding *Urocyon webbi*, *U. galushai*, and *U. citrinus*, three species that are highly incomplete in the matrix), which yielded 249 trees of length 149, a strict consensus of which is shown in figure 62. The consensus tree contains a series of multichotomies bound together by dichotomous regions. Bootstrap analysis (100 replicates, heuristic search) was performed on a reduced data matrix that eliminated eight taxa. These taxa tended to reduce resolution in the initial PAUP analysis (fig. 62) and to make the bootstrap computation prohibitively expensive. Numbers at the nodes indicate percentage bootstrap support from a heuristic search based on 100 replicates (fig. 63). Only clades with a frequency of more than 50% are retained.

Further analysis involved using the branch-and-bound option of PAUP to explore segments of the tree to ensure that no shorter tree was missed by the heuristic search. We began with an examination of the relationships within the species of *Canis* beginning with *Canis arnensis* and ending with *Lycaon pictus* (*C. lepophagus* as an outgroup). This resulted in eight trees of 74 steps each, a consensus of which was identical in form to that found by heuristic search (fig. 64). A second run using the branch-and-bound option began at the vulpines and proceeded downward through the stem group (*Leptocyon* species). In this analysis *Vulpes stenognathus* was as often (50% of trees) attached to the Canini as to the Vulpini largely on the basis of its Canini-like frontal sinus (fig. 60B) and Vulpini-like large paroccipital process (the living species of *Vulpes* unequivocally lack the frontal sinus).

At this point the data were transported to the MacClade program (version 3 of Maddison and Maddison, 1992) so that relative stratigraphic data (last column in data matrix, 64 of table 2) could be incorporated to test the various arrangements within the multichotomy for the greatest congruence with stratigraphic occurrence. We manually searched the composite morphological and stratigraphical data matrix for the shortest tree among those suggested by the six most parsimonious trees in the *Canis* group based on morphology alone. The arrangement shown in figure 65 is the most congruent

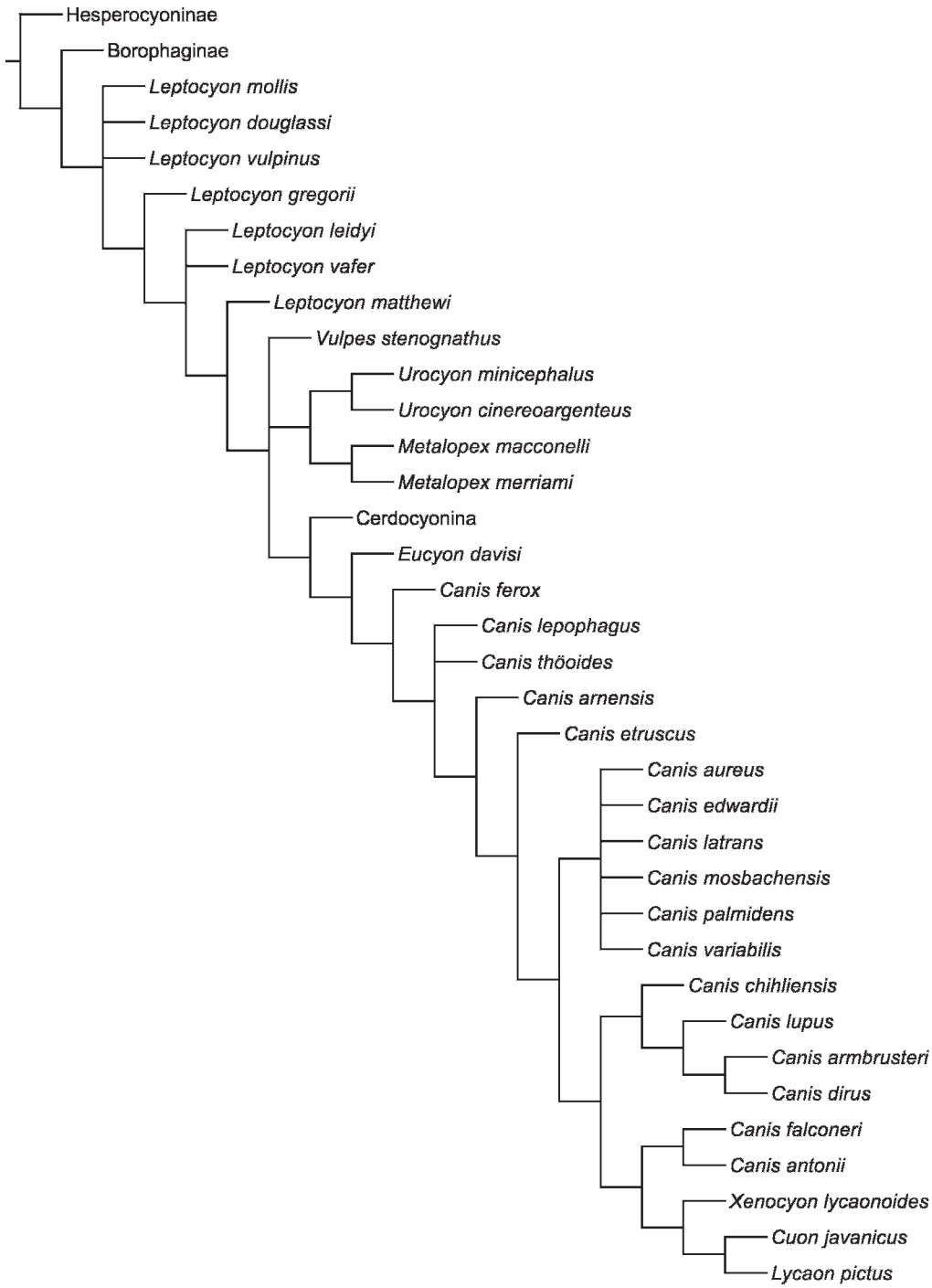

Fig. 62. Strict consensus of 248 shortest trees (length = 49) derived from heuristic search in the PAUP program. Data matrix of 36 taxa by 63 characters is derived from table 1 but excludes three poorly represented taxa, *Urocyon webbi*, *Urocyon galushai*, and *U. citrinus*, and one character (number 64), the stratigraphic character. All characters are unordered and unweighted.

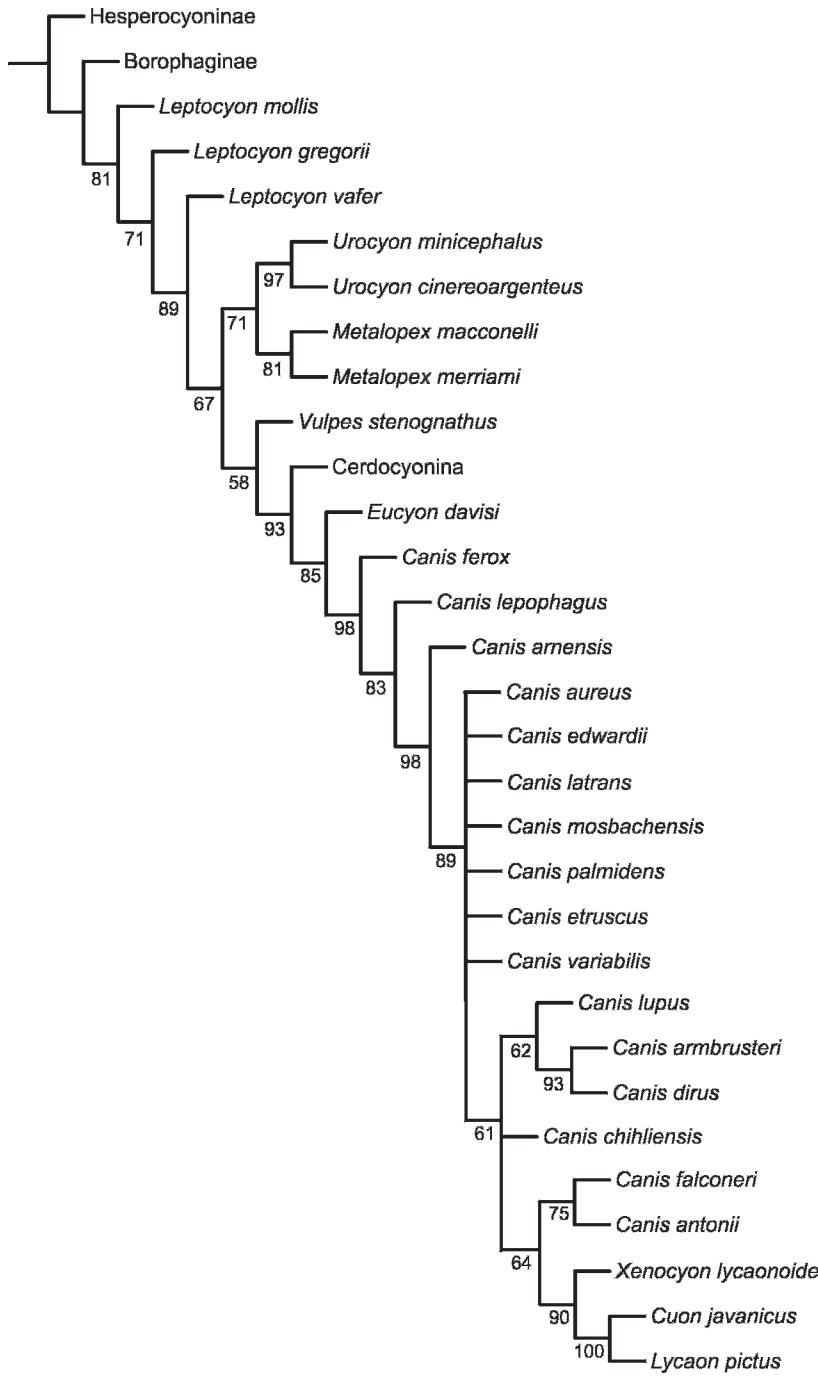

Fig. 63. Bootstrap analysis using the PAUP program on a subset of the data matrix in table 1 (8 taxa excluded: *Leptocyon douglassi*, *L. vulpinus*, *L. leidyi*, *L. matthewi*, *Urocyon webbi*, *U. galushai*, *U. citrinus*, and *Canis thöoides*; stratigraphic character excluded). Numbers to the left of the nodes indicate the percentage of bootstrap support from heuristic search of 100 replicates. Only nodes with a frequency of greater than 50% are retained.

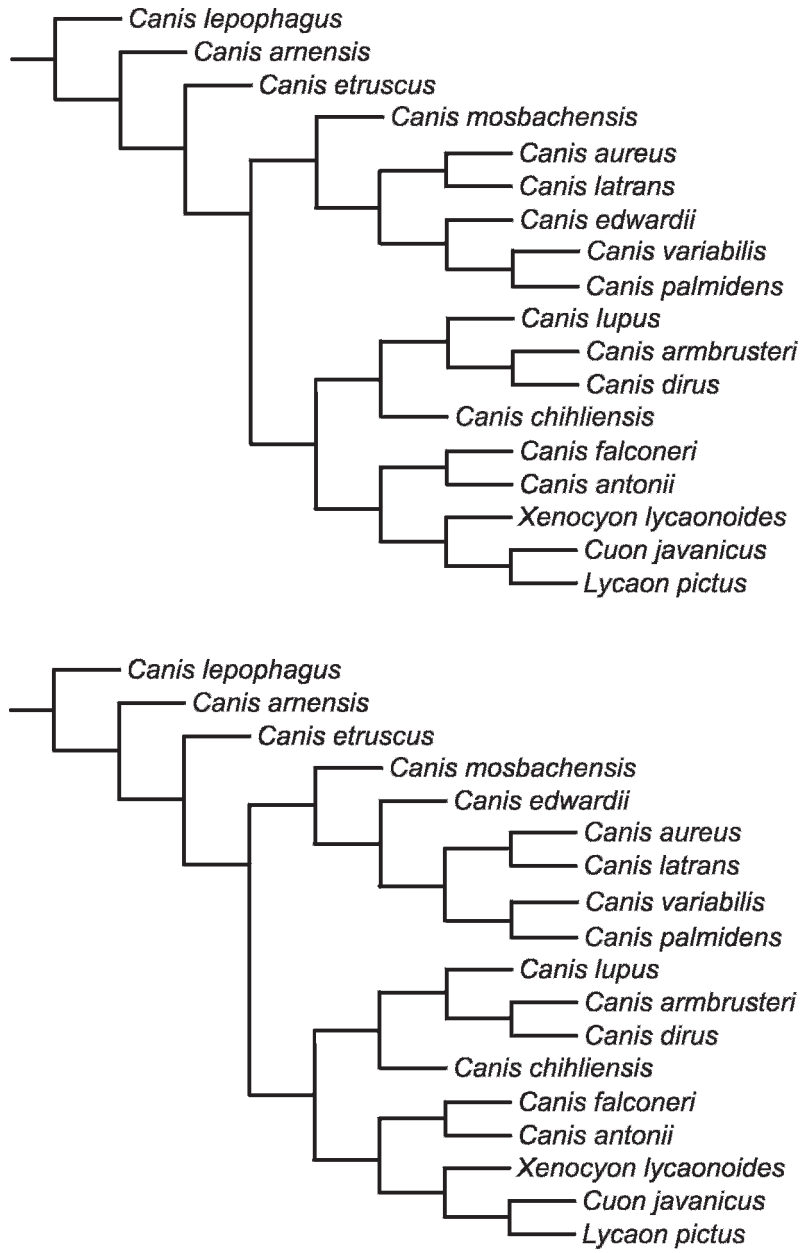

Fig. 64. Two of the eight trees found by the branch-and-bound search option in the PAUP program on a subset of the data matrix (table 1) consisting of the species of *Canis* used in this analysis. These two trees are the most resolved topologies, with the rest having at least one unresolved node. The upper tree is preferred when the stratigraphic characters are taken into consideration (see below).

between morphological and stratigraphical data with a new length of 185 steps (157 steps if the stratigraphic character is not counted).

We reaffirmed the phyletic relationships of the outgroup subfamilies (Hesperocyoninae and Borophaginae), their relationship to the Caninae, and support for the latter as a monophyletic group in more detail elsewhere (Wang, 1994; Wang and Tedford, 1994, 1996; Wang et al., 1999). Three characters define

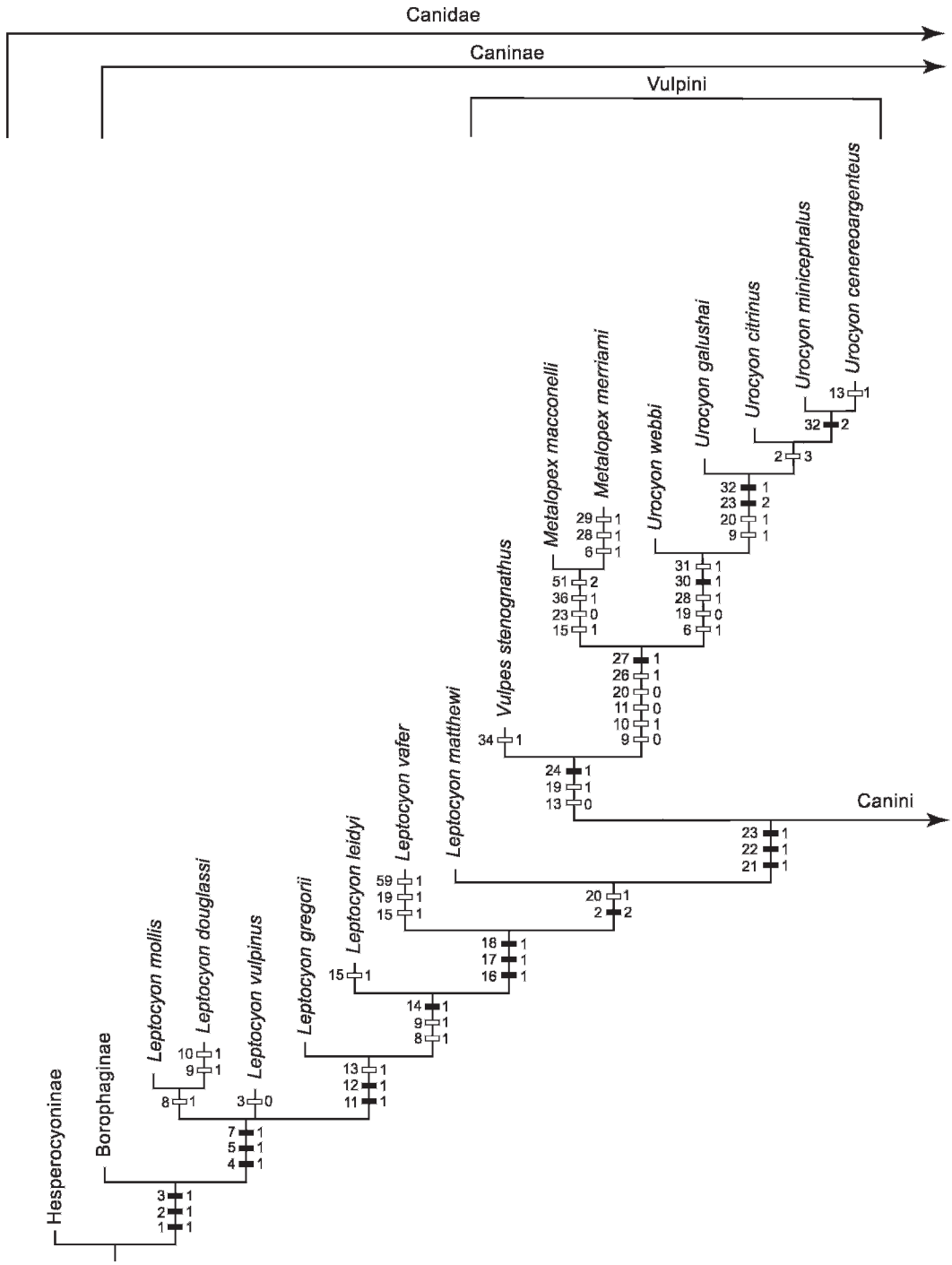

Fig. 65. Proposed cladogram for the subfamily Caninae, derived from combined analyses of morphology (PAUP analysis) and stratigraphy (manual search in MacClade program). Character distributions are mapped by ClaDos program (version 1.2 by Kevin C. Nixon), and all characters are unordered and unweighted. *Leptocyon tejonensis*, *Vulpes kernensis*, and *Metalopex bakeri* are omitted.

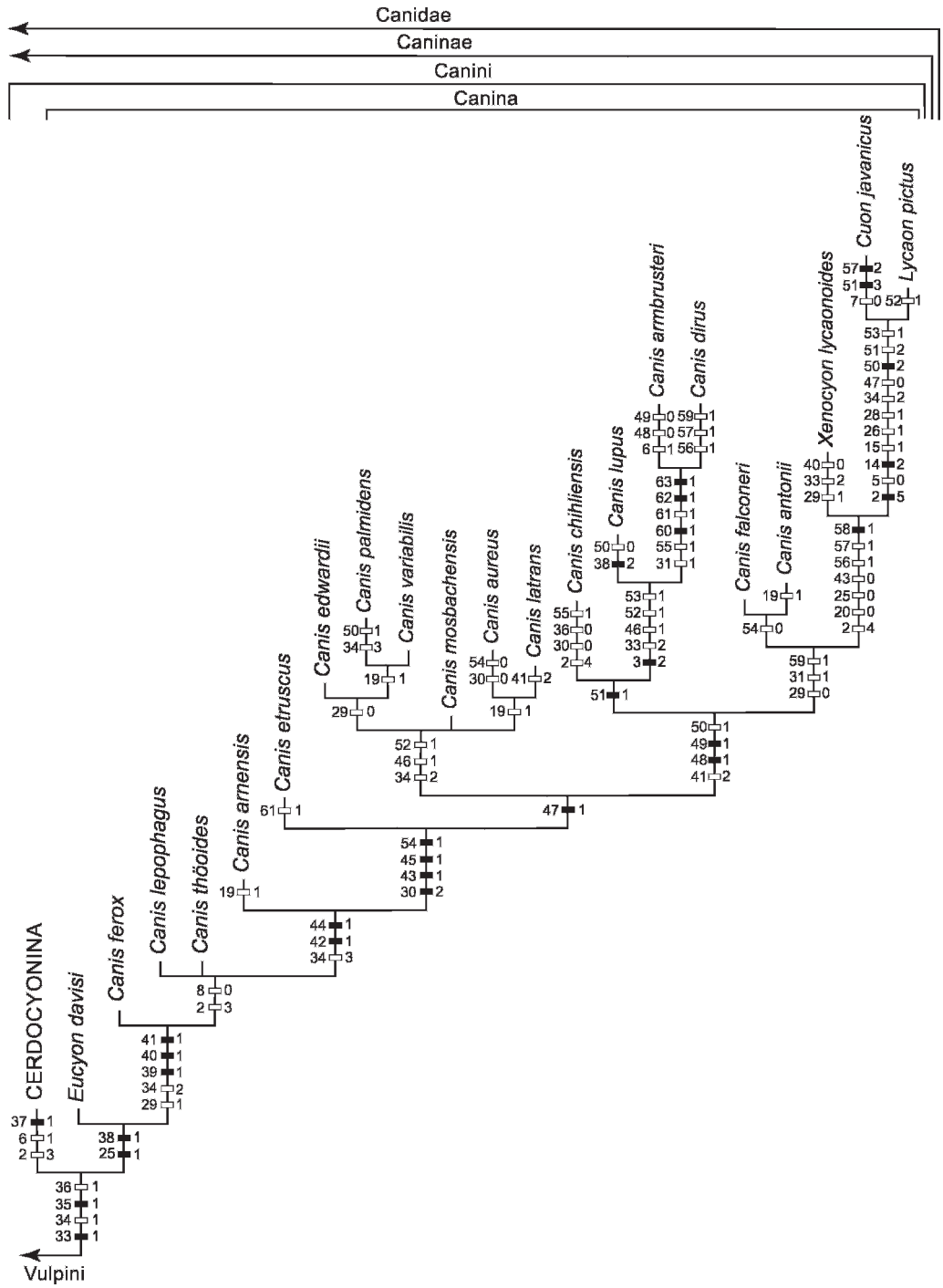

Fig. 65. *Continued.* Numbers above the branches represent characters and those below represent character states (all numbers correspond to those in table 1; character 64, the stratigraphic character, is not mapped in this tree). Solid boxes indicate synapomorphies and empty boxes indicate homoplasies (parallelisms or reversals). Tree statistics: length, 157; consistency index, 51; retention index, 84.

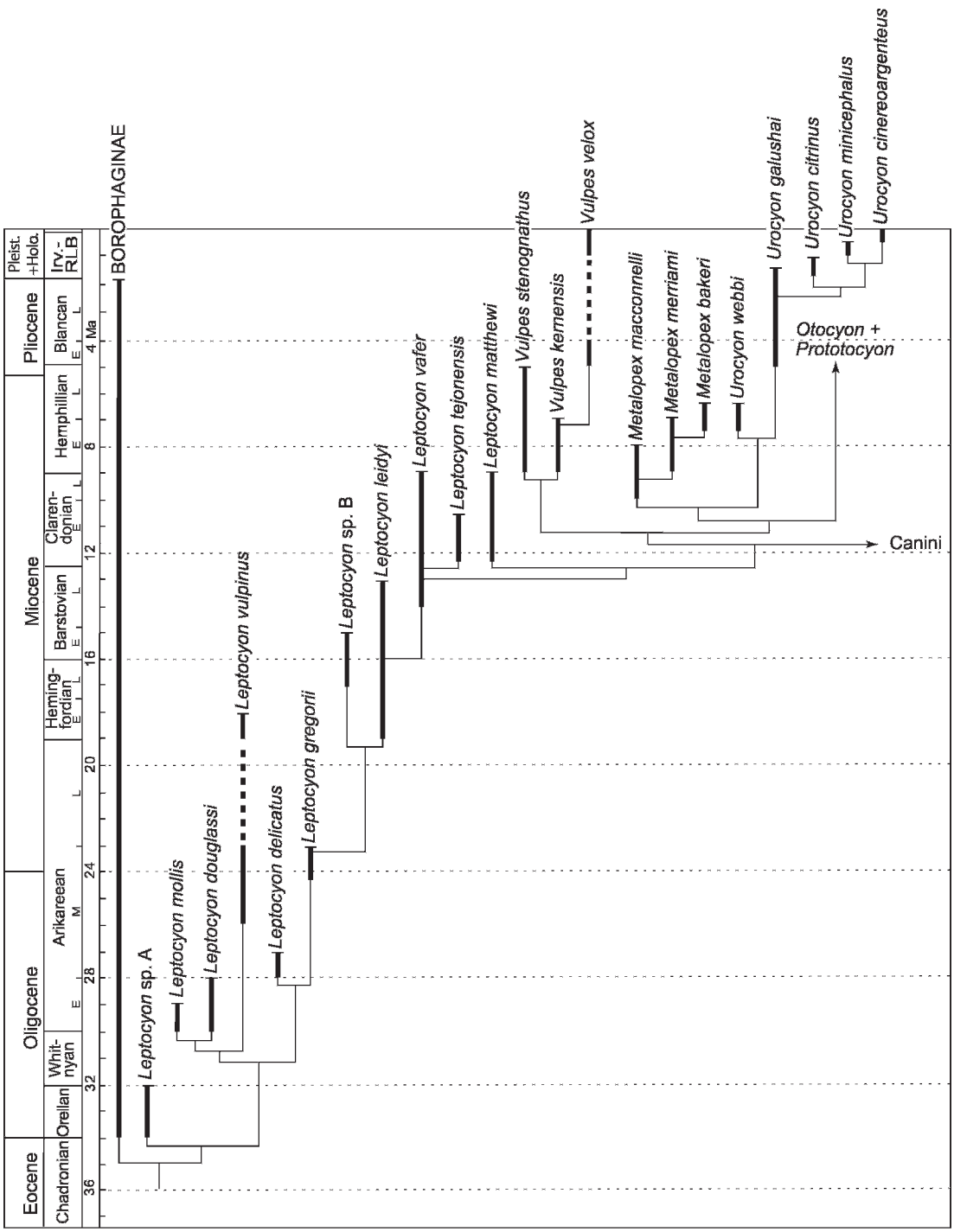

Fig. 66. Stratigraphic ranges and postulated phyletic relationships for taxa of the subfamily Caninae discussed in this report. The relationship is largely based on the preferred cladogram in figure 65, modified by speculations about cladogenetic or anagenetic events. These speculations are based on morphologic features too subtle to be coded in the data matrix but which, nonetheless, offer clues about possible relationships.

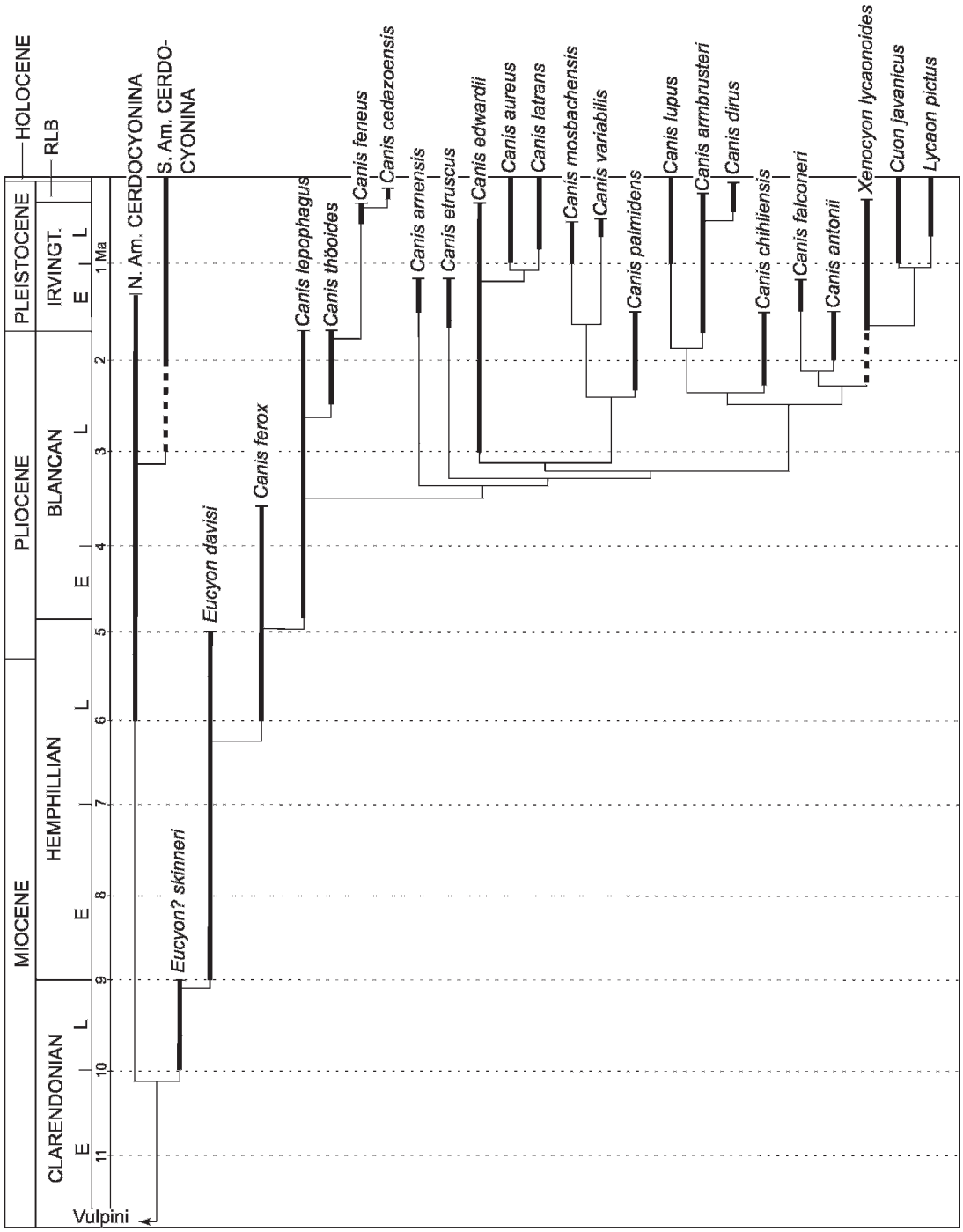

Fig. 66. *Continued.* Taxa that are too poorly known to be included in the phylogenetic analysis are also plotted on this chart. Chronologic framework is based on Tedford et al. (2004). Geographic range changes of Cerdocyonina are shown that schematically reflect dispersal to South America and extinction in North America.

the basal taxa of the Caninae: the shallow ramus, narrow and elongate premolars, and the presence of diastemata between these teeth. As in the borophagines, the basal taxa form a multichotomy, partly the result of the incompleteness of their remains, but possibly also the presence of few synapomorphies that would resolve their relationship. *Leptocyon mollis* and *L. douglassi* are weakly united by the loss of the posterior cusp on P3. Retention of primitive features of the Canidae is shown by *Leptocyon vulpinus* with its large M1 parastyle and well-developed preparacrista. Additional bushiness is hinted at by taxa not complete enough for cladistic analysis (see fig. 66A): the diminutive *Leptocyon delicatus* and *Leptocyon* sp. B, and especially *Leptocyon* sp. A, the oldest canine, which shares the morphology of its lower carnassial with the borophagines.

Above this level *Leptocyon* species have a more resolved pectinate relationship. *Leptocyon gregorii* lies between the basal multichotomy and younger *Leptocyon* species. *Leptocyon leidyi* and *L. vafer* share the loss of the postprotocrista as well as the metaconule on M2, features that unite them in some cladograms. However, *Leptocyon gregorii* through *L. matthewi* can also be resolved in pectinate order that correlates with their relative geological ranges. Missing data for the upper incisors and postcrania of *L. matthewi* allow that taxon to be a part of the quadrichotomy of the Vulpini and Canini (fig. 62) under the assumption that it possesses derived states of these features, but in the resolved cladogram (fig. 65) this taxon assumes a position below the major tribal dichotomy. The limited data available for *L. tejonensis* would place it in a position between *L. vafer* and *L. matthewi*. As mentioned, the relationship of the fossil *Vulpes*, *V. stenognathus*, is complicated by the presence of a frontal sinus in an otherwise vulpine taxon. In this case we have chosen to ally *Vulpes stenognathus* with the living *Vulpes* species and regard the sinus as an autapomorphy acquired independently of the Canini.

The clade containing *Metalopex* and *Urocyon* species is well differentiated from other vulpines and maintains its integrity even in the consensus tree (fig. 62). Despite this, it has been difficult to resolve the total array of species assigned to the clade largely because one-third are known from limited evidence (at the 40% level of completeness or below). However, some estimation can be made of the possible relationships of *Urocyon webbi*, *U. galushai*, and *U. citrinus*, as they show a relative temporal sequence of development of the subangular lobe characteristic of *Urocyon*.

As a consequence of the history of the Caninae, nearly half of the species dealt with in this report belong to the tribe Canini and most of these to the genus *Canis*. The late Miocene to Recent diversification of this group is largely the result of the enormous increase in their geographic range during this span. While endeavoring to focus on the North American record, we have also explored the rooting of the South American clade (Cerdocyonina, new subtribe, previously analyzed by Tedford et al., 1995) by incorporating the perspective of the fossil record. This clade consistently stands in sister relationship to *Eucyon* plus the *Canis* group in the consensus and in more resolved trees.

It appears that species of the genus *Eucyon* are more diverse in Eurasia than in North America, and species of the genus continue into the Pliocene there (Tedford and Qiu, 1996; Rook, 1992). We treat the *Eucyon* clade as monophyletic, as the Eurasian species give no evidence of a special relationship to *Canis*. *Eucyon davisi*, the most completely represented species in that genus, is consistently placed in a sister relationship with the species of *Canis* rather than at the base of the Canini. It lies in a dichotomous region beneath the first multichotomy of *Canis* species. *Canis ferox*, the most primitive member of the genus, is defined by posterior enlargement of the fossa on the angular process for the superior branch of the medial pterygoid muscle; lengthening of the radius in comparison with the tibia; and loss of a prominent lateral process of the nuchal crest so that the supraoccipital shield assumes a more triangular form when viewed from the rear. Above this level lie taxa with the m1 hypoconid and entoconid consistently joined by cristids and having a posterior cusp on P3 (a reversal). Two taxa stand at this node, both of North American occurrence and

presumed origin: *C. lepophagus* and *C. thöoides*.

Above the initial multichotomous region lie two contemporary European taxa, *C. arnensis* and *C. etruscus*, that record important steps in the evolution of the frontal sinus and dentition that characterize higher *Canis* species: extension of the frontal sinus to the frontoparietal suture, enlargement of the I3 relative to I1–I2, and lingual orientation of the protocone of P4 occur at the *C. arnensis* node; significant reduction of the metaconid of m2; the principal cusp of the p3 lies below that of p2 and p4; and marked enlargement of the paracone of M1 relative to the metacone occurs at the *C. etruscus* node. Higher in the *Canis* clade, at the base of the upper multichotomy (fig. 65), the medium-sized *Canis* species of the multichotomy are nearly resolved by single characters mediated by their stratigraphic relationships. Above this, the crown group (*Canis chihliensis* through *Lycaon pictus*) is defined by two dental characters that signal the hypercarnivorous nature of this clade (reduction of the labial cingulum of M1, and reduction of the metaconid of m1), in addition to further elongation of the radius and a wider palate. The crown group is characterized by taxa that show acquisition of the dental characters typical of hypercarnivory coupled with a marked tendency for reversal of many of the derived features acquired earlier in the *Canis* clade. However, the presence of nonhomoplastic features gives the branches of the crown group strong support leading to their integrity even in consensus trees (fig. 62) involving the entire data set utilized here.

DISCUSSION AND CONCLUSIONS

To present our summary of the evolutionary history of the Caninae we have redrafted the cladogram onto a time scale and shown the known chronologic ranges of the taxa subjected to phyletic analysis as well as those too incomplete for such treatment (fig. 66A–B). These transformations yield hypotheses of the evolution of the Caninae and in so doing introduce more subjective elements than allowed in the parsimony-directed dichotomous format of the cladogram. Statements about anagenetic as well as cladogenetic relationships can be presented when such conclusions are permitted by the morphological evidence. We will discuss the history of the Caninae in these terms in the text that follows.

The incomplete evidence at hand points to an origin of the Caninae at the beginning of the Oligocene, more or less coincidental with that of its sister taxon, the Borophaginae (Wang et al., 1999), whose first appearance was also obtained from the Brule Formation of the northern Great Plains. The single ramal fragment of *Leptocyon* sp. A shows only the characteristic jaw and premolar features of the Caninae. Its carnassial bears a bicuspid talonid, but otherwise this tooth, by itself, cannot be unequivocally assigned to the Caninae.

The record is discontinuous above this single Orellan occurrence but resumes in the early and medial Arikareean of northern regions of the United States where the appearance of taxa gives evidence of unrecorded cladogenesis in the early Oligocene. A similar gap in the record is shown by the Borophaginae. Some of these canines retain primitive features, shared with the hesperocyonines, that were otherwise lost prior to the Miocene. Early in this history we see two size groups among the *Leptocyon* species: *L. delicatus* is half the size of *L. gregorii*.

The record in the Great Plains resumes in the early Hemingfordian with *L. vulpinus*, as a holdover taxon, joined by *L. leidyi*. We show the latter arising directly, and possibly anagenetically, from *L. gregorii*, as permitted by the structural sequence in our cladistic analysis and the lack of autapomorphies visible in the latter. Likewise, *L. leidyi* and *L. vafer* are linked in sharing the loss of the metaconule and postprotocrista on M2. Again a small taxon, *Leptocyon* sp. B, partially overlaps *L. leidyi*. We regard these small forms as independent cladogenetic events rather than evidence of a lineage of small taxa, largely because they seem morphologically close to their larger partners.

With *L. leidyi*, and especially *L. vafer*, the geographic range of *Leptocyon* species broadens to include the Great Basin of California, Nevada, and New Mexico. Unlike the borophagines, species of *Leptocyon* have not been recorded on the East and Gulf

coasts of the United States. At no time in this long span from Oligocene through early Miocene are there more than four contemporary species of *Leptocyon* known and none shows adaptations beyond that of mesocarnivorous small canids, in contrast to the great cladogenetic and adaptive breadth achieved by the borophagines over the same span (Wang et al., 1999). However, there is clear evidence of major cladogenetic events in the late Barstovian and Clarendonian. The final steps in the evolution of *Leptocyon* take place during this span with the appearance of *L. matthewi*, which in the morphology of its m1 talonid has a link to the Vulpini. Likewise, the premolar morphology of the small *L. tejonensis* foreshadows trends in the hypocarnivorous Vulpini.

The earliest known hypocarnivorous lineage in the Caninae appears in the late Clarendonian, along with the earliest species that mark the origin of components of the modern Vulpini. The oldest vulpine is a species of the extinct genus *Metalopex*, *M. macconnelli*, that first appears in the late Clarendonian of the Great Basin of California, Oregon, and Arizona. By early Hemphillian time, *M. merriami* and *M. bakeri* show that species of this genus have spread eastward into the Great Plains. *Urocyon*, the genus containing the living gray fox, appears in the Hemphillian of Florida as *U. webbi*, but its sister relationship with *Metalopex* implies a similar Clarendonian time of origin for both groups and for the Vulpini as a whole. The fossil record of *Urocyon* species shows that they have not moved significantly outside of the southern North American range containing the living races of *Urocyon cinereoargenteus*.

In our analysis of living canids (Tedford et al., 1995) we postulated that the living African bat-eared fox, *Otocyon megalotis*, was a sister taxon of *Urocyon cinereoargenteus*. Fossil evidence from India and Africa shows that this clade can be traced into *Prototocyon* Pohle, 1928 (nec *Sivacyon* Pilgrim, 1929; *P. recki* Olduvai Bed I, and possibly *P. curvipalatus* Bose, 1880, Upper Siwalik, but see Petter, 1964: 342), of the late Pliocene. *Prototocyon* species show the trend toward molarization of P4/p4 and modification of the molars in the direction of the singular dentition of *Otocyon*, including a small M3, but they lack the subangular lobe of the lower jaw (Petter, 1964).

Early in the North American record of *Vulpes* two species are evident, a red fox-sized form, *V. stenognathus*, and a swift fox-sized taxon, *V. kernensis*. The large form does not appear to continue into the Pliocene of North America, but rare remains of a smaller taxon (or taxa), grouped in this work as *Vulpes* sp. cf. *V. velox*, range from the early Blancan to Recent, especially in the mid-continent where swift foxes have their present distribution. Foxes of this size and morphology are also widely known in the Eurasian fossil record (*Vulpes praeglacialis* Kormos, 1932, is closely similar). Larger foxes reenter mid-continent North America only in the late Rancholabrean (last glacial cycle) when *Vulpes vulpes* becomes part of the fauna (Kurtén and Anderson, 1980).

Molecular estimates of divergence of the *Vulpes* and *Urocyon* clades (Bininda-Emonds et al., 1999) at 8.4 Ma (9.5 Ma in Wayne et al., 1997) are slightly younger than ours, which includes the extinct *Metalopex* at 11–12 Ma (fig. 66A). Since the Vulpini and Canini, as recognized here, are sister taxa, the fossil record permits an estimation of this divergence close to 12 Ma, in agreement with the estimate of Bininda-Emonds et al. (1999) at 12.5 Ma for the origin of living canids.

The South American Canini (subtribe Cerdocyonina) includes the most primitive members of the tribe Canini. Members are represented by North American records attributed to *Cerdocyon* (*C. texanus*) in the earliest Pliocene (late Hemphillian), *Chrysocyon* (*C. nearcticus*) in the early Pliocene (early Blancan), and possibly *Theriodictis* (*T.? floridanus*) in the early Pleistocene. As these taxa represent crown elements within the South American clade (Tedford et al., 1995), their appearance predicts the presence of the so far undiscovered stem taxa in North America before the emergence of the Isthmus of Panama in the medial Pliocene (Keigwin, 1978). The robust placement of the South American clade and *Eucyon davisi* as sister taxa (fig. 63) also predicts that these two groups are equally ancient, diverging before the beginning of the Hemphillian, early in late Miocene time at least 4 m.y. prior to the

appearance of the earliest member of the South American clade in the fossil record (fig. 66B).

The occurrence in the Pliocene of Eurasia of species that are traditionally placed in *Nyctereutes*, the sister taxon of *Cerdocyon*, suggests a wider unrecorded geographic range for taxa that have affinity with *Cerdocyon* in the Northern Hemisphere (Tedford et al., 1995). *Nyctereutes donnezani* (Deperet, 1890–1897) from Perpignan, France, and *N. tingi* Tedford and Qiu, 1991, from Yushe, China, are closely similar in morphology. Material attributed to *N. donnezani* has been obtained from deposits of early Pliocene age (the type locality and the Layna fissures of Spain are both ca. 4.0 Ma; Soria and Aguirre, 1976), whereas the Chinese counterpart (*N. tingi*) is known from the latest Miocene to medial Pliocene (5.5–3.0 Ma; Tedford and Qiu, 1991). Taxa clearly attributed to *Nyctereutes* sensu stricto (*N. megamastoides* and *N. sinense*) first occur in the medial Pliocene in Eurasia but in China they co-occur in the same deposits with the plesiomorphic *N. tingi* beginning in the early Pliocene. A phyletic relationship between *N. donnezani* and *N. megamastoides*, as envisioned by Soria and Aguirre (1976), is supported by their morphological, geographical, and temporal affinities. Lacking evidence of *Nyctereutes* in North America, we see paleontological support for the origin of *Nyctereutes* in Eurasia.

The poorly known *Eucyon*? *skinneri* seems best compared with *E. davisi* and probably lies close to the point of origin of *Eucyon*. We postulate an anagenetic relationship of *skinneri* and *davisi* and extend the range of *Eucyon* into the late Clarendonian on this evidence (fig. 66B). *Eucyon davisi* has a long late Miocene range in North America, but gives rise to species of *Canis* toward the end of its span, coexisting with them for a short time at the end of the Hemphillian. Surprisingly, Tedford and Qiu (1996) found *E. davisi* in the medial Pliocene of China and realized that the genus includes a taxon previously referred to *Nyctereutes donnezani* from late Miocene deposits at Venta de Moro, Spain (Morales and Aguirre, 1976), as well as a related Italian late Miocene species, *E. monticinensis* (Rook, 1992), and a closely related Ukrainian Pliocene form, *E. odessana* (Odintzov, 1967). Other north China Pliocene species, *Eucyon zhoui* Tedford and Qiu, 1996, and *E. minor* (Teilhard de Chardin and Piveteau, 1930), suggest an adaptive radiation within the genus during the early Pliocene in Eurasia well after its extinction in North America.

The earliest record in Eurasia of putative *Canis* is in the Teruel Basin of central Spain in deposits of Turolian age (late Miocene) between 8.2 and 7.1 Ma (Steininger et al., 1996). Our knowledge of the enigmatic "*Canis*" *cipio* (Crusafont-Pairó, 1950) is limited to the holotype maxillary fragment with P3–M2 from Concud and a referred lower carnassial from the Los Mansuetos site (Pons-Moya and Crusafont-Pairó, 1978). This is a coyote-sized member of the Canini, relatively primitive in morphology in terms of the characters used here for phyletic analysis: the P3 has a large but low posterior cusp [our character code 8(0)]; P4 has a small, anterolingually directed protocone that just extends beyond the anterior border of the paracone [44(0)]; the M1 has a continuous lingual cingulum [49(0)] that terminates at the large metaconule; the paracone is not markedly enlarged relative to the metacone [54(0)]; M2 is not strongly reduced in size relative to M1 and, although worn, it appears to have a postprotocrista [15(0)], but may not have a metaconule [13(1)]. The paraconid of the lower carnassial curves backward [47(1)], but the talonid cusps are not united by a transverse cristid [2(2)]; the metaconid is not greatly reduced [50(0)]; the entoconid is large and placed opposite the hypoconid, and there is a hypoconulid shelf [20(1)]. The characters displayed by the upper dentition suggest that the holotype of "*Canis*" *cipio* lies at the base of the stem group of *Canis* species or below. Except for the curving face of the paraconid, the morphology of the lower carnassial lies in approximately the same phylogenetic position. The lack of cristids connecting the talonid cusps would relegate "*C.*" *cipio* to the level of *Eucyon*. Rook (1992) questioned the placement of *cipio* in *Canis*, but did not offer an opinion about its affinities. Previous describers of "*C.*" *cipio* (Crusafont-Pairó, 1950; Pons-Moya and Crusafont-Pairó, 1978) have unquestionably assigned it to

Canis and regarded it as ancestral to such Pleistocene forms as *C. etruscus*.

The earliest North American record of *Canis* is that of *C. ferox* Miller and Carranza-Casteñeda, 1998, from terminal Miocene (late Hemphillian) deposits of the southwestern United States and Mexico. During the latest Miocene or earliest Pliocene, cladogenesis within *Canis* in North America gave rise to the geographically widespread *Canis lepophagus*, whose close morphological relationship with *C. ferox* suggests a phyletic origin within the latter as shown in figure 66B. Toward the end of the Blancan (late Pliocene), we postulate that *C. thöoides* arises, beginning a lineage of small jackal-like taxa that are very rare in the fossil record but seem to continue into the medial (*C. feneus*) and late Pleistocene (*C. cedazoensis*) in the Great Plains and central Mexico.

During the medial Pliocene, between 3 and 4 Ma, *Canis* species extended their geographic range to Eurasia, opening a vigorous episode of cladogenesis, the earliest manifestation of which is visible in eastern Asia during the Nihewanian mammal age (ca. 2.5–2.0 Ma) and later in Europe in the late Villafranchian (ca. 2.0–1.0 Ma). In the early Pleistocene of Europe *Canis arnensis* and *C. etruscus* retain evidence of the steps in the transformations that lie in the early phase of this Plio-Pleistocene cladogenetic event, particularly the posterior expansion of the frontal sinus and modifications along the whole dental battery.

Above this pectinate region of the phylogeny, *Canis edwardii* and its living sister taxa, the golden jackal, *C. aureus*, and coyote, *C. latrans*, form a small clade showing some reversals and precociously derived states for characters that appear later in the crown group. *Canis edwardii* is the earliest occurring taxon in this clade, ranging from the mid-Blancan (late Pliocene) to the close of the Irvingtonian (late Pleistocene) exclusively in North America. It is tempting to regard this taxon as a North American autochthone with an origin in *C. lepophagus* as proposed by Kurtén (1974, although he used the nomen dubium *C. priscolatrans* for *C. edwardii*) in his history of the "coyote-like dogs."

The *Canis edwardii* clade is weakly held together by a reversal in the otherwise orderly increase in size of the frontal sinus. Likewise, the golden jackal and coyote are held together by the common possession of relatively short nasal bones, a feature that has proved to be highly homoplastic so that the assumption of synapomorphy in this instance is weak. Nevertheless, it is interesting to consider a linkage of *C. edwardii* and *C. latrans* as envisioned by Kurtén (1974). Coyotes indistinguishable from *C. latrans* first appear in North America at the close of the Irvingtonian where they are contemporaneous with *C. edwardii* and occur over much of the same geographic range. A possible phyletic origin of the coyote from *C. edwardii* in the New World has some support in this analysis and should be further tested.

The golden jackal, *C. aureus*, is the only smaller *Canis* species with a geographic distribution both in Asia and Africa. The morphological relationship with the African jackals was not explored in this work. However, molecular studies (Wayne et al., 1997; Zrzavý and Řičánková, 2004) group the golden jackal more closely with the coyote (and wolf) than with other jackal species, suggesting some phyletic diversity within the jackals and calling into question assumptions of their monophyly.

The *C. edwardii* to *C. latrans* clade (fig. 65) is held together by three synapomorphies, all of which represent features that appear elsewhere in the cladogram. Resolution within this clade is minimal. The contained taxa form a multichotomy in the initial shortest tree (fig. 62), although analysis of the crown group of *Canis* does present some fully resolved (fig. 64) arrangements, one of which we have chosen as plausible based on single synapomorphies (fig. 65). In the more subjective arrangement of figure 66B we have used zoogeography to group the Eurasian small wolves as a sister taxon of *C. aureus* and the New World *Canis* (*C. edwardii* and *C. latrans*). The association of the Eurasian small wolves (*C. mosbachensis*, *C. variabilis*, and *C. palmidens*) is favored mostly by zoogeography and overall morphological similarity that invites hypotheses of close, if not conspecific, relationship (see remarks, appendix 1, *C. variabilis*).

The crown group of *Canis* is made up of large wolflike species showing hypercarnivorous dental trends, including a clade that is particularly marked by those features. Within this group two clades are supported by parsimony analysis (fig. 63). One clade contains *C. lupus* and fossil sister taxa, and the other contains *Xenocyon* and the living hypercarnivores *Cuon* and *Lycaon*.

Canis armbrusteri is the earliest member of the *lupus* clade to appear in North America. It enters the fossil record at the beginning of the Irvingtonian (earliest Pleistocene) in the southwest United States and expands to the northeast by the late Irvingtonian. It is displaced from much of its range by its sister taxon *C. dirus* in the late Irvingtonian, but continues just into the early Rancholabrean in the eastern part of the United States. The appearance of *C. armbrusteri* in mid-latitude North America is considered an allochthonous element in the canid fauna accompanying the contemporary appearance of *Mammuthus* species near the beginning of the Irvingtonian. In China the Pliocene wolf *C. chihliensis*, a sister taxon of the *lupus* clade, may have been the Old World source for *C. armbrusteri* and *C. lupus*.

There is good evidence of the evolution of *Canis dirus* from *C. armbrusteri* in mid-latitude North America. These taxa share a number of synapomorphies, which suggests an origin of *C. dirus* in the late Irvingtonian, probably in more open terrain in the mid-continent, and subsequent range extension to the east displacing *C. armbrusteri*. In South America (Berta, 1988) *C. dirus* appears in Lujanian (late Pleistocene) coastal sites in the northwestern part of the continent and is probably represented in the southern part by *C. nehringi*, a taxon we cannot clearly separate from *C. dirus*. The older Pleistocene (Ensenadan) member of this clade, *C. gezi*, known only from a single Argentine specimen, is not referable to *C. dirus*. Its presence suggests some diversification of large *Canis* in southern South America.

Canis lupus appears toward the end of the medial Pleistocene in Europe (*C. lupus lunellensis* Bonifay, 1971), but not until the latest Pleistocene (late Rancholabrean) in mid-latitude North America. In arctic Beringia the early to medial Pleistocene Olyor Fauna of Siberia and its correlate in Alaska (Cripple Creek Sump Fauna) contain an older record of *Canis lupus*, pointing to the origin of wolves in Beringia perhaps in coevolution with the large ungulate assemblage of the arctic biome. Wolves seem to have invaded mid-latitudes of North America, as did many of their prey, the large Beringian ungulates, only during the last glacial cycle when they became characteristic elements of the Rancholabrean and living fauna.

Large canines appear in the medial and late Pliocene in eastern Asia (Nihewanian) and as allochthones in the early Pleistocene of Europe (the ''wolf event'' of the early late Villafranchian). These animals form a clade characterized by hypercarnivorous dentitions that culminate in taxa representing the extremes of this adaptation among the Caninae, comparable to the Aelurodontina within the Borophaginae. Curiously, this clade is distinguished by reversals to the primitive state in 8 of the 27 characters (30%) used to define nodes among the five taxa. Two-thirds of these reversals are unique to this clade and thus appear to be true reversals that behave robustly in parsimony analysis. Rook (1994) recognized the essential unity of this clade as ''*Canis* (*Xenocyon*) ex gr. *falconeri*'', even suggesting a possible derivation of *Lycaon* within it. Our analysis also indicates the sister taxon relationship of *C. falconeri* and *antonii*. Cranially and dentally these taxa are so closely related that they may only represent geographic varieties within a single species. *Canis antonii* is a late Pliocene to early Pleistocene (Nihewanian) taxon in Asia, whereas *C. falconeri* occurs abruptly (the ''wolf event'') in Europe at ca. 1.6 Ma in the early Pleistocene (late Villafranchian; Turner, 1990), perhaps representing a marked westward range extension.

Underlining the importance of eastern Asia in the evolution of large hypercarnivorous taxa is the appearance of species of *Xenocyon* in the medial Pliocene of China. The union of *Xenocyon lycaonoides* with *Cuon* and *Lycaon* is robustly supported by dental characters related to their hypercarnivorous adaptation, especially the central position of the hypoconid in the m1 talonid and suppression of lingual cuspids. The

oldest remains referable to *Xenocyon* are those of *X. dubius* (Teilhard de Chardin, 1940) from the Nihewanian fissure fill at Zhoukoudian locality 18 near Beijing. This occurrence extends the genus into the late Pliocene in China, but knowledge of it is restricted to the mandible and its dentition and a referred M1. *Xenocyon dubius* and *X. lycaonoides* differ largely in size as far as the preserved remains admit comparison, suggesting a possible anagenetic relationship between them. The origin of *X. lycaonoides* lies near the beginning of the medial Pleistocene; it seems restricted to the medial Pleistocene (1.0–0.5 Ma) in Eurasia, occurring from Spain (as "*Cuon*" *rosi* Pons-Moya and Moya-Sola, 1978) to Beringian North America where it accompanies *Canis lupus*. There is an important geographic range extension of a similar form in the late Irvingtonian of North America south of the continental ice sheets in southern Saskatchewan and the panhandle of Texas (as the closely related *X. texanus* (Troxell), 1915) where it is associated with *Canis armbrusteri*.

The cladogram implies a close phyletic relationship between *Cuon* and *Lycaon* as well as a probable origin within *Xenocyon*. This cladogenesis occurred before *Cuon* appears in the fossil record in the medial Pleistocene in Europe (*C. alpinus priscus*) and southeastern Asia (*C. javanicus fossilis*). The fossil record of *Lycaon* is poor in Africa, but possibly the genus occurs as early as the medial Pleistocene at the Elandsfontein site in South Africa (Ewer and Singer, 1956). The geographically widespread presence of species of the sister genus *Xenocyon* makes it seem likely that *Cuon* and *Lycaon* arose in allopatry from *Xenocyon* populations at the limits of their distribution. The characters defining their sister relationship predict the morphology of this common ancestor. This is most closely approached by *Cuon alpinus priscus* Thenius, 1954, from the medial Pleistocene deposits at Hundesheim in Austria. Although the m3 in that taxon is absent, as in the dhole, the m2 is relatively large in comparison with the m1 and retains a well-developed talonid; the p4 has an anterior cusp; and the premolars are slender and separated by diastemata as in *Lycaon pictus*.

In conclusion, the fossil record of the Caninae shows a number of interesting features in comparison with the rest of the Canidae: (1) it shows low taxonomic diversity over most of its history; (2) it begins a marked evolutionary expansion only in the last 20% of its history, an event that may in part be related to the extinction of its sister taxon, the Borophaginae (fig. 2); (3) the Caninae have a spectacular intercontinental expansion during the late Miocene, Pliocene, and Pleistocene epochs, which results in the formation of partially endemic canid faunas in the Pleistocene and Recent of Africa, Eurasia, and South America; and (4) elements of the Eurasian radiation of Canina reenter North America at various times during the late Pliocene and Pleistocene and come to dominate the large canid niche during that span.

Although the paleontological evidence makes a clear case for the origin of the genera *Vulpes* and *Canis* within North America, the Pliocene and Pleistocene history of these clades fails to indicate the origin of any real diversity within North America. *Vulpes* is restricted to small species during the Pleistocene comparable to the living swift fox (*V. velox*) and kit-fox (*V. macrotis*), which have a surprisingly sparse geologic record. Only during the later Pleistocene do northern foxes (*Vulpes vulpes* and *V. allopex*) enlarge the fox fauna. Likewise, *Canis* is limited to the coyote (*C. latrans*) and the extinct *C. edwardii*. The appearance of the large wolf *C. armbrusteri* in the early Pleistocene of North America is phyletically "out of place" in a canid fauna consisting of coyote and jackal-sized species. Its phyletic relationships are with *C. lupus* and its eastern Asian sister taxon, *C. chihliensis* (including *C. teilhardi*, see appendix 1). *Canis armbrusteri* and, later, its descendant, *C. dirus*, were the only large *Canis* in the New World, other than during occasional visitations of the Asian hypercarnivorous clades (*Xenocyon* and *Cuon*) during the Pleistocene. These North American occurrences rarely seem to last beyond a few glacial cycles. The wolf, *Canis lupus*, is the latest immigrant to North America, perhaps following the arctic ungulates that enter the mid-continent during the last glacial cycle. *Canis lupus* was early dominated by *C. dirus*,

the largest member of the genus, but in postglacial times they were followed by humans and their domesticated wolf, the dog, and a consequent wave of extinction that continues today.

ACKNOWLEDGMENTS

We acknowledge our debt to Childs Frick for the persistence with which he searched for the remains of Carnivora. The success of his field parties with respect to the Canidae are illustrated and described in Wang (1994) and Wang et al. (1999) and form the major basis of this work. One of us (B.E.T.) had the privilege of working on the Canidae under his guidance, and this earlier study has aided our efforts in many ways.

We again thank the indefatible contributors to of the Frick Collection, especially Dr. and Mrs. Morris F. Skinner and Mr. and Mrs. Theodore Galusha, who not only collected most of the material herein described, but obtained the vital stratigraphic data necessary for its interpretation.

During the years that our work was in progress we benefited from the generosity of colleagues who have discussed the subject with us and who have allowed us to use specimens in their care. Among those who have been especially helpful we must single out Dr. Ronald Nowak (U.S. Fish and Wildlife) who graciously permitted us full use of his important study of Quaternary and living *Canis* of North America before its publication. Dr. Annalisa Berta (San Diego State University, California) kept us apprised of her work on the larger South American Quaternary canids and provided us with casts of Argentine fossil canids that were of great value in comparing the history of the canids in North and South America. Dr. Karl Koopman, Dr. Nancy Neff, and Henry Galiano (while at the American Museum of Natural History) and Dr. Alfredo Languth (University of Montevideo, Uruguay) provided stimulating discussions of canid phylogeny. Dr. Bjorn Kurtèn (University of Helsinki) generously sent preprints of his work on coyotelike dogs as well as his summaries of North American Quaternary canids, which helped keep us abreast of developing ideas of Quaternary canid relationships. Drs. Danillo Torre and Lorenzo Rook (University of Florence) supplied measurements of the dentitions of the Valdarno canids and provided preprints of their work on Eurasian canids. Dr. Marina Sotnikova (Geological Institute, Russian Academy of Sciences, Moscow) also provided information on Eurasian canids in advance of publication, and Drs. F. Clark Howell (University of California) and Germaine Petter (Museum National d'Histoire Naturelle, Paris) provided notes and bibliographical material relative to Asian and African canids.

The following colleagues have generously made specimens and data available to us during the course of this work: S. Anderson (Department of Mammalogy, American Museum of Natural History), W.W. Dalquest (Midwestern University, Texas), P.D. Gingerich (University of Michigan), R.M. Hunt, Jr. (University of Nebraska), L.R. Kittleman (University of Oregon), G.E. Lewis (U.S. Geological Survey, Denver), J.A. Lillegraven (University of Wyoming), E.H. Lindsay (University of Arizona), C. Ray (National Museum of Natural History), C.A. Repenning (U.S. Geological Survey, Denver, Colorado), D.-E. Savage (University of California, Berkeley), G.E. Schultz (West Texas State University, Canyon), D.P. Whistler (Los Angeles County Museum of Natural History), and M.O. Woodburne (University of California, Riverside).

Most of the illustrations were prepared by the late Raymond J. Gooris, venerable artist of the Frick Laboratory, whose comprehensive work on these canid monographs provided most of the essential imagery. One of us (X.W.) prepared the graphics and filled in the illustrations of some important specimens acquired during the later phase of this work. Lorraine Meeker provided the excellent photos included herein.

The collection could not be so completely described without the skillful work of the Frick Laboratory preparators Otto Simonis and Ernest Heying and, more recently, Edward Pedersen, who undertook much casting and preparation of loaned material that informs this work.

Alejandra Lora and Judy Galkin undertook the enormous burden of getting the

manuscript of this study translated from the complexities of the editorial work and the handwriting of one of us.

REFERENCES

Adam, K.D. 1959. Mitt–elpleistozäne Caniden aus dem Heppenloch bei Gutenberg (Württemberg). Stuttgart Beitrage Naturkunden 27: 1–46.

Akersten, W.A. 1970. Red light local fauna (Blancan) of the Love Formation, southeastern Hudspeth County, Texas. Bulletin of the Texas Memorial Museum 20: 1–52.

Albright, L.B., III. 1999. Magnetostratigraphy and biochronology of the San Timoteo Badlands, southern California, with implications for local Pliocene-Pleistocene tectonic and depositional patterns. Geological Society of America Bulletin 111: 1265–1293.

Allen, J.A. 1905. Reports of the Princeton University Expeditions to Patagonia: mammalia of southern Patagonia. Vol. 3. Zoology pt. 1: 1–210.

Anderson, E. 1996. Preliminary report on the Carnivora of Porcupine cave, Park County, Colorado. *In* K.M. Stewart and K.L. Seymour (editors), Palaeocology and palaeoenvironments of Late Cenozoic mammals: tributes to the career of C.S. Churcher, 259–282. Toronto: University of Toronto Press.

Arambourg, C. 1979. Vertebrés Villafranchiens d'Afrique du Nord (Artiodactyles, Carnivores, Primates, Reptiles, Oiseaux). Paris: Edition de la Fondation Singer-Palignac, 141 pp.

Arroyo-Cabrales, J., E. Johnson, H. Haas, M. de los Rios-Paredes, R.W. Ralph, and W.T. Hartwell. 1995. First radiocarbon dates for San Josecito Cave, Nuevo León, Mexico. Quaternary Research 43: 255–258.

Audubon, J.J., and J. Bachman. 1851. The viviparous quadrupeds of North America. Vol. 2. New York: Audubon, 344 pp.

Azzaroli, A., C. de Giuli, G. Ficarelli, and D. Torre. 1988. Late Pliocene to early mid-Pleistocene mammals in Eurasia: faunal succession and dispersal events. Palaeogeography Palaeoclimatology Palaeoecology 66: 77–100.

Baird, S.F. 1857. Mammals: upon the zoology of the several Pacific railroad routes. Reports, explorations and surveys for railroad route from Mississippi River to Pacific Ocean Vol. 8, pt. 1: xix–xlviii, 1–757. Washington, DC: Tucker.

Barbour, G.B. 1926. Deposition and erosion in the Huai-lai Basin and their bearing on the Pleistocene history of north China. Geological Society of China Bulletin 5: 47–55.

Barbour, G.B., E. Licent, and P. Teilhard de Chardin. 1926. Geological study of the deposits of the Sangkanho basin. Geological Society of China Bulletin 5: 263–278.

Barendregt, R.W., F.F. Thomas, E. Irving, J. Baker, A. Macs Stalker, and C.S. Churcher. 1991. Stratigraphy and paleomagnetism of the Jaw Face section, Wellsch Valley site, Saskatchewan. Canadian Journal of Earth Sciences 28: 1353–1364.

Bartow, J.A. 1984. Geologic map and cross-sections of the southeastern margin of the San Joaquin Valley, California. U. S. Geological Survey Miscellaneous Investigations Series Map I-1496.

Bartow, J.A., and K. McDougall. 1984. Tertiary stratigraphy of the southeastern San Joaquin Valley, California. U. S. Geological Survey Bulletin 1529-J: 1–41.

Becker, J.J., and H.G. McDonald. 1998. The Star Valley local fauna (early Hemphillian) southwestern Idaho. *In* W.A. Akersten, H.G. McDonald, D.J. Meldrum, and M.E.T. Flint (editors), And whereas…: papers on the vertebrate paleontology of Idaho honoring John A. White. Idaho Museum of Natural History Occasional Papers 36: 25–49.

Benés, J. 1972. Die Füchse im Mitteleuropäischen Pleistozän. Časopis Nārodniho Musea Oddil Přiŕodovedny 140: 191–196.

Berggren, W.A., D.K. Kent, C.C. Swisher, III, and M.-P. Aubry. 1995. A revised Cenozoic geochronology and chronostratigraphy. *In* W.A. Berggren, D.V. Kent, M.P. Aubry, and J. Hardenbol (editors), Geochronology, timescales and global stratigraphic correlation. Society for Sedimentary Geology Special Publication 54: 129–212.

Berta, A. 1981. Evolution of large canids in South America. Anais de Congreso Latino-Americano de Paleontologia 2: 835–845.

Berta, A. 1987. Origin, diversification, and zoogeography of the South American Canidae. *In* B.D. Patterson and R.M. Timm (editors), Studies in Neotropical mammalogy: essays in Honor of Philip Hershkovitz. Fieldiana Zoology New Series 39: 455–471.

Berta, A. 1988. Quaternary evolution and biogeography of the large South American Canidae (Mammalia: Carnivora). University of California Publiations in Geological Sciences 132: 1–49.

Berta, A. 1995. Fossil carnivores from the Leisey Shell Pits, Hillsborough County, Florida. *In* R.C. Hulbert, Jr., G.S. Morgan, and S.D. Webb (editors), Paleontology and geology of the Leisey Shell Pits, early Pleistocene of Florida.

Bulletin of the Florida Museum of Natural History 37: 463–499.

Berta, A., and L.G. Marshall. 1978. South American Carnivora. Fossilium Catalogus 1. Animalia pt. 125: i–ix, 1–48.

Bever, G.S. 2005. Morphometric variation in the cranium, mandible, and dentition of *Canis latrans* and *Canis lepophagus* (Carnivora: Canidae) and its implications for the identification of isolated fossil specimens. Southwestern Naturalist 50: 42–56.

Bininda-Emonds, O.R.P., J.L. Gittleman, and A. Purvis. 1999. Building large trees by combining phylogenetic information: a complete phylogeny of extant Carnivora (Mammalia). Biological Reviews 74: 143–175.

Bishop, M.J. 1982. The mammal fauna of the early middle Pleistocene cavern infill site of Westbury-Sub-Mendip, Somerset. Special Papers in Palaeontology 28: 1–108.

Bjork, P.R. 1970. The Carnivora of the Hagerman local fauna (late Pliocene) of southwestern Idaho. American Philosophical Society Transactions 60: 1–54.

Bjork, P.R. 1974. Additional carnivores from the Rexroad Formation (Upper Pliocene) of southwestern Kansas. Transactions of the Kansas Academy of Sciences 76: 24–38.

Bohlin, B. 1938. Einige Jungtertiäre und Pleistozäm Cavicorner aus Nord-China. Nova Acta Regiae Societatis Scientarium 11(2): 1–54.

Bonifay, M.-F. 1971. Carnivores Quaternaires du Sud-est de la France. Memoires du Museum Naturelle d'Histoir Naturelle Series C Sciences de la Terre 21: 43–377.

Bose, P.N. 1880. Undescribed fossil Carnivora from the Siwalik Hills in the collection of the British Museum. Quarterly Journal of the Geological Society of London 36: 110–136.

Brown, B. 1908. The Conard fissure, a Pleistocene bone deposit in northern Arkansas: with descriptions of the two new genera and twenty new species of mammals. American Museum of Natural History Memoirs 9(4): 155–208.

Cady, R.C., and O.J. Scherer. 1946. Geology and ground-water sources of Box Butte County, Nebraska. U.S. Geological Survey Water-Supply Paper 969: 1–102.

Cande, S.C., and D.V. Kent. 1995. Revised calibration of the geomagnetic polarity timescale for the late Cretaceous and Cenozoic. Journal of Geophysical Research 100: 6093–6095.

Churcher, C.S. 1959. The specific status of the New World red fox. Journal of Mammalogy 40: 513–520.

Clutton-Brock, J., G.B. Corbet, and M. Hills. 1976. A review of the Family Canidae, with a classification by numerical methods. Bulletin of the British Museum (Natural History) 29(3): 117–199.

Cook, H.J., and J.R. Macdonald. 1962. New Carnivora from the Miocene and Pliocene of western Nebraska. Journal of Paleontology 36: 560–567.

Cope, E.D. 1895. Extinct Bovidae, Canidae and Felidae from the Pleistocene of the Plains. Journal of the Academy of Natural Sciences of Philadelphia 9: 453–459.

Cope, E.D. 1899. Vertebrate remains from Port Kennedy bone deposit. Journal of the Academy of Natural Sciences of Philadelphia 11: 193–267.

Crusafont-Pairó, M. 1950. El primer representante del género *Canis* en el Pontiense eurasiático (*Canis cipio* nova sp.). Boletin de la Real Sociedad Española de Historia Natural Seccion Geologica 48: 43–51.

Crusafont-Pairó, M., and J. Truyols-Santana. 1956. A biometric study of the evolution of fissiped carnivores. Evolution 10: 314–332.

Dalquest, W.W. 1967. Mammals of the Pleistocene Slaton local fauna of Texas. Southwestern Naturalist 12: 1–30.

Dalquest, W.W. 1978. Early Blancan mammals of the Beck Ranch local fauna of Texas. Journal of Mammalogy 59: 269–298.

Dalquest, W.W., and G.E. Schultz. 1992. Ice Age mammals of northwestern Texas. Wichita Falls, TX: Midwestern University Press.

Dayan, T., D. Simberloff, E. Tchernov, and Y. Yom-Tov. 1992. Canine carnassials; character displacement in wolves, jackals and foxes of Israel. Biological Journal of the Linnean Society 45: 315–331.

Dayan, T., E. Tchernov, Y. Yom-Tov, and D. Simberloff. 1989. Ecological character displacement in Saharo-Arabian Vulpes: outfoxing Bergmann's Rule. Oikos 55: 265–272.

Del Campana, D. 1913. I cani pliocenici di Toscana. Palaeontographia Italica 19: 189–254.

Del Campana, D. 1924. Nuovi resti di cani pliocenici del Valdarno Superiore. Rivista Italiana Paleontologia. fasc 3–4: 47–51.

Depéret, C. 1890–97. Les animaux Pliocene du Roussilon. Mémoires de la Société Géologique de France 3: 1–164.

Dundas, R.G. 1999. Quaternary records of the dire wolf, *Canis dirus*, in North and South America. Boreas 28: 375–385.

Dundas, R.G., R.B. Smith, and K.L. Verosub. 1996. The Fairmead Landfill (Pleistocene, Irvingtonian), Madera County, California: preliminary report and significance. Paleobios 17: 50–58.

Evans, H.E., and G.C. Christensen. 1979. Miller's anatomy of the dog. Philadelphia: W. B. Sanders.

Ewer, R.F., and R. Singer. 1956. Fossil Carnivora from Hopefield. Annales of the South African Museum 42: 335–347.

Fischer de Waldheim, G. 1817. Adversaria zoological. Memoir Societe Naturelle (Moscow) 5: 368–428.

Fisher, R.V., and J.M. Rensberger. 1972. Physical stratigraphy of the John Day Formation, central Oregon. University of California Publications in Geological Sciences 101: v–33.

Flower, W.H. 1869. On the value of the characters of the base of the cranium in the classification of the Order Carnivora, and on the systematic position of Bassaris and other disputed forms. Proceedings of the Zoological Society of London 1869: 4–37.

Forsythe-Major, C.J. 1877. Considerazioni sulle faune dei mammiferi pliocenici e postpliocenici della Toscana. Pisa: Atti della Società Toscana di sciencze naturali, Memorie, III: 207–227. 82 pp.

Fremd, T., E.A. Bestland, and G.J. Retallack. 1994. John Day Basin paleontological field trip guide and log. Seattle, WA: Society of Vertebrate Paleontology 1994 Annual Meeting.

Frick, C. 1930. Alaska's frozen fauna. Natural History 30: 71–80.

Galusha, T. 1975. Stratigraphy of the Box Butte Formation, Nebraska. Bulletin of the American Museum of Natural History 156(1): 1–68.

Galusha, T., and J.C. Blick. 1971. Stratigraphy of the Santa Fe Group, New Mexico. Bulletin of the American Museum Natural History 144(1): 1–127.

Galusha, T., N.M. Johnson, E.H. Lindsay, N.O. Opdyke, and R.H. Tedford. 1984. Biostratigraphy and magnetostratigraphy, late Pliocene rocks, 111 Ranch, Arizona. Bulletin of the Geological Society of America 95: 714–722.

Gaspard, M. 1964. La region de l'angle mandibulaire chez les Canidae. Mammalia 28: 249–329.

Gazin, C.L. 1942. The late Cenozoic vertebrate faunas from the San Pedro Valley, Ariz. Proceedings of the United States National Museum 92: 475–518.

Geraads, D. 1997. Carnivores du Pliocene Terminal de Ahi al Oughlam (Casablanca, Maroc). Geobios 30: 127–164.

Getz, L.L. 1960. Middle Pleistocene carnivores from southwestern Kansas. Journal of Mammalogy 41: 361–365.

Gidley, J.W. 1913. Preliminary report on a recently discovered Pleistocene cave deposit near Cumberland, Maryland. Proceedings of the United States National Museum 46: 93–102.

Gidley, J.W., and C.L. Gazin. 1933. New Mammalia in the Pleistocene fauna from Cumberland Cave. Journal of Mammalogy 14: 343–357.

Gidley, J.W., and C.L. Gazin. 1938. The Pleistocene vertebrate fauna from Cumberland Cave, Maryland. Bulletin of the United States National Museum 171: 1–99.

Giles, E. 1960. Multivariate analysis of Pleistocene and recent coyotes (*Canis latrans*) from California. University of California Publications in Geological Sciences 36: 369–390.

Gray, J.E. 1821. On the natural arrangement of vertebrose animals. London Medical Repository 15: 296–310.

Gregory, J.T. 1942. Pliocene vertebrates from Big Spring Canyon, South Dakota. University of California Publications in Geological Sciences 26: 307–446.

Gustafson, E.P. 1978. The vertebrate faunas of the Pliocene Ringold Formation, south-central Washington. University of Oregon Museum of Natural History Bulletin 23: 1–62.

Harington, C.R. 1978. Quaternary vertebrate faunas of Canada and Alaska and their suggested chronological sequence. National Museum of Natural Sciences (Ottawa) Syllogeus Series 15: 1–105.

Harington, C.R. 1981. Pleistocene Saiga Antelopes in North America and their paleoenvironmental implications. *In* W.C. Mahaney (editor), Quaternary paleoclimate, 193–225. Norwich: Geo Books, University of East Anglia.

Henshaw, P.C. 1939. A Tertiary mammalian fauna from the Avawatz Mountains, San Bernardino County, California. Carnegie Institute of Washington Publication 514: 1–30.

Henshaw, P.C. 1942. A Tertiary mammalian fauna from the San Antonio Mountains near Tonopah, Nevada. Carnegie Institution of Washington Publication 530: 79–168.

Hibbard, C.W. 1937. Additional fauna of Edson Quarry of the Middle Pliocene of Kansas. American Midland Naturalist 18: 460–464.

Hibbard, C.W. 1953. *Equus* (*Asinus*) *calobatus* Troxell and associated vertebrates from the Pleistocene of Kansas. Transactions of the Kansas Academy of Sciences 56: 111–126.

Hibbard, C.W., and W.W. Dalquest. 1966. Fossils from the Seymour Formation of Knox and Baylor Counties, Texas, and their bearing on the late Kansan climate of that region. Contributions from the Museum of Paleontology University of Michigan 21: 1–66.

Hildebrand, M. 1952. An analysis of body proportions in the Canidae. American Journal of Anatomy 90: 217–256.

Hough, J.R. 1948. The auditory region in some members of the Procyonidae, Canidae, and Ursidae: its significance in the phylogeny of

the Carnivora. Bulletin of the American Museum of Natural History 92(2): 67–118.

Hulbert, R.C., Jr., and G.S. Morgan. 1993. Qualitative evolution in the giant armadillo *Holmesina* (Edentata, Pampatheriidae) in Florida. *In* R.A. Martin and A.D. Barnosky (editors), Morphological change in Quaternary mammals of North America, 134–177. New York, NY: Cambridge University Press.

Hunt, R.M., Jr. 1974. The auditory bulla in Carnivora: an anatomical basis for reappraisal of carnivore evolution. Journal of Morphology 143: 21–76.

Hunt, R.M., Jr. 2001. Small Oligocene amphicyonids from North America (*Paradaphoenus*, Mammalia, Carnivora). American Museum Novitates 3331: 1–20.

Hunt, R.M., Jr., and E. Stepleton. 2004. Geology and paleontology of the Upper John Day beds, John Day River Valley, Oregon: lithostratigraphy and biochronologic revision in the Haystack Valley and Kimberly areas (Kimberly at Mr. Misery quadrangles). Bulletin of the American Museum of Natural History 282: 1–90.

Huxley, T.H. 1880. On the cranial and dental characters of the Canidae. Proceedings of the Zoological Society of London 16: 238–288.

Illiger, K. 1815. Überblick der Säugethiere nach ihrer Verteilung über die Welttheile. Abhandlungen der Königlichen Akademie der Wissenschaffen in Berlin aus den Jähren 1804–1811: 39–159.

International Commission on Zoological Nomenclature, International Code of Zoologic Nomenclature. 3rd ed. Adopted by the 20th International Union of Biological Sciences, Helsinki, August 1979. London: International Trust for Zoological Nomenclature, 338 pp.

Jefferson, G.T. 1991. A catalogue of late Quaternay vertebrates from California. Part 2. Mammals. Natural History Museum of Los Angeles County Technical Report 7: 1–129.

Johnston, C.S. 1938. Preliminary report on the vertebrate type locality of Cita Canyon, and the description of an ancestral coyote. American Journal of Science 35: 383–390.

Keigwin, L.D., Jr. 1978. Pliocene closing of the Isthmus of Panama, based on biostratigraphic evidence from nearby Pacific Ocean and Caribbean Sea cores. Geology 6: 630–634.

Kormos, T. 1932. Die Füchse des ungarischen Oberpliozäns. Folia Zoolica et Hydrobiolica 4: 167–188.

Koufos, G.D. 1997. The canids *Eucyon* and *Nyctereutes* from the Ruscinian of Macedonia, Greece. Paleontologia i Evolució 30–31: 39–48.

Kraglievich, J.L. 1952. Un canido del Eocuartario de Mar del Plata y sus relaciones con otras formas Brasilenas y Norteamericanas. Revista Museo Mar del Plata 1: 53–70.

Kretzoi, M. 1938. Die Raubtiere von Gombaszög nebst einer übersicht der Gesamtfauna. Annales Historico-Naturales Musei Nationalis Hungarici Pars Minerales Geologie et Palaeontology 31: 88–157.

Kretzoi, M. 1941. Weitere Beiträge zur Kenntnis der Fauna von Gombaszög. Annales Historico-Naturales Musei Nationalis Hungarici Pars Minerales Geologie et Paleonology 34: 105–139.

Kretzoi, M. 1942. Präokkupierte und durch ältere zu ersetzende Säugetiernamen. Földtany Közlöny 72: 345–349.

Kurtén, B. 1974. A history of the coyote-like dogs (Canidae; Mammalia). Acta Zoologica Fennica 140: 1–37.

Kurtén, B. 1984. Geographic differentiation in the Rancholabrean dire wolf (*Canis dirus* Leidy) in North America. Carnegie Museum of Natural History Special Publication 8: 218–227.

Kurtén, B., and E. Anderson. 1980. Pleistocene mammals of North America. New York: Columbia University Press, i–xvii, 1442 pp.

Langguth, A. 1969. Die Südamerikanischen Canidae unter besonderer Berücksichtigung des Mähnenwolfes *Chrysocyon brachyurus* Illiger (morphologische, systematische und phylogenetische untersuchungen). Zeifschrift für Wissenschafflichen Zoologie 179: 1–188.

Leidy, J. 1854. Note on some fossil bones discovered by Mr. Francis A. Lincke in the banks of the Ohio River, Indiana. Proceedings of the Academy of Natural Sciences of Philadelphia 7: 199–201.

Leidy, J. 1858. Notice of remains of extinct Vertebrata, from the valley of the Niobrara River, collected during the exploring expedition of 1857, in Nebraska, under the command of Liet. G. K. Warren, U. S. Topographical Engineer, by Dr. F. V. Hayden, Geologist to the expedition. Proceedings of Academy of Natural Sciences of Philadelphia 10: 20–29.

Leidy, J. 1869. The extinct mammalian fauna of Dakota and Nebraska, including an account of some allied forms from other localities, together with a synopsis of the mammalian remains of North America. Journal of the Academy of Natural Sciencesof Philadelphia 7: 1–472.

Linnaeus, C. 1758. Systema naturae per regna tria naturae, secundum classes, ordines genera, species cum characteribus, differentis, synonyms, locis. Vol. 1 [10th ed.]. Stockholm: L. Salvii, 824 pp.

Linnaeus, C. 1766. Systema naturae. [12th ed.]. Stockholm: L Salvii, 532 pp.

Lönnberg, E. 1916. A remarkable occurrence of the first hind toe in the common fox (*Vulpes vulpes*). Arkiv for Zoologi 10: 1–5.

Loomis, F.B. 1932. The small carnivores of the Miocene. American Journal of Science 25: 316–329.

Lozinsky, R.P., and R.H. Tedford. 1991. Geology and paleontology of the Santa Fe Group, southwestern Albuquerque basin, Valencia County, New Mexico. New Mexico Bureau of Mines and Mineral Resources Bulletin 132: 1–35.

Macdonald, J.R. 1948. The Pliocene carnivores of the Black Hawk Ranch fauna. University of California Publications in Geological Sciences 28(3): 53–80.

Macdonald, J.R. 1963. The Miocene faunas from the Wounded Knee area of western South Dakota. Bulletin of the American Museum of Natural History 125(3): 139–238.

Macdonald, J.R. 1970. Review of the Miocene Wounded Knee faunas of southwestern South Dakota. Bulletin of the Los Angeles County Museum of Natural History Science 8: 1–82.

MacFadden, B.J., and R.M. Hunt, Jr. 1998. Magnetic polarity stratigraphy and correlation of the Arikaree Group, Arikareean (late Oligocene-early Miocene) of northwestern Nebraska. *In* D.O. Terry, H.E. LaGarry, and R.M. Hunt, Jr (editors), Depositional environments, lithostratigraphy and biostratigraphy of the White River and Arikaree Groups (late Eocene to early Miocene), North America. Geological Society of America Special Paper 325: 143–166.

Maddison, W.P., and D.R. Maddison. 1992. MacClade: analysis of phylogeny and character evolution. Sunderland, MA: Sinauer Associates.

Marshall, L.G., R.F. Butler, R.E. Drake, and G.H. Curtis. 1982. Geochronology of type Uquian (Late Cenozoic) land mammal age, Argentina. Science 216: 986–989.

Martin, L.D. 1972. The microtine rodents of the Mullen assemblage from the Pleistocene of north-central Nebraska. Bulletin of the University of Nebraska State Museum 9: 173–182.

Martin, L.D. 1989. Fossil history of the Terrestrial Carnivora. *In* J.L. Gittleman (editor), Carnivore behavior, ecology, and evolution Vol. 1: 536–568. Ithaca, NY: Cornell University Press.

Martin, R.A. 1974. Fossil mammals from the Coleman IIA Fauna, Sumter County. *In* S.D. Webb (editor), Pleistocene mammals of Florida, 35–99. Gainesville: University of Florida Press.

Martin, R.A., and S.D. Webb. 1974. Late Pleistocene mammals from the Devil's Den Fauna, Levy County. *In* S.D. Webb (editor), Pleistocene mammals of Florida, 114–145. Gainesville: University of Florida Press.

Masini, F., and D. Torre. 1989. Large mammal dispersal events at the beginning of the late Villafranchian. *In* E.H. Lindsay, V. Fahlbusch, and P. Mein (editors), European Neogene mammal chronology, 131–138. New York: Plenum Press.

Matthew, W.D. 1907. A lower Miocene fauna from South Dakota. Bulletin of the American Museum of Natural History 23(9): 169–219.

Matthew, W.D. 1909. Faunal lists of the Tertiary Mammalia of the west. U.S. Geological Survey Bulletin 361: 91–138.

Matthew, W.D. 1918. Contributions to the Snake Creek Fauna. Bulletin of the American Museum of Natural History 38(7): 183–229.

Matthew, W.J., and W. Granger. 1923. New fossil mammals from the Pliocene of Sze-chuan, China. Bulletin of the American Museum of Natural History 48(17): 563–598.

McDonald, J.N., and C.E. Ray. 1989. The autochthonous North American Musk Oxen (*Bootherium*, *Symbos* and *Gidleya* (Mammalia: Artiodactyla: Bovidae). Smithsonian Contributions to Paleobiology 66: 1–77.

McDonald, J.N., C.E. Ray, and C.R. Harington. 1991. Taxonomy and zoogeography of the musk ox genus *Praeovibos* Staudinger, 1908. *In* J.R. Purdue, W.E. Klippel, and B.W. Styles (editors), Beamers, bobwhites and blue-points: tributes to the career of Paul W. Parmalee. Illinois State Museum Science Paper 23: 285–314.

McKenna, M.C. 1965. Stratigraphic nomenclature of the Miocene Hemingford Group, Nebraska. American Museum Novitates 2228: 1–21.

McKenna, M.C., and S.K. Bell. 1997. Classification of mammals above the species level. New York: Columbia University Press, xii+631 pp.

Merriam, J.C. 1906. Carnivora from the Tertiary Formation of the John Day Region. Bulletin of the Department of Geology of the University of California 5: 1–64.

Merriam, J.C. 1911. Tertiary mammal beds of Virgin Valley and Thousand Creek in northwestern Nevada. Part 2. Vertebrate faunas. Bulletin of the Department of Geology of the University of California 11: 199–304.

Merriam, J.C. 1912. The fauna of Rancho La Brea. Part 2. Canidae. Memoirs of the University of California 1: 217–262.

Merriam, J.C. 1918. Note on the systematic position of the wolves of the *Canis dirus* group. Bulletin of the Department of Geology of the University of California 10: 531–533.

Merriam, J.C. 1919. Tertiary mammalian faunas of the Mohave Desert. University of California

Publications in Geological Sciences 11: 437a–437e, 438–585.

Miller, W.E. 1980. The late Pliocene Las Tunas Local Fauna from southernmost Baja California, Mexico. Journal of Paleontology 54: 762–805.

Miller, W.E., and O. Carranza-Castañeda. 1998. Late Tertiary canids from central Mexico. Journal of Paleontology 72: 546–556.

Mooser, O., and W.W. Dalquest. 1975. Pleistocene mammals from Aguascalientes, central Mexico. Journal of Mammalogy 56: 781–820.

Morales, J., and E. Aguirre. 1976. Carnívoros de Venta del Moro. Trabajos sobre Neogene-Cuaternario 5: 31–80.

Morgan, G.S., and R.C. Hulbert, Jr. 1995. Overview of the geology and vertebrate biochronology of the Leisey Shell Pit Local Fauna, Hillsborough County, Florida. *In* R.C. Hulbert, Jr., G.S. Morgan, and S.D. Webb (editors), Paleontology and geology of the Leisey Shell Pits, early Pleistocene of Florida. Bulletin of the Florida Museum of Natural History 37: 1–92.

Morgan, G.S., P.L. Sealey, S.G. Lucas, and A.B. Heckert. 1997. Pliocene (latest Hemphillian and Blancan) vertebrate fossils from the Mangas Basin, southwestern New Mexico. *In* S.G. Lucas, T.E. Williamson, and G.S. Morgan (editors), New Mexico's fossil record 1. New Mexico Museum of Natural History and Science Bulletin 11: 97–128.

Musil, R. 1972. Die Caniden der Stránská Skála. *In* R. Musil (editor), Stránská Skála 1, 1910–1945. Studia Musei Moraviae. Anthropos 20: 77–106.

Naeser, N.D., J.A. Westgate, O.L. Hughes, and T. Péwé. 1982. Fission-track ages of late Cenozoic distal tephra beds in the Yukon Territory and Alaska. Canadian Journal of Earth Sciences 19: 2167–2178.

Nehring, C.W.A. 1890. Über *Cuon alpinus fossilus* Nehring, rebst Bemerkungen über einige andere fossile caniden. Neues Jahrbuch Mineralogie und Palaentologie 1890(2): 34–52.

Neville, C., N.D. Opdyke, E.H. Lindsay, and N.M. Johnson. 1979. Magnetic stratigraphy of Pliocene deposits of the Glenn's Ferry Formation, Idaho, and its implications for North American mammalian biostratigraphy. American Journal of Science 279: 503–526.

Nowak, R.M. 1979. North American Quaternary *Canis*. University of Kansas Museum of Natural History Monograph 6: 1–154.

Nowak, R.M. 2002. The original status of wolves in eastern North America. Southeastern Naturalist 1: 95–130.

Odintzov, I.A. 1967. New species of Pliocene Carnivora, *Vulpes odessana* sp. nov. from the karst caves of Odessa. Paleontologichesky Sbornik 4: 130–137.

Olsen, S.J., J.W. Olsen, and G.-Q. Qi. 1982. The position of *Canis lupus variabilis* from Zhoukoudian in the ancestral lineage of the domestic dog, *Canis familiaris*. Vertebrata Palasiatica 20: 264–267. [in Chinese with English abstract]

Patterson, B. 1932. Upper Molars of *Canis armbrusteri* Gidley from Cumberland Cave, Maryland. American Journal of Science 23: 334–336.

Pavlinov, I.Y. 1975. Tooth anomalies in some Canidae. Acta Theriologica 20: 507–519.

Pei, W.-C. 1934. On the Carnivora from locality 1 of Choukoutien. Palaeontologia Sinica Series C 8: 1–166.

Pei, W.-C. 1939. New fossil material and artifacts collected from the Choukoutien region during the years 1937 to 1939. Bulletin of the Geological Society of China 19: 207–232.

Petter, G. 1964. Origine du genre *Otocyon* (Canidae Africain de la sous-famille des Otocyoninae). Mammalia 28: 330–344.

Péwé, T.L. 1975a. Quaternary geology of Alaska. U. S. Geological Survey Professional Paper 835: 1–145.

Péwé, T.L. 1975b. Quaternary stratigraphic nomenclature in unglaciated Central Alaska. U.S. Geological Survey Professional Paper 862: 1–32.

Péwé, T.L. 1989. Quaternary stratigraphy of The Fairbanks area, Alaska. U.S. Geological Survey Circular 1026: 72–77.

Péwé, T.L., and D.M. Hopkins. 1967. Mammal remains of pre-Wisconsin Age in Alaska. *In* D.M. Hopkins (editor), the Bering land bridge, 266–271. Stanford, CA: Stanford University Press.

Pilgrim, G.E. 1929. The fossil Carnivora of India. Palaeontologica Indica 18: 1–232.

Pinsof, J.D. 1996. Current status of north American Sangamonian local faunas and vertebrate taxa. *In* K.M. Stewart and K.L. Seymour (editors), Paleoecology and paleoenvironments of late Cenozoic mammals: tribute to the career of C. S. (Rufus) Churcher, 156–190. Toronto: University of Toronto Press.

Pocock, R.I. 1936. The Asiatic wild dog or dhole (*Cuon javavicus*). Proceedings of the Zoological Society of London 1936: 35–55.

Pohle, H. 1928. Die Raubtiere von Oldoway. Wissenschaftlichen Ergebnisse der Oldoway Expedition Neuefolge Hefte 3: 45–54.

Pons-Moya, J., and M. Crusafont Paíro. 1978. El *Canis cipio* Crusafont (1950), comparación con los canides del Plioceno y Pleistoceno europeo. Acta Geologica Hispanica 13: 133–136.

Pons-Moya, J., and S. Moya-Sola. 1978. La fauna de Carnívoros del Pleistoceno medio (Mindel) de la cueva Victoria (Cartagena) España. Acta Geológica Hispánica 13: 54–58.

Prothero, D.R., and C.C. Swisher, III. 1992. Magnetostratigraphy and geochronology of the terrestrial Eocene-Oligocene transition in North America. *In* D.R. Prothero and W.A. Berggren (editors), Eocene-Oligocene c limatic and biotic evolution, 46–73. Princeton, NJ: Princeton University Press.

Qiu, Z.-X., T. Deng, and B.-Y. Wang. 2004. Early Pleistocene mammalian fauna from Longdon, Dongxiang, Gansu, China. Palaeontologica Sinica [Whole no.] 191(n. ser. C 27): 1–198.

Qiu, Z.-X., and R.H. Tedford. 1990. A Pliocene species of *Vulpes* from Yushe, Shanxi. Vertebrate Palasiatica 10: 245–258. [in Chinese with English summary]

Rabeder, G. 1976. Die Carnivoren (Mammalia) an den Altpleistozän von Deutsch-Altenburg 2. Mit Beiträgen zur Systematik einiger Musteliden und Caniden. Beiträge Päläontologishen Österreich 1: 5–119.

Ray, C.E. 1958. Additions to the Pleistocene mammalian fauna from Melbourne, Florida. Bulletin of the Museum of Comparative Zoology 119: 421–444.

Repenning, C.A. 1967. Palearctic-Nearctic mammalian dispersal in the late Cenozoic. *In* D.M. Hopkins (editor), The Bering land bridge, 288–311. Stanford, CA: Stanford University Press.

Repenning, C.A. 1987. Biochronology of the microtine rodents of the United States. *In* M.O. Woodburne (editor), Cenozoic mammals of north America: geochronology and biostratigraphy, 236–268. Berkeley: University of California Press.

Repenning, C.A. 1992. *Allophaiomys* and the age of the Olyor Suite, Krestovka sections, Yakutia. U.S. Geological Survey Bulletin 2037: 1–98.

Robinson, G.D. 1963. Geology of the Three Forks quadrangle, Montana. U.S. Geological Survey Professional Paper 370: 1–143.

Rook, L. 1992. "*Canis*" *monticinensis* sp. nov., a new Canidae (Carnivora: Mammalia) from the late Messinian of Italy. Bolletino della Societa de Paleontologica Italiana 31: 151–156.

Rook, L. 1994. The Plio-Pleistocene Old World *Canis* (*Xenocyon*) ex gr. *falconeri*. Bollettino della Societa de Paleontologica Italiana 33: 71–82.

Savage, D.E. 1941. Two new middle Pliocene carnivores from Oklahoma with notes on the Optima Fauna. American Midland Naturalist 25: 692–710.

Savage, D.E. 1951. Late Cenozoic vertebrates of the San Francisco Bay Region. University of California Publications in Geological Sciences 28: 215–314.

Schultz, C.B., and C.H. Falkenbach. 1949. Promerycochoerinae: a new subfamily of oreodonts. Bulletin of the American Museum of Natural History 93(3): 69–198.

Schultz, H.A. Semken, S.D. Webb, and R.J. Zakrzewski. 1987. The North American Quaternary sequence. *In* M.O. Woodburne (editor), Ceaphy, 211–235. Berkeley: University of California Press.

Schultz, J.R. 1938. A late Quaternary mammal fauna from the tar seeps of McKittrick, California. Carnegie Institution of Washington Contributions in Paleontology 487: 112–215.

Schütt, G. 1973. Revision der *Cuon-* und *Xenocyon-* funde (Canidae, Mammalia) aus den AltPleistozänen Mosbacher Sanden (Wiesbaden, Hessen). Mainzer Naturwissenschaftliches Archiv 12: 49–77.

Schütt, G. 1974. Die Carnivoren von Würzburg-Schalksberg: mit einem Beitrag zur biostratigraphischen und zoogeographischen Stellung der altpleistozanen Wirbeltierfaunen von Mittelmain (Unterfranken). Neues Jahrbuch der Geologie und Paläontologie Abhandlungen 147: 61–90.

Sclater, P.L. 1859. On the general geographical distribution of the members of the Class Aves. Journal and Proceedings of the Linnean Society (Zoology) 2: 130 (for 1857) pp.

Segall, W. 1943. The auditory region of the arctoid carnivores. Field Museum of Natural History Publications Zoological Series 29(3): 33–59.

Sellards, E.H. 1916. Human remains and associated fossils from the Pleistocene of Florida. Annual Report of the Florida Geological Survey 8: 123–160.

Shen, G.-J., T.-L. Ku, H. Cheng, R.L. Edwards, Z.-X. Yuan, and Q. Wang. 2001. High-precision U-series dating of locality 1 at Zhoukoudian, China. Journal of Human Evolution 41: 679–688.

Sher, A.V. 1986. Olyorian land mammal age of north-eastern Siberia. Palaeontologia Italica 74: 97–112.

Shotwell, J.A. 1956. Hemphillian mammalian assemblage from northeastern Oregon. Bulletin of the Geological Society of America 67: 717–733.

Simpson, G.G. 1941. Large Pleistocene felines in North America. American Museum Novitates 1136: 1–27.

Simpson, G.G. 1945. The principles of classification and a classification of mammals. Bulletin of

the American Museum of Natural History 85: i–xvi, 1–350.

Simpson, G.G., A. Roe, and R.C. Lewontin. 1960. Quantitative zoology. Revised ed. New York: Harcourt, Brace, 440 pp.

Skinner, M.F., and C.W. Hibbard. 1972. Early Pleistocene pre-glacial rocks and faunas of north-central Nebraska. Bulletin of the American Museum of Natural History 148(1): 1–148.

Skinner, M.F., and F.W. Johnson. 1984. Tertiary stratigraphy and the Frick Collection of fossil vertebrates from north-central Nebraska. Bulletin of the American Museum of Natural History 178(3): 215–368.

Skinner, M.F., M.S. Skinner, and R.W. Gooris. 1977. Stratigraphy and biostratigraphy of late Cenozoic deposits in central Sioux County, western Nebraska. Bulletin of the American Museum of Natural History 158(5): 263–371.

Smith, C. Hamilton. 1839. The Canine Family in general or the genus *Canis*. *In* W. Jardine (editor), The naturalist's library, vol. 18. Natural history of dogs, vol. 1. Edinburgh: W. H. Lizars, 267 pp.

Soergel, W. 1925. Die Säugetierfauna des altdiluvialen Tonlages von Jockgrim in des Pfalz. Zeitschrift der Deutischen Geologischen Gesellschaft 77: 405–438.

Soria, D., and E. Aguirre. 1976. El canido de Layna: revision de los *Nyctereutes* fosiles. Trabajos sobre Neogene-Quaternario 5: 83–107.

Sotnikova, M.Y. 2001. Remains of Canidae from the lower Pleistocene site of Untermassfeld. Monographien Römisch-Germanisches Zentralmuseum Mainz, Forschungsinstitut für Vor- und Frühgeschicte 40: 607–632.

Sotnikova, M.Y. 2006. A new canid *Nurocyon chonokhariensis* gen. et sp. nov. (Canini, Canidae, Mammalia) from the Pliocene of Monglia. Courier Forschungsinstitut Senckenberg 256: 11–21.

Spassov, N., and L. Rook. 2006. *Eucyon marinae* sp. nov. (Mammalia, Carnivora) a new canid species from the Pliocene of Mongolia with a review of forms referable to the genus. Rivista Italiana di Paleontologia e Stratigrafia 1/2(1): 123–133.

Steininger, F.F., W.A. Berggren, D.V. Kent, R.L. Bernor, S. Sen, and J. Agusti. 1996. Circum-Mediterraneum Neogene (Miocene and Pliocene) marine-continental chronologic units. *In* R.L. Bernor, V. Fahlbusch, V., and H.-W. Mittman (editors), The evolution of western Eurasian Neogene: mammal faunas, 7–46. New York: Columbia University Press.

Stevens, M.S. 1965. A new species of *Urocyon* from the upper Pliocene of Kansas. Journal of Mammalogy 46: 265–269.

Stirton, R.A., and P.O. McGrew. 1935. A preliminary notice of the Miocene and Pliocene mammalian faunas near Valentine, Nebraska. American Journal of Science 29: 125–132.

Swofford, D.L. 1993. Phylogenetic analysis using parsimony. Version 3.1.1. Urbana: Illinois Natural History Survey.

Tedford, R.H. 1992. Neogene stratigraphy of the northwestern Albuquerque Basin. New Mexico Geological Society Guidebook 33: 273–278.

Tedford, R.H., S.B. Albright, III, A.P. Barnosky, I. Ferrusquía-Villafranca, R.M. Hunt, Jr., J.E. Storer, C.C. Swisher, III, M.R. Voorhies, S.D. Webb, and D.P. Whistler. 2004. Mammalian biochronology of the Arikareean through Hemphillian interval (Late Oligocene through Early Pliocene epochs). *In* M.O. Woodburne (editor), Late Cretaceous and Cenozoic mammals of North America: biostratigraphy and geochronology, 169–231. New York: Columbia University Press.

Tedford, R.H., and S. Barghoorn. 1993. Neogene stratigraphy and mammalian biochronology of the Espanola Basin, northern New Mexico. *In* S.G. Lucas and J. Zidek (editors), Vertebrate paleontology in New Mexico. New Mexico Museum of Natural History and Science 2: 159–168.

Tedford, R.H., and S. Barghoorn. 1999. Santa Fe Group (Neogene), Ceja del Rio Puerco, northwestern Albuquerque Basin, Sandoval County, New Mexico. New Mexico Geological Society Guidebook, 50th Field Conference, Albuquerque Geology, 327–335.

Tedford, R.H., T. Galusha, M.F. Skinner, B.E. Taylor, R.W. Fields, J.R. Macdonald, J.M. Rensberger, S.D. Webb, and D.P. Whistler. 1987. Faunal succession and biochronology of the Arikareean through Hemphillian interval (late Oligocene through earliest Pliocene epochs) in North America. *In* M.O. Woodburne (editor), Cenozoic mammals of North America: geochronology and biostratigraphy, 153–210. Berkeley: University of California Press.

Tedford, R.H., and Z.-X. Qiu. 1991. Pliocene *Nyctereutes* (Carnivora: Canidae) from Yushe, Shanxi, with comments on Chinese fossil raccoon-dogs. Vertebrata Palasiatica 29: 176–189. [in Chinese with English summary]

Tedford, R.H., and Z.-X. Qiu. 1996. A new canid genus from the Pliocene of Yushe, Shanxi Province. Vertebrata Palasiatica 34: 27–48. [in Chinese with English summary]

Tedford, R.H., J.B. Swinehart, C.C. Swisher, III, D.R. Prothero, S.A. King, and T.E. Tierney. 1996. The Whitneyan-Arikareean transition in the High Plains. *In* D.R. Prothero and R.J. Emry (editors), The terrestrial Eocene-Oligo-

cene transition in North America, 312–334. New York: Cambridge University Press.

Tedford, R.H., B.E. Taylor, and X.-M. Wang. 1995. Phylogeny of the Caninae (Carnivora: Canidae): the living taxa. American Museum Novitates 3146: 1–37.

Tedford, R.H., and X.-M. Wang. 2008. *Metalopex* a new genus of fox (Vulpini, Canidae, Carnivora) from the late Miocene of western North America. Natural History Museum of Los Angeles County Science Series 41: 273–278.

Teilhard de Chardin, P. 1936. Fossil mammals from locality 9 of Choukoutien. Palaeontologica Sinica Series C 7: 1–60.

Teilhard de Chardin, P. 1940. The fossils from locality 18 near Peking. Paleontologica Sinica Series C 9: 1–94.

Teilhard de Chardin, P., and P. Leroy. 1942. Chinese fossil mammals. Institut de Géo-biologie, Pekin. 8. Shanghai: Pax Publishing and Printing Co., 142 pp.

Teilhard de Chardin, P., and W.-C. Pei. 1941. The fossil mammals from locality 13 of Choukoutien. Palaeontologica Sinica Series C 11: 1–106.

Teilhard de Chardin, P., and J. Piveteau. 1930. Les mammiféres fossils de Nihowan (China). Annales de Paleontologie 19: 1–134.

Thenius, E. 1954. Die Caniden (Mammalia) aus dem Altquartär Von Hundesheim (Niederösterreich) nebst Bemerkungen zur Stammesgeschiehte der Gattung *Cuon*. Neues Jarhbuch fűr Geologie und Paläontologie Abhandlungen 99: 230–286.

Tonni, E.P., M.T. Alberdi, J.L. Prado, M.S. Bargo, and A.L. Cione. 1992. Changes of mammal assemblages in the Pampean region (Argentina) and their relation with the Plio-Pleistocene boundary. Palaeogeography Palaeoclimatology Palaeoecology 95: 179–194.

Tonni, E.P., P. Nabel, A.L. Cione, M. Etchichury, R. Tofalo, G.S. Yané, San. Cristobal, A. Carlini, and D. Vargas. 1999. The Ensenada and Buenos Aires formations (Pleistocene) in a quarry near La Plata, Argentina. Journal of South American Earth Sciences 12: 273–291.

Torre, D. 1974. Affinitá dentali del cane della grotta di "L'Escale." Rivista Italiana Paleontologia 80: 147–156.

Torre, D. 1967. I cani Villafranchiani della Toscana. Palaeontologia Italica 68: 113–138.

Torres, V. 1980. El significado paleontológico-estratigráfico de la mastofáunula local Algodones, Pliocene Tardio de Baja California Sur, México. Tesis Professional, Facultad de Ciencias, Universidad Nacional Autónoma de México.

Torres, V., and I. Ferrusquía. 1981. *Cerdocyon* sp. nov. A (Mammalia, Carnivora) en México y su sifnificatión evolutiva y zoogeographica en relación a los cánidos sudamericanos. Anais de Congreso Latino-Americano Paleontologia, Porte Alegre, 1981 2: 709–719.

Trouessart, E.L. 1897. Catalogus mammalium tam viventium quom fossilium. Nova ed. Berlin: Berolini, 8 vols., 1264 pp.

Troxell, E.L. 1915. The vertebrate fossils of Rock Creek, Texas. American Journal of Science 39: 632–634.

Turner, A. 1990. The evolution of the guild of larger terrestrial carnivores during the Plio-Pleistocene in Africa. Geobios 23: 349–368.

Turner, H.N. 1848. Observations relating to some of the foramina at the base of the skull in Mammalia, and on the classification of the order Carnivora. Proceedings of the Zoological Society of London 1848: 63–88.

VanderHoof, V.L. 1933. Additions to the fauna of the Tehama Upper Pliocene of northern California. American Journal of Science 25: 382–384.

Van der Klaauw, C.J. 1931. The auditory bulla in some fossil mammals, with a general introduction to this region of the skull. Bulletin of the American Museum of Natural History 62(1): 1–352.

Van Kampen, P.N. 1905. Die Tympanalgegend des Säugetierschädels. Morphologisches Jahrbuch 34: 321–722.

Von Reichenau, W. 1906. Beiträge zur näheren Kenntnis der Carnivoren aus den Sanden von Mauer und Mosbach. Abhandlungen der Grossherzoglich-hessischen Landdesanstalt zu Darmstadt 5: 185–313.

Voorhies, M.R. 1990. Vertebrate paleontology of the proposed Norden Reservor Area: Brown, Cherry and Keya Paha Counties, Nebraska. University of Nebraska Division of Archaeological Research Technical Report 82-09: 1–138, A1–A592.

Voorhies, M.R., and R.G. Corner. 1986. *Megatylopus* (?) *cochrani* (Mammalia: Camelidae): a re-evaluation. Journal of Vertebrate Paleontology 6: 65–75.

Wang, X.-M. 1994. Phylogenetic systematics of the Hesperocyoninae (Carnivora: Canidae). Bulletin of the American Museum of Natural History 221: 1–207.

Wang, X.-M., and B.M. Rothschild. 1992. Multiple hereditary osteochondromata of Oligocene *Hesperocyon* (Carnivora: Canidae). Journal of Vertebrate Paleontology 12: 387–394.

Wang, X.-M., and R.H. Tedford. 1992. The status of genus *Nothocyon* Matthew, 1899 (Carnivora): an arctoid not a canid. Journal of Vertebrate Paleontology 12: 223–229.

Wang, X.-M., and R.H. Tedford. 1994. Basicranial anatomy and phylogeny of primitive canids and

closely related miacids (Carnivora: Mammalia). American Museum Novitates 3092: 1–34.

Wang, X.-M., and R.H. Tedford. 1996. Canidae. *In* D.R. Prothero and R.J. Emry (editors), The terrestrial Eocene-Oligocene transition in North America, 433–452. New York: Cambridge University Press.

Wang, X.-M., R.H. Tedford, and B.E. Taylor. 1999. Phylogenetic systematics of the Borophaginae (Carnivora: Canidae). Bulletin of the American Museum of Natural History 243: 1–391.

Wang, X.-M., R.H. Tedford, B. Van Valkenburgh, and R.K. Wayne. 2004. Ancestry: evolutionary history, molecular systematics, and evolutionary ecology of Canidae. *In* D.W. Macdonald and Cladio. Sillero-Zubiri (editors), The biology and conservation of wild canids, 39–54. New York: Oxford University Press.

Wayne, R.K., E. Gefen, D.J. Girman, K.P. Koepfli, L.M. Lau, and C.R. Marshall. 1997. Molecular systematics of the Canidae. Systematic Biology 46: 622–653.

Wayne, R.K., B. Van Valkenburg, P.W. Kat, T.K. Fuller, W.E. Johnson, and S.J. O'Brien. 1989. Genetic and morphological divergence among sympatric Canids. Journal of Heredity 80: 447–454.

Webb, S.D. 1969. The Buge and Minnechaduza Clarendonian mammalian faunas of north-central Nebraska. University of California Publications in Geological Sciences 78: 1–191.

Westgate, J.A., B.A. Stemper, and T.L. Péwé. 1990. A 3 m.y. record of Pliocene-Pleistocene loess in interior Alaska. Geology 18: 858–861.

Youngman, P.M. 1993. The Pleistocene small carnivores of eastern Beringia. Canadian Field Naturalist 107: 139–163.

Zdansky, O. 1924. Jungtertiäre Carnivoren Chinas. Paleontologia Sinica Series C 2: 1–149.

Zdansky, O. 1928. Die Säugetiere der Quartärfauna Von Chou-k'ou-tien. Palaeontologia Sinica Series C 5: 1–146.

Zdansky, O. 1935. *Equus* und andere Perissodactyla. Palaeontologia Sinica Series C 6: 1–54.

Zhou, C.-l., Z.-C. Liu, Y.-J. Wang, and Q.-H. Huang. 2000. Climatic cycles investigated by sediment analysis in Peking Man's Cave, Zhoukoudian, China. Journal of Archaeological Science 27: 101–109.

Zrzavý, J., and V. Řičánková. 2004. Phylogeny of Recent Canidae (Mammalia, Carnivora): relative reliability and utility of morphological and molecular datasets. Zoologica Scripta 33: 311–333.

Zymela, S.H., P. Schwarz, R. Grün, A.M. Stalker, and C.S. Churcher. 1988. ESR dating of Pleistocene fossil teeth from Alberta and Saskatchewan. Canadian Journal of Earth Sciences 25: 235–245.

APPENDIX 1

Eurasian Species of *Canis* Used in Phyletic Analysis

The following notes give the essential bibliographical information regarding the Eurasian species of *Canis* used in our phyletic analysis of the Caninae. These taxa are not individually dealt with in the systematics section of this work, although they have been referred to in the wider comparison of the North American taxa.

Canis etruscus Forsyth-Major, 1877
Canis etruscus: Del Campana, 1913: 192.
Canis olivolanus Del Campana, 1913: 192.
Canis majori Del Campana, 1913: 192.
Canis etruscus: Del Campana, 1924: 48.
Canis olivolanus: Del Campana, 1924: 47.
Canis etruscus: Torre, 1967: 116.

Holotype: IGF 12867, cranium (fig. 67A–C) and associated mandible (fig. 67D–E). Holotype selected by Torre (1967: 118).

Type Locality: "Ostine" near Renacci (Figline), upper Valdarno, Tuscany, Italy.

Age: Late Villafranchian; Olivola, Tasso, and Farneta faunal units; early Pleistocene (ca. 1.2–1.7 Ma).

Remarks: Torre (1967) recognized the synonomy of Del Campana's *Canis majori* and *C. olivolanus* with Forsyth-Major's *C. etruscus*. A cast of the holotype is available in the AMNH collection (F:AM 89777), and the better preserved material in the Italian sample from Valdarno has been figured and described by Del Campana (1913, 1924) and Torre (1967) so that 95% of the characters used in the present analysis can be obtained from this material. As in the case of *C. arnensis*, Torre (1967) gave a largely biometric definition of *C. etruscus*, but a morphological characterization is inherent in the matrix (table 2) and cladogram provided herein (fig. 65).

A large population sample from the medial Pleistocene deposits in the cave at L'Escale, central France, attributed to *C. etruscus* by Bonifay (1971), has been regarded as intermediate between *C. etruscus* and *C. lupus* in a biometric analysis by Torre (1974), supporting a widespread belief of the origin of *C. lupus* within *C. etruscus* (cf. Kurtén and Anderson, 1980: 170). Sotnikova (2001), after comparison of the L'Escale population with the large sample of *C. mosbachensis* from Untermassfeld, concluded that the L'Escale material should be assigned to the latter taxon.

Canis falconeri Forsyth-Major, 1877
Canis falconeri: Del Campana, 1913: 220.
Canis falconeri: Torre, 1967: 132.
Canis (*Xenocyon*) *falconeri:* Rook, 1994: 71.

Holotype: IGF 883, a palate with right I1–I3 roots, C broken, P1 absent, P2, P3–M2 broken; left I1–I3 and C crowns broken, P1–P2 missing, P3–P4, M1–M2.

Referred Specimen: IGF 865, a mandible lacking only i2.

Type Locality: Both from upper Valdarno; holotype possibly near S. Giovanni; the referred mandible from "il Tasso", near Terranuova Bracciolini, Tuscany, Italy.

Age: Late Villafranchian; Tasso faunal unit; early Pleistocene (ca. 1.5 Ma).

Remarks: The cited remains from the type region are the only useful topotypes. Casts of these specimens are available in the AMNH (F:AM 102519, holotype; F:AM 102520, mandible). The limited material allows examination of only 73% of the characters used in the phyletic analysis. Most recently Rook (1994) has used *C. falconeri* to contain his grouping of Old World species including *C. antonii*, *C. africanus*, and *Xenocyon lycaonoides* as "*Canis* (*Xenocyon*) ex gr. *falconeri*", characterized as "large sized species with robust dentitions and the tendency to develop blade-like carnassials" (p. 81).

Canis arnensis Del Campana, 1913
Canis arnensis: Del Campana, 1924: 48.
Canis arnensis: Torre, 1967: 133.

Holotype: IGF 867 cranium and mandible of a single individual. Holotype selected by Torre (1967: 134).

Type Locality: "il Tasso", upper Valdarno, Tuscany, Italy.

Age: Late Villafranchian; Tasso faunal unit; early Pleistocene (ca. 1.5 Ma); so far known only from the early Pleistocene of Europe.

Remarks: This taxon was described and figured in the cited publications based on numerous referred specimens. A cast of the holotype is available at the AMNH (F:AM 102521) from which other features could be obtained to yield 89% of characters coded. Although not formally diagnosed here, the essential characters needed for the present analysis can be read from the matrix (table 2) or cladogram (fig. 65). This taxon has been related to the jackals (Torre, 1967) or to the "coyote-like dogs" (Kurtén, 1974).

Canis antonii Zdansky, 1924
Canis (*Xenocyon*) *antonii:* Rook, 1994: 76.

Holotype: Paleontological Museum, Upsala, Sweden, M3514, palate with partial alveoli of right I1–I2, I3 root, C (erupting), P1 alveolus, P2, P3 alveolus, P4–M1, M2 alveolus, left I1–I2 broken crowns, I3–P4 alveoli, M1–M2. A cast of the holotype dentition is available at the AMNH.

Type Locality: Holotype from one-third of a mile ("1 li") south of Yangshao village, Mienchi County, Henan Province, east-central China (from label on holotype, Zdansky 1924: pl. II, fig. 5); "Locality A" in locality list (Zdansky, 1924, unnumbered pages between text and plates).

Age: The holotype is associated (Zdansky, 1935; Bohlin, 1938) with *Nyctereutes sinensis*, *Ursus arctos*, *Crocuta honanensis*, *Dinofelis abeli*, *Felis palaeosinensis*, rhinocerotid, *Proboscidipparion sinense*, *Equus* cf. *sanmenensis*, *Paracamelus gigas*, *Cervus* sp., *Gazella* cf.

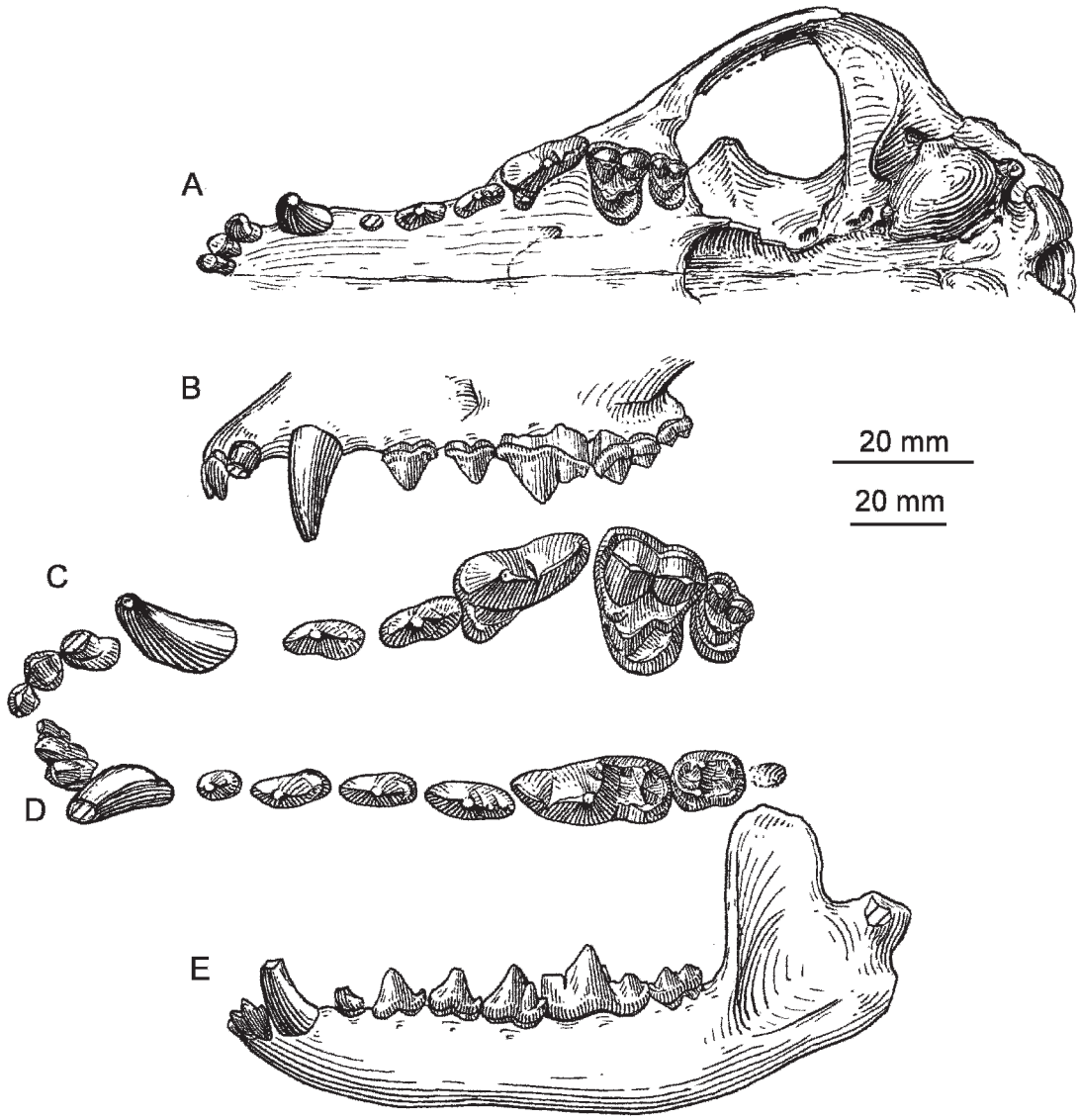

Fig. 67. **A–E**. *Canis etruscus*, upper Valdarno, Italy. **A**. IGF 12867 (AMNH cast 89779), palatal view. **B–E**. IGF 12334 (AMNH cast 89777). **B**. Lateral view, reversed. C–D. Occlusal views, reversed. **E**. Lateral view, reversed. The longer (upper) scale is for C and D, and the shorter scale is for the rest.

paragutturosa, an ovibovine, and *Ovis shantungensis*, suggesting a late Nihewanian (early Pleistocene) age.

Remarks: Zdansky (1924: 10–11) also referred a snout with anterior dentition: I2–I3, C, P1–P2 (not figured) from ''Locality 33'': Ma-ti, near Lungwagou village in Jiangning County, southwestern Shanxi Province, where it is associated only with *Bison palaeosinensis*, a largely Nihewanian taxon. A skull and mandible (F:AM 97052), figured and partially described by Rook (1994), was found near Taigu, Shanxi Province, associated with the myospalacine cricetid rodent *Youngia omegodon* whose biochron is restricted to the early Matuyama Chron. Rook (1994) attributed this skull to *C. antonii* Zdansky, 1924, described from post-Olduvai early Pleistocene strata in Henan Province. He also included *C. chihliensis* Zdansky, 1924, from early Pleistocene strata in Hebei Province in the same taxon. These two taxa had not been previously synonymized by investigators working with Chinese collections (viz. Teilhard de Chardin and Pei, 1941: 10) and they appear to us to represent distinct forms.

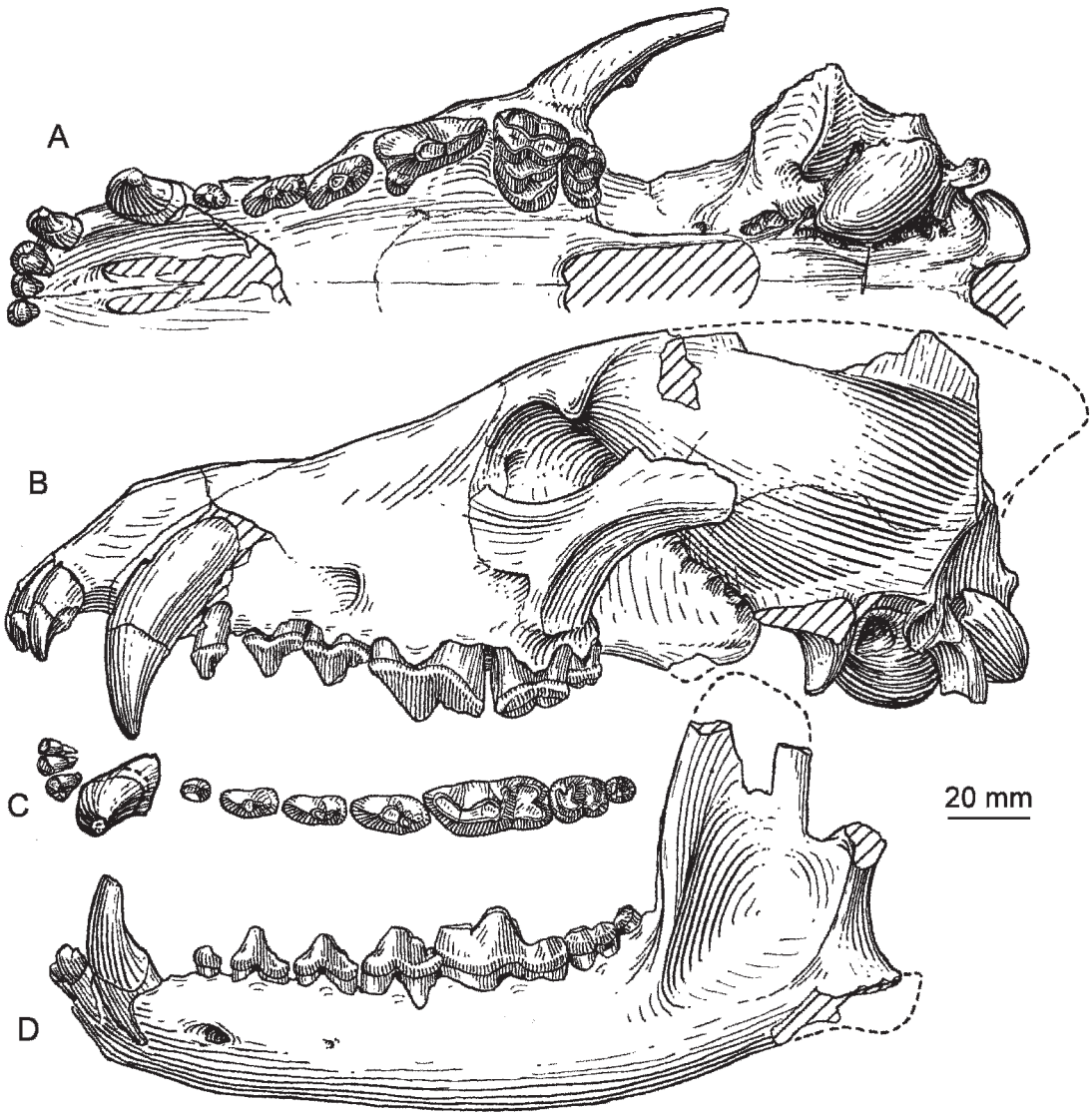

Fig. 68. **A–D**. *Canis antonii*, skull and mandible, F:AM 97052, Nihewanian, Shanxi Province, China. **A**. Palatal view. **B**. Lateral view. **C**. Occlusal view. **D**. Lateral view.

The late Pliocene Taigu specimen (fig. 68A–D) represents a sister species of the crown group (including *Canis armbrusteri*) in most cranial characters. It differs from *C. armbrusteri* in aspects of the cheek tooth dentition, which appears to retain (or have reverted to) primitive states: the m1 metaconid is small but still placed high on the flank of the protoconid; m2 metaconid is subequal in size to the protoconid; the m3 bears two cusps (as far as wear will allow judgment), the tip of p3 is not markedly lower than p2; the p3 and P3 have posterior cusps, the p4 has a second posterior cusp lying anterior to the posterior cingulum; judging from the backward slant of the anterior edge of the m1 paraconid, the p4 did not exceed the former in height; the P4 protocone is salient, pointed anterolingually and separated from the paracone by a notch. The paracone of M1–M2 is not markedly enlarged relative to the metacone; a strong metaconule is retained on M1; the postprotocrista of M2 extends to the base of the metacone (although there is no metaconule); the labial cingulum is subdued but complete on M1 and the parastyle is connected to the paracone by the preparacrista; and the M1 lingual cingulum is complete across the protocone. The possession of these features allies the Taigu large *Canis* with *C. falconeri* at the base of the crown group within the genus.

Canis chihliensis Zdansky, 1924

Canis chihliensis chihliensis Teilhard and Piveteau, 1930: 56.

Canis (*Xenocyon*) *antonii* (in part) Rook, 1994: 76.

Holotype: Paleontological Museum, Upsala, Sweden, M3496, right maxillary fragment with P3–P4, M1–M2.

Locality: ''Locality 64'' (Zdansky, 1924, unnumbered pages between the text and plates), Fengwo near Huanglu village in Huailai County near the Sangkanhe, about 80 km north of Beijing, northwestern Chihli (now Hebei) Province. The general geology and relationship of the fossiliferous deposits to adjacent basins are treated by Barbour (1926).

Age: Zdansky (1924: 13) mentioned that the holotype was associated with ''bovines but not *Hipparion*''. In 1935 he listed *Equus* cf. *sanmenensis*, and Bohlin (1938) recorded *Gazella paragutterosa* and cf. *Bison palaeosinensis* from the type locality. These are Nihewanian taxa, perhaps late Nihewanian; early Pleistocene.

Remarks: Although the taxa were comparable in size, Zdansky (1924: 13014) noted certain differences between the holotypes of *C. antonii* and *C. chihliensis*, particularly the stronger P4 protocone and lesser reduction of M2 relative to M1 that implied that *C. chihliensis* was a more primitive form.

Teilhard de Chardin and Piveteau (1930: 96) referred several specimens from Nihewan to ''*Canis chihliensis* form typique.'' Their concept centered around three Tianjin Museum specimens: a skull, TNP 00162 (''specimen 1'' in table on p. 96, pl. XIX, fig. 4), the rami, TNP 00163 (''specimen a'', table p. 96, pl. XIX, fig. 2) and TNP 00161 (''specimen b'', table p. 96, pl. XIX, fig. 3), all of which we have examined. Unfortunately, most of these specimens fall within the size and range of variation of the new taxon *Canis chihliensis palmidens* Teilhard de Chardin and Piveteau, 1930, typified by TNP 00198, a skull referred to as ''Crâne A'' and illustrated on their plate XIX, figure 1–1a. Of the specimens mentioned by Teilhard de Chardin and Piveteau (1930), only the ramus, TNP 00161 (''specimen b'', measurements in table on p. 96 and illustrated in fig. 3 of pl. XIX), is markedly larger as appropriate for *C. chihliensis*. This ramus was collected at Nihewan locality 15 in 1925, probably near Xiashagou, along with a palate (TNP 18706, 18685) and a right premaxillary and associated maxillary (TNP 18720), all of which we think belong to a single taxon that, on comparison with the holotype of *C. chihliensis*, seems appropriately assigned to that taxon. Teilhard de Chardin and Piveteau (1930) gave little morphological evidence for assignment to Zdansky's taxon. They rejected assignment to *Canis etruscus* (or its synonym *C. olivolanus*) despite their inability to distinguish them from the Chinese form. They used the name *C. chihliensis* more on zoogeographic than on morphologic grounds.

As we have remarked above, Rook (1994) synonymized *C. chihliensis* and *C. antonii* using the latter name, which has page priority as the senior synonym. We, however, return to the recognition of both species based on our study of the Chinese material mentioned in comparison with casts of the holotypes. Our assessment of *C. chihliensis* recognizes the large Nihewan taxon as morphologically subsuming the holotype as an individual within the range of variation shown by these examples. Our coding of the characters analyzed (table 2) is based primarily on the Tianjin Museum material from Nihewan. This gives us 95% of the features used, lacking only postcranial characters. A cast of the dentition of the holotype resides in the AMNH collection.

Canis mosbachensis Soergel, 1925

Canis neschersensis (in part): von Reichenau, 1906: 185.

Canus lupus mosbachensis: Thenius, 1954: 232.

Canis mosbachensis: Sotnikova, 2001: 608.

Holotype: Not selected from the sample of the five rami available to Soergel in 1925 in the collections of the museum at Mainz.

Type Locality: Mosbach (Weisbaden), Germany; from the middle layers of sand pit where the ''main fauna'' was obtained.

Age: Early medial Pleistocene (early Biharian).

Remarks: Soergel separated this taxon in the course of comparing a ramus from Jockgrim (Pfalz), Germany, subsequently referred to *C. neschersensis*, with the sample from Mosbach previously referred to the latter species (von Reichenau, 1906). *Canis mosbachensis* has been widely recognized in Europe, mostly as a full species, although Thenius (1954) labeled it a race of *C. lupus*, recalling the similarity of *C. mosbachensis* to the living small, southern races of the wolf.

The best sample (more than 300 specimens) of *C. mosbachensis* is that described by Sotnikova (2001) from the medial Pleistocene deposits at Untermassfeld near Meiningen (southern Thuringia), Germany. Through the generosity of that researcher we have also been able to examine central Asian examples of this species. These data allow observation of about 89% of the characters used in the phyletic analysis and provide a characterization of the taxon in the matrix (table 2).

Canis palmidens (Teilhard de Chardin and Piveteau), 1930

Canis chihliensis palmidens Teilhard de Chardin and Piveteau, 1930: 97.

Canis chihliensis palmidens: Torre, 1967: 113ff.

Lectotype: TNP 00198, skull (''Crâne A'', pl. XIX, fig. 1–1a, Teilhard de Chardin and Piveteau, 1930: 97–99).

Referred Specimens: TNP 00162, skull (Teilhard de Chardin and Piveteau, 1930: pl XIX, fig. 4) and its mandible, THP 00163, left ramus (op.cit. fig. 2) and THP 18752, right ramus assigned to ''*Canis chihliensis* form typique'', but, as explained above in the account of that species, these remains are clearly the same taxon as ''Crâne A''. Further confusion was introduced by the assignment to *Canis palmidens* of ''Crâne

B'' by Teilhard de Chardin and Piveteau (1930: 97, pl. XVII, fig. 1 and 1a), a specimen clearly referable to *Nyctereutes sinensis*.

Locality: North of the Sangkanhe, near Nihewan and Xiashagou villages. These specimens were collected from different sites lying at correlative levels within 2000 yards of Xiashagou (Barbour et al., 1926: 272), northwestern Hebei Province, China.

Age: Late Pliocene; late Gauss and early Matuyama geomagnetic chrons.

Remarks: Reference of *C. palmidens* as a ''race'' of *C. chihliensis* was based on the ''notably smaller size'' of the former and its ''longer and clearly more cuspidate'' premolars. At the same time its authors pointed out the close resemblance to such European taxa as *C. arnensis* and *C. nescherensis* and suggested that separation of *C. palmidens* rested mainly on its geographic location. Torre (1976) held a similar view, considering that the validity of the Chinese taxon was in doubt.

The sample of *C. palmidens* from Nihewan used in this study allows us to code 95% of the features used in our analysis. The diagnosis of *C. palmidens* is contained within the matrix of table 2.

Canis variabilis Pei, 1934

Canis sp. cf. *C. dingo* Zdansky, 1928: 27.
Canis lupus variabilis Pei, 1934: 13.
Canis lupus (in part) Pei, 1934: 10.
Canis cyonoides Pei, 1934: 18.
Canis lupus variabilis Teilhard de Chardin: p. 7.
Canis variabilis: Teilhard de Chardin and Pei, 1941: 8.
Canis sp. Teilhard de Chardin and Leroy, 1942: 40.

Lectotype: Unfortunately, much of the original topotypic material from Zhoukoudian locality 1 was misplaced during the chaotic years during and following World War II; none of the eight ''partly broken skulls'' is now at IVPP in Beijing. Nevertheless, the name *variabilis* needs to be stabilized by selection of a lectotype from what remains of the hypodigm of 1934. We were able to find the maxillary fragments illustrated by Pei (1934: pl. 1, figs. 2–4) and here select the subject of figure 2, IVPP C1570, a right maxillary fragment with P3–P4 and M1–M2 in early wear as the lectotype. Fortunately, this taxon is abundantly characterized by the material from locality 13 (Teilhard de Chardin and Pei, 1941). We have mainly used the latter sample to typify the skull, mandible, and postcrania while checking the ranges of variation within and between both samples.

Type Locality: Zhoukoudian locality 1, the famous ''*Sinanthropus*'' site, first monographed by Zdansky (1928) and later by Pei (1934) and other authors. The site is in a region of limestone quarries along the foot of the Western Hills, 47 km southwest of Beijing. The localities are fillings in a karst developed in the Paleozoic limestone. The canid fossils were collected from layers 3–9 of the cave-fill but most abundantly in layers 8 and 9 in the Lower Cave. Localities 13 and 9, slightly older than locality 1, occur about a kilometer south of locality 1 and have also provided samples of *Canis variabilis*.

Age: Medial Pleistocene. Many attempts have been made to provide a reliable age for locality 1. Recognition of the position of the boundary between the geomagnetic Matuyama and Brunhes chrons within layer 14 and recent U-series dating (Shen et al., 2001), corroborated by paleoclimatic analysis (Zhou et al., 2000, which includes previous literature on dating), give the age range for *C. variabilis* at locality 1 as 470–660 Ka.

Remarks: Pei (1934) recognized three species of *Canis* in his monograph on the Carnivora of locality 1. Subsequently ''*Canis* cf. *lupus*'' was recognized as a variant of *C. variabilis* (Teilhard de Chardin and Pei, 1941). Later, Teilhard de Chardin and Leroy (1942: 40) regarded *Canis cyonoides* Pei, 1934, as a taxon ''insufficiently characterized to be of practical use, and which may have to be dropped later on.'' We think the latter taxon to be a slightly hypercarnivorous variant within the population of *C. variabilis*. Similarly, the upper teeth separated as ''Canidae gen. et sp. indet.'' by Pei (1934: 43) and relegated to ''*Canis* sp.'' by Teilhard de Chardin and Leroy (1942: 40) seem to us to represent not too uncommon variants within *Canis* populations and are assigned to *C. variabilis* on the basis of size. In the ensuing years little has been directly written regarding *Canis variabilis*, and no reviews of the Chinese collection of this taxon have been made. Olsen et al. (1982) speculated that ''*Canis lupus variabilis*'' might resemble the stock from which the domestic dog originated. Sotnikova (2001), in her study of the large sample of *C. mosbachensis* from the fissure-fill at Untermassfeld, southern Thuringia, Germany, pointed out the similarity of that form and *C. variabilis* but, lacking a detailed study of the latter, her comparisons were necessarily based on the original literature. Our study accumulated sufficient information on these wolves to be able to compare them across the characters used in our phyletic analysis. *Canis variabilis* and *C. mosbachensis* are closely similar chronological contemporaries at mid-latitude Eurasia, differing only in that *C. variabilis* has nasal bones that terminate at or anterior to the most posterior position of the frontal-maxillary suture. This character is among the more homoplastic features accepted for analysis in this work. These taxa group in a common region on the cladogram and could represent variation in a geographically widespread mid-Pleistocene wolf.

Canis teilhardi Qiu, Deng and Wang, 2004

Canis cf. *chihliensis* Teilhard de Chardin, 1940: 5.

Holotype: Hezheng Paleozoological Museum (HMV) 1144, skull and associated left ramus.

Type Locality: East slope of Longdan, 2.5 km south of Walesi Township, southern Dongxiang Autonomous County, Linxia Hui Nationality Autonomous Prefecture, Gansu Province.

Age: Lower part of the Wucheng Loess, early Matuyama Chron. Two levels yielding *C. teilhardi* are separated by 12 m. The oldest (''L5'') is just above the Gauss–Matuyama boundary (ca. 2.55 Ma) and the youngest (''L9'') is within the Reunion subchron

(ca. 2.16 Ma). The holotype of *C. teilhardi* is from level 5, latest Pliocene (earliest Pleistocene, sensu China).

Remarks: More than 40 topotypes were obtained from the two levels at the type locality, making evidence of this taxon the most abundantly represented fossil *Canis* species described from north China. From an examination of a topotypic skull (''upper level'') and Qiu et al.'s (2004) diagnosis and description, we could code 95% of the characters used in our analysis. This places *C. teilhardi* as a sister taxon to *C. chihliensis* and thus to the *C. lupus* clade of the crown group within the genus.

Teilhard de Chardin (1940) compared a skull and mandible (his ''skull A'', now IVPP RV40005) from locality 18, Zhoukoutian, with large Chinese *Canis* spp. described up to that time and designated it *Canis* cf. *chihliensis*. This specimen closely resembles *C. teilhardi*, as Qiu et al. (2004) have pointed out, and may represent another late Pliocene occurrence of this taxon. We have tentatively included the Zhoukoutian 18 form in *C. teilhardi*.

APPENDIX 2

Cranial Measurements

In all of our studies of the Canidae, we have used Nowak's system (1979) of skull measurements (units in millimeters), slightly modified by addition and deletion as appropriate to our fossil samples, so that interested parties could carry out comparative biometrical work using his extensive data and ours. The following list details the cranial variates and their acronyms used in this paper. Reference points for these measurements are diagrammed in the accompanying figure (70A–B) and the measurements are presented in tables 3 and 4.

BW: Braincase width—Maximum breadth of the braincase across the level of parietal-squamosal suture.

FSW: Frontal shield width—Maximum breadth across the postorbital processes of the frontals.

GSL: Greatest skull length—Length from anterior tip of premaxillae to the posterior point of the inion.

JD: Jugal depth—Mininum depth of the jugal anterior to the postorbital process, at a right angle to its anteroposterior axis.

LB: Bulla length—Length from the median lacerate foramen to the suture of the bulla with the paroccipital process.

LCM: Length, post. C to for. mag. notch—Distance from the posterior border of the canine alveolus to the foramen magnum notch.

LPM: Maxillary toothrow length—Distance from the anterior edge of the alveolus of P1 to the posterior edge of the alveolus of M2.

M2B: Length, M2 to bulla—Mininum distance from the posterior edge of the alveolus of M2 to depression in front of the bulla.

M2W: M2 width—Maxinum transverse diameter.

MOH: Height, maxillary toothrow to orbit—Mininum distance from the outer alveolar margin of M1 to the most ventral point of orbit.

MW: Maximum skull width across cheek teeth—Greatest breadth between the outer sides of the most widely separated upper teeth (P4 or M1).

P4L: P4 length—Maximum anteroposterior length of crown measured on the outer side.

PCW: Postorbital constriction width—Least width across the frontals at the constriction behind the postorbital processes.

PWP1: Palatal width at P1—Mininum width between the inner margins of the alveoli of the first upper premolars.

ZW: Zygomatic width—Greatest distance across the zygoma.

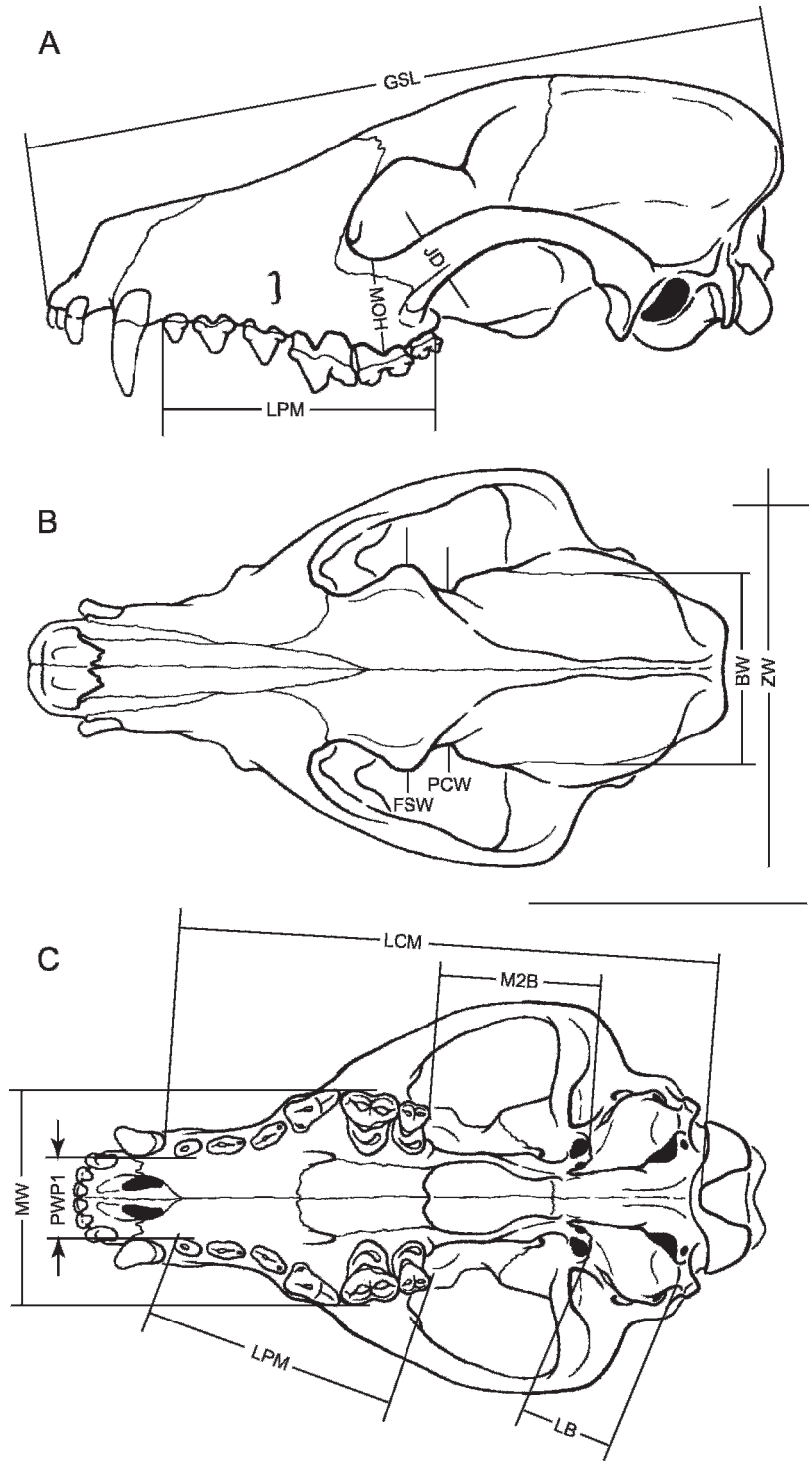

Fig. 69. Cranial dimensions used in this report. **A**. Lateral view. **B**. Dorsal view. **C**. Ventral view. Measurement acronyms are detailed in appendix 2.

TABLE 3
Summary of Cranial and Selected Dental Measurements Used to Typify Taxa Recognized in this Work

	LCM	GSL	ZW	BW	LPM	PWP4	PWP1	FSW	PCW	M2B	MOH	JD	P4L	M2W	LB
Leptocyon mollis															
UCMP 90 (type)	83.0	102.0	54.0	32.0	37.5	32.2	11.0	25.0	16.0	22.3	11.5	5.7	9.5	7.2	18.0
Leptocyon gregorii															
AMNH 12779								22.0	12.0	22.0	12.0				20.5
F:AM 49063	82.5	96.0		30.0	37.0	26.0	9.5	21.0	14.5	20.3	10.5	5.2	9.5	5.6	19.0
Mean	82.5	96.0		30.0	37.0	26.0	9.5	21.5	13.3	21.2	11.3	5.2	9.5	5.6	19.8
SD	0.00	0.00		0.00	0.00	0.00	0.00	0.50	1.25	0.85	0.75	0.00	0.00	0.00	0.75
CV	0.00	0.00		0.00	0.00	0.00	0.00	2.33	9.43	4.02	6.67	0.00	0.00	0.00	3.80
Leptocyon leidyi, n. sp.															
UNSM 25715	89.0		54.0		38.5				13.0		13.5	7.5	9.1	6.2	
Leptocyon vafer															
UCMP 77703	89.0	107.0	56.0	37.0	41.0	29.0	10.0	25.0	16.5	24.0	14.5	7.5	11.0	7.0	19.0
Vulpes stenognathus															
F:AM 49284	109.0	135.0	73.0	41.5	52.0	39.0	12.0	34.0	24.0	31.0	16.5	7.6	14.0	8.8	20.0
Metalopex macconnelli, n. sp.															
UA 361-49	100.0			40.2	45.3	32.6	10.3	27.0	19.0	29.2	13.3		11.5	7.8	16.4
Eucyon davisi (N. Am.)															
F:AM 63010	114.0	143.0			56.0					31.0		9.0	15.8	10.2	23.0
F:AM 63007	124.0	159.0	80.0	50.0	59.0		18.0		27.0	36.0	22.0	10.0	16.5	9.8	23.0
F:AM 63009	120.0	150.0	80.0	43.0	51.0	49.0	16.0	36.0	26.0	40.0	20.0	9.0	15.3	10.0	23.5
Mean	119.3	150.7	80.0	46.5	55.3	49.0	17.0	36.0	26.5	35.7	21.0	9.3	15.9	10.0	23.2
SD	4.11	6.55	0.00	3.50	3.30	0.00	1.00	0.00	0.50	3.68	1.00	0.47	0.49	0.16	0.24
CV	3.44	4.35	0.00	7.53	5.96	0.00	5.88	0.00	1.89	10.32	4.76	5.05	3.10	1.63	1.02
Canis ferox															
UNSM 26107	139.0	176.0	78.0	44.0	66.0	51.0		46.0	30.0	40.0	23.0	10.5	18.0	10.8	21.0
F:AM 49298	140.0	176.0	99.0	52.0	67.0	53.0	21.3	44.0	23.5	40.0	26.0	11.0	18.5	9.5	24.0
Mean	139.5	176.0	88.5	48.0	66.5	52.0	21.3	45.0	26.8	40.0	24.5	10.8	18.3	10.2	22.5
SD	0.50	0.00	10.50	4.00	0.50	1.00	0.00	1.00	3.25	0.00	1.50	0.25	0.25	0.65	1.50
CV	0.36	0.00	11.86	8.33	0.75	1.92	0.00	2.22	12.15	0.00	6.12	2.33	1.37	6.40	6.67

TABLE 3
(Continued)

	LCM	GSL	ZW	BW	LPM	PWP4	PWP1	FSW	PCW	M2B	MOH	JD	P4L	M2W	LB
Canis lepophagus															
WTU 881	148.0	189.0	97.5	54.0	69.0	53.0	19.6	48.0	33.0	49.8	23.7	11.6	18.8	11.4	19.5
WTU 722	146.5	192.0	102.6	60.0	67.0	59.0	20.5	55.0	39.0	46.5	25.5	13.1	18.3	11.0	23.0
WTU 760	144.0	186.5		59.8	64.5	56.5	20.0		33.0	45.5	25.9	12.9	18.2	10.8	20.8
WTU 2523	155.0			59.0	71.8	59.0	21.0	57.2	35.1	51.7			19.5	11.3	24.5
UNSM 26111	147.0	190.0			67.0	52.0	20.0	52.0			26.0	13.8	19.0	11.0	
F:AM 49295	147.0	190.0			67.0	52.0	16.0	52.0		46.0		11.5	18.0	11.0	23.0
F:AM 63091	130.0	178.0		51.5	66.0				32.0				20.5		
Mean	145.4	187.6	100.1	56.9	67.5	55.3	19.5	52.8	34.4	47.9	25.3	12.6	18.9	11.1	22.2
SD	7.01	4.59	2.55	3.46	2.16	3.05	1.63	3.11	2.50	2.42	0.93	0.89	0.81	0.20	1.78
CV	4.83	2.44	2.55	6.09	3.21	5.52	8.37	5.89	7.27	5.06	3.67	7.10	4.29	1.84	8.02
Canis edwardii															
F:AM 63100		195.0	102.0	53.0	70.0	60.0	22.9	55.0	34.4	49.0	27.0	12.0	21.8	11.0	
USNM 12862	170.0		118.0		77.0	65.0	22.2	58.0		57.0	29.0	13.7	23.8	12.6	
USNM 23898	156.0			60.5	77.5	68.0	19.0	50.8	38.5	49.9	29.0		23.5	13.2	26.0
UA 23402	152.0	198.0	110.0	57.5	74.8	65.0	18.3	58.0	32.9	46.6	24.7	12.0	20.9		25.7
UF 11516			99.0	62.0	76.7	63.6	23.0	50.6	40.6	57.0	26.8	14.3	20.9	12.0	
Mean	159.3	196.5	107.3	58.3	75.2	64.3	21.1	54.5	36.6	51.9	27.3	13.0	22.2	12.2	25.9
SD	7.72	1.50	7.40	3.44	2.76	2.59	2.02	3.28	3.09	4.30	1.60	1.02	1.25	0.81	0.15
CV	4.84	0.76	6.90	5.90	3.67	4.03	9.56	6.01	8.44	8.29	5.88	7.86	5.63	6.66	0.58
Canis latrans (Irvingtonian)															
NMNH 7660				59.7					38.5		32.0	15.5			
Canis armbrusteri															
UF 11519	185.0	240.0	132.0	66.5	86.0	77.5	29.0	60.0	45.0	60.0	37.0	18.2	25.0	15.5	27.5
F:AM 67286	195.0		133.0	69.5	90.5		29.0	65.0	41.0		35.0	21.5	26.4	14.1	30.5
Mean	190.0	240.0	132.5	68.0	88.3	77.5	29.0	62.5	43.0	60.0	36.0	19.9	25.7	14.8	29.0
SD	5.00	0.00	0.50	1.50	2.25	0.00	0.00	2.50	2.00	0.00	1.00	1.65	0.70	0.70	1.50
CV	2.63	0.00	0.38	2.21	2.55	0.00	0.00	4.00	4.65	0.00	2.78	8.31	2.72	4.73	5.17
Canis dirus (Irvingtonian)															
F:AM 25511					95.5		40.5				42.0		27.5	13.5	

TABLE 4
Summary of Cranial and Selected Dental Measurements of Living Canid Taxa Used for Comparison in This Work

	LCM	GSL	ZW	BW	LPM	PWP4	PWP1	FSW	PCW	M2B	MOH	JD	P4L	M2W	LB
Vulpes vulpes fulva (New England)															
Mean	108.94	136.65	68.77	45.78	51.41	38.57	13.74	31.68	22.38	30.98	17.93	8.15	13.13	7.78	20.96
SD	3.82	5.39	2.77	1.41	2.21	1.35	1.14	1.99	1.03	1.62	0.91	0.62	0.66	0.67	0.50
CV	3.51	3.94	4.03	3.09	4.31	3.49	8.29	6.28	4.62	5.23	5.09	7.62	5.05	8.61	2.41
Max.	115.0	145.5	73.1	48.5	55.4	40.7	16.0	35.6	24.5	33.5	20.0	9.4	14.5	8.7	22.0
Min.	102.0	127.3	64.2	44.0	48.0	37.0	12.0	29.3	21.0	28.2	16.5	7.3	12.0	6.3	20.0
n	12	12	12	12	12	12	12	12	12	12	12	12	12	12	12
Canis latrans (Nevada)															
Mean	144.04	187.55	90.32	55.56	67.55	52.37	18.97	42.67	32.95	43.16	24.37	11.48	19.30	11.04	23.78
SD	2.85	4.43	3.98	1.00	1.97	1.42	1.07	3.07	2.54	1.73	0.98	0.43	0.85	0.64	0.79
CV	1.98	2.36	4.40	1.79	2.92	2.71	5.63	7.20	7.70	4.00	4.02	3.73	4.39	5.84	3.31
Max.	151.0	195.6	98.8	57.5	72.4	55.2	21.5	47.5	36.4	45.0	26.0	12.3	21.1	12.3	25.5
Min.	139.5	181.0	84.8	53.4	64.8	50.3	17.3	37.8	27.0	39.0	22.8	10.8	18.0	10.0	22.8
n	12	12	12	12	12	12	12	12	12	12	12	12	12	12	12
Canis lupus occidentalis (western Canada)															
Mean	191.78	255.39	138.62	67.20	87.83	82.99	32.26	60.91	42.67	66.72	40.92	18.33	25.83	13.54	28.42
SD	6.19	9.25	5.77	1.64	2.56	3.45	2.39	3.27	3.33	2.89	1.42	1.25	1.25	0.47	1.28
CV	3.23	3.62	4.17	2.43	2.92	4.16	7.41	5.37	7.81	4.33	3.46	6.84	4.83	3.45	4.50
Max.	202.0	270.0	148.5	69.5	92.0	89.3	37.0	66.5	48.0	70.5	43.0	20.3	28.0	14.3	31.0
Min.	182.0	241.0	129.5	64.5	83.5	78.3	29.0	54.5	36.2	62.0	38.0	16.0	24.0	12.7	26.5
n	9	9	9	9	9	9	9	9	9	9	9	9	9	9	9

APPENDIX 3

Statistical Summaries of Dental Measurements

The following tooth measurements were used in this study. These are summarized in tables 5 and 6. Reference points are shown in the accompanying figure (fig. 71). Specimens listed in the hypodigm and marked with an asterisk there were too incomplete to be measured. These data were prepared nearly exclusively by one of us (B.E.T.) following the methods indicated. Measurements are in millimeters.

LP1, LP2, LP3: Maximum anteroposterior diameter along the major axis of each upper premolar.

LP4: Maximum anteroposterior diameter from the parastyle to the metastyle corners with the calipers held parallel to the base of the P4.

WP4: Maxinum transverse diameter taken just posterior to the protocone.

LM1: Maximum anteroposterior diameter of the M1 from the parastyle to the metastyle corners with the calipers held parallel to the labial border.

WM1: Maximum transverse diameter of M1 from the labial cingulum to the lingual border with the calipers held perpendicular to the paracone and metacone.

LM2: Maximum anteroposterior diameter of M2 from the parastyle to the metasyle corners with the calipers held parallel to the labial border.

WM2: Maximum transverse diameter of M2 from the labial cingulum to the lingual border with the calipers held perpendicular to the paracone and metacone.

Lp1, Lp2, Lp3, Lp4: Maximum anteroposterior diameter on the major axis of each lower premolar.

Wp4: Maximum transverse diameter of p4.

Lm1: Maximum anteroposterior diameter of m1.

Wm1tr: Maximum transverse diameter of m1 trigonid at the carnassial notch.

Wm1tl: Maximum transverse diameter of the m1 talonid.

Lm2: Maximum anteroposterior diameter of m2 on the main axis of the tooth from the paraconid to the posterior cingulum or hypoconulid.

Wm2: Maximum transverse diameter of m2.

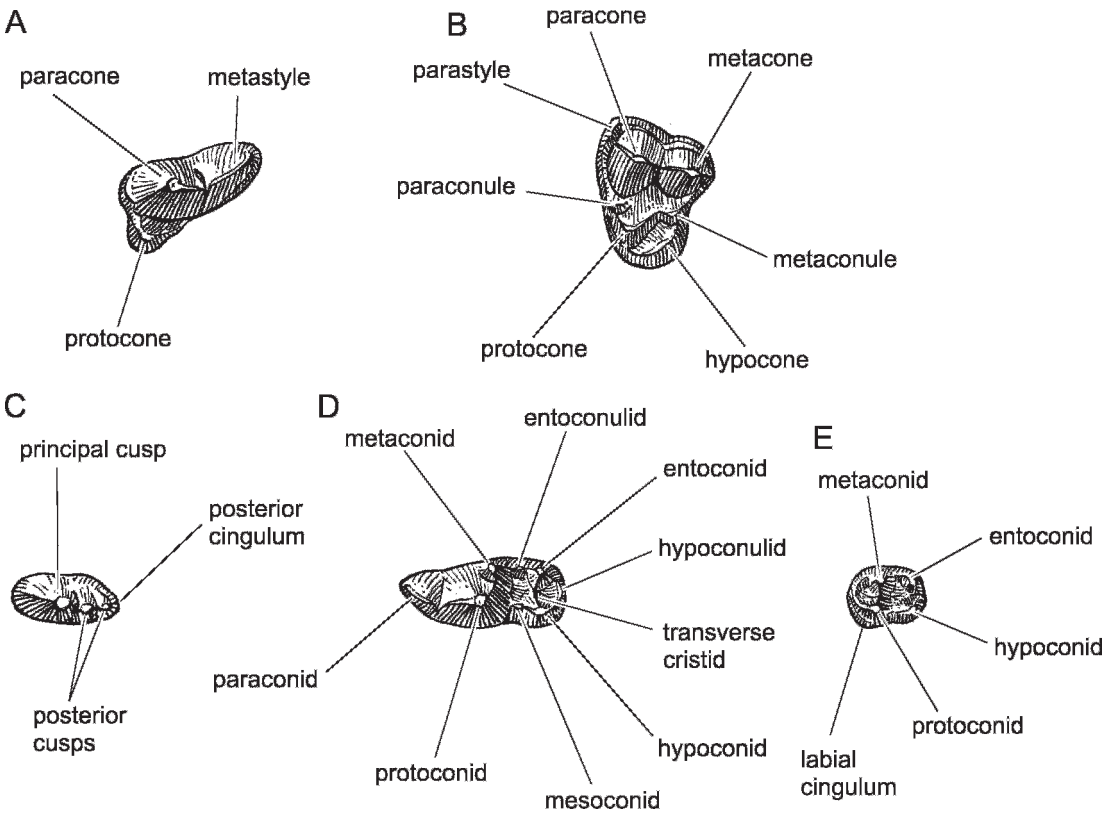

Fig. 70. Dental nomenclature used in this report.

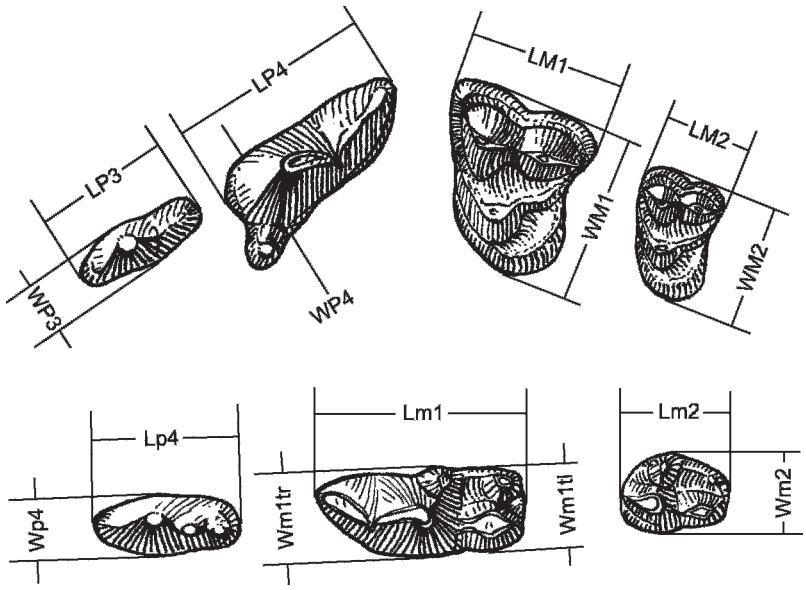

Fig. 71. Dental dimensions used in this report. Measurement acronyms are detailed in appendix 3.

TABLE 5
Summary of Dental Measurements Used to Typify Taxa Recognized in This Work

	Bl	LP1	LP2	LP3	LP4	WP4	LM1	WM1	LM2	WM2	Lp1	Lp2	Lp3	Lp4	Wp4	Lm1	Wm1tr	Wm1tl	Lm2	Wm2
Archaeocyon pavidus																				
Mean	69.67	2.03	3.68	4.44	6.73	3.14	5.20	6.94	3.47	5.22	2.14	3.71	4.49	5.18	2.23	7.36	2.95	3.13	4.28	2.76
SD	1.25	0.18	0.15	0.27	0.45	0.27	0.37	0.24	0.17	0.46	0.23	0.34	0.42	0.40	0.23	0.38	0.28	0.25	0.28	0.17
CV	1.79	8.87	4.08	6.08	6.69	8.60	7.12	3.46	4.90	8.81	10.75	9.16	9.35	7.72	10.31	5.16	9.49	7.99	6.54	6.16
Max.	71.0	2.3	3.8	5.0	7.6	3.5	5.5	7.3	3.8	5.8	2.5	4.2	5.5	6.1	2.6	7.9	3.5	3.7	4.7	3.0
Min.	68.0	1.80	3.4	4.1	6.3	2.8	4.5	6.6	3.3	4.4	1.8	3.0	4.0	4.6	1.8	6.5	2.5	2.7	3.8	2.3
n	3	4	5	7	8	5	6	5	7	6	5	8	10	12	12	16	13	14	16	14
Leptocyon sp. A																				
UNSM 25354													5.3	6.0	2.4	7.6	3.7	3.4		
Leptocyon mollis																				
UCMP 90																				
(type)			5.2	6.3	9.5	4.6	7.8	9.0	4.8	7.0										
Leptocyon douglassi																				
USNM 19931																				
(type)					9.5	4.2	6.7	8.0	3.9	6.0		5.4	6.6	7.2	2.5	10.0	3.5	3.6	5.5	3.4
Mean			5.10	5.80	8.93	4.00	6.55	7.70	4.00	6.10	2.70	5.23	6.37	6.83	2.58	9.82	3.54	3.62	5.28	3.18
SD			0.00	0.00	0.42	0.14	0.45	0.19	0.10	0.10	0.00	0.31	0.26	0.38	0.13	0.60	0.26	0.32	0.32	0.23
CV			0.00	0.00	4.69	3.54	6.87	2.43	2.50	1.64	0.00	5.91	4.12	5.52	5.04	6.09	7.28	8.81	6.04	7.17
Max.			5.1	5.8	9.5	4.2	7.2	8.0	4.1	6.2	2.7	5.5	6.6	7.2	2.8	10.7	4.0	4.0	5.6	3.4
Min.			5.1	5.8	8.5	3.9	6.0	7.5	3.9	6.0	2.7	4.8	6.0	6.4	2.5	8.9	3.2	3.1	4.8	2.8
n			1	1	3	3	4	4	2	2	1	3	3	4	4	5	5	5	5	4
Leptocyon vulpinus																				
AMNH 12883																				
(type)		3.2			10.4	4.4	8.5				3.0	5.8	6.9	7.5	3.1	11.5	4.3	4.5	7.0	3.8
Mean		3.20			10.40	4.40	8.50				3.00	5.68	6.58	7.43	3.23	11.27	4.47	4.59	6.35	3.63
SD		0.00			0.00	0.00	0.00				0.00	0.18	0.25	0.18	0.25	0.50	0.44	0.49	0.44	0.30
CV		0.00			0.00	0.00	0.00				0.00	3.15	3.77	2.41	7.71	4.44	9.76	10.58	6.91	8.36
Max.		3.2			10.4	4.4	8.5				3.0	5.9	6.9	7.7	3.6	11.8	4.9	5.0	7.0	4.0
Min.		3.20			10.4	4.4	8.5				3.0	5.5	6.2	7.2	2.8	10.3	3.5	3.5	5.9	3.2
n		1			1	1	1				1	4	5	6	6	7	7	7	4	4
Leptocyon delicatus																				
ACM 31102																				
(type)												2.9	3.4	3.7	1.5	5.6	2.2	2.0	2.7	1.6

TABLE 5
(Continued)

	Bl	LP1	LP2	LP3	LP4	WP4	LM1	WM1	LM2	WM2	Lp1	Lp2	Lp3	Lp4	Wp4	Lm1	Wm1tr	Wm1tl	Lm2	Wm2
Leptocyon sp. B																				
F:AM 97247																8.0	2.5	2.7		
Leptocyon gregorii																				
AMNH 12879																				
(type)				6.0	10.2	4.0	7.1	8.5	4.1	5.4				6.5		11.0	4.1		5.3	3.2
Mean	90.00	3.10	5.40	6.05	9.85	3.85	7.05	8.60	4.20	5.50	3.00	5.33	6.13	6.73	2.70	10.45	3.88	3.93	5.50	3.40
SD	0.00	0.00	0.00	0.05	0.35	0.15	0.05	0.10	0.10	0.10	0.00	0.12	0.29	0.19	0.20	0.39	0.33	0.32	0.51	0.36
CV	0.00	0.00	0.00	0.83	3.55	3.90	0.71	1.16	2.38	1.82	0.00	2.34	4.68	2.86	7.41	3.78	8.46	8.13	9.27	10.47
Max.	90.0	3.1	5.4	6.1	10.2	4.0	7.1	8.7	4.3	5.6	3.0	5.5	6.5	7.0	2.9	11.0	4.5	4.4	6.2	3.9
Min.	90.0	3.10	5.4	6.0	9.5	3.7	7.0	8.5	4.1	5.4	3.0	5.2	5.8	6.5	2.5	10.1	3.5	3.5	5.0	3.1
n	1	1	1	2	2	2	2	2	2	2	1	3	3	4	2	6	6	4	3	3
Leptocyon leidyi, n. sp.																				
UNSM 25715																				
(type)	100.0	3.0	5.0	6.0	9.1	4.1	6.9	8.2	4.0	6.2										
Mean	100.00	2.83	5.45	6.14	9.54	3.95	7.09	8.61	4.06	6.34	2.63	5.50	6.51	7.23	3.00	10.64	4.06	4.05	5.60	3.49
SD	0.00	0.12	0.29	0.47	0.35	0.13	0.28	0.27	0.35	0.44	0.23	0.54	0.41	0.58	0.23	0.66	0.28	0.35	0.42	0.27
CV	0.00	4.40	5.27	7.61	3.71	3.19	3.95	3.13	8.61	6.92	8.68	9.88	6.26	8.03	7.82	6.23	7.03	8.64	7.56	7.78
Max.	100.0	3.0	5.7	6.6	10.3	4.1	7.5	9.0	4.8	7.1	3.0	6.2	7.1	8.1	3.5	12.0	4.6	4.8	6.3	4.0
Min.	100.0	2.70	5.0	5.3	9.1	3.8	6.6	8.2	3.5	5.7	2.4	4.7	5.7	6.3	2.6	9.5	3.4	3.4	4.7	3.0
n	1	3	4	5	7	6	7	7	8	8	6	12	12	22	20	38	32	34	25	24
Leptocyon vafer																				
USNM 126																				
(type)												6.3	7.4	8.2	3.2	11.5	4.7	4.8	6.3	4.1
Mean	98.75	2.97	5.77	7.17	10.54	4.29	7.67	9.20	4.59	6.68	2.59	5.98	6.95	7.68	3.18	11.75	4.43	4.28	6.00	3.75
SD	5.97	0.33	0.32	0.49	0.48	0.40	0.45	0.38	0.31	0.35	0.23	0.30	0.38	0.40	0.24	0.58	0.30	0.30	0.40	0.26
CV	6.05	11.12	5.63	6.80	4.54	9.41	5.81	4.15	6.69	5.18	8.98	5.04	5.40	5.22	7.49	4.96	6.68	6.98	6.61	6.96
Max.	108.0	3.4	6.3	7.9	11.4	5.0	8.5	10.0	5.2	7.3	3.0	6.5	7.5	8.5	4.0	13.3	5.4	5.0	7.0	4.5
Min.	93.0	2.60	5.3	6.4	9.3	3.4	6.7	8.2	4.0	6.1	2.2	5.2	6.0	6.7	2.7	10.5	3.8	3.5	5.0	3.2
n	4	3	6	14	32	29	27	26	18	18	17	31	35	52	45	98	68	77	79	67
Leptocyon matthewi, n. sp.																				
F:AM 25198																				
(type)												6.5	8.1	9.1	4.0	14.0	5.6	5.5	7.0	5.5
Mean					11.69	4.60	8.42	10.50	5.17	7.95	2.86	6.37	7.35	8.13	3.36	13.09	5.02	4.94	6.44	4.24

TABLE 5
(Continued)

	Bl	LP1	LP2	LP3	LP4	WP4	LM1	WM1	LM2	WM2	Lp1	Lp2	Lp3	Lp4	Wp4	Lm1	Wm1tr	Wm1tl	Lm2	Wm2
SD					0.36	0.28	0.72	0.49	0.24	0.05	0.23	0.32	0.39	0.46	0.31	0.69	0.30	0.34	0.40	0.44
CV					3.05	5.99	8.61	4.71	4.56	0.63	8.16	4.97	5.31	5.69	9.37	5.31	6.05	6.98	6.28	10.45
Max.					12.1	5.0	9.3	11.3	5.5	8.0	3.2	6.9	8.1	9.1	4.0	14.0	5.6	5.5	7.4	5.5
Min.					11.0	4.2	7.5	10.0	5.0	7.9	2.5	5.8	7.0	7.5	2.8	11.2	4.3	4.3	5.8	3.5
n					7	5	5	4	3	2	5	9	10	12	12	28	21	23	20	18
Leptocyon tejonensis, n. sp.																				
LACM 16719 (type)												5.3	6.0	6.8	3.0	11.2	4.2	4.1	6.0	3.8
Mean				6.30	10.10	4.15	7.87	9.10	4.60	6.50		5.43	6.20	6.93	3.23	11.80	4.44	4.40	5.75	3.75
SD				0.00	0.50	0.15	0.21	0.46	0.51	0.14		0.12	0.16	0.09	0.17	0.52	0.33	0.32	0.25	0.05
CV				0.00	4.92	3.61	2.71	5.10	11.08	2.18		2.30	2.63	1.36	5.26	4.40	7.50	7.31	4.35	1.33
Max.				6.3	10.8	4.3	8.2	9.8	5.2	6.7		5.6	6.4	7.0	3.4	12.5	4.9	5.0	6.0	3.8
Min.				6.3	9.7	4.0	7.6	8.5	3.8	6.3		5.3	6.0	6.8	3.0	11.1	3.8	4.0	5.5	3.7
n				1	3	2	6	4	4	4		3	3	3	3	8	7	6	2	2
Vulpes kernensis, n. sp.																				
LACM 55215 (type)				7.1	11.2	4.7	7.5	9.0	4.0	6.8										
LACM 55216														7.0		11.8	3.9	4.0		
Vulpes stenognathus																				
OMP 40-4-S24 (type)												7.1	8.2	9.4	3.8	13.9	5.5	0.0	7.5	5.8
Mean	122.00	4.95	8.08	9.24	13.27	4.87	9.55	11.18	6.06	8.49	3.42	7.63	8.57	9.75	3.73	14.90	5.42	5.46	7.48	4.81
SD	5.00	0.15	0.42	0.35	0.73	0.49	0.62	0.63	0.36	0.60	0.39	0.54	0.56	0.55	0.26	0.80	0.32	0.34	0.44	0.52
CV	4.10	3.03	5.25	3.76	5.53	9.97	6.46	5.63	5.96	7.02	11.46	7.04	6.57	5.67	7.05	5.38	5.98	6.25	5.95	10.81
Max.	127.0	5.1	8.8	9.6	14.5	6.0	10.5	12.3	6.8	9.4	4.3	8.7	9.5	10.7	4.2	16.2	6.0	6.2	8.5	5.8
Min.	117.0	4.80	7.5	8.5	11.8	3.9	8.4	10.0	5.2	7.0	2.7	6.4	7.2	8.0	3.2	12.5	4.5	4.5	6.2	3.8
n	2	2	9	10	31	26	24	23	17	19	10	19	27	28	20	70	59	53	32	27
Vulpes sp. *V.* cf. *velox*																				
Mean					12.00	4.70	7.30	9.20				7.20	7.30	8.17	3.27	13.25	4.50	4.48	5.85	3.90
SD					0.00	0.00	0.00	0.00				0.00	0.90	0.63	0.29	0.54	0.25	0.33	0.35	0.10
CV					0.00	0.00	0.00	0.00				0.00	12.33	7.77	8.78	4.08	5.67	7.47	5.98	2.56
Max.					12.0	4.7	7.3	9.2				7.2	8.2	8.8	3.6	13.9	4.9	4.9	6.2	4.0
Min.					12.0	4.7	7.3	9.2				7.2	6.4	7.3	2.9	12.5	4.2	4.1	5.5	3.8
n					1	1	1	1				2	2	3	3	4	4	4	2	2

TABLE 5
(Continued)

	Bl	LP1	LP2	LP3	LP4	WP4	LM1	WM1	LM2	WM2	Lp1	Lp2	Lp3	Lp4	Wp4	Lm1	Wm1tr	Wm1tl	Lm2	Wm2
Metalopex macconnelli, n. sp.																				
LACM 55237																				
(type)			6.6	7.5	11.4	4.5	9.0	9.6	5.6	6.9										
Mean		3.70	6.03	7.37	10.89	4.77	8.42	9.74	5.24	7.33	3.25	6.10	7.00	8.29	3.41	12.37	4.52	4.71	6.92	4.24
SD		0.00	0.38	0.42	0.77	0.37	0.58	0.35	0.39	0.52	0.15	0.16	0.16	1.02	0.65	0.73	0.35	0.46	0.48	0.39
CV		0.00	6.25	5.69	7.04	7.74	6.94	3.64	7.40	7.06	4.62	2.59	2.26	12.36	19.18	5.89	7.86	9.77	6.92	9.27
Max.		3.7	6.6	8.3	12.0	5.6	9.4	10.4	5.8	8.6	3.4	6.3	7.2	10.4	4.8	13.5	5.4	5.3	8.0	4.8
Min.		3.7	5.4	7.0	9.7	4.3	7.4	9.0	4.5	6.8	3.1	5.9	6.8	7.5	2.8	11.1	4.0	3.8	6.3	3.7
n		1	6	9	11	11	12	12	10	10	2	4	4	9	8	13	13	13	10	10
Metalopex merriami																				
F:AM 49282																				
(type)			7.8	8.5	13.5	5.0	10.7	11.4	8.1	9.3		8.0	8.6	9.8	4.0	15.5		6.1	9.5	5.5
Mean			7.70	8.70	13.50	5.00	10.63	11.37	7.67	9.03	4.00	6.98	7.78	8.87	3.68	14.55	5.32	5.80	9.18	5.48
SD			0.10	0.20	0.00	0.00	0.57	0.37	0.31	0.60	0.00	0.90	0.68	0.75	0.28	0.78	0.35	0.44	0.77	0.04
CV			1.30	2.30	0.00	0.00	5.39	3.24	4.03	6.66	0.00	12.95	8.69	8.48	7.57	5.36	6.66	7.65	8.35	0.79
Max.			7.8	8.9	13.5	5.0	11.3	11.8	8.1	9.6	4.0	8.0	8.6	9.8	4.0	15.6	6.0	6.4	10.0	5.5
Min.			7.6	8.5	13.5	5.0	9.9	10.9	7.4	8.2	4.0	5.8	7.0	7.6	3.3	13.5	5.0	5.3	7.8	5.4
n			2	2	1	1	3	3	3	3	1	5	5	6	5	6	5	6	6	4
Metalopex bakeri, n. sp.																				
F:AM 62970																				
(type)												6.5	7.8	8.4	3.8	12.5				
F:AM 62971					11.7	5.0	10.0	11.4	6.8	8.5										
Urocyon webbi, n. sp.																				
UF 19407																				
(type)												5.0	6.5	7.5	3.5	12.3	5.0	5.7	8.5	5.3
UF 19408				6.3	10.5	4.5														
Urocyon galushai, n. sp.																				
F:AM 63104																				
(type)				7.3	10.8	4.9	9.2	10.0				6.5	6.8	8.0	3.3	12.5			7.3	4.8
Mean				7.30	10.80	4.90	9.30	10.50				6.50	6.55	7.65	3.15	11.75		4.45	6.87	4.33
SD				0.00	0.00	0.00	0.10	0.50				0.00	0.25	0.35	0.15	0.75		0.45	0.42	0.46
CV				0.00	0.00	0.00	1.08	4.76				0.00	3.82	4.58	4.76	6.38		10.11	6.10	10.71
Max.				7.3	10.8	4.9	9.4	11.0				6.5	6.8	8.0	3.3	12.5		4.9	7.3	4.8

TABLE 5
(Continued)

	Bl	LP1	LP2	LP3	LP4	WP4	LM1	WM1	LM2	WM2	Lp1	Lp2	Lp3	Lp4	Wp4	Lm1	Wm1tr	Wm1tl	Lm2	Wm2
Min.				7.3	10.8	4.9	9.2	10.0				6.5	6.3	7.3	3.0	11.0		4.0	6.3	3.7
n				1	1	1	2	2				2	2	2	2	2		2	3	3
Urocyon citrinus, n. sp.																				
UF 19294 (type)												5.5	6.0	7.5	3.2	12.0	4.0	5.0	7.8	4.9
Urocyon minicephalus																				
UF 13146 (type)			5.2	6.0	9.8	4.7	8.9	10.4	6.0	8.0										
Mean			5.20	6.45	9.86	4.51	8.46	9.72	6.05	7.50		5.28	5.97	7.45	3.43	11.65	4.34	4.90	6.75	5.10
SD			0.00	0.45	0.21	0.16	0.24	0.42	0.05	0.50		0.25	0.21	0.27	0.19	0.38	0.24	0.23	0.25	0.30
CV			0.00	6.98	2.16	3.44	2.86	4.29	0.83	6.67		4.82	3.44	3.61	5.41	3.30	5.52	4.68	3.70	5.88
Max.			5.2	6.9	10.3	4.7	8.9	10.4	6.1	8.0		5.7	6.2	8.0	3.7	12.3	4.7	5.2	7.0	5.4
Min.			5.2	6.0	9.6	4.3	8.2	9.3	6.0	7.0		5.0	5.7	7.0	3.2	11.2	4.0	4.5	6.5	4.8
n			1	2	7	7	5	5	2	2		6	6	8	8	8	8	8	2	2
Cerdocyon texanus, n. sp.																				
F:AM 62984-5 (type)		4.9	6.9	7.8	13.8	5.3						7.4	7.6	9.5	4.3	14.7	5.9	5.7	8.2	5.7
NMNH 26861																14.6	6.9	5.9		
Cerdocyon avius																				
IGM 2903 (type)							9.2	10.8								12.8				
Chrysocyon nearcticus, n. sp.																				
UA 12610 (type)												11.5	12.5	13.8	5.6	21.3	8.3	7.8	10.5	7.0
Mean											5.10	11.80	13.33	14.15	6.15	21.90	8.70	8.25	11.05	7.75
SD											0.00	0.30	0.62	0.35	0.55	0.60	0.40	0.45	0.55	0.75
CV											0.00	2.54	4.68	2.47	8.94	2.74	4.60	5.45	4.98	9.68
Max.											5.1	12.1	14.0	14.5	6.7	22.5	9.1	8.7	11.6	8.5
Min.											5.1	11.5	12.5	13.8	5.6	21.3	8.3	7.8	10.5	7.0
n											1	2	3	2	2	2	2	2	2	2
Theriodictis? floridanus, n. sp.																				
UF 19324 (type)																			11.6	8.3
UF 133922																24.10	10.50	8.10		

TABLE 5
(Continued)

	Bl	LP1	LP2	LP3	LP4	WP4	LM1	WM1	LM2	WM2	Lp1	Lp2	Lp3	Lp4	Wp4	Lm1	Wm1tr	Wm1tl	Lm2	Wm2
Eucyon? *skinneri*, n. sp.																				
F:AM 25143																				
(type)												7.0	8.4	9.0	4.0	14.8	6.3	6.0		
Eucyon davisi																				
UO F3241																				
(type)																			8.3	4.5
Mean	136.00	4.98	9.13	10.34	15.69	5.99	10.93	12.93	6.77	9.76	4.19	8.74	10.03	11.21	4.53	17.07	6.35	6.23	8.71	5.77
SD	6.54	0.37	0.62	0.45	0.91	0.53	0.80	0.91	0.56	0.76	0.51	0.59	0.70	0.67	0.42	1.01	0.57	0.48	0.57	0.48
CV	4.81	7.34	6.78	4.37	5.79	8.78	7.33	7.07	8.25	7.74	12.09	6.77	6.97	5.96	9.27	5.91	8.91	7.73	6.55	8.24
Max.	148.0	5.8	10.4	11.3	18.0	7.5	12.5	16.4	8.1	11.8	5.4	10.3	11.5	12.8	5.3	19.2	7.7	7.4	9.8	6.7
Min.	128.0	4.40	8.0	9.4	14.0	4.6	9.0	11.6	6.0	7.5	3.4	7.6	8.5	9.7	3.8	15.0	4.7	4.5	7.5	4.5
n	5	10	24	28	61	45	62	60	52	49	33	53	72	94	72	134	109	109	81	66
Canis ferox																				
IGM 1130																				
(type)				11.7	16.3		11.7	15.0	6.4	9.9			11.0			19.2	7.4	6.8	8.9	5.8
Mean	169.67	6.30	11.00	12.30	18.06	7.07	12.48	14.67	7.53	10.47	5.00	9.95	11.68	12.85	5.28	19.93	7.43	7.07	9.31	6.43
SD	8.73	0.20	1.47	1.32	1.04	0.62	0.83	1.28	0.70	0.94	0.87	0.75	0.73	1.05	0.57	1.47	0.73	0.58	0.67	0.45
CV	5.15	3.17	13.38	10.74	5.78	8.80	6.61	8.76	9.24	8.97	17.49	7.58	6.27	8.16	10.89	7.36	9.78	8.18	7.21	6.94
Max.	182.0	6.5	12.2	14.3	19.5	8.0	14.3	16.0	8.6	12.0	6.5	11.1	13.0	14.5	6.2	23.0	8.6	8.5	10.0	7.1
Min.	163.0	6.1	8.5	10.0	16.0	5.8	11.4	12.5	6.4	9.2	4.4	8.6	10.0	11.1	4.3	17.4	5.9	5.8	8.0	5.5
n	3	2	4	6	13	11	11	11	10	10	4	11	13	11	11	18	14	14	14	13
Canis thöoides, n. sp.																				
F:AM 63101																				
(type)			8.9	10.5	16.7	7.2	11.0	13.3	6.7	10.0	4.9	8.5	10.0	11.4	5.5	18.0	7.6	8.0	8.5	6.1
Mean			8.90	10.50	16.70	7.20	11.00	13.30	6.70	10.00	4.90	8.50	10.20	11.80	5.65	18.35	7.50	7.60	8.65	6.30
SD			0.00	0.00	0.00	0.00	0.00	0.00	0.00	0.00	0.00	0.00	0.20	0.40	0.15	0.35	0.10	0.40	0.15	0.20
CV			0.00	0.00	0.00	0.00	0.00	0.00	0.00	0.00	0.00	0.00	1.96	3.39	2.65	1.91	1.33	5.26	1.73	3.17
Max.			8.9	10.5	16.7	7.2	11.0	13.3	6.7	10.0	4.9	8.5	10.4	12.2	5.8	18.7	7.6	8.0	8.8	6.5
Min.			8.9	10.5	16.7	7.2	11.0	13.3	6.7	10.0	4.9	8.5	10.0	11.4	5.5	18.0	7.4	7.2	8.5	6.1
n			1	1	1	1	1	1	1	1	1	2	2	2	2	2	2	2	2	2

TABLE 5
(Continued)

	Bl	LP1	LP2	LP3	LP4	WP4	LM1	WM1	LM2	WM2	Lp1	Lp2	Lp3	Lp4	Wp4	Lm1	Wm1tr	Wm1tl	Lm2	Wm2
Canis feneus, n. sp.																				
F:AM 25515																				
(type)				10.2	15.5	6.5	11.0	13.4	7.5	11.0	4.0	9.0	10.0	11.2		16.5			9.4	6.0
Canis cedazoensis																				
TMM 41536-																				
41 (type)				10.5	16.7	6.9	10.3	12.0												
Canis lepophagus																				
WTUC 881																				
(type)	171.5	6.0	10.0	12.9	18.8	7.5	12.6	15.9	8.0	11.4										
Mean	172.84	5.43	10.53	12.14	18.94	7.49	12.91	14.88	7.68	10.86	4.98	10.42	11.67	12.89	5.50	20.63	7.66	8.00	10.10	7.06
SD	4.64	0.60	0.45	0.68	1.10	0.61	0.73	0.99	0.51	0.66	0.43	0.62	0.57	0.57	0.37	1.04	0.51	0.50	0.54	0.54
CV	2.68	11.08	4.30	5.63	5.84	8.17	5.64	6.63	6.69	6.08	8.67	5.98	4.93	4.39	6.68	5.05	6.62	6.19	5.32	7.63
Max.	180.0	6.0	11.1	12.9	20.6	8.2	14.5	16.0	8.4	11.5	5.6	11.6	12.7	14.0	6.2	22.6	8.5	9.0	11.0	8.0
Min.	166.2	4.60	9.9	10.8	16.6	6.5	11.6	13.2	6.5	9.3	4.3	9.2	10.8	12.0	4.8	18.8	6.7	7.0	9.0	6.0
n	5	3	6	7	14	14	16	14	9	9	13	20	22	27	25	37	33	30	29	27
Canis edwardii																				
NMNH 12862																				
(type)	200.0	7.0	12.5	15.0	23.8	9.4	14.5	18.0	8.5	12.1	6.0	12.3	13.6	15.5	7.3	25.0	9.7	9.5	11.4	8.0
Mean	191.50	6.46	12.27	14.31	21.76	8.66	14.26	16.81	8.16	11.36	5.53	11.20	12.74	14.03	6.38	24.95	9.45	8.95	10.43	7.43
SD	8.50	0.49	0.78	1.30	1.23	0.73	1.05	1.25	0.40	1.05	0.46	1.01	0.76	0.97	0.60	1.52	0.79	0.74	0.53	0.56
CV	4.44	7.56	6.38	9.11	5.64	8.47	7.34	7.41	4.87	9.24	8.26	9.06	6.00	6.93	9.35	6.10	8.34	8.26	5.11	7.58
Max.	200.0	7.1	13.8	16.5	23.8	9.8	16.1	18.7	8.8	13.5	6.0	13.5	14.5	16.2	7.3	28.0	10.6	10.1	11.6	8.8
Min.	183.0	6.00	11.2	11.7	18.8	7.5	11.5	13.5	7.4	10.0	4.5	9.8	11.5	12.5	5.5	22.0	8.0	7.5	9.5	6.3
n	2	5	7	9	21	21	25	25	18	18	9	15	20	23	21	34	28	31	24	23
Canis latrans (fossils)																				
Mean					19.95	8.13	12.63	15.83	7.57	10.50		10.30	11.17	12.89	6.09	21.97	8.36	8.11	9.73	6.77
SD					0.86	0.43	0.85	1.35	1.17	1.02		1.23	0.82	0.82	0.50	1.31	0.77	0.64	0.63	0.43
CV					4.29	5.32	6.76	8.55	15.42	9.74		11.91	7.34	6.36	8.29	5.96	9.26	7.84	6.46	6.30
Max.					21.2	8.6	13.6	17.5	8.8	11.8		11.7	12.3	14.0	6.9	24.0	9.7	9.6	10.6	7.3
Min.					18.9	7.6	11.0	13.5	6.0	9.3		8.2	9.6	11.5	5.2	19.9	7.1	6.7	8.9	6.1
n					4	4	6	6	3	3		8	9	10	10	20	19	19	8	7

TABLE 5
(Continued)

	Bl	LP1	LP2	LP3	LP4	WP4	LM1	WM1	LM2	WM2	Lp1	Lp2	Lp3	Lp4	Wp4	Lm1	Wm1tr	Wm1tl	Lm2	Wm2
Canis latrans orcutti																				
Mean	177.50		11.90	13.14	21.01	8.05	13.43	15.88	7.71	11.38	5.00	10.89	11.85	12.82	5.98	23.10	8.41	7.92	10.19	6.75
SD	4.32		0.27	0.64	0.59	0.52	0.70	0.72	0.48	0.40	0.25	0.51	0.63	0.62	0.29	0.92	0.46	0.34	0.62	0.35
CV	2.43		2.30	4.87	2.83	6.50	5.19	4.52	6.28	3.48	5.10	4.65	5.31	4.85	4.83	3.99	5.41	4.29	6.13	5.16
Max.	183.5		12.3	13.9	22.1	9.0	14.5	17.0	8.5	12.0	5.3	12.3	13.3	14.1	6.5	24.5	9.5	8.8	11.2	7.6
Min.	173.5		11.6	11.8	19.6	6.8	12.1	14.6	7.0	11.0	4.6	9.9	10.9	11.3	5.4	20.0	7.7	7.4	9.0	6.0
n	3		4	9	14	14	13	13	13	13	4	14	17	26	25	33	32	30	24	24
Canis armbrusteri																				
NMNH 7662 (type)														18.1	9.4	31.0		12.0	12.8	9.8
Mean	253.50	7.33	13.50	16.83	27.05	11.30	17.39	20.91	9.79	14.49	6.54	13.37	14.94	16.78	8.36	29.54	11.45	10.97	12.30	9.05
SD	3.50	1.33	0.65	1.25	1.27	0.78	1.16	1.26	0.88	1.45	0.10	0.72	1.02	1.33	1.06	1.85	0.82	0.93	1.11	0.88
CV	1.38	18.10	4.85	7.43	4.71	6.91	6.65	6.04	8.98	9.99	1.56	5.42	6.80	7.92	12.68	6.27	7.13	8.47	9.05	9.70
Max.	257.0	8.6	14.5	18.5	29.0	13.0	19.8	23.5	11.0	17.0	6.7	14.2	16.3	18.5	9.8	32.0	13.0	12.5	14.0	10.0
Min.	250.0	5.50	12.5	14.6	25.2	10.0	15.8	18.8	8.4	11.9	6.4	12.4	13.4	14.3	6.6	27.0	10.2	9.8	10.0	7.4
n	2	3	5	8	14	14	15	14	10	9	5	6	8	12	12	14	13	15	14	13
Canis armbrusteri (Cumberland Cave)																				
Mean	253.50	7.05	13.85	17.70	28.06	11.57	18.37	22.08	10.28	15.24	6.55	13.47	15.04	17.73	9.12	30.16	12.00	12.05	13.04	9.62
SD	3.50	1.55	0.65	0.51	0.68	0.81	0.75	0.77	0.63	1.14	0.05	0.77	0.88	0.80	0.70	1.33	0.87	0.11	0.42	0.43
CV	1.38	21.99	4.69	2.88	2.43	6.99	4.06	3.50	6.14	7.45	0.76	5.73	5.85	4.53	7.69	4.42	7.26	0.93	3.24	4.48
Max.	257.0	8.6	14.5	18.5	29.0	13.0	19.8	23.5	11.0	17.0	6.6	14.2	16.0	18.5	9.8	31.5	13.0	12.2	13.5	10.0
Min.	250.0	5.50	13.2	17.0	26.8	10.2	17.3	21.0	9.1	13.5	6.5	12.4	13.4	16.0	7.7	27.9	10.6	11.9	12.4	8.8
n	2	2	2	5	7	7	7	6	6	5	2	3	5	6	6	5	4	4	5	5
Canis dirus (Irvingtonian)																				
Mean		8.90	14.80	17.95	29.84	12.84	19.14	22.76	9.28	13.03	6.60	13.38	14.52	18.59	9.50	32.07	12.24	11.90	11.86	9.33
SD		0.00	0.00	0.75	1.32	0.94	1.25	1.57	0.64	1.29	0.41	0.67	0.53	1.11	0.59	1.73	0.65	0.58	0.61	0.51
CV		0.00	0.00	4.18	4.41	7.35	6.53	6.92	6.92	9.88	6.19	5.03	3.68	5.97	6.16	5.40	5.33	4.84	5.16	5.44
Max.		8.9	14.8	18.7	31.4	14.3	21.0	25.6	10.2	14.8	7.1	14.4	15.4	20.5	10.1	34.7	13.5	12.9	13.0	10.2
Min.		8.90	14.8	17.2	27.5	11.4	17.6	20.2	8.5	11.3	6.1	12.6	13.9	17.0	8.3	29.7	11.6	11.0	10.9	8.6
n		1	2	2	5	5	8	8	4	4	3	4	6	7	7	7	5	7	8	8
Canis dirus (Rancholabrean)																				
Mean			15.20	18.16	31.58	13.40	19.29	22.89	9.59	14.30		15.11	16.02	19.38	9.79	34.31	12.90		12.74	9.48
SD			0.50	0.48	1.22	0.78	0.59	1.34	0.69	0.89		0.84	0.86	0.64	0.26	1.91	0.78		0.32	0.36

TABLE 5
(Continued)

	Bl	LP1	LP2	LP3	LP4	WP4	LM1	WM1	LM2	WM2	Lp1	Lp2	Lp3	Lp4	Wp4	Lm1	Wm1tr	Wm1tl	Lm2	Wm2
CV			3.29	2.67	3.87	5.85	3.08	5.87	7.15	6.20		5.53	5.34	3.31	2.64	5.58	6.08		2.48	3.82
Max.			15.7	19.0	33.8	15.3	20.0	25.0	10.8	15.4		17.0	18.0	20.3	10.2	38.6	14.3		13.3	10.0
Min.			14.7	17.5	29.2	13.0	18.5	21.0	8.6	12.6		14.1	14.9	18.3	9.4	31.5	11.8		12.3	8.9
n			2	5	8	7	8	7	7	6		8	9	9	7	10	9		7	6
Canis lupus (Cripple Creek Sump)																				
Mean					23.20	9.60	14.10	17.70	8.10	11.50	6.40	12.65	14.15	15.73	8.13	27.03	10.43	9.20	10.80	8.13
SD					0.00	0.00	0.00	0.00	0.00	0.00	0.00	0.05	0.05	0.49	0.54	0.17	0.12	0.16	0.66	0.22
CV					0.00	0.00	0.00	0.00	0.00	0.00	0.00	0.40	0.35	3.13	6.68	0.63	1.20	1.77	6.11	2.66
Max.					23.2	9.6	14.1	17.7	8.1	11.5	6.4	12.7	14.2	16.3	8.9	27.2	10.6	9.4	11.5	8.4
Min.					23.2	9.6	14.1	17.7	8.1	11.5	6.4	12.6	14.1	15.1	7.7	26.8	10.3	9.0	10.0	7.8
n					1	1	1	1	1	1	1	2	2	3	3	3	3	3	4	4
Xenocyon texanus																				
YPM 10058 (type)											6.8	12.2	14.3	16.7	8.8	28.3	10.2	9.8	11.4	8.2
Xenocyon lycaonoides																				
Mean														14.70	6.90	24.80	10.00	8.50	12.30	8.35
SD														0.10	0.20	0.00	0.00	0.00	0.50	0.55
CV														0.68	2.90	0.00	0.00	0.00	4.07	6.59
Max.														14.8	7.1	24.8	10.0	8.5	12.8	8.9
Min.														14.6	6.7	24.8	10.0	8.5	11.8	7.8
n														2	2	1	1	1	2	2
Cuon alpinus																				
Mean							12.70	13.70				8.95	10.50	13.65	6.95	22.18	8.68	7.80	7.07	
SD							0.00	0.00				0.05	0.36	0.15	0.05	0.25	0.15	0.07	0.40	
CV							0.00	0.00				0.56	3.39	1.10	0.72	1.12	1.70	0.91	5.70	
Max.							12.7	13.7				9.0	10.8	13.8	7.0	22.6	8.9	7.9	7.4	
Min.							12.7	13.7				8.9	10.0	13.5	6.9	22.0	8.5	7.7	6.5	
n							1	1				2	3	2	2	4	4	4	3	

TABLE 6
Summary of Dental Measurements of Living Canid Taxa Used for Comparison in This Work

	Bl	LP1	LP2	LP3	LP4	WP4	LM1	WM1	LM2	WM2	Lp1	Lp2	Lp3	Lp4	Wp4	Lm1	Wm1tr	Wm1tl	Lm2	Wm2
Vulpes v. fulva (Georgia)																				
Mean	127.79	4.51	8.30	9.26	12.81		9.24	10.74	5.11	7.74	3.77	8.13	8.74	9.39	3.89	14.43	5.30	5.54	6.74	4.70
SD	5.48	0.16	0.30	0.35	0.80		0.54	0.65	0.31	0.52	0.20	0.33	0.36	0.41	0.27	0.90	0.36	0.32	0.28	0.21
CV	4.29	3.64	3.64	3.78	6.22		5.81	6.09	6.13	6.72	5.25	4.04	4.14	4.32	7.07	6.26	6.77	5.77	4.11	4.55
Max.	134.0	4.8	8.8	9.8	14.3		10.3	12.0	5.5	8.5	4.1	8.7	9.3	10.0	4.3	16.5	6.0	6.3	7.0	5.0
Min.	118.5	4.2	8.0	8.9	12.2		8.6	10.0	4.5	6.7	3.5	7.8	8.2	8.8	3.5	13.5	5.0	5.3	6.2	4.3
n	7	7	7	7	7		7	7	7	7	7	7	7	7	7	7	7	7	7	7
Vulpes velox (western N. Am.)																				
Mean	103.30	3.65	7.25	7.63	10.98	4.12	7.53	8.95	4.77	6.63	3.10	6.97	7.45	7.80	3.27	12.42	4.55	4.50	5.72	3.93
SD	5.42	0.50	0.60	0.36	0.48	0.23	0.31	0.24	0.27	0.43	0.28	0.35	0.38	0.52	0.14	0.51	0.18	0.23	0.30	0.27
CV	5.25	13.68	8.30	4.70	4.35	5.51	4.17	2.64	5.77	6.44	8.93	5.09	5.13	6.66	4.21	4.09	3.96	5.13	5.29	6.99
Max.	109.3	4.5	8.4	8.2	11.5	4.5	8.0	9.3	5.0	7.0	3.3	7.5	8.0	8.6	3.4	13.3	4.9	4.8	6.1	4.3
Min.	93.5	2.8	6.6	7.0	10.3	3.8	7.0	8.7	4.3	6.0	2.5	6.3	6.9	7.1	3.0	11.9	4.3	4.2	5.2	3.5
n	6	6	6	6	6	6	6	6	6	6	6	6	6	6	6	6	6	6	6	6
Vulpes macrotis (southwest U.S.)																				
Mean	104.50	3.27	5.87	6.90	10.28	3.57	7.10	8.40	4.07	6.17	2.85	6.08	6.80	7.58	2.95	11.75	4.07	4.10	5.63	3.65
SD	4.05	0.15	0.29	0.23	0.28	0.18	0.26	0.38	0.27	0.58	0.13	0.30	0.17	0.33	0.22	0.35	0.14	0.16	0.36	0.20
CV	3.88	4.56	4.89	3.35	2.72	5.03	3.64	4.51	6.61	9.35	4.42	4.97	2.55	4.40	7.39	2.98	3.38	3.98	6.45	5.42
Max.	111.5	3.5	6.4	7.2	10.5	3.9	7.6	8.9	4.3	7.0	3.0	6.4	7.0	8.0	3.2	12.3	4.3	4.4	6.0	3.9
Min.	99.0	3.0	5.5	6.5	9.8	3.4	6.8	7.8	3.5	5.3	2.7	5.7	6.6	7.0	2.6	11.2	3.9	3.9	4.9	3.3
n	5	6	6	6	6	6	6	6	6	6	6	6	6	6	4	6	6	6	6	6
Urocyon c. floridanus (Georgia)																				
Mean	112.05	3.58	5.61	6.19	10.39	4.43	8.72	10.04	5.96	7.90	3.08	5.38	5.98	7.48	3.68	12.35	4.59	5.18	7.14	4.60
SD	3.34	0.29	0.36	0.44	0.42	0.26	0.38	0.44	0.37	0.54	0.33	0.34	0.36	0.41	0.18	0.50	0.31	0.26	0.31	0.31
CV	2.98	8.03	6.42	7.16	4.06	5.96	4.38	4.42	6.22	6.81	10.58	6.26	6.06	5.46	4.86	4.03	6.70	5.02	4.29	6.78
Max.	118.5	4.2	6.6	7.2	11.4	5.1	9.7	10.9	6.8	9.5	3.9	6.2	6.8	8.7	4.0	13.5	5.3	5.9	7.7	5.5
Min.	104.0	2.9	4.9	5.1	9.4	3.9	7.8	9.0	5.0	6.5	2.3	4.7	5.1	6.8	3.4	11.2	3.8	4.7	6.6	4.0
n	66	69	67	68	70	70	70	70	69	69	63	68	64	69	12	70	70	70	69	69

TABLE 6
(Continued)

	Bl	LP1	LP2	LP3	LP4	WP4	LM1	WM1	LM2	WM2	Lp1	Lp2	Lp3	Lp4	Wp4	Lm1	Wm1tr	Wm1tl	Lm2	Wm2
Canis latrans (Nevada)																				
Mean	166.86	5.56	10.94	12.28	19.71	7.17	12.85	15.21	7.48	10.96	4.59	9.83	11.15	12.39	5.44	21.63	7.90	7.81	9.66	6.53
SD	7.70	0.37	0.63	0.57	0.86	0.36	0.65	0.66	0.49	0.57	0.49	0.55	0.56	0.56	0.31	0.77	0.41	0.44	0.51	0.45
CV	4.62	6.63	5.72	4.68	4.37	5.09	5.03	4.34	6.57	5.23	10.63	5.56	5.01	4.50	5.64	3.57	5.14	5.64	5.26	6.86
Max.	181.0	6.2	12.0	13.3	21.3	8.0	14.5	16.5	8.5	12.3	5.8	11.1	12.3	13.5	5.9	23.0	9.0	9.0	10.7	7.6
Min.	145.0	4.8	9.8	11.0	18.1	6.4	11.1	13.4	6.4	9.6	3.8	8.8	10.0	11.0	4.5	20.0	7.1	7.0	8.5	5.5
n	38	35	32	37	38	30	37	37	38	38	29	32	34	36	34	37	32	32	36	34
Canis lupus occidentalis (western Canada)																				
Mean	228.70	8.92	15.36	16.66	26.05	11.95	17.53	20.62	9.18	13.67	6.72	13.67	14.94	16.19	8.06	29.28	11.16	10.84	12.17	8.62
SD	8.17	0.56	0.52	0.58	1.35	0.58	1.06	1.00	0.46	0.58	0.53	0.54	0.89	0.69	0.32	1.81	0.46	0.76	0.56	0.55
CV	3.57	6.26	3.40	3.49	5.18	4.88	6.03	4.87	5.03	4.25	7.83	3.93	5.94	4.23	3.92	6.19	4.14	7.05	4.60	6.42
Max.	242.0	10.0	16.5	17.7	28.0	13.3	20.0	22.3	9.8	14.8	7.7	14.5	16.5	17.4	8.5	32.5	12.0	12.0	13.2	10.0
Min.	217.0	7.9	14.6	16.0	24.0	11.1	15.8	18.9	8.4	12.7	6.0	12.6	13.8	15.0	7.5	26.5	10.5	9.3	11.5	7.8
n	10	10	10	10	10	10	10	10	10	10	9	9	9	9	8	9	9	9	9	9
Mean + STD	236.87	9.48	15.88	17.24	27.40	12.53	18.59	21.62	9.64	14.25	7.25	14.20	15.83	16.87	8.38	31.09	11.62	11.61	12.73	9.18
Mean - STD	220.53	8.36	14.84	16.08	24.70	11.37	16.47	19.62	8.72	13.09	6.20	13.13	14.06	15.50	7.75	27.47	10.69	10.08	11.61	8.07

APPENDIX 4

Measurements of Limb Bones

The maximum lengths of the limbs bones listed in table 7 are indicated by the measurements given there. These data have principally been used to calculate certain ratios indicated in the text and graphically displayed in figure 52.

TABLE 7
Means of Measurements of Total Length of Limb Bones of Taxa Recognized in This Work
Sizes of samples are contained in parentheses. Radius/tibia ratios are in final column.

	Humerus	Radius	Ulna	MC III	Femur	Tibia	MT III	Radius/Tibia
Leptocyon vulpinus	98.0 (1)	82.0 (1)	96.0 (1)					
Leptocyon leidyi, n. sp.	96.0 (2)	81.5 (2)	95.5 (1)		110.5 (1)	102.2 (2)		0.80
Leptocyon vafer	88.0 (1)	74.1 (1)	103.8 (1)			110.5 (3)	49.3 (1)	0.67
Leptocyon matthewi, n. sp.			87.0 (1)	46.5 (1)	112.0 (1)			
Vulpes stenognathus		100.8 (1)	135.0 (1)	41.5 (1)	119.3 (1)	116.6 (1)	54.6 (1)	0.86
Eucyon davisi	119.8 (2)	114.6 (6)	138.5 (4)	49.4 (6)	133.9 (5)	138.1 (8)	62.6 (12)	0.83
Canis ferox	141.4 (2)	132.0 (2)	151.3 (1)	54.5 (2)		168.0 (1)	73.0 (1)	0.79
Canis thöoides, n. sp.	124.5 (1)	122.0 (1)		51.5 (1)		138.0 (1)	61.5 (1)	0.88
Canis lepophagus	144.0 (2)	136.5 (2)	152.5 (2)	60.4 (2)		156.7 (1)	66.0 (1)	0.87
Canis latrans	164.5 (1)	150.0 (1)		69.3 (1)			73.5 (1)	
Canis edwardii	189.0 (1)	166.2 (6)	181.0 (1)	72.7 (3)	170.9 (2)	183.9 (4)	78.3 (4)	0.90
Canis armbrusteri	192.8 (6)	195.7 (3)	228.7 (3)	83.0 (7)	226.8 (5)	222.5 (2)	99.0 (1)	0.88
Canis armbrusteri (Cumberland Cave)	193.8 (5)	183.5 (2)	228.7 (3)	83.0 (5)	218.0 (3)	222.5 (2)	99.0 (1)	0.82